UNIVERSITY OF CALIFORNIA

Los Angeles

Complexity-Generating Annulation Reactions in the Synthesis of Natural Products and Materials Scaffolds

A dissertation submitted in partial satisfaction of the

requirements for the degree Doctor of Philosophy

in Chemistry

by

Robert Bergstrand Susick

2020

© Copyright by

Robert Bergstrand Susick

2020

ABSTRACT OF THE DISSERTATION

Complexity-Generating Annulation Reactions in the Synthesis

of Natural Products and Materials Scaffolds

by

Robert Bergstrand Susick

Doctor of Philosophy in Chemistry

University of California, Los Angeles, 2020

Professor Neil Kamal Garg, Chair

This dissertation encompasses several studies pertaining to natural product total synthesis, reaction methodology development, and organic materials. Given that natural product structures inspire the development of new agrochemicals and pharmaceuticals, their syntheses remain a worthwhile pursuit in organic chemistry. Furthermore, the successful completion of a total synthesis endeavor can confirm proposed molecular structures and biological activities, in addition to serving as a testing ground for new synthetic methods. Similarly, organic materials impact many areas of humanity, including technology, health, and energy conversion. Therefore, developing new reaction methodologies is crucial for expanding the architectures, and thereby properties, of organic materials. Specifically, photocatalysts and organic light-emitting diodes

(OLEDs) often rely on photophysical properties imparted by *N*-containing polycyclic aromatic hydrocarbon (PAH) ligands. As such, new methods that provide access to unique *N*-containing heterocyclic scaffolds are highly desirable.

Chapter one offers a current perspective on the field of natural product total synthesis. Although historically viewed as a highly competitive field, several recent syntheses demonstrate a growing spirit of collaboration in total synthesis. By forming alliances with chemists in other fields, industries, or laboratories, total synthesis chemists have made many breakthroughs that would arguably not have been possible if working independently.

Chapter two describes our laboratory's total syntheses of several bioactive akuammiline alkaloids, including strictamine, 2(*S*)-cathafoline, akuammiline, Ψ-akuammigine, and 10-demethoxyvincorine. Our strategic approach to the natural products focused on the use of a modern variant of a classic reaction, the Fischer indolization, to install several rings and the common quaternary center found in each target. This strategy allowed for the first total syntheses of akuammilines bearing a methanoquinolizidine core, as well as those that bear vicinal quaternary centers. In addition, rearrangements of the methanoquinolizidine core were developed that allowed us to access pyrrolidinoindoline-containing akuammilines.

Chapter three describes synthetic studies of the reactive intermediates 2,3-pyridyne and 4,5-pyrimidyne. Heterocycles bearing one or more nitrogen atom are privileged motifs in natural products and pharmaceuticals. Therefore, methodologies that decorate such heterocycles are of great interest to the synthetic and biological communities. Arynes are highly reactive, transient species that can efficiently build multiple bonds in a single transformation, and our lab is particularly interested in accessing new, heterocyclic arynes to study their reactivity. This study

demonstrates the synthetic utility of 2,3-pyridyne and the undesired reactivity of a 4,5-pyrimidyne precursor.

Chapter four describes synthetic studies toward the development of new methods to manipulate polypyridyl organometallic scaffolds. Ruthenium- and iridium-based polypyridyl organometallic complexes have been known for nearly a century and have broadly impacted the scientific community, including the areas of catalysis, bioimaging, and energy conversion. Despite decades of study, methods to synthesize polypyridyl ligands are limited to relatively few transformations, particularly when extending π-conjugation. We detail the use of arynes to extend the conjugation of polypyridyl ligands "on-the-complex," thereby overcoming traditional limitations in ligand synthesis. We also disclose the first generation and trapping of a ligand-bound aryne on an organometallic complex.

Chapter five describes the synthesis of a novel π-extended carbazole ligand for the study of structure-property relationships in two-coordinate metal complexes. Recently, linear two-coordinate metal complexes of the general structure donor–metal–acceptor have been identified as promising dopants for OLEDs. Both the donor and acceptor ligand play a crucial role in tuning the photophysical properties of these complexes. However, donor ligands with extended π-conjugation have not been studied in this context. Our approach leverages heterocyclic arynes to synthesize π-extended donor ligands in a modular fashion, which can also apply to other PAHs. Subsequent photophysical studies of π-extended two-coordinate metal complexes identify a new dopant that displays up to 80% photoluminescence efficiency.

The dissertation of Robert Bergstrand Susick is approved.

Patrick Harran

Kendall Houk

Yi Tang

Neil Kamal Garg, Committee Chair

University of California, Los Angeles

2020

"Hard choices, easy life. Easy choices, hard life."

– Jerzy Gregorek

For my parents: Kris Bergstrand and Bob Susick

TABLE OF CONTENTS

Abstract....ii

Committee Page....v

Dedication Page....vi

Table of Contents....vii

List of Figures....xi

List of Schemes....xx

List of Tables....xxii

List of Abbreviations....xxiii

Acknowledgements....xxviii

Biographical Sketch....xxxvi

CHAPTER ONE: Total Synthesis as a Vehicle for Collaboration....1

1.1 Abstract....1

1.2 Introduction....1

1.3 Collaborative Synthesis of (+)-Chlorolissoclimide....6

1.4 Collaborative Total Synthesis of Nigelladine A....11

1.5 Collaborative Total Synthesis of Artemisinin....15

1.6 Total Synthesis of Ingenol....20

1.7 Total Synthesis of Hippolachnin A....24

1.8 Biosynthesis of Natural and Unnatural Communesin Scaffolds....28

1.9 Total Synthesis of Cyclopiamine B and Biogenetic Studies....34

1.10 Conclusion....43

1.11 Notes and References.....43

CHAPTER TWO: Enantioselective Total Syntheses of Methanoquinolizidine-Containing Akuammiline Alkaloids and Related Studies.....56

2.1 Abstract.....56

2.2 Introduction.....57

2.3 (+)-Strictamine and (–)-2(*S*)-Cathafoline: Background and Retrosynthetic Analysis.....59

2.4 Enantioselective Synthesis of the Fischer Indolization Substrate.....61

2.5 Reductive Interrupted Fischer Indolization Reaction.....64

2.6 Undesired C16 Epimerization and Synthesis of Unnatural C16 Epimers of Strictamine and 2(*S*)-Cathafoline.....66

2.7 Enantioselective Syntheses of (+)-Strictamine and (–)-2(*S*)-Cathafoline.....69

2.8 (–)-Ψ-Akuammigine: Isolation, Biological Activity, and Retrosynthetic Analysis.....71

2.9 Attempted Introduction of the Furoindoline Motif.....73

2.10 Enantioselective Total Synthesis of (–)-Ψ-Akuammigine.....75

2.11 Enantioselective Total Synthesis of (+)-Akuammiline.....78

2.12 Structural Rearrangement of Methanoquinolizidines to Pyrrolidinoindolines.....80

2.13 Conclusion.....81

2.14 Experimental Section.....82

2.14.1 Materials and Methods.....82

2.14.2 Experimental Procedures.....84

2.15 Spectra Relevant to Chapter Two.....117

2.16 Notes and References.....147

CHAPTER THREE: Synthetic Studies Pertaining to the 2,3-Pyridyne and 4,5-Pyrimidyne.....155

3.1 Abstract.....155

3.2 Introduction.....155

3.3 Synthesis of 2,3-Pyridyne Precursor.....158

3.4 Generation & Trapping of 2,3-Pyridyne.....158

3.5 Synthesis of 4,5-Pyrimidyne Precursors & Trapping Experiments.....161

3.6 Conclusion.....164

3.7 Experimental Section.....165

3.7.1 Materials and Methods.....165

3.7.2 Experimental Procedures.....166

3.8 Spectra Relevant to Chapter Three.....174

3.9 Notes and References.....185

CHAPTER FOUR: Aryne-Driven Approach for the Synthesis and Manipulation of Polypyridyl Metal Complexes.....190

4.1 Abstract.....190

4.2 Introduction.....191

4.3 Annulation Optimization.....196

4.4 Scope of Aryne Annulation Partners.....197

4.5 Scope of Polypyridyl Annulation Partners.....199

4.6 Synthesis and Trapping of Ligand-Bound Aryne Precursor.....201
4.7 Conclusion.....204
4.8 Experimental Section.....205
4.8.1 Materials and Methods.....205
4.8.2 Experimental Procedures.....206
4.8.2.1 Halobipyridine Organometallic Complex Synthesis.....206
4.8.2.2 Reaction Optimization.....216
4.8.2.3 Scope of Pd-Catalyzed Aryne Annulation.....218
4.8.2.4 Synthesis of Ligand-Bound Silyl Triflate and Trapping of Organometallic Aryne.....224
4.9 Spectra Relevant to Chapter Four.....230
4.10 Notes and References.....246

CHAPTER FIVE: Heterocyclic Aryne Annulations for the π-Extension of Donor Ligands in Two-Coordinate Metal Comlpexes.....250
5.1 Abstract.....250
5.2 Introduction.....250
5.3 Annulation of Heterocycles.....253
5.4 Carbazolyne Silyl Triflate Precursor Synthesis.....254
5.5 Pd-Catalyzed Carbazolyne Annulations.....255
5.6 Two-Coordinate Metal Complex Synthesis and Photophysical Characterization.....256
5.7 Conclusion.....260
5.8 Experimental Section.....261
5.8.1 Materials and Methods.....261

5.8.2 Experimental Procedures.....263

5.8.3 Computational Data.....278

5.9 Spectra Relevant to Chapter Five.....279

5.10 Notes and References.....292

LIST OF FIGURES

CHAPTER ONE

Figure 1.1. The remarkable structure of vitamin B_{12} (**1.1**).....2

Figure 1.2. Woodward–Eschenmoser approach to vitamin B_{12} (**1.1**) and the infamous "Black Friday" loss of material.....4

Figure 1.3. Natural products **1.8**–**1.14** synthesized via collaborations.....6

Figure 1.4. (+)-Chlorolissoclimide (**1.8**) and site-selective halogenation methodology.....7

Figure 1.5. C–H chlorination methodology and gram-scale synthesis of (+)-2-chlorosclareolide (**1.23**).....9

Figure 1.6. A robust route to (+)-chlorolissoclimide (**1.8**).....10

Figure 1.7. Collaborative total synthesis of nigelladine (A) (**1.9**) by the Stoltz and Arnold laboratories.....11

Figure 1.8. Stoltz's synthesis of tricycle **1.29**.....12

Figure 1.9. The crucial site-selective, late-stage oxidation of tricycle **1.29** was achieved using an enzymatic oxidation and allowed for the total synthesis of nigelladine A (**1.9**).....14

Figure 1.10. Artemisinin (**1.10**) accessed through a collaboration between the Keasling laboratory and Sanofi–Aventis, in addition to unnatural derivatives **1.36** and **1.37**.....16

Figure 1.11. Keasling's contribution: an efficient biosynthetic route to artemisinic acid (**1.42**).....18

Figure 1.12. The finishing touches by Sanofi: industrial scale conversion of artemisinic acid (**1.42**) to artemisinin (**1.10**).....19

Figure 1.13. (–)-Ingenol (**1.11**) and medicinally important derivatives.....21

Figure 1.14. Expedient total synthesis of (+)-ingenol (**1.11**).....22

Figure 1.15. Synthesis of ingenol derivative **1.53** bearing a photoaffinity probe.....23

Figure 1.16. Collaborative total synthesis of hippolachnin A (**1.12**).....25

Figure 1.17. Shared retrosynthetic analysis of hippolachnin A (**1.12**).....26

Figure 1.18. Collaborative route to achieve the total synthesis of hippolachnin A (**1.12**).....27

Figure 1.19. Biosynthetic studies of the heterodimeric scaffolds of communesin indole alkaloids.....29

Figure 1.20. Feeding studies of P450 oxidoreductase with analogs.....31

Figure 1.21. Mechanistic studies on communesin scaffold formation by the Houk laboratory.....33

Figure 1.22. Reported structures of natural products **1.83**–**1.85** and revised structure of citrinalin B (**1.14**).....35

Figure 1.23. Overview of Sarpong's synthesis of spirooxindole precursor **1.90** and unsuccessful oxidation attempts.....37

Figure 1.24. Successful oxidation to give **1.92** using Miller's peptide catalyst and challenges encountered in attempted rearrangement toward **1.96**.....39

Figure 1.25. Successful spirooxindole formation and total syntheses of *ent*-citrinalin B (*ent*-**1.14**) and cyclopiamine B (**1.85**).....41

Figure 1.26. Results of feeding studies of *P. citrinum* F53 with ^{13}C labeled precursors.....42

CHAPTER TWO

Figure 2.1. Representative methanoquinolizidine-containing akuammilines.....58

Figure 2.2. Synthetic routes to 16-*epi*-2(*S*)-cathafoline (**2.35**).....69

Figure 2.3. Structural rearrangement to access pyrrolidinoindolines.....81

Figure 2.4. ^{1}H NMR (500 MHz, $CDCl_3$) of compound **2.26**.....118

Figure 2.5. ^{13}C NMR (125 MHz, $CDCl_3$) of compound **2.26**.....118

Figure 2.6. ^{1}H NMR (500 MHz, $CDCl_3$) of compound **2.27**.....119

Figure 2.7. ^{13}C NMR (125 MHz, $CDCl_3$) of compound **2.27**.....119

Figure 2.8. ^{1}H NMR (500 MHz, $CDCl_3$) of compound **2.29**.....120

Figure 2.9. ^{13}C NMR (125 MHz, $CDCl_3$) of compound **2.29**.....120

Figure 2.10. ^{1}H NMR (500 MHz, $CDCl_3$) of compound **2.31**.....121

Figure 2.11. ^{13}C NMR (125 MHz, $CDCl_3$) of compound **2.31**.....121

Figure 2.12. ^{1}H NMR (500 MHz, $CDCl_3$) of compound **2.34**.....122

Figure 2.13. ^{13}C NMR (125 MHz, $CDCl_3$) of compound **2.34**.....122

Figure 2.14. ^{1}H NMR (500 MHz, $CDCl_3$) of compound **2.35**.....123

Figure 2.15. ^{13}C NMR (125 MHz, $CDCl_3$) of compound **2.35**.....123

Figure 2.16. ^{1}H NMR (500 MHz, $CDCl_3$) of compound **2.36**.....124

Figure 2.17. ^{13}C NMR (125 MHz, $CDCl_3$) of compound **2.36**.....124

Figure 2.18. ^{1}H NMR (500 MHz, $CDCl_3$) of compound **2.42**.....125

Figure 2.19. ^{13}C NMR (125 MHz, $CDCl_3$) of compound **2.42**.....125

Figure 2.20. ^{1}H NMR (500 MHz, $CDCl_3$) of compound **2.43**.....126

Figure 2.21. ^{13}C NMR (125 MHz, $CDCl_3$) of compound **2.43**.....126

Figure 2.22. ^{1}H NMR (500 MHz, $CDCl_3$) of compound **2.44**.....127

Figure 2.23. ^{13}C NMR (125 MHz, $CDCl_3$) of compound **2.44**.....127

Figure 2.24. ^{1}H NMR (500 MHz, $CDCl_3$) of compound **2.45**.....128

Figure 2.25. ^{13}C NMR (125 MHz, $CDCl_3$) of compound **2.45**.....128

Figure 2.26. ^{1}H NMR (500 MHz, $CDCl_3$) of compound **2.46**.....129

Figure 2.27. ^{13}C NMR (125 MHz, $CDCl_3$) of compound **2.46**.....129

Figure 2.28. ^{1}H NMR (500 MHz, $CDCl_3$) of compound **2.49**.....130

Figure 2.29. ^{13}C NMR (125 MHz, $CDCl_3$) of compound **2.49**.....130

Figure 2.30. ^{31}P NMR (202 MHz, $CDCl_3$) of compound **2.49**.....131

Figure 2.31. ^{1}H NMR (500 MHz, $CDCl_3$) of compound **2.50**.....132

Figure 2.32. ^{13}C NMR (125 MHz, $CDCl_3$) of compound **2.50**.....132

Figure 2.33. ^{11}B NMR (160 MHz, $CDCl_3$) of compound **2.50**.....133

Figure 2.34. ^{1}H NMR (500 MHz, $CDCl_3$) of compound **2.51**.....134

Figure 2.35. ^{13}C NMR (125 MHz, $CDCl_3$) of compound **2.51**.....134

Figure 2.36. ^{11}B NMR (160 MHz, $CDCl_3$) of compound **2.51**.....135

Figure 2.37. ^{1}H NMR (500 MHz, $CDCl_3$) of compound **2.53**.....136

Figure 2.38. ^{13}C NMR (125 MHz, $CDCl_3$) of compound **2.53**.....136

Figure 2.39. ^{11}B NMR (160 MHz, $CDCl_3$) of compound **2.53**.....137

Figure 2.40. ^{1}H NMR (500 MHz, $CDCl_3$) of compound **2.4**.....138

Figure 2.41. ^{13}C NMR (125 MHz, $CDCl_3$) of compound **2.4**.....138

Figure 2.42. ^{1}H NMR (500 MHz, $CDCl_3$) of compound **2.54**.....139

Figure 2.43. ^{13}C NMR (125 MHz, $CDCl_3$) of compound **2.54**.....139

Figure 2.44. ^{11}B NMR (160 MHz, $CDCl_3$) of compound **2.54**.....140

Figure 2.45. ^{1}H NMR (500 MHz, C_6D_6) of compound **2.55**.....141

Figure 2.46. ^{13}C NMR (125 MHz, $CDCl_3$) of compound **2.55**.....141

Figure 2.47. ^{11}B NMR (160 MHz, C_6D_6) of compound **2.55**.....142

Figure 2.48. ^{1}H NMR (500 MHz, $CDCl_3$) of compound **2.3**.....143

Figure 2.49. ^{13}C NMR (125 MHz, $CDCl_3$) of compound **2.3**.....143

Figure 2.50. ^{1}H NMR (500 MHz, $CDCl_3$) of compound **2.56**.....144

Figure 2.51. ^{13}C NMR (125 MHz, $CDCl_3$) of compound **2.56**.....144

Figure 2.52. ^{1}H NMR (500 MHz, $CDCl_3$) of compound **2.57**.....145

Figure 2.53. ^{13}C NMR (125 MHz, $CDCl_3$) of compound **2.57**.....145

Figure 2.54. ^{1}H NMR (500 MHz, $CDCl_3$) of compound **2.58**.....146

Figure 2.55. ^{13}C NMR (125 MHz, $CDCl_3$) of compound **2.58**.....146

CHAPTER THREE

Figure 3.1. Natural products **3.1**–**3.4** and heterocyclic arynes **3.5**–**3.7**.....157

Figure 3.2. Unsuccessful cycloadditions using silyl triflate **3.10**.....161

Figure 3.3. Unsuccessful attempts to generate and trap the 4,5-pyrimidyne from silyl triflate **3.37**.....164

Figure 3.4. ^{1}H NMR (500 MHz, $CDCl_3$) of compound **3.13**.....175

Figure 3.5. ^{13}C NMR (125 MHz, $CDCl_3$) of compound **3.13**.....175

Figure 3.6. ^{1}H NMR (500 MHz, $CDCl_3$) of compound **3.15**.....176

Figure 3.7. ^{13}C NMR (125 MHz, $CDCl_3$) of compound **3.15**.....176

Figure 3.8. ^{1}H NMR (500 MHz, $CDCl_3$) of compound **3.18**.....177

Figure 3.9. ^{13}C NMR (125 MHz, $CDCl_3$) of compound **3.18**.....177

Figure 3.10. ^{1}H NMR (500 MHz, $CDCl_3$) of compound **3.20**.....178

Figure 3.11. ^{13}C NMR (125 MHz, $CDCl_3$) of compound **3.20**.....178

Figure 3.12. ^{1}H NMR (500 MHz, $CDCl_3$) of compound **3.22**.....179

Figure 3.13. ^{13}C NMR (125 MHz, $CDCl_3$) of compound **3.22**.....179

Figure 3.14. ^{1}H NMR (500 MHz, $CDCl_3$) of compound **3.24**.....180

Figure 3.15. ^{13}C NMR (125 MHz, $CDCl_3$) of compound **3.24**.....180

Figure 3.16. ^{1}H NMR (500 MHz, $CDCl_3$) of compound **3.33**.....181

Figure 3.17. ^{13}C NMR (125 MHz, $CDCl_3$) of compound **3.33**.....181

Figure 3.18. ^{1}H NMR (500 MHz, $CDCl_3$) of compound **3.34**.....182

Figure 3.19. ^{13}C NMR (125 MHz, $CDCl_3$) of compound **3.34**.....182

Figure 3.20. ^{1}H NMR (500 MHz, MeOD) of compound **3.35**.....183

Figure 3.21. ^{13}C NMR (125 MHz, MeOD) of compound **3.35**.....183

Figure 3.22. ^{1}H NMR (500 MHz, $CDCl_3$) of compound **3.37**.....184

Figure 3.23. ^{13}C NMR (125 MHz, $CDCl_3$) of compound **3.37**.....184

CHAPTER FOUR

Figure 4.1. Polypyridyl metal complexes used as therapeutics and in bioimaging....192

Figure 4.2. A) Strategies for the synthesis of polypyridyl metal complexes. B) Aryne and cyclic alkyne intermediates. C) Synthetic designs for the direct manipulation of photoactive metal complexes using arynes and Pd catalysis.....195

Figure 4.3. Scope of aryne annulation partners.....199

Figure 4.4. Scope of organometallic complex reaction partners.....201

Figure 4.5. Synthesis of Ru-polpyridyl silyl triflate.....202

Figure 4.6. Mild generation of the first ligand-bound aryne, and future trapping partners.....203

Figure 4.7. ^{1}H NMR (500 MHz, CD_3CN) of compound **4.20**.....231

Figure 4.8. ^{13}C NMR (125 MHz, CD_3CN) of compound **4.20**.....231

Figure 4.9. ^{1}H NMR (500 MHz, CD_3CN) of compound **4.25**.....232

Figure 4.10. ^{1}H NMR (500 MHz, CD_3CN) of compound **4.26**.....233

Figure 4.11. ^{13}C NMR (125 MHz, CD_3CN) of compound **4.26**.....233

Figure 4.12. ^{1}H NMR (500 MHz, CD_3CN) of compound **4.27**.....234

Figure 4.13. ^{13}C NMR (125 MHz, CD_3CN) of compound **4.27**.....234

Figure 4.14. ^{1}H NMR (600 MHz, CD_3CN) of compound **4.28**.....235

Figure 4.15. ^{1}H NMR (600 MHz, CD_3CN) of compound **4.29**.....235

Figure 4.16. ^{1}H NMR (500 MHz, CD_3CN) of compound **4.30**.....236

Figure 4.17. ^{13}C NMR (125 MHz, CD_3CN) of compound **4.30**.....236

Figure 4.18. ^{1}H NMR (500 MHz, CD_3CN) of compound **4.31**.....237

Figure 4.19. ^{13}C NMR (125 MHz, CD_3CN) of compound **4.31**.....237

Figure 4.20. ^{1}H NMR (500 MHz, CD_3CN) of compound **4.32**.....238

Figure 4.21. ^{13}C NMR (125 MHz, CD_3CN) of compound **4.32**.....238

Figure 4.22. ^{1}H NMR (600 MHz, CD_3CN) of compound **4.33**.....239

Figure 4.23. ^{13}C NMR (125 MHz, CD_3CN) of compound **4.33**.....239

Figure 4.24. ^{1}H NMR (500 MHz, CD_3CN) of compound **4.34**.....240

Figure 4.25. ^{13}C NMR (125 MHz, CD_3CN) of compound **4.34**.....240

Figure 4.26. ^{1}H NMR (500 MHz, CD_3CN) of compound **4.36**.....241

Figure 4.27. ^{1}H NMR (500 MHz, $CDCl_3$) of compound **4.37**.....242

Figure 4.28. ^{13}C NMR (125 MHz, $CDCl_3$) of compound **4.37**.....242

Figure 4.29. ^{1}H NMR (500 MHz, CD_3CN) of compound **4.38**.....243

Figure 4.30. ^{1}H NMR (500 MHz, CD_3CN) of compound **4.40**.....243

Figure 4.31. ^{1}H NMR (500 MHz, $CDCl_3$) of compound **4.49**.....244

Figure 4.32. ^{1}H NMR (500 MHz, $CDCl_3$) of compound **4.51**.....244

Figure 4.33. ^{1}H NMR (500 MHz, CD_3CN) of compound **4.53**.....245

Figure 4.34. ^{13}C NMR (125 MHz, CD_3CN) of compound **4.53**.....245

CHAPTER FIVE

Figure 5.1. A) Linear two-coordinate metal complexes. B) Previous donor studies. C) A modular platform for studying conjugation effects of donors in two-coordinate metal complexes.....252

Figure 5.2. Scope of biaryl annulation partners..... 254

Figure 5.3. Annulation with *N*-substituted carbazolynes.....256

Figure 5.4. Synthesis of novel two-coordinate organometallic complexes.....257

Figure 5.5. A) Absorbance spectra in methylcyclohexane (MeCy) and 2-methyl-tetrahydrofuran (MeTHF). B) Previously studied carbazole–Au–MAC complex **5.32** and

carbazole–Au–BZI complex **5.33**. C) Emission spectra of MAC complexes **5.29** and **5.32**. D) Emission spectra of BZI complexes **5.31** and **5.33**.....259

Figure 5.6. ^{1}H NMR (500 MHz, $CDCl_3$) compound **5.13**.....280

Figure 5.7. ^{13}C NMR (125 MHz, $CDCl_3$) compound **5.13**.....280

Figure 5.8. ^{1}H NMR (500 MHz, $CDCl_3$) compound **5.14**.....281

Figure 5.9. ^{1}H NMR (500 MHz, C_6D_6) compound **5.15** and **5.36**.....282

Figure 5.10. ^{13}C NMR (125 MHz, C_6D_6) compound **5.15** and **5.36**.....282

Figure 5.11. ^{1}H NMR (500 MHz, $CDCl_3$) compound **5.16** and **5.38**.....283

Figure 5.12. ^{13}C NMR (125 MHz, $CDCl_3$) compound **5.16** and **5.38**.....283

Figure 5.13. ^{1}H NMR (500 MHz, $CDCl_3$) compound **5.17** and **5.40**.....284

Figure 5.14. ^{13}C NMR (125 MHz, $CDCl_3$) compound **5.17** and **5.40**.....284

Figure 5.15. ^{1}H NMR (500 MHz, C_6D_6) compound **5.18** and **5.42**.....285

Figure 5.16. ^{13}C NMR (125 MHz, C_6D_6) compound **5.18** and **5.42**.....285

Figure 5.17. ^{1}H NMR (500 MHz, C_6D_6) compound **5.19** and **5.44**.....286

Figure 5.18. ^{13}C NMR (125 MHz, C_6D_6) compound **5.19** and **5.44**.....286

Figure 5.19. ^{1}H NMR (500 MHz, C_6D_6) compound **5.20** and **5.46**.....287

Figure 5.20. ^{13}C NMR (125 MHz, C_6D_6) compound **5.20** and **5.46**.....287

Figure 5.21. ^{1}H NMR (500 MHz, $CDCl_3$) compound **5.48**.....288

Figure 5.22. ^{1}H NMR (500 MHz, $CDCl_3$) compound **5.23**.....288

Figure 5.23. ^{1}H NMR (500 MHz, $CDCl_3$) compound **5.24**.....289

Figure 5.24. ^{1}H NMR (500 MHz, $CDCl_3$) compound **5.25**.....289

Figure 5.25. ^{1}H NMR (500 MHz, $CDCl_3$) compound **5.26**.....290

Figure 5.26. ^{1}H NMR (500 MHz, $CDCl_3$) compound **5.27**.....290

Figure 5.27. ^{1}H NMR (500 MHz, $CDCl_3$) compound **5.29**.....291

Figure 5.28. ^{1}H NMR (500 MHz, $CDCl_3$) compound **5.31**.....291

LIST OF SCHEMES

CHAPTER ONE

CHAPTER TWO

Scheme 2.1. Retrosynthetic analysis of (+)-strictamine (**2.1**) and (–)-2(*S*)-cathafoline (**2.2**).....60

Scheme 2.2. Trost desymmetrization and synthesis of enone **2.16**.....61

Scheme 2.3. Gold-catalyzed construction of the [3.3.1]-azabicycle and elaboration to enal **2.20**.....63

Scheme 2.4. Synthesis of reductive Fischer indolization reaction substrate, ketolactone **2.9**.....64

Scheme 2.5. Reductive interrupted Fischer indolization reaction delivers **2.6**.....66

Scheme 2.6. Undesired C16 epimerization.....67

Scheme 2.7. Synthesis of 16-*epi*-strictamine (**2.34**).....68

Scheme 2.8. Total syntheses of (+)-strictamine (**2.1**) and (–)-2(*S*)-cathafoline (**2.2**).....71

Scheme 2.9. Retrosynthetic analysis of (–)-Ψ-akuammigine (**2.4**).....73

Scheme 2.10. Scalable preparation of aldehyde **2.42**.....74

Scheme 2.11. Introduction of the furoindoline motif and undesired isomerization to afford **2.46**.....75

Scheme 2.12. Reassessment of synthetic approach.....76

Scheme 2.13. Introduction of methanoquinolizidine framework and amine-borane complexation.....77

Scheme 2.14. Total synthesis of (–)-Ψ-akuammigine (**2.4**).....78

Scheme 2.15. Total synthesis of (+)-akuammiline (**2.3**).....79

CHAPTER THREE

Scheme 3.1. Synthesis of silyl triflate **3.10**.....158

Scheme 3.2. Approaches to 4,5-pyrimidyne (**3.7**) from silyl triflate precursors **3.30** and **3.31**.....161

Scheme 3.3. Synthesis of silyl triflate **3.34** and undesired Fries rearrangement.....163

Scheme 3.4. Synthesis of silyl triflate **3.37**.....163

CHAPTER FOUR

CHAPTER FIVE

Scheme 5.1. Synthesis of carbazolyne silyl triflate precursors.....255

LIST OF TABLES

CHAPTER ONE

CHAPTER TWO

Table 2.1. Fischer indolization reaction between ketolactone **2.9** and hydrazine **2.8**.....65

Table 2.2. Interrupted Fischer indolization reaction optimization.....85

Table 2.3. Comparison of ^{13}C NMR data for the natural vs synthetic (–)-Ψ-akuammigine (**2.4**).....107

Table 2.4. Comparison of ^{13}C NMR data for the natural vs synthetic (+)-akuammiline (**2.3**).....112

Table 2.5. Comparison of ^{13}C NMR data for the natural vs synthetic (–)-10-demethoxyvincorine (**2.57**).....115

CHAPTER THREE

Table 3.1. Trapping of 2,3-pyridyne (**3.6**) with nucleophiles.....159

Table 3.2. Annulation reactions of 2,3-pyridyne (**3.6**).....160

CHAPTER FOUR

Table 4.1. Optimization studies for Pd-catalyzed annulation of benzyne onto Ru-polypyridyl complexes **4.18**.....197

Table 4.2. Optimization studies of Br-Ru(bpy)$_3$ annulation with benzyne.....217

CHAPTER FIVE

Table 5.1. Photophysical measurements for MAC-based complexes **5.29** and **5.32**.....259

Table 5.2. Photophysical measurements for BZI-based complexes **5.31** and **5.32**.....260

Table 5.3. Calculated frontier molecular orbitals, singlet (S_1), and triplet (T_1) energies.....278

LIST OF ABBREVIATIONS

α	alpha
$[\alpha]_D$	specific rotation at wavelength of sodium D line
Å	angstrom
β	beta
c	concentration for specific rotation measurements
γ	gamma
m/z	mass to charge ratio
μ	micro
π	pi
Ac	acetyl, acetate
AcOH	acetic acid
AIBN	azobisisobutyronitrile
app.	apparent
aq.	aqueous
bpy	2,2'-bipyridyne
BHT	butylated hydroxytoluene
Boc	*tert*-butoxycarbonyl
Boc_2O	di-*tert*-butyl dicarbonate
Bn	benzyl

br	broad
BTPP	(*tert*-butylimino)tris(pyrrolidino)phosphorane
Bu	butyl
i-Bu	isobutyl
n-Bu	butyl (linear)
t-Bu	*tert*-butyl
t-BuOH	*tert*-butyl alcohol
Bz	benzoyl
BZI	1,3-bis(2,6-diisopropylphenyl)-1-H-benzo[d]imidazole-2-ylidene
°C	degrees Celsius
calcd	calculated
CAN	cerium (IV) ammonium nitrate
cat.	catalytic
CCDC	Cambridge Crystallographic Data Centre
cod	1,5-cyclooctadiene
DACH	daminocyclohexane
d	doublet
dba	dibenzylideneacetone
DCE	1,2-dichloroethane
Dess–Martin	Dess–Martin Periodinane
$(DHQ)_2PHAL$	hydroquinine 1,4-phthalazinediyl diether
DIBAL-H	diisobutylaluminium hydride
DIC	*N,N*′-diisopropylcarbodiimide
dig	digonal
DMA	dimethylacetamide
DMAP	4-dimethylaminopyridine
DMF	*N*,*N*-dimethylformamide
DMPU	1,3-dimethyl-3,4,5,6-tetrahydro-2(1H)-pyrimidinone
DMSO	dimethyl sulfoxide
dppf	1,1′-bis(diphenylphosphino)ferrocene
DFT	density functional theory
ee	enantiomeric excess
equiv	equivalent
EDC•HCl	1-ethyl-3-(3-dimethylaminopropyl)carbodiimide hydrochloride

ESI	electrospray ionization
Et	ethyl
EtOAc	Ethyl acetate
g	gram(s)
Glc	glucosyl
h	hour(s)
HMPA	hexamethylphosphoramide
HOBt	hydroxybenzatriazole
HRMS	high resolution mass spectroscopy
Hz	hertz
imid.	imidazole
IBX	2-iodoxybenzoic acid
ICT	inter-ligand charge transfer
IR	infrared (spectroscopy)
J	coupling constant
L	liter
LiHMDS	lithium hexamethyldisilazide
m	meta
MAC	1,3-bis(2,6-diisopropylphenyl)-5,5-dimethyl-4-keto-tetrahydropyridylidene
MeCy	methylcyclohexane
MeTHF	2-methyl-tetrahydrofuran
m-CPBA	3-chloroperbenzoic acid
m	multiplet or milli
min	minute(s)
mol	mole(s)
mp	melting point
M	molecular mass
Me	methyl
MHz	megahertz
MOM	methoxymethyl ether
MS	molecular sieves
N	Nucleophilicity Parameter
NF-κB	nuclear Factor kappa B
NIS	*N*-iodosuccinimide

NMO	4-methylmorpholine *N*-oxide
NMR	nuclear magnetic resonance
Ns	2-nitrobenzenesulfonyl
OAc	acetate
[O]	oxidation
OLED	organic light-emitting diode
OTf	trifluoromethanesulfonate (triflate)
p	para-toluenesulfonic acid
Ph	phenyl
pH	hydrogen ion concentration in aqueous solution
ppm	parts per million
PCC	pyridinium chlorochromate
Ph	phenyl
Piv	pivaloyl
Pr	propyl
i-Pr	isopropyl
PMP	1,2,2,6,6-pentamethylpiperidine
PPTS	pyridinium *p*-toluenesulfonate
PSI	Pounds per square inch
q	quartet
quint.	quintet
R_f	retention factor
s	singlet
sat.	saturated
sext.	sextet
SGLT2	sodium-glucose linked transporter 2
s_N	Nucleophile-specific susceptibility
t	triplet
TADF	thermally activated delayed fluorescence
trig	trigonal
TBAB	tetra-*n*-butylammonium bromide
TBDPS	*tert*-butyldiphenylsilyl
TBS	*tert*-butyldimethylsilyl
TBSCl	*tert*-butyldimethylsilyl chloride

TDDFT	time-dependent density functional theory
TES	triethylsilyl
TESCl	triethylsilyl chloride
Tf	trifluoromethanesulfonyl (trifyl)
TFA	trifluoroacetic acid
THF	tetrahydrofuran
TLC	thin layer chromatography
TMS	trimethylsilyl
TMSCl	trimethylsilyl chloride
TMSOTf	trimethylsiyl triflate
TMP	2,2,6,6-tetramethylpiperidine
Trost Ligand	(*R*, *R*)-DACH-phenyl Trost ligand
Ts	*p*-toluenesulfonyl (tosyl)
UV	ultraviolet

ACKNOWLEDGEMENTS

Beyond the coursework, the science, and the accolades that define a PhD, I am most thankful for the relationships that I have made in the last five years. The scientific state-of-the-art may change, but I will be forever indebted to the following mentors, peers, family, and friends whose guidance, camaraderie, love, and support made this journey possible.

In hindsight, it's difficult to imagine completing my PhD with any other advisor than Professor Neil Garg. I came to UCLA to learn how to make molecules, but got so much more from your laboratory. I fondly remember writing papers in your office, hunting for the perfect phrasing, recording videos, and running crazy errands, like purchasing the UCLA store's entire stock of Joe Bruin gummy bears to give to elementary school visitors. I also remember mingling with prospective students together during recruitments, and reflecting on all we had accomplished in the last year. Thank you for cultivating an environment that fosters camaraderie and communication, enabling a powerful engine of scientific discovery and support (and legendary celebrations). Lastly, thank you for taking me on as a graduate student, despite my limited synthetic training, and believing I had the skills to succeed when I doubted myself on numerous occasions. I wouldn't have accomplished nearly as much without your encouragement.

To my doctoral committee, thank you for supporting me and always providing valuable feedback during critical points in my academic training. Professor Harran, I think I speak for many of my classmates when I say your Synth II class was a beacon of light in the murky waters that could be described as the first year of graduate school. Thank you for reaffirming that total synthesis is indeed one of the most elegant and gratifying endeavors that we can pursue as synthetic chemists. Professor Houk, I am grateful for our stimulating discussions about both chemistry and cars, as well as your sense of humor during departmental functions. Professor

Tang, thank you for being so encouraging and friendly throughout my progress in the program, especially during my candidacy exam.

To my parents, Kris and Bob, I am so fortunate to have grown up with you both as outstanding, complementary role models. Your example has always guided me towards a more fulfilling life, and completing this program has been the largest step I've taken toward that end. Growing up, you entertained my every interest, no matter how fleeting, with unwaivering love and support. It was easy for me to find my passion for the sciences through our trips to museums, watching countless nature documentaries, and even from our conversations at the dinner table. Now that path has led me into the family business, pharmaceuticals! I know this chapter of my life was taxing on our time together, but it means so much that you were always there when I needed you. I love you both.

To my sister, Emma, and brother-in-law, Ian, thank you for always allowing me to crash at your house after so many red-eye flights back to North Carolina over the last five years. I cannot express how excited I am to begin the next chapter of my life closer to you all and little Liam, at a time when he will really come into his own! I promise to be a good influence and ensure he has better rhythm than his father.

My extended family has also been incredibly supportive. Thank you, Karen, for the frequent care packages of baked goods and exotic hot sauces. Thank you, Doug, for sharing the extraordinary beauty of Yosemite with me on multiple occasions, and for providing much needed respite from the hustle and bustle of Los Angeles. Deb and Bob, I'm honored to be joining you in the upper echealon of academia! Thank you for being so supportive during my transition out to California, and I hope to rely on your support once again when we become neighbors in the

greater Philadelphia area – I hope Julia is ready for some serious "Sushi Go!" competition. Lastly, Grandma Betty, thank you for always being my cheerleader!

I would also be remiss to not thank many friends of the family, who have watched me grow up and celebrated many milestones with me. To Pat and Steve Bocckino, thank you for believing in me, and of course you were right when you told me, "patience, grasshopper." To the Ludlows, I am grateful for your friendship over the years and taking me out on the town whenever Nick was home. Bennett Love, I'm so glad we reconnected at TRC 6 years ago! I'm grateful to have shared in your perspective on life, rock climbing, and the pharmaceutical industry. Sue and Chris Brown, thank you for making me feel like a third son over the years, and including me with your family to the Bar Lazy J ranch when I really needed a break from the daily grind. Amy and Morgan Ryan, your house was always a place for us neighborhood boys to let our imaginations run wild and build, or sometimes destroy, whatever came to our minds. I'm so grateful we had that space, and your patience. And finally, to Bushra Agha, I consider you my chemical Godmother, and I'm so grateful for all your wisdom and support throughout my professional and academic career. Although I'm starting a new phase in my life now, I'm still counting on crashing Thanksgiving dinners with the usual crew at your house.

The bridge between my undergraduate and doctoral studies, Cirrus Pharmaceuticals, was instrumental in preparing me for the rigor of graduate school. There, I met many incredible scientists who entertained my curiosities and encouraged my decision to pursue a PhD. Ramil, your example as a manager was truly inspiring. Working under you, designing experiments, and solving problems gave me my first taste of what it meant to do research, and your confidence in my decision to pursue a PhD was invaluable. Murali, you warned me that research required motivation and unquenchable curiousity, but that I had the mind to be successful. Neha, you

were right about so many things during my transition to graduate school, such as becoming addicted to caffeine. Thank you for always offering sage advice when I was stressed out.

As I alluded to above, the Garg laboratory comes with a strong culture of camaraderie. Beyond helping me navigate the milestones of the graduate program, I am most thankful for the friends who made the last five years as enjoyable as they were productive. To Liana and Tejas, you went out of your way to help me acclimate to my new life in Los Angeles by showing me around the city, and organizing trips to great restaurants. I am so grateful for your friendship and mentorship during my first year. Tejas, thank you for teaching me how to use a manifold and set up my first reactions. To Nick, Jose, Mike, and Jesus, your class was a bastion of synthetic prowess, and each of you played critical roles in my development as an organic chemist, both intellectually and experimentally. Shout out to Jesus "Josh Marungo" Moreno, for making MSB 5234 the most fun room with your exceptional levity and sense of humor, often during inappropriate situations.

To Elias, Junyong, and Emma, it was through your class that I first witnessed the trials and tribulations of advancing to candidacy, and you all set a super high bar! Thank you for being productive role models. Elias and Junyong, it still blows my mind that we went to Vegas and saw the League of Legends semi-finals match in a packed Mandalay Bay Arena. To Joyann, Bryan, and Lucas, yours was the recruiting class that got me so hyped to join the Garg lab, and it was hard to believe I would ever achieve your proficiency by the time I finished my first year. Joyann, thank you for always having a keen eye for typos in my documents, and introducing me to "Sushi Go!", it has become a family favorite on game nights. Bryan, thank you for bringing the perfect balance of sarcasm and sincerity to the lab, as well as looking out for us younger students. Lastly, Lucas, you were my go-to lab mate when things got crazy. Thank you for going

the extra mile when I needed help in the lab, or in my personal life. The akuammiline team thrived by your example, and I really hope we can work together again one day.

With each passing generation, a new class arrived. Even when it was my turn to play mentor, I continued to learn from and rely on the younger Gargoyles. Sarah, Melissa, and Tim, your class brought a diversity of interests and expertise to the group. From computations, to catalysis, to total synthesis, you all continue to propel the lab forward. Sarah, thank you for blasting Paul Simon or other feel good songs in lab when we needed a pick-me-up. I'm not sure if I'll ever have another coworker whom I can communicate with as effectively using only single syllable sounds. Melissa, I'm so glad we got to share a workspace in 5229. You're one of the most dedicated chemists I know, and your drive to keep learning and improving is infectious! Tim, when it comes to self-improvement both in- and outside the lab, you are the most committed person I've ever met. You've come a long way from sleeping in a closet, to now stand as an intellectual gatekeeper for the lab. I'm grateful that we not only worked together, but also lived together, and I know our paths will cross again in the future.

Rachel, Francesca, and Jason, your class brought a diversity of personalities that really livened up the lab culture. Francesca and Rachel, you are both responsible for significantly "classing up" our lab events, which is something I will surely miss. Jason, working with you on so many different projects was so much fun. Your creativity and enthusiasm for chemistry is relentless, which made it impossible for me to ever feel jaded about research. Your crazy ideas worked surprisingly often, and I'm grateful that I got to finish out my research on such unique, surprising chemistry with you.

Andrew, Katie, and Milauni, your class came in hungry for research, and I have no doubt you'll accomplish great things during your time in the Garg lab. Katie, I've seen you tackle some

pretty crazy chemistry, and your drive to get results was invaluable to our projects together. Milauni, you boldly asserted yourself as an honorary member of the senior class, and kept us all up-to-date with the latest youth culture, for which my tired vernacular was very grateful. You are one of the most driven people I know, and I can't wait to see who you become after graduate school. Andrew, I'm glad we could work in the same room together, otherwise I may never have gotten to know you. Also, I wouldn't have had anyone else to jam out to TOOL with. You're a brilliant chemist, and I can't wait to see what you discover throughout your PhD. To the newest members of the lab, Matthew, Ana, and Laura, our time together has been short, especially given the COVID-19 circumstances. Regardless, you all bring an enthusiasm that revitalizes the entire program, especially for us at the top, for which I am very grateful. Remember Matt, "it's just a wall!"

I had the fortune to work along side many postdoctoral researchers from across the globe during my PhD studies. They brought unique backgrounds in synthesis that enriched the chemistry of the Garg lab, literally and figuratively. Marie, thank you for pushing me to rely on my brain rather than SciFinder throughout my first year. Sophie and Maude, I am grateful for our scientific discussions, as well as my lessons on cultures abroad. Darzi, thank you for bringing an insane enthusiasm and a deep knowledge of organic materials to the laboratory. You were an invaluable resource for many of the projects in this thesis, and for that I am extremely grateful. Veronica, thank you for teaching me Italian, and making me feel important by asking me so many questions about UCLA, California, and life in the US. You made the day-to-day grind far more entertaining! Logan, thanks for getting me back into rock climbing, a hobby I had neglected since beginning graduate school, and for helping make the 257th National ACS conference legendary.

Last, but not least, to my comrades in the trenches, Jordan, Michael, and Jacob, a.k.a. the Fellahs. Without your fellowship, this journey would really not have been possible. I didn't realize how important such a fellowship could be when I moved across the country and met you all. In fact, it was often overwhelming to have such gifted and talented chemists as my closest friends. However, we marched our way through the program together. I think it's safe to say that we set a new bar for throwing candidacy parties and group field trips. Michael Yamano, the master of acronyms, you are the most loyal friend I have ever had and constantly make the rest of us feel like inadequate friends. You can catalyze any gathering, with any assortment of people, into a memorable party, which was so important to me while I adjusted to my new life in California. You are the sharpest chemist that I know, even though you should have gone to law school, and you are the ultimate guide for Las Vegas – I will never play craps without you! Jacob "Bahhb" Dander, you are the most gifted entertainer I've ever met, a true thespian. You are also the most thoughtful person I know, and despite being my least favorite friend in the lab, you were a great roommate. I couldn't ask for a better person to have in my corner when things got tough. Also, your incessant need to check boxes saved our cohort multiple times in the last 5 years. Jordan, I'm so glad you joined our trifecta after candidacy. Not only did you bring a bottomless pit of physical organic chemistry knowledge, complete with memorized references, but you also brought a competitive nature that rivaled Michael's, which took a lot of much needed pressure off of me and Jacob. Our time together became more selective as we progressed through the program, but our bond never faded. No matter the distance or future careers, we'll always have the legendary 257th National ACS conference. Thanks for the ride boys.

Chapter One is a version of Morrill, L. A.[†]; Susick, R. B.[†]; Chari, J. V.; Garg, N. K. *J. Am. Chem. Soc.* **2019**, *141*, 12423–12443. Morrill, Susick, Chari, and Garg were responsible for writing. *([†] Denotes equal authorship)*

Chapter Two is a version of Picazo, E.[†]; Morrill, L. A.[†]; Susick, R. B.; Moreno, J.; Smith, J. M.; Garg, N. K. *J. Am. Chem. Soc.* **2018**, *140*, 6483–6492. Picazo, Morrill, Susick, Moreno, and Smith were responsible for experimental studies. *([†] Denotes equal authorship)*

Chapter Three is a version of Medina, J. M.; Jackl, M. J.; Susick, R. B.; Garg, N. K. *Tetrahedron* **2016**, *72*, 3629–3634. Medin, Jackl, and Susick were responsible for experimental studies.

Chapter Four describes unpublished studies. Jason V. Chari, Robert B. Susick, and Katie A. Spence were responsible for experimental studies under the supervision of Prof. Neil Garg.

Chapter Five describes unpublished studies. Robert B. Susick, Jason V. Chari, and Katie A. Spence were responsible for experimental studies under the supervision of Prof. Neil Garg. Narcisse Ukwitegetse and Mattia Diniro were responsible for organometallic synthesis and photophysical characterization under the supervision of Prof. Mark E. Thompson (University of Southern California).

BIOGRAPHICAL SKETCH

Education:

University of California, Los Angeles, CA

- PhD in Chemistry, anticipated Spring 2020
- Current GPA: 3.73/4.00

North Carolina State University, Raleigh, NC

- Bachelor's of Science in Chemistry, May 2013
- Cumulative GPA: 3.60/4.00

Professional and Academic Experience:

Graduate Research Assistant: University of California, Los Angeles, CA

- July 2015 – present; Advisor: Prof. Neil K. Garg
- Developed an efficient biologically inspired structural rearrangement to convert one class of akuammiline alkaloids to another. This enabled the first total synthesis of (–)-10-demethoxyvincorine, (–)-10-demethoxynorvincorine, and unnatural akuammiline derivatives.
- Synthesized over two grams of material en route to the enantioselective total synthesis of (–)-pseudoakuammigine. Elucidated late-stage discoveries that informed the first successful synthesis of the natural product.
- Optimized the synthesis of the first ligand-bound aryne precursor, enabling a new method for chemistry "on-the-complex," and divergent access to exotic, π-extended photoactive metal complexes.
- Designed novel π-extended ligands to study the structure-property relationships of two-coordinate metal complexes for applications in OLED technology.
- Managed laboratory inspections with Environmental Health & Safety department as the Laboratory Safety Officer and updated Standard Operating Procedures.
- Maintained and organized an inventory of over 2000 compounds as Inventory Manager for the laboratory.

Honors and Awards:

- Pfizer-UCLA Dissertation Award for Excellence in Organic Synthesis, Spring 2020
- UCLA Chemistry and Biochemistry Excellence in Research Fellowship, Spring 2020
- UCLA Graduate Research Showcase Travel Grant, 2019
- UCLA Hanson-Dow Award for Excellence in Teaching, 2018
- 2018 Safety Initiative Award
- UCLA University Fellowship, 2015–2017.

Publications:

1. **Heterocyclic Aryne Annulations for the π-Extension of Donor Ligands in Two-Coordinate Metal Complexes.** Robert B. Susick[†], Jason V. Chari[†], Katie A. Spence, Narcisse Ukwitegetse,

Mattia Diniro, Mark E. Thomspon, and Neil K. Garg. *Manuscript in preparation. († Denotes equal authorship)*

2. **Aryne-Driven Approach for the Structural Manipulation of Polypyridyl Metal Complexes.** Jason V. Chari†, Robert B. Susick†, Katie A. Spence, Neil K. Garg. *Manuscript in preparation. († Denotes equal authorship)*

3. **Total Synthesis as a Vehicle for Collaboration**. Lucas A. Morrill,† Robert B. Susick,† Jason V. Chari, Neil K. Garg. *J. Am. Chem. Soc.* **2019**, *141*, 12423–12443. *(† Denotes equal authorship)*

4. **Canvass: A Crowd-Sourced, Natural-Product Screening Library for Exploring Biological Space**. Sarah E. Kearney, Gergely Zahoránszky-Köhalmi, Kyle R. Brimacombe, Mark J. Henderson, Caitlin Lynch, Tongan Zhao, Kanny K. Wan, Zina Itkin, Christopher Dillon, Min Shen, Dorian M. Cheff, Tobie D. Lee, Danielle Bougie, Ken Cheng, Nathan P. Coussens, Dorjbal Dorjsuren, Richard T. Eastman, Ruili Huang, Michael J. Iannotti, Surendra Karavadhi, Carleen Klumpp-Thomas, Jacob S. Roth, Srilatha Sakamuru, Wei Sun, Steven A. Titus, Adam Yasgar, Ya-Qin Zhang, Jinghua Zhao, Rodrigo B. Andrade, M. Kevin Brown, Noah Z. Burns, Jin K. Cha, Emily E. Mevers, Jon Clardy, Jason A. Clement, Peter A. Crooks, Gregory D. Cuny, Jake Ganor, Jesus Moreno, Lucas A. Morrill, Elias Picazo, Robert B. Susick, Neil K. Garg, Brian C. Goess, Robert B. Grossman, Chambers C. Hughes, Jeffrey N. Johnston, Madeleine M. Joullie, A. Douglas Kinghorn, David G. I. Kingston, Michael J. Krische, Ohyun Kwon, Thomas J. Maimone, Susruta Majumdar, Katherine N. Maloney, Enas Mohamed, Brian T. Murphy, Pavel Nagorny, David E. Olson, Larry E. Overman, Lauren E. Brown, John K. Snyder, John A. Porco Jr., Fatima Rivas, Samir A. Ross, Richmond Sarpong, Indrajeet Sharma, Jared T. Shaw, Zhengren Xu, Ben Shen, Wei Shi, Corey R. J. Stephenson, Alyssa L. Verano, Derek S. Tan, Yi Tang, Richard E. Taylor, Regan Thomson, David A. Vosburg, Jimmy Wu, William M. Wuest, Armen Zakarian, Yufeng Zhang, Tianjing Ren, Zhong Zuo, James Inglese, Sam Michael, Anton Simeonov, Wei Zheng, Paul Shinn, Ajit Jadhav, Matthew B. Boxer, Matthew D. Hall, Menghang Xia, Rajarshi Guha, Jason M. Rohde. *ACS Cent. Sci.* **2018**, *4*, 1727–1741.

5. **Enantioselective Total Syntheses of Methanoquinolizidine-Containing Akuammiline Alkaloids and Related Studies**. Elias Picazo†, Lucas A. Morrill†, Robert B. Susick, Jesus Moreno, Joel M. Smith, and Neil K. Garg. *J. Am. Chem. Soc.* **2018**, *140*, 6483–6492.

6. **Pardon the Interruption: A Modification of Fischer's Venerable Reaction for the Synthesis of Heterocycles and Natural Products.** Robert B. Susick†, Lucas A. Morrill†, Elias Picazo†, and Neil K. Garg. *Synlett* **2017**, *28*, 1–11. *(† Denotes equal authorship)*

7. **Synthetic Studies Pertaining to the 2,3-Pyridyne and 4,5-Pyrimidyne.** Jose M. Medina, Moritz K. Jackl, Robert B. Susick, and Neil K. Garg. *Tetrahedron* **2016**, *72*, 3629–3634.

Patents:

1. **Methods for the Synthesis of Heteroatom Containing Polycyclic Aromatic Hydrocarbons.** Robert B. Susick, Jason V. Chari, Katie A. Spence; Neil K. Garg, Evan R. Darzi, and Joyann S. Barber. *WO2020041369*.

CHAPTER ONE

Total Synthesis as a Vehicle for Collaboration

Lucas A. Morrill, Robert B. Susick, Jason V. Chari, and Neil K. Garg.

J. Am. Chem. Soc. **2019**, *141*, 12423–12443.

1.1 Abstract

"Collaboration" is not the first word most would associate with the field of total synthesis. In fact, the spirit of total synthesis is all-too-often reputed as being more competitive, rather than collaborative, sometimes even within individual laboratories. However, recent studies in total synthesis have inspired a number of collaborative efforts that strategically blend synthetic methodology, biocatalysis, biosynthesis, computational chemistry, and drug discovery with complex molecule synthesis. This chapter highlights select recent advances in these areas, including collaborative syntheses of chlorolissoclimide, nigelladine A, artemisinin, ingenol, hippolachnin A, communesin A, and citrinalin B. The legendary Woodward–Eschenmoser collaboration that led to the total synthesis of vitamin B_{12} is also discussed.

1.2 Introduction

One of the most stunning scientific achievements of the 20th century is the landmark total synthesis[1] of vitamin B_{12} (**1.1**, Figure 1.1).[2,3] Vitamin B_{12} (**1.1**) is the largest and most structurally complex vitamin known and is comprised of a number of structural challenges, including 63 carbons, 14 nitrogens, a cobalt center, and 14 stereocenters. The vitamin, which

plays a critical role in metabolism, was first isolated in pure form in 1948.[4] Subsequently, Nobel Laureate Dorothy Hodgkin determined the structure of **1.1** using X-ray crystallography in 1956.[5] In turn, the remarkable structure of the natural product captivated the minds of the legendary synthetic chemists R. B. Woodward (Harvard, USA) and Albert Eschenmoser (ETH Zurich, Switzerland). The two would initially pursue the synthesis of **1.1** independently, but ultimately realized the difficulty was too great for either group to bear independently. Thus, an international collaboration was formed between the two laboratories in 1965.[2]

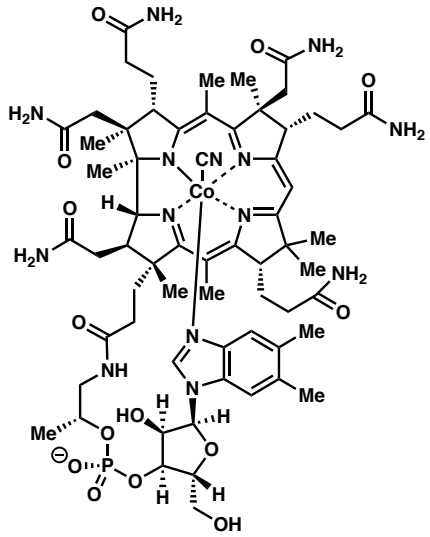


Figure 1.1. The remarkable structure of vitamin B_{12} (**1.1**).

Two of the most memorable moments of the epic vitamin B_{12} collaboration are summarized in Figure 1.2. The groups had decided to each prepare one half of the molecule. Woodward's group arrived at cyanobromide **1.2**, whereas Eschenmoser's team prepared thiodextrolin **1.3**. The two units were then successfully joined using Eschenmoser's sulfide contraction methodology.[6] This transformation delivered product **1.4** bearing the necessary A–D

rings, which, in turn, was elaborated to cobalt derivative **1.5**. The synthesis of **1.5**, bearing much of the natural product's core, constituted an amazing achievement toward the natural product. The second aspect of the highlighted chemistry reflects a somewhat tragic incident. Eschenmoser's group had developed a new, high yielding set of conditions for adding a carbon to each of the one-carbon linkers between the A–B and C–D ring systems. This information was given to Woodward's group, as they had significant quantities of **1.5** on hand, while the Eschenmoser group completed the characterization. Using IR spectroscopy, it was regrettably realized that the nitrile unit stemming off of the D ring had been unintentionally converted to a methyl ester, giving rise to **1.6**. This marked a dead-end, as moving forward it would be impossible to differentiate the newly formed methyl ester from the other esters in **1.6**. Eschenmoser tried to call Woodward immediately, but it was too late. One of Woodward's postdoctoral scholars had come to the laboratory early (ca. 3:30 A.M.) to start the alkylation sequence. Almost all of the material was lost in the incident commonly referred to by the groups as "Black Friday" (July 9, 1971).[3b]

Despite the "Black Friday" setback, the team ultimately persevered and developed an alternate protocol to give the desired alkylated product **1.7** by simply using $ClCH_2OBn$ in place of $ClCH_2OCH_3$.[3b] They would go on to complete the total synthesis of **1.1** in 1972, which remains the only total synthesis of vitamin B_{12} (**1.1**) to date.[7] The total synthesis is said to have involved a remarkable team of 103 co-workers over the course of 12 years, representing 19 countries. Overall the Woodward–Eschenmoser collaborative synthesis of **1.1** would be an incredible feat, even if accomplished today.

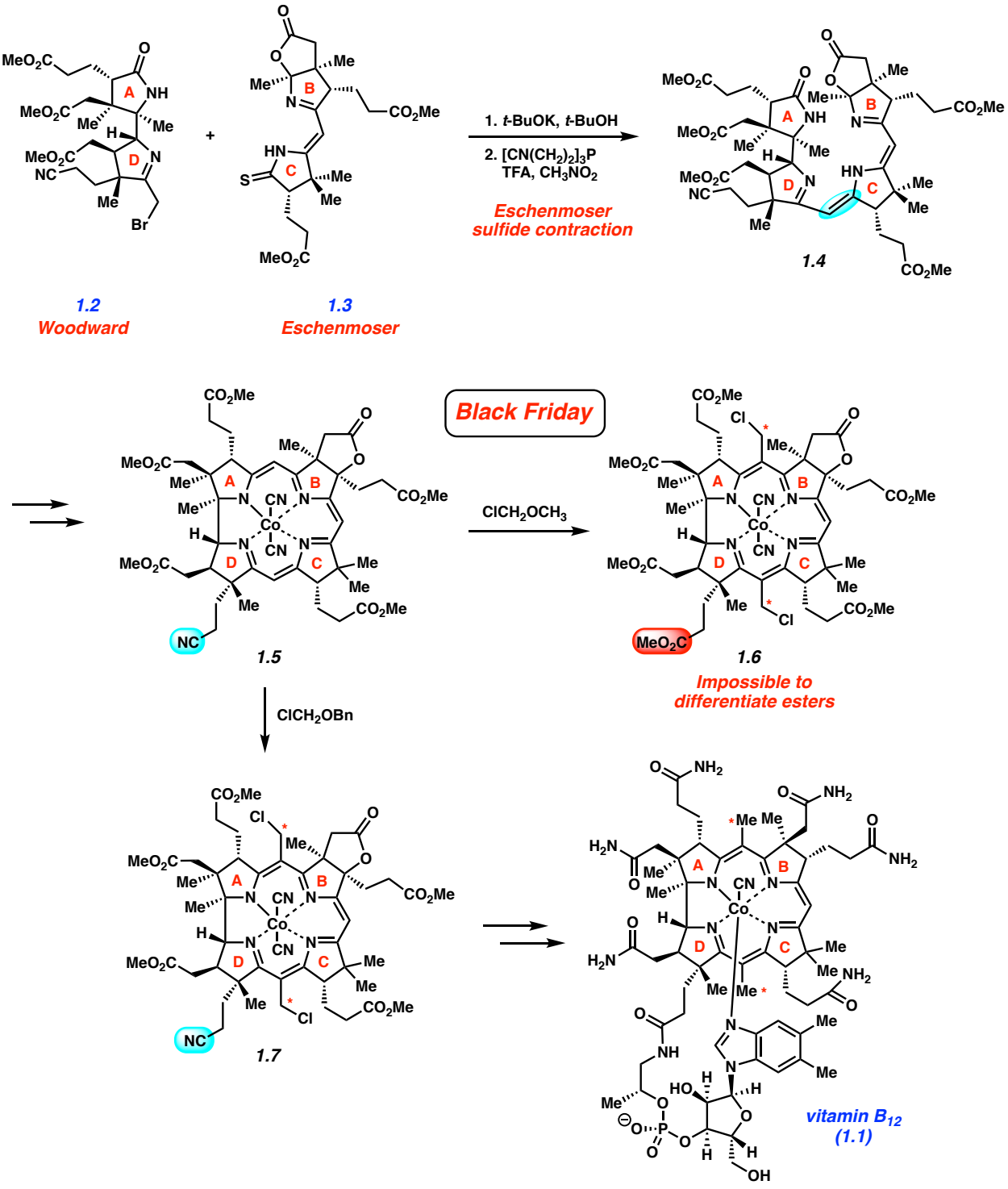


Figure 1.2. Woodward–Eschenmoser approach to vitamin B_{12} (**1.1**)

and the infamous "Black Friday" loss of material.

In the modern era, "collaboration" is perhaps not the first word one would associate with the field of total synthesis. Even practioners like us might think of the field as being more competitive, rather than collaborative, in general. *Who will make the molecule first? Whose synthesis is more elegant? Which synthesis is shorter or more efficient?* Such questions are commonplace amongst total synthesis chemists, and the resulting discussions do ultimately prompt innovations and achievements. That being said, we admire the glory days of collaboration in total synthesis pioneered by Woodward and Eschenmoser. Although we may never see a collaboration of such magnitude within the field of total synthesis again, a number of striking collaborations surrounding total synthesis have been reported in recent years. We describe some of our favorite examples in this chapter that tie together synthetic methodology, biocatalysis, biosynthesis, computations, and pharmaceutical science with total synthesis. The specific targets described are chlorolissoclimide (**1.8**),[8] nigelladine A (**1.9**),[9] artemisinin (**1.10**),[10] ingenol (**1.11**),[11] hippolachnin A (**1.12**),[12] communesin A (**1.13**),[13] and citrinalin B (**1.14**),[14] as highlighted in Figure 1.3.

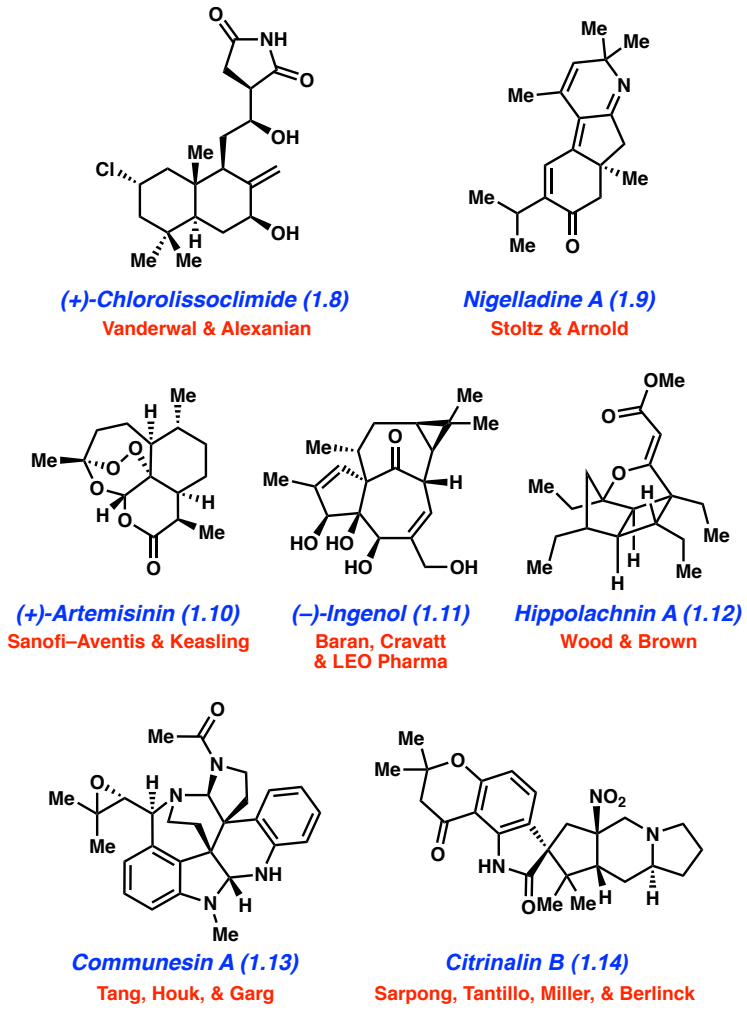


Figure 1.3. Natural products **1.8**–**1.14** synthesized via collaborations.

1.3 Collaborative Synthesis of (+)-Chlorolissoclimide

An elegant collaboration between the Alexanian and Vanderwal laboratories[8] nicely showcases the modern synergy between methodology and total synthesis. (+)-Chlorolissoclimide (**1.8**) (Figure 1.4) was first isolated in the early 1990s from *Lissoclinum voeltzkowi* Michaelson, a coral reef ascidian found in New Caledonia.[15] It displays potent activity against the P388 murine leukemia and KB human oral carcinoma cell lines.[15d,16] The natural product, bearing three rings and 7 stereogenic centers, poses a formidable challenge for total synthesis.[17] One of the

stereocenters is quaternary, whereas another is a secondary stereocenter bearing an alkyl chloride. The latter challenge provided an opportunity for the Alexanian and Vanderwal groups to join forces. Vanderwal's group had already displayed an affinity for chlorinated natural products, which led to several completed total syntheses.[18] Fortuitously, Alexanian's team had established an innovative means to carry out site- and stereoselective halogenation of aliphatic carbons.[19] A compelling example of Alexanian's methodology is shown in Figure 1.4, where (+)-sclareolide (**1.15**) was treated with *N*-bromoamide **1.16** in the presence of visible light to yield bromide **1.17** in 67% yield.[19] A chlorinative counterpart to this methodology did not exist at the time, but if available, could enable the synthesis of (+)-chlorolissoclimide (**1.8**).

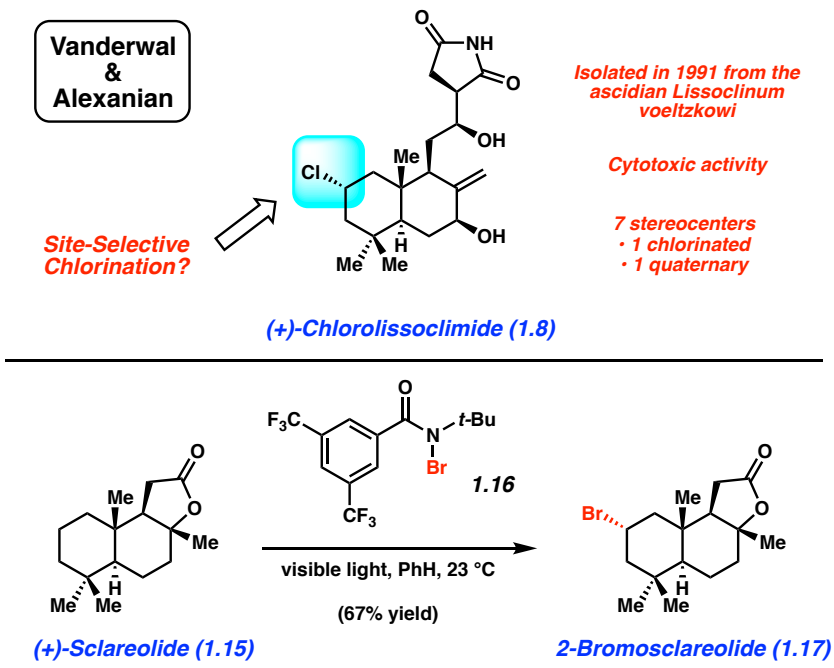


Figure 1.4. (+)-Chlorolissoclimide (**1.8**) and site-selective halogenation methodology.

The success of the Vanderwal–Alexanian collaboration would hinge upon the development of a site-selective, stereocontrolled C–H chlorination reaction. Although highly predictable and chemoselective aliphatic C–H bromination reactions had been developed,[19] aliphatic C–H chlorination reactions remained challenging. Existing methods required the use of strongly acidic conditions or the presence of highly reactive reagents to enable such transformations.[20]

Ultimately, the Alexanian group was able to identify suitable conditions using *N*-chloroamide **1.18** to enable efficient C–H chlorination, which was evaluated on a range of substrates (Figure 1.5). Several products are shown (**1.19**–**1.22**), which reflect that the reaction primarily leads to monochlorination and is sensitive to sterics. It was envisioned that this strategy could be applied to (+)-sclareolide (**1.15**), which has become a popular testing ground as a substrate for C–H functionalization protocols that rely on radical intermediates.[21] Impressively, applying their optimal chlorination reaction conditions to (+)-sclareolide (**1.15**) furnished chloride **1.23** in 82% yield. For gram-scale reactions, an alternate procedure was developed wherein benzoyl peroxide was used in place of visible light for radical initiation. This flexibility underscores the robustness of the Alexanian C–H functionalization protocol.

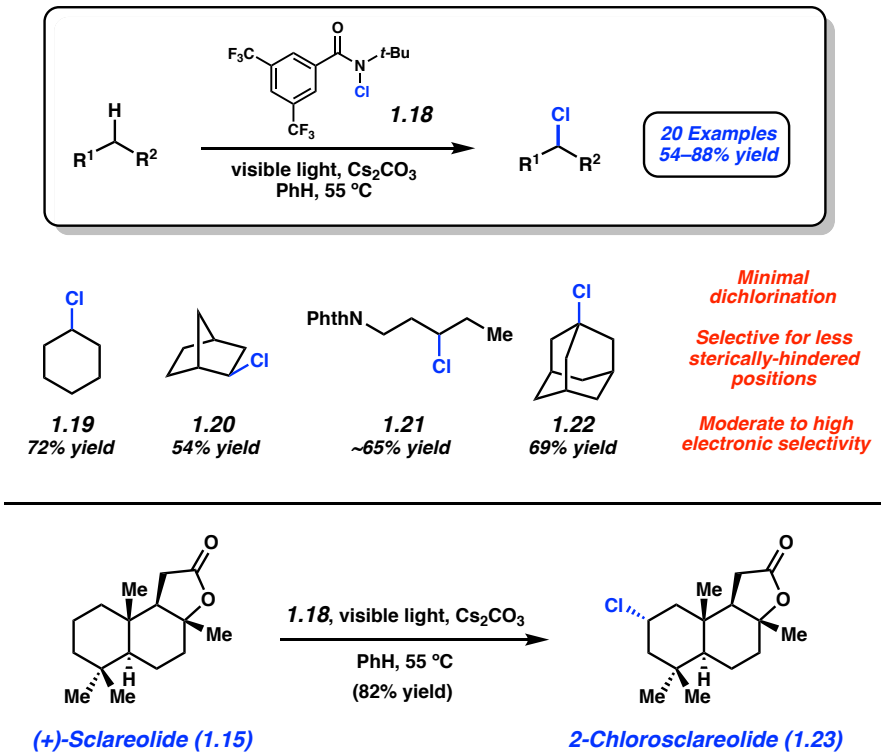


Figure 1.5. C–H chlorination methodology and gram-scale synthesis of (+)-2-chlorosclareolide (**1.23**).

Following the development of the successful C–H chlorination step as the first step of the total synthesis, Vanderwal's team was well poised to develop the necessary synthetic steps to access (+)-chlorolissoclimide (**1.8**) (Figure 1.6). 2-Chlorosclareolide (**1.23**) was elaborated to Weinreb amide **1.24** using a two-step sequence. This set the stage for a site-selective C–H oxidation,[22] followed by Swern oxidation, to deliver enone **1.25**. Further modification gave rise to aldehyde **1.26**, which underwent an Evans aldol reaction with **1.27**.[23] This allowed for the introduction of two new stereocenters and generated alcohol **1.28**. The final steps, involving ammonolysis of the chiral auxillary and ring closure, provided (+)-chlorolissoclimide (**1.8**).

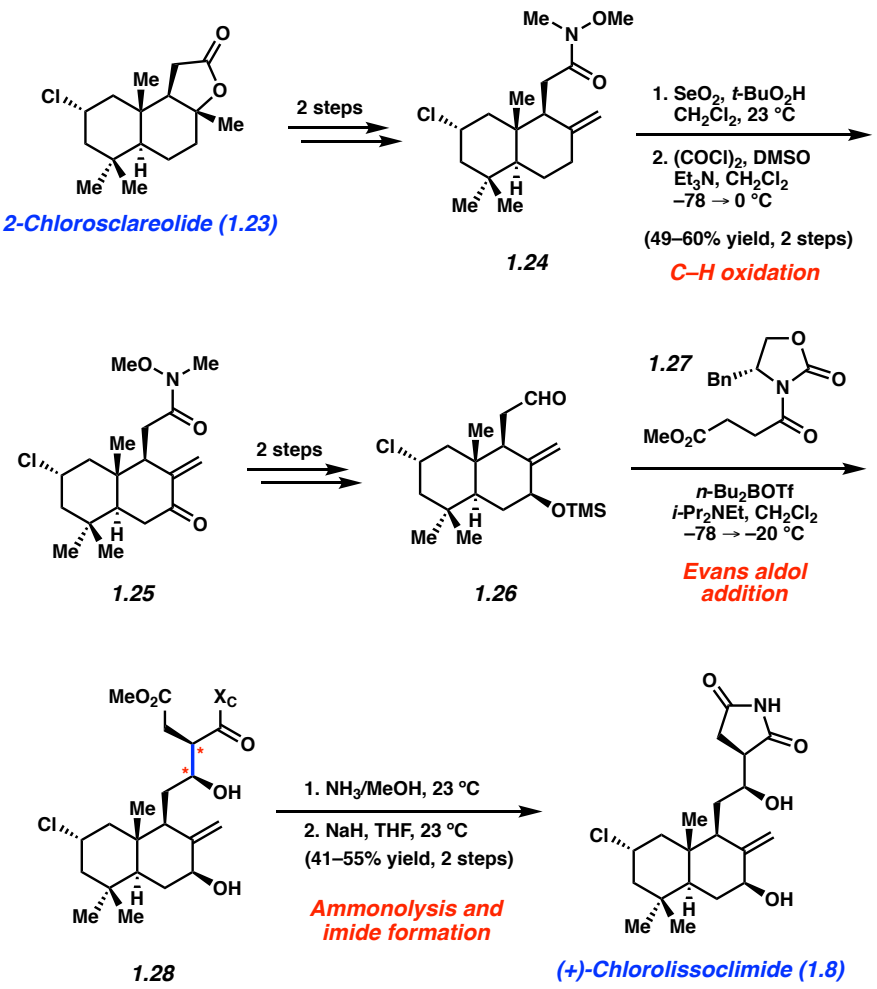


Figure 1.6. A robust route to (+)-chlorolissoclimide (**1.8**).

The Alexanian–Vanderwal collaboration provides a striking example of the synergy between methods development and total synthesis between two different research groups. The effort led to a powerful new methodology for achieving site-selective and stereoselective chlorination, while also facilitating a concise total synthesis of (+)-chlorolissoclimide (**1.8**). The authors were also able to prepare unnatural analogs that show promise as cytotoxic agents toward melanoma and prostate cancer cell lines.[8,24]

1.4 Collaborative Total Synthesis of Nigelladine A

The collaborative synthesis of nigelladine A (**1.9**) (Figure 1.7) by the Stoltz and Arnold laboratories presents a compelling example of synergy between biocatalysis and total synthesis.[9] The natural product, **1.9**, a norditerpenoid alkaloid, was first isolated in 2014 from *Nigella glandulifera* and exhibits potent protein tyrosine phosphatase 1B (PTP1B) inhibitory activity.[25] Nigelladine A (**1.9**) bears a highly conjugated tricyclic skeleton and a quaternary stereocenter, thus offering an intriguing synthetic challenge. Moreover, the natural product possesses oxidation at C7, which the Stoltz group viewed as a potential testing ground for late-stage C–H oxidation protocols. Ultimately, this challenge proved to be a formidable one and could not be easily resolved using conventional synthetic chemistry. This difficulty was eventually resolved using a biocatalytic oxidation.

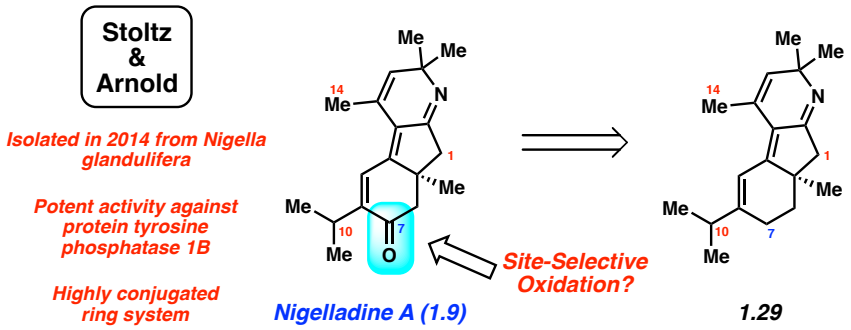


Figure 1.7. Collaborative total synthesis of nigelladine A (**1.9**) by the Stoltz and Arnold laboratories.

With the aim of testing late-stage oxidation chemistry, the Stoltz laboratory first developed the synthetic sequence shown in Figure 1.8. Beginning with known enone **1.30**,[26] a four-step sequence provided multigram quantities of β-ketoester **1.31**. Next, to establish a key

quaternary stereocenter, an asymmetric allylic alkylation was performed.[27] This furnished allylated product **1.32** in 96% yield and 87% ee. Enone **1.32** was further elaborated to vinyl bromide **1.33**, which set the stage for a Suzuki–Miyaura cross-coupling. In the event, treatment of **1.33** with vinyl boronate **1.34** using palladium catalysis delivered triene **1.35**.[28] Lastly, the Boc group was removed using TFA (trifluoroacetic acid). Upon neutralization and exposure to SiO_2, the amine underwent cyclization with subsequent olefin isomerization to provide iminium salt **1.29**.

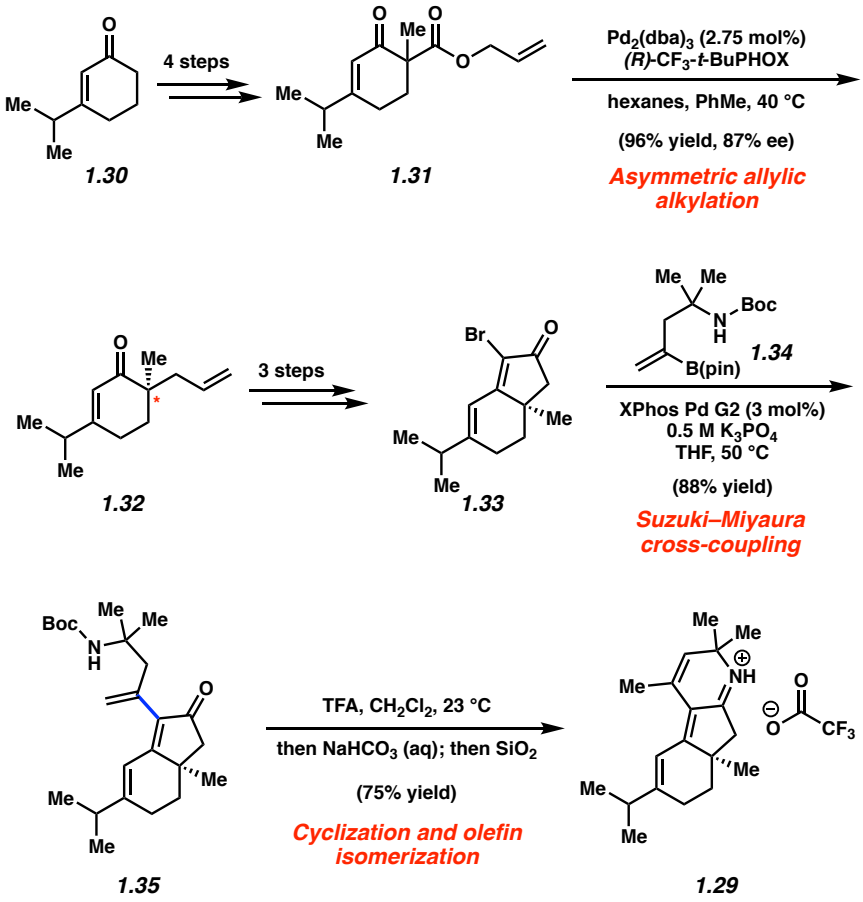


Figure 1.8. Stoltz's synthesis of tricycle **1.29**.

With **1.29** in hand, the Stoltz group was just an oxidation step away from completing the total synthesis of **1.9** (Figure 1.9). The group examined a number of conditions to effect the desired oxidation of neutral imine **1.29** to deliver the natural product nigelladine A (**1.9**).[29] Unfortunately, these efforts were hampered by low yields and poor site-selectivity. At best, nigelladine A (**1.9**) could be obtained in 10% yield using a Rh-catalyzed oxidation protocol. Faced with near defeat, the graduate student lead, Steven Loskot, approached the Arnold laboratory and connected with Dr. David Romney, who coincidentally performed research with Stoltz as an undergraduate student. Together, they envisioned carrying out the key oxidation step enzymatically.[30] A select library of mutated cytochrome P450 enzymes was evaluated and, fortunately, several delivered the desired secondary alcohol. P450 8C7 was identified as the enzyme of choice. In their optimal sequence, the enzymatic oxidation was followed directly by a Dess–Martin oxidation to give nigelladine A (**1.9**) in 21% yield (43% based on recovered starting material **1.29**). This result not only allowed for the completed total synthesis, but also provides a persuasive example of how biocatalysis can be used to effect a challenging late-stage transformation in target-oriented synthesis.

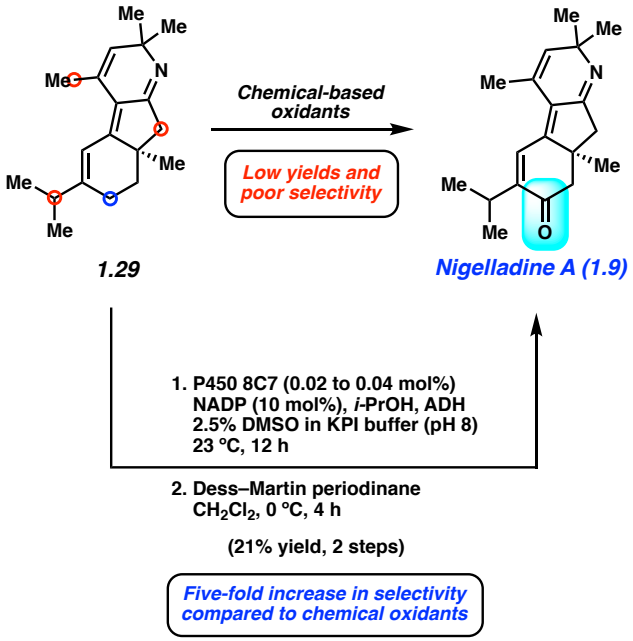


Figure 1.9. The crucial site-selective, late-stage oxidation of tricycle **1.29** was achieved using an enzymatic oxidation and allowed for the total synthesis of nigelladine A (**1.9**).

The alliance between the Stoltz and Arnold laboratories proved instrumental in enabling the first total synthesis of nigelladine A (**1.9**). More specifically, the synthetic expertise of the Stoltz group, including their enantioselective allylation methodology, was leveraged in combination with the Arnold laboratory's proficiency in biocatalysis using mutated enzymes to concisely deliver the natural product. Stoltz notes, "I hope this effort will influence the synthetic community to not only use biocatalysis when faced with a synthetic obstacle, but also to more frequently consider the use of biocatalysis and particularly engineered enzymes during strategic planning."[31]

1.5 Collaborative Total Synthesis of Artemisinin

One of the most exciting collaborations reported in recent years involves the Keasling laboratory and the pharmaceutical giant Sanofi, who came together to develop a semisynthetic route to artemisinin (**1.10**) (Figure 1.10).[10] Artemisinin (**1.10**) is a naturally occurring small molecule first isolated in 1971 in an effort to boost anti-malarial medicinal abilities during the Vietnam War.[32] Artemisinin (**1.10**) and its derivatives display exceptional potency, showing low nanomolar EC_{50} values with regard to their inhibition of the parasitic cause of malaria *Plasmodium falciparum*.[33] Although the development of resistance has historically made malaria difficult to treat, the discovery of artemisinin (**1.10**) and derivatives, such as artesunate (**1.36**) and artemether (**1.37**), has been a tremendous breakthrough for humanity. These compounds function through a novel mode of action relative to previously used anti-malarial drugs.[34] Thus, therapies involving the combination of **1.36** or **1.37** alongside drugs with separate modes of action, termed artemisinin-based combination therapy (ACT), have revolutionized modern malarial treatments. ACTs have led to reduced treatment times, diminished parasite recurrence, and lower resistance development. The impact of these therapies cannot be understated, and was recognized by the awarding of the 2015 Nobel Prize in Physiology or Medicine to Youyou Tu "for her discoveries concerning a novel therapy against malaria."[35] Despite these remarkable advances, malaria continues to be a deadly threat to people, especially children, in the developing world.

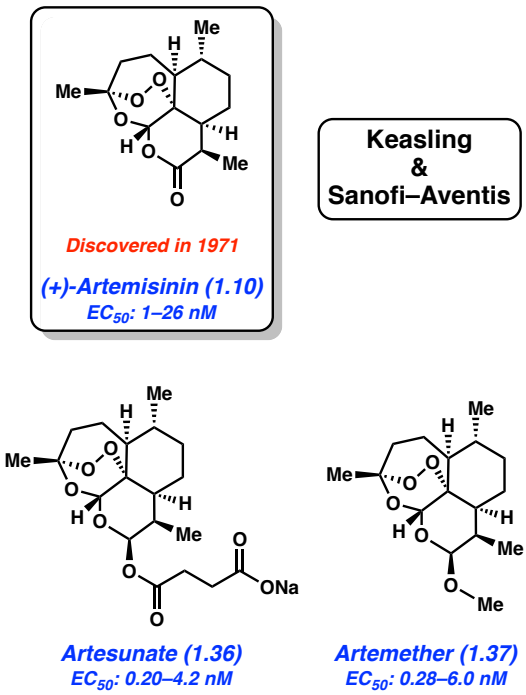


Figure 1.10. Artemisinin (**1.10**) accessed through a collaboration between the Keasling laboratory and Sanofi–Aventis, in addition to unnatural derivatives **1.36** and **1.37**.

ACTs have proven difficult to access for the developing world due to challenges in obtaining reliable supplies of artemisinin (**1.10**).[36] The industrial production of artemisinin (**1.10**) has long relied on isolation from *Artemisia annua*, which gives low and inconsistent yields. This has led to fluctuations in price and availability, which, in turn, has prompted research efforts towards alternative sources of the compound. One such approach involves chemical synthesis, an avenue which has been explored for many years due in part to the provocative structure of artemisinin (**1.10**). The natural product contains four rings and seven stereocenters, as well as a unique endoperoxide bridge. To date, more than 10 completed syntheses have been reported,[37] including those by the laboratories of Schmid and Hofheinz,[38] Yadav,[39] and Cook.[40] Despite these breakthroughs, an approach based solely on synthetic chemistry has yet to meet the high global demand for artemisinin (**1.10**). In addition, synthetic biology on its own has not provided

a cost-efficient synthesis of **1.10**. However, an approach that utilizes both synthetic chemistry and synthetic biology in a synergistic fashion had tremendous potential to unlock a low-cost production route.

The tag-team approach taken by Keasling and Sanofi involved a strategic blend of engineered biosynthesis and organic synthesis. First, the Keasling laboratory and Amyris[41] developed the conversion of glucose (**1.38**) to artemisinic acid (**1.42**) (Figure 1.11). After initial optimization studies performed in *E. Coli* yielded high titres of key intermediate amorphadiene (**1.41**, 25 g/L), the Keasling lab made a pivotal discovery in performing the engineered biosynthesis in a less common strain (CEN.PK2) of *S. cerevisiae*. This switch, driven by the need to express downstream enzymes, allowed for the entire engineered biosynthesis to take place in a single organism. In the final process, glucose (**1.38**) was used as a precursor to acetyl-CoA (**1.39**), which provided an entryway into terpene biosynthesis. A variety of different enzymes then transform acetyl-CoA into amorphadiene (**1.41**) via intermediate farnesyl pyrophosphate (**1.40**). After extensive optimization, the Keasling lab was able to obtain amorphadiene (**1.41**) in a remarkable 40 g/L titre. Further downstream enzymatic oxidations, performed by enzymes characterized in *A. annua* and expressed in yeast, provided artemisinic acid (**1.42**) in an overall isolation of 25 g/L.

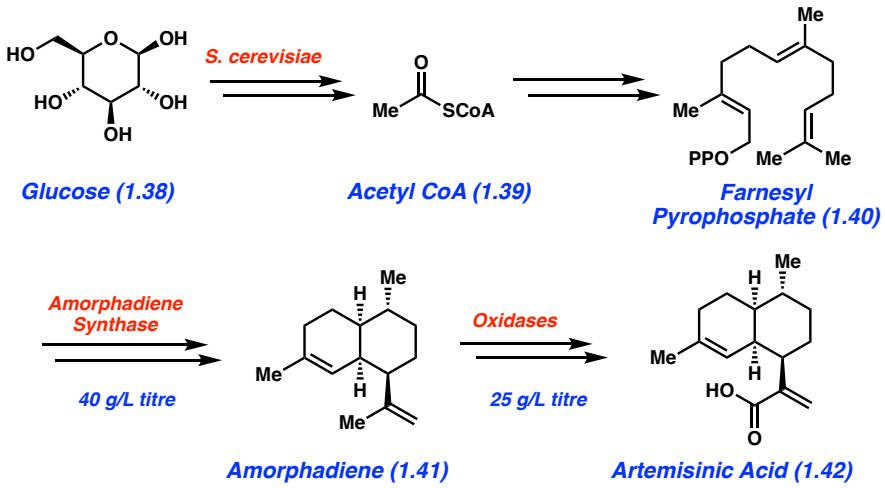


Figure 1.11. Keasling's contribution: an efficient biosynthetic route to artemisinic acid (**1.42**).

With Keasling's biosynthetic efforts providing artemisinic acid (**1.42**), Sanofi took to the task of developing the chemical conversion of **1.42** to artemisinin (**1.10**). Original efforts by Acton and Roth[42] had established the viability of this route, but were not commercially feasible. Thus, over several years, Sanofi optimized the sequence shown in Figure 1.12.[10] First, reduction of **1.42** with a Ru-Segphos catalytic system proceeds in nearly quantitative yield to give acid **1.43** with excellent diastereoselectivity. Activation of **1.43** provides the corresponding mixed anhydride, **1.44**, thus setting the stage for a key photocyclization. Such a photocyclization is thought to occur naturally when **1.44** is exposed to sunlight[43] and has been shown to be viable in a flow process.[44] In the Sanofi procedure, **1.44** is exposed to a sensitizer and light in a semi-batch reactor, with exposure to oxygen. The resulting hydroperoxide intermediate **1.45** then reacts with another equivalent of oxygen to ultimately provide artemisinin (**1.10**). This three-step sequence is remarkably efficient, furnishing the desired natural product in 55% yield. Notably, single batches of 600 kg of artemisinic acid (**1.42**) have delivered 370 kg of artemisinin (**1.10**) using this approach.

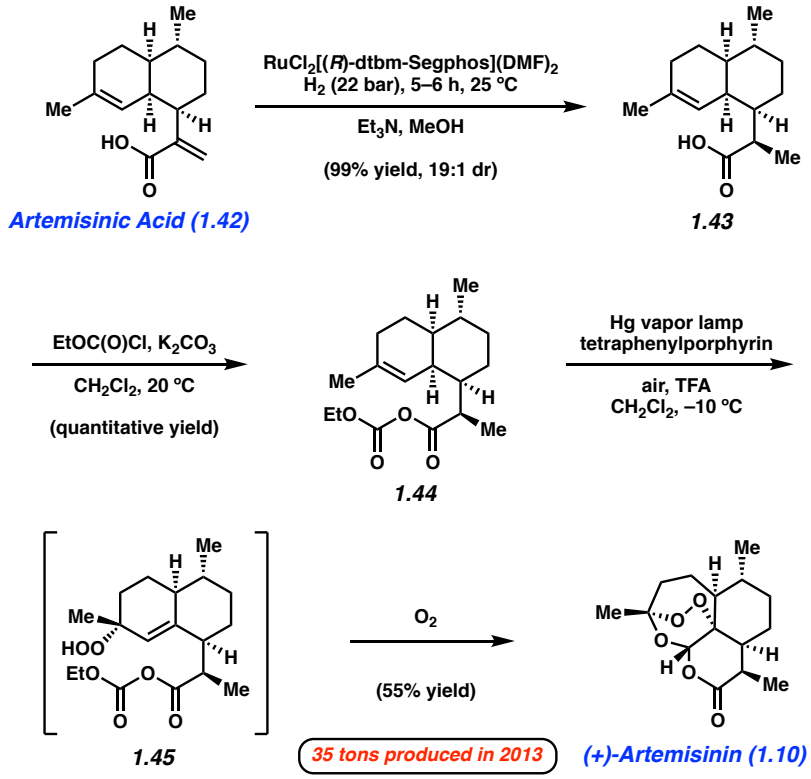


Figure 1.12. The finishing touches by Sanofi: industrial scale conversion of artemisinic acid (**1.42**) to artemisinin (**1.10**).

There have been relatively few collaborations between academic laboratories and industrial laboratories that blend biosynthesis and chemical synthesis to solve a production problem in the pharmaceutical field. Perhaps the most classic example of such a collaboration is the production route to Taxol devised by Holten[45] and licensed by Bristol-Myers Squibb in the 1990s. The collaboration described herein that addresses the artemisinin production problem sets another gold standard for this type of blended approach. The Keasling/Sanofi collaboration delivered 35 tons of artemisinin (**1.10**) in 2013, with the potential to produce up to 60 tons annually. Although the amounts of synthetic artemisinin needed to complement natural material

will vary annually and may even be negligible at times,[46] having a scalable route offers long-term stability to the artemisinin supply problem.

1.6 Total Synthesis of Ingenol

Another exciting collaboration between the pharmaceutical industry and academia is presented in the efficient total synthesis of (+)-ingenol (**1.11**) in 2013 via a partnership between the Baran and Cravatt laboratories and LEO Pharma (Figure 1.13).[11] (+)-Ingenol (**1.11**) was first isolated from *Euphorbia ingens* in 1968,[47] and its derivatives have since been employed as effective treatments for the precancerous skin condition actinic keratosis. The potent analog, ingenol mebutate (**1.46**), marketed as Picato® by LEO Pharma, is an FDA-approved topical treatment for the disease, whereas isoxazole derivative ingenol disoxate (**1.47**) is currently undergoing clinical trials for the same ailment.[48] The preparation of these therapeutic agents presented a major obstacle for LEO Pharma, as only 275 milligrams of ingenol (**1.11**) can be isolated per kilogram of plant material.[11] Artemisinin, in comparison, can be accessed in recovery yields of about 5 grams per kilogram.[49] In addition to this crucial isolation problem, previous synthetic approaches[50] were lengthy due to the complex architecture of the molecule that contains four interconnected rings including an *in/out*-[4.4.1]bicycloundecane core and eight stereocenters, one of which is quaternary and five of which are contiguous. Further, structure–activity relationships were not fully understood, and structural analogs could only be accessed through derivatization of (+)-ingenol (**1.11**) itself.[11] To address these challenges, LEO Pharma partnered with the Baran laboratory to devise a concise, enantioselective total synthesis of (+)-ingenol (**1.11**).

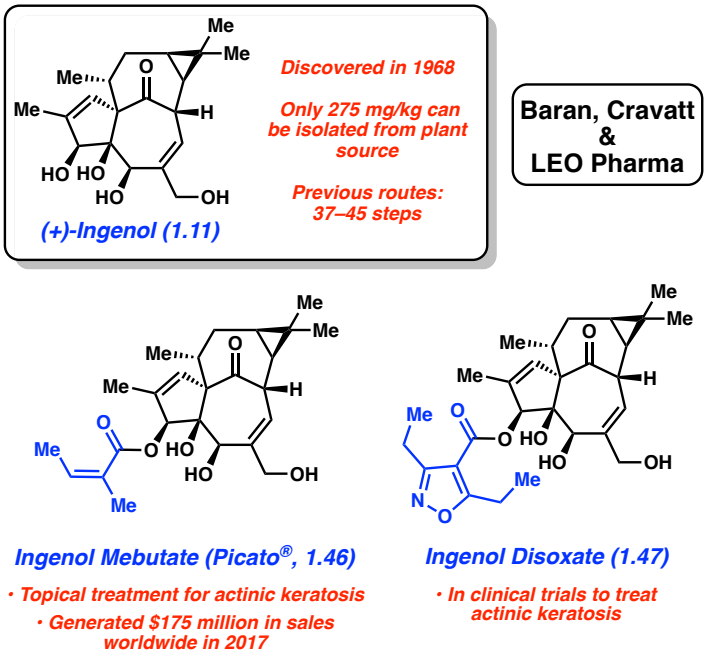


Figure 1.13. (–)-Ingenol (**1.11**) and medicinally important derivatives.

(+)-3-Carene (**1.48**) was identified as a cost-effective starting material for the synthesis of (+)-ingenol (**1.11**) (Figure 1.14).[11] From **1.48**, elaboration to allene **1.49** was achieved through a five-step alkylation sequence, which established four contiguous stereocenters and set the stage for a key allenic Pauson–Khand cyclization.[51] Treatment of **1.49** with an appropriate rhodium catalyst under an atmosphere of CO furnished the 5/7-fused ring system of the natural product to deliver dienone **1.50** in 72% yield. After elaboration to **1.51**, a semi-pinacol rearrangement was employed to furnish **1.52**. Of note, this crucial step assembles the necessary 7-membered ring and the notorious *in/out*-[4.4.1]bicycloundecane. Selective allylic oxidations and protecting group removal ultimately gave rise to (+)-ingenol (**1.11**) in a total of 14 steps from (+)-3-carene (**1.48**).

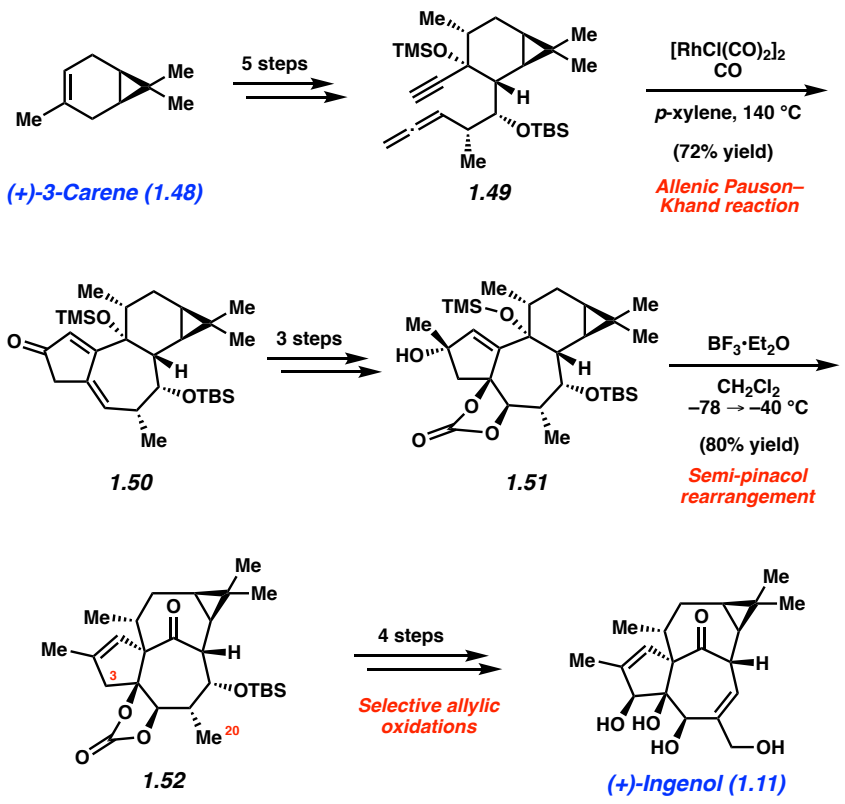


Figure 1.14. Expedient total synthesis of (+)-ingenol (**1.11**).

The newly developed synthetic route to (+)-ingenol (**1.11**) enabled the synthesis of unnatural derivatives for biological investigations. One prominent example is related to the aforementioned analog ingenol mebutate (**1.46**) (Figure 1.15), which is an effective treatment for actinic keratosis commercialized by LEO Pharma. Whereas the general mode of action for **1.46** had been well characterized,[52] the specific proteins it targets within cancer cells had not been identified. In collaboration with the Cravatt laboratory, a suitable substrate for chemical proteomic discovery was synthesized to enable the identification of ingenol mebutate (**1.46**) binding proteins. A "fully functionalized" probe was realized in the ingenol mebutate derivative **1.53**, which harbors a photoreactive dialkyl diazirine and clickable alkyne for visualization of the binding proteins.[53] This derivative was accessed from allylic alcohol **1.54**, available from the

route described above,[11] by treatment with MsCl, followed by TBACl and LiN_3, to provide azide **1.55** in 60% yield over two steps. Further elaboration generated "azido-ingenol" (**1.56**), which, in turn, underwent a copper-catalyzed click reaction[54] with bis(alkyne) **1.57** to furnish clickable probe **1.53** in 37% yield. Empowered with the ingenol-based probe, Cravatt and co-workers employed quantitative mass spectrometry-based proteomics to discover a new protein target for ingenol mebutate (**1.46**).[55] Specifically, the mitochondrial carnitine/acylcarnitine carrier protein SLC25A20 was identified as a highly ligandable site for **1.46** and **1.53**. Further studies revealed that ingenol mebutate (**1.46**) inhibits SLC25A20, thereby perturbing mitochondrial function and leading to necrotic cell death in a pathway independent of that known via protein kinase C agonism.

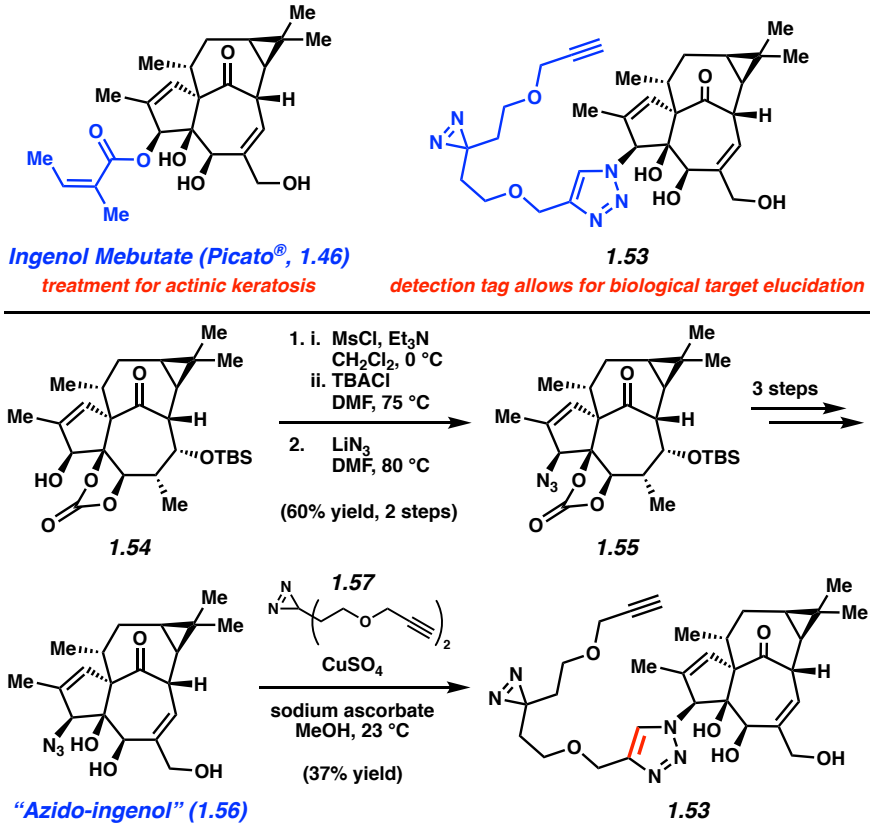


Figure 1.15. Synthesis of ingenol derivative **1.53** bearing a photoaffinity probe.

The partnership between the Baran laboratory, the Cravatt laboratory, and LEO Pharma illustrates the effectiveness of leveraging academic resources to solve critical problems in the pharmaceutical industry. The concise total synthesis of (+)-ingenol (**1.11**) delivered an attractive solution to access valuable material.[11] Additionally, the synthetic route enabled further biological studies by the Cravatt laboratory to elucidate the molecular targets of ingenol derivatives, including that of the FDA-approved drug ingenol mebutate (**1.46**). In turn, this effort led to the elucidation of a novel mechanism of action. The Baran–LEO Pharma team subsequently synthesized the classic target (+)-phorbol, where LEO Pharma provided large quantities of **1.50**, a common intermediate from their synthesis of (+)-ingenol (**1.11**).[56] The total syntheses of several other terpene targets have also been achieved as a result of this collaboration.[57]

1.7 Total Synthesis of Hippolachnin A

Collaboration between two total synthesis groups is rare today, despite the precedent set by Eschenmoser and Woodward decades earlier. Nonetheless, the Wood and Brown laboratories reported a particularly successful example with their total synthesis of hippolachnin A (**1.12**) described in 2016 (Figure 1.16).[12,58] The natural product was first isolated in 2013 from *Hippospongia lachne*. Hippolachnin A (**1.12**) bears a densely functionalized polycyclic core, which presents a challenge for chemical synthesis. Notably, **1.12** possesses six contiguous stereocenters, one of which is quaternary, and a structurally unique, highly congested tricyclic skeleton. In addition to its unique structure, **1.12** was initially reported to display potent antifungal activity against several pathogenic fungi, in particular *Cryptococcus neoformans*.[59] Thus, developing a synthetic strategy to access the scaffold of **1.12** was highly desirable.

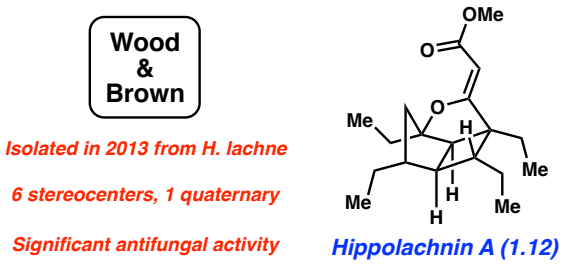


Figure 1.16. Collaborative total synthesis of hippolachnin A (**1.12**).

The collaboration between the Wood and Brown groups was spurred by a serendipitous meeting during a poster session at the 2015 National Organic Symposium.[12,60] The lead graduate students on the project realized their synthetic designs toward hippolachnin A (**1.12**) were nearly identical, including the non-obvious use of quadricyclane (**1.60**) as the starting material (Figure 1.17). Although one could imagine each group trying to reach the finish line first, the researchers took the opportunity to work together. Ultimately, they were able to combine the strengths of each independent synthesis to formulate an improved and elegant route to hippolachnin A (**1.12**). The natural product, **1.12**, was envisioned to arise from fused-[3.2.0]-bicyclic intermediate **1.58** through a late-stage C–H oxidation. Fused bicycle **1.58** could be traced back to bridged-[2.2.1]-bicycle **1.59**. In the forward sense, ring-opening metathesis of the bridged bicycle present in **1.59** would yield **1.58**. Lastly, the cyclobutane found in **1.59** would arise from quadricyclane (**1.60**). In the Brown laboratory's route, quadricyclane (**1.60**) would undergo a [2+2+2] cycloaddition with acid chloride **1.61** to generate the desired cyclobutane intermediate. Separately, the Wood laboratory envisioned a [2+2+2] cycloaddition between quadricyclane (**1.60**) and diester **1.62**, with further manipulations, would deliver the key cyclobutane intermediate **1.59**.

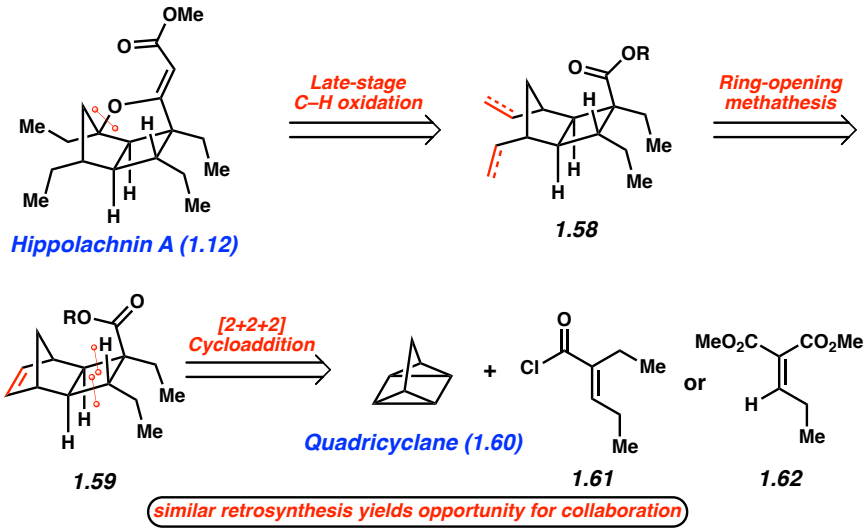


Figure 1.17. Shared retrosynthetic analysis of hippolachnin A (**1.12**).

Figure 1.18 provides a summary of the collaborative route to hippolachnin A (**1.12**) devised by the Brown and Wood laboratories. Using Brown's initial step, quadricyclane (**1.60**) underwent a [2+2+2] cycloaddition[61] with acid chloride **1.61**, thus forming carboxylic acid **1.59** in 50% yield after hydrolysis of the acid chloride. This remarkable key reaction installed all six stereocenters of the natural product in a single transformation. From **1.59**, ring-opening metathesis of the bridged bicycle in the presence of ethylene delivered fused-[3.2.0]-bicycle **1.58** with high efficiency.[62] This set the stage for a key C–H oxidation developed by the Wood laboratory. In the event, **1.58** was treated with a modification of White's conditions using catalyst **1.63** to generate lactone **1.64** in 70% yield.[63] With lactone **1.64** in hand, a three-step sequence involving a condensation, reduction, and transesterification produced hippolachnin A (**1.12**). Interestingly, the reported antifungal activity of hippolachnin A (**1.12**) could not be reproduced using synthetic material.[64] This same observation was verified independently by Trauner's laboratory during bioactivity studies of synthetic analogs of **1.12**.[65] In fact, none of the analogs displayed antifungal activity, and only weakly potent growth inhibition of the nematode

Caenorhabditis elegans was observed. This clarification of the biological activity of hippolachnin A (**1.12**) and derivatives underscores the utility of total synthesis in enabling bioactivity studies.

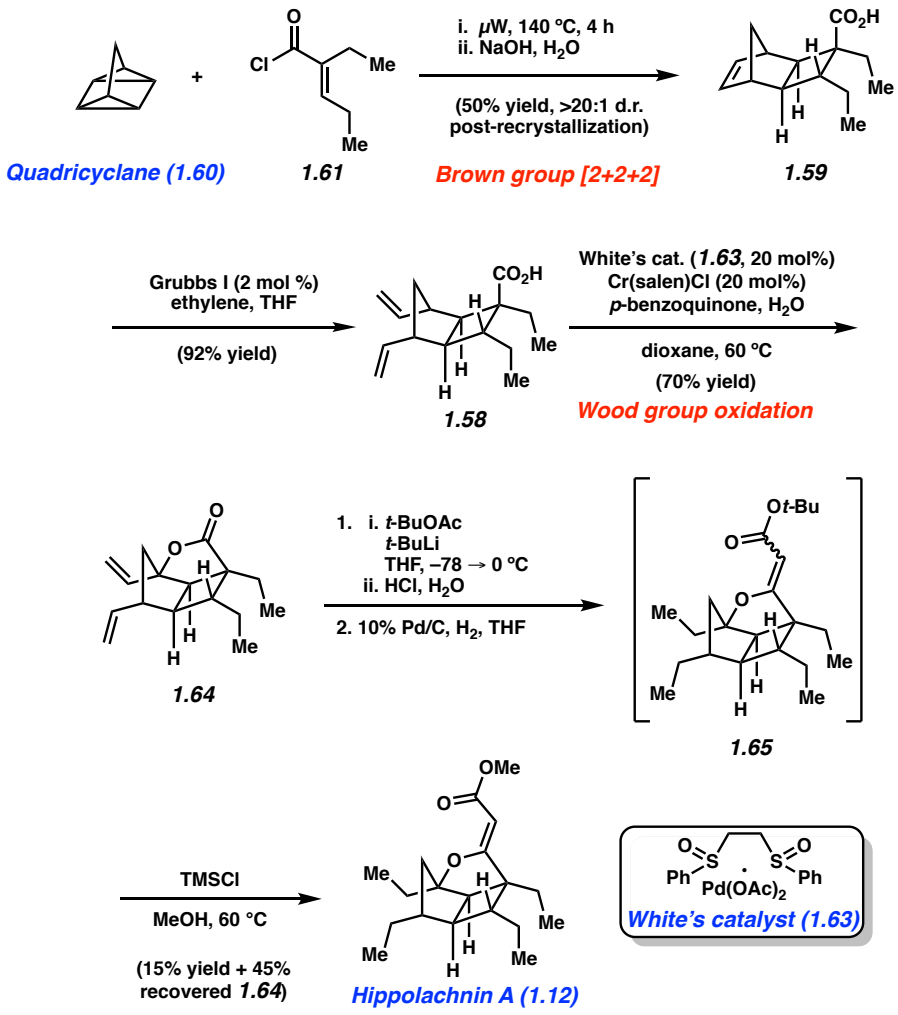


Figure 1.18. Collaborative route to achieve the total synthesis of hippolachnin A (**1.12**).

Overall, the joint synthetic route developed by the Brown and Wood laboratories represents an uncommon synergetic relationship between two synthetic research groups. The individual laboratories' total syntheses of hippolachnin A (**1.12**) each totaled nine steps. Upon

collaborating and finding advantageous portions of each route, the team was able to establish a six-step route to **1.12**. The final synthesis featured impressive [2+2+2] cycloaddition chemistry using quadricyclane (Brown laboratory) in combination with an elegant C–H oxidation and subsequent elaboration (Wood laboratory). Moreover, the joint effort provided students with many opportunities to exchange ideas beyond the confines of their individual institutions. Although collaborations of this nature between total synthesis groups remain rare, the elegant Brown and Wood synthesis of **1.12** underscores the value of such partnerships.

1.8 Biosynthesis of Natural and Unnatural Communesin Scaffolds

Understanding the biosynthetic origins of highly intricate natural product scaffolds can require collaboration across synthetic, computational, and enzymatic chemists. A compelling example of this cooperation that was borne out of a total synthesis endeavour is exemplified by the investigation of the communesin alkaloid biosynthesis recently reported by the Houk and Tang laboratories, together with our laboratory.[13] The communesins possess daunting chemical structures and promising biological activities, and have therefore been popular targets for synthetic chemists.[66] With regard to their structural features, the communesin scaffold **1.68** (Figure 1.19) bears four nitrogen atoms and a multitude of stereocenters embedded in a heptacyclic framework. The vicinal quaternary centers at C3 and C3' are particularly challenging to install.

The nature of how this particular collaboration arose deserves special mention. Garg had studied in two laboratories where the communesin alkaloids were being pursued.[67] In addition, his own laboratory had devised a synthetic route to the communesin scaffold using the so-called interrupted Fischer indolization methodology.[68] When this synthetic methodology failed to

generate scaffolds containing vicinal quaternary stereocenters, over a casual lunch meeting, Professors Tang and Garg decided the problem should be investigated biosynthetically. Tang procured the necessary fungus and a joint student was able to isolate communesin alkaloids in a matter of weeks. Both research groups became fascinated by the remarkable ability of Nature to generate vicinal quaternary stereocenters and the challenging communesin framework.

The Tang group went on to identify the biosynthetic gene cluster for quaternary stereocenter formation.[69] However, the exact mechanism of formation of these quaternary centers remained elusive (**1.66** + **1.67** → **1.68**, R=H, Figure 1.19). Thus, the Houk laboratory was also recruited and together, the team performed a combination of feeding studies, computations, and mechanism of action studies that ultimately led to new insights and access to a novel communesin scaffold (i.e., **1.69**).

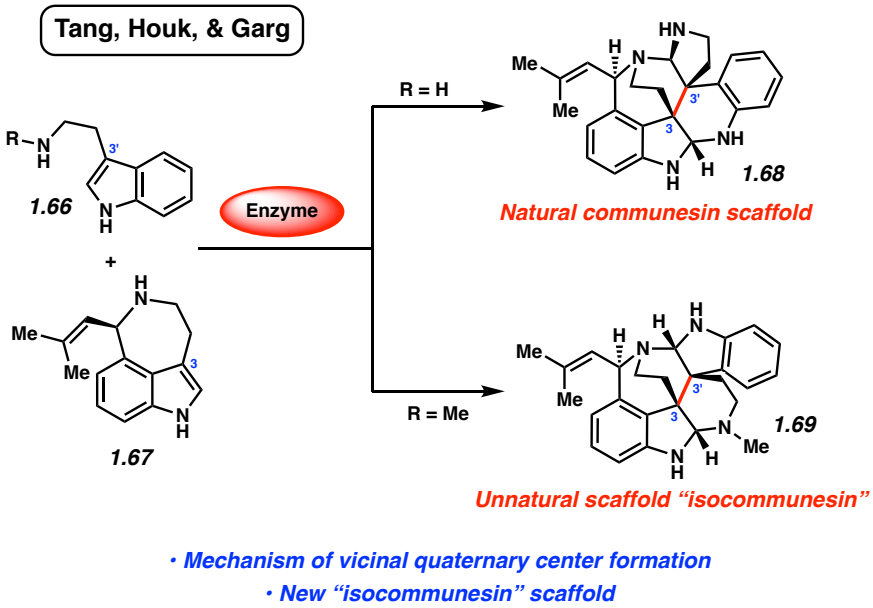


Figure 1.19. Biosynthetic studies of the heterodimeric scaffolds of communesin indole alkaloids.

To determine the order of bond forming steps, the Tang laboratory engineered yeast to express the cytochrome P450 oxidoreductase. Concurrently, the Garg laboratory synthesized substrate analogs for feeding studies. Several key results are depicted in Figure 1.20. For example, when N10' methylated tryptamine derivative **1.70** was employed in the enzymatic coupling with aurantioclavine (**1.67**), a new oxidatively coupled product was obtained. This compound, **1.69**, bears a new scaffold that was termed "isocommunesin". An analogous outcome was seen when tryptophol (**1.71**) was utilized, which gave rise to "isocommunesin" **1.72**. Interestingly, isocommunesins were obtained when ω-*N*-dimethyl-tryptamine (**1.73**) and 3-(2-azidoethyl)-indole (**1.74**) were used, whereas no product was seen if N1 and N1' methylated derivatives of tryptamine or aurantioclavine were employed (**1.75** or **1.76**, respectively). The latter results indicate that the indole hydrogens are essential for coupling and supports previous hypotheses.[70,71] Overall, the fact that a new communesin-type framework could be accessed through the use of natural enzymes showcases the power of this strategy for accessing new chemical space.

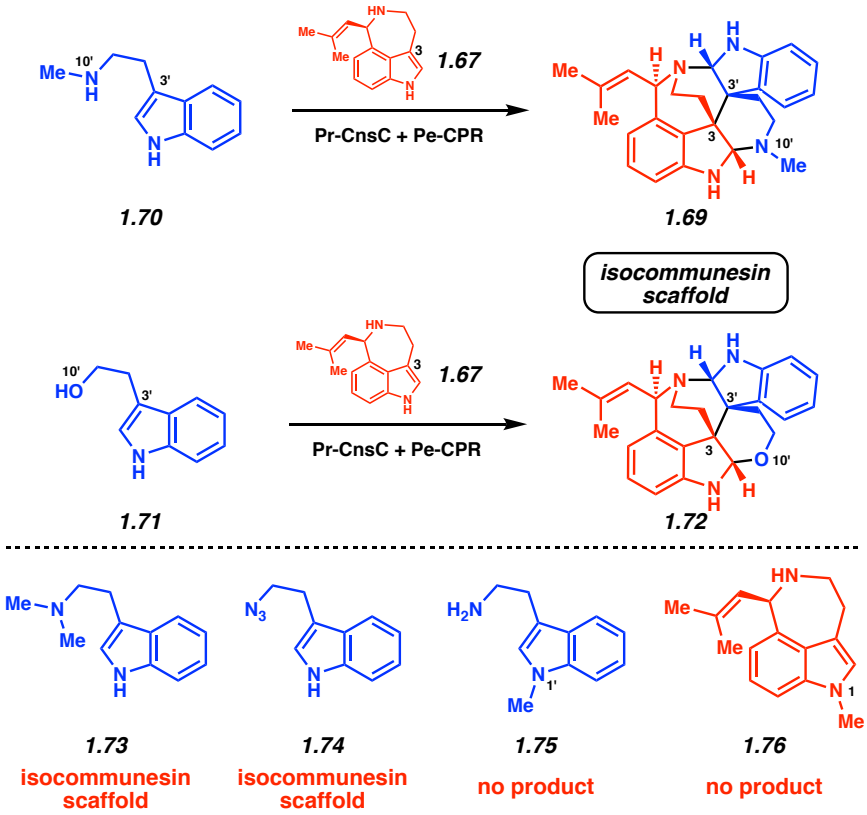


Figure 1.20. Feeding studies of P450 oxidoreductase with analogs.

With access to both communesin and "isocommunesin" scaffolds, the researchers questioned what factors govern the formation of one scaffold over the other as a function of substituents. As such, the Houk laboratory performed computations to determine the energetics of the two competing pathways in the absence of enzymes (Figure 1.21). Although no transition states were identified, it was assumed that the activation energy of each step was proportional to the energy of formation for each intermediate in the proposed reaction pathway. Given the commonality of the C3–C3' linkage in both scaffolds, the indole coupling step is proposed to occur first in the active site of CnsC. Beginning from **1.66** and **1.67**, two sequential one-electron transfer processes lead to aza-allyl radicals **1.77** and **1.78** (with net two-electron reduction of Fe), which combine to generate the vicinal quaternary stereocenters in **1.79**. From heterodimer **1.79**,

two possible intramolecular aminal formations can occur that lead to either the communesin or isocommunesin scaffold. It was found that aminal formation between N10' and C2 is more energetically favored, leading to the unnatural isocommunesin scaffold **1.80**. The competing process involving aminal formation between N10' and C2' (leading to the natural communesin scaffold **1.81**) is actually less energetically favorable. Thus, it is thought that elaboration to the communesin scaffold **1.82** requires the CnsC enzyme to override the inherent thermodynamic preference of the system. As observed in the feeding studies, the enzyme's substrate specificity about N10' is limited to R=H.

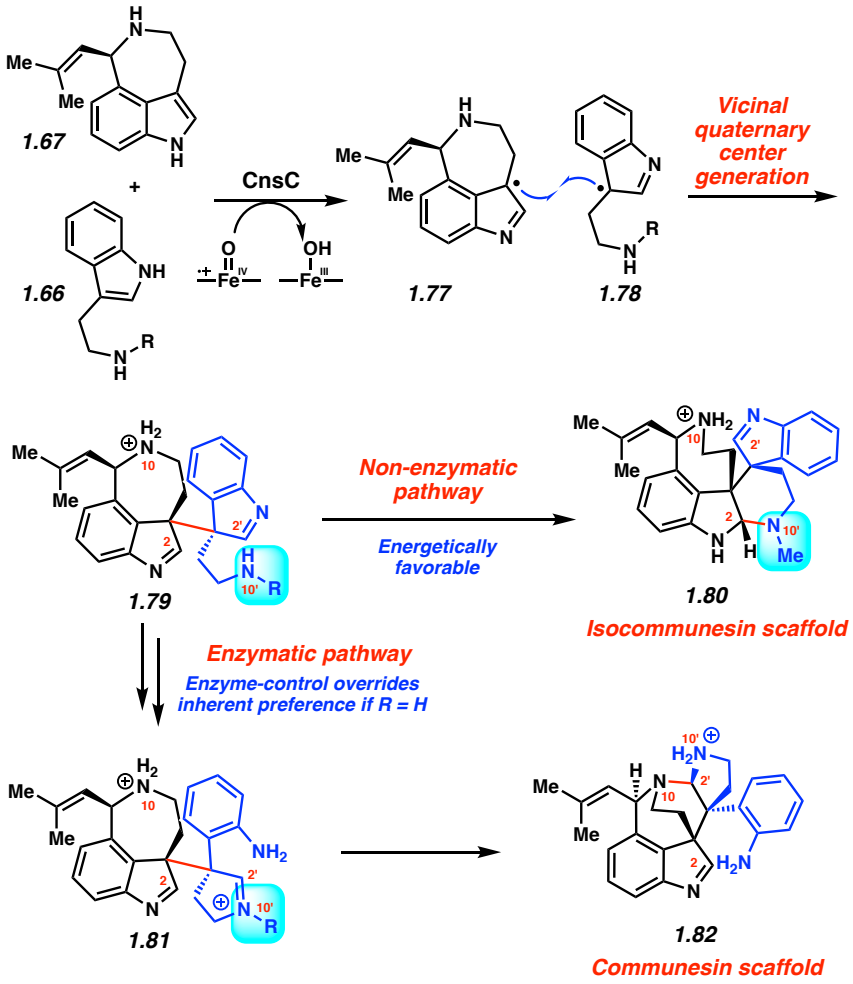


Figure 1.21. Mechanistic studies on communesin scaffold formation by the Houk laboratory.

The collaboration between the Tang, Garg, and Houk laboratories does not necessarily fall under the general category of total synthesis. However, the study is an important one in the area of natural products, as it strategically leverages the collective powers of synthetic chemistry, biosynthetic chemistry, and computational chemistry to furnish access to natural products, new and highly complex natural product analogs, and mechanistic insights. Moreover, the enzymatic coupling of two indole units to generate vicinal quaternary stereocenters sets a high bar for synthetic chemists in pursuit of such alkaloids.

1.9 Total Synthesis of Cyclopiamine B and Biogenetic Studies

The final collaboration we discuss involves research performed by four teams pertaining to the citrinalin and cyclopiamine natural products. Here, Sarpong, Tantillo, Miller, and Berlinck[14] demonstrated the interplay between total synthesis, computational tools, peptide catalysis, and natural product biosynthesis. Ultimately, these efforts led to a natural product structural revision, seminal total syntheses, discoveries in peptide-based catalysis, and insights into natural product biosynthesis.

The specific targets accessed in this endeavour using total synthesis are the indole alkaloids citrinalin B (**1.14**) and cyclopiamine B (**1.85**) (Figure 1.22).[72] Both the originally assigned structure **1.83** and the revised structure for citrinalin B (**1.14**) are depicted. Citrinalin B (**1.14**) was first isolated in 2010 from *Penicillium citrinum*[73] and cyclopiamine B (**1.85**) was isolated from a toxinogenic strain of *Penicillium cyclopium* in 1979.[74] The natural products have six rings, and each bears four stereocenters, including one quaternary stereocenter as part of the spirooxindole framework. In addition, citrinalin B (**1.14**) and cyclopiamine B (**1.85**) each possess three distinct nitrogen substituents. One of the substituents is an alkyl nitro group, which is rarely seen in natural products.[75] From a biosynthetic perspective, **1.14** and **1.85** are curiosities because they lack the typical bicyclo[2.2.2]diazaoctane moiety present in many congeners,[76] such as citrinalin C (**1.84**).

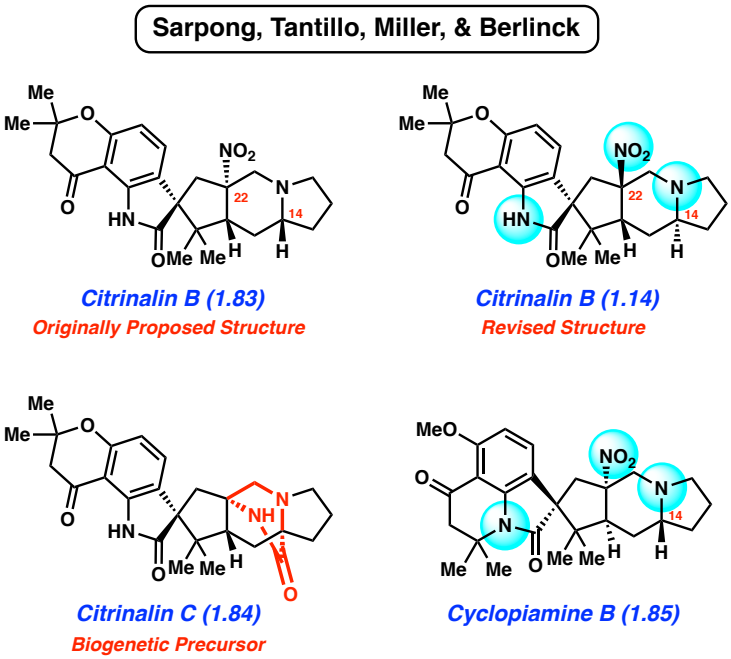


Figure 1.22. Reported structures of natural products **1.83**–**1.85** and revised structure of citrinalin B (**1.14**).

With the aim of completing the total syntheses and exploring various biosynthetic considerations, the Sarpong laboratory devised a synthetic strategy wherein *ent*-citrinalin B (*ent*-**1.14**) would first be synthesized and then converted to cyclopiamine B (**1.85**) using a chromanone rearrangement. However, based on biosynthetic hypotheses and known transformations across the cyclopiamine family,[74] the group suspected that the stereocenters at C22 and C14 in the originally proposed structure of citrinalin B (**1.83**) were incorrect. Instead, they proposed **1.14** as the revised natural product structure. To validate this hypothesis, the Tantillo laboratory performed computations to predict the ^{1}H and ^{13}C NMR spectra for both **1.83** and **1.14**, which were then compared to experimentally reported NMR data. Tantillo's findings supported the revised structural assignment of **1.14** and enabled the Sarpong laboratory to aggressively launch their synthetic campaign targeting *ent*-**1.14**.[77] Moreover, these results

underscore the value of computations in the determination and revision of natural product structures.[78]

The early stages of Sarpong's synthetic sequence are shown in Figure 1.23. D-Proline (**1.86**) was first elaborated to vinyl iodide **1.87** over a series of transformations. Next, vinyl iodide **1.87** underwent Suzuki–Miyaura cross-coupling with known boronic ester **1.88**[79] to give adduct **1.89** in 95% yield. **1.89** was converted to the fused indole **1.90** using two sequential reductions, setting the stage for spirooxindole formation. Face-selective oxygenation of a C2–C3-fused indole to the hydroxyindolenine, followed by spirooxindole formation is well established.[80] It was envisioned that the carbamate would direct oxidation to the alpha face of the indole. However, attempts to employ typical heteroatom-directed oxygenation using Davis' oxaziridines[81] did not provide the desired stereoselectivity. Instead, hydroxyindolenine **1.91** was typically observed as the major product, with only trace amounts of the desired hydroxyindolenine **1.92**, as well as undesired spirooxindole **1.93**.

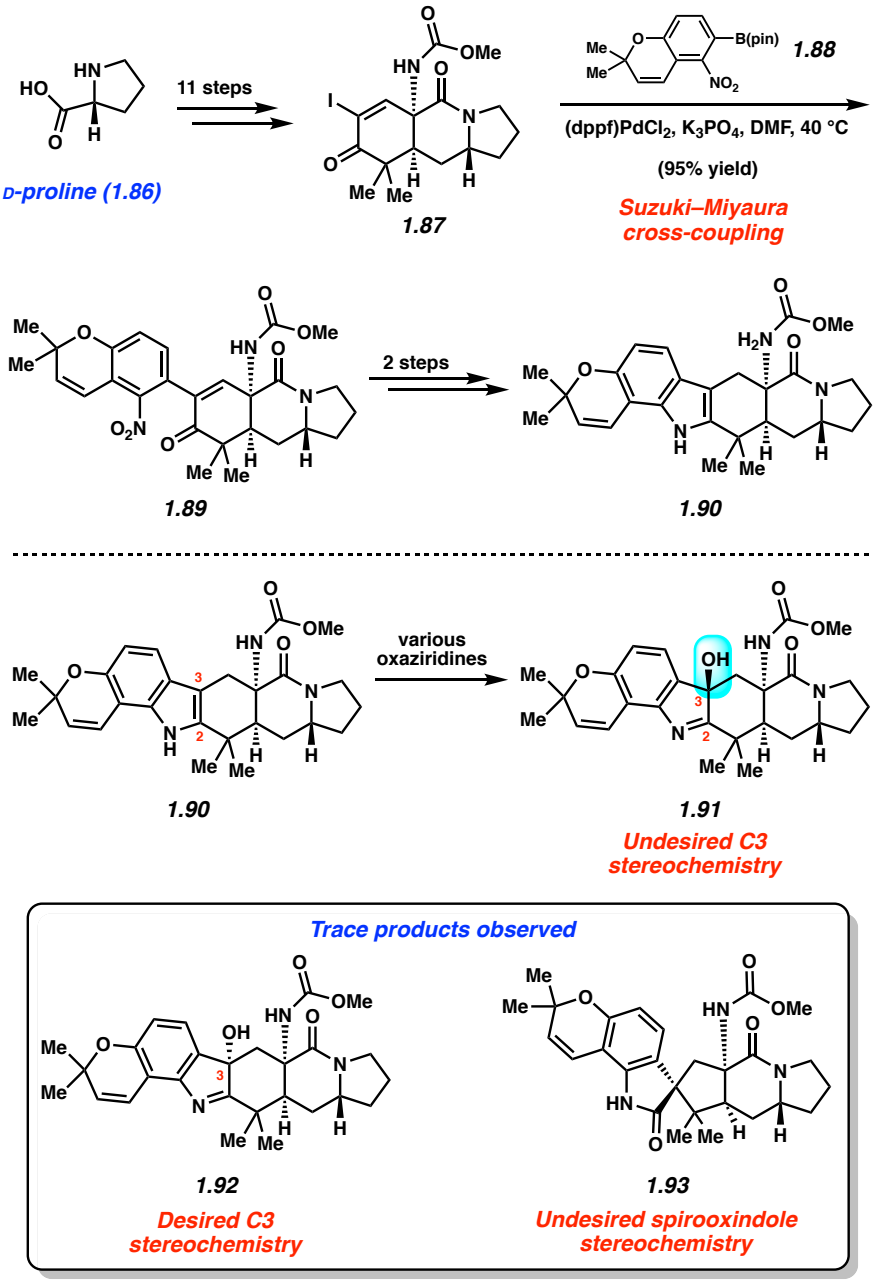


Figure 1.23. Overview of Sarpong's synthesis of spirooxindole precursor **1.90** and unsuccessful oxidation attempts.

Following a fruitful conversation at a Gordon Research Conference between Professors Richmond Sarpong and Scott Miller, the Sarpong laboratory bridged a collaboration with Miller's laboratory at Yale University.[82] The groups hoped to employ Miller's peptide catalysts

to achieve the stereoselective oxidation of substrate **1.90** (Figure 1.24).[83] Ironically, the experimental effort was carried out by graduate student David Romney, who was mentioned earlier as a key player in the nigelladine A collaboration. After screening a library of peptide catalysts, it was found that desired hydroxyindolenine **1.92** could be obtained in 83% yield upon oxidation of fused indole **1.90** in the presence of peptide catalyst **1.94** and H_2O_2. With desired stereoisomer **1.92** in hand, attempted formation of the spirooxindole was pursued. However, attempts to perform the rearrangement led only to intermediate pseudoindoxyl **1.95**, which did not undergo further rearrangement to oxindole **1.96**.[84] The failure of **1.95** to rearrange was posited to be the result of a stabilizing hydrogen bond between the carbonyl of the pseudoindoxyl and carbamate N–H (calculated to be 2.24 Å apart). Although the peptide-based catalysis would ultimately not be used to achieve the total syntheses at hand, the collaboration with the Miller laboratory demonstrated the high selectivity of peptide catalysts in an extraordinarily complex environment. Moreover, the failed conversion of **1.95** to **1.96** informed the Sarpong laboratory's efforts and prompted them to design a more viable substrate for attempted spirooxindole formation.

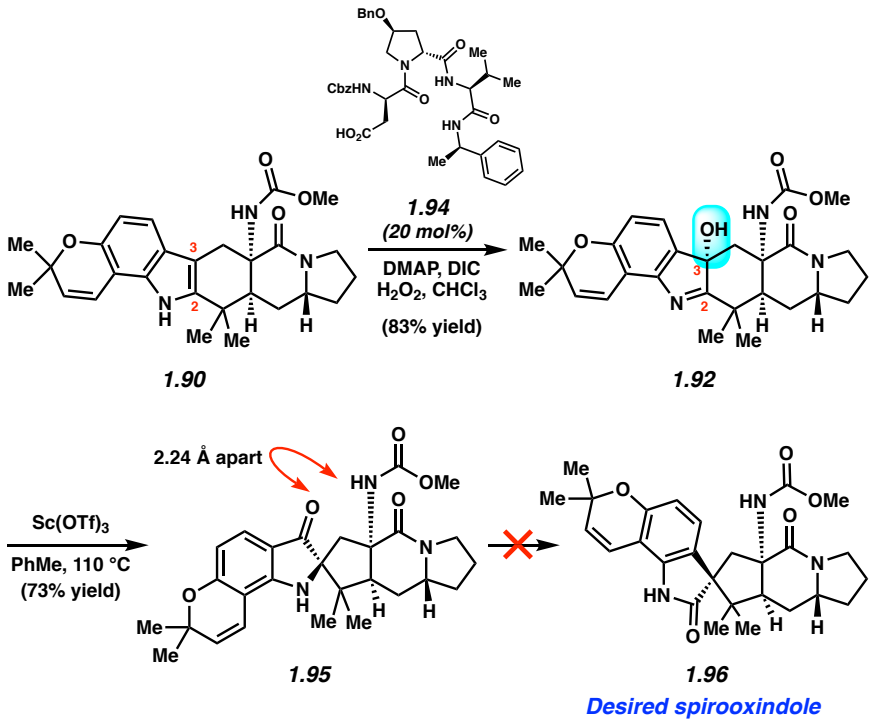


Figure 1.24. Successful oxidation to give **1.92** using Miller's peptide catalyst and challenges encountered in attempted rearrangement toward **1.96**.

The Sarpong laboratory identified indole **1.97** as a revised precursor to construct the desired spirooxindole and set out to complete the syntheses (Figure 1.25). It was believed that the free amine of **1.97** could still serve as a hydrogen-bond donor to effect stereoselective oxidation of the C2–C3 face of the indole. However, it could also be oxidized to the nitro group present in the natural product in situ. Importantly, the presence of the nitro group would subvert the hypothesized hydrogen bond stabilization effect mentioned earlier, which was thought to prevent pseudoindoxyl rearrangement to the spirooxindole. Indole **1.97** was prepared in two steps from **1.90** via Wacker oxidation[85] and carbamate cleavage. Remarkably, **1.97** was transformed to spirooxindole **1.98** with simultaneous introduction of the nitro group in a single step. Using excess dimethyldioxirane (DMDO) generated in situ,[86] the rearrangement proceeded

in 56% yield to give **1.98** as a mixture of diastereomers in a 4:1 ratio favoring the desired compound. To complete the synthesis of *ent*-citrinalin B (*ent*-**1.14**), the group performed a selective two-step reduction of the tertiary amide.[87] Spectral data for *ent*-**1.14** matched those of the isolated material,[73] but with the opposite sign of optical rotation. Moreover, *ent*-**1.14** was unambiguously characterized by X-ray crystallographic analysis. *ent*-Citrinalin B (*ent*-**1.14**) was then converted to cyclopiamine B (**1.85**) in 78% yield over two additional steps involving chromanone rearrangement. The completed syntheses of *ent*-citrinalin B (*ent*-**1.14**) and cyclopiamine B (**1.85**) provided unambiguous structural confirmation of these natural products, while also lending support to the notion that the cyclopiamines may arise from the citrinalin family of alkaloids.

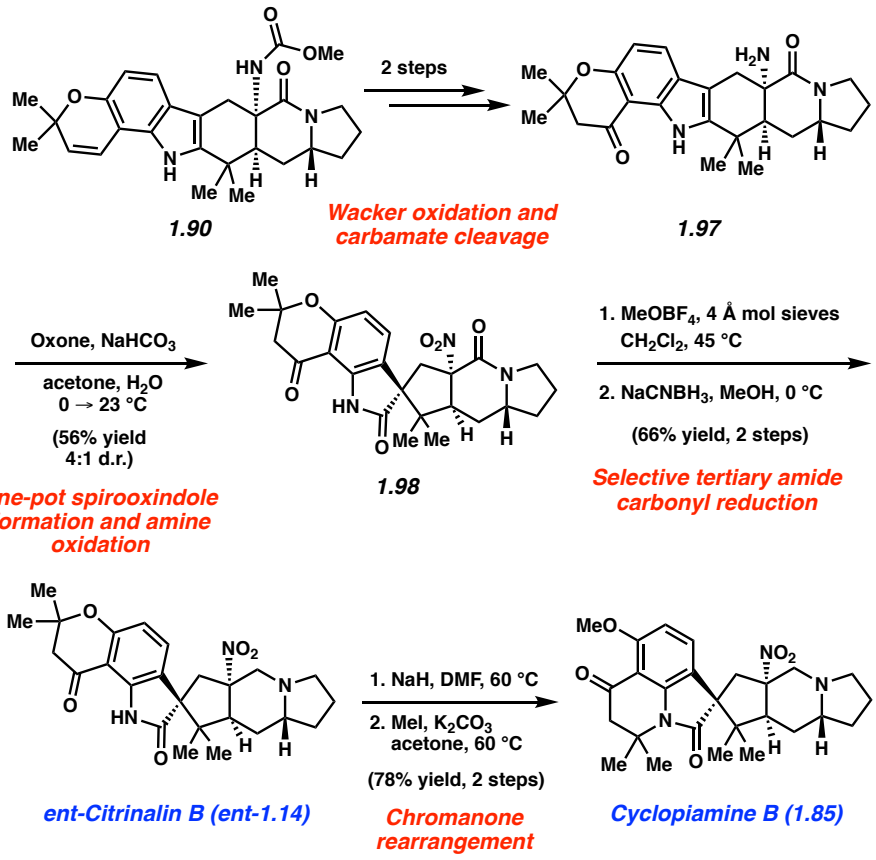


Figure 1.25. Successful spirooxindole formation and total syntheses of *ent*-citrinalin B (*ent*-**1.14**) and cyclopiamine B (**1.85**).

The final part of the collaboration was spearheaded by the Berlinck laboratory and focused on establishing the biosynthetic origins of the natural products in question (Figure 1.26). In a key finding, employing ^{13}C labeled glucose (**1.99**), anthranilic acid (**1.100**), and ornithine (**1.101**), in feeding studies gave rise to citrinalin A (**1.102**), citrinalin B (**1.14**), and two new metabolites that were determined to be citrinalin C (**1.84**) and **1.103**. Upon refractionation and re-analysis of secondary metabolites from *P. citrinum* F53, both **1.84** and **1.103** were found. Interestingly, although ^{13}C labeled ornithine (**1.101**) was incorporated, the use of ^{13}C labeled proline in feeding studies was unsuccessful. This suggests that ornithine is not converted to

proline in the biosynthesis of the citrinalins, despite proline being a known biosynthetic derivative of ornithine. Lastly, and perhaps most importantly, the isolation of citrinalin C (**1.84**) among congeners like 17-hydroxycitrinalin B (**1.103**)[88] provides support for the notion that **1.102** and other family members may arise from biosynthetic precursors that contain bicyclo[2.2.2]diazaoctane units.[89]

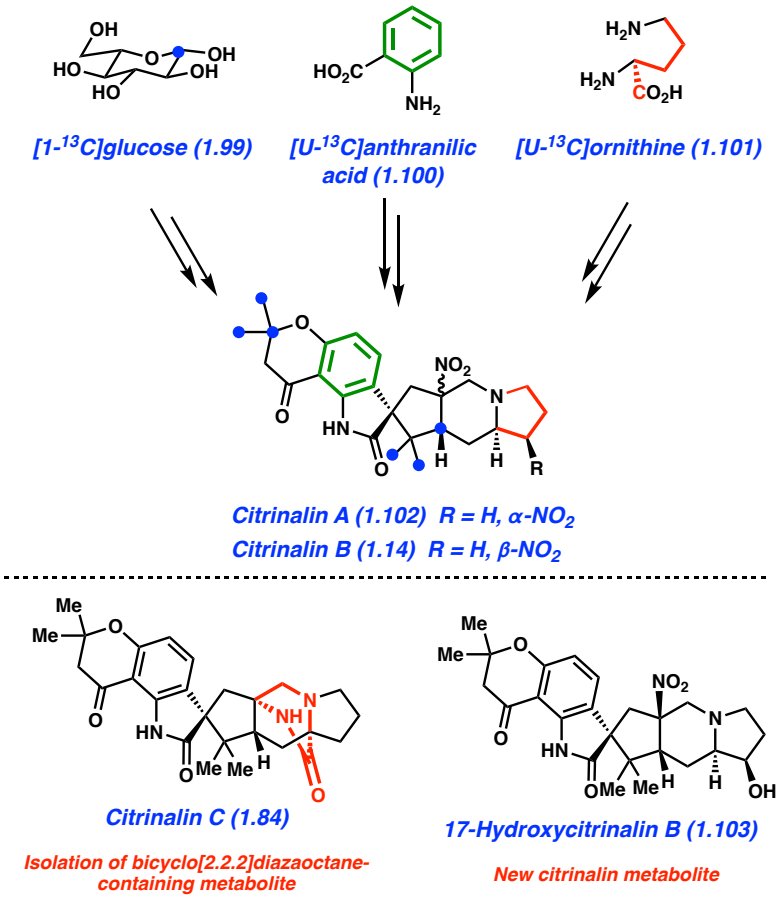


Figure 1.26. Results of feeding studies of *P. citrinum* F53 with ^{13}C labeled precursors.

The combined efforts of the Sarpong, Tantillo, Miller, and Berlinck laboratories led to many advances. These include a computationally-supported structural revision of a natural product (Tantillo), a peptide-mediated oxidation reaction of a complex substrate (Miller), the

completed total syntheses of two indole alkaloids using a late-stage stereoselective spirooxindole-forming reaction (Sarpong), and insight into the biosynthetic origins of the targeted natural products (Berlinck). Overall, these collective studies beautifully intertwine the expertise of four laboratories, leading to new knowledge and achievements, in addition to the interdisciplinary training of many talented coworkers.

1.10 Conclusion

We have described a collection of recent total synthesis-related efforts that were performed in highly collaborative manners. These efforts showcase how collaborations in areas such as synthetic methodology, biocatalysis, biosynthesis, computations, and pharmaceutical research can lead to new insights and ultimately facilitate our ability to access intricate chemical structures. Moreover, such collaborations allow for students and postdoctoral scholars to be exposed to new areas of science, while benefiting from interactions with scientists from other groups and institutions. We hope this perspective will help to prompt synthetic chemists to further build a growing spirit of collaboration in the future.

1.11 Notes and References

(1) For recent reviews, views, and perspectives on total synthesis, see: a) Seebach, D. *Angew. Chem., Int. Ed.* **1990**, *29*, 1320–1367. b) Nicolaou, K. C.; Vourloumis, D.; Winssinger, N.; Baran, P. S. *Angew. Chem., Int. Ed.* **2000**, *39*, 44–122. c) Nicolaou, K. C.; Snyder, S. A. *Angew. Chem., Int. Ed.* **2005**, *44*, 1012–1044. d) Roush, W. R. *J. Am. Chem. Soc.* **2008**, *130*, 6654–6656. e) Hale, K. J. *Org. Lett.* **2013**, *15*, 3181–3198. f) Molinski, T. F. O*rg. Lett.* **2014**, *16*, 3849–3855. g) Notman, N. https://www.chemistryworld.com/features/unpicking-natural-product-

synthesis/7663.article. (accessed April 22, 2019). h) Ball, P. *Nature* **2015**, *528*, 327–329. i) Denmark, S. E. *Isr. J. Chem.* **2018**, *58*, 61–72. j) Baran, P. S. *J. Am. Chem. Soc.* **2018**, *140*, 4751–4755.

(2) a) Woodward, R. B. *Pure Appl. Chem.* **1968**, *17*, 519–547. b) Eschenmoser, A. *Quart. Rev.* **1970**, *24*, 366–415. c) Woodward, R. B. *Pure Appl. Chem.* **1971**, *25*, 283–304. d) Eschenmoser, A. Studies on Organic Synthesis. *XXIIIrd International Congress of Pure and Applied Chemistry: special lectures presented at Boston, USA, 26-30 July 1971, Vol 2*. **1971**, *2*, 69–106. e) Woodward, R. B. *Pure. Appl. Chem.* **1973**, *33*, 145–178. f) Eschenmoser, A. *Naturwissenschaften* **1974**, *61*, 513–525. g) Eschenmoser, A.; Wintner, C. E. *Science* **1977**, *196*, 1410–1420.

(3) For book chapters regarding the total synthesis of vitamin B_{12} (**1.1**), see: a) Nicolaou, K. C.; Sorensen, E. J. Vitamin B_{12}. In *Classics in Total Synthesis: Targets, Strategies, Methods*, 1st edn. VCH Publishers: New York, NY. b) Benfey, O. T.; Morris, P. J. T. eds Vitamin B_{12}. In *Robert Burns Woodward: Architect and Artist in the World of Molecules*, 1st edn. Chemical Heritage Foundation: Philadelphia, PA.

(4) Rickes, E. L.; Brink, N. G.; Koniuszy, F. R.; Wood, T. R.; Folkers, K. *Science* **1948**, *107*, 396–397.

(5) Hodgkin, D. C.; Kamper, J.; Mackay, M.; Pickworth, J.; Trueblood, K. N.; White, J. G. *Nature* **1956**, *178*, 64–66.

(6) Yamada, Y.; Miljkovic, D.; Wehrli, P.; Golding, B.; Löliger, P.; Keese, R.; Müller, K.; Eschenmoser, A. *Angew. Chem., Int. Ed.* **1969**, *8*, 343–348.

(7) The total synthesis of vitamin B_{12} (**1.1**) actually represents a formal synthesis through cobyric acid. The conversion of cobyric acid to vitamin B_{12} (**1.1**) had been reported previously, see: Friedrich, W.; Gross, G.; Bernhauer, K.; Zeller, P. *Helv. Chim. Acta* **1960**, *43*, 704.

(8) Quinn, R. K.; Könst, Z. A.; Michalak, S. E.; Schmidt, Y.; Szklarski, A. R.; Flores, A. R.; Nam, S.; Horne, D. A.; Vanderwal, C. D.; Alexanian, E. J. *J. Am. Chem. Soc.* **2016**, *138*, 696–702.

(9) Loskot, S. A.; Romney, D. A.; Arnold, F. H.; Stoltz, B. M. *J. Am. Chem. Soc.* **2017**, *139*, 10196–10199.

(10) Turconi, J.; Griolet, F.; Guevel, R.; Oddon, G.; Villa, R.; Geatti, A.; Hvala, M.; Rossen, K.; Göller, R.; Burgard, A. *Org. Process Res. Dev.* **2014**, *18*, 417–422.

(11) a) Jorgensen, L.; McKerrall, S. J.; Kuttruff, C. A.; Ungeheuer, F.; Felding, J.; Baran, P. S. *Science* **2013**, *341*, 878–882. b) McKerral, S. J.; Jorgensen, L.; Kuttruff, C. A.; Ungeheuer, F.; Baran, P. S. *J. Am. Chem. Soc.* **2014**, *136*, 5799–5810.

(12) McCallum, M. E.; Rasik, C. M.; Wood, J. L.; Brown, M. K. *J. Am. Chem. Soc.* **2016**, *138*, 2437–2442.

(13) Lin, H.-C.; McMahon, T. C.; Patel, A.; Corsello, M.; Simon, A.; Xu, W.; Zhao, M.; Houk, K. N.; Garg, N. K.; Tang, Y. *J. Am. Chem. Soc.* **2016**, *138*, 4002–4005.

(14) Mercado-Marin, E. V.; Garcia-Reynaga, P.; Romminger, S.; Pimenta, E. F.; Romney, D. K.; Lodewyk, M. W.; Williams, D. E.; Andersen, R. J.; Miller, S. J.; Tantillo, D. J.; Berlinck, R. G. S.; Sarpong, R. *Nature* **2014**, *509*, 318–324.

(15) a) Malochet-Grivois, C.; Cotelle, P.; Biard, J. F.; Henichart, J. P.; Debitus, C.; Roussakis, C.; Verbist, J.-F. *Tetrahedron Lett.* **1991**, *32*, 6701–6702. b) Malochet-Grivois, C.; Roussakis, C.; Robillard, N.; Biard, J. F.; Riou, D.; Debitus, C.; Verbist, J.-F. *Anti-Cancer Drug Des.* **1992**,

7, 493–502. c) Roussakis, C.; Charrier, J.; Riou, D.; Biard, J. F.; Malochet, C.; Meflah, K.; Verbist, J. F. *Anti-Cancer Drug Des.* **1994**, *9*, 119–128. d) Biard, J.-F.; Malochet-Grivois, C.; Roussakis, C.; Cotelle, P.; Hénichart, J.-P.; Débitus, C.; Verbist, J.-F. *Nat. Prod. Lett.* **1994**, *4*, 43–50.

(16) Uddin, J.; Ueda, K.; Siwu, E. R. O.; Kita, M.; Uemura, D. *Bioorg. Med. Chem.* **2006**, *14*, 6954–6961.

(17) For relevant synthetic studies, see: a) Jung, M. E.; Gomez, A. V. *Tetrahedron Lett.* **1993**, *34*, 2891–2894. b) González, M. A.; Romero, D.; Zapata, B.; Bentancur-Galvis, L. *Lett. Org. Chem.* **2009**, *6*, 289–292.

(18) a) Bedke, D. K.; Shibuya, G. M.; Pereira, A.; Gerwick, W. H.; Haines, T. H.; Vanderwal, C. D. *J. Am. Chem. Soc.* **2009**, *131*, 7570–7572. b) Bedke, D. K.; Shibuya, G. M.; Pereira, A. R.; Gerwick, W. H.; Vanderwal, C. D. *J. Am. Chem. Soc.* **2010**, *132*, 2542–2543. c) Chung, W.-J.; Carlson, J. S.; Bedke, D. K.; Vanderwal, C. D. *Angew. Chem., Int. Ed.* **2013**, *52*, 10052–10055. d) Chung, W.-J.; Vanderwal, C. D. *Acc. Chem. Res.* **2014**, *47*, 718–728. e) Chung, W.-J.; Carlson, J. S.; Vanderwal, C. D. *J. Org. Chem.* **2014**, *79*, 2226–2241. f) Vogel, C. V.; Pietraszkiewicz, H.; Sabry, O. M.; Gerwick, W. H.; Valeriote, F. A.; Vanderwal, C. D. *Angew. Chem., Int. Ed.* **2014**, *53*, 12205–12209. g) Daub, M. E.; Prudhomme, J.; Le Roch, K.; Vanderwal, C. D. *J. Am. Chem. Soc.* **2015**, *137*, 4912–4915.

(19) Schmidt, V. A.; Quinn, R. K.; Bruscoe, A. T.; Alexanian, E. J. *J. Am. Chem. Soc.* **2014**, *136*, 14389–14392.

(20) a) Minisci, F.; Galli, R.; Galli, A.; Bernardi, R. *Tetrahedron Lett.* **1967**, *8*, 2207–2209. b) Deno, N. C.; Fishbein, R.; Wyckoff, J. C. *J. Am. Chem. Soc.* **1971**, *93*, 2065–2066.

(21) For select examples of 2-functionalization of sclareolide, see the following. Oxygenation: a) Chen, M. S.; White, M. C. *Science* **2010**, *327*, 566–571. Fluorination: b) Liu, W.; Huang, X.; Cheng, M.-J.; Nielsen, R. J.; Goddard, W. A., III; Groves, J. T. *Science* **2012**, *337*, 1322–1325. c) Halperin, S. D.; Fan, H.; Chang, S.; Martin, R. E.; Britton, R. *Angew. Chem., Int. Ed.* **2014**, *53*, 4790–4693. d) Bloom, S.; Knippel, J. L.; Lectka, T. *Chem. Sci.* **2014**, *5*, 1175–1178. e) Xia, J.-B.; Ma, Y.; Chen, C. *Org. Chem. Front.* **2014**, *2*, 806–810. Chlorination: f) Liu, W.; Groves, J. T. *J. Am. Chem. Soc.* **2010**, *132*, 12847–12849. Bromination: g) Kee, C. W.; Chan, K. M.; Wong, M. W.; Tan, C.-H. *Asian J. Org. Chem.* **2014**, *3*, 536–544. Azidation: h) Huang, X.; Bergsten, T. M.; Groves, J. T. *Org. Lett.* **2015**, *17*, 5828–5831.

(22) Umbreit, M. A.; Sharpless, K. B. *J. Am. Chem. Soc.* **1977**, *99*, 5526–5528.

(23) a) Nguyen, T. M.; Vu, N. Q.; Youte, J.-J.; Lau, J.; Cheong, A.; Ho, Y. S.; Tan, B. S. W.; Yogonathan, K.; Butler, M. S.; Chai, C. L. L. *Tetrahedron* **2010**, *66*, 9270–9276. b) Hajra, S.; Giri, A. K.; Karmakar, A.; Khatua, S. *Chem. Commun.* **2007**, *23*, 2408–2410.

(24) Konst, Z. A.; Szklarski, A. R.; Michalak, S. E.; Pellegrino, S.; Meyer, M.; Zanette, C.; Cencil, R.; Nam, S.; Voora, V.; Horne, D. A.; Pelletier, J.; Mobley, D. L.; Yusupov, M.; Vanderwal, C. D. *Nat. Chem.* **2017**, *9*, 1140–1149.

(25) Chen, Q.-B.; Xin, X.-L.; Yang, Y.; Lee, S.-S.; Aisa, H. A. *J. Nat. Prod.* **2014**, *77*, 807–812.

(26) Stork, G.; Danheiser, R. L. *J. Org. Chem.* **1973**, *38*, 1775–1776.

(27) McDougal N. T.; Streuff, J.; Mukherjee, H.; Virgil, S. C.; Stoltz, B. M. *Tetrahedron Lett.* **2010**, *51*, 5550–5554.

(28) Bruno, N. C.; Tudge, M. T.; Buchwald, S. L. *Chem. Sci.* **2013**, *4*, 916–920.

(29) Oxidation of imine **1.29** was attempted using a variety of chemical methods, including the use of SeO_2, Pd/C and TPHP, Cr(V), $Rh_2(esp)_2$ and T-HYDRO, and CrO_3-based reaction

conditions. The rhodium-catalyzed oxidation protocol gave the desired product in 10% isolated yield.

(30) a) Roiban, G.-D.; Reetz, M. T. *Chem. Commun*. **2015**, *51*, 2208–2224. b) Lewis, J. C.; Mantovani, S. M.; Fu, Y.; Snow, C. D.; Komor, R. S.; Wong, C.-H.; Arnold, F. H. *ChemBioChem* **2010**, *11*, 2502–2505. c) Rentmeister, A.; Arnold, F. H.; Fasan, R. *Nat. Chem. Biol.* **2009**, *5*, 26–28. d) Lewis, J. C.; Bastian, S.; Bennett, C. S.; Fu, Y.; Mitsuda, Y.; Chen, M. M.; Greenberg, W. A.; Wong, C.-H.; Arnold, F. H. *Proc. Natl. Acad. Sci. U.S.A.* **2009**, *106*, 16550–16555. e) Kille, S.; Zilly, F. E.; Acevedo, J. P.; Reetz, M. T. *Nat. Chem.* **2011**, *3*, 738–743.

(31) Stoltz, B. M. California Institute of Technology, Pasadena CA. Personal communication, 2019.

(32) a) Qinghaosu Antimalaria Coordinating Research Group, Antimalaria Studies on Qinghaosu. *Chin. Med. J.* **1979**, *92*, 811–816. b) White, N. J. *Science* **2008**, *320*, 330–334. c) Tu, Y. *Nat. Med.* **2011**, *17*, 1217–1220.

(33) Guidelines for the Treatment of Malaria, World Health Organization, Geneva, 2nd ed, 2010.

(34) a) Meshnick, S. R. *Int. J. Parasitol.* **2002**, *32*, 1655–1660. b) Cui, L.; Su, X.-Z. *Expert Rev. Anti Infect. Ther.* **2009**, *7*, 999–1013. c) Edikpo, N.; Ghasi, S.; Elias, A.; Oguanobi, N. *Mol. Cell. Pharmacol.* **2013**, *5*, 75–89.

(35) Nobel Prize Press Release https://www.nobelprize.org/nobel_prizes/medicine/laureates/2015/press.pdf, accessed March 2018.

(36) Enserink, M. *Science* **2005**, *307*, 33.

(37) a) Xu, X.-X.; Zhu, J.; Huang, D.-Z.; Zhou, W.-S. *Tetrahedron* **1986**, *42*, 819–828. b) Avery, M. A.; Jennings-White, C.; Chong, W. K. M. *Tetrahedron Lett.* **1987**, *28*, 4629–4632. c)

Ravindranathan, T.; Kumar, M. A.; Menon, R. B.; Hiremath, S. V. *Tetrahedron Lett.* **1990**, *31*, 755–758. d) Avery, M. A.; Chong, W. K. M.; Jennings-White, C. *J. Am. Chem. Soc.* **1992**, *114*, 974–979. e) Liu, H. J.; Yeh, W. L.; Chew, S. Y. *Tetrahedron Lett.* **1993**, *34*, 4435–4438. f) Constantino, M. G.; Beltrame, M.; da Silva, G. V. J.; Zukerman-Schepector, J. *Synth. Commun.* **1996**, *26*, 321–329.

(38) Schmid, G.; Hofheinz, W. *J. Am. Chem. Soc.* **1983**, *105*, 624–625.

(39) a) Yadav, J. S.; Babu, R. S.; Sabitha, G. *Tetrahedron Lett.* **2003**, *44*, 387–389. b) Yadav, J. S.; Thirupathaiah, B.; Srihari, P. *Tetrahedron* **2010**, *66*, 2005–2009.

(40) Zhu, C.; Cook, S. P. *J. Am. Chem. Soc.* **2012**, *134*, 13577–13579.

(41) Paddon, C. J.; Westfall, P. J.; Pitera, D. J.; Benjamin, K.; Fisher, K.; McPhee, D.; Leavell, M. D.; Tai, A.; Main, A.; Eng, D.; Polichuk, D. R.; Teoh, K. H.; Reed, D. W.; Treynor, T.; Lenihan, J.; Fleck, M.; Bajad, S.; Dang, G.; Dengrove, D.; Diola, D.; Dorin, G.; Ellens, K. W.; Fickes, S.; Galazzo, J.; Gaucher, S. P.; Geistlinger, T.; Henry, R.; Hepp, M.; Horning, T.; Iqbal, T.; Jiang, H.; Kizer, L.; Lieu, B.; Melis, D.; Moss, N.; Regentin, R.; Secrest, S.; Tsuruta, H.; Vazquez, R.; Westblade, L. F.; Xu, L.; Yu, M.; Zhang, Y.; Zhao, L.; Lievense, J.; Covello, P. S.; Keasling, J. D.; Reiling, K. K.; Renninger, N. S.; Newman, J. D. *Nature* **2013**, *496*, 528–532.

(42) a) Acton, N.; Roth, R. J. *J. Nat. Prod.* **1989**, *52*, 1183–1185. b) Acton, N.; Roth, R. J. *J. Org. Chem.* **1992**, *57*, 3610–3614.

(43) a) Bertea, C. M.; Freije, J. R.; van der Woude, H.; Verstappen, F. W.; Perk, L.; Marqeuz, V.; De Kraker, J. W.; Posthumus, M. A.; Jansen, B. J.; de Groot, A.; Franssen, M. C.; Bouwmeester, H. J. *Planta Med*. **2005**, *71*, 40–47. b) Brown, G. D. *Molecules* **2010**, *15*, 7603–7698.

(44) a) Lévesque, F.; Seeberger, P. H. *Angew. Chem., Int. Ed.* **2012**, *51*, 1706–1709. b) Kopetzki, D.; Lévesque, F.; Seeberger, P. H. *Chem. Eur. J.* **2013**, *19*, 5450–5456. c) Lévesque, F.; Seeberger, P. H. *Org. Lett.* **2011**, *13*, 5008–5011. d) McQuade, D. T.; Seeberger, P. H. *J. Org. Chem.* **2013**, *78*, 6384–6389.

(45) Holton, R. A. Patent US005254703A, (Oct. 19, 1993).

(46) At the present time, the yield of natural artemisin is such that the synthetic route is not essential to meet the current demand. For a pertinent discussion, see: Peplow, M. *Chem. Eng. News* **2018**, *96*, 29–31.

(47) Hecker, E. *Cancer Res*. **1968**, *28*, 2338–2348.

(48) Bertelsen, M.; Stahlhut, M.; Grue-Sorensen, G.; Liang, X.; Christensen, G. B.; Skak, K.; Engell, K. M.; Högberg, T. *Dermatol. Ther.* **2016**, *6*, 599–626.

(49) Hale, V.; Keasling, J. D.; Renninger, N.; Diagana, T. T. *Am. J. Trop. Med. Hyg.* **2007**, *77 (suppl. 6)*, 198–202.

(50) a) Winkler, J. D.; Rouse, M. B.; Greaney, M. F.; Harrison, S. J.; Jeon, Y. T. *J. Am. Chem. Soc.* **2002**, *124*, 9726–9728. b) Tanino, K.; Onuki, K; Asano, K.; Miyashita, M.; Nakamura, T.; Takahashi, Y.; Kuwajima, I. *J. Am. Chem. Soc.* **2003**, *125*, 1498–1500. c) Nickel, A.; Maruyama, T.; Tang, H.; Murphy, P. D.; Greene, B.; Yusuff, N.; Wood, J. L. *J. Am. Chem. Soc.* **2004**, *126*, 16300–16301. d) Watanabe, K.; Suzuki, Y.; Aoki, K.; Sakakura, A.; Suenaga, K.; Kigoshi, H. *J. Org. Chem.* **2004**, *69*, 7802–7808.

(51) a) Mukai, C.; Nomura, I.; Yamanishi, K.; Hanaoka, M. *Org. Lett.* **2002**, *4*, 1755–1758. b) Brummond, K. M.; Chen, H.; Fisher, K. D.; Kerekes, A. D.; Rickards, B.; Sill, P. C.; Geib, S. J. *Org. Lett.* **2002**, *4*, 1931–1934. c) Mukai, C.; Nomura, I.; Kitagaki, S. *J. Org. Chem.* **2003**, *68*, 1376–1385. d) Brummond, K. M.; Chen, D.; Davis, M. M. *J. Org. Chem.* **2008**, *73*, 5064–5068.

(52) a) Gillespie, S. K.; Zhang, X. D.; Hersey, P. *Mol. Cancer Ther.* **2004**, *3*, 1651−1658. b) Rosen, R. H.; Gupta, A. K.; Tyring, S. K. *J. Am. Acad. Dermatol.* **2012**, *66*, 486−493. c) Ogbourne, S. M.; Suhrbier, A.; Jones, B.; Cozzi, S.-J.; Boyle, G. M.; Morris, M.; McAlpine, D.; Johns, J.; Scott, T. M.; Sutherland, K. P., Gardner, J. M.; Le, T. T. T.; Lenarczyk, A.; Aylward, J. H.; Parsons, P. G. *Cancer Res.* **2004**, *64*, 2833−2839.

(53) a) Parker, C. G.; Galmozzi, A.; Wang, Y.; Correia, B. E.; Sasaki, K.; Joslyn, C. M.; Kim, A. S.; Cavallaro, C. L.; Lawrence, R. M.; Johnson, S. R.; Narvaiza, I.; Saez, E.; Cravatt, B. F. *Cell* **2017**, *168*, 527−541. b) Horning, B. D.; Suciu, R. M.; Ghadiri, D. A.; Ulanovskaya, O. A.; Matthews, M. L.; Lum, K. M.; Backus, K. M.; Brown, S. J.; Rosen, H.; Cravatt, B. F. *J. Am. Chem. Soc.* **2016**, *138*, 13335−13343. c) Hulce, J. J.; Cognetta, A. B.; Niphakis, M. J.; Tully, S. E.; Cravatt, B. F. *Nat. Methods* **2013**, *10*, 259−264. d) Li, Z.; Hao, P.; Li, L.; Tan, C. Y. J.; Cheng, X. M.; Chen, G. Y. J.; Sze, S. K.; Shen, H. M.; Yao, S. Q. *Angew. Chem., Int. Ed.* **2013**, *52*, 8551−8556. e) Li, Z.; Wang, D.; Li, L.; Pan, S.; Na, Z.; Tan, C. Y. J.; Yao, S. Q. *J. Am. Chem. Soc.* **2014**, *136*, 9990−9998. f) Niphakis, M. J.; Lum, K. M.; Cognetta, A. B.; Correia, B. E.; Ichu, T. A.; Olucha, J.; Brown, S. J.; Kundu, S.; Piscitelli, F.; Rosen, H.; Cravatt, B. F. *Cell* **2015**, *161*, 1668−1680. g) Shi, H.; Zhang, C.-J.; Chen, G. Y. J.; Yao, S. Q. *J. Am. Chem. Soc.* **2012**, *134*, 3001−3014.

(54) Rostovtsev, V. V.; Green, L. G.; Fokin, V. V.; Sharpless, K. B. *Angew. Chem., Int. Ed.* **2002**, *41*, 2596−2599.

(55) Parker, C. G.; Kuttruff, C. A.; Galmozzi, A.; Jorgensen, L.; Yeh, C.-H.; Hermanson, D. J.; Wang, Y.; Artola, M.; McKerrall, S. J.; Josyln, C. M.; Norremark, B.; Dunstl, G.; Felding, J.; Saez, E.; Baran, P. S.; Cravatt, B. F. *ACS Cent. Sci.* **2017**, *3*, 1276–1285.

(56) Kawamura, S.; Chu, H.; Felding, J.; Baran, P. S. *Nature* **2016**, *532*, 90–93.

(57) a) Foo, K.; Usui, I.; Götz, D. C. G.; Werner, E. W.; Holte, D.; Baran, P. S.; *Angew. Chem., Int. Ed.* **2012**, *51*, 11491–11495. b) Dixon, D. D.; Lockner, J. W.; Zhou, Q.; Baran, P. S. *J. Am. Chem. Soc.* **2012**, *134*, 8432–8435. c) Rosen, B. R.; Simke, L. R.; Thuy-Boun, P. S.; Dixon, D. D.; Yu, J.-Q.; Baran, P. S. *Angew. Chem., Int. Ed.* **2013**, *52*, 7317–7310. d) Renata, H.; Zhou, Q.; Baran, P. S. *Science* **2013**, *339*, 59–63. e) Michaudel, Q.; Ishihara, Y.; Baran, P. S. *Acc. Chem. Res.* **2015**, *48*, 712–721.

(58) Piao, S.-J.; Song, Y-L.; Jiao, W.-H.; Yang, F.; Liu, X.-F.; Chen, W.-S.; Han, B.-N. Lin, H.-W. *Org. Lett.* **2013**, *15*, 3526–3529.

(59) Piao, S.-J.; Song, Y.-L.; Jiao, W.-H.; Yang, F.; Liu, X.-F.; Chen, W.-S.; Han, B.-N.; Lin, H. W. *Org. Lett.* **2013**, *15*, 3526–3529.

(60) a) Rasik, C. M.; Brown, M. K. Total Synthesis of Gracilioether F and (±)-Hippolachnin A. Poster presentation at the 44th National Organic Chemistry Symposium, University of Maryland, College Park, MD, USA, June 28th, 2015. b) McCallum, M. E.; Wood, J. L. Total Synthesis of Hippolachnin A. Poster presentation at the 44th National Organic Chemistry Symposium, University of Maryland, College Park, MD, USA, June 28th, 2015.

(61) For seminal reports regarding cycloadditions with quadricyclane, see: (a) Smith, C. D. *J. Am. Chem. Soc.* **1966**, *88*, 4273−4274. (b) Tabushi, I.; Yamamura, K.; Yoshida, Z. *J. Am. Chem. Soc*. **1972**, *94*, 787−792. For a review, see: (c) Petrov, V. A.; Vasil'ev, N. V. *Curr. Org. Synth.* **2006**, *3*, 215–259.

(62) Schwab, P. E.; Grubbs, R. H.; Ziller, J. W. *J. Am. Chem. Soc.* **1996**, *118*, 100–110.

(63) a) Gormisky, P. E.; White, M. C. *J. Am. Chem. Soc.* **2013**, *135*, 14052–14055. b) Osberger, T. J.; White, M. C. *J. Am. Chem. Soc.* **2014**, *136*, 11176–11181. c) Ammann, S. E.; Rice, G. T.;

White, M. C. *J. Am. Chem. Soc.* **2014**, *136*, 10834–10837. d) Malik, M.; Witkowski, G.; Jarosz, S. *Org. Lett.* **2014**, *16*, 3816–3819.

(64) Timmerman, J. C.; Wood, J. L. *Org. Lett.* **2018**, *20*, 3788–3792.

(65) Winter, N.; Rupcic, Z.; Stadler, M.; Trauner, D. *J. Antibiot.* **2019**, *72*, 375–383.

(66) For synthetic studies and completed syntheses of communesins, see: a) Zuo, Z.; Ma, D. *Isr. J. Chem.* **2011**, *51*, 434–441. b) Suetsugu, S.; Tsukano, C.; Takemoto, Y. *Eur. J. Org. Chem.* **2016**, *1*, 108–115.

(67) a) May, J. A.; Zeidan, R. K.; Stoltz, B. M. *Tetrahedron Lett.* **2003**, *44*, 1203–1205. b) Peterson, E. A. Formation of Contiguous Stereogenic Quaternary Carbon Centers in Natural Products Synthesis: the Enantioselective Total Synthesis of (–)-Idiospermuline and Approaches Toward the Total synthesis of Communesins A and B. Ph.D. Thesis, University of California, Irvine, 2005. c) May, J. A.; Stoltz, B. M. *Tetrahedron* **2006**, *62*, 5262–5271. d) Han, S.-J.; Vogt, F.; Krishnan, S.; May, J. A.; Gatti, M.; Virgil, S. C.; Stoltz, B. M. *Org. Lett.* **2014**, *16*, 3316–3319. e) Han, S.-J.; Vogt, F.; May, J. A.; Krishnan, S.; Gatti, M.; Virgil, S. C.; Stoltz, B. M. *J. Org. Chem.* **2015**, *80*, 528–547.

(68) a) Boal, B. W.; Schammel, A. W.; Garg, N. K. *Org. Lett.* **2009**, *11*, 3458–3461. b) Schammel, A. W.; Boal, B. W.; Zu, L.; Mesganaw, T.; Garg, N. K. *Tetrahedron* **2010**, *66*, 4687–4695. c) Schammel, A. W.; Chiou, G.; Garg, N. K. *Org. Lett.* **2012**, *14*, 4556–4559. d) Susick, R. B.; Morrill, L. A.; Picazo, E.; Garg, N. K. *Synlett* **2017**, *28*, 1–11.

(69) Lin, H.-C.; Chiou, G.; Chooi, Y.-H.; McMahon, T. C.; Xu, W.; Garg, N. K.; Tang, Y. *Angew. Chem., Int. Ed.* **2015**, *54*, 3004–3007.

(70) Gerken, T.; Walsh, C. T. *ChemBioChem*, **2013**, *14*, 2256–2258.

(71) Walsh, C. T. *ACS Chem. Biol.* **2014**, *9*, 2718–2728.

(72) For a pertinent review, see: Miller, K. A.; Williams, R. M. *Chem. Soc. Rev.* **2009**, *38*, 3160–3174.

(73) Pimenta, E. F.; Vita-Marques, A. M.; Tininis, A.; Seleghim, M. H. R.; Sette L. D.; Veloso, K.; Ferreira, A. G.; Williams, D. E.; Patrick, B. O.; Dalisay, D. S.; Andersen, R. J.; Berlinck, R. G. S. *J. Nat. Prod.* **2010**, *73*, 1821–1832.

(74) Bond, R. F.; Boeyens, J. C. A.; Holzapfel, C. W.; Steyn, P. S. *J. Chem. Soc. Perkin Trans. I* **1979**, *0,* 1751–1761.

(75) Parry, R.; Nishino, S.; Spain, J. *Nat. Prod. Rep.* **2011**, *28*, 152–167.

(76) Finefield, J. M.; Frisvad, J. C.; Sherman, D. H.; Williams, R. M. *J. Nat. Prod.* **2012**, *75*, 812–833.

(77) Though *ent*-citrinalin B (*ent*-**1.14**) is not the natural configuration of the natural product, it bears the correct stereochemistry as cyclopiamine B (**1.85**), thus *ent*-**1.14** was targeted for total synthesis.

(78) Lodwyk, M. W.; Siebert, M. R.; Tantillo, D. J. *Chem. Rev.* **2012**, *112*, 1839–1862.

(79) Herzon, S. B.; Myers, A. G. *J. Am. Chem. Soc.* **2005**, *127*, 5342–5344.

(80) Marti, C.; Carreira, E. *Eur. J. Org. Chem.* **2003**, *12,* 2209–2219.

(81) Davis, F. A.; Stringer, O. D. *J. Org. Chem.* **1982**, *47*, 1774–1775.

(82) Sarpong, R. University of California, Berkeley, Berkeley CA. Personal communication, 2019.

(83) Kolundzic, F.; Noshi, M. N.; Meiliana, T.; Movassaghi, M.; Miller, S. J. *J. Am. Chem. Soc.* **2011**, *133*, 9104–9111.

(84) a) Guller, R.; Borschberg, H.-J. *Tetrahedron Lett.* **1994**, *35*, 865–868. b) Movassaghi, M.; Schmidt, M. A.; Ashenhurst, J. A. *Org. Lett.* **2008**, *10*, 4009–4012.

(85) Miller, D. G.; Wayner, D. D. M. *J. Org. Chem.* **1990**, *55*, 2924–2927.

(86) Zhang, X.; Foote, C. S. *J. Am. Chem. Soc.* **1993**, *115*, 8867–8868.

(87) Borch, R. F. *Tetrahedron Lett.* **1968**, *9*, 61–65.

(88) For subsequent total synthesis, see: Mercado-Marin, E. V.; Sarpong, R. *Chem. Sci.* **2015**, *6*, 5048–5052.

(89) Ding, Y.; de Wet, J. R.; Cavalcoli, J.; Li, S.; Greshock, T. J.; Miller, K. A.; Finefield, J. M.; Sunderhaus, J. D.; McAfoos, T. J.; Tsukamoto S.; Williams, R. M.; Sherman, D. H. *J. Am. Chem. Soc.* **2010**, *132*, 12733–12740.

CHAPTER TWO

Enantioselective Total Syntheses of Methanoquinolizidine-Containing Akuammiline Alkaloids and Related Studies

Elias Picazo,[†] Lucas A. Morrill,[†] Robert B. Susick,

Jesus Moreno, Joel M. Smith, and Neil K. Garg.

J. Am. Chem. Soc. **2018**, *140*, 6483–6492.

2.1 Abstract

The akuammiline alkaloids are a structurally diverse class of bioactive natural products isolated from plants found in various parts of the world. A particularly challenging subset of akuammiline alkaloids are those that contain a methanoquinolizidine core. We describe a synthetic approach to these compounds that has enabled the first total syntheses of (+)-strictamine, (–)-2(*S*)-cathafoline, (+)-akuammiline, and (–)-Ψ-akuammigine. Our strategy relies on the development of the reductive interrupted Fischer indolization reaction to construct a common pentacyclic intermediate bearing five contiguous stereocenters, in addition to late-stage formation of the methanoquinolizidine framework using a deprotection–cyclization cascade. The total syntheses of (–)-Ψ-akuammigine and (+)-akuammiline mark the first preparations of akuammiline alkaloids containing both a methanoquinolizidine core and vicinal quaternary centers. Lastly, we describe the bioinspired reductive rearrangements of (+)-strictamine and (+)-akuammiline to ultimately provide (–)-10-demethoxyvincorine and a new analogue thereof.

2.2 Introduction

The akuammiline alkaloids are an important class of natural products isolated from plants found in India, Africa, and Southeast Asia. These alkaloids, thought to be the active ingredients in traditional medicines used to treat a multitude of ailments in humans and livestock,[1] have been the subject of intense investigations spanning structural elucidation, biosynthesis, biological evaluation, and chemical synthesis.[2] More than 75 akuammilines have now been unambiguously characterized,[3] many of which display exciting biological profiles, and all of which possess provocative chemical structures. Despite their enticing characteristics and biosynthetic relation to the popular *Strychnos* alkaloids,[4] the akuammiline family has been comparatively less studied by synthetic chemists relative to the *Strychnos* alkaloids. It was not until recently that the synthetic community launched efforts toward the akuammiline alkaloids, which have now culminated in total syntheses of several subclasses.[5] This is particularly noteworthy, as even the simplest akuammilines contain at least five interconnected rings, a multitude of stereocenters, and one or more basic nitrogen atoms.

We became interested in a subset of the akuammiline alkaloids that possess a methanoquinolizidine core. This cage-like scaffold and several methanoquinolizidine-containing akuammilines are shown in Figure 2.1 (i.e., **2.1**–**2.4**).[6] (+)-Strictamine (**2.1**)[7] features an indolenine and four stereocenters, whereas (–)-2(*S*)-cathafoline (**2.2**)[8] has an indoline core resulting in five contiguous stereocenters. (+)-Akuammiline (**2.3**) and (–)-Ψ-akuammigine (**2.4**)[9] display an additional layer of complexity with vicinal quaternary centers at C7 and C16. Moreover, (–)-Ψ-akuammigine (**2.4**) also bears a furoindoline motif, leading to six interconnected rings and five contiguous stereocenters, thereby rendering it the most complex member of this akuammiline subclass.

The complexity of **2.1**–**2.4**, coupled with attractive biological activities (vide infra), have prompted numerous synthetic efforts. Following seminal studies by Dolby,[10] Bosch and Bennasar,[11] and Sakai[12] beginning more than four decades ago, the laboratories of Cook,[13] Tokuyama,[14] and Matsuo[15] have more recently described promising synthetic approaches. However, a total synthesis of any methanoquinolizidine-containing akuammiline alkaloid had proven elusive.[16] Moreover, to date, no total syntheses of methanoquinolizidine-containing akuammilines that also bear vicinal quaternary centers (e.g., **2.3** and **2.4**) have been reported.

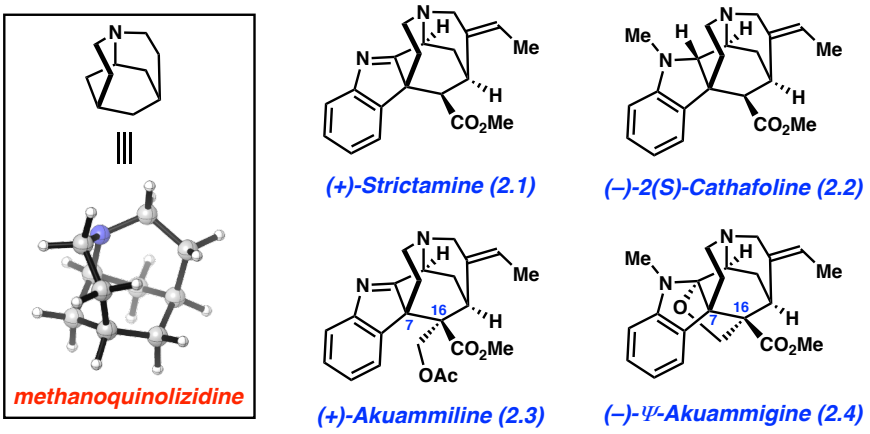


Figure 2.1. Representative methanoquinolizidine-containing akuammiline alkaloids.

Herein, we describe a full account of our enantioselective approach to several methanoquinolizidine-containing akuammilines and subsequent biomimetic manipulations. Key to the success of these studies is the development of the reductive interrupted Fischer indolization reaction[17,18,19] to construct a complex pentacyclic intermediate, as well as the late-stage formation of the methanoquinolizidine framework using a deprotection–cyclization cascade. These studies result in the first total syntheses of (+)-strictamine (**2.1**) and (–)-2(*S*)-cathafoline (**2.2**), which we communicated in 2016.[51] We then exploit a previously undesired epimerization event to access

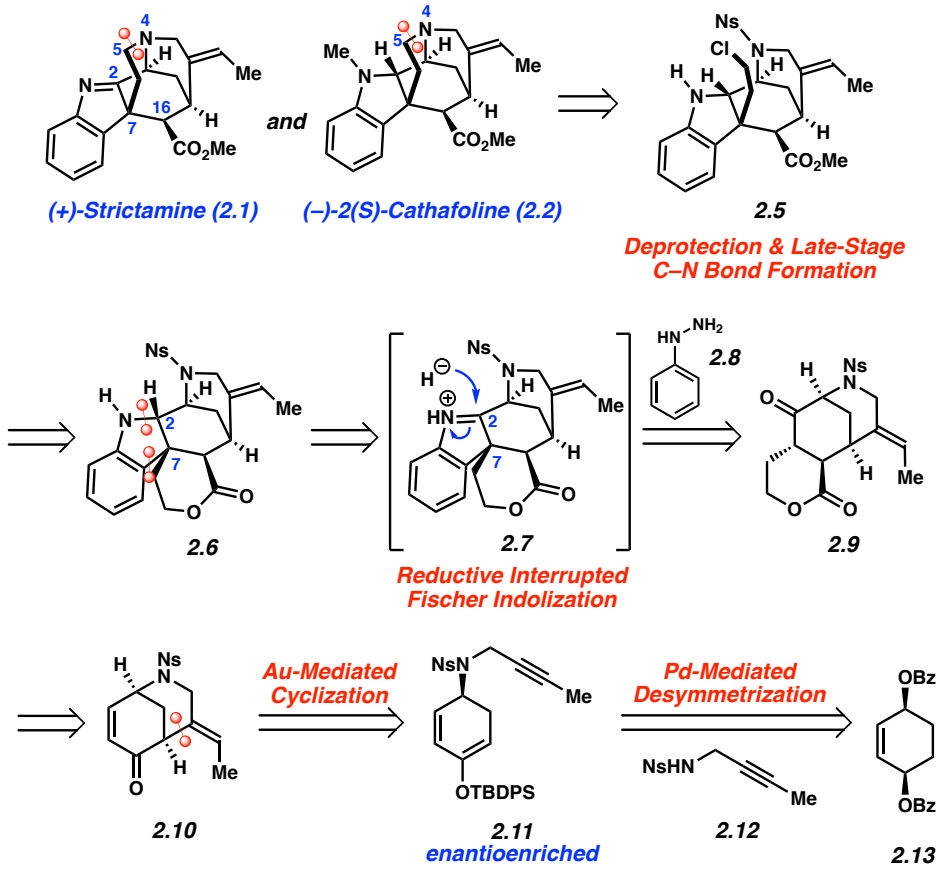
(+)-akuammiline (**2.3**) and (–)-Ψ-akuammigine (**2.4**), each of which bear vicinal quaternary stereocenters embedded in their methanoquinolizidine cores. Lastly, we describe late-stage reductive rearrangements of (+)-strictamine (**2.1**) and (+)-akuammiline (**2.3**), inspired by the proposed biosynthesis of akuammiline alkaloids[20] to give pyrrolidinoindoline scaffolds.

2.3 (+)-Strictamine and (–)-2(*S*)-Cathafoline: Background and Retrosynthetic Analysis

(+)-Strictamine (**2.1**) and (–)-2(*S*)-cathafoline (**2.2**) were selected as our initial synthetic targets. (+)-Strictamine (**2.1**) was isolated in 1966[7] from the plant *Rhazya stricta*, whereas (–)-2(*S*)-cathafoline (**2.2**) was extracted from *Alstonia macrophylla* in 2014.[8] (+)-Strictamine (**2.1**) inhibits the transcription factor NF-κB,[21] and may therefore serve as a lead compound for the discovery of new drugs for the treatment of cancer or inflammatory diseases. (–)-2(*S*)-Cathafoline (**2.2**) shows moderate activity in overturning drug resistance in vincristine-resistant KB cells.[8] Despite the aforementioned synthetic pursuits, neither **2.1** nor **2.2** had succumbed to total synthesis. In the case of (+)-strictamine (**2.1**), this is especially noteworthy given that the compound had been known for more than 50 years.

Our retrosynthetic analysis of (+)-strictamine (**2.1**) and (–)-2(*S*)-cathafoline (**2.2**) is shown in Scheme 2.1. We envisioned forming the methanoquinolizidine scaffold by late-stage construction of the C5–N4 bond. Thus, **2.1** and **2.2** would be accessed from primary alkyl chloride **2.5** through a tandem deprotection–cyclization reaction, followed by manipulation of the indoline ring system. Chloride **2.5** would derive from indoline lactone **2.6** through methanolysis and halide formation. In a key retrosynthetic disconnection, we envisaged indoline lactone **2.6** arising from ketolactone **2.9** and phenylhydrazine (**2.8**) via a reductive interrupted Fischer indolization reaction.[16] If successful, this transformation would introduce two new rings.

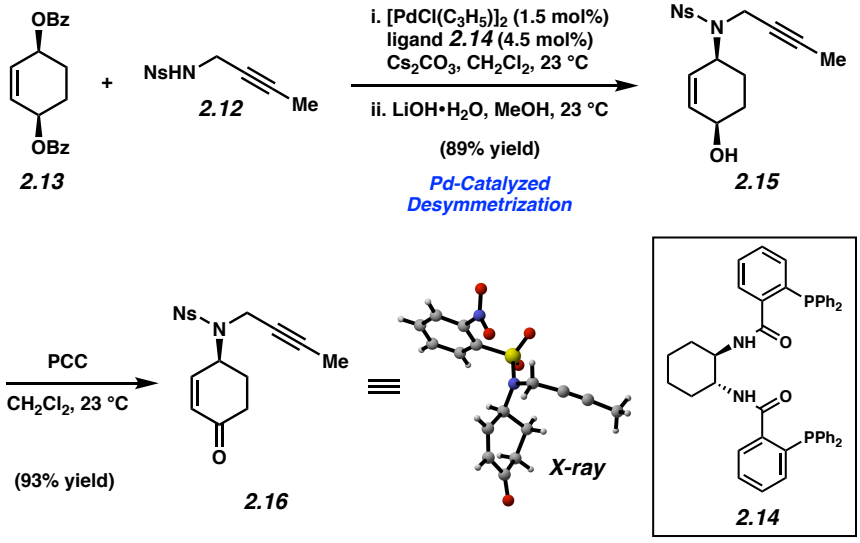
Moreover, two stereogenic centers would be generated, including the C2 stereocenter seen in 2(*S*)-cathafoline (**2.2**) (via transition structure **2.7**) and the challenging C7 quaternary center common to all akuammilines. Ketolactone **2.9** would ultimately be obtained from enone **2.10**, which, in turn, would arise from a gold-catalyzed cyclization of silyl enol ether **2.11**.[22] Finally, **2.11** would be accessed in enantioenriched fashion from sulfonamide **2.12** and dibenzoate **2.13** via a Pd-catalyzed desymmetrization and subsequent manipulations.[23]



Scheme 2.1. Retrosynthetic analysis of (+)-strictamine (**2.1**) and (–)-2(*S*)-cathafoline (**2.2**).

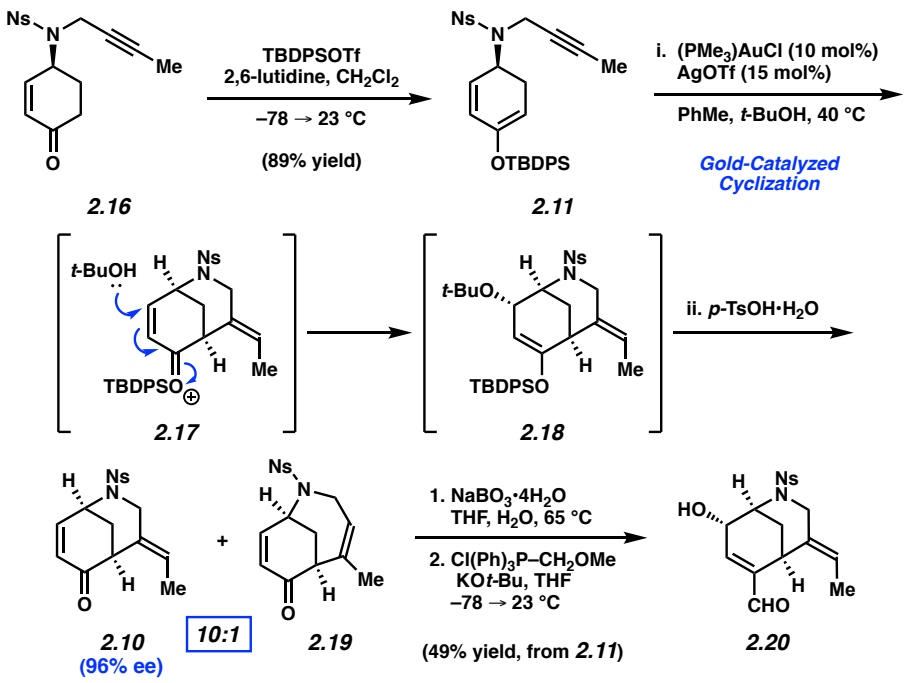
2.4 Enantioselective Synthesis of the Fischer Indolization Substrate

To initiate our forward synthetic studies, we sought to prepare enone **2.16** in enantioenriched form, as this could serve as a precursor for later construction of the necessary [3.3.1]-azabicycle (Scheme 2.2). Although we initially examined several possible routes, including enzymatic desymmetrization[24] and the use of Koga bases,[25] we found a Pd-catalyzed Trost desymmetrization[22] was ultimately most successful. Upon treatment of dibenzoate **2.13** and sulfonamide **2.12** with a suitable Pd precatalyst and (*R*,*R*)-DACH-phenyl Trost ligand **2.14**, the desired desymmetrization took place. Direct saponification of the product furnished alcohol **2.15** in 89% yield. Subsequent PCC-mediated oxidation of the resultant secondary alcohol delivered enone **2.16** in excellent yield. Enone **2.16** could be crystallized at the interface of EtOAc and heptane; X-ray diffraction studies confirmed the desired absolute stereochemistry had been obtained in the desymmetrization reaction.[26]



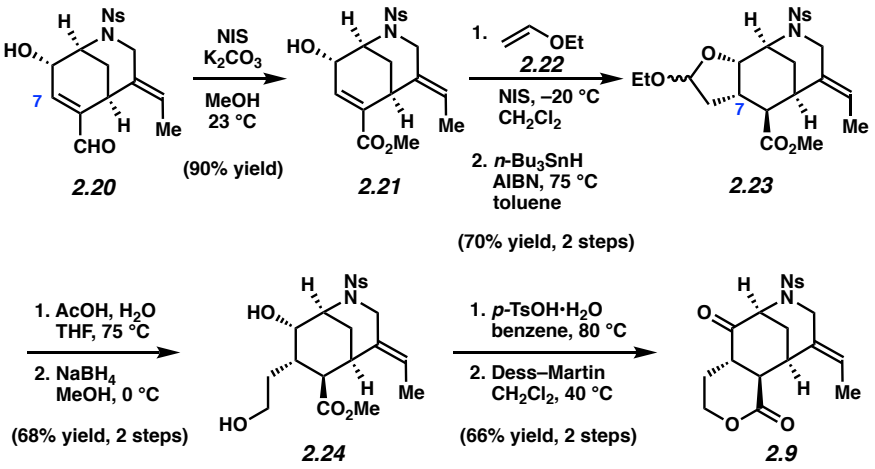
Scheme 2.2. Trost desymmetrization and synthesis of enone **2.16**.

Having synthesized enone **2.16**, we sought to introduce the [3.3.1]-azabicycle of the natural product and perform further elaborations (Scheme 2.3). Upon treatment with TBDPSOTf and 2,6-lutidine, enone **2.16** was converted to silyl enol ether **2.11** in high yield. This set the stage for a pivotal gold-mediated cyclization, inspired by precedent from Li and coworkers.[21] Using our optimized protocol, silyl enol ether **2.11** was treated with $(PMe_3)AuCl$ and AgOTf, followed by quenching with tosic acid hydrate in the same pot, to ultimately afford bicycle **2.10** as the major product. This sequence is thought to proceed by initial formation of oxocarbenium ion intermediate **2.17**, which undergoes nucleophilic attack by *t*-BuOH to give silyl enol ether **2.18**. In the presence of acid and water, **2.18** is hydrolyzed to give the desired enone **2.10**. Chiral SFC analysis at this stage revealed that **2.10** had been prepared in 96% ee. It should also be noted that the key gold-mediated cyclization gave an undesired product, **2.19**, in minor quantities. Although **2.10** and **2.19** were inseparable, the mixture could be taken forward through an epoxidation and Wittig homologation.[5h,k] Aqueous workup of the Wittig product led to enol ether hydrolysis with epoxide fragmentation to cleanly deliver enal **2.20** as a single constitutional isomer in 49% yield from silyl enol ether **2.11**.



Scheme 2.3. Gold-catalyzed construction of the [3.3.1]-azabicycle and elaboration to enal **2.20**.

Using the sequence shown in Scheme 2.4, enal **2.20** was elaborated to ketolactone **2.9**, the substrate for our key reductive interrupted Fischer indolization reaction. One of the synthetic challenges we encountered was the introduction of a hydroxyethyl group on C7. Initial approaches using metal-mediated conjugate addition strategies were met without success, so instead we targeted Ueno–Stork cyclization methodology.[27] En route to testing this approach, aldehyde **2.20** was converted to the corresponding methyl ester, **2.21**, using an NIS-based oxidative esterification protocol.[28] Next, **2.21** was treated with ethyl vinyl ether (**2.22**) and NIS to give a mixed iodoacetal intermediate. Subsequent reaction with tributyltin hydride and AIBN led to cyclization at C7 to deliver acetal **2.23** as an inconsequential mixture of diastereomers.[27] Acid-mediated hydrolysis of the acetal and reduction of the resultant lactol provided diol **2.24**. Finally, lactonization, followed by alcohol oxidation, afforded the desired ketolactone **2.9**.



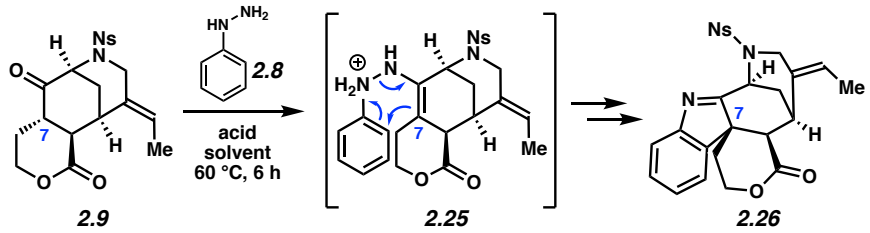
Scheme 2.4. Synthesis of reductive Fischer indolization reaction substrate, ketolactone **2.9**.

2.5 Reductive Interrupted Fischer Indolization Reaction

With ketolactone **2.9** in hand, we developed the key reductive interrupted Fischer indolization reaction. Our laboratory had extensive experience in developing Fischer indolizations in the context of methodology[17] and complex molecule synthesis.[5b,h,k] Thus we began by surveying a range of acid sources that were utilized in the Fischer indolization reaction literature and those we had previously deemed most promising. As shown in Table 2.1, the reactions of phenylhydrazine (**2.8**) and ketolactone **2.9** were performed at 60 °C for 6 h to provide meaningful comparison data. Most attempts, including those with Lewis acids and very strong protic acids, were met with disappointment (entries 1–5). Whereas the use of AcOH gave modest yield using water as the solvent (entry 6), an improvement was seen in switching the solvent to acetic acid (entry 7). Lastly, the use of TFA gave the most promising result, delivering Fischer indolization product **2.26** in 38% yield (entry 8). It should be noted that this transformation proceeds with complete diastereoselectivity and sets the C7 quaternary stereocenter. The diastereoselectivity is thought to be governed by approach of the phenyl ring on the less hindered face of the [3.3.1]-

azabicycle during the charge-accelerated [3,3]-sigmatropic rearrangement (see transition structure **2.25**).

Table 2.1. Fischer indolization reaction between ketolactone **2.9** and hydrazine **2.8**.

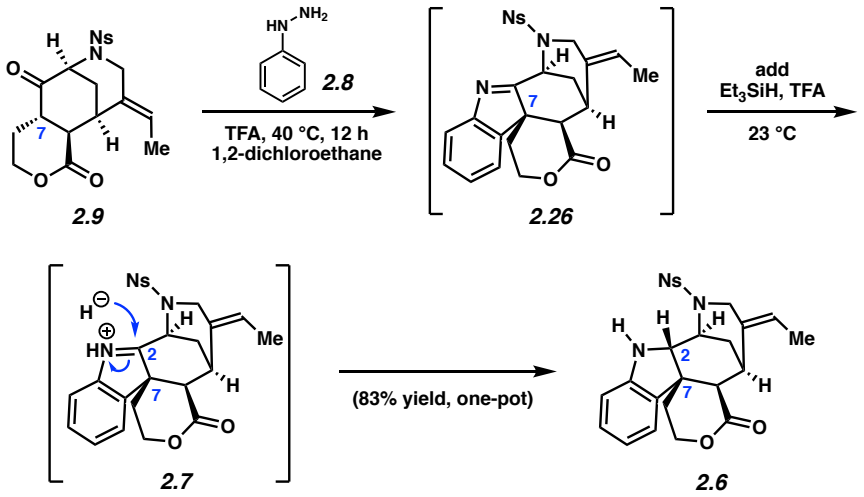


entry	*acid source*	*solvent*	*yield[a] (%)*
1	PCl_3	benzene	<5
2	$ZnCl_2$	EtOH	<5
3	*p*-TsOH·H_2O	EtOH, H_2O	<5
4	5% HCl	CH_3CN	<5
5	4% H_2SO_4	CH_3CN	<5
6	AcOH	H_2O	9
7	AcOH	AcOH	14
8	TFA	1,2-dichloroethane	38

[a] Yields were determined by ^{1}H NMR analysis using 1,3,5-trimethoxybenzene as an external standard.

Our next objective was to further optimize the Fischer indolization reaction and develop the desired reductive variant.[16] We were delighted to find that slight changes in our reaction conditions (i.e., 40 °C and 12 h), greatly improved conversion to indolenine lactone **2.26** (Scheme 2.5). Moreover, it was found that by simply adding triethylsilane and additional TFA to the Fischer indolization reaction with stirring at 23 °C, we obtained the reductive Fischer indolization product **2.6** in 83% yield. Overall, the conversion of ketolactone **2.9** to indoline **2.6** proceeds with installation of two new rings, three new bonds, and two new stereocenters, all with complete diastereoselectivity. This transformation represents one of the most complex Fischer indolization

reactions reported in the literature.[29] Interestingly, hydride approach from the more congested face of the [3.3.1]-azabicycle appears to be favorable (see transition structure **2.7**). Although counterintuitive in some respects, the stereochemical outcome may be rationalized by the kinetic preference for the formation of a cis ring juncture between the pyrrolidine and cyclohexyl units. The stereochemical outcome is consistent with reports from the *Strychnos* alkaloid literature[30] as well as a similar C2 reduction in akuammiline synthesis.[5v]

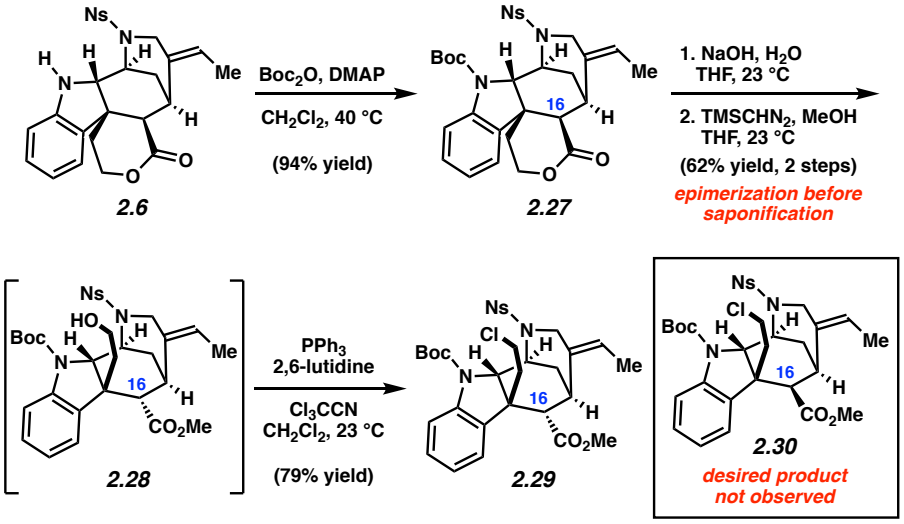


Scheme 2.5. Reductive interrupted Fischer indolization reaction delivers **2.6**.

2.6 Undesired C16 Epimerization and Synthesis of Unnatural C16 Epimers of Strictamine and 2(*S*)-Cathafoline

Having executed the key reductive interrupted Fischer indolization reaction, we sought to prepare chloroester **2.30** en route to the desired natural products through a seemingly straightforward sequence (Scheme 2.6). Boc protection of indoline **2.6** proceeded smoothly to furnish **2.27**. Subsequently, a two step hydrolysis/methylation protocol was used to arrive at hydroxyester **2.28**. Although we found **2.28** to be somewhat unstable, we found it could be used

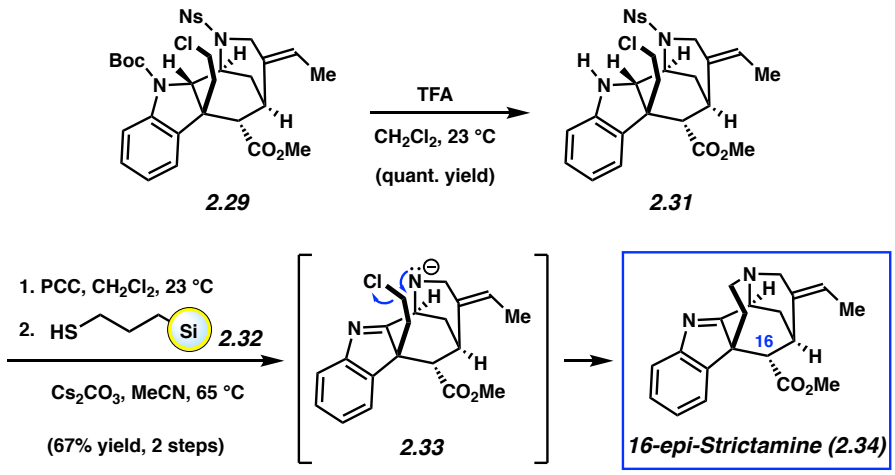
directly in the subsequent step. Treatment under Appel-like conditions cleanly provided **2.29**, which unfortunately possessed the undesired stereochemistry at C16. Despite a survey of alternative methanoloysis conditions prior to performing the chlorination, the undesired C16 epimer, **2.29**, was routinely formed as the major product. We surmise that C16 epimerization of **2.27** occurs more favorably than methanolysis or hydrolysis of the lactone. Several workarounds were pursued, such as attempted lactone opening via amidation,[31] Pd-catalyzed ring-opening,[32] or S_N2 displacements,[33] none of which were successful. Additionally, efforts to epimerize C16 of **2.29** and related compounds to provide the desired C16 epimer also proved fruitless.



Scheme 2.6. Undesired C16 epimerization.

Faced with the undesired epimerization leading to chloroester **2.29**, we saw an opportunity to develop late-stage transformations and synthesize unnatural epimeric analogs of strictamine and 2(*S*)-cathafoline. As shown in Scheme 2.7, the C16 epimer of strictamine **2.34** could be accessed in three steps from chloroester **2.29**. Deprotection of **2.29** furnished indoline **2.31** in quantitative yield. Treatment of **2.31** with PCC led to indoline oxidation, thus providing the

corresponding indolenine motif. Lastly, we pursued the key deprotection–cyclization step, analogous to that outlined in our retrosynthetic analysis (see Scheme 2.1). Exposure of the indolenine intermediate to solid-supported thiol resin **2.32**[34] and Cs_2CO_3 in acetonitrile at 65 °C delivered 16-*epi*-strictamine (**2.34**), presumably by way of transition structure **2.33**. Analogous to our earlier study toward the total synthesis of picrinine,[5h,k] the use of **2.32** proved instrumental in facilitating purification of the basic tertiary amine product. More importantly, this sequence demonstrated that our overall approach involving a late-stage deprotection–cyclization could be used to access the challenging methanoquinolizidine framework.



Scheme 2.7. Synthesis of 16-*epi*-strictamine (**2.34**).

We also explored two complementary routes to the C16 epimer of 2(*S*)-cathafoline **2.35**, which are depicted in Figure 2.2. Beginning from intermediate alkyl chloride **2.31**, reductive amination using formaldehyde led to *N*-methylation.[5c] Subsequent deprotection–cyclization provided **2.35**, albeit in only 10% yield. Given the modest synthetic efficiency of this sequence, we pursued an alternative path that involved methanoquinolizidine formation prior to *N*-methylation. Deprotection–cyclization of sulfonamide **2.29**, followed by acidic deprotection of

the indoline, furnished the methanoquinolizidine-containing product **2.36** in 76% yield over two steps. Finally, a reductive amination involving the indoline nitrogen afforded 16-*epi*-2(*S*)-cathafoline (**2.35**). The synthetic routes to **2.34** and **2.35** not only permitted access to unnatural analogs of strictamine and 2(*S*)-cathafoline, but also gave us critical experience in performing late-stage operations, particularly for introduction of the methanoquinolizidine unit and purification of polar natural product-like compounds.

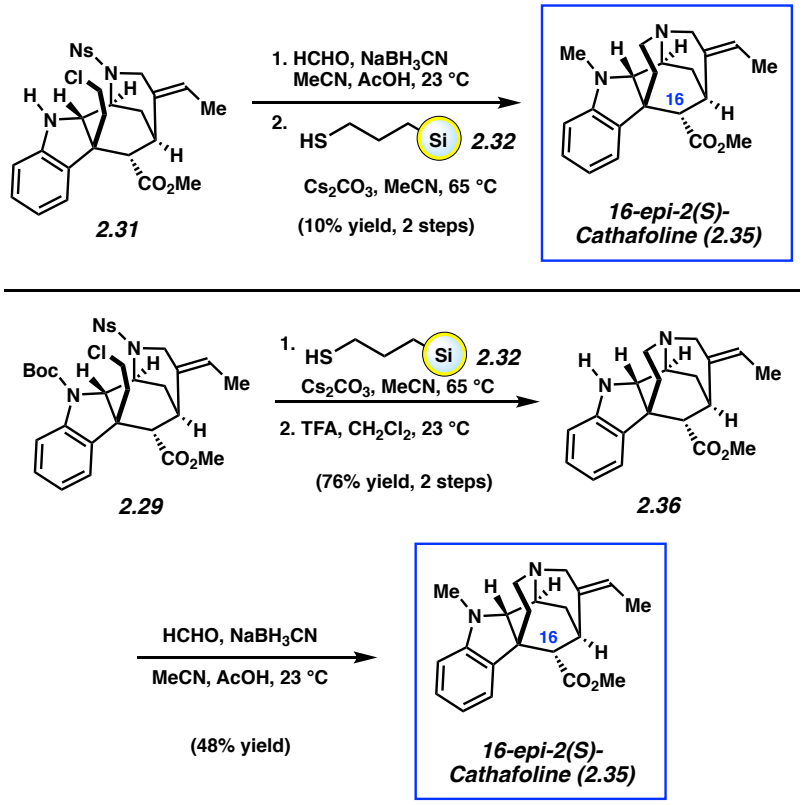
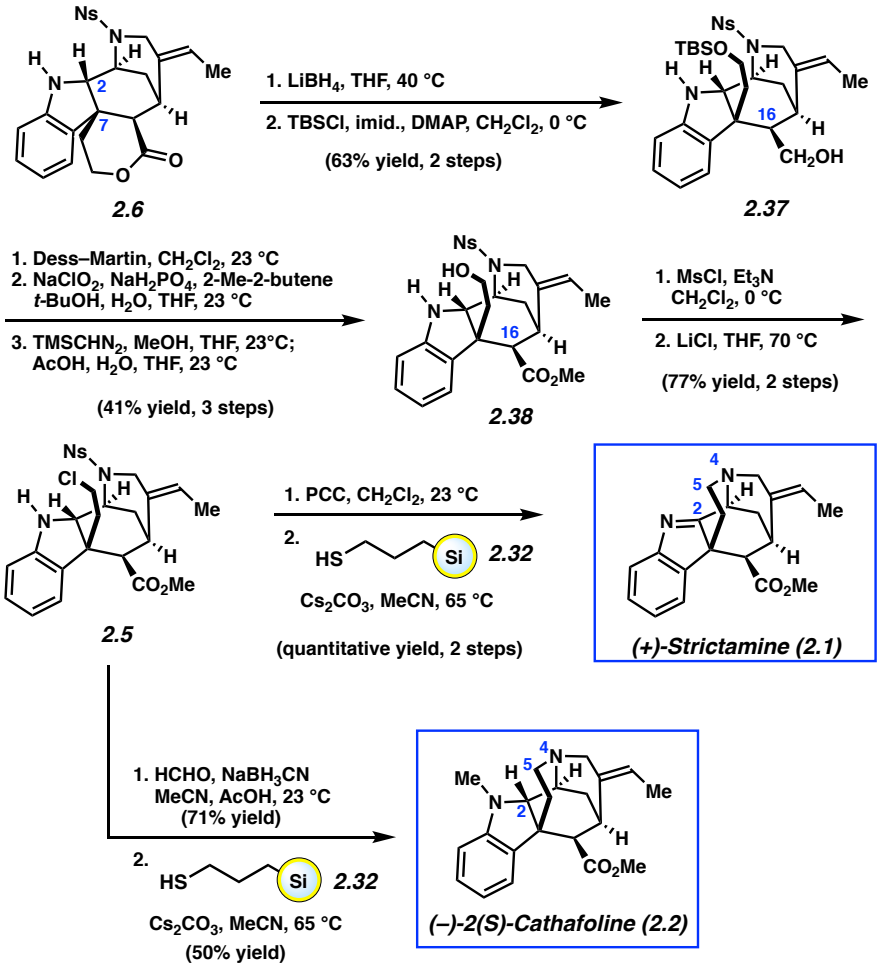


Figure 2.2. Synthetic routes to 16-*epi*-2(*S*)-cathafoline (**2.35**).

2.7 Enantioselective Total Syntheses of (+)-Strictamine and (–)-2(*S*)-Cathafoline

Despite the C16 epimerization setback, we returned to the primary task of completing the total syntheses of (+)-strictamine and (–)-2(*S*)-cathafoline (Scheme 2.8). We first sought a means

to open the lactone ring of **2.6** under non-basic reaction conditions, to hopefully avoid the undesired epimerization. To this end, indoline lactone **2.6** was treated with lithium borohydride to give the corresponding diol with the C16 stereochemistry unperturbed. Subsequent protection of the more accessible primary alcohol furnished silyl ether **2.37**. Next, a straightforward three-step sequence was performed to elaborate the C16 hydroxymethyl group of **2.37** to the corresponding methyl ester, **2.38**. From hydroxy ester **2.38**, a two-step chlorination protocol gave alkyl chloride **2.5**,[35] which proceeded in the presence of the free N–H of the indoline unit and set the stage for the final steps of the total syntheses. (+)-Strictamine (**2.1**) was accessed in quantitative yield from **2.5** by indoline oxidation, followed by deprotection–cyclization. Similarly, the total synthesis of (–)-2(*S*)-cathafoline (**2.2**) was achieved by *N*-methylation of **2.5**, followed by deprotection–cyclization. In both cases, the pentacyclic methanoquinolizidine framework was established in the final step of the total synthesis. NMR spectra of synthetic (+)-**2.1** and (–)-**2.2** correlated with spectra of the natural samples. This synthetic effort marked the first total syntheses of **2.1** and **2.2**, which was initially communicated concurrently with Zhu's synthesis of **2.1**.[16] Other synthetic routes to **2.1** have subsequently been reported by the labs of Fujii and Ohno,[5o] Gaich,[5p,t] Snyder,[5r] Qin,[5u,z] and Zu.[5v]



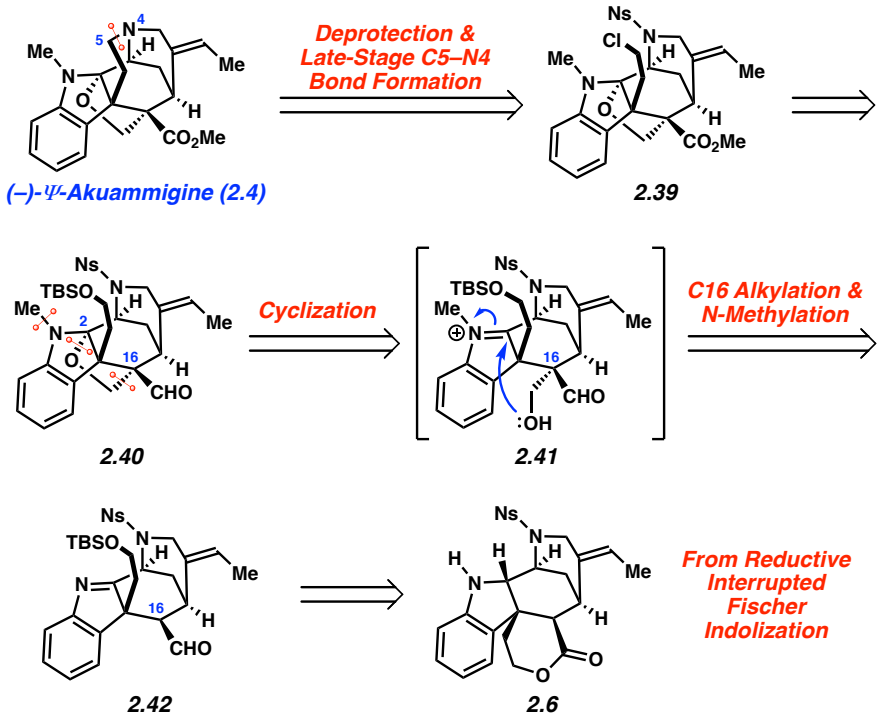
Scheme 2.8. Total syntheses of (+)-strictamine (**2.1**) and (–)-2(*S*)-cathafoline (**2.2**).

2.8 (–)-Ψ-Akuammigine: Isolation, Biological Activity, and Retrosynthetic Analysis

Having validated our strategy toward the total syntheses of natural products containing the methanoquinolizidine core, we directed our attention toward (–)-Ψ-akuammigine (**2.4**), the most structurally complex of the methanoquinolizidine-containing akuammiline alkaloids. (–)-Ψ-Akuammigine (**2.4**) was isolated from *Picralima klaineana* in 1932.[9] Biological studies later revealed promising activity as an anti-inflammatory agent.[36] Moreover, (–)-Ψ-akuammigine (**2.4**) belongs to a subset of akuammilines bearing vicinal quaternary centers, a structural motif which continues to be a notable synthetic challenge. In fact, only recently have there been reported total

syntheses of akuammiline alkaloids bearing this motif.[5w–y] Despite these triumphant efforts, akuammilines containing both the methanoquinolizidine and vicinal quaternary centers have yet to succumb to total synthesis.[37]

Our initial retrosynthetic analysis of (–)-Ψ-akuammigine (**2.4**) is shown in Scheme 2.9. The natural product (**2.4**) was proposed to arise from late-stage intermediate **2.39**, possessing a furoindoline motif and an alkyl chloride. In the forward sense, removal of the nosyl group was expected to enable C5–N4 bond formation and forge the methanoquinolizidine core, analogous to the strategy used to synthesize (+)-strictamine (**2.1**) and (–)-2(*S*)-cathafoline (**2.2**). Chloride **2.39** would be synthesized from furoindoline **2.40** through oxidative esterification and elaboration of the silyl ether. In a key maneuver, furoindoline **2.40** would ultimately be derived from aldehyde **2.42** through a sequence involving C16 hydroxymethylation, followed by *N*-methylation and cyclization (see transition structure **2.41**). Although not depicted, it was envisioned that the namesake of the natural product family, (+)-akuammiline (**2.3**), could also be accessed from **2.42** or derivatives thereof. Finally, aldehyde **2.42** was anticipated to be available from indoline lactone **2.6**, the product of the reductive interrupted Fischer indolization reaction[16] described above (see Scheme 2.5).

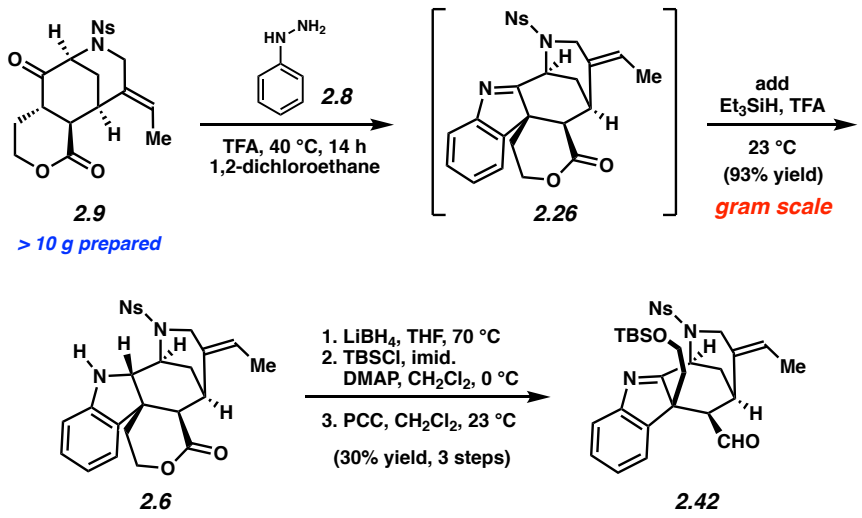


Scheme 2.9. Retrosynthetic analysis of (–)-Ψ-akuammigine (**2.4**).

2.9 Attempted Introduction of the Furoindoline Motif

To initiate our studies toward (–)-Ψ-akuammigine (**2.4**), we focused on the scalable preparation of aldehyde **2.42** following the route shown in Scheme 2.10. Knowing the commonly encountered difficulties associated with late-stage endeavors in akuammiline total synthesis, we expected our expedition would require us to perform the key reductive interrupted Fischer indolization[16] step on a large scale. Thus, we first prepared more than 10 grams of ketolactone **2.9**. In the key reductive Fischer indolization step, we were heartened to find that gram-scale reaction of ketolactone **2.9** and phenylhydrazine (**2.8**) under acidic conditions proceeded smoothly to deliver intermediate indolenine **2.26**. Reduction in the same pot using triethylsilane then furnished the pentacyclic indoline lactone **2.6** in 93% yield. Elaboration of indoline lactone **2.6** through a 3-

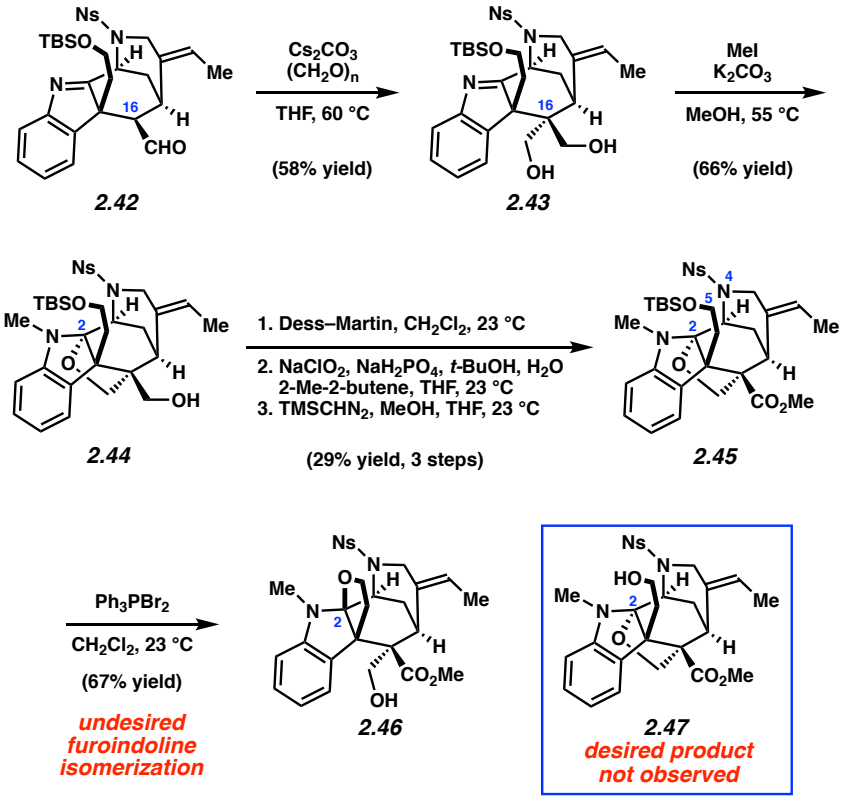
step sequence involving lactone reduction, selective alcohol protection, and simultaneous oxidation of the indoline and remaining alcohol afforded indolenine aldehyde **2.42**.



Scheme 2.10. Scalable preparation of aldehyde **2.42**.

With aldehyde **2.42** in hand, we sought to tackle three structural challenges presented by Ψ-akuammigine (**2.4**): the vicinal quaternary centers, the furoindoline moiety, and the methanoquinolizidine core. As shown in Scheme 2.11, treatment of aldehyde **2.42** with paraformaldehyde under basic conditions[5w,x] provided diol **2.43** in 58% yield. Of note, this transformation establishes the second of the vicinal quaternary centers and proceeds with Tischenko-type reduction of the aldehyde.[38] Next, we pursued introduction of the furoindoline moiety by exposing diol **2.43** to excess methyl iodide and K_2CO_3.[39] This allowed for differentiation of the C16 hydroxymethyl groups and furnished furoindoline alcohol **2.44** in 66% yield. Lastly, we sought to forge the methanoquinolizidine core of the natural product. A three-step oxidation/esterification sequence delivered ester **2.45**, which was poised to undergo C5–N4 bond formation upon C5 activation and removal of the nosyl group. Unfortunately, removal of the

silyl ether group present in **2.45** failed to deliver the desired alcohol **2.47**. Instead, we exclusively obtained an undesired isomer, furoindoline **2.46**, in 67% yield using Ph_3PBr_2,[40] and in high efficiencies under other conditions (e.g., acetic acid, TBAF). It is hypothesized that the presumed in situ structural rearrangement of furoindoline **2.47** to isomer **2.46** is thermodynamically driven, with **2.46** being significantly more stable.[41]

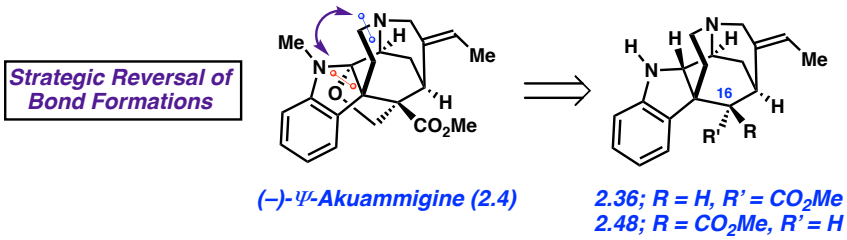


Scheme 2.11. Introduction of the furoindoline motif and undesired isomerization to afford **2.46**.

2.10 Enantioselective Total Synthesis of (–)-Ψ-Akuammigine

The discovery of the undesired furoindoline isomerization prompted us to reassess our synthetic approach toward (–)-Ψ-akuammigine (**2.4**) (Scheme 2.12). Rather than installing the furoindoline prior to the methanoquinolizidine, we sought to reverse the order in which these key

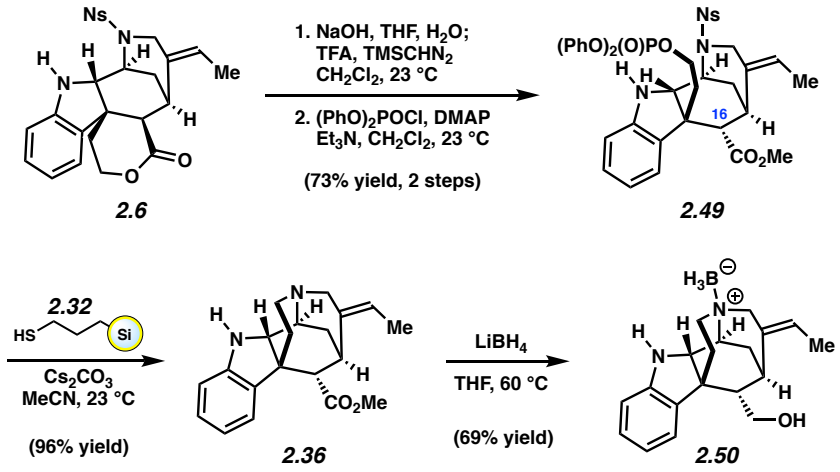
structural features were formed. Thus, we targeted epimeric esters **2.36** or **2.48** and derivatives thereof that contain the methanoquinolizidine core, but lack the vicinal quaternary centers and furoindoline, as potential precursors to (–)-Ψ-akuammigine (**2.4**).[42] It should be noted that the C16 stereochemistry was considered inconsequential, as this stereocenter would be controlled during a subsequent alkylation step. However, the strategy would likely require the handling and purification of polar compounds due to the earlier installation of the tertiary amine. Given limited options, we pursued this revised strategy.



Scheme 2.12. Reassessment of synthetic approach.

With the aim of installing the methanoquinolizidine and setting the stage for furoindoline formation, we developed the sequence described in Scheme 2.13. Beginning with the product of our reductive interrupted Fischer indolization reaction, indoline lactone **2.6**, we performed a one-pot saponification/methylation reaction. This net methanolysis of the lactone proceeded smoothly, with the expected epimerization of the C16 stereocenter. Several attempts were made to activate the resultant primary alcohol (e.g., tosylate, mesylate, halides, etc.), but the desired products of such efforts were highly unstable and could not be isolated. We ultimately found that the alcohol intermediate could be activated by conversion to diphenyl phosphate ester **2.49**.[43] This set the stage for methanoquinolizidine formation. Treatment of **2.49** with solid-supported thiol resin **2.32** under basic conditions provided ester **2.36**.[5h,k,l] Reduction of ester **2.36** with $LiBH_4$ afforded the

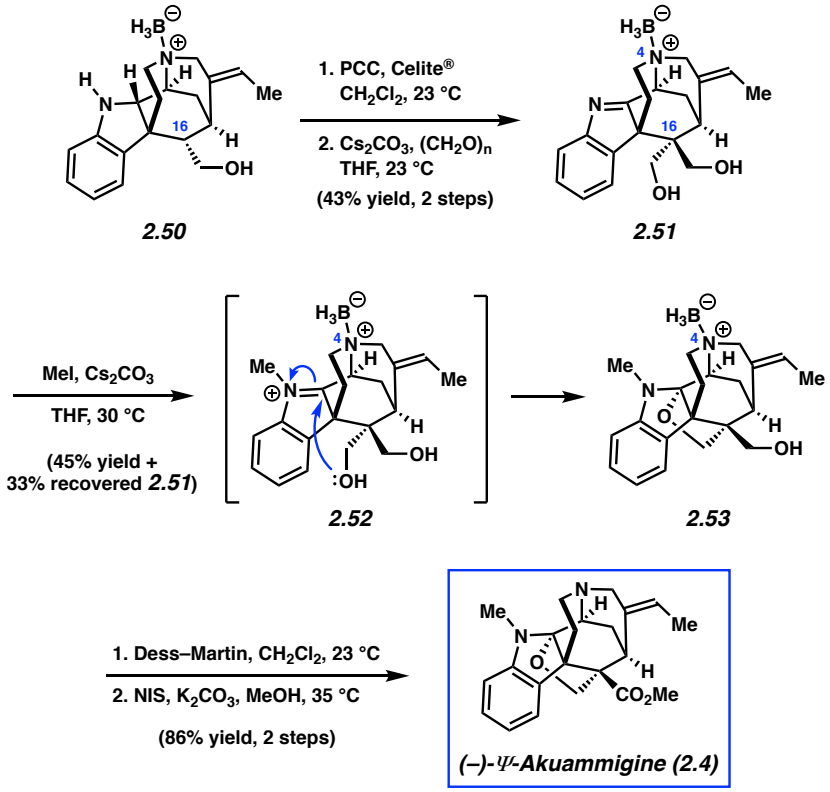
corresponding alcohol with concomitant borylation of the tertiary amine to give indoline alcohol **2.50** in 69% yield.[44] Although unintentional, the introduction of the amine-borane functional group proved beneficial, as it masked the basic tertiary amine and dramatically facilitated purification of late-stage intermediates.



Scheme 2.13. Introduction of methanoquinolizidine framework and amine-borane complexation.

The final steps to complete the total synthesis of (–)-Ψ-akuammigine (**2.4**) focused on installation of the C16 quaternary stereocenter and the furoindoline motif (Scheme 2.14). Double oxidation of indoline alcohol **2.50** with PCC yielded the corresponding indolenine aldehyde, which was a suitable substrate for C16 alkylation. Exposure of the indolenine aldehyde to paraformaldehyde (9 equivalents) and Cs_2CO_3 provided diol **2.51** in 43% yield over two steps. In a key ploy, we pursued furoindoline formation by exposing **2.51** to methyl iodide under basic conditions.[39] This gave rise to the desired product, furoindoline alcohol **2.53**, in 45% yield, with 33% recovered **2.51**. We presume the reaction proceeds through activated indoleninium **2.52** to deliver an intricate scaffold bearing both the methanoquinolizidine and the furoindoline motifs. Notably, if the reaction was allowed to proceed with higher conversion, borane removal and N4-

methylation occured to give an undesired ammonium salt byproduct. Nonetheless, oxidation to the aldehyde, followed by oxidative esterification[28] with borane removal,[45] furnished (–)-Ψ-akuammigine (**2.4**) in 86% yield over two steps. All spectral data for (–)-Ψ-akuammigine (**2.4**) were consistent with reported data and authentic samples.[46]



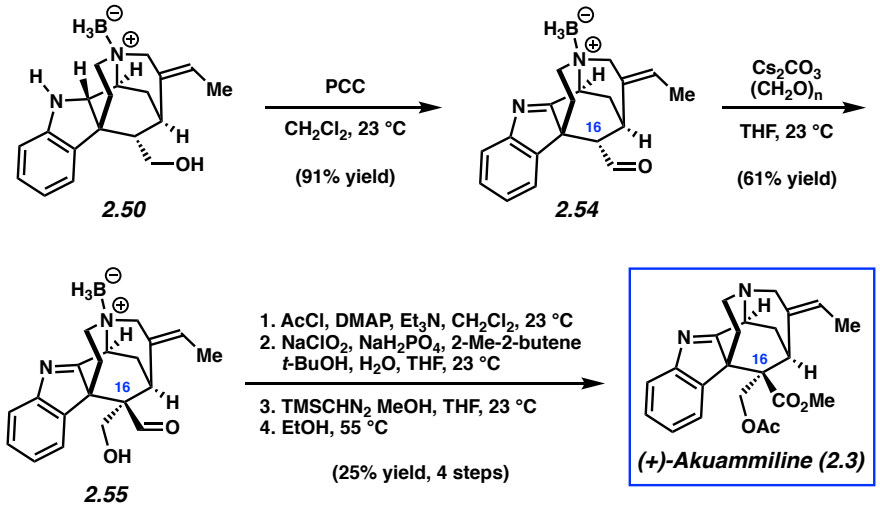
Scheme 2.14. Total synthesis of (–)-Ψ-akuammigine (**2.4**).

2.11 Enantioselective Total Synthesis of (+)-Akuammiline

Lastly with regard to the synthesis of methanoquinolizidine-containing akuammilines, we sought to prepare (+)-akuammiline (**2.3**, Scheme 2.15), the namesake of the natural product family. Akuammiline (**2.3**) was isolated alongside (–)-Ψ-akuammigine (**2.4**) in 1932 and has not

been synthesized.[9] (+)-Akuammiline (**2.3**) is structurally similar to (–)-Ψ-akuammigine (**2.4**), but possesses a C16 acetoxymethyl group, rather than a furoindoline unit.

We were delighted to find that late-stage intermediate alcohol **2.50** served as a suitable precursor to (+)-akuammiline (**2.3**) (Scheme 2.15). Double oxidation of indoline alcohol **2.50** provided borane-protected indolenine aldehyde **2.54**. C16 alkylation of **2.54** proceeded smoothly to establish the vicinal quaternary centers and provide aldehyde **2.55**.[47] It was optimal to use only 1.2 equivalents of paraformaldehyde to preserve the aldehyde moiety and avoid reduction to the corresponding diol as we had observed earlier (see **2.51**, Scheme 2.14). To complete the total synthesis of (+)-akuammiline (**2.3**), aldehyde **2.55** was elaborated through a multistep protocol involving acetylation, conversion to the methyl ester, and borane removal.[48] Synthetic (+)-akuammiline (**2.3**) was spectroscopically comparable to an authentic sample of the natural product.[49]



Scheme 2.15. Total synthesis of (+)-akuammiline (**2.3**).

2.12 Structural Rearrangement of Methanoquinolizidines to Pyrrolidinoindolines

One interesting notion regarding the methanoquinolizidine-containing akuammiline alkaloids is that, biosynthetically, they serve as precursors to the pyrrolidinoindoline-containing akuammilines.[19] As such, we wondered if structural rearrangements could efficiently be performed in the laboratory under mild reaction conditions. Exciting precedent for such conversions exist from the Zn/AcOH-mediated rearrangement of strictamine reported by Banerji and Chakrabarti in 1966, albeit without a reported yield.[50] We were particularly enticed to attempt the rearrangement of the methanoquinolizidine-containing natural products (+)-strictamine (**2.1**) and (+)-akuammiline (**2.3**) using the mild reducing agent samarium diiodide[51] (Figure 2.3). Samarium diiodide has been utilized to reductively cleave C–N bonds of α-amino carbonyls, even in the context of akuammiline chemistry.[5v,52] However, there have been no previous examples of the corresponding reductive cleavage of C–N bonds with SmI_2 using α-amino imine substrates. Given that previous reductive rearrangements of the methanoquinolizidine core have been low yielding,[50] we viewed this as an opportunity to improve their efficiencies.

The results of our rearrangement studies are shown in Figure 2.3. Upon treatment of (+)-strictamine (**2.1**) with SmI_2 in THF and methanol at 23 °C, the desired reductive rearrangement took place to furnish pyrrolidinoindoline compound **2.56**. Subsequent methylation afforded (–)-10-demethoxyvincorine (**2.57**), a bioactive natural product isolated in 2014[8] from *Alstonia macrophylla*, that had yet to be synthesized. Next, we applied the same reductive rearrangement conditions to (+)-akuammiline (**2.3**). To our delight, the rearrangement proceeded in quantitative yield to provide the unnatural akuammiline derivative **2.58**. Of note, **2.58** bears a pyrrolidinoindoline core with vicinal quaternary stereocenters at C7 and C16, and is therefore reminiscent of complex akuammilines bearing those structural features.[53]

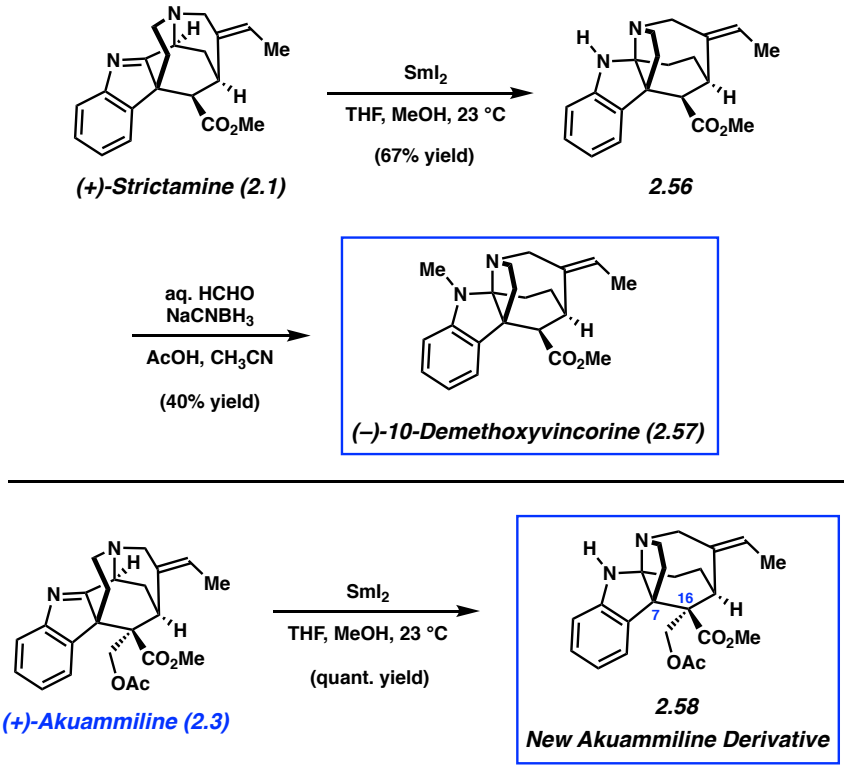


Figure 2.3. Structural rearrangement to access pyrrolidinoindolines.

2.13 Conclusion

We have completed the first enantioselective total syntheses of five akuammiline alkaloids, in addition to several unnatural compounds. Our synthetic approach to the methanoquinolizidine-containing natural products **2.1**–**2.4** features a number of key steps, including: a) a Trost desymmetrization to govern absolute stereochemistry, b) a gold-mediated cyclization to construct the [3.3.1]-azabicycle, c) a reductive interrupted Fischer indolization to arrive at pentacycle **2.6**, and d) late-stage formation of the methanoquinolizidine using a deprotection–cyclization cascade. In the case of (+)-akuammiline (**2.3**) and what is arguably the most complex methanoquinolizidine-containing alkaloid, (–)-Ψ-akuammigine (**2.4**), late-stage introduction of the vicinal quaternary stereocenters was achieved by employing challenging C16

alkylations. Additionally, in the case of (–)-Ψ-akuammigine (**2.4**), a means to install the furoindoline was crafted, while avoiding an undesired furoindoline isomerization that plagued our early approaches. Lastly, bioinspired reductive rearrangements of (+)-strictamine (**2.1**) and (+)-akuammiline (**2.3**) provided (–)-10-demethoxyvincorine (**2.57**) and a C16 analogue thereof, by rearrangement of the methanoquinolizidine core to pyrrolidinoindoline scaffolds.

These efforts mark the first total syntheses of some of the most complex akuammilines known, including those that possess both a methanoquinolizidine core and vicinal quaternary stereocenters. It is expected that our studies will enable biological investigations of akuammilines and unnatural analogs. Moreover, the lessons learned from our synthetic endeavors, including the delicate late-stage manipulations and various undesired setbacks, should inform synthetic forays toward akuammilines and other challenging natural products.

2.14 Experimental Section

2.14.1 Materials and Methods

Unless stated otherwise, reactions were conducted in flame-dried glassware under an atmosphere of nitrogen using anhydrous solvents (either freshly distilled or passed through activated alumina columns). All commercially obtained reagents were used as received unless otherwise specified. Dess–Martin periodinane (DMP) was prepared following a literature procedure.[54] *N*-Iodosuccinimide was purchased from Oakwood Chemical and recrystallized from dioxane–CCl_4 prior to use. $PhNHNH_2$ (**2.8**) was obtained from Sigma Aldrich and purified by flash chromatography (4:1 hexanes:EtOAc) prior to use. Methyl iodide was purchased from Alfa Aesar and distilled prior to use. Cs_2CO_3 Puratronic® 99.994% (metals basis) and paraformaldehyde were purchased from Alfa Aesar. K_2CO_3 was purchased from Alfa Aesar and

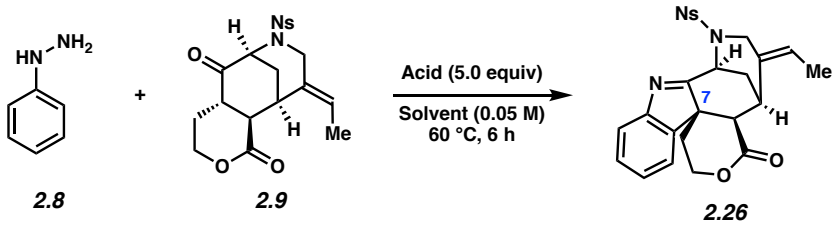
ground prior to use. Solid supported thiol-resin, MetSThiol® (**2.32**), was obtained from SiliCycle (Product # R51030B). Et_3SiH, TBSCl, TFA, and DMAP were obtained from Oakwood Chemical and used as received. $NaClO_2$, Ph_3PBr_2, and $(PhO)_2POCl$ were purchased from Sigma Aldrich and used as received. 2-methyl-2-butene, PCC, imidazole, absolute ethanol, and $LiBH_4$ were obtained from Acros Organics. NaH_2PO_4, 1,2-dichloroethane, Celite®, and acetyl chloride were used as received from Fisher Scientific. $TMSCHN_2$ was used as received from TCI America. NaOH was purchased from EMD Millipore. Reaction temperatures were controlled using an IKAmag temperature modulator, and unless stated otherwise, reactions were performed at room temperature (rt, approximately 23 °C). Thin-layer chromatography (TLC) was conducted with EMD gel 60 F254 pre-coated plates (0.25 mm) and visualized using a combination of UV, anisaldehyde, iodine, phosphomolybdic acid and cerium (IV) sulfate in water with sulfuric acid (Seebach), and potassium permanganate staining. Silicycle P60 (particle size 0.040–0.063 mm) silica gel was used for flash column chromatography. ^1H NMR spectra were recorded on Bruker spectrometers (at 500 MHz) and are reported relative to deuterated solvent signals (7.26 ppm for $CDCl_3$, 7.16 ppm for C_6D_6). Data for ^1H NMR spectra are reported as follows: chemical shift (δ ppm), multiplicity, coupling constant (Hz), and integration. ^{13}C NMR spectra were recorded on Bruker spectrometers (at 125 MHz) and are reported relative to deuterated solvent signals (77.16 ppm for $CDCl_3$, 128.06 ppm for C_6D_6). Data for ^{13}C NMR spectra are reported in terms of chemical shift, and when necessary, multiplicity, coupling constant (Hz) and carbon type. ^{11}B NMR spectra were recorded on Bruker spectrometers (at 160 MHz) and are reported relative to an external standard (0.00 ppm for $BF_3 \bullet Et_2O$). Data for ^{11}B NMR spectra are reported in terms of chemical shift. ^{31}P NMR spectra were recorded on Bruker spectrometers (at 202 MHz) and are reported relative to an external standard (0.00 ppm for 85% H_3PO_4). Data for ^{31}P NMR spectra

are reported in terms of chemical shift. IR spectra were recorded on a Perkin-Elmer 100 spectrometer and are reported in terms of frequency of absorption (cm^{-1}). DART-MS spectra were collected on a Thermo Exactive Plus MSD (Thermo Scientific) equipped with an ID-CUBE ion source and a Vapur Interface (IonSense Inc.). Both the source and MSD were controlled by Excalibur software v. 3.0. The analyte was spotted onto OpenSpot sampling cards (IonSense Inc.) using $CHCl_3$ or CH_2Cl_2 as the solvent. Ionization was accomplished using UHP He plasma with no additional ionization agents. The mass calibration was carried out using Pierce LTQ Velos ESI (+) and (–) Ion calibration solutions (Thermo Fisher Scientific). Optical rotations were measured with a Rudolf Autopol III Automatic Polarimeter. Melting points were determined using a DigiMelt MPA160 melting point apparatus.

2.14.2 Experimental Procedures

Note: Experimental information for compounds **2.1**, **2.2**, **2.5**, **2.6**, **2.9**, **2.10**, **2.11**, **2.12**, **2.13**, **2.15**, **2.16**, **2.19**, **2.20**, **2.21**, **2.23**, **2.24**, **2.37**, and **2.38** have previously been reported.[51]

Table 2.2 Interrupted Fischer Indolization Reaction Optimization.

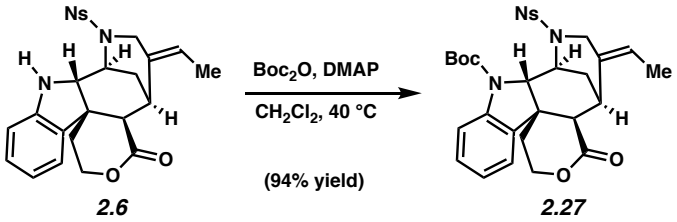


2.8 *2.9* *2.26*

entry	acid source	conditions	yield (%)
1	PCl_3	benzene, 60 °C	<5
2	$ZnCl_2$	EtOH, 60 °C	<5
3	*p*-TsOH·H_2O	EtOH, H_2O, 60 °C	<5
4	5% HCl	CH_3CN, 60 °C	<5
5	4% H_2SO_4	CH_3CN, 60 °C	<5
6	AcOH	H_2O, 60°C	9
7	AcOH	AcOH, 60 °C	14
8	TFA	DCE, 60 °C	38

Indolenine lactone 2.26. General Procedure. To a solution of ketolactone **2.9**[51] (5.0 mg, 0.012 mmol, 1.0 equiv) in 1,2-dichloroethane (0.25 mL) was added TFA (5 µL, 0.059 mmol, 5.0 equiv) and $PhNHNH_2$ (**2.8**) (3.5 µL, 0.036 mmol, 3.0 equiv). The resulting mixture was degassed via the freeze-pump-thaw method (3 cycles) using a –78 °C bath. After warming to 23 °C, the reaction was backfilled with N_2 for 1 min and heated to 60 °C. After stirring for 6 h, the reaction was cooled to 23 °C, at which point it was quenched with sat. aq. $NaHCO_3$ (1 mL). The layers were separated and the aqueous layer was extracted with CH_2Cl_2 (3 x 1 mL). The organic layers were combined, dried over Na_2SO_4, and concentrated under reduced pressure. Yields were determined by ^1H NMR analysis using 1,3,5-trimethoxybenzene as an internal standard. An analytically pure sample was obtained by combining the crude mixtures and purifying via flash chromatography (1:1 hexanes:EtOAc → 1:2 hexanes:EtOAc) to afford indolenine lactone **2.26** as a yellow oil. Indolenine lactone **2.26**: R_f 0.30 (3:1 EtOAc:hexanes); ^1H NMR (500 MHz, $CDCl_3$): δ 8.24–8.18 (m, 1H), 7.76–7.70 (m, 3H), 7.69–7.64 (m, 1H), 7.43 (td, *J* = 7.6, 1.2, 1H), 7.33 (d, *J* = 7.5, 1H), 7.26 (td, *J* = 7.5, 1.0, 1H), 5.86 (q, *J* = 7.4, 1H), 5.02 (dd, *J* = 4.1, 2.3 1H), 4.77 (td, *J* = 12.2, 4.7,

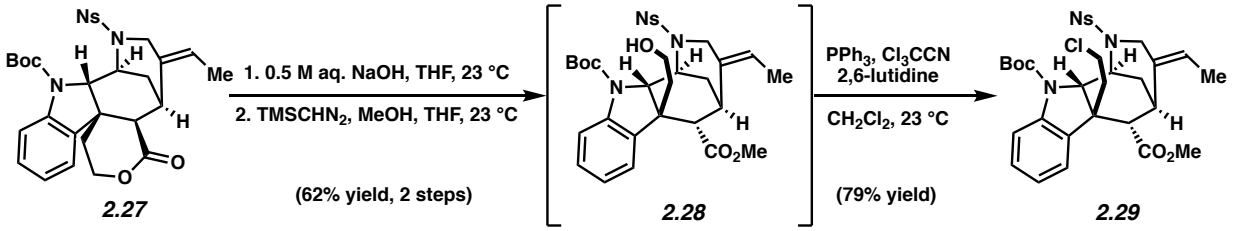
1H), 4.66 (dd, *J* = 12.2, 7.1, 1H), 4.50 (d, *J* = 15.6, 1H), 4.17 (br d, *J* = 15.1, 1H), 3.69 (br s, 1H), 3.20 (qd, *J* = 7.4, 4.3, 1H), 2.66 (dt, *J* = 14.5, 3.8, 1H), 2.45 (dd, *J* = 4.4, 1.8, 1H), 1.83 (dt, *J* = 14.5, 2.6, 1H), 1.74 (dd, *J* = 7.4, 2.5, 3H), 1.34 (m, 1H); ^{13}C NMR (125 MHz, $CDCl_3$): δ 181.4, 170.1, 153.5, 148.4, 142.3, 134.2, 132.5, 132.0, 131.5, 131.45, 129.3, 127.3, 126.5, 124.4, 122.8, 122.2, 67.5, 55.2, 53.4, 51.4, 48.2, 34.3, 31.6, 25.9, 14.5; IR (film): 2923, 2854, 1733, 1544, 1360, 1215, 1169 cm^{-1}; HRMS–APCI (m/z) $[M + H]^+$ calcd for $C_{25}H_{24}N_3O_6S^+$, 493.1380; found 494.1297; $[\alpha]^{22.7}_D$ –8.67° (c = 0.1, CH_2Cl_2).



2.6 *2.27*

Indoline lactone 2.27. To a solution of known lactone **2.6**[51] (800 mg, 1.6 mmol, 1.0 equiv) in CH_2Cl_2 (120 mL) was added Boc_2O (512 mg, 2.4 mmol, 1.5 equiv), and DMAP (191 mg, 1.6 mmol, 1.0 equiv). The golden brown solution became bright yellow and was placed into a preheated oil bath set to 40 °C. Additional aliquots of Boc_2O (512 mg, 2.4 mmol, 1.5 equiv) were added after the reaction had been stirring for 1, 13, 17 h. After stirring for 20 h total, the reaction was concentrated under reduced pressure and the crude mixture was purified by flash chromatography (1:1 hexanes:EtOAc) to afford indoline lactone **2.27** (900 mg, 94% yield) as a yellow oil. Indoline lactone **2.27**: R_f 0.84 (7:3 EtOAc:hexanes); ^{1}H NMR (500 MHz, $CDCl_3$): δ 8.10 (d, *J* = 7.2, 1H), 7.70–7.62 (m, 3H), 7.51 (br s, 1H), 7.21 (td, *J* = 7.6, 1.4, 1H), 7.10–7.07 (m, 1H), 7.04 (td, *J* = 7.4, 0.9, 1H), 5.60 (q, *J* = 6.8, 1H), 4.63 (dt, *J* = 12.0, 2.4, 1H), 4.48 (br s, 1H), 4.42 (dt, *J* = 12.2, 3.9, 1H), 4.34 (d, *J* = 15.9, 1H), 4.23 (br s, 1H), 3.86–3.79 (m, 2H), 3.70–3.64 (m, 1H), 2.00 (dt, *J* = 14.9, 2.5, 1H), 2.91–1.84 (m, 2H), 1.68–1.62 (m, 4H), 1.49 (s, 9H); ^{13}C

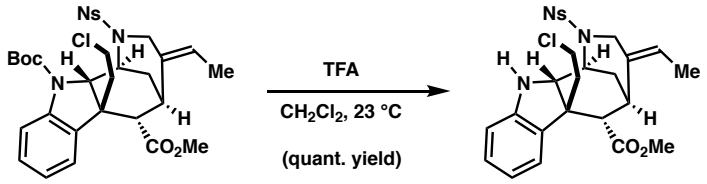
NMR (125 MHz, $CDCl_3$): (27 of 28 signals observed) δ 170.5, 151.5, 148.1, 139.5, 139.3, 134.4, 133.2, 131.6, 131.5, 128.8, 125.8, 124.3, 123.5, 121.9, 115.6, 82.6, 67.8, 65.3, 54.7, 47.9, 45.1, 42.8, 37.3, 30.1, 29.7, 28.3, 12.7; IR (film): 2958, 2923, 2854, 1735, 1698, 1547, 1373 cm^{-1}; HRMS–APCI (m/z) $[M - C_5H_7O_2]^+$ calcd for $C_{25}H_{26}N_3O_6S^+$, 496.1537; found 496.1498; $[\alpha]^{25.4}_D$ 223.33° (c = 0.1, CH_2Cl_2).



Indoline chloride 2.29. To a solution of lactone **2.27** (415 mg, 0.68 mmol, 1.0 equiv) in THF (34 mL) was added 0.5 M aq. NaOH (34 mL). The yellow solution was stirred for 12 h at 23 °C. Then the mixture was quenched with sat. aq. NH_4Cl (100 mL) and the layers were separated. The aqueous layer was extracted with EtOAc (3 x 100 mL) and the combined organic layers were dried over Na_2SO_4, and concentrated under reduced pressure. The residue was then resuspended in methanol (19 mL) and THF (52 mL). Trimethylsilyldiazomethane (0.6 M in hexanes, 0.81 mmol, 1.2 equiv) was added to the solution and the reaction was stirred for 1 h at 23 °C. Then the mixture was diluted with sat. aq. NaCl (100 mL). The layers were separated and the aqueous layer was extracted with EtOAc (3 x 50 mL). The combined organic layers were dried over Na_2SO_4, and concentrated under reduced pressure. The crude mixture was purified via column chromatography (7:3 hexanes:EtOAc) to afford alcohol **2.28** (270 mg, 62% yield) as a yellow oil. *Note*: Upon extensive purification, alcohol **2.28** decomposed to lactone intermediates such as **2.27** and its presumed epimer.

To a solution of alcohol **2.28** (270 mg, 0.42 mmol, 1.0 equiv) in CH_2Cl_2 (60 mL) was added triphenylphosphine (220 mg, 0.84 mmol, 2.0 equiv), 2,6-lutidine (0.10 mL, 0.84 mmol, 2.0

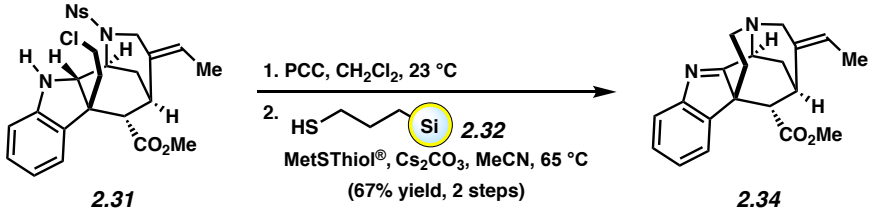
equiv), and trichloroacetonitrile (85 μL, 0.84 mmol, 2.0 equiv). The solution was stirred for 2 h at 23 °C. Then the mixture was diluted with sat. aq. NaCl (100 mL). The layers were separated and the aqueous layer was extracted with CH_2Cl_2 (3 x 50 mL). The combined organic layers were dried over Na_2SO_4 and concentrated under reduced pressure. The crude mixture was purified via column chromatography (7:3 hexanes:EtOAc) to afford indoline chloride **2.29** (219 mg, 79% yield) as a yellow oil. R_f 0.50 (4:6 EtOAc:hexanes); ^{1}H NMR (500 MHz, $CDCl_3$): δ 8.60 (d, *J* = 6.1, 1H), 7.74–7.67 (m, 2H), 7.62 (dd, *J* = 7.5, 1.6, 1H), 7.52 (d, *J* = 8.3, 1H), 7.22–7.17 (m, 2H), 6.70 (t, *J* = 7.5, 1H), 5.31 (q, *J* = 6.7, 1H), 4.91 (br s, 1H), 4.22–4.14 (m, 2H), 3.92 (d, *J* = 15.0, 1H), 3.76 (s, 3H), 3.50 (ddd, *J* = 16.6, 11.1, 5.3, 1H), 3.41 (t, *J* = 5.3 1H), 3.17–3.06 (m, 2H), 2.24–2.15 (m, 1H), 2.15–2.05 (m, 1H), 1.74 (dd, *J* = 14.2, 4.5, 1H), 1.62 (s, 9H), 1.54–1.51 (m, 4H); ^{13}C NMR (125 MHz, $CDCl_3$): δ 174.2, 152.2, 148.5, 142.2, 135.2, 133.8, 133.2, 131.4, 131.1, 128.7, 124.1, 124.0, 123.0, 119.1, 115.2, 82.7, 66.5, 54.5, 52.4, 48.5, 48.2, 47.0, 45.3, 39.6, 29.7, 29.2, 28.4, 23.0, 12.7 ; IR (film): 2957, 2922, 2857, 1736, 1699, 1547, 1371 cm^{-1}; HRMS–APCI (m/z) $[M - C_5H_8ClO_2]^+$ calcd for $C_{26}H_{28}N_3O_6S^+$, 510.1693; found 510.1653; $[\alpha]^{22.7}_D$ – 34.67° (c = 0.1, CH_2Cl_2).



2.29 ***2.31***

Alkyl chloride 2.31. To a solution of chloride **2.29** (30.0 mg, 0.045 mmol, 1.0 equiv) in CH_2Cl_2 (2.3 mL) was added TFA (2.3 mL). The yellow solution was stirred for 5 min at 23 °C. Then the mixture was quenched with sat. aq. $NaHCO_3$ (10 mL). The layers were separated and the aqueous layer was extracted with CH_2Cl_2 (3 x 10 mL). The combined organic layers were dried over Na_2SO_4, and concentrated under reduced pressure. The crude mixture was purified via column

chromatography (9:1 hexanes:EtOAc) to afford alkyl chloride **2.31** (26 mg, quant. yield) as a yellow oil. Alkyl chloride **2.31**: R_f 0.42 (3:2 hexanes:EtOAc); ^{1}H NMR (500 MHz, $CDCl_3$): δ 8.04–8.01 (m, 1H), 7.78–7.71 (m, 2H), 7.65–7.61 (m, 1H), 7.06–7.01 (m, 2H), 6.72 (td, *J* = 7.5, 1.0, 1H), 6.63 (d, *J* = 7.8, 1H), 5.58 (q, *J* = 7.2, 1H), 4.26–4.21 (m, 1H), 4.16 (d, *J* = 13.8, 1H), 4.04 (d, *J* = 1.8, 1H), 3.77 (dq, *J* = 13.9, 2.3, 1H), 3.55 (ddd, *J* = 16.1, 10.6, 5.7, 1H), 3.24–3.20 (m, 1H), 3.19 (s, 3H), 3.05 (s, 1H), 2.97 (dt, *J* = 14.5, 2.8, 1H), 2.86 (d, *J* = 1.4, 1H), 2.66 (ddd, *J* = 17.9, 12.2, 5.8, 1H), 2.37–2.29 (m, 1H), 1.74–1.67 (m, 4H); ^{13}C NMR (125 MHz, $CDCl_3$): (25 of 26 signals observed) δ 173.6, 150.0, 134.9, 134.2, 131.8, 131.2, 130.94, 130.91, 128.9, 124.2, 124.2, 123.4, 118.9, 110.1, 64.5, 54.1, 52.1, 51.4, 48.2, 46.5, 43.7, 40.8, 28.7, 19.8, 13.4; IR (film): 2925, 2853, 1729, 1545, 1374, 1165 cm^{-1}; HRMS-APCI (*m/z*) $[M - Cl]^+$ calcd for $C_{26}H_{28}N_3O_6S^+$, 510.1693; found, 510.1625; $[\alpha]^{22.0}_D$ 11.33° (c = 0.1, CH_2Cl_2).

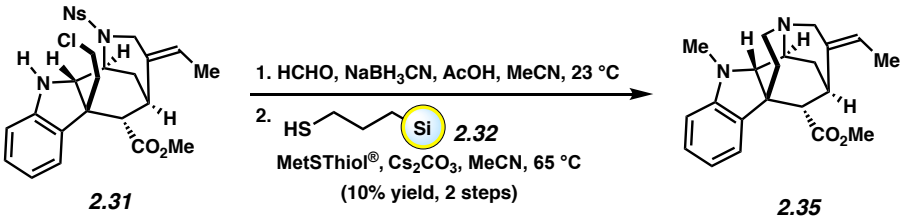


2.31 *2.34*

16-Epi-strictamine 2.34. To a solution of indoline **2.31** (13.0 mg, 0.023 mmol, 1.0 equiv) in CH_2Cl_2 (2.3 mL) was added PCC (10.0 mg, 0.046 mmol, 2.0 equiv). The solution was stirred for 20 min at 23 °C. Then the mixture was filtered through a plug of basic alumina (2 g) and eluted with EtOAc (10 mL). The volatiles were removed under reduced pressure to afford the corresponding indolenine (13.0 mg, quant. yield) as a yellow oil, which was taken forward with no further purification.

To a solution of indolenine (13.0 mg, 0.023 mmol) in MeCN (3.2 mL) was added Cs_2CO_3 (25.0 mg, 0.077 mmol, 3.0 equiv), and SiliaMetS Thiol® **2.32** (0.10 mmol, 4.0 equiv). The solution was then placed into a preheated aluminum block set at 65 °C and stirred for 9 h. Then

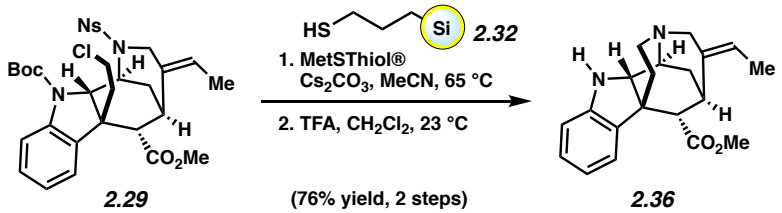
the mixture was filtered through a plug of Celite® (1 g) and eluted with MeCN (10 mL). The volatiles were removed under reduced pressure and the crude material was purified by column chromatography (9:1 acetone:MeOH) to afford 16-epi-strictamine **2.34** (5.0 mg, 67% yield) as a colorless oil. 16-Epi-strictamine **2.34**: R_f 0.20 (9:1 acetone:MeOH); ^{1}H NMR (500 MHz, $CDCl_3$): δ 7.62 (dt, *J* = 7.0, 0.8, 1H), 7.32–7.27 (m, 2H), 7.15 (td, *J* = 7.4, 1.0, 1H), 5.48 (q, *J* = 7.0, 1H), 4.74–4.70 (m, 1H), 4.10 (d, *J* = 16.4, 1H), 3.48 (s, 1H), 3.15–3.09 (m, 4H), 3.03–2.96 (m, 1H), 2.77–2.71 (m, 2H), 2.48 (t, *J* = 2.5, 2H), 2.07–2.01 (m, 1H), 1.76 (dd, *J* = 7.0, 2.5, 3H), 1.72–1.65 (m, 1H); ^{13}C NMR (125 MHz, $CDCl_3$): δ 189.9, 171.8, 156.2, 145.4, 142.0, 128.1, 125.2, 122.0, 120.9, 118.8, 58.4, 55.3, 54.0, 53.9, 51.8, 51.4, 41.8, 31.6, 31.1, 12.8; IR (film): 2928, 2863, 1736, 1594, 1453, 1165 cm^{-1}; HRMS-APCI (*m/z*) $[M + H]^+$ calcd for $C_{20}H_{23}N_2O_2^+$, 323.1754; found, 323.1710; $[\alpha]^{22.6}_D$ 141.33° (c = 0.1, CH_2Cl_2).



16-Epi-2(*S*)-cathafoline 2.35. To a solution of indoline **2.31** (13.0 mg, 0.023 mmol, 1.0 equiv) in MeCN (2.3 mL) was added HCHO (37 wt. % in water, 0.40 mL), AcOH (0.23 mL), and $NaBH_3CN$ (4.4 mg, 0.069 mmol, 3.0 equiv). The solution was stirred for 10 min at 23 °C. Then the mixture was filtered through a plug of sodium sulfate (5 g) and eluted with EtOAc (10 mL). The volatiles were removed under reduced pressure. The resultant solution was suspended in sat. aq. $NaHCO_3$ (5 mL) and EtOAc (5 mL). The layers were separated and the aqueous layer was extracted with EtOAc (3 x 5 mL). The organic layers were combined and dried over Na_2SO_4. The organic solvent was evaporated under reduced pressure to afford a crude residue, which was

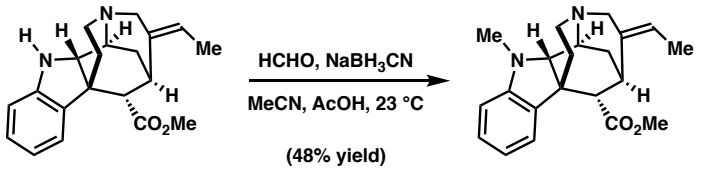
purified via column chromatography (9:1 hexanes:EtOAc) to afford the corresponding *N*-Me-indoline (13.3 mg, quant. yield) as a yellow oil.

To a solution of the *N*-Me-indoline intermediate (13.3 mg, 0.023 mmol) in MeCN (2.9 mL) was added Cs_2CO_3 (23.0 mg, 0.070 mmol, 3.0 equiv), and SiliaMetSThiol® (**2.32**) (0.093 mmol, 4.0 equiv). The solution was then placed into a preheated aluminum block set at 65 °C and stirred for 9 h. Then the mixture was filtered over a plug of Celite® (1 g) and eluted with MeCN (10 mL). The volatiles were removed under reduced pressure and the crude material was purified by column chromatography (9:1 acetone:MeOH) to afford 16-epi-2(*S*)-cathafoline (**2.35**) (1.0 mg, 10% yield) as a colorless oil. 16-Epi-2(*S*)-cathafoline (**2.35**): R_f 0.22 (9:1 acetone:MeOH); ^{1}H NMR (500 MHz, $CDCl_3$): δ 7.13–7.05 (m, 2H), 6.81–6.73 (dt, *J* = 7.4, 0.9, 1H), 6.59 (d, *J* = 7.8, 1H), 5.32 (q, *J* = 6.8, 1H), 4.0 (t, *J* = 5.0, 1H), 3.95 (d, *J* = 15.9, 1H), 3.55 (ddd, *J* = 18.6, 11.2, 7.7, 1H), 3.34 (d, *J* = 4.6, 1H), 3.13 (s, 1H), 2.97 (s, 3H), 2.94 (d, *J* = 15.8, 1H), 2.76 (dd, *J* = 13.8, 3.0, 1H), 2.67 (s, 3H), 2.64 (d, *J* = 7.2, 1H), 2.61 (s, 1H), 2.41–2.26 (m, 2H), 1.87–1.81 (m, 1H), 1.58–1.55 (m, 3H); ^{13}C NMR (125 MHz, $CDCl_3$): δ 175.0, 153.6, 142.9, 136.6, 128.0, 123.8, 118.8, 117.5, 109.2, 70.2, 57.0, 56.7, 51.0, 48.7, 46.9, 42.9, 38.6, 34.3, 30.9, 20.6, 12.8; IR (film): 2947, 2925, 2856, 1738, 1465, 1158 cm^{-1}; HRMS-APCI (*m/z*) $[M + H]^+$ calcd for $C_{21}H_{27}N_2O_2^+$, 339.2067; found, 339.2022; $[\alpha]^{21.6}_D$ – 204.67° (c = 0.1, CH_2Cl_2).

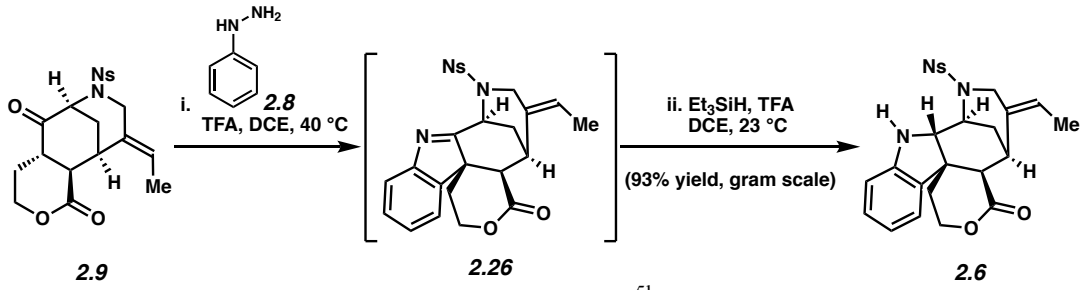


Methanoquinolizidine 2.36. To a solution of indoline **2.29** (297 mg, 0.459 mmol, 1.0 equiv) in MeCN (15.0 mL) was added Cs_2CO_3 (299 mg, 0.918 mmol, 2.0 equiv), and SiliaMetSThiol® (**2.32**) (2.294 mmol, 5.0 equiv). The solution was then placed into a preheated aluminum block set

at 65 °C and stirred for 17 h, at which point, the reaction mixture was cooled to 23 °C and a second addition of Cs_2CO_3 (299 mg, 0.918 mmol, 2.0 equiv), and SiliaMetSThiol® (**2.32**) (2.294 mmol, 5.0 equiv) were added. The reaction was then placed into a preheated aluminum block set at 65 °C and stirred for 24 h. Then the mixture was filtered through a plug of Celite® (5 grams) and eluted with MeCN (40 mL). The volatiles were removed under reduced pressure. The crude oil was suspended in CH_2Cl_2 (20.0 mL) and TFA (10.0 mL) was added. The solution was then stirred at 23 °C for 1 h. The reaction was quenched with sat. aq. $NaHCO_3$ (200 mL) and diluted with CH_2Cl_2 (40 mL). The layers were separated and the aqueous layer was extracted with CH_2Cl_2 (3 x 40 mL). The organic layers were combined and dried over Na_2SO_4. The volatiles were removed under reduced pressure to afford a crude mixture, which was purified via column chromatography (EtOAc → 1:4 MeOH:$CHCl_3$) to afford methanoquinolizidine **2.36** (113.4 mg, 76% yield, over two steps) as a colorless oil. Methanoquinolizidine **2.36**: R_f 0.10 (3:7 MeOH:EtOAc); ^{1}H NMR (500 MHz, $CDCl_3$): δ 7.11 (d, *J* = 7.4, 1H), 7.04 (t, *J* = 7.8, 1H), 6.81 (t, *J* = 7.5, 1H), 6.75 (d, *J* = 7.8, 1H), 5.34 (q, *J* = 6.8, 1H), 4.08 (d, *J* = 4.7, 1H), 3.92–4.02 (m, 2H), 3.51–3.61 (m, 1H), 3.13 (br s, 1H), 2.99 (s, 3H), 2.86–2.96 (m, 2H), 2.60–2.68 (m, 2H), 2.30–2.43 (m, 2H), 1.87 (d, *J* = 14.0, 1H), 1.58 (dd, *J* = 6.9, 1.7, 3H); ^{13}C NMR (125 MHz, $CDCl_3$): δ 175.2, 150.8, 142.4, 136.8, 127.9, 124.3, 119.7, 117.9, 111.7, 63.9, 56.9, 56.6, 51.1, 50.3, 46.9, 43.4, 38.8, 30.7, 20.6, 12.8; IR (film): 2947, 2918, 2856, 1733, 1612, 1462, 1249, 1158 cm^{-1}; HRMS-APCI (*m/z*) $[M + H]^+$ calcd for $C_{20}H_{25}N_2O_2^+$, 325.1911; found, 325.1890; $[\alpha]^{24.5}_D$ –75.3° (c = 0.1, CH_2Cl_2).

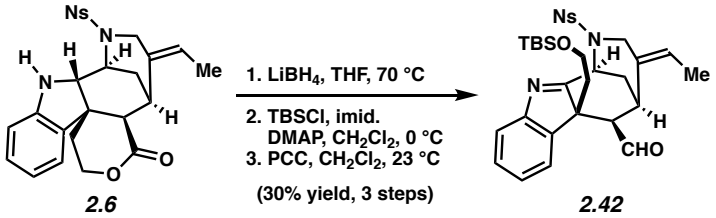


16-Epi-2(*S*)-cathafoline 2.35. To a solution of methanoquinolizidine **2.36** (4.0 mg, 0.012 mmol, 1.0 equiv) in MeCN (1.2 mL) was added HCHO (37 wt. % in water, 0.22 mL), AcOH (0.12 mL), and $NaBH_3CN$ (2.3 mg, 0.037 mmol, 3.0 equiv). The solution was stirred for 10 min at 23 °C. Then the mixture was filtered through a plug of sodium sulfate (5 g) and eluted with EtOAc (10 mL). The volatiles were removed under reduced pressure. The resultant solution was suspended in sat. aq. $NaHCO_3$ (5 mL) and EtOAc (5 mL). The layers were separated and the aqueous layer was extracted with EtOAc (3 x 5 mL). The organic layers were combined and dried over Na_2SO_4. The volatiles were removed under reduced pressure to afford a crude residue, which was purified via column chromatography (9:1 acetone:MeOH) to afford 16-epi-2(*S*)-cathafoline **2.35** (2.0 mg, 48% yield) as a colorless oil. 16-Epi-2(*S*)-cathafoline **2.35** is characterized above, vide supra.



Indoline lactone 2.6. To a solution of ketolactone **2.9**[51] (1.00 g, 2.40 mmol, 1.0 equiv) in 1,2-dichloroethane (120 mL) was added TFA (0.900 mL, 12.0 mmol, 5.0 equiv) and $PhNHNH_2$ (**2.8**) (472 μL, 4.76 mmol, 2.0 equiv). The resulting mixture was degassed via the freeze-pump-thaw method (3 cycles) using a –78 °C bath. After warming to 23 °C, the reaction was backfilled with N_2 for 1 min and heated to 40 °C. After stirring for 14 h, the reaction was cooled to 23 °C, at which point additional TFA (19.0 mL, 246 mmol, 103.0 equiv) and Et_3SiH (19.0 mL, 119 mmol,

50.0 equiv) were added. The reaction was flushed with N_2 for 1 min and stirred at 23 °C. After 1 h of stirring, the reaction was quenched with sat. aq. $NaHCO_3$ (400 mL) and diluted with CH_2Cl_2 (200 mL). The layers were separated and the aqueous layer was extracted with CH_2Cl_2 (3 x 200 mL). The organic layers were combined, dried over Na_2SO_4, and concentrated under reduced pressure. The crude mixture was purified via flash chromatography (3:1 hexanes:EtOAc → 2:1 hexanes:EtOAc) to afford indoline lactone **2.6** (1.10 g, 93% yield) as a yellow solid. Indoline lactone **2.6**: mp: 135–137 °C; R_f 0.30 (1:1 EtOAc:hexanes); ^{1}H NMR (500 MHz, $CDCl_3$): δ 8.07–8.03 (m, 1H), 7.78–7.70 (m, 2H), 7.68– 7.65 (m, 1H), 7.10–7.04 (m, 2H), 6.75 (dt, *J* = 7.5, 0.9, 1H), 6.66 (d, *J* = 7.8, 1H), 5.62 (q, *J* = 7.2, 1H), 4.72–4.64 (m, 1H), 4.61–4.53 (m, 1H), 4.21 (s, 1H), 4.18 (d, *J* = 2.4, 1H), 4.06 (d, *J* = 14.6, 1H), 3.95 (s, 1H), 3.82 (dt, *J* = 14.5, 1.3, 1H), 3.55–3.49 (m, 1H), 3.08 (d, *J* = 6.4, 1H), 2.51–2.43 (m, 1H), 2.11 (dt, *J* = 13.9, 2.8, 1H), 2.07–1.98 (m, 1H), 1.87 (dtd, *J* = 13.9, 3.8, 1.3, 1H), 1.68 (d, *J* = 7.1, 3H). The spectral data match those previously reported in the literature.[51]



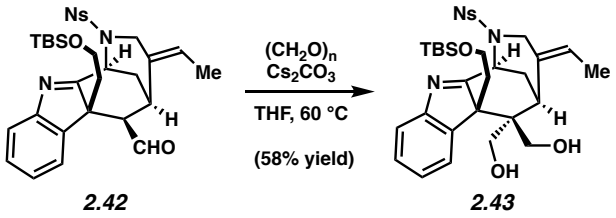
2.6 *2.42*

Indolenine aldehyde 2.42. To a solution of indoline lactone **2.6** (255 mg, 0.499 mmol, 1.0 equiv) in THF (20 mL) was added $LiBH_4$ (43.0 mg, 2.0 mmol, 4.0 equiv). The reaction was placed in a preheated oil bath at 40 °C. After stirring for 5 h, the reaction was cooled to 23 °C, poured into deionized water (25 mL), and diluted with EtOAc (20 mL). The layers were separated and the aqueous layer was extracted with EtOAc (3 x 20 mL). The organic layers were combined, dried over $MgSO_4$, and evaporated under reduced pressure. The crude residue was purified via flash chromatography (3:7 hexanes:EtOAc) to afford the corresponding diol.

To a solution of the diol in CH_2Cl_2 (10 mL) was added imidazole (28.5 mg, 0.418 mmol, 1.2 equiv) and DMAP (43.0 mg, 0.350 mmol, 1.0 equiv). The reaction was cooled to 0 °C and stirred. After 1 min, TBSCl (74.0 mg, 0.500 mmol, 1.4 equiv) was added. The reaction was allowed to warm to 23 °C. After 1 h the reaction was poured into deionized water (12 mL). The layers were separated and the aqueous layer was extracted with CH_2Cl_2 (3 x 12 mL). The organic layers were combined, dried over $MgSO_4$, and evaporated under reduced pressure. The crude residue was purified via flash chromatography (4:1 hexanes:EtOAc → 3:1 hexanes:EtOAc) to afford the corresponding silyl ether.

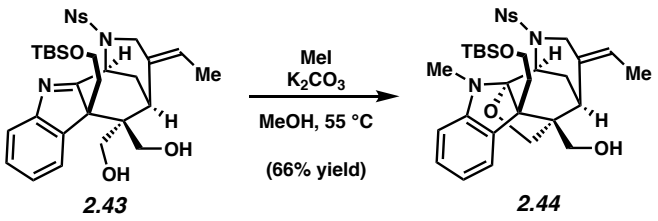
To a solution of the silyl ether in CH_2Cl_2 (30 mL) was added PCC (0.200 g, 0.800 mmol, 2.5 equiv). After 45 min, Celite® (200 mg) was added to the reaction and the contents of the flask were filtered through a pad of Celite® (2 g) and basic alumina (4 g). The pad was eluted with EtOAc (100 mL) and the filtrate was concentrated under reduced pressure. The crude mixture was purified via flash chromatography (1:3 hexanes:EtOAc) to afford indolenine aldehyde **2.42** (99.7 mg, 30% yield, 3 steps) as a colorless oil. Indolenine aldehyde **2.42**: R_f 0.70 (1:1 hexanes:EtOAc); ^{1}H NMR (500 MHz, $CDCl_3$): δ 10.15 (d, *J* = 3.3, 1H), 8.21–8.15 (m, 1H), 7.78–7.70 (m, 2H), 7.67–7.61 (m, 2H), 7.38–7.31 (m, 2H), 7.23 (td, *J* = 7.5, 1.1, 1H), 5.79 (q, *J* = 7.4, 1H), 5.22 (dd, *J* = 4.1, 2.7, 1H), 4.47 (d, *J* = 15.0, 1H), 4.10–4.00 (m, 1H), 3.55–3.47 (m, 1H), 3.41 (s, 1H), 2.94–2.84 (m, 1H), 2.69–2.59 (m, 2H), 2.47 (dd, *J* = 14.0, 3.7, 1H), 1.98 (t, *J* = 3.5, 1H), 1.82 (dt, *J* = 14.1, 3.0, 1H), 1.69 (dd, *J* = 7.3, 2.4, 3H), 0.70 (s, 9H), –0.18 (s, 3H), –0.22 (s, 3H); ^{13}C NMR (125 MHz, $CDCl_3$): δ 201.8, 182.4, 153.6, 148.8, 143.6, 134.2, 132.0, 131.8, 131.2, 131.0, 128.5, 126.4, 125.1, 124.4, 123.5, 121.5, 63.2, 59.1, 58.9, 54.5, 47.7, 35.5, 35.1, 29.5, 26.1, 18.4, 15.0, –5.4, –5.5; IR (film): 2955, 2930, 2856, 1715, 1544, 1443, 1371, 1175,

1091 cm^{-1}; HRMS-APCI (*m/z*) $[M + H]^+$ calcd for $C_{31}H_{40}N_3O_6SSi^+$, 610.2402; found, 610.2361; $[\alpha]^{23.2}_D$ 16.00° (c = 0.1, CH_2Cl_2).



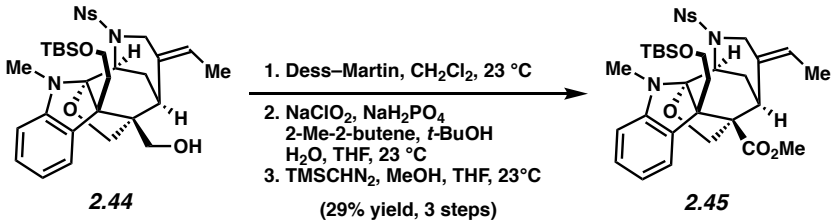
2.42 *2.43*

Diol 2.43. To a solution of indolenine aldehyde **2.42** (47 mg, 0.077 mmol, 1.0 equiv) in THF (8 mL) was added Cs_2CO_3 (250 mg, 0.77 mmol, 10.0 equiv) and paraformaldehyde (23 mg, 0.77 mmol, 10.0 equiv). The reaction was heated to 60 °C. After stirring for 2.5 h, the reaction was cooled to 23 °C, filtered over Celite®(2 g), and evaporated under reduced pressure. The crude mixture was purified via preparative thin layer chromatography (3:2 benzene:MeCN) to afford diol **2.43** (28.7 mg, 58% yield) as a pale yellow oil. Diol **2.43**: R_f 0.30 (1:3 hexanes:EtOAc); ^1H NMR (500 MHz, $CDCl_3$) δ 8.19–8.12 (m, 1H), 7.76–7.71 (m, 2H), 7.70–7.66 (d, *J* = 7.7, 1H), 7.65–7.60 (m, 1H), 7.53 (d, *J* = 7.4, 1H), 7.37 (td, *J* = 7.6, 1.3, 1H), 7.25 (td, *J* = 7.5, 1.1, 1H), 5.79 (q, *J* = 7.4, 1H), 5.13 (t, *J* = 3.3, 1H), 4.45 (d, *J* = 15.2, 1H), 4.31 (dd, *J* = 10.6, 3.4, 1H), 4.21 (dd, *J* = 10.5, 5.3, 1H), 4.06 (dt, *J* = 15.1, 2.5, 1H), 3.47 (ddd, *J* = 10.0, 9.1, 5.9, 1H), 3.34 (s, 1H), 3.07 (dd, *J* = 12.0, 2.7, 1H), 2.69–2.58 (m, 2H), 2.45 (dd, *J* = 5.6, 3.8, 1H), 2.37 (td, *J* = 9.8, 4.6, 1H), 2.10 (dt, *J* = 14.6, 3.3, 1H), 2.03 (ddd, *J* = 13.5, 9.1, 4.7, 1H), 1.97 (dt, *J* = 14.6, 3.2, 1H), 1.86 (d, 7.1, 3H), 1.82 (dd, *J* = 9.8, 3.1, 1H), 0.69 (s, 9H), –0.21 (s, 3H), –0.24 (s, 3H); ^{13}C NMR (125 MHz, $CDCl_3$): δ 182.8, 154.4, 148.9, 141.3, 134.0, 131.86, 131.84, 131.7, 131.1, 128.7, 126.3, 125.8, 124.3, 124.1, 122.1, 64.9, 64.7, 62.2, 58.7, 54.2, 52.3, 47.6, 35.4, 30.6, 30.2, 26.1, 18.4, 14.4, –5.3, –5.5; IR (film): 3376, 2928, 1546, 1467, 1373, 1170, 1071 cm^{-1}; HRMS-APCI (*m/z*) $[M + H]^+$ calcd for $C_{32}H_{44}N_3O_7SSi^+$, 642.2664; found, 642.2617; $[\alpha]^{25.3}_D$ 4.00° (c = 0.1, CH_2Cl_2).



2.43 *2.44*

Furoindoline 2.44. To a solution of diol **2.43** (9.5 mg, 0.0150 mmol, 1.0 equiv) in MeOH (1.4 mL) was added K_2CO_3 (20.0 mg, 1.50 mmol, 1.5 equiv) and MeI (1.5 mL, 22.0 mmol, 22.0 equiv). The reaction was heated to 55 °C. After stirring for 4 h, the reaction was cooled to 23 °C and concentrated under reduced pressure. The crude solid was washed with EtOAc (5 x 2 mL) and the organic wash was filtered over a plug of silica (2 g). The filtrate was concentrated under reduced pressure and purified via column chromatography (1:1 hexanes:EtOAc) to afford furoindoline **2.44** (6.4 mg, 66% yield) as a colorless oil. Furoindoline **2.44**: R_f 0.60 (EtOAc); ^{1}H NMR (500 MHz, $CDCl_3$): δ 8.08–8.02 (m, 1H), 7.75–7.65 (m, 2H), 7.63–7.57 (m, 1H), 7.21–7.14 (m, 2H), 6.76 (td, *J* = 7.5, 1.0, 1H), 6.71 (d, *J* = 8.4, 1H), 5.51 (q, *J* = 7.0, 1H), 4.84–4.78 (m, 1H), 4.28 (dd, *J* = 10.8, 3.6, 1H), 4.22–4.12 (m, 2H), 3.83 (d, *J* = 7.5, 1H), 3.68 (dt, *J* = 14.7, 2.1, 1H), 3.55 (ddd, *J* = 10.0, 8.1, 4.6, 1H), 3.46 (d, *J* = 7.2, 1H), 3.42 (s, 1H), 2.95 (s, 3H), 2.79 (m, 1H), 2.47 (dt, *J* = 14.2, 3.9, 1H), 2.19 (ddd, *J* = 14.3, 7.7, 4.6, 1H), 2.03 (ddd, *J* = 14.3, 8.2, 7.0, 1H), 1.83 (dd, *J* = 7.1, 2.3, 3H), 1.72 (t, *J* = 4.4, 1H), 1.64 (dt, *J* = 14.1, 2.4, 1H), 0.79 (s, 9H), –0.09 (s, 3H), -0.11 (s, 3H); ^{13}C NMR (125 MHz, $CDCl_3$): δ 151.9, 148.8, 135.3, 134.1, 133.7, 132.2, 131.2, 131.0, 127.6, 124.6, 124.0, 121.6, 118.8, 110.5, 106.8, 75.4, 62.5, 60.7, 58.8, 56.5, 52.2, 48.2, 33.8, 33.5, 30.5, 27.3, 26.0, 18.4, 13.8, –5.3, –5.4; IR (film): 3438, 2928, 1542, 1470, 1371, 1071 cm^{-1}; HRMS-APCI (*m/z*) $[M + H]^+$ calcd for $C_{33}H_{46}N_3O_7SSi^+$, 656.2820; found, 656.2777; $[\alpha]^{27.6}_D$ 14.00° (c = 0.1, CH_2Cl_2).

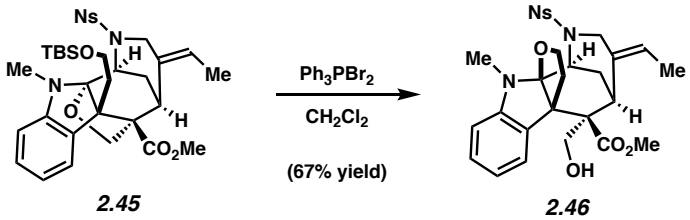


Ester 2.45. To a solution of furoindoline **2.44** (7.2 mg, 0.011 mmol, 1.0 equiv) in CH_2Cl_2 (1.0 mL) was added Dess–Martin periodinane (5.8 mg, 0.014 mmol, 1.3 equiv). After stirring for 20 min, the reaction was quenched with sat. aq. $Na_2S_2O_3$ (1.5 mL) and diluted with CH_2Cl_2 (1.5 mL). The layers were separated and the aqueous layer was extracted with CH_2Cl_2 (3 x 1.5 mL). The organic layers were combined, dried over Na_2SO_4, and evaporated under reduced pressure. The crude residue was purified via flash chromatography (1:1 hexanes:EtOAc) to afford the corresponding furoindoline aldehyde.

To a solution of the furoindoline aldehyde in *t*-butanol (0.24 mL), 2-methyl-2-butene (2.0 M in THF, 0.24 mL), and deionized water (0.24 mL), was added $NaClO_2$ (3.7 mg, 0.040 mmol, 5.5 equiv), and NaH_2PO_4 (5.7 mg, 0.048 mmol, 6.5 equiv). After stirring for 14 h, the reaction was diluted with deionized water (2 mL) and CH_2Cl_2 (2 mL). The layers were separated and the aqueous layer was extracted with CH_2Cl_2 (3 x 2 mL). The organic layers were combined, dried over Na_2SO_4, and evaporated under reduced pressure. The corresponding furoindoline carboxylic acid intermediate was used in the subsequent step without further purification.

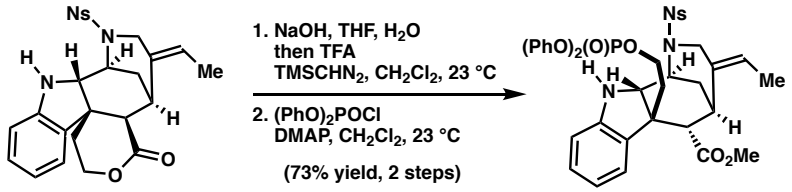
To a solution of the crude furoindoline carboxylic acid in THF (0.5 mL) and methanol (0.3 mL) was added $TMSCHN_2$ (0.6 M in THF, 0.020 mL, 0.12 mmol, 1.6 equiv). After stirring for 40 min, the reaction was quenched with deionized water (1.5 mL) and diluted with CH_2Cl_2 (1.5 mL). The layers were separated and the aqueous layer was extracted with CH_2Cl_2 (3 x 1.5 mL). The organic layers were combined, dried over Na_2SO_4, and evaporated under reduced pressure. The crude material was purified via preparative thin layer chromatography (1:4

hexanes:EtOAc) to afford ester **2.45** (2.2 mg, 29% yield, 3 steps) as a colorless oil. Ester **2.45**: R_f 0.75 (1:3 hexanes:EtOAc); ^{1}H NMR (500 MHz, $CDCl_3$): (42 of 45 protons observed) δ 8.10–8.04 (m, 1H), 7.76–7.64 (m, 2H), 7.63–7.57 (m, 1H), 7.20–7.12 (m, 2H), 6.75 (td, *J* = 7.5, 0.8, 1H), 6.68 (d, *J* = 8.2, 1H), 5.54 (q, *J* = 6.8, 1H), 4.84 (s, 1H), 4.20 (d, *J* = 14.3, 1H), 3.87 (d, *J* = 7.7, 1H), 3.80 (s, 3H), 3.70 (d, *J* = 14.3, 1H), 3.58–3.45 (m, 3H), 3.08 (ddd, *J* = 11.0, 9.7, 4.9, 1H), 2.94 (s, 3H), 2.57 (dt, *J* = 14.2, 3.9, 1H), 2.47 (ddd, *J* = 14.2, 10.9, 4.9, 1H), 2.39 (ddd, *J* = 14.2, 11.0, 5.4, 1H), 1.67 (dt, *J* = 14.2, 2.4, 1H), 0.74 (s, 9H), –0.16 (s, 3H), –0.18 (s, 3H); ^{13}C NMR (125 MHz, $CDCl_3$): δ 172.1, 151.9, 148.9, 134.7, 134.2, 133.9, 132.5, 131.4, 130.9, 127.8, 124.1, 123.8, 123.0, 119.6, 110.1, 106.9, 73.2, 60.8, 58.7, 58.1, 52.3, 51.7, 48.4, 38.4, 34.8, 30.3, 27.5, 26.2, 18.4, 13.3, –5.1, –5.2; IR (film): 2955, 2928, 2853, 1741, 1542, 1470, 1371, 1254, 1172, 1075 cm^{-1}; HRMS-APCI (*m/z*) $[M + H]^+$ calcd for $C_{34}H_{46}N_3O_8SSi^+$, 684.2769; found, 684.2732; $[\alpha]^{29.2}_D$ 8.00° (c = 0.1, CH_2Cl_2).



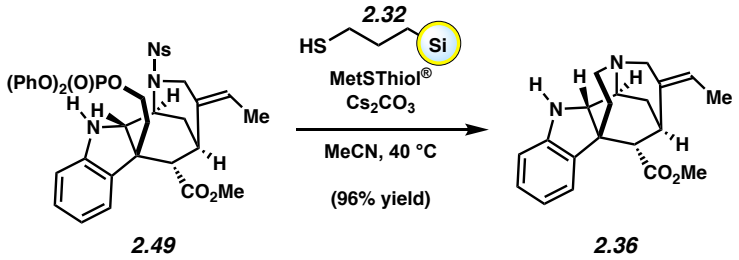
Furoindoline isomer 2.46. To a solution of ester **2.45** (2.7 mg, 0.039 mmol, 1.0 equiv) in CH_2Cl_2 (0.4 mL) was added Ph_3PBr_2 (8.3 mg, 0.20 mmol, 0.5 equiv). After stirring for 20 min, the reaction was quenched with deionized water (1.5 mL) and diluted with CH_2Cl_2 (1.5 mL). The layers were separated and the aqueous layer was extracted with CH_2Cl_2 (3 x 1.5 mL). The organic layers were combined, dried over Na_2SO_4, and evaporated under reduced pressure. The crude mixture was purified via preparative thin layer chromatography (1:3 hexanes:EtOAc) to afford furoindoline isomer **2.46** (1.5 mg, 67% yield) as a colorless oil. Furoindoline isomer **2.46**: R_f 0.70

(1:3 hexanes:EtOAc); ^{1}H NMR (500 MHz, $CDCl_3$): δ 8.16–8.09 (m, 1H), 7.71–7.64 (m, 3H), 7.36–7.32 (m, 1H), 7.17 (td, *J* = 7.7, 1.3, 1H), 6.77 (td, *J* = 7.5, 1.0, 1H), 6.54 (dd, *J* = 8.0, 1.0, 1H), 5.48 (q, *J* = 6.8, 1H), 4.62 (t, *J* = 3.5, 1H), 4.10 (dt, *J* = 14.7, 2.3, 1H), 4.00 (t, *J* = 8.2, 1H), 3.77 (s, 3H), 3.72 (d, *J* = 14.7, 1H), 3.65 (dd, *J* = 11.7, 4.1, 1H), 3.62 (t, *J* = 3.4, 1H), 3.28 (ddd, *J* = 11.5, 8.6, 5.8, 1H), 3.16 (dd, *J* = 11.6, 8.9, 1H), 2.88 (s, 3H), 2.67 (ddd, *J* = 13.1, 11.4, 8.0, 1H), 2.53 (dd, *J* = 13.2, 5.6, 1H), 2.14 (dt, *J* = 14.3, 3.2, 1H), 1.79 (dt, *J* = 14.3, 3.7, 1H), 1.66 (dd, *J* = 6.9, 2.1, 3H), 1.64–1.61 (m, 1H); ^{13}C NMR (125 MHz, $CDCl_3$): δ 173.9, 151.9, 147.9, 134.1, 133.3, 131.73, 131.70, 131.2, 130.1, 129.3, 126.0, 125.2, 124.7, 119.2, 108.7, 105.1, 68.2, 67.1, 57.5, 56.6, 51.9, 51.4, 49.7, 39.4, 30.8, 30.4, 26.9, 13.5; IR (film): 3545, 2950, 2925, 1742, 1720, 1542, 1490, 1351, 1163, 1125 cm^{-1}; HRMS-APCI (*m/z*) $[M + H]^+$ calcd for $C_{28}H_{32}N_3O_8S^+$, 570.1905; found, 570.1863; $[\alpha]^{29.5}_D$ –50.00° (c = 0.1, CH_2Cl_2).

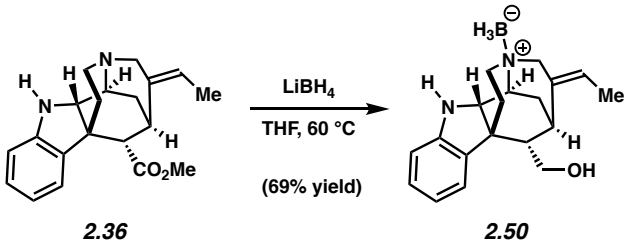


Phosphate ester 2.49. To a solution of indoline lactone **2.6** (50.0 mg, 0.10 mmol, 1.0 equiv) in THF (5.0 mL) was added aq. NaOH (0.5 M, 5.0 mL). After stirring for 14 h at 23 °C, the reaction was neutralized with TFA (190 μL) and diluted with brine (2.0 mL) and CH_2Cl_2 (2.0 mL). The aqueous layer was removed by pipette and $TMSCHN_2$ (0.6 M in hexanes, 3.30 mL, 1.98 mmol, 20.0 equiv) was added. The reaction was stirred at 23 °C for 30 min then dried over Na_2SO_4. The solution was concentrated under reduced pressure and the crude mixture was purified via flash chromatography (1:1 EtOAc:hexanes) to afford the corresponding ester.

To a solution of the ester in CH_2Cl_2 (8.0 mL), was added diphenyl phosphoryl chloride (26 μL, 0.13 mmol, 1.5 equiv), triethylamine (29 μL, 0.20 mmol, 2.5 equiv), and DMAP (2.5 mg, 0.021 mmol, 0.5 equiv). After stirring for 1 h at 23 °C, additional diphenyl phosphoryl chloride (26 μL, 0.13 mmol, 1.5 equiv), triethylamine (29 μL, 0.20 mmol, 2.5 equiv), and DMAP (2.5 mg, 0.021 mmol, 0.5 equiv) were added and the reaction was stirred for 1 h. Then the reaction was concentrated under reduced pressure and the crude material was purified by flash chromatography (1:1:18 acetone:CH_2Cl_2:benzene) to afford phosphate ester **2.49** (55.9 mg, 73% yield, 2 steps) as a colorless oil. Phosphate ester **2.49**: R_f 0.70 (1:1 hexanes:EtOAc); ^{1}H NMR (500 MHz, $CDCl_3$): δ 8.01–7.95 (m, 1H), 7.76–7.68 (m, 2H), 7.62–7.57 (m, 1H), 7.36–7.28 (m, 4H), 7.22–7.12 (m, 6H), 7.06–6.98 (m, 2H), 6.68 (t, *J* = 7.3, 1H), 6.61 (d, *J* = 7.6, 1H), 5.49 (q, *J* = 7.1, 1H), 4.37–4.28 (m, 1H), 4.21 (br s, 1H), 4.17–3.96 (m, 4H), 3.77 (d, *J* = 13.9, 1H), 3.17 (s, 3H), 3.04 (br s, 1H), 2.93 (dt, *J* = 14.2, 2.5, 1H), 2.86 (br s, 1H), 2.68–2.58 (m, 1H), 2.38–2.28 (m, 1H), 1.71–1.62 (m, 4H); ^{13}C NMR (125 MHz, $CDCl_3$): δ 173.6, 150.6 (t, *J* = 6.6), 149.8, 149.0, 134.7, 134.2, 131.7, 131.0, 130.9, 130.7, 129.9, 128.9, 125.3, 124.4, 124.2, 123.4, 120.3 (t, *J* = 4.9), 119.0, 110.1, 66.5 (d, *J* = 6.3), 65.0, 53.9, 52.2, 51.4, 48.3, 45.2, 40.4 (d, *J* = 6.9), 28.6, 19.8, 13.4; ^{31}P NMR (202 MHz, $CDCl_3$): δ –12.4; IR (film): 2923, 1735, 1590, 1543, 1487, 1189, 1163, 1024 cm^{-1}; HRMS-APCI (*m/z*) $[M + H]^+$ calcd for $C_{38}H_{39}N_3O_{10}PS^+$, 760.2088; found, 760.2043; $[\alpha]^{25.9}_D$ – 2.0° (c = 0.1, CH_2Cl_2).

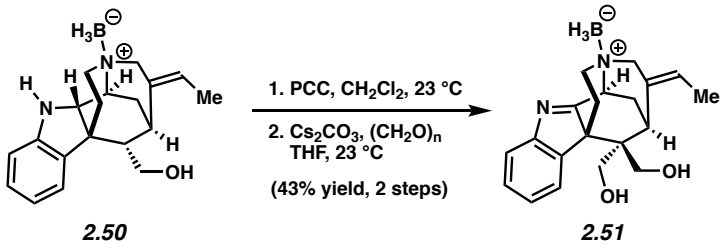


Methanoquinolizidine 2.36. To a solution of phosphate ester **2.49** (8.5 mg, 0.011 mmol, 1.0 equiv) and Cs_2CO_3 (15.0 mg, 0.045 mmol, 4.0 equiv) in MeCN (1.0 mL) was added SiliaMetS Thiol® **2.32** (0.033 mmol, 3.0 equiv). The reaction was heated to 40 °C. After stirring for 46 h, the reaction was cooled to 23 °C, and filtered through a plug of Celite® (1 g). The plug was washed with MeCN (15 mL) and the filtrate was concentrated under reduced pressure. The crude mixture was purified via flash chromatography (1:19 MeOH:$CHCl_3$) to afford methanoquinolizidine **2.36** (3.5 mg, 96% yield) as a colorless oil. Methanoquinolizidine **2.36** is characterized above, vide supra.



Indoline alcohol 2.50. To two separate solutions of ester **2.36** (35.3 mg, 0.109 mmol, 1.0 equiv) in THF (10.9 mL each) was added $LiBH_4$ (47.4 mg, 2.18 mmol each, 20.0 equiv). The mixtures were each heated to 60 °C. Additional aliquots of $LiBH_4$ (47.4 mg, 2.18 mmol each, 20.0 equiv) were added to each mixture after 14, 24, 27, and 30 h. After stirring for 32 h total, the reactions were cooled to 23 °C and poured into deionized water (30 mL each) and diluted with CH_2Cl_2 (30 mL). The layers were separated and the aqueous layer was extracted with CH_2Cl_2 (3 x 30 mL). The organic layers were combined, dried over Na_2SO_4, and evaporated under reduced pressure. The crude mixtures were combined and purified via flash chromatography (4:1 → 7:3

hexanes:EtOAc) to afford indoline alcohol **2.50** (46.2 mg total, 69% yield) as a colorless oil. Indoline alcohol **2.50**: R_f 0.70 (1:1 hexanes:EtOAc); ^{1}H NMR (500 MHz, $CDCl_3$): δ 7.14 (t, *J* = 7.5, 1H), 7.04 (d, *J* = 7.1, 1H), 6.92 (t, *J* = 7.5, 1H), 6.83 (d, *J* = 7.7, 1H), 5.49 (q, *J* = 6.8, 1H), 4.04–4.11 (m, 2H), 4.01 (br s, 1H), 3.92 (t, *J* = 3.7, 1H), 3.54–3.67 (m, 1H), 3.20–3.31 (m, 3H), 3.05–3.13 (m, 1H), 2.90 (dd, *J* = 15.0, 7.7, 1H), 2.34–2.51 (m, 3H), 2.27 (dd, *J* = 7.0, 4.0, 1H), 1.97 (d, *J* = 14.6, 1H), 1.76 (t, *J* = 4.8, 1H), 1.68 (dd, *J* = 7.1, 2.0, 3H); ^{13}C NMR (125 MHz, $CDCl_3$): (18 of 19 signals observed) δ 149.8, 137.7, 136.9, 128.2, 122.8, 121.7, 121.3, 112.2, 64.8, 61.6, 60.0, 56.3, 53.5, 41.8, 35.2, 29.9, 20.3, 13.1; ^{11}B NMR (160 MHz, $CDCl_3$): δ 6.8; IR (film): 3330, 2924, 2354, 1463, 1168, 1011, 746 cm^{-1}; HRMS-APCI (*m/z*) $[M - H]^-$ calcd for $C_{19}H_{26}BN_2O^-$, 309.2144; found, 309.2139; $[\alpha]^{24.3}_D$ –42.0° (c = 0.1, CH_2Cl_2).

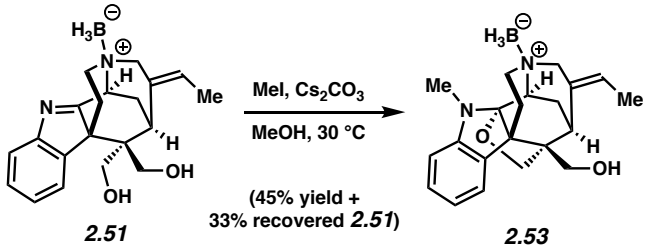


2.50 ***2.51***

Diol 2.51. To a solution of indoline alcohol **2.50** (9.3 mg, 0.030 mmol, 1.0 equiv) in CH_2Cl_2 was added PCC (32.0 mg, 0.15 mmol, 5.0 equiv) and Celite® (30 mg). The reaction mixture was stirred at 23 °C for 2 h. The mixture was filtered over a pad of Celite® (1 g) and basic alumina (2 g), and then washed with 75% EtOAc in hexanes (12 mL). Evaporation of the solvent under reduced pressure afforded the corresponding indolenine aldehyde intermediate, which was used in the subsequent step without further purification.

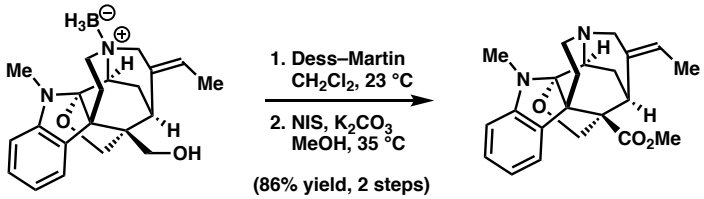
To a solution of the crude indolenine aldehyde in THF (3.0 mL) was added Cs_2CO_3 (39.0 mg, 0.121 mmol, 4.0 equiv) and paraformaldehyde (8.2 mg, 0.273 mmol, 9.0 equiv). The reaction

mixture was stirred at 23 °C for 16 h, at which point it was poured into sat. aq. NaCl (5 mL) and diluted with EtOAc (5 mL). The layers were separated and the aqueous layer was extracted with EtOAc (3 x 5 mL). The organic layers were combined, dried over $MgSO_4$, and evaporated under reduced pressure. The resulting residue was purified via flash chromatography (4:1 → 1:2 hexanes:EtOAc) to afford diol **2.51** (4.4 mg, 43% yield, 2 steps) as a colorless oil. Diol **2.51**: R_f 0.20 (1:1 hexanes:EtOAc); ^{1}H NMR (500 MHz, $CDCl_3$): δ 7.71 (d, *J* = 7.8, 1H), 7.50 (d, *J* = 7.6, 1H), 7.42 (t, *J* = 7.6, 1H), 7.26 (d, *J* = 7.5, 1H), 5.73 (q, *J* = 7.2, 1H), 4.79 (d, *J* = 4.2, 1H), 4.30 (dd, *J* = 10.8, 4.2, 1H), 4.20–4.28 (m, 2H), 3.49 (d, *J* = 17.0, 1H), 3.39 (br s, 1H), 3.07 (dd, *J* = 12.3, 3.1, 1H), 2.88–3.02 (m, 3H), 2.74 (tdd, *J* = 13.9, 4.6, 1.5, 1H), 2.51 (ddd, *J* = 15.0, 4.2, 2.7, 1H), 2.43 (dd, *J* = 5.8, 4.2, 1H), 1.97 (d, *J* = 15.0, 1H), 1.87 (dd, *J* = 7.2, 2.7, 3H), 1.73 (dd, *J* =14.7, 5.4, 1H), 1.60 (dd, *J* =9.8, 3.2, 1H); ^{13}C NMR (125 MHz, $CDCl_3$): δ 184.3, 155.5, 143.5, 133.7, 129.2, 126.5, 124.2, 123.6, 122.6, 64.4, 64.2, 62.4, 61.9, 59.7, 56.9, 52.0, 30.8, 29.7, 28.1, 14.0; ^{11}B NMR (160 MHz, $CDCl_3$): δ 6.8; IR (film): 3332, 2922, 2854, 2378, 1450, 1170, 1016, 751 cm^{-1}; HRMS-APCI (*m/z*) $[M - H]^-$ calcd for $C_{20}H_{26}BN_2O_2^-$, 337.2093; found, 337.2085; $[\alpha]^{24.5}_D$ 68.0° (c = 0.1, CH_2Cl_2).



Furoindoline 2.53. To a solution of diol **2.51** (4.5 mg, 0.013 mmol, 1.0 equiv) in MeOH (0.2 mL) was added Cs_2CO_3 (43.0 mg, 0.13 mmol, 10.0 equiv) and MeI (1.0 mL, 16 mmol, 1200 equiv). The reaction was heated to 30 °C. After stirring for 18 h, the reaction was cooled to 23 °C and

poured into brine (0.5 mL) and diluted with CH_2Cl_2 (0.5 mL). The layers were separated and the aqueous layer was extracted with CH_2Cl_2 (5 x 1 mL). The organic layers were combined, dried over Na_2SO_4, and evaporated under reduced pressure. The crude mixture was purified via preparative thin layer chromatography (3:7 hexanes:EtOAc) to afford furoindoline **2.53** (2.1 mg, 45% yield) as a colorless oil and diol **2.51** (1.5 mg, 33% yield). Furoindoline **2.53**: R_f 0.60 (1:1 hexanes:EtOAc); ^{1}H NMR (500 MHz, $CDCl_3$): δ 7.17 (t, *J* = 7.7, 1H), 7.08 (d, *J* = 7.5, 1H), 6.78 (t, *J* = 7.5, 1H), 6.68 (d, *J* = 7.8, 1H), 5.51 (q, *J* = 6.9, 1H), 4.39 (dd, *J* = 10.2, 3.5, 1H), 4.34 (br s, 1H), 4.08 (dd, *J* = 10.2, 4.5, 1H), 4.01 (d, *J* = 16.5, 1H), 3.97 (d, *J* = 7.7, 1H), 3.78 (td, *J* = 14.0, 4.1, 1H), 3.57 (d, *J* = 7.7, 1H), 3.52 (br s, 1H), 3.15 (d, *J* = 17.0, 1H), 2.98 (td, *J* = 15.1, 5.5, 1H), 2.90 (s, 3H), 2.77 (dd, *J* = 13.1, 5.2, 1H), 2.32 (d, *J* = 14.8, 1H), 2.04 (d, *J* = 14.2, 1H), 1.85 (dd, *J* = 7.1, 1.9, 3H), 1.45 (t, *J* = 4.1, 1H), 1.34 (dd, *J* = 15.9, 4.9, 1H); ^{13}C NMR (125 MHz, $CDCl_3$): δ 151.2, 137.9, 137.6, 128.1, 123.5, 120.3, 120.2, 110.6, 103.4, 63.7, 61.2, 60.7, 58.1, 55.9, 52.4, 34.1, 29.9, 29.3, 28.7, 26.3, 13.5; ^{11}B NMR (160 MHz, $CDCl_3$): δ 7.7; IR (film): 3455, 2922, 1556, 1454, 1375, 1095 cm^{-1}; HRMS-APCI (*m/z*) $[M - H]^-$ calcd for $C_{21}H_{28}BN_2O_2^-$, 351.2249; found, 351.2237; $[\alpha]^{24.7}_D$ –13.3° (c = 0.1, CH_2Cl_2).



2.53 ***(–)-Ψ-Akuammigine (2.4)***

(–)-Ψ-Akuammigine (2.4). To a solution of furoindoline **2.53** (1.0 mg, 0.0028 mmol, 1.0 equiv) in CH_2Cl_2 (0.3 mL) was added Dess–Martin periodinane (2.4 mg, 0.0057 mmol, 2.0 equiv). The reaction mixture was stirred at 23 °C for 1 h. The reaction was quenched with sat. aq. $Na_2S_2O_3$ (1

mL) and diluted with CH_2Cl_2 (0.5 mL). The resulting layers were separated and the aqueous layer was extracted with CH_2Cl_2 (5 x 1 mL). The organic layers were combined, dried over Na_2SO_4, and concentrated under reduced pressure. The crude residue was purified via flash chromatography (4:1 hexanes:EtOAc) to afford the corresponding indolenine aldehyde.

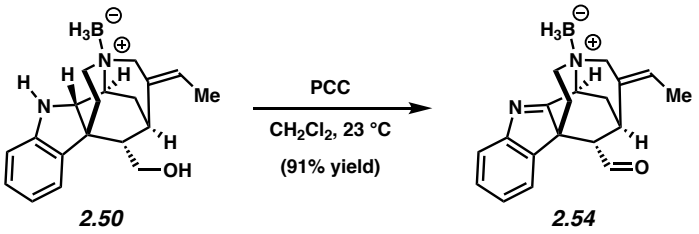
To a solution of the indolenine aldehyde in MeOH (0.3 mL) was added K_2CO_3 (7.9 mg, 0.057 mmol, 20.0 equiv) and NIS (12.8 mg, 0.057 mmol, 20.0 equiv). Following 3 h of stirring at 35 °C, additional K_2CO_3 (7.9 mg, 0.057 mmol, 20.0 equiv) and NIS (12.8 mg, 0.057 mmol, 20.0 equiv) were added. Following 5 h of additional stirring at 35 °C, the reaction was quenched with sat. aq. $Na_2S_2O_3$ (0.5 mL) and aq. NaOH (15%, 0.5 mL) and diluted with CH_2Cl_2 (1.0 mL). The layers were separated and the aqueous layer was extracted with CH_2Cl_2 (5 x 1 mL). The organic layers were combined, dried over Na_2SO_4, and evaporated under reduced pressure. The resulting residue was purified via flash chromatography (0:100 → 1:4 MeOH:$CHCl_3$) to afford (–)-Ψ-Akuammigine (**2.4**) (0.9 mg, 86% yield, 2 steps) as a colorless oil.

* The tertiary amine of (–)-Ψ-Akuammigine (**2.4**) causes significant pH-dependent variation in chemical shifts during NMR analysis. In order to observe consistent NMR data, the natural product (~1 mg) was partitioned between 15% aq. NaOH (1 mL) and $CHCl_3$ (1 mL; pre-basified with K_2CO_3). The layers were separated and the aqueous layer was extracted with $CHCl_3$ (3 x 1 mL). The organic layers were combined, dried over Na_2SO_4, and evaporated under reduced pressure. The NMR spectra were obtained using $CDCl_3$, which had been filtered over basic alumina immediately prior to use. Spectral data for synthetic **2.4** were consistent with literature reports[46] and a natural sample provided by L. Evanno. (–)-Ψ-Akuammigine (**2.4**): R_f 0.40 (1:9 MeOH:$CHCl_3$); ^{1}H NMR (500 MHz, $CDCl_3$): δ 7.12 (td, *J* = 7.3, 1.3, 1H), 7.07 (dd, *J* = 7.7, 1.2, 1H), 6.73 (td, *J* = 7.5, 1.0, 1H), 6.64 (d, *J* = 7.8, 1H), 5.40 (q, *J* = 7.0, 1H), 4.18 (br s, 1H), 3.95

(d, J = 7.5, 1H), 3.92 (m, 1H, partially overlapped with the signal at 3.95), 3.82 (s, 3H), 3.59 (d, J = 7.6, 1H), 3.58 (m, 1H, partially overlapped with the signal at 3.59), 3.48 (br s, 1H), 3.31 (td, J = 14.3, 6.0, 1H), 2.83 (s, 3H), 2.82 (d, J = 16.6, 1H, partially overlapped with the signal at 2.83), 2.57 (dd, J = 13.4, 5.7, 1H), 2.31 (d, J = 14.7, 1H), 2.06 (ddd, J = 14.0, 3.7, 2.0, 1H), 1.52 (dd, J = 7.1, 2.5, 3H), 1.45 (dd, J = 15.3, 4.6, 1H); ^{13}C NMR (125 MHz, $CDCl_3$): δ 172.3, 151.9, 142.4, 139.4, 127.5, 122.6, 120.0, 118.4, 110.0, 104.0, 74.5, 58.5, 54.7, 53.8, 52.8, 52.1, 50.9, 41.1, 31.4, 29.1, 28.2, 13.1; IR (film): 2922, 2854, 1738, 1467, 1455, 1276, 1259, 1107, 1075 cm^{-1}; HRMS-APCI (*m/z*) [M + H] $^{+}$ calcd for $C_{22}H_{27}N_2O_3^{+}$, 367.2016; found, 367.1993; $[\alpha]^{25.4}_D$ –14.0° (c = 0.1, CH_2Cl_2).

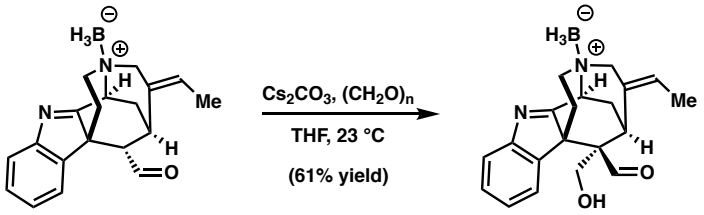
Table 2.3. Comparison of ^{13}C NMR data for natural vs. synthetic (–)-Ψ-akuammigine (**2.4**).

Natural (–)-Ψ-Akuammigine (**2.4**) (From Hesse, et. al. Report)[46] ^{13}C NMR, 50.4 MHz, $CDCl_3$	Synthetic (–)-Ψ-Akuammigine (**2.4**) ^{13}C NMR, 125 MHz, $CDCl_3$
172.8	172.3
151.9	151.9
142.6	142.4
139.4	139.4
127.3	127.5
122.4	122.6
119.9	120.0
118.0	118.3
109.8	110.0
103.8	104.0
74.3	74.5
58.4	58.5
54.5	54.7
53.7	53.8
52.7	52.8
51.7	52.1
50.8	50.9
41.0	41.1
31.4	31.4
28.6	29.1
28.0	28.2
12.8	13.1



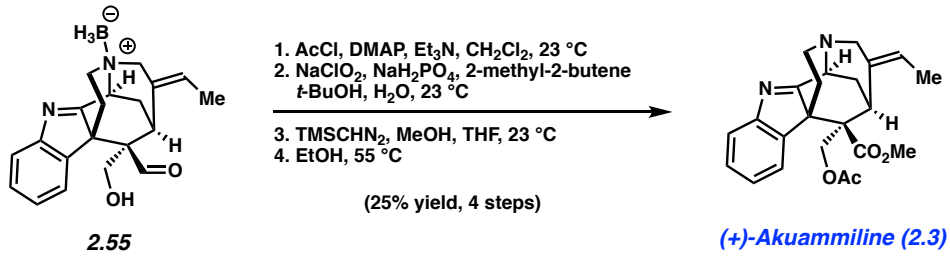
2.50 *2.54*

Aldehyde 2.54. To solution of indoline alcohol **2.50** (20.0 mg, 0.064 mmol, 1.0 equiv) in CH_2Cl_2 (6.0 mL), was added PCC (69.0 mg, 0.32 mmol, 5.0 equiv). After stirring for 2 h at 23 °C, the reaction was filtered over basic alumina (2 g) and eluted with EtOAc (20 mL). The solution was concentrated under reduced pressure and the crude material was purified by flash chromatography (7:3 hexanes:EtOAc) to afford aldehyde **2.54** (18 mg, 91% yield) as a colorless oil. Aldehyde **2.54**: R_f 0.50 (1:1 hexanes:EtOAc); ^{1}H NMR (500 MHz, $CDCl_3$): δ 8.64 (d, *J* = 2.8, 1H), 7.73 (d, *J* = 7.7, 1H), 7.43 (td, *J* = 7.6, 1.2, 1H), 7.40 (d, *J* = 7.7, 1H), 7.30 (td, *J* = 7.5, 0.9, 1H), 5.65 (q, *J* = 7.1, 1H), 4.93 (d, *J* = 4.6, 1H), 4.22 (d, *J* = 16.7, 1H), 3.50 (d, *J* = 16.5, 1H), 3.38 (br s, 1H), 3.19 (q, *J* = 2.0, 1H), 3.02–3.13 (m, 2H), 2.83–2.92 (m, 1H), 2.65 (dquint, *J* = 15.7, 2.5, 1H), 1.99–2.09 (m, 2H), 1.80 (dd, *J* = 7.0, 2.7, 3H); ^{13}C NMR (125 MHz, $CDCl_3$): δ 200.1, 183.7, 155.2, 142.9, 134.9, 129.4, 127.2, 122.7, 122.5, 122.4, 62.6, 62.3, 61.3, 59.8, 52.3, 34.4, 31.2, 29.2, 13.1; ^{11}B NMR (160 MHz, $CDCl_3$): δ 6.4; IR (film): 2920, 2364, 1721, 1448, 1170, 750 cm^{-1}; HRMS-APCI (*m/z*) $[M - H]^-$ calcd for $C_{19}H_{22}BN_2O^-$, 295.1805; found, 295.1788; $[\alpha]^{22.1}_D$ – 81.3° (c = 0.1, CH_2Cl_2).



2.54 *2.55*

Alcohol 2.55. To a solution of aldehyde **2.54** (18.0 mg, 0.059 mmol) in THF (6.0 mL) was added Cs_2CO_3 (29.0 mg, 0.088 mmol, 1.5 equiv) and paraformaldehyde (2.0 mg, 0.068 mmol, 1.2 equiv). After stirring for 12 h, the reaction was filtered over Na_2SO_4 (2 g) and eluted with CH_2Cl_2 (20 mL). The volatiles were evaporated under reduced pressure and the crude mixture was purified via flash chromatography (1:1 hexanes:EtOAc) to afford alcohol **2.55** (12 mg, 61% yield) as a colorless oil. Alcohol **2.55**: R_f 0.20 (1:1 hexanes:EtOAc); ^{1}H NMR (500 MHz, C_6D_6): δ 9.69 (s, 1H), 7.69 (d, J = 7.7, 1H), 7.52 (d, J = 7.6, 1H), 7.07 (td, J = 7.7, 1.1, 1H), 6.94 (td, J = 7.6, 1.0, 1H), 4.98 (d, J = 4.3, 1H), 4.76 (q, J = 7.2, 1H), 3.93 (d, J = 16.9, 1H), 3.22 (br s, 1H), 3.02 (d, J = 16.9, 1H), 2.85 (td, J = 15.2, 5.5, 1H), 2.55 (d, J = 7.2, 1H), 2.47–2.52 (m, 1H), 2.36–2.43 (m, 2H), 1.84 (ddd, J = 15.2, 4.9, 3.0, 1H), 1.31–1.45 (m, 2H), 1.20 (dd, J = 7.1, 2.8, 3H), 0.20 (dd, J = 6.3, 4.1, 1H); ^{13}C NMR (125 MHz, C_6D_6): (19 of 20 signals observed) δ 201.8, 183.3, 156.5, 143.7, 134.1, 126.5, 125.5, 122.4, 120.8, 63.7, 62.1, 61.6, 61.2, 59.9, 55.5, 30.3, 29.3, 28.4, 14.2; ^{11}B NMR (160 MHz, C_6D_6): δ 6.3; IR (film): 3310, 2923, 2853, 1721, 1444, 1169, 1030 cm^{-1}; HRMS-APCI (*m/z*) [M – H]$^-$ calcd for $C_{20}H_{24}BN_2O_2^-$, 335.1936; found, 335.1927; $[\alpha]^{24.7}_D$ –2.0° (c = 0.1, CH_2Cl_2).



2.55 *(+)-Akuammiline (2.3)*

(+)-Akuammiline 2.3. A stock solution of acetyl chloride (51 μL, 0.71 mmol, 20.0 equiv), triethylamine (250 μL, 1.8 mmol, 50.0 equiv), and DMAP (87.0 mg, 0.71 mmol, 20.0 equiv) in CH_2Cl_2 (36 mL) was prepared. To a separate vial containing alcohol **2.55** (12.0 mg, 0.036 mmol, 1.0 equiv) was added 3.6 mL of the aforementioned stock solution. The reaction was stirred at 23 °C for 15 min and then filtered over Na_2SO_4 (2 g). The solution was concentrated under reduced pressure and the crude product was purified via flash chromatography (1:1 hexanes:EtOAc) to afford the corresponding acetylated product.

To a solution of acetylated product in *t*-butanol (0.70 mL), was added 2-methyl-2-butene (2.0 M in THF, 0.70 mL), water (0.70 mL), $NaClO_2$ (11.0 mg, 0.12 mmol, 6.0 equiv), and NaH_2PO_4 (17.0 mg, 0.14 mmol, 7.0 equiv). After stirring for 12 h, $NaClO_2$ (11.0 mg, 0.12 mmol, 6.0 equiv), and NaH_2PO_4 (17.0 mg, 0.14 mmol, 7.0 equiv) were added. The resultant mixture was stirred for an additional 6 h. Then the reaction was diluted with EtOAc (5 mL) and the layers were separated. The aqueous layer was extracted with EtOAc (3 x 5 mL) and the organic layers were combined, dried over Na_2SO_4, and evaporated under reduced pressure. The corresponding carboxylic acid intermediate was used in the subsequent step without further purification.

To a solution of the crude carboxylic acid in THF (1.0 mL), was added methanol (1.0 mL) and $TMSCHN_2$ (0.6 M in THF, 0.050 mL, 0.030 mmol, 1.5 equiv). After stirring for 15 min, the reaction was quenched with water (2.0 mL) and diluted with CH_2Cl_2 (5.0 mL). The layers were separated and the aqueous layer was extracted with CH_2Cl_2 (3 x 5.0 mL). The organic layers were combined, dried over Na_2SO_4, and evaporated under reduced pressure. The crude material

was purified via flash chromatography (1:1 hexanes:EtOAc) to afford the corresponding methyl ester.

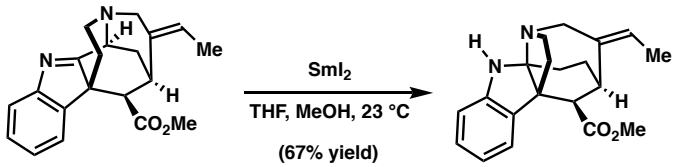
To a vial containing the methyl ester was added ethanol (0.9 mL). The solution was heated to 55 °C and stirred for 7 h. Then the reaction was concentrated under reduced pressure and suspended in EtOAc (2.0 mL) and aq. NaOH (1 M, 2.0 mL). The layers were separated and the aqueous layer was extracted with EtOAc (3 x 5 mL). The organic layers were combined, dried over Na_2SO_4, and evaporated under reduced pressure. The crude mixture was purified via flash chromatography (9:1 acetone:MeOH) to afford (+)-Akuammiline (**2.3**) (2.0 mg, 25% yield, 4 steps) as a colorless oil.

* The tertiary amine of Akuammiline (**2.3**) causes significant pH-dependent variation in chemical shifts during NMR analysis. In order to observe consistent NMR data, the natural product (~1 mg) was partitioned between 1 M NaOH (1 mL) and ethyl acetate (1 mL). The layers were separated and the aqueous layer was extracted with ethyl acetate (3 x 1 mL). The organic layers were combined, dried over Na_2SO_4, and evaporated under reduced pressure. The NMR spectra were obtained using $CDCl_3$, which had been filtered over basic alumina immediately prior to use. Spectral data for synthetic **2.3** were consistent with literature reports[55] and a natural sample provided by L. Evanno. Akuammiline (**2.3**): R_f 0.26 (9:1 acetone:MeOH); ^{1}H NMR (500 MHz, $CDCl_3$): δ 7.64 (d, *J* = 7.5, 1H), 7.58 (d, *J* = 7.8, 1H), 7.29 (t, *J* = 7.5, 1H), 7.15 (t, *J* = 7.8, 1H), 5.49 (q, *J* = 7.4, 1H), 4.62 (d, *J* = 4.8, 1H), 4.10 (d, *J* = 17.2, 1H), 3.76 (s, 3H), 3.64–3.47 (m, 4H), 3.15 (d, *J* = 16.9, 1H), 2.67–2.58 (m, 2H), 2.48 (ddd, *J* = 14.6, 4.9, 2.2, 1H), 2.12 (dd, *J* = 14.9, 3.7, 1H), 1.89 (dd, *J* = 15.4, 3.9, 1H) 1.65 (dd, *J* = 7.0, 2.5, 3H), 1.57 (s, 3H); ^{13}C NMR (125 MHz, $CDCl_3$): δ 189.5, 171.6, 169.5, 155.6, 144.9, 139.4, 128.2, 126.1, 125.5, 121.2, 120.3, 66.3, 59.3, 58.8, 54.6, 54.0, 52.3, 51.9, 37.8, 37.1, 31.0, 20.2, 13.6; IR (film): 2928, 2860, 1738,

1445, 1237, 753 cm^{-1}; HRMS-APCI (*m/z*) $[M + H]^+$ calcd for $C_{23}H_{27}N_2O_4^+$, 395.1965; found, 395.1944. $[\alpha]^{23.7}_D$ 50.0° (c = 0.1, MeOH).

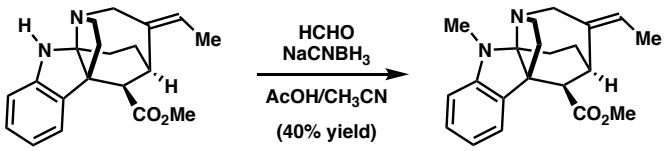
Table 2.4. Comparison of ^{13}C NMR data for natural vs. synthetic (+)-akuammiline (**2.3**).

Natural (+)-Akuammiline (**2.3**) (From Benayad, et. al. Report)[55b] ^{13}C NMR, 101 MHz, $CDCl_3$	Synthetic (+)-Akuammiline (**2.3**) ^{13}C NMR, 125 MHz, $CDCl_3$
189.4	189.5
171.5	171.6
169.4	169.5
155.5	155.6
144.9	144.9
139.3	139.4
128.2	128.2
126.1	126.1
125.5	125.5
121.2	121.2
120.3	120.3
66.3	66.3
59.3	59.3
58.8	58.8
54.6	54.6
54.0	54.0
52.3	52.3
51.9	51.9
37.8	37.8
37.1	37.1
31.0	31.0
20.2	20.2
13.6	13.6



(+)-Strictamine (2.1) *2.56*

Pyrrolidinoindoline 2.56. To a solution of (+)-strictamine (**2.1**) (8.6 mg, 0.027 mmol, 1.0 equiv) in MeOH (138 μL) was added SmI_2 (0.37 M in THF, 1.1 mL, 15 equiv). The dark blue solution was stirred at 23 °C and gradually became clear after 30 min. Then the mixture was quenched with sat. aq. $NaHCO_3$ (1.5 mL). The layers were separated and the aqueous layer was extracted with $CHCl_3$ (3 x 1.5 mL). The organic layers were combined, dried over Na_2SO_4, and then concentrated under reduced pressure. The crude residue was purified via column chromatography (acetone) to afford the corresponding pyrrolidinoindoline **2.56** (5.7 mg, 67% yield) as a white film. Pyrrolidinoindoline **2.56**: R_f 0.25 (9:1 acetone:MeOH); ^{1}H NMR (500 MHz, $CDCl_3$): δ 7.27–7.26 (m, 1H), 7.01 (td, *J* = 7.7, 1.1, 1H), 6.66 (td, *J* = 7.5, 1.0, 1H), 6.53 (d, *J* = 7.6, 1H), 5.39 (q, *J* = 6.8, 1H), 3.85 (d, *J* = 15.3, 1H), 3.80 (s, 3H), 3.71–3.66 (m, 1H), 3.64 (d, *J* = 4.9, 1H), 3.52 (td, *J* = 11.4, 8.7, 1H), 2.97 (d, *J* = 15.1, 1H), 2.85 (s, 1H), 2.75 (dd, *J* = 12.0, 9.0, 1H), 2.56–2.49 (m, 1H), 2.33 (ddd, *J* = 14.1, 10.7, 2.5, 1H), 2.05–1.95 (m, 2H), 1.84 (tdd, *J* = 13.8, 5.3, 2.4, 1H), 1.80–1.72 (m, 1H), 1.59 (dd, *J* = 6.9, 1.8, 3H); ^{13}C NMR (125 MHz, $CDCl_3$): δ 173.9, 148.1, 139.3, 137.4, 127.8, 124.7, 122.5, 118.8, 109.1, 94.3, 58.2, 57.6, 55.0, 51.8, 50.8, 41.5, 35.5, 26.6, 26.7, 13.6; IR (film): 2923, 2853, 1734, 1581, 1465, 1436, 743 cm^{-1}; HRMS-APCI (*m/z*) $[M + H]^+$ calcd for $C_{20}H_{25}N_2O_2^+$, 325.19105; found, 325.1874; $[\alpha]^{23.9}_D$ – 48.00° (c = 0.1, CH_2Cl_2).

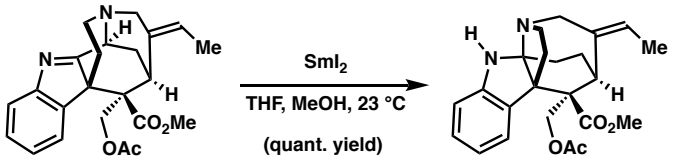


2.56 *(–)-10-Demethoxyvincorine (2.57)*

(–)-10-Demethoxyvincorine 2.57. A stock solution of reagents was prepared by combining MeCN (930 µL), HCHO (37 wt. % in water, 40 µL, 30 equiv), and AcOH (30 µL, 30 equiv). To a solution of pyrrolidinoindoline **2.56** (5.5 mg, 0.017 mmol, 1.0 equiv) in MeCN (0.18 mL) was added 100 µL of stock solution and $NaBH_3CN$ (3.2 mg, 0.051 mmol, 3.0 equiv). The solution was stirred for 60 min at 23 °C. Then the mixture was quenched with sat. aq. $NaHCO_3$ (1.5 mL). The layers were separated and the aqueous layer extracted with $CHCl_3$ (3 x 1.5 mL). The organic layers were combined, dried over Na_2SO_4, and then concentrated under reduced pressure. The crude residue was purified via column chromatography (acetone) to afford (–)-10-Demethoxyvincorine (**2.57**) (2.3 mg, 40% yield) as a white film. Although a natural sample was not obtained, spectral data for synthetic **2.57** were consistent with literature reports.[8] (–)-10-Demethoxyvincorine (**2.57**): R_f 0.28 (1:1 EtOAc:Hexanes); ^{1}H NMR (500 MHz, $CDCl_3$): δ 7.22 (dd, *J* = 7.4, 1.1, 1H), 7.06 (td, *J* = 7.7, 1.3, 1H), 6.57 (td, *J* = 7.4, 1.0, 1H), 6.27 (d, *J* = 7.8, 1H), 5.39 (q, *J* = 6.8, 1H), 3.84–3.76 (m, 4H), 3.60 (d, *J* = 4.7, 1H), 3.31 (td, *J* = 11.4, 8.9, 1H), 2.99 (d, *J* = 15.3, 1H), 2.83 (d, *J* =1.3, 1H), 2.76–2.69 (m, 1H), 2.61 (s, 3H), 2.54–2.44 (m, 1H), 2.36–2.26 (m, 1H), 1.97 (ddd, *J* = 14.0, 8.9, 1.4, 1H), 1.80–1.64 (m, 3H), 1.58 (dd, *J* = 6.9, 1.9, 3H); ^{13}C NMR (125 MHz, $CDCl_3$): δ 174.0, 149.3, 139.4, 137.3, 127.9, 123.7, 122.4, 116.9, 105.4, 97.5, 58.5, 57.2, 55.3, 51.7, 50.9, 41.4, 35.0, 27.4, 26.5, 21.1, 13.7; IR (film): 3049, 2950, 2876, 2855, 1737, 1505, 1487, 1175 cm^{-1}; HRMS-APCI (*m/z*) $[M + H]^+$ calcd for $C_{21}H_{27}N_2O_2^+$, 339.2067; found, 339.2051; $[\alpha]^{24.3}_D$ – 80.00° (c = 0.1, CH_2Cl_2).

Table 2.5. Comparison of ^{13}C NMR data for natural vs. synthetic (–)-10-Demethoxyvincorine (**2.57**).

Natural (–)-10-Demethoxyvincorine (**2.57**) (From Lim, et. al. Report)[8] ^{13}C NMR, 100 MHz, $CDCl_3$	Synthetic (–)-10-Demethoxyvincorine (**2.57**) ^{13}C NMR, 125 MHz, $CDCl_3$
173.8	174.0
149.0	149.3
138.9	139.4
137.0	137.3
127.8	127.9
123.5	123.7
122.4	122.4
116.9	116.9
105.3	105.4
97.4	97.5
58.3	58.5
57.0	57.2
55.0	55.3
51.5	51.7
50.6	50.9
41.0	41.4
34.8	35.0
27.3	27.4
26.2	26.5
20.8	21.1
13.5	13.7



(+)-Akuammiline (2.3) ***2.58***

Pyrrolidinoindoline 2.58. To a solution of (+)-akuammiline (**2.3**) (2.3 mg, 0.0058 mmol, 1.0 equiv) in MeOH (35 µL) was added SmI_2 (0.37 M in THF, 0.24 mL, 15 equiv). The dark blue solution was stirred at 23 °C and gradually became clear after 30 min. Then the mixture was quenched with sat. aq. $NaHCO_3$ (1.5 mL). The layers were separated and the aqueous layer was extracted with $CHCl_3$ (3 x 1.5 mL). The organic layers were combined, dried over Na_2SO_4, and

then concentrated under reduced pressure. The crude residue was purified via column chromatography (acetone) to afford the corresponding pyrrolidinoindoline **2.58** (2.4 mg, quant. yield) as a white film. Pyrrolidinoindoline **2.58**: R_f 0.16 (5% MeOH in acetone); ^{1}H NMR (500 MHz, $CDCl_3$): δ 7.72 (dd, *J* = 7.6,1.0, 1H), 7.01 (td, *J* = 7.6, 1.2, 1H), 6.67 (td, *J* = 7.5, 1.1, 1H), 6.49 (dd, *J* = 7.9, 0.6, 1H), 5.37 (q, *J* = 6.7, 1H), 4.81 (d, *J* = 12.0, 1H), 4.03–3.95 (m, 1H), 3.88 (d, *J* = 12.1, 1H), 3.79 (m, 4H), 3.71 (d, *J* = 4.7, 1H), 3.41–3.22 (m, 1H), 3.02 (d, *J* = 16.1, 1H), 2.71 (dd, *J* = 12.3, 8.3, 1H), 2.47 (ddd, *J* = 14.8, 11.6, 2.3, 1H), 2.15–2.07 (m, 1H), 2.05 (s, 3H), 2.04–1.99 (m, 2H), 1.93 (tdd, *J* = 14.6, 5.3, 2.0, 1H), 1.76 (dd, *J* = 7.0, 2.2, 3H) 1.66–1.61 (m, 1H); ^{13}C NMR (125 MHz, $CDCl_3$): δ 174.1, 170.7, 148.9, 139.6, 131.0, 128.4, 127.9, 123.1, 118.6, 109.3, 92.2, 67.3, 60.7, 58.5, 54.3, 53.9, 52.0, 46.6, 35.3, 28.0, 21.7, 21.2, 14.9; IR (film): 3359, 3193, 2952, 2918, 1744, 1630, 1468, 1247, 1034, 806 cm^{-1}; HRMS-APCI (*m/z*) $[M + H]^+$ calcd for $C_{23}H_{29}N_2O_4^+$, 397.2122; found, 397.2088; $[\alpha]^{21.8}_D$ – 56.00° (c = 0.1, CH_2Cl_2).

2.15 Spectra Relevant to Chapter Two:

Enantioselective Total Syntheses of Methanoquinolizidine-Containing Akuammiline Alkaloids and Related Studies

Elias Picazo,[†] Lucas A. Morrill,[†] Robert B. Susick,

Jesus Moreno, Joel M. Smith, and Neil K. Garg.

J. Am. Chem. Soc. **2018**, *140*, 6483–6492.

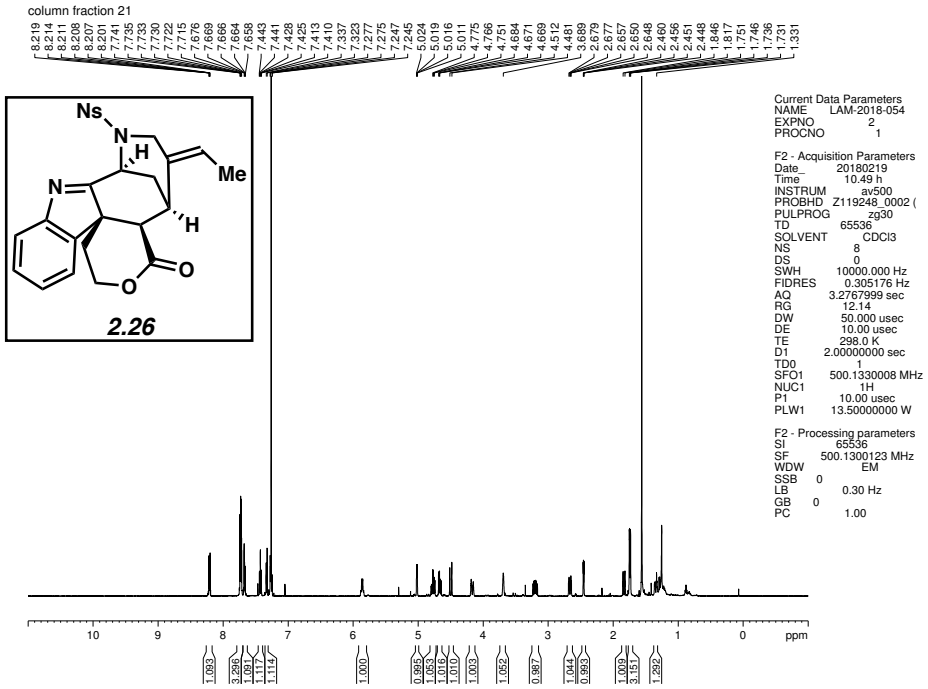


Figure 2.4. ^{1}H NMR (500 MHz, $CDCl_3$) of compound **2.26**.

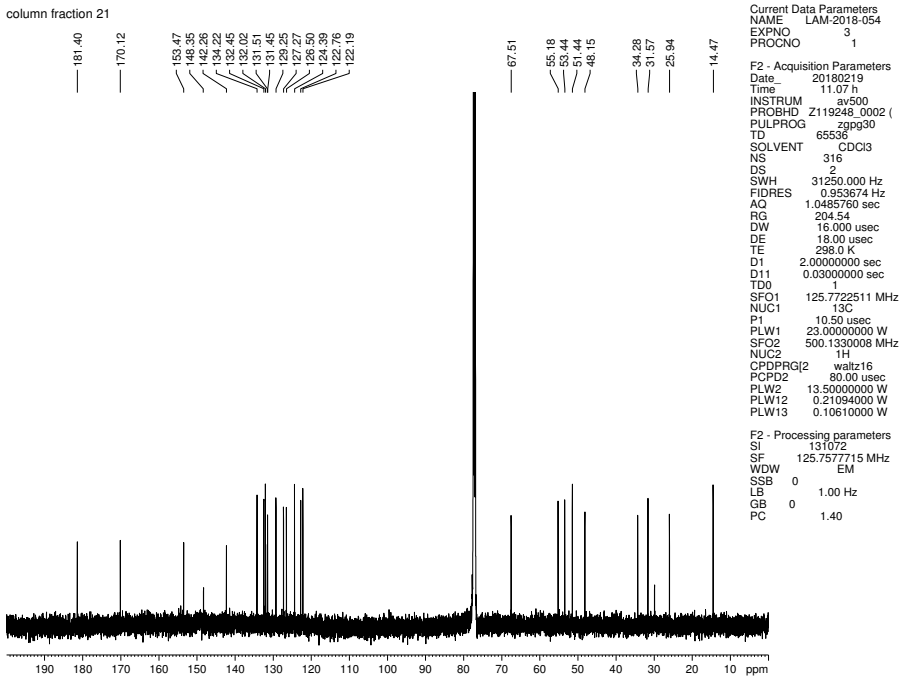


Figure 2.5. ^{13}C NMR (125 MHz, $CDCl_3$) of compound **2.26**.

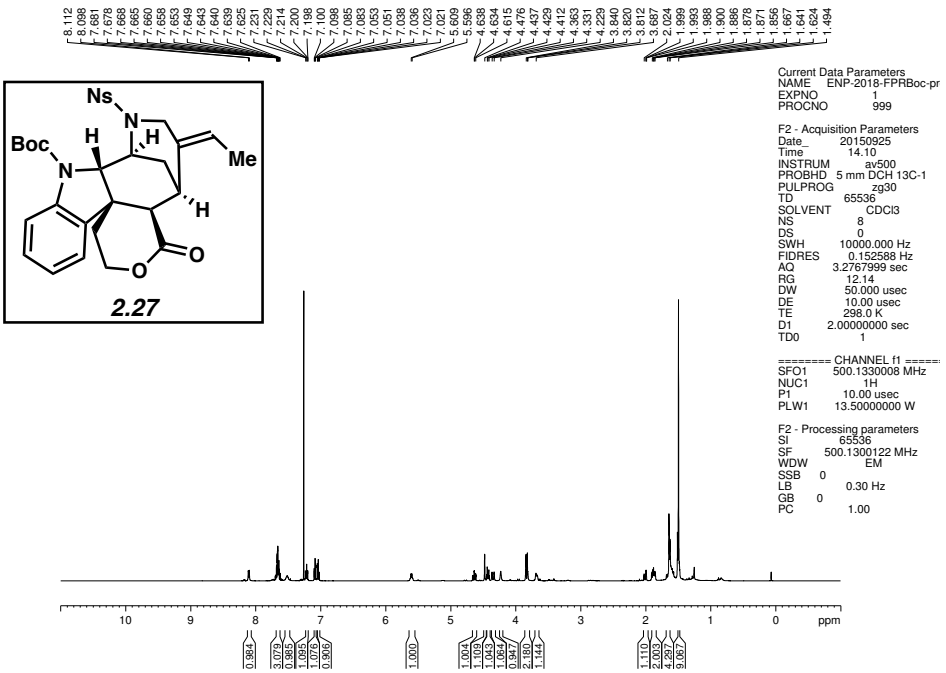


Figure 2.6. ^{1}H NMR (500 MHz, $CDCl_3$) of compound **2.27**.

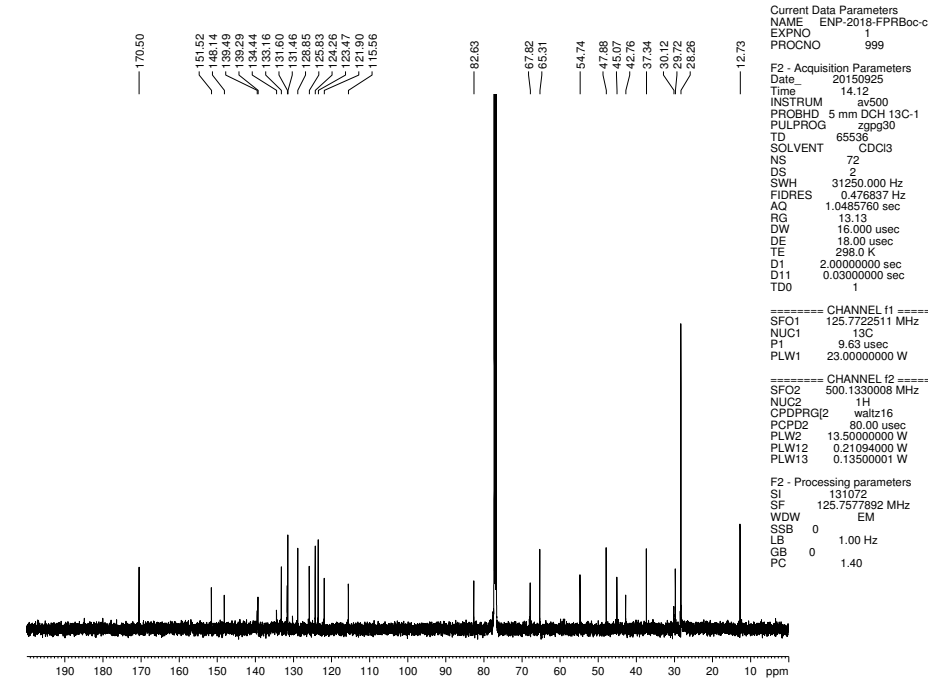


Figure 2.7. ^{13}C NMR (125 MHz, $CDCl_3$) of compound **2.27**.

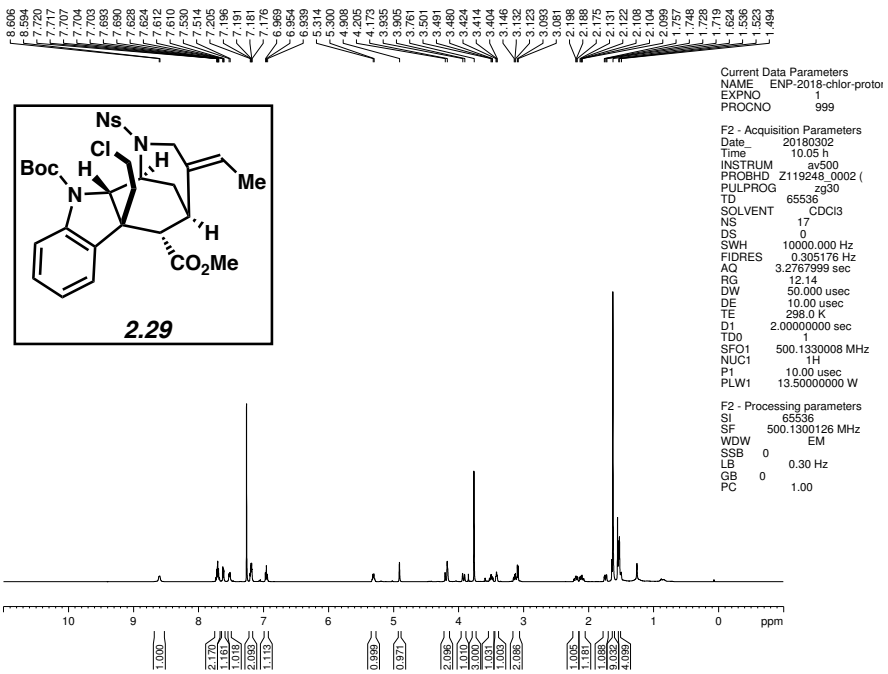


Figure 2.8. ^{1}H NMR (500 MHz, $CDCl_3$) of compound **2.29**.

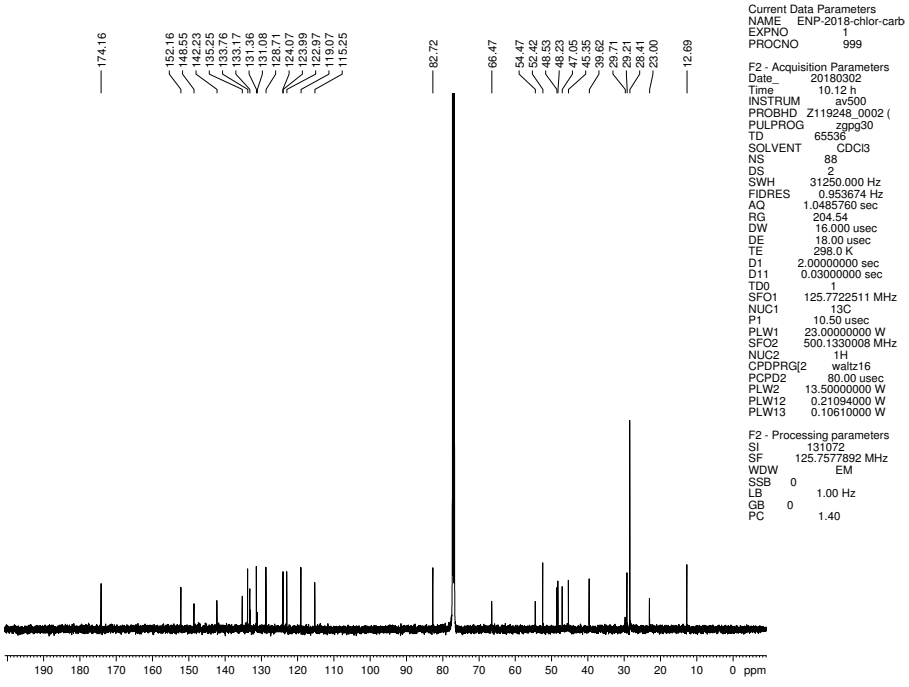


Figure 2.9. ^{13}C NMR (125 MHz, $CDCl_3$) of compound **2.29**.

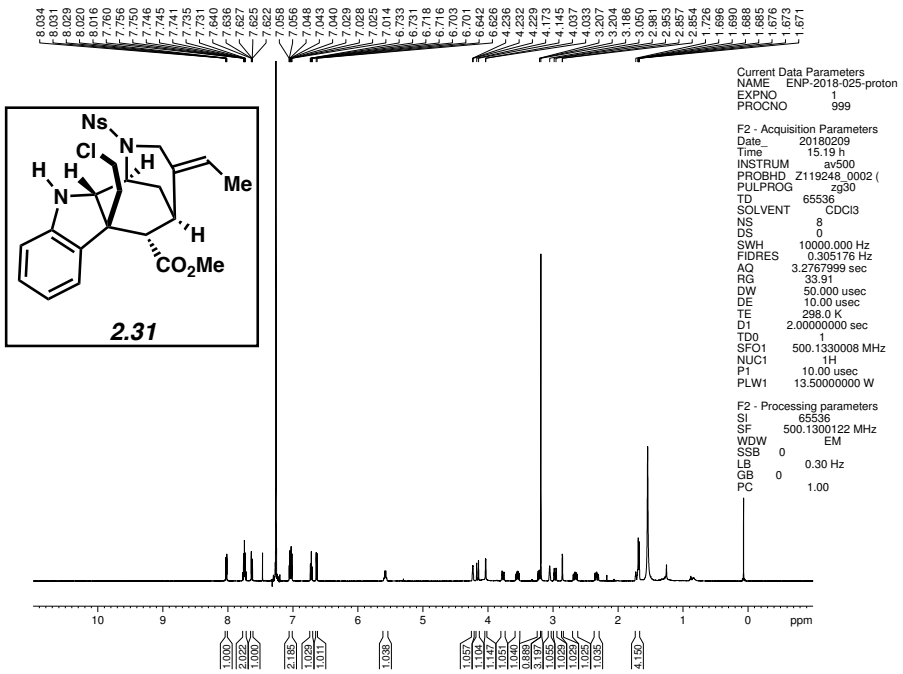


Figure 2.10. ^{1}H NMR (500 MHz, $CDCl_3$) of compound **2.31**.

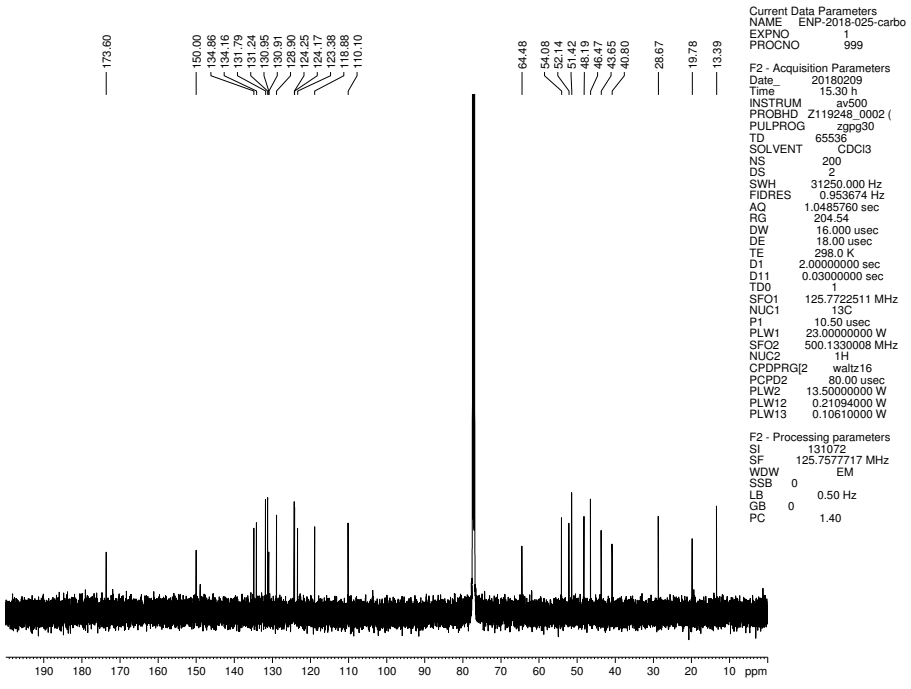


Figure 2.11. ^{13}C NMR (125 MHz, $CDCl_3$) of compound **2.31**.

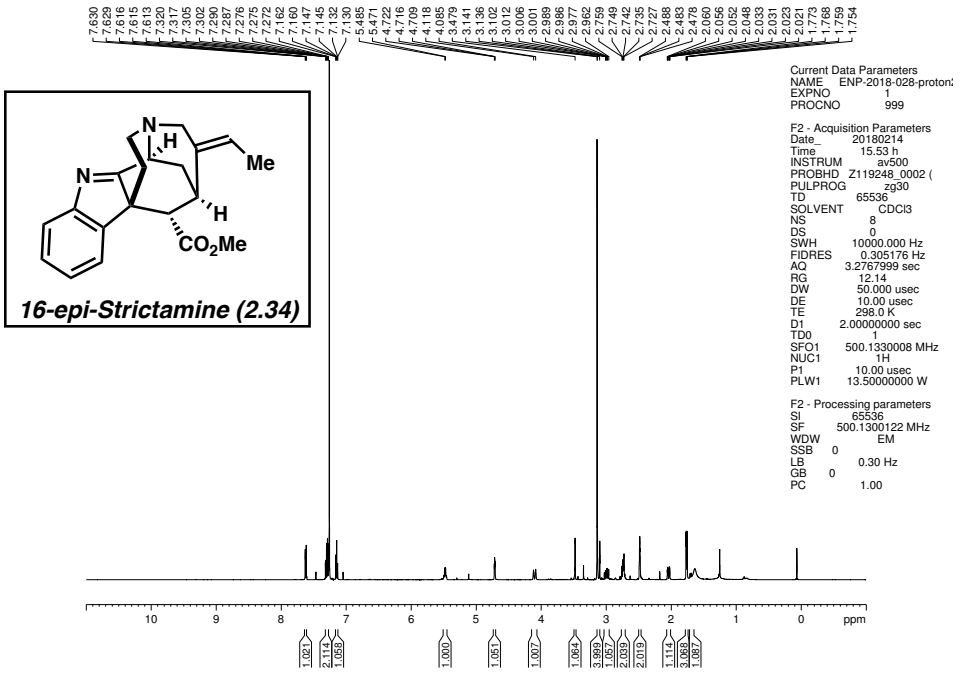


Figure 2.12. ^{1}H NMR (500 MHz, $CDCl_3$) of compound **2.34**.

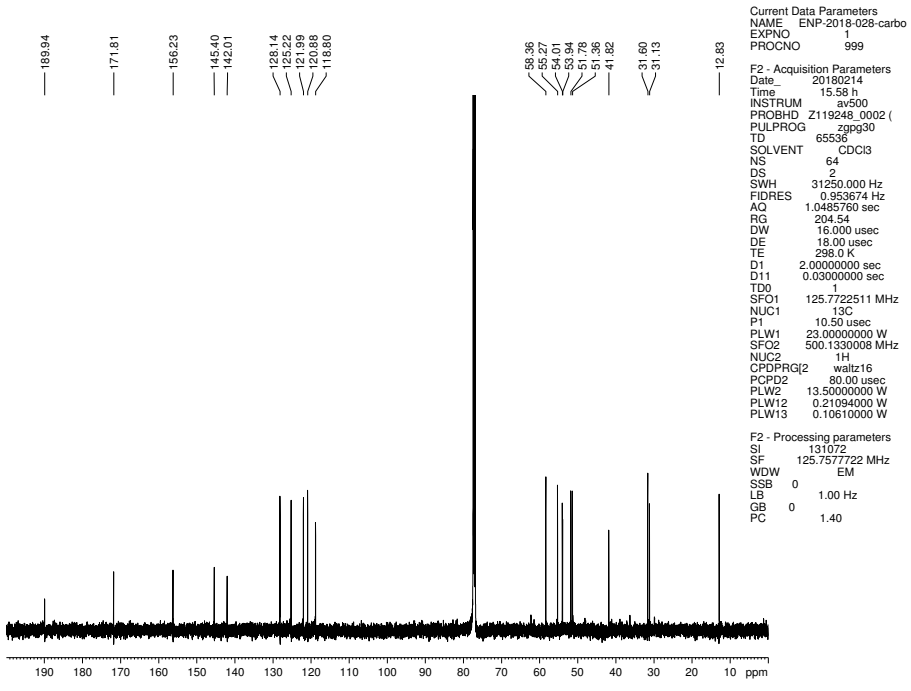


Figure 2.13. ^{13}C NMR (125 MHz, $CDCl_3$) of compound **2.34**.

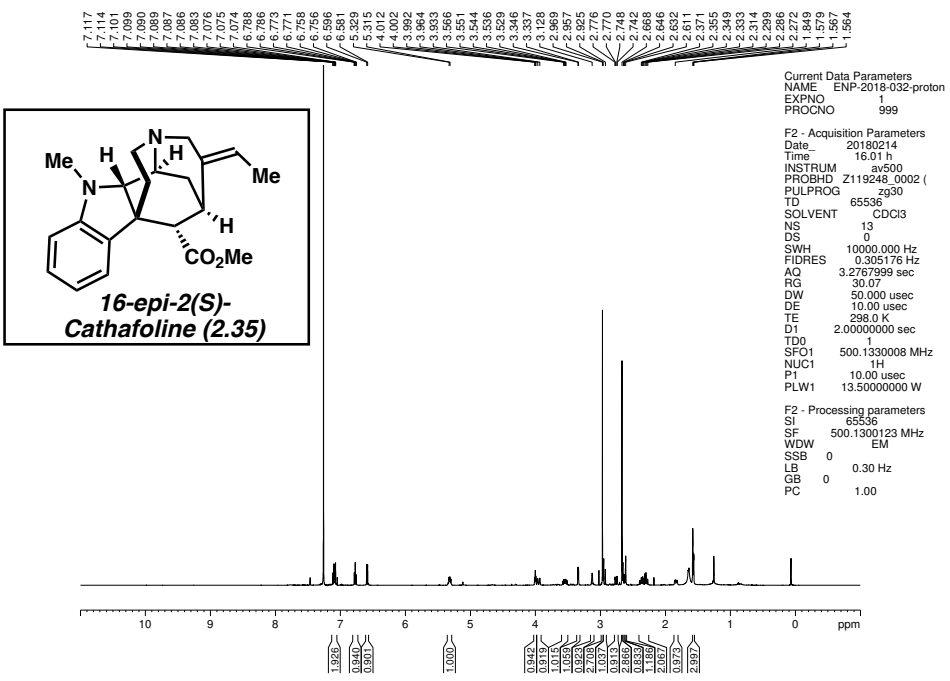


Figure 2.14. ^{1}H NMR (500 MHz, $CDCl_3$) of compound **2.35**.

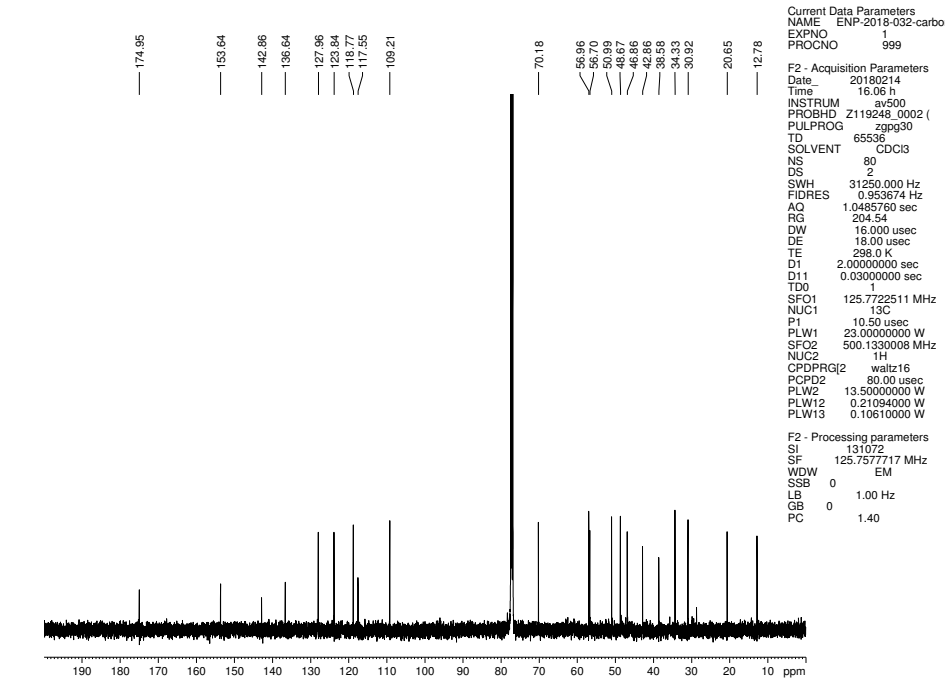


Figure 2.15. ^{13}C NMR (125 MHz, $CDCl_3$) of compound **2.35**.

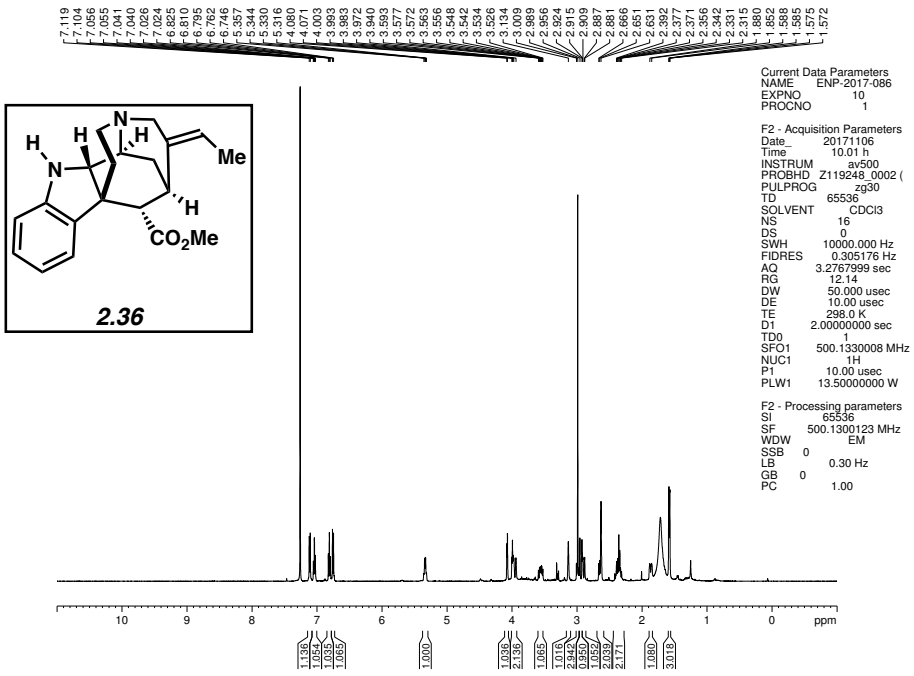


Figure 2.16. ^{1}H NMR (500 MHz, $CDCl_3$) of compound **2.36**.

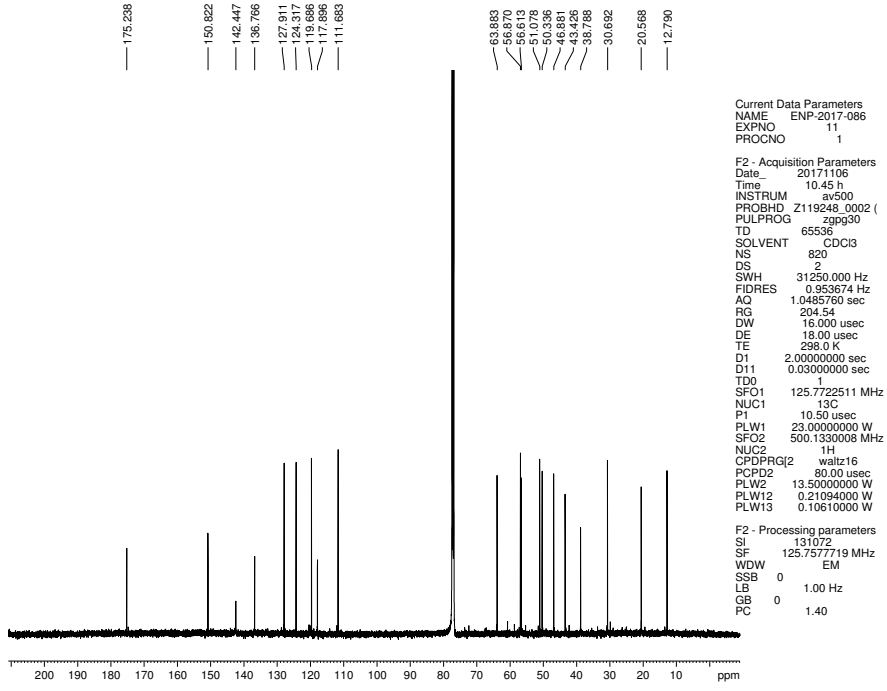


Figure 2.17. ^{13}C NMR (125 MHz, $CDCl_3$) of compound **2.36**.

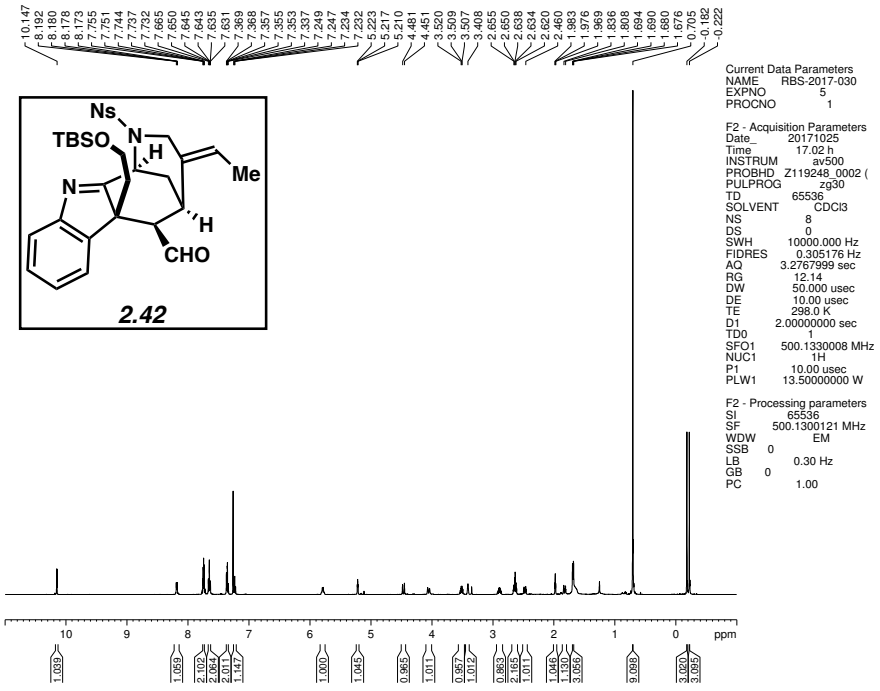


Figure 2.18. ^{1}H NMR (500 MHz, $CDCl_3$) of compound **2.42**.

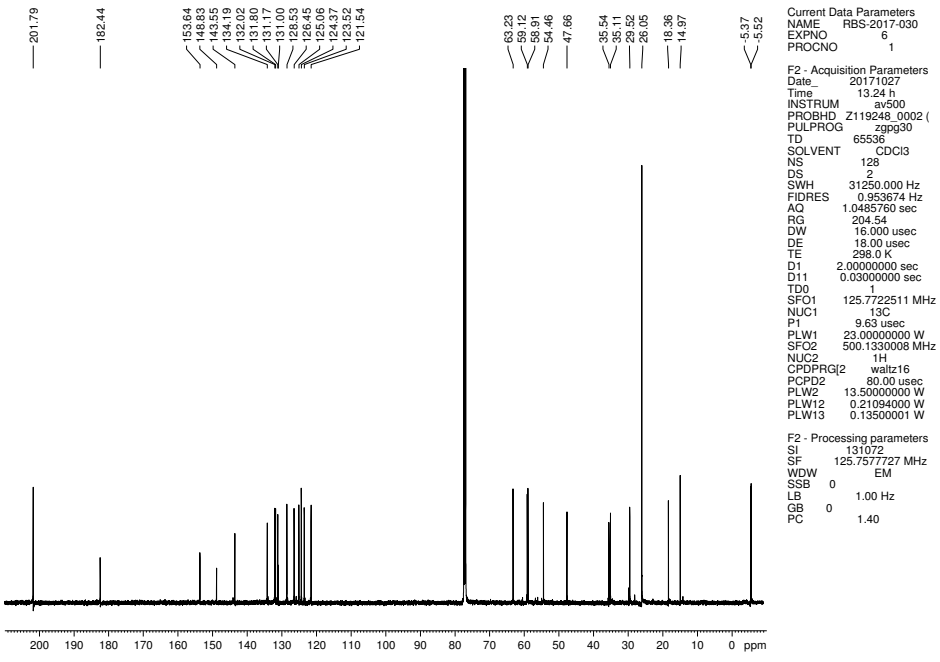


Figure 2.19. ^{13}C NMR (125 MHz, $CDCl_3$) of compound **2.42**.

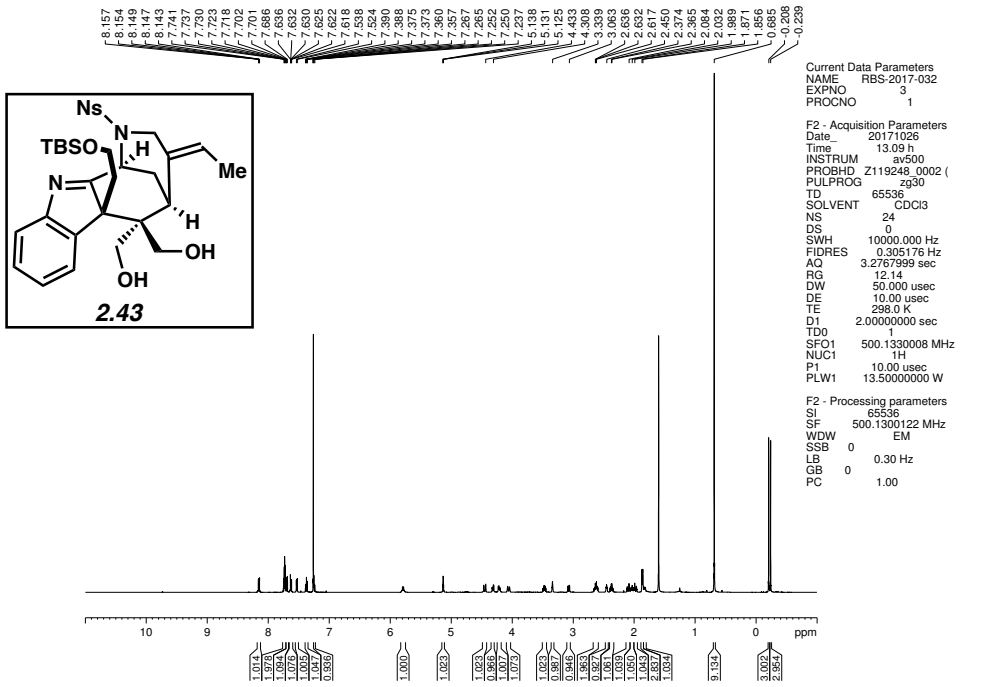


Figure 2.20. ^{1}H NMR (500 MHz, $CDCl_3$) of compound **2.43**.

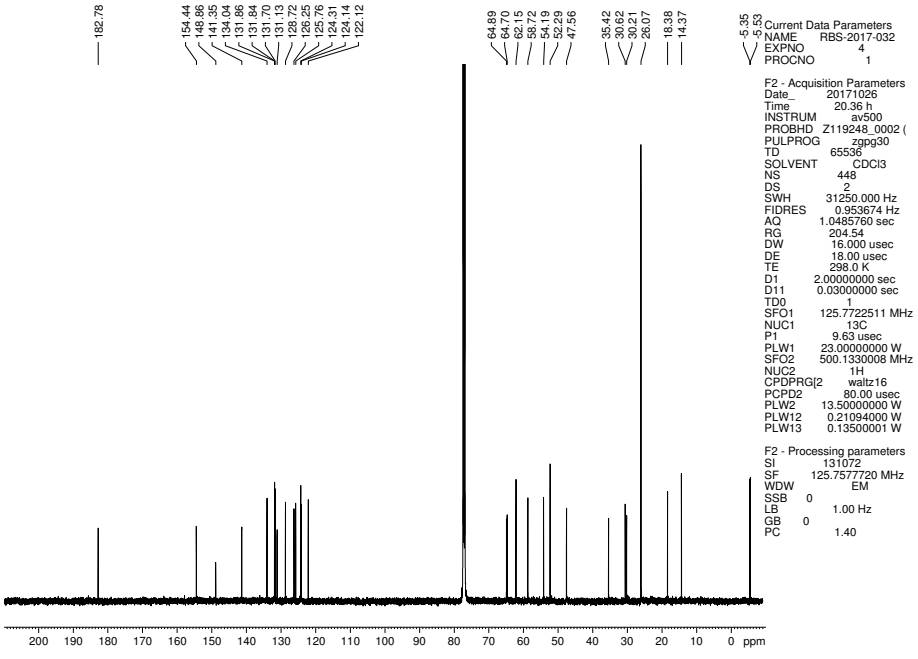


Figure 2.21. ^{13}C NMR (125 MHz, $CDCl_3$) of compound **2.43**.

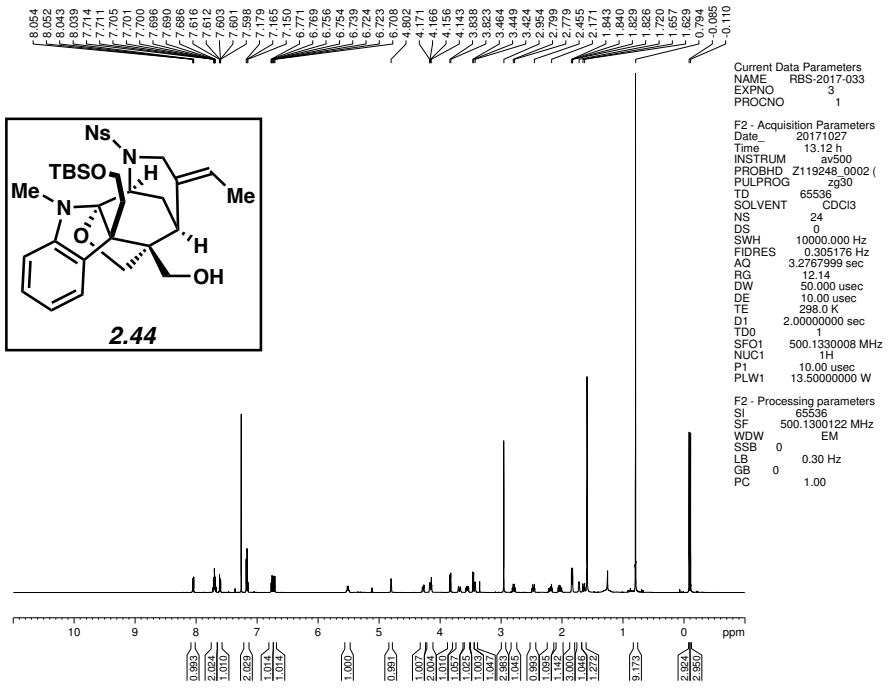


Figure 2.22. ^{1}H NMR (500 MHz, $CDCl_3$) of compound **2.44**.

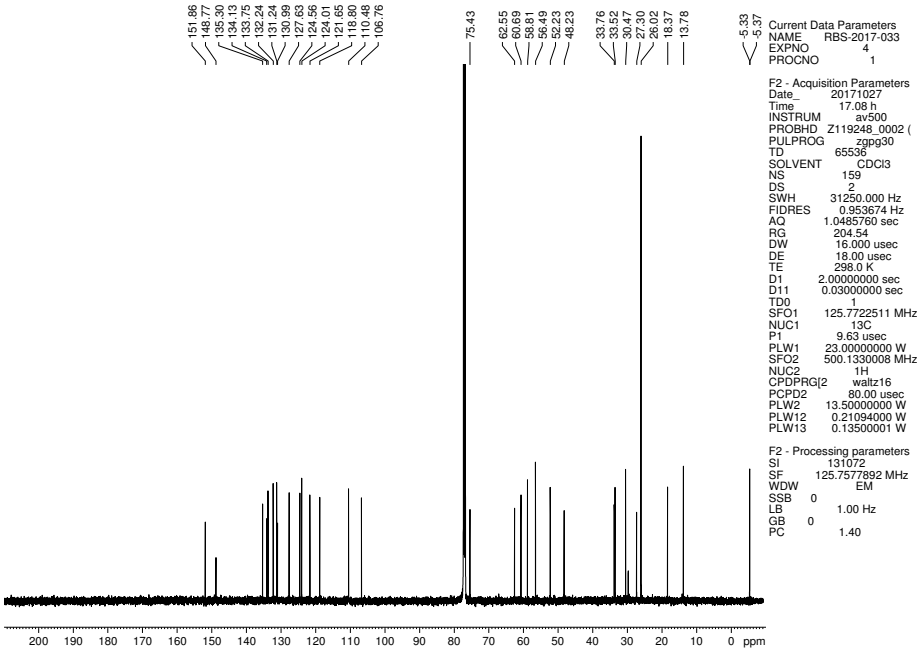


Figure 2.23. ^{13}C NMR (125 MHz, $CDCl_3$) of compound **2.44**.

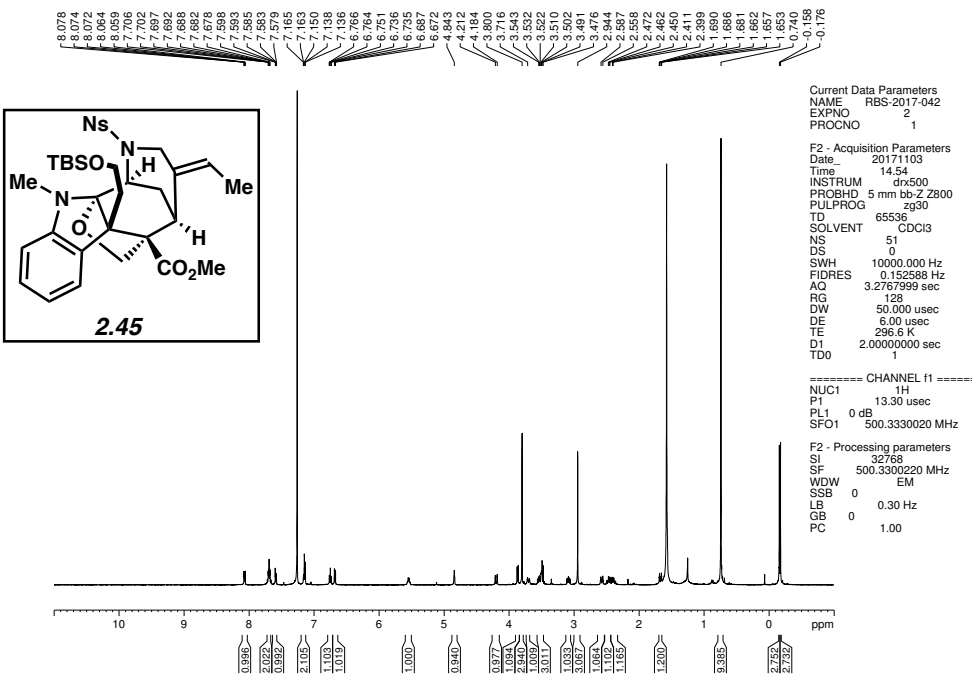


Figure 2.24. ^{1}H NMR (500 MHz, $CDCl_3$) of compound **2.45**.

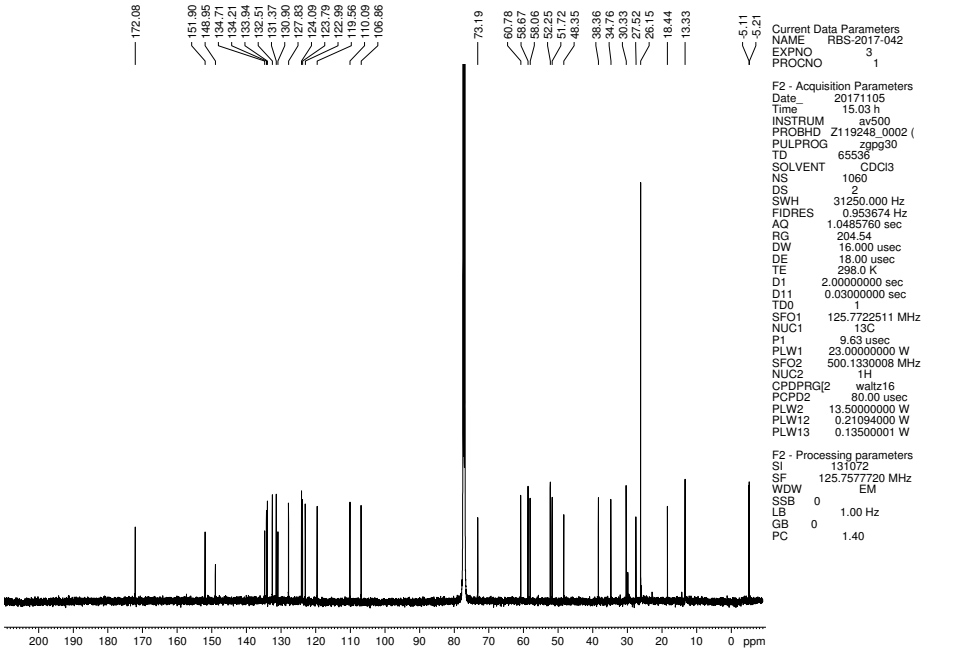


Figure 2.25. ^{13}C NMR (125 MHz, $CDCl_3$) of compound **2.45**

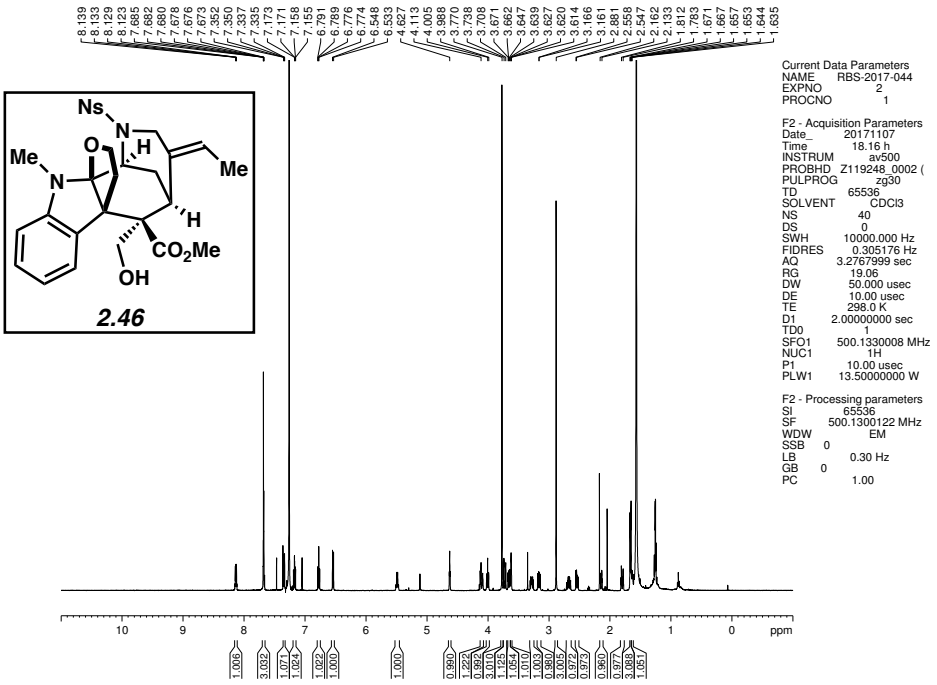


Figure 2.26. ^{1}H NMR (500 MHz, $CDCl_3$) of compound **2.46**.

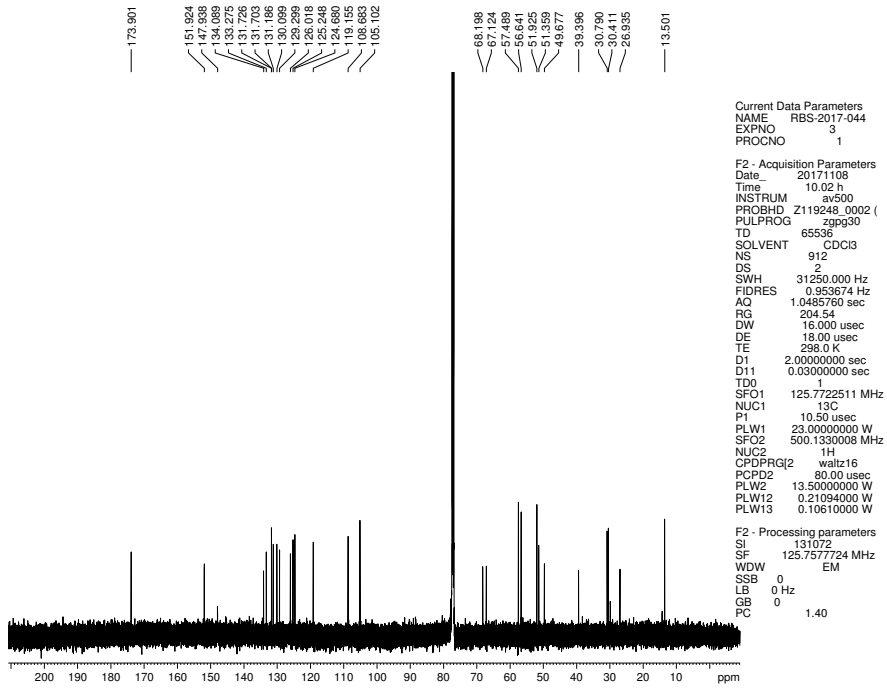


Figure 2.27. ^{13}C NMR (125 MHz, $CDCl_3$) of compound **2.46**.

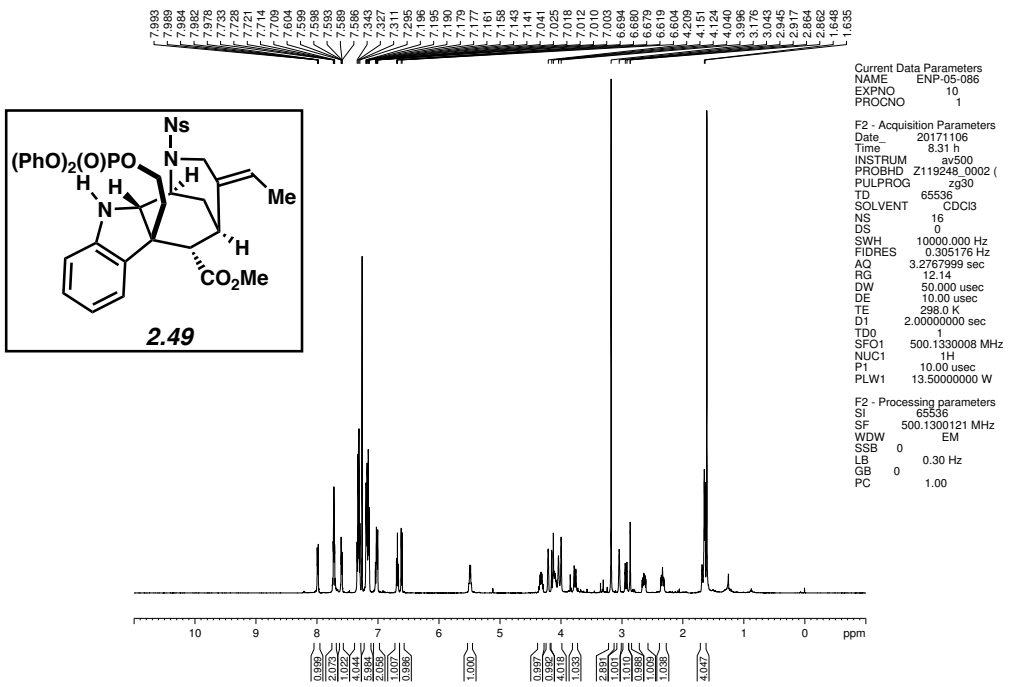


Figure 2.28. ^{1}H NMR (500 MHz, $CDCl_3$) of compound **2.49**.

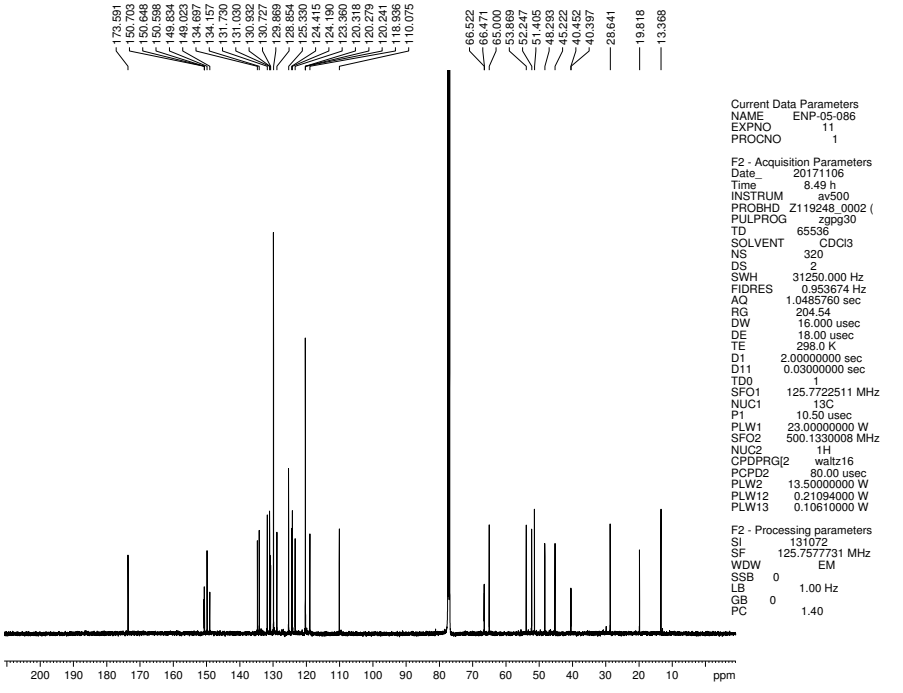


Figure 2.29. ^{13}C NMR (125 MHz, $CDCl_3$) of compound **2.49**.

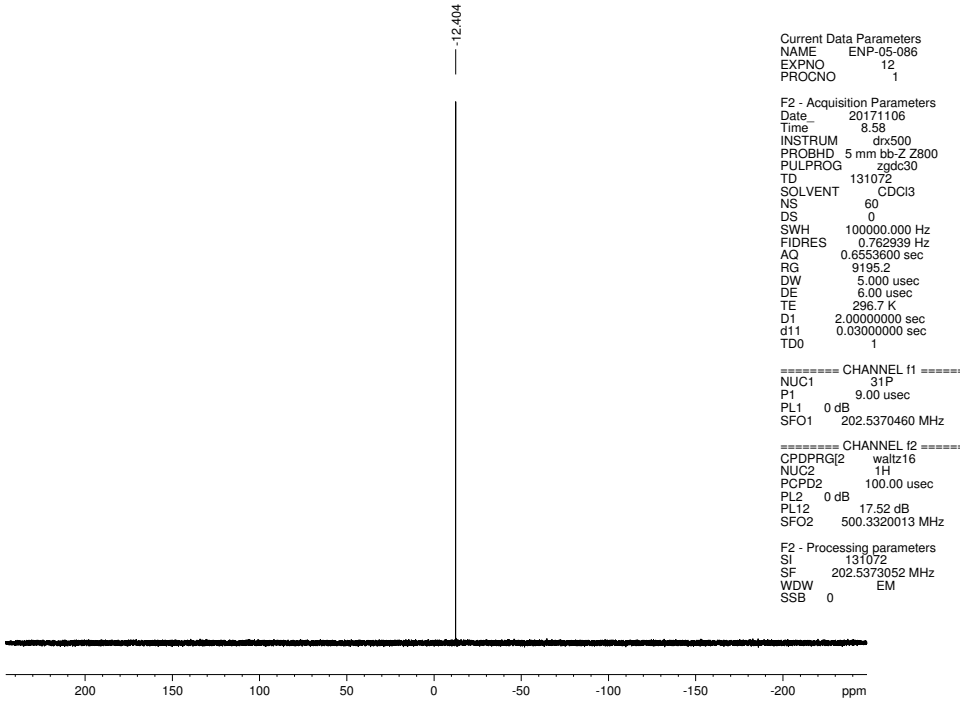


Figure 2.30. ^{31}P NMR (202 MHz, $CDCl_3$) of compound **2.49**.

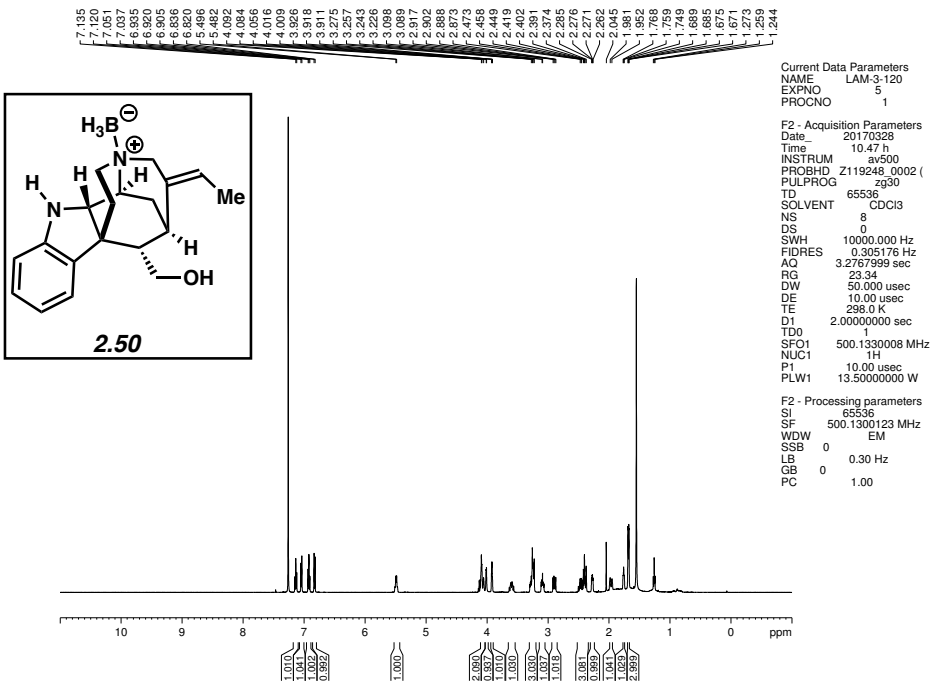


Figure 2.31. ^{1}H NMR (500 MHz, $CDCl_3$) of compound **2.50**.

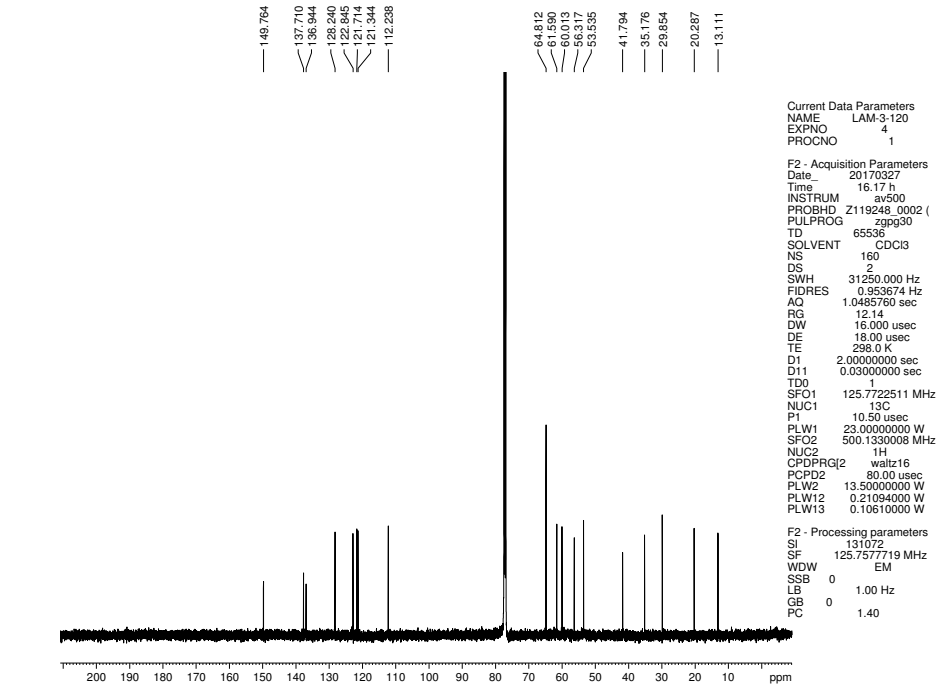


Figure 2.32. ^{13}C NMR (125 MHz, $CDCl_3$) of compound **2.50**.

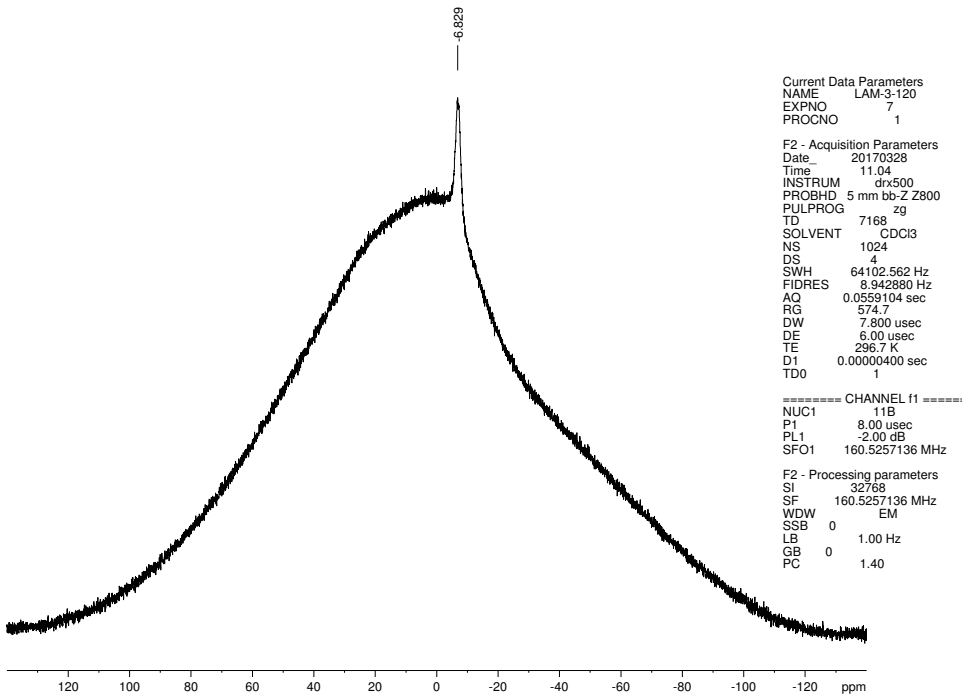


Figure 2.33. ^{11}B NMR (160 MHz, $CDCl_3$) of compound **2.50**.

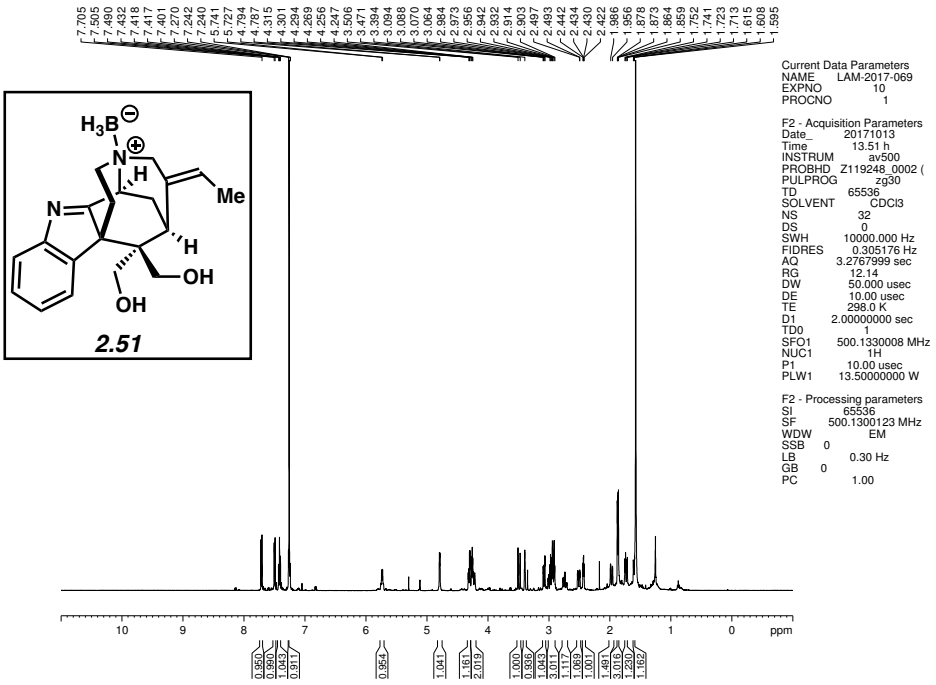


Figure 2.34. ^{1}H NMR (500 MHz, $CDCl_3$) of compound **2.51**.

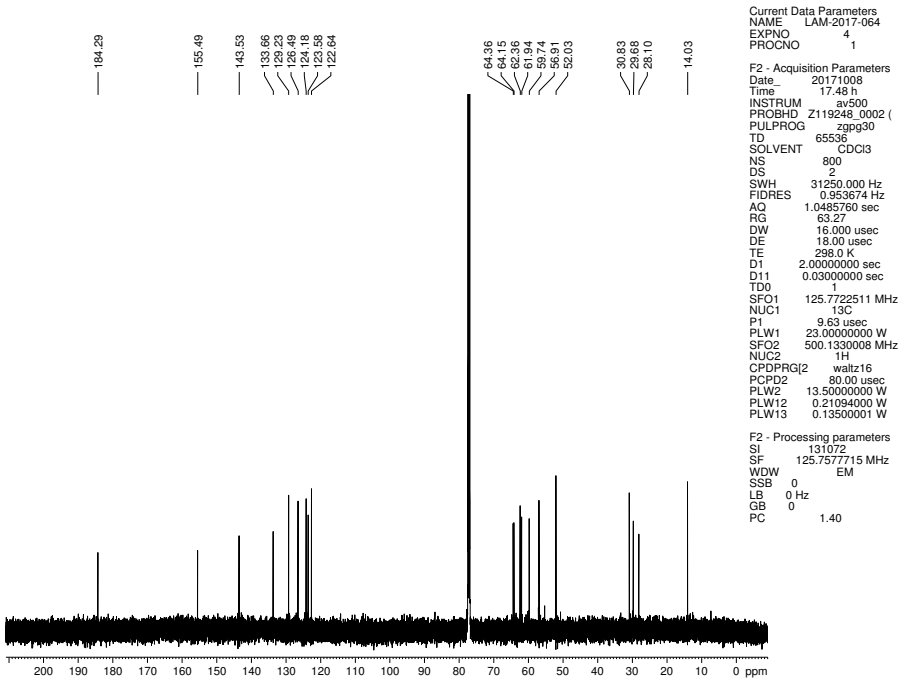


Figure 2.35. ^{13}C NMR (125 MHz, $CDCl_3$) of compound **2.51**.

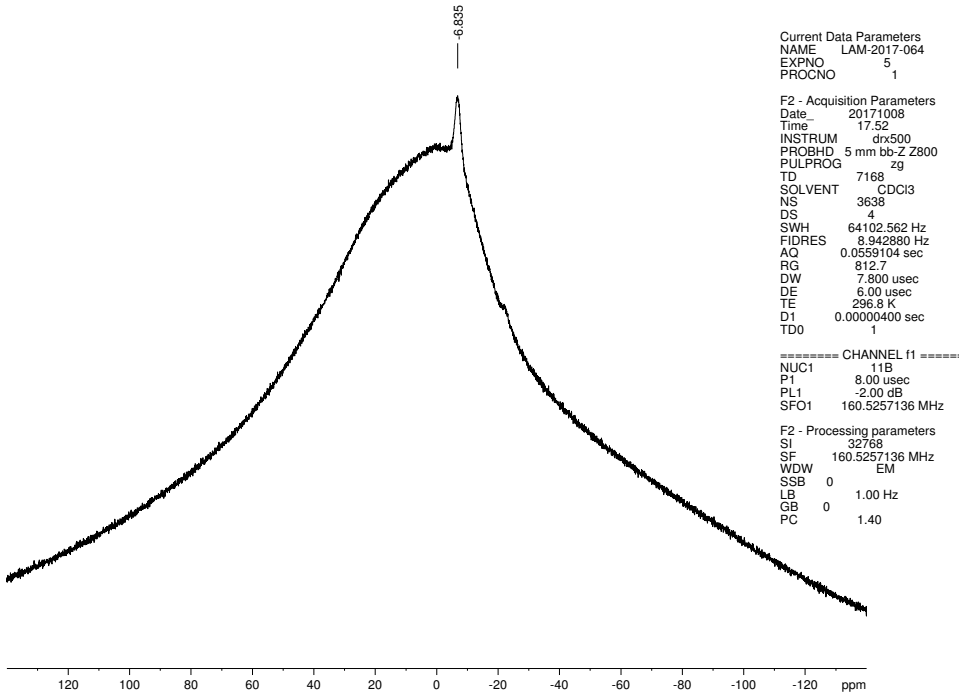


Figure 2.36. ^{11}B NMR (160 MHz, $CDCl_3$) of compound **2.51**.

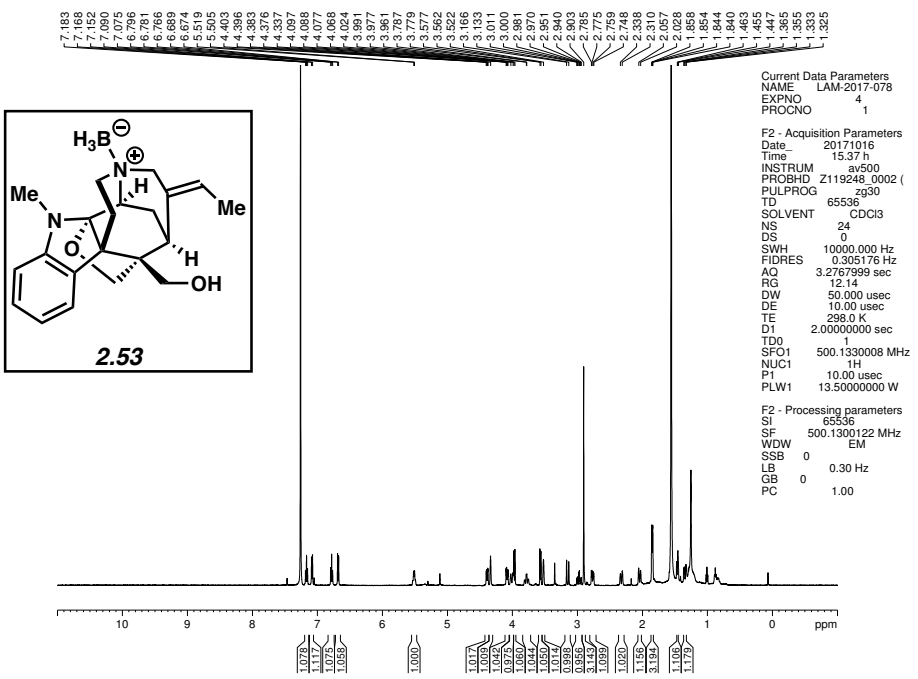


Figure 2.37. ^{1}H NMR (500 MHz, $CDCl_3$) of compound **2.53**.

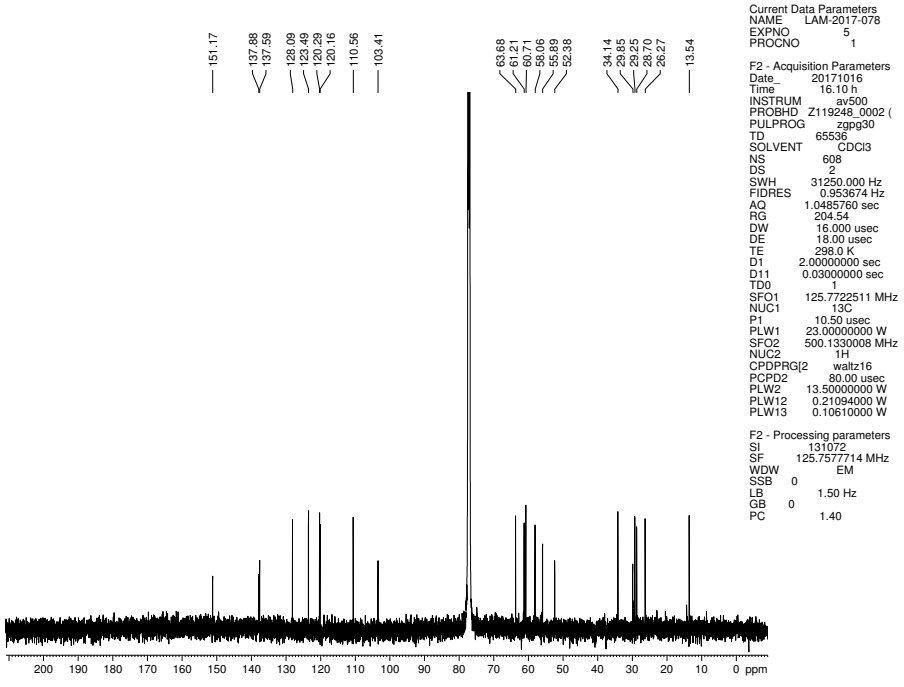


Figure 2.38. ^{13}C NMR (125 MHz, $CDCl_3$) of compound **2.53**.

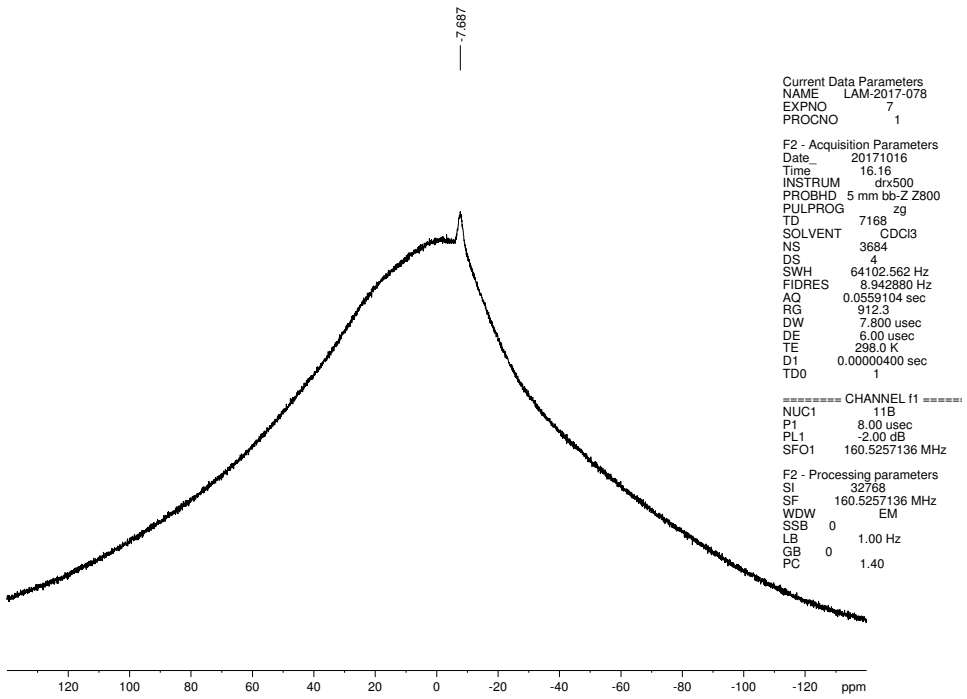


Figure 2.39. ^{11}B NMR (160 MHz, $CDCl_3$) of compound **2.53**.

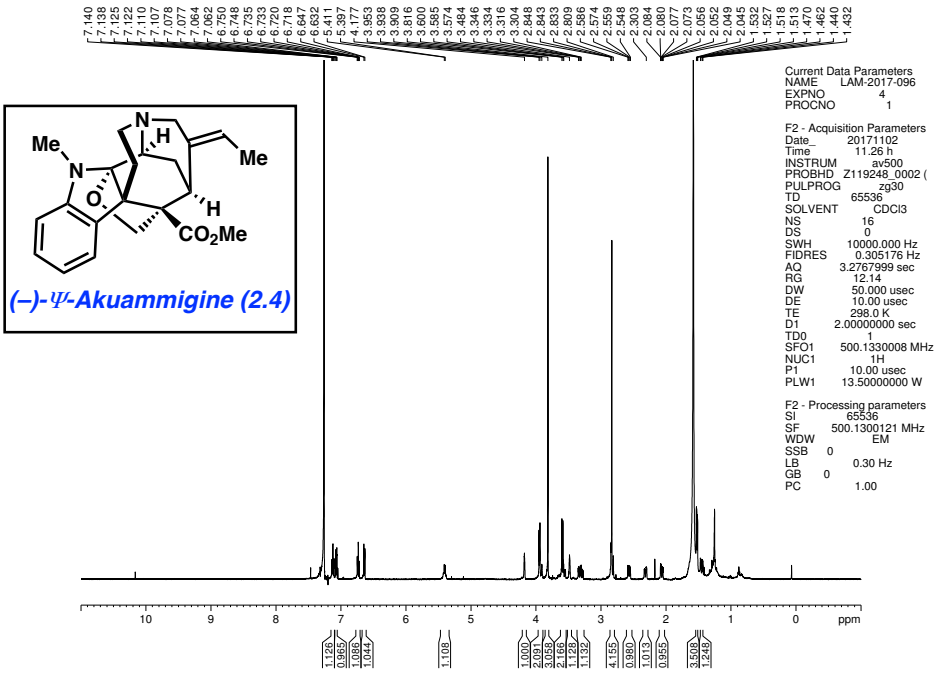


Figure 2.40. ^{1}H NMR (500 MHz, $CDCl_3$) of compound **2.4**.

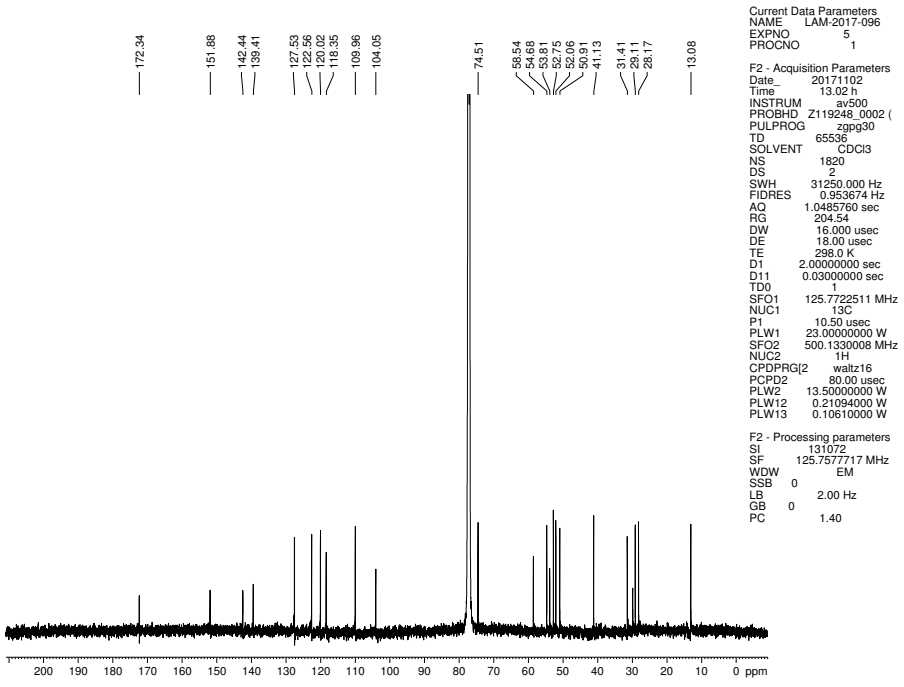


Figure 2.41. ^{13}C NMR (125 MHz, $CDCl_3$) of compound **2.4**.

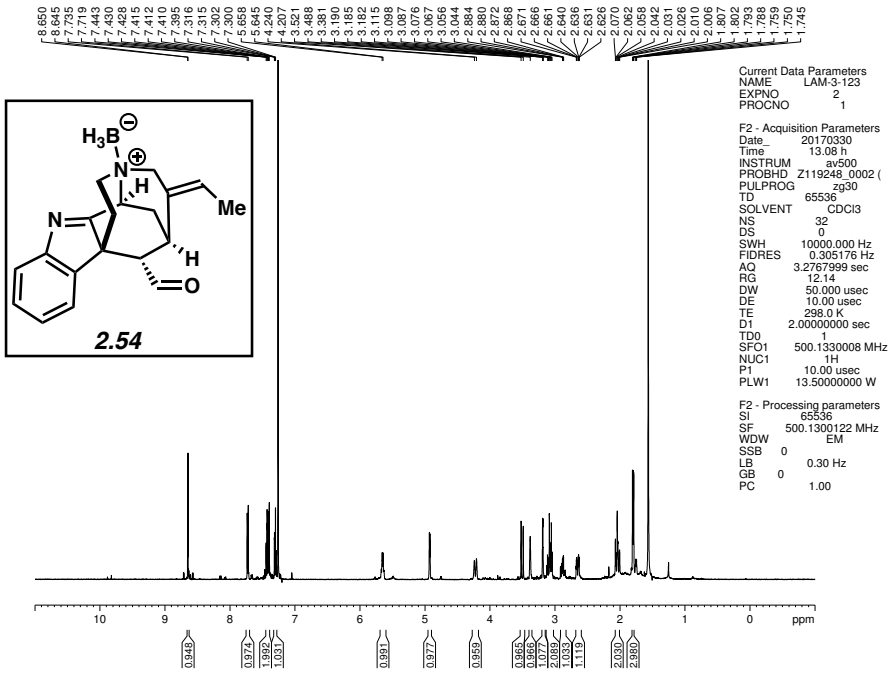


Figure 2.42. ^{1}H NMR (500 MHz, $CDCl_3$) of compound **2.54**.

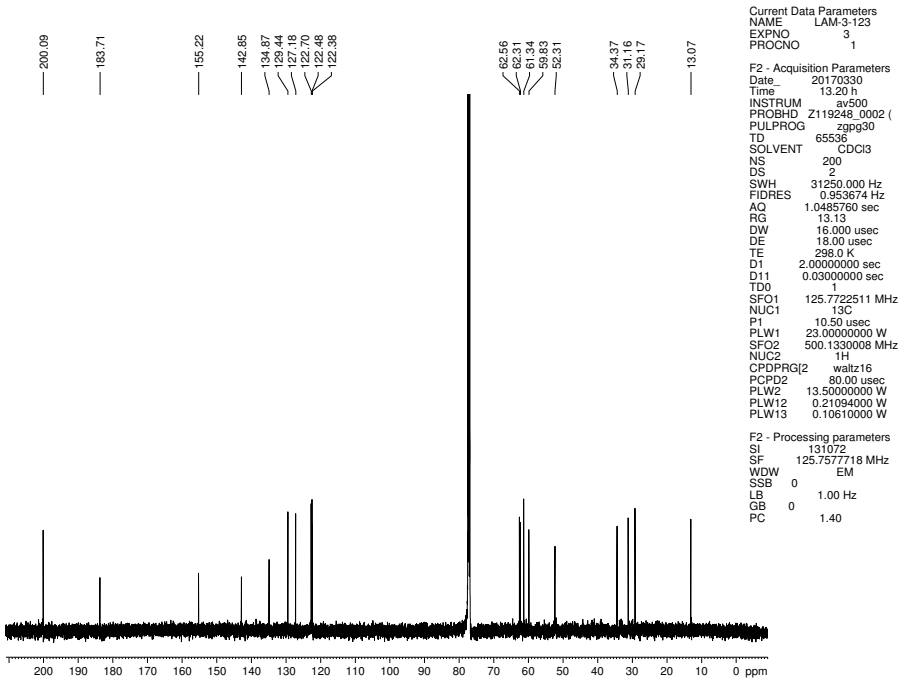


Figure 2.43. ^{13}C NMR (125 MHz, $CDCl_3$) of compound **2.54**.

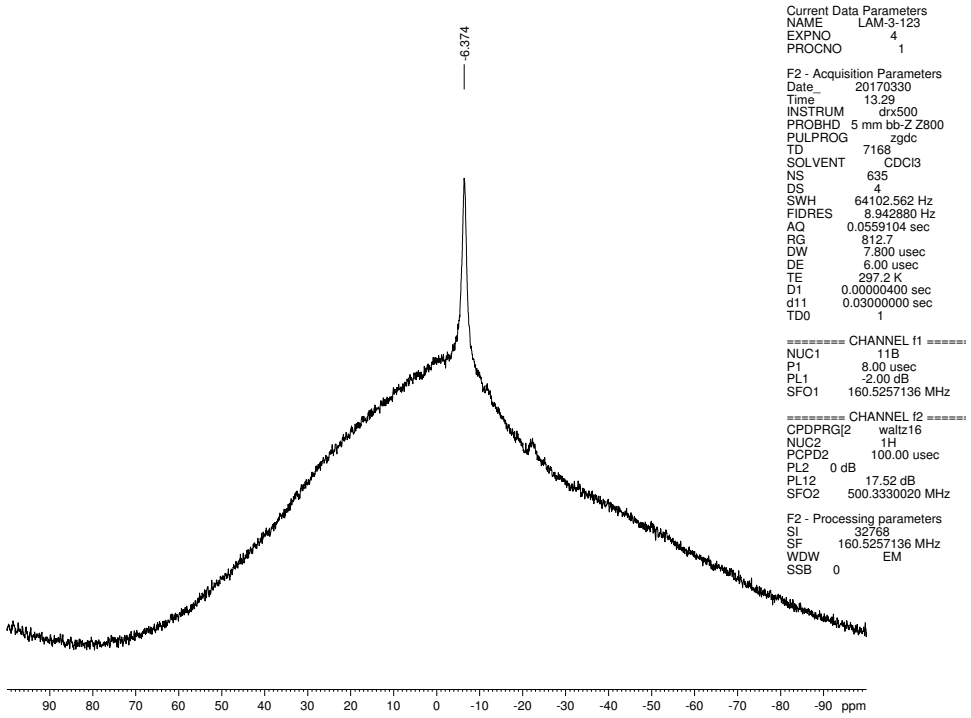


Figure 2.44. ^{11}B NMR (160 MHz, $CDCl_3$) of compound **2.54**.

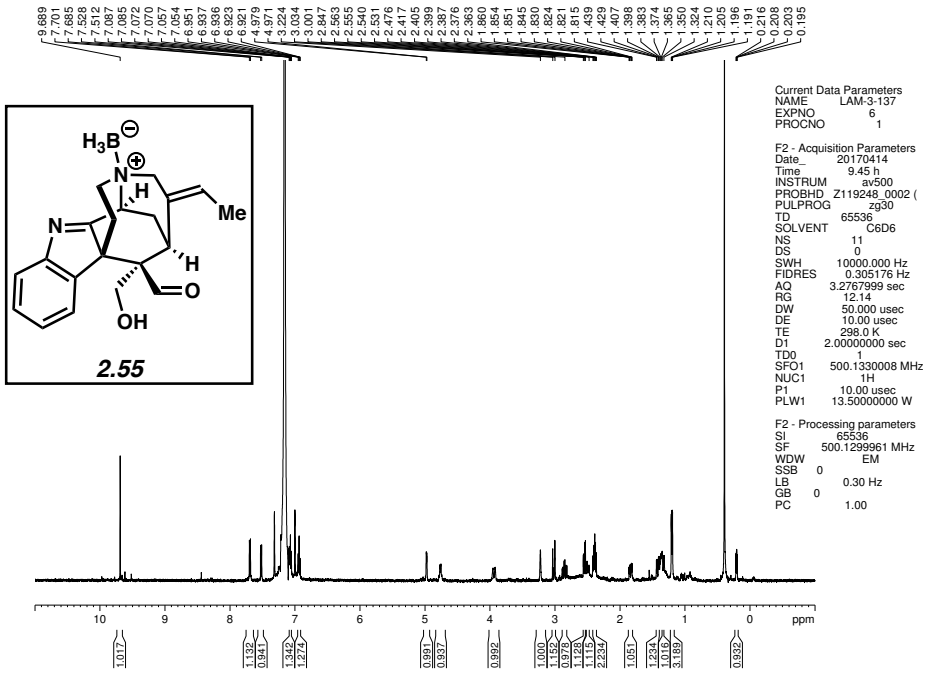


Figure 2.45. ^{1}H NMR (500 MHz, C_6D_6) of compound **2.55**.

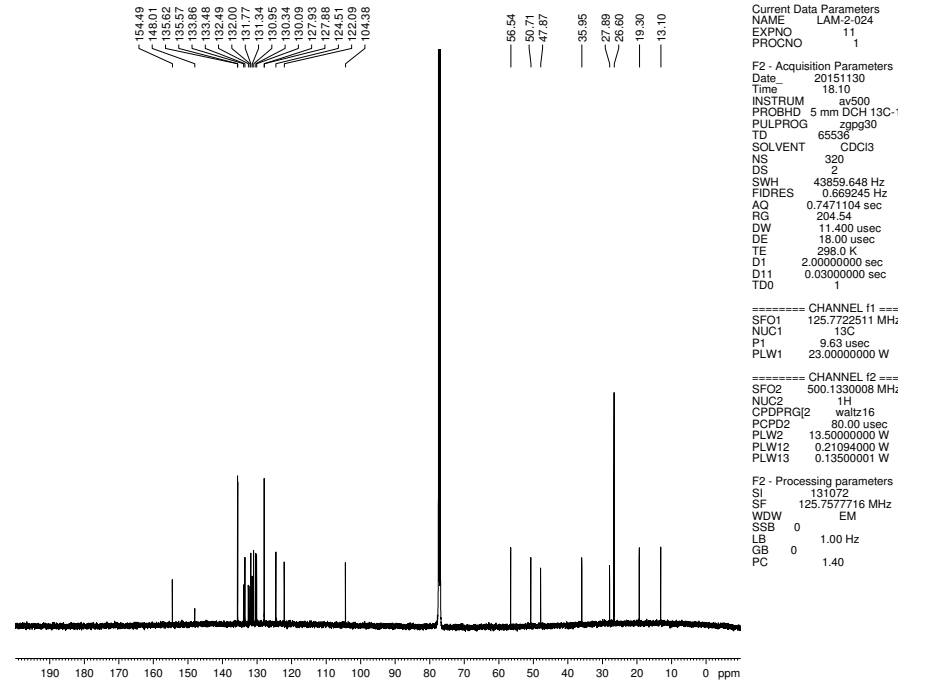


Figure 2.46. ^{13}C NMR (125 MHz, $CDCl_3$) of compound **2.55**.

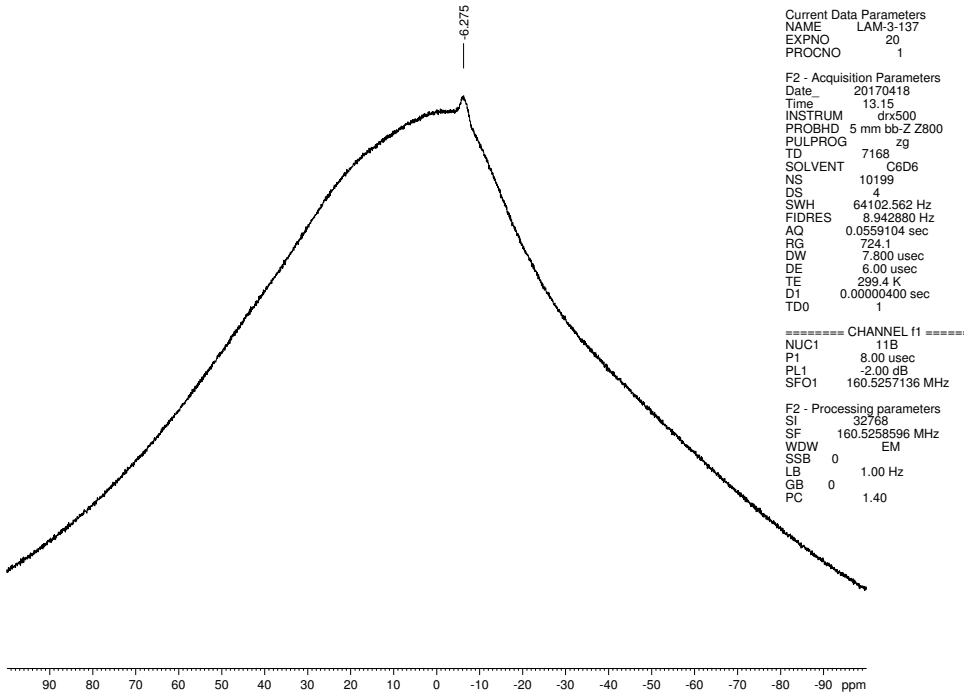


Figure 2.47. ^{11}B NMR (160 MHz, C_6D_6) of compound **2.55**.

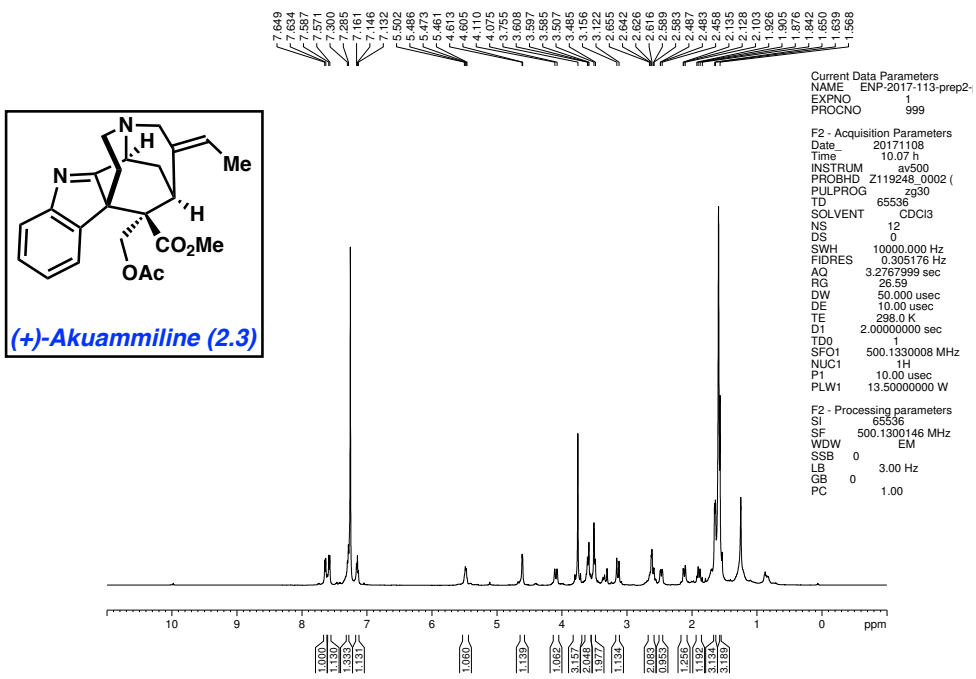


Figure 2.48. ^{1}H NMR (500 MHz, $CDCl_3$) of compound **2.3**.

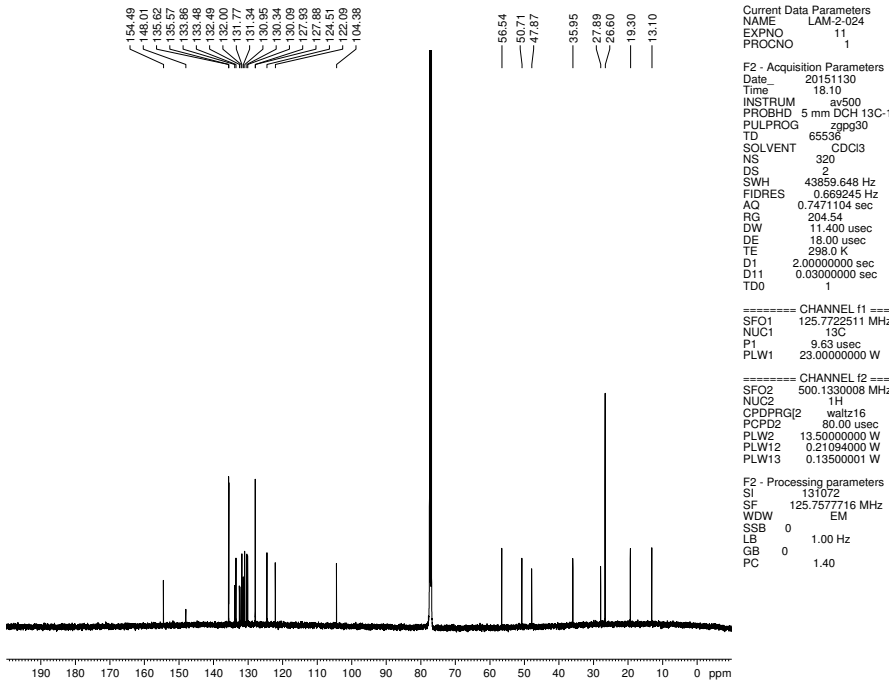


Figure 2.49. ^{13}C NMR (125 MHz, $CDCl_3$) of compound **2.3**.

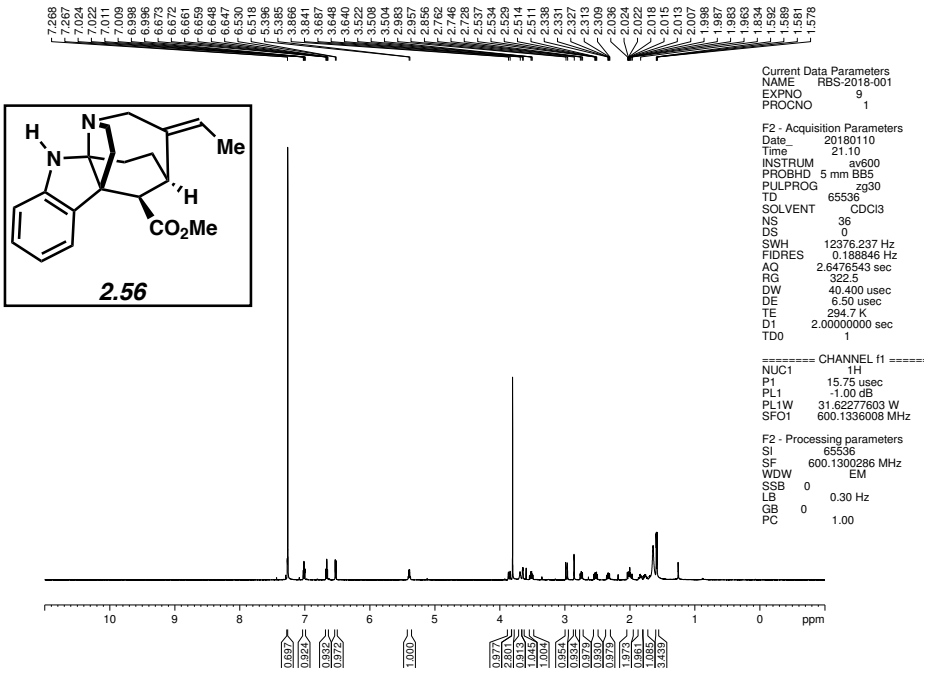


Figure 2.50. ^{1}H NMR (500 MHz, $CDCl_3$) of compound **2.56**.

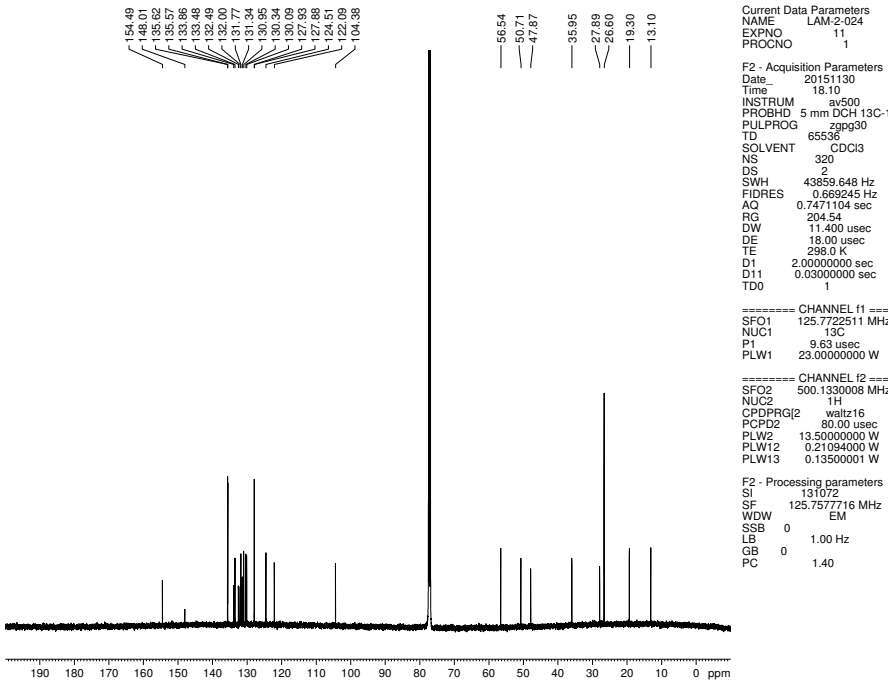


Figure 2.51. ^{13}C NMR (125 MHz, $CDCl_3$) of compound **2.56**.

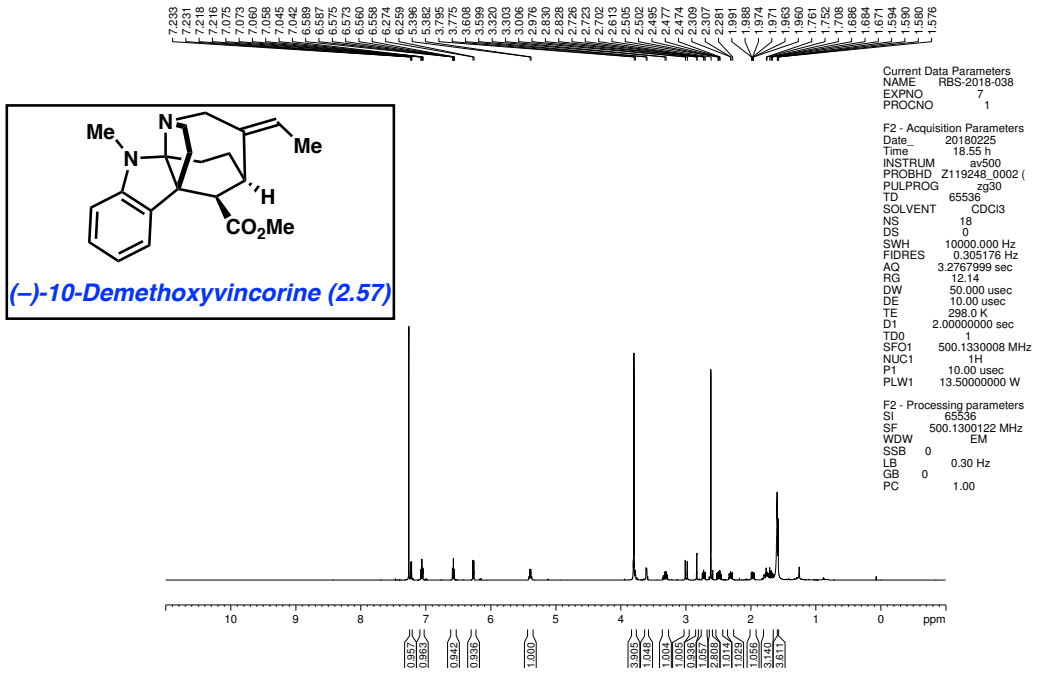


Figure 2.52. ^{1}H NMR (500 MHz, $CDCl_3$) of compound **2.57**.

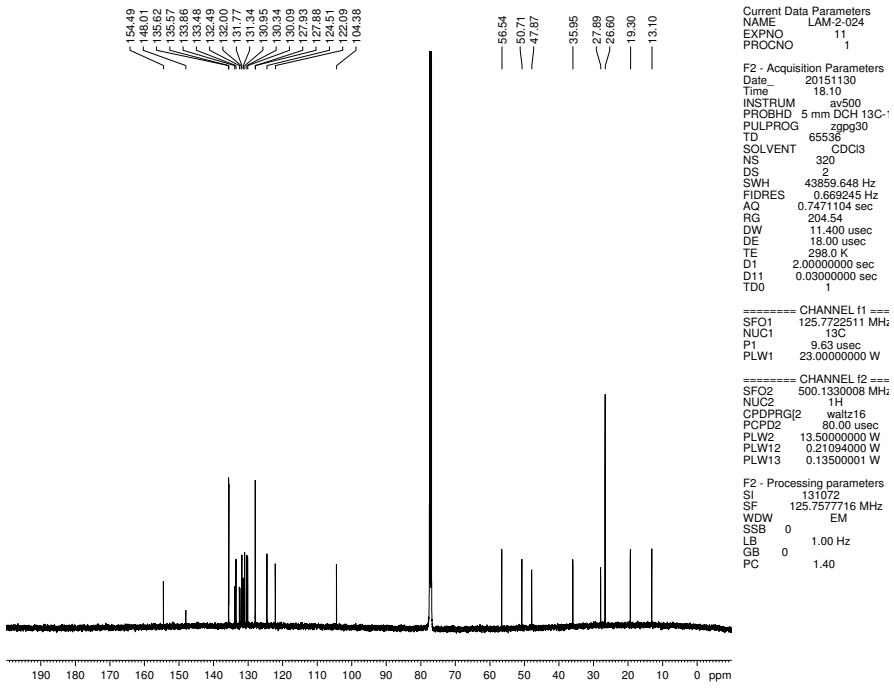


Figure 2.53. ^{13}C NMR (125 MHz, $CDCl_3$) of compound **2.57**.

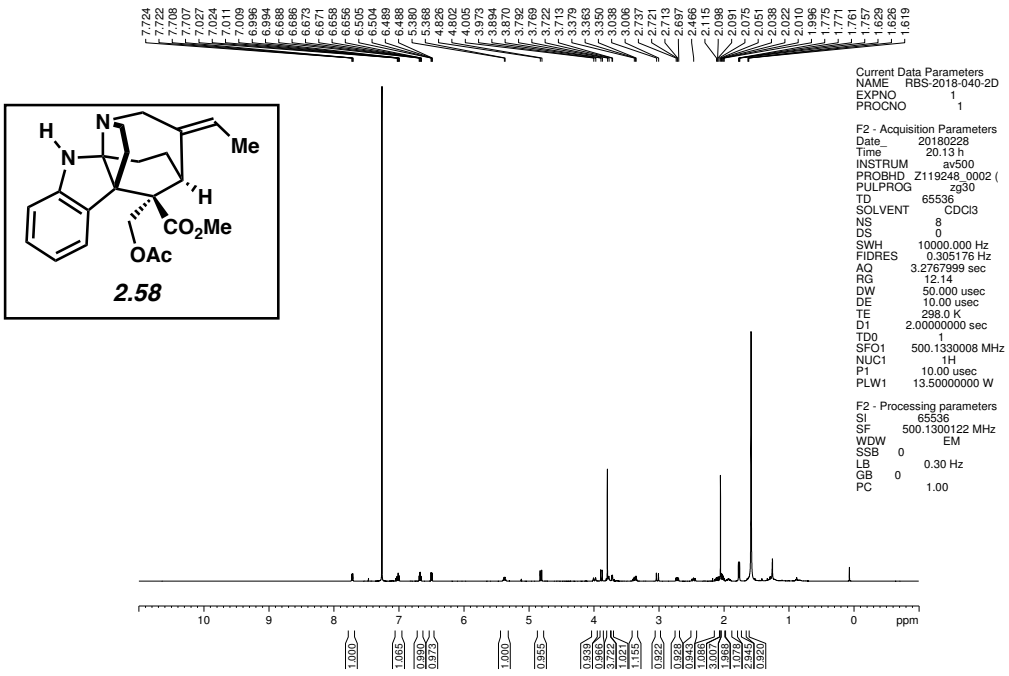


Figure 2.54. ^{1}H NMR (500 MHz, $CDCl_3$) of compound **2.58**.

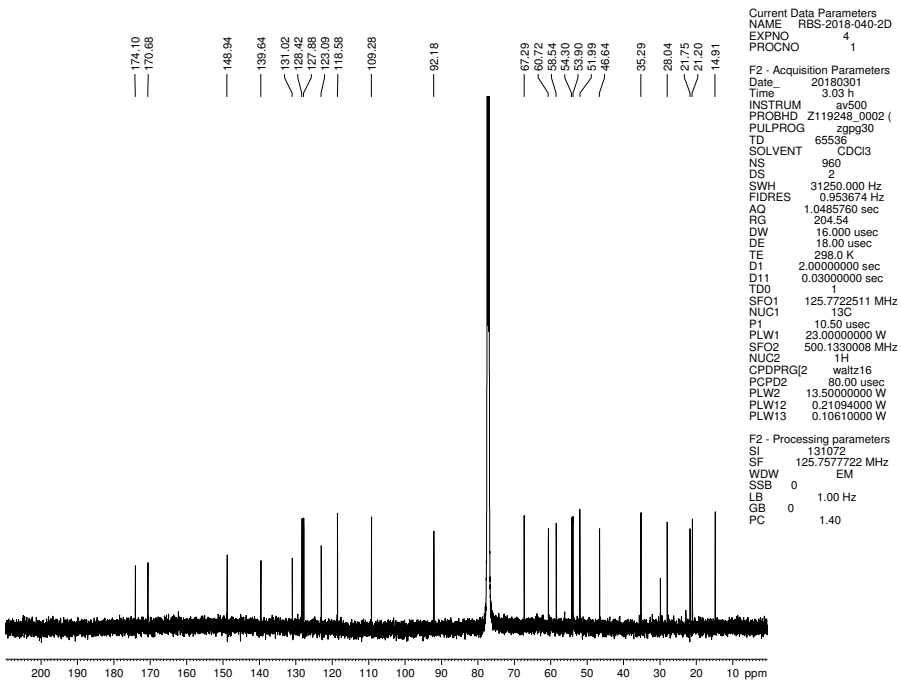


Figure 2.55. ^{13}C NMR (125 MHz, $CDCl_3$) of compound **2.58**.

2.16 Notes and References

(1) Baliga, M. S. *Chin. J. Integr. Med.* **2012**, DOI: 10.1007/s11655-011-0947-0.

(2) For reviews on akuammiline alkaloids, see: a) Ramírez, A.; García–Rubio, S. *Curr. Med. Chem.* **2003**, *10*, 1891–1915. b) Eckermann, R.; Gaich, T. *Synthesis* **2013**, *45*, 2813–2823. c) Smith, J. M.; Moreno, J.; Boal, B. W.; Garg, N. K. *Angew. Chem., Int. Ed.* **2015**, *54*, 400–412. d) Adams, G. L.; Smith, A. B. III The Chemistry of the Akuammiline Alkaloids. In *The Alkaloids*; Knolker, H.-J., Ed.; Elsevier: New York, 2016; Vol. *76*, p 171.

(3) www.reaxys.com (accessed March 26, 2018).

(4) Bonjoch, J.; Solé, D. *Chem. Rev*. **2000**, *100*, 3455–3482.

(5) a) Zhang, M.; Huang, X.; Shen, L.; Qin, Y. *J. Am. Chem. Soc*. **2009**, *131*, 6013–6020. b) Zu, L.; Boal, B. W.; Garg, N. K. *J. Am. Chem. Soc*. **2011**, *133*, 8877–8879. c) Zi, W.; Xie, W.; Ma, D. *J. Am. Chem. Soc*. **2012**, *134*, 9126–9129. d) Adams, G. L.; Carroll, P. J.; Smith III, A. B. *J. Am. Chem. Soc*. **2012**, *134*, 4037–4040. e) Horning, B. D.; MacMillan, D. W. C. *J. Am. Chem. Soc*. **2013**, *135*, 6442–6445. f) Adams, G. L.; Carroll, P. J.; Smith III, A. B. *J. Am. Chem. Soc*. **2013**, *135*, 519–528. g) Smith, M. W.; Snyder, S. A. *J. Am. Chem. Soc*. **2013**, *135*, 12964–12967. h) Smith, J. M.; Moreno, J.; Boal, B. W.; Garg, N. K. *J. Am. Chem. Soc*. **2014**, *136*, 4504–4507. i) Teng M.; Zi, W.; Ma, D. *Angew. Chem., Int. Ed*. **2014**, *53*, 1814–1817. j) Ren, W.; Wang, Q.; Zhu, J. *Angew. Chem., Int. Ed*. **2014**, *53*, 1818–1821. k) Smith, J. M.; Moreno, J.; Boal, B. W.; Garg, N. K. *J. Org. Chem.* **2015**, *80*, 8954–8967. l) Moreno, J.; Picazo, E.; Morrill, L. A.; Smith, J. M.; Garg, N. K. *J. Am. Chem. Soc.* **2016**, *138*, 1162–1165. m) Ren, W.; Wang, Q.; Zhu, J. *Angew. Chem., Int. Ed.* **2016**, *55*, 3500–3503. n) Jiang, S.-Z.; Zeng, X.-Y.; Liang, X.; Lei, T.; Wei, K.; Yang, Y.-R. *Angew. Chem.,*

Int. Ed. **2016***, 55,* 4044–4048. o) Nishiyama, D.; Ohara, A.; Chiba, H.; Kumagai, H.; Oishi, S.; Fujii, N.; Ohno, H. *Org. Lett.* **2016**, *18*, 1670–1673. p) Eckermann, R.; Breunig, M.; Gaich, T. *Chem. Commun.* **2016**, *52*, 11363–11365. q) Wang, T.; Duan, X.; Zhao, H.; Zhai, S.; Tao, C.; Wang, H.; Li, Y.; Cheng, B.; Zhai, H. *Org. Lett.* **2017**, *19*, 1650–1653. r) Smith, M. W.; Zhou, Z.; Gao, A. X.; Shimbayashi, T.; Snyder, S. A. *Org. Lett.* **2017**, *19*, 1004–1007. s) Wang, D.; Hou, M.; Ji, Y.; Gao, S. *Org. Lett.* **2017**, *19*, 1922–1925. t) Eckermann, R.; Breunig, M.; Gaich, T. *Chem. Eur. J.* **2017**, *23*, 3938–3949. u) Xiao, T.; Chen, Z.-T.; Deng, L.-F.; Zhang, D.; Liu, X.-Y.; Song, H.; Qin, Y. *Chem. Commun.* **2017**, *53*, 12665–12667. v) Xie, X.; Wei, B.; Li, G.; Zu, L. *Org. Lett.* **2017**, *19*, 5430–5433. w) Li, Y.; Zhu, S.; Li, J.; Li, A. *J. Am. Chem. Soc.* **2016**, *138*, 3982–3985. x) Li, G.; Xie, X.; Zu, L. *Angew. Chem., Int. Ed.* **2016**, *55*, 10483–10486. y) Zhang, B.; Wang, X, Cheng, C.; Sun, D.; Li, C. *Angew. Chem., Int. Ed.* **2017**, *56*, 7484–7487. z) Chen, Z.-T.; Xiao, T.; Tang, P.; Zhang, D.; Qin, Y. *Tetrahedron* **2018**, *74*, 1129–1134.

(6) Equilibrium geometry calculations for the methanoquinolizidine scaffold were performed using Spartan ’16 (B3LYP/6-31(G)). The 3D representation was prepared from the calculated equilibrium geometry using CYLview. For CYLview, see: Legault, C. Y. CYLview, 1.0b; Université de Sherbrooke: Quebec, 2009; http://www.cylview.org.

(7) For the initial isolation of (+)-strictamine (**2.1**), see: a) Schnoes, H. K.; Biemann, K.; Mokrý, J.; Kompis, I.; Chatterjee, A.; Ganguli, G. *J. Org. Chem.* **1966**, *31*, 1641–1642. For the X-ray structure of strictamine, see: b) Ahmad, Y.; Fatima, K.; Occolowitz, J. L.; Solheim, B. A.; Clardy, J.; Garnick, R. L.; Le Quesne, P. W. *J. Am. Chem. Soc.* **1977**, *99*, 1943–1946.

(8) For the initial isolation of (–)-2(*S*)-cathafoline (**2.2**), see: Lim, S.-H.; Low, Y.-Y.; Sinniah, S. K.; Yong, K.-T.; Sim, K.-S.; Kam, T.-S. *Phytochemistry* **2014**, *98*, 204–215.

(9) For the initial isolation of (+)- akuammiline (**2.3**) and (–)-Ψ-akuammigine (**2.4**), see: Henry, T. A. *J. Chem. Soc.* **1932**, 2759–2768.

(10) a) Dolby, L. J.; Esfandiabi, Z. *J. Org. Chem.* **1972**, *37*, 43–46. b) Dolby, L. J.; Nelson, S. J. *J. Org. Chem.* **1973**, *38*, 2882–2887.

(11) a) Bennasar, M.-L.; Zulaica, E.; López, M.; Bosch, J. *Tetrahedron Lett.* **1988**, *29*, 2361–2364. b) Bennasar, M.-L.; Zulaica, E.; Ramírez, A.; Bosch, J. *J. Org. Chem.* **1996**, *61*, 1239–1251.

(12) Koike, T.; Takayama, H.; Sakai, S.-I. *Chem. Pharm. Bull.* **1991**, *39*, 1677–1681.

(13) Edwankar, R. V.; Edwankar, C. R.; Namjoshi, O. A.; Deschamps, J. R.; Cook, J. M. *J. Nat. Prod.* **2012**, *75*, 181–188.

(14) Komatsu, Y.; Yoshida, K.; Ueda, H.; Tokuyama, H. *Tetrahedron Lett.* **2013**, *54*, 377–380.

(15) Kawano, M.; Kiuchi, T.; Negishi, S.; Tanaka, H.; Hoshikawa, T.; Matsuo, J.; Ishibashi, H. *Angew. Chem., Int. Ed*. **2013**, *52*, 906–910.

(16) For our laboratory's communication detailing the first total syntheses of (+)-strictamine and (–)-2(*S*)-cathafoline, see ref 5l. Simultaneously Zhu's group reported the total synthesis of (±)-strictamine, see ref 5m.

(17) For the reductive interrupted Fischer indolization reaction, see: Maligres, P. E.; Houpis, I.; Rossen, K.; Molina, A.; Sager, J.; Upadhyay, V.; Wells, K. M.; Reamer, R. A.; Lynch, J. E.; Askin, D.; Volante, R. P.; Reider, P. J.; Houghton, P. *Tetrahedron* **1997**, *53*, 10983−10992.

(18) For methodology studies of the interrupted Fischer indolization, see: a) Boal, B. W.; Schammel, A. W.; Garg, N. K. *Org. Lett.* **2009**, *11*, 3458–3461. b) Schammel, A. W.; Boal, B. W.; Zu, L.; Mesganaw, T.; Garg, N. K. *Tetrahedron* **2010**, *66*, 4687–4695. c) Simmons, B. J.; Hoffmann, M.; Champagne, P. A.; Picazo, E.; Yamakawa, K.; Morrill, L. A.; Houk, K. N.; Garg, N. K. *J. Am. Chem. Soc.* **2017**, *139*, 14833–14836.

(19) For a pertinent review of our laboratory's Fischer indolization studies, see: Susick, R. B.; Morrill, L. A.; Picazo, E.; Garg, N. K. *Synlett* **2017**, *28*, 1–11.

(20) Scott, A. I. *Acc. Chem. Res.* **1970**, *3*, 151–157.

(21) Hou, Y.; Cao, X.; Wang, L.; Cheng, B.; Dong, L.; Luo, X.; Bai, G.; Giao, W. *J. Chromatogr. B* **2012**, *908*, 98–104.

(22) a) Lu, Z.; Li, Y.; Deng, J.; Li, A. *Nat. Chem*. **2013**, *5*, 679–683. b) Xiong, X.; Li, Y.; Lu, Z.; Wan, M.; Deng, J.; Wu, S.; Shao, H.; Li, A. *Chem. Commun*. **2014**, *50*, 5294–5297.

(23) For a review on catalytic asymmetric allylic alkylation employing heteroatom nucleophiles, see: Trost, B. M.; Zhang, T.; Sieber, J. D. *Chem. Sci.* **2010**, *1*, 427–440.

(24) Ohno, M.; Otsuka, M. *Org. React.* **1989**, *37*, 1–55.

(25) Aoki, K.; Koga, K. *Chem. Pharm. Bull*. **2000**, *48*, 571–574.

(26) For the crystallographic data of **3.16**, refer to CCDC number 1440684.

(27) Salom-Roig, X. J.; Dénès, F.; Renaud, P. *Synthesis* **2004**, 1903–1928.

(28) McDonald, C.; Holcomb, H.; Kennedy, K.; Kirkpatrick, E.; Leathers, T.; Vanemon, P. *J. Org. Chem.* **1989**, *54*, 1213–1215.

(29) For examples of the Fischer indolization being employed in late-stage total synthesis, see references 5b, h, k, and l, in addition to the following: a) Ueda, H.; Satoh, H.; Matsumoto, K.; Sugimoto, K.; Fukuyama, T.; Tokuyama, H. *Angew. Chem., Int. Ed.* **2009**, *48*, 7600−7603. b) Satoh, H.; Ueda, H.; Tokuyama, H. *Tetrahedron* **2013**, *69*, 89−95. (c) Krüger, S.; Gaich, T. *Eur. J. Org. Chem.* **2016**, 4893–4899.

(30) For an example of an indolenine reduction to an indoline in *Strychnos* alkaloid synthesis, see: Kim, J.-Y.; Suhl, C.-H.; Lee, J.-H.; Cho, C.-G. *Org. Lett.* **2017**, *19*, 6168–6171; see also references therein.

(31) a) Basha, A.; Lipton, M.; Weinreb, S. M. *Tetrahedron Lett.* **1977**, *18*, 4171–4174. b) Shimizu, T.; Osako, K.; Nakata, T. *Tetrahedron Lett.* **1997**, *38*, 2685–2688.

(32) Iwata, A.; Oshita, J.; Tang, H.; Kunai, A. *J. Org. Chem.* **2002**, *67*, 3927–3929.

(33) a) Liotta, D.; Sunay, U.; Santiesteban, H.; Markiewicz, W. *J. Org. Chem.* **1981**, *46*, 2605–2610. b) McMurry, J. *Org. React.* **1976**, *24*, 187–224.

(34) For the removal of nosyl groups using a solid-supported thiol reagent, see: Cardullo, F.; Donati, D.; Merlo, G.; Paio, A.; Salaris, M.; Taddei, M. *Synlett* **2005**, 2996−2998.

(35) Wang, H.; Reisman, S. E. *Angew. Chem., Int. Ed.* **2014**, *53*, 6206–6210.

(36) Duwiejua, M.; Woode, E.; Obiri, D. D. *J. Ethnopharmacol.* **2002**, *81*, 73–79.

(37) For a reported effort toward (–)-Ψ-akuammigine (**2.4**), see: Andreansky, E. S.; Blakey, S. B. *Org. Lett.* **2016**, *18*, 6492–6495.

(38) a) Sung, M. J.; Lee, H. I.; Lee, H. B.; Cha, J. K. *J. Org. Chem.* **2003**, *68*, 2205–2208. b) Shimada, K.; Kaburagi, Y.; Fukuyama, T. *J. Am. Chem. Soc.* **2003**, *125*, 4048–4049. c) Yu,

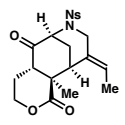
J.; Wearing, X. Z.; Cook, J. M. *J. Am. Chem. Soc.* **2004**, *126*, 1358–1359. d) Yu, J.; Wearing, X. Z.; Cook, J. M. *J. Org. Chem.* **2005**, *70*, 3963–3979.

(39) García, A.; Castedo, L.; Domínguez, D. *Tetrahedron* **1996**, *52*, 5929–5932.

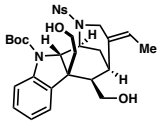
(40) Le, D. D.; Cortesi, A. T.; Myers, S. A.; Burlingame, A. L.; Fujimori, D. G. *J. Am. Chem. Soc.* **2013**, *135*, 2879–2882.

(41) Equilibrium geometry calculations were performed using Spartan '16 (B3LYP/6-31(G)). The results indicated that furoindoline **2.46** is nearly 8 kcal/mol lower in energy than desired furoindoline **2.47**.

(42) Additional strategies were investigated. For example, we attempted to introduce the C16 quaternary stereocenter prior to Fischer indolization on a model system. However, Fischer indolization efforts using **i** were unsuccessful, presumably due to the difficulty of performing the [3,3]-sigmatropic rearrangement when trying to access vicinal quaternary stereocenters. With regard to late-stage efforts, intermediates such as diol **ii** could not be elaborated to substrates suitable for methanoquinolizidine formation.



i



ii

(43) Wilk, A.; Grajkowski, A.; Phillips, L. R.; Beaucage, S. L. *J. Org. Chem.* **1999**, *64*, 7515–7522.

(44) a) Stotter, P. L.; Friedman, M. D.; Dorsey, G. O.; Shiely, R. W.; Williams, R. F.; Minter, D. E. *Heterocycles* **1987**, *25*, 251–258. b) Lu, X.; Cook, J. M. *Org. Lett.* **2001**, *3*, 4023–4026. c)

Lu, X.; Deschamp, J. R.; Cook, J. M. *Org. Lett.* **2002**, *4*, 3339–3342. d) Liao, X.; Zhou, H.; Wearing, X. Z.; Ma, J.; Cook, J. M. *Org. Lett.* **2005**, *7*, 3501–3504.

(45) Schwartz, M. A.; Rose, B. F.; Vishnuvajjala, B. *J. Am. Chem. Soc.* **1973**, *95*, 612–613.

(46) For (–)-Ψ-akuammigine (**2.4**) characterization data, see: Hu, W.-L.; Zhu, J.-P.; Hesse, M. *Planta Med.* **1989**, *55*, 463–466.

(47) Attempts to install the furoindoline from aldehyde **2.55** en route to (–)-Ψ-akuammigine (**2.4**) were unsuccessful.

(48) Picot, A.; Lusinchi, X. *Bull. Soc. Chim. Fr.* **1977**, 1227–1234.

(49) For (+)-akuammiline (**2.3**) characterization data, see: Benayad, S.; Ahamada, K.; Lewin, G.; Evanno, L.; Poupon, E. *Eur. J. Org. Chem.* **2016**, 1494–1499.

(50) For the Zn / strong acid-promoted rearrangement of the methanoquinolizidine in low yield (or no reported yield), see ref 7a and: a) Savaskan, S.; Kompis, I.; Hesse, M.; Schmid, H. *Helv. Chim. Acta* **1972**, *55*, 2861–2867. b) Banerji, J.; Chakrabarti, R. *Indian J. Chem. Sect. B* **1984**, *23B*, 453–454.

(51) Honda, T.; Ishikawa, F. *Chem. Commun.* **1999**, *1065–1066.*

(52) Xie, X.; Zu, L. *Synlett* **2018**, *29*, 1008–1013.

(53) An exemplary akuammiline natural product of this variety is echitamine, first isolated in 1875. For the seminal isolation report, see: Group-Besanez, v. *Justus Liebigs Ann. Chem.* **1875**, *176*, 88−89.

(54) Niu, C.; Pettersson, T.; Miller, M. J. *J. Org. Chem.* **1996**, *61*, 1014–1022.

(55) a) Dugan, J. J.; Hesse, M.; Renner, U.; Schmid, H. *Helv. Chim. Acta* **1969**, *52*, 701–707. b) Benayad, S.; Ahamada, K.; Lewin, G.; Evanno, L.; Poupon, E. *Eur. J. Org. Chem.* **2016**, 1494–1499.

CHAPTER THREE

Synthetic Studies Pertaining to the 2,3-Pyridyne and 4,5-Pyrimidyne

Jose M. Medina, Moritz K. Jackl, Robert B. Susick, and Neil K. Garg

Tetrahedron **2016**, *72*, 3629–3634.

3.1 Abstract

We report synthetic studies pertaining to two heterocyclic aryne intermediates: the 2,3-pyridyne and the 4,5-pyrimidyne. First, a 2,3-pyridyne precursor was readily accessed from 2-pyridone using a known procedure. Subsequently, 2,3-pyridyne generation and trapping were used to access several functionalized pyridines in a regioselective manner. In addition, we report synthetic routes to two isomeric silyl triflates, which were intended to serve as precursors to the 4,5-pyrimidyne. Consecutive 4,5-pyrimidyne generation and trapping experiments were ultimately deemed unfruitful. We expect these findings will promote the use of 2,3-pyridyne and other heterocyclic arynes as building blocks for the synthesis of functionalized heterocycles.

3.2 Introduction

The synthesis of heterocycles continues to be a vital area of research. Heterocycles, especially *N*-containing compounds, are commonly seen in a variety of important molecules including medicines, natural products, and agrochemicals.[1] One exciting approach to the synthesis of decorated heterocycles involves the trapping of in situ generated heterocyclic

arynes, commonly referred to as hetarynes.[2,3] This strategy was well studied several decades ago,[4] but only led to modest synthetic utility.

More recently, the chemistry of heterocyclic arynes has undergone a revival. Methodological studies pertaining to indolynes[5,6] and 3,4-pyridynes[7] have been disclosed and several silyl triflate precursors to these intermediates are now commercially available.[8] Moreover, heterocyclic arynes have been used to synthesize several natural products (e.g., **3.1**–**3.4**, Figure 3.1).[2,9,10] One particularly attractive subclass of heterocyclic arynes are those that possess one or more nitrogen atoms in a 6-membered ring (e.g., **3.5**–**3.7**). The successful generation and trapping of such species via cycloaddition processes would provide a powerful means to build medicinally privileged scaffolds, including compounds that may be difficult to access by other means.

We have been particularly interested in the chemistry of pyridynes and pyrimidynes, each of which are classes of heterocyclic arynes with an interesting history. The 3,4-pyridyne (**3.5**) was first generated in 1955[11] and has subsequently been the subject of numerous investigations, including one by our own laboratory.[7] The 3,4-pyridyne (**3.5**) and substituted versions can now be used to access polysubstituted pyridines in a controlled and predictable way by virtue of the aryne distortion model[5,12] using robust silyl triflate precursors.[7] Similarly, the 2,3-pyridyne (**3.6**) has been known for several decades.[13] In more recent efforts, Walters and Shay reported the synthesis of a silyl triflate precursor to **3.6**.[14] In turn, a few examples where **3.6** can be used in Diels–Alder reactions or other annulations are available.[14,15,16,17,18,19] The least well-studied of our targets is the 4,5-pyrimidyne (**3.7**). Substituted derivatives have been accessed by dehydrohalogenation under strongly basic reaction conditions or by oxidation of an

aminotriazole precursor.[20] Prior experiments involving 4,5-pyrimidynes have led to amination or low yields of annulated products.[20]

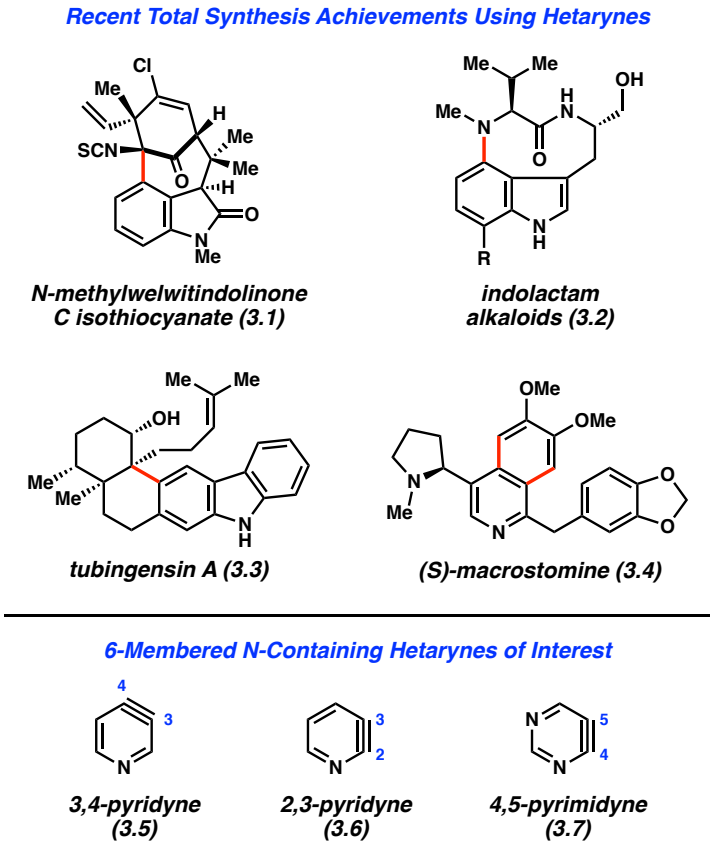
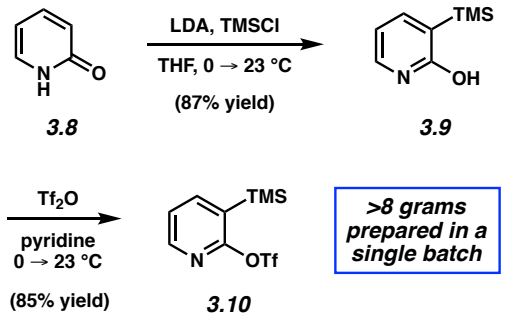


Figure 3.1. Natural products **3.1**–**3.4** and heterocyclic arynes **3.5**–**3.7**

Given the earlier promising results involving the 2,3-pyridyne (**3.6**) and 4,5-pyrimidyne (**3.7**), we sought to further expand the utility of these intermediates for the synthesis of functionalized heterocycles. Herein, we report new trapping experiments involving 2,3-pyridyne (**3.6**), in addition to efforts toward 4,5-pyrimidyne (**3.7**).

3.3 Synthesis of 2,3-Pyridyne Precursor

To study annulations of 2,3-pyridyne, it was first necessary to prepare a suitable silyl triflate precursor. Thus, silyl triflate **3.10** was synthesized using a known procedure (Scheme 3.1).[14] Beginning from 2-pyridone (**3.8**), a lithiation and silylation sequence provided silylhydroxypyridine **3.9**. Subsequent reaction with triflic anhydride furnished silyl triflate **3.10**. This high-yielding two-step sequence provides a reliable method to access **3.10** in multigram quantities. It should be noted that **3.10** is now also commercially available.[21]

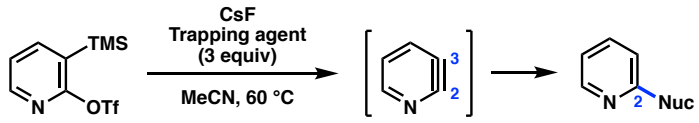


Scheme 3.1. Synthesis of silyl triflate **3.10**

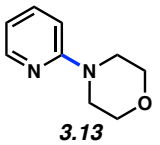
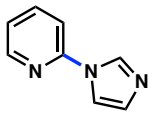
3.4 Generation & Trapping of 2,3-Pyridyne

Silyl triflate **3.10** was examined in nucleophilic trapping experiments as shown in Table 3.1. Trapping with morpholine (**3.12**) led to the formation of **3.13** in 55% yield (entry 1), whereas use of imidazole (**3.14**) as the trapping agent delivered **3.15** in 63% yield (entry 2). In both cases, the 2-substituted pyridine products were obtained, with no evidence of the formation of 3-substituted adducts. This regioselectivity trend is consistent with prior observations[2c] and predictions made by the aryne distortion model.[12c]

Table 3.1. Trapping of 2,3-Pyridyne (**3.6**) with nucleophiles



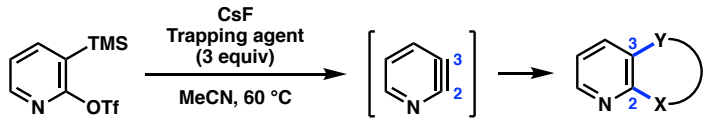
3.10 *3.6* *3.11*

Entry	*Trapping agent*	*Product*	*Yield*[a]
1	 *3.12*	 *3.13*	*55%*
2	 *3.14*	 *3.15*	*63%*

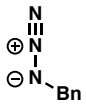
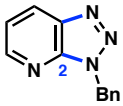
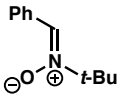
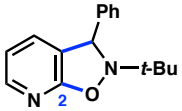
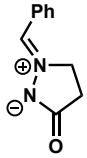
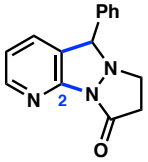
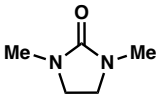
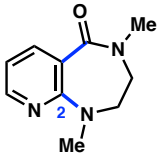
[a] Reported yields are the average of two experiments and are based on the amounts of isolated product.

We were delighted to find that silyl triflate **3.10** could also be employed in cycloaddition reactions (Table 3.2). For example, interception of pyridyne **3.6** by benzylazide (**3.17**)[22] furnished annulated product **3.18**, albeit in low yield (entry 1). Alternatively, trapping with nitrone **3.19**[23] provided the unusual heterocycle **3.20** (entry 2). We also tested an azomethine imine cycloaddition[24] using **3.21**, which gave rise to tricycle **3.22** in 42% yield (entry 3). More synthetically useful yields were obtained when dimethylurea **3.23**[16] was utilized in the trapping experiments. This reaction gave fused bicyclic pyridine derivative **3.24** in 75% yield (entry 4). In all cases, only one regioisomer of annulated product was detected, indicative of preferential nucleophilic attack occurring at C2 of the 2,3-pyridyne intermediate.

Table 3.2. Annulation reactions of 2,3-pyridyne (**3.6**)



3.10 *3.6* *3.16*

Entry	*Trapping agent*	*Product*	*Yield*[a]
1	 *3.17*	 *3.18*	*20%*
2	 *3.19*	 *3.20*	*33%*
3	 *3.21*	 *3.22*	*42%*
4	 *3.23*	 *3.24*	*75%*

[a] Reported yields are the average of two experiments and are based on the amounts of isolated product.

Despite the success of the aforementioned trapping experiments, it should be noted that silyl triflate **3.10** could not be employed successfully in other attempted 2,3-pyridyne trapping experiments (Figure 3.2). For example, the use of nitrile oxide precursor **3.25**, diazoester **3.26**, or enamide **3.27** in attempted annulations led only to decomposition. Similarly, efforts to utilize sydnone **3.28** in a Diels–Alder trapping or β-ketoester **3.29**[25] in a formal (2+2) cycloaddition

were unsuccessful. Nonetheless, the knowledge gained from our 2,3-pyridyne studies should enable the judicious use of **3.10** in synthetic applications.

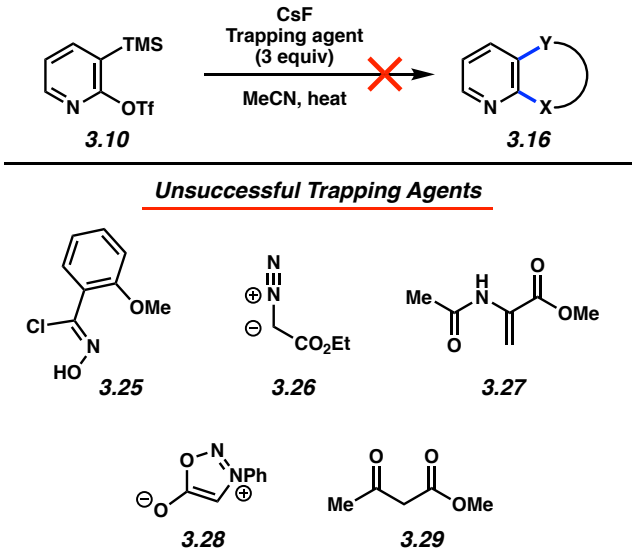
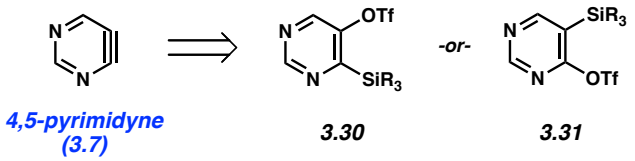


Figure 3.2. Unsuccessful cycloadditions using silyl triflate **3.10**

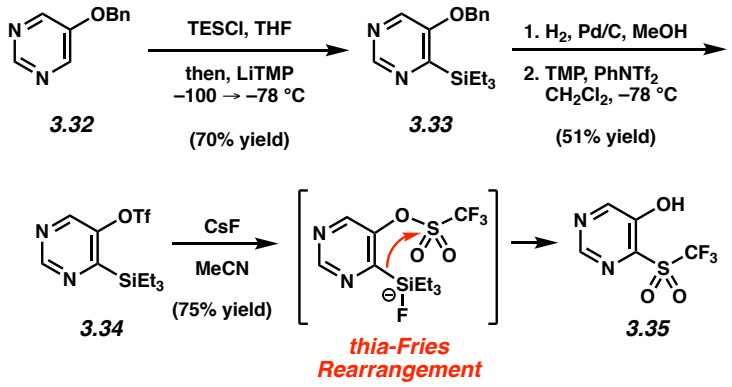
3.5 Synthesis of 4,5-Pyrimidyne Precursors & Trapping Experiments

As noted earlier, we were also eager to expand the limited scope of 4,5-pyrimidyne trapping experiments.[20] As such, we pursued the notion suggested in Scheme 3.2. Specifically, we envisioned that 4,5-pyrimidyne (**3.7**) could be prepared in situ from silyl triflate **3.30** or its constitutional isomer **3.31**.



Scheme 3.2. Approaches to 4,5-pyrimidyne (**3.7**) from silyl triflate precursors **3.30** and **3.31**

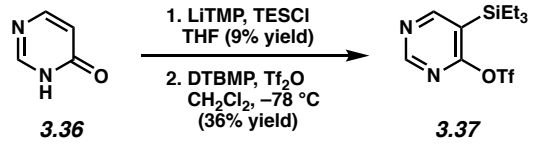
In our initial approach, we sought to access a silyl triflate precursor from known benzyloxypyrimidine **3.32**[26] (Scheme 3.3). As such, 5-benzyloxypyrimidine (**3.32**) was synthesized from the corresponding commercially available bromide using an Ullmann coupling.[26] With **3.32** in hand, extensive efforts were put forth to effect silylation. It was ultimately found that the desired triethylsilylated product **3.33** could be obtained using a one-pot procedure involving mixing of **3.32** with TESCl, followed by low temperature lithiation, with in situ silylation.[27] From **3.33**, debenzylation and subsequent triflation delivered the desired silyl triflate **3.34**. Eager to attempt pyrimidyne generation, **3.34** was subjected to a battery of experiments involving variation of fluoride sources, trapping agents, and other reaction conditions. Unfortunately, no products indicative of pyrimidyne formation were observed. Instead, it was found that **3.34** was prone to readily undergo thia-Fries rearrangement in the presence of fluoride sources. For example, treatment of **3.34** with CsF in acetonitrile gave **3.35** as the major product.[28] Greaney and coworkers have also observed thia-Fries rearrangement in attempted aryne generation from silyl triflate precursors.[29]



3.32 3.33 3.34 3.35

Scheme 3.3. Synthesis of silyl triflate **3.34** and undesired Fries rearrangement

With our initial efforts thwarted, we pursued the synthesis of an isomeric silyl triflate, as shown in Scheme 3.4. 2-Pyrimidone (**3.36**) was found to undergo lithiation/silylation using a protocol similar to the one described previously to access pyridyne precursor **3.10** (see Scheme 3.1). Subsequent triflation of the remaining hydroxyl group furnished silyl triflate **3.37**.[30]



3.36 3.37

Scheme 3.4. Synthesis of silyl triflate **3.37**

With the desired isomeric silyl triflate **3.37** available in just two steps from commercially available material, we pursued pyrimidyne generation and trapping (Figure 3.3). Thus, **3.37** was exposed to fluoride sources (e.g., CsF) in the presence of trapping agents. However, in all attempts, we were unable to observe any of the desired cycloaddition adducts. Instead, only substantial non-specific decomposition or formation of 2-pyrimidone was observed.[31]

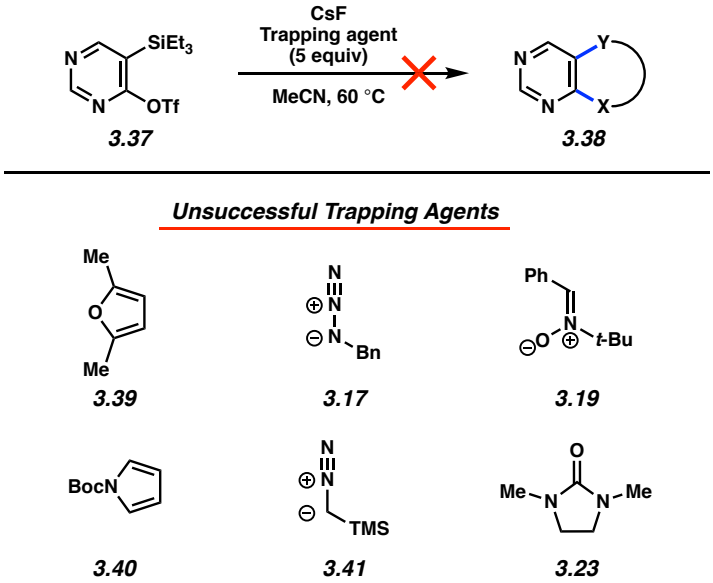


Figure 3.3. Unsuccessful attempts to generate and trap the 4,5-pyrimidyne from silyl triflate **3.37**

3.6 Conclusion

In summary, we have performed studies pertaining to two interesting heterocyclic aryne intermediates: 2,3-pyridyne and 4,5-pyrimidyne. We have shown that 2,3-pyridyne can be employed in various trapping experiments involving nucleophiles or cycloaddition partners. Several of the products obtained are unique scaffolds that would arguably be difficult to access by other means. In addition, we have developed synthetic routes to two plausible silyl triflate precursors to the 4,5-pyrimidyne, although no evidence of pyrimidyne formation was noted in attempted trapping experiments. We expect our findings will promote the use of 2,3-pyridyne and other strained heterocyclic intermediates in the synthesis of functionalized heterocycles.

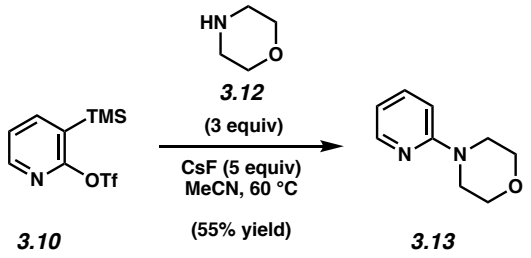
3.7 Experimental Section

3.7.1 Materials and Methods

Unless stated otherwise, reactions were conducted in flame-dried glassware under an atmosphere of nitrogen using anhydrous solvents (freshly distilled or passed through activated alumina columns). All commercially obtained reagents were used as received unless otherwise specified. Cesium fluoride (CsF) was obtained from Strem Chemicals. Trifluoromethanesulfonic anhydride (Tf_2O), trimethylsilyl chloride (TMSCl), 2,2,6,6-tetramethylpiperidine (TMP) and triethylsilyl chloride (TESCl) were obtained from Oakwood Products, Inc. and distilled over before use. *N*-tert-butyl-α-phenylnitrone and methyl 2-acetamidoacrylate were obtained from Alfa Aesar. Ethyl diazoacetate, (trimethylsilyl) diazomethane (1 M in Et_2O), 2,5-dimethylfuran, imidazole, and *N*-Boc-pyrrole were obtained from Sigma-Aldrich. Morpholine was obtained from Spectrum Chemical and distilled before use. Reaction temperatures were controlled using an IKAmag temperature modulator and, unless stated otherwise, reactions were performed at room temperature (rt, approximately 23 °C). Thin layer chromatography (TLC) was conducted with EMD gel 60 F254 pre-coated plates (0.25 mm) and visualized using a combination of UV light and potassium permanganate staining. Preparative thin layer chromatography (TLC) was conducted with EMD gel 60 F254 pre-coated plates (0.5 mm) and visualized using UV light. Silicycle Siliaflash P60 (particle size 0.040–0.063 mm) was used for flash column chromatography. ^{1}H NMR spectra were recorded on Bruker spectrometers (500 MHz) and are reported relative to deuterated solvent signals. Data for ^{1}H NMR spectra are reported as follows: chemical shift (δ ppm), multiplicity, coupling constant (Hz) and integration. ^{13}C NMR spectra were recorded on Bruker spectrometers (125 MHz) and are reported relative to deuterated solvent signals. Data for ^{13}C NMR spectra are reported in terms of chemical shift and, when

necessary, multiplicity, and coupling constant (Hz). IR spectra were obtained using a Perkin-Elmer 100 spectrometer or a Perkin-Elmer UATR two spectrometer, and are reported in terms of frequency absorption (cm^{-1}). DART-MS spectra were collected on a Thermo Exactive Plus MSD (Thermo Scientific) equipped with an ID-CUBE ion source and a Vapur Interface (IonSense Inc.). Both the source and MSD were controlled by Excalibur software v. 3.0. The analyte was spotted onto OpenSpot sampling cards (IonSense Inc.) using $CDCl_3$ as the solvent. Ionization was accomplished using UHP He (Airgas Inc.) plasma with no additional ionization agents. The mass calibration was carried out using Pierce LTQ Velos ESI (+) and (–) Ion calibration solutions (Thermo Fisher Scientific).

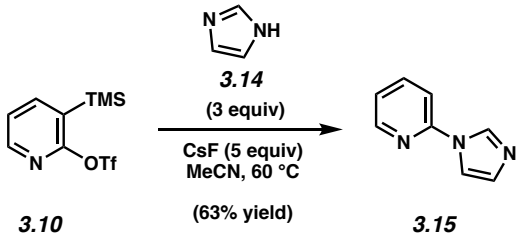
3.7.2 Experimental Procedures



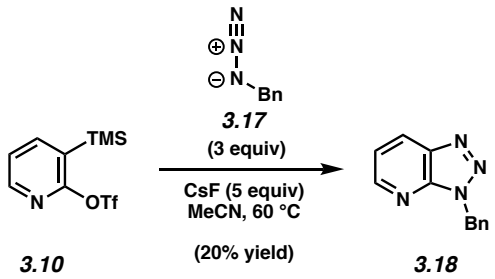
Representative Procedure for 2,3-Pyridyne Trappings. Adduct 3.13 (Table 3.1, Entry 1). To a stirred solution of silyl triflate **3.10**[14] (51.1 mg, 0.172 mmol, 1.0 equiv) and morpholine (**3.12**, 48.0 μL, 0.516 mmol, 3.0 equiv) in MeCN (7.0 mL) was added CsF (128 mg, 0.840 mmol, 5.0 equiv). The reaction vessel was sealed and placed in a preheated aluminum heating block maintained at 60 °C for 2 h. After cooling to 23 °C, the reaction mixture was filtered over silica gel (EtOAc eluent, 12 mL). Evaporation under reduced pressure and further purification by preparative thin layer chromatography (2:1 hexanes:EtOAc) afforded **3.13** as a colorless oil

(55% yield, average of two experiments). **3.13**: R_f 0.48 (3:1 hexanes:EtOAc); ^{1}H NMR (500 MHz, $CDCl_3$): δ 8.19 (ddd, *J* = 4.9, 2.0, 0.8, 1H), 7.49 (ddd, *J* = 9.0, 7.2, 2.0, 1H), 6.65 (ddd, *J* = 7.2, 4.9, 0.8, 1H), 6.62 (d, *J* = 8.7, 1H), 3.82 (t, *J* = 5.0, 4H), 3.49 (t, *J* = 5.0, 4H); ^{13}C NMR (125 MHz, $CDCl_3$): δ 159.7, 148.1, 137.6, 113.9, 107.0, 66.9, 45.7; IR (film): 1593, 1481, 1437, 1376, 1312, 1243 cm^{-1}; HRMS-APCI (*m/z*) $[M + H]^+$ calcd for $C_9H_{13}N_2O^+$, 165.1022; found 165.1024.

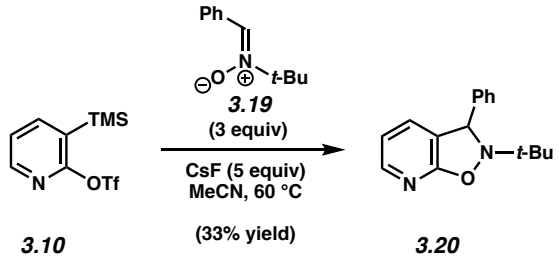
Any modifications of the conditions shown in this representative procedure are specified in the following schemes, which depict all of the results shown in Tables 3.1 and 3.2.



Adduct 3.15 (Table 3.1, Entry 2). Purification by preparative thin layer chromatography (6:3:1 EtOAc:PhH:MeOH) afforded **3.15** (63% yield, average of two experiments) as a light orange oil. **3.15**: R_f 0.62 (9:1 EtOAc:MeOH); ^{1}H NMR (500 MHz, $CDCl_3$): δ 8.49 (ddd, *J* = 4.9, 1.8, 0.9, 1H), 8.35 (s, 1H), 7.83 (dt, *J* = 7.5, 1.8, 1H), 7.65 (s, 1H), 7.36 (d, *J* = 8.2, 1H), 7.24 (ddd, *J* = 7.5, 4.9, 0.8, 1H), 7.20 (s, 1H); ^{13}C NMR (125 MHz, $CDCl_3$): δ 149.4, 149.3, 139.1, 135.1, 130.9, 122.1, 116.3, 112.5; IR (film): 1598, 1578, 1487, 1444, 772, 738 cm^{-1}; HRMS-APCI (*m/z*) $[M + H]^+$ calcd for $C_8H_8N_3^+$, 146.0713; found 146.0714.

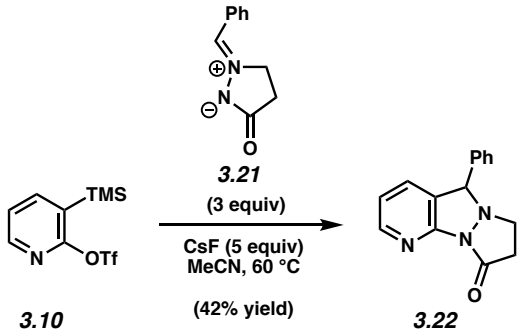


Adduct 3.18 (Table 3.2, Entry 1). Purification by preparative thin layer chromatography (3:1 hexanes:EtOAc) afforded **3.18** (20% yield, average of two experiments) as a light yellow oil. **3.18**: R_f 0.35 (3:1 hexanes:EtOAc); ^{1}H NMR (500 MHz, $CDCl_3$): δ 8.69 (dd, J = 4.5, 1.4, 1H), 8.37 (dd, J = 8.2, 1.4, 1H), 7.46 (d, J = 7.2, 2H), 7.36–7.28 (m, 4H), 5.92 (s, 2H); ^{13}C NMR (125 MHz, $CDCl_3$): δ 150.5, 145.8, 137.2, 135.2, 129.0, 128.7, 128.5, 128.4, 120.0, 50.6; IR (film): 3032, 2927, 2852, 1591, 1216 cm^{-1}; HRMS-APCI (*m/z*) $[M + H]^+$ calcd for $C_{12}H_{11}N_4^+$, 211.0978; found 211.0974.

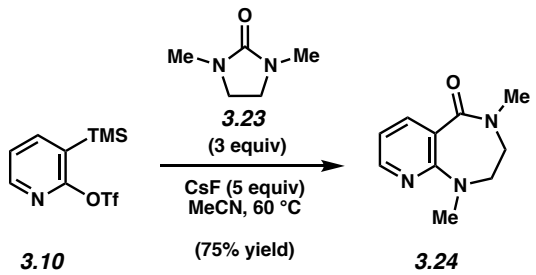


Adduct 3.20 (Table 3.2, Entry 2). Purification by preparative thin layer chromatography (3:1 hexanes:EtOAc) afforded **3.20** (33% yield, average of two experiments) as an amorphous white solid. **3.20**: R_f 0.52 (3:1 hexanes:EtOAc); ^{1}H NMR (500 MHz, $CDCl_3$): δ 8.04 (d, J = 5.0, 1H), 7.42 (d, J = 7.2, 2H), 7.35 (t, J = 7.2, 2H), 7.28 (tt, J = 7.2, 1.2, 1H), 7.19 (dt, J = 7.3, 1.3, 1H), 6.74 (dd, J = 7.3, 5.0, 1H), 5.62 (s, 1H), 1.20 (s, 9H); ^{13}C NMR (125 MHz, $CDCl_3$): δ 165.1, 147.9, 143.0, 132.8, 128.9, 127.9, 127.4, 123.0, 116.8, 66.3, 61.4, 25.5; IR (film): 1604, 1420,

1282, 1270, 775, 739 cm^{-1}; HRMS-APCI (*m/z*) $[M + H]^+$ calcd for $C_{16}H_{19}N_2O^+$, 255.1492; found 255.1492.

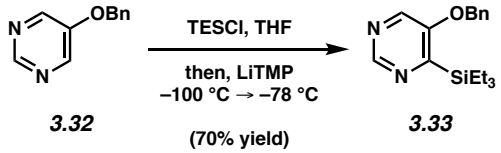


Adduct 3.22 (Table 3.2, Entry 3). Purification by preparative thin layer chromatography (95:5 EtOAc:MeOH) afforded **3.22** (42% yield, average of two experiments) as a colorless amorphous solid. **3.22**: R_f 0.48 (95:5 EtOAc:MeOH); ^{1}H NMR (500 MHz, $CDCl_3$): δ 8.32 (dt, *J* = 5.1, 1.1, 1H), 7.44–7.38 (m, 5H), 7.18 (dt, *J* = 7.5, 1.3, 1H), 6.94 (dd, *J* = 7.5, 5.1, 1H), 5.16 (s, 1H), 3.64–3.60 (m, 1H), 3.19–3.06 (m, 2H), 2.89–2.83 (m, 1H); ^{13}C NMR (125 MHz, $CDCl_3$): δ 163.2, 148.8, 148.5, 137.6, 132.5, 129.2, 129.1, 128.8, 128.4, 119.7, 73.5, 52.5, 36.9; IR (film): 1708, 1597, 1460, 1430, 1388, 1308 cm^{-1}; HRMS-APCI (*m/z*) $[M + H]^+$ calcd for $C_{15}H_{14}N_3O^+$, 252.1131; found 252.1126.



Adduct 3.24 (Table 3.2, Entry 4). Purification by preparative thin layer chromatography (95:5 EtOAc:MeOH) afforded **3.24** (75% yield, average of two experiments) as a colorless oil. **3.24**: R_f

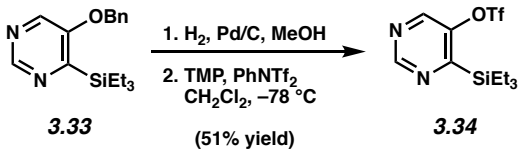
0.45 (95:5 EtOAc:MeOH); ^{1}H NMR (500 MHz, $CDCl_3$): δ 8.29 (dd, J = 4.9, 2.0, 1H), 8.01 (dd, J = 7.6, 2.0, 1H), 6.76 (dd, J = 7.6, 4.9, 1H), 3.61–3.57 (m, 2H), 3.57–3.52 (m, 2H), 3.18 (s, 3H), 3.05 (s, 3H); ^{13}C NMR (125 MHz, $CDCl_3$): δ 169.2, 155.7, 150.9, 140.7, 119.4, 114.6, 56.3, 48.1, 38.9, 35.6; IR (film): 1633, 1504, 1408, 1385, 1247, 1208 cm^{-1}; HRMS-APCI (*m/z*) [M + H]$^{+}$ calcd for $C_{10}H_{14}N_3O^{+}$, 192.1131; found 192.1131.



3.32 ***3.33***

Pyrimidine 3.33 (Scheme 3.3). To a stirred solution of freshly distilled 2,2,6,6-tetramethylpiperidine (1.97 g, 14.0 mmol, 1.4 equiv) in THF (50 mL) at 0 °C was added *n*-BuLi in hexanes (2.3 M, 5.65 mL, 13.0 mmol, 1.3 equiv). The resulting solution was allowed to stir at 0 °C for 30 min. A separate flask was charged with 5-benzyloxypyrimidine **3.32** (2.00 g, 10.0 mmol, 1.0 equiv), TESCl (4.53 g, 30.0 mmol, 3.0 equiv), and THF (50 mL). The resulting solution was cooled to –100 °C and the LiTMP solution was added dropwise via cannula over 20 min. The resulting solution was warmed to –78 °C and allowed to stir for 3.5 h. The solution was then allowed to warm to 0 °C and quenched with saturated NH_4Cl (25 mL). The volatiles were removed under reduced pressure and EtOAc (75 mL) was added. The organic phase was separated and the aqueous layer was extracted with EtOAc (3 x 50 mL). The combined organic layers were dried with $MgSO_4$ and concentrated under reduced pressure. The resulting oil was further purified by column chromatography (5:1 hexanes:EtOAc) to yield pyrimidine **3.33** (2.09 g, 70% yield) as a colorless oil. **3.33**: R_f 0.41 (3:1 hexanes:EtOAc); ^{1}H NMR (500 MHz, $CDCl_3$): δ 8.95 (s, 1H), 8.24 (s, 1H), 7.42–7.34 (m, 5H), 5.12 (s, 2H), 0.95–0.91 (m, 9H), 0.91–0.86 (m, 6H); ^{13}C NMR (125 MHz, $CDCl_3$): δ 165.5, 158.4, 151.7, 137.6, 135.7, 128.9, 128.6,

127.7, 70.6, 7.5, 3.0; IR (film): 2953, 2874, 1558, 1456, 1397, 1284 cm^{-1}; HRMS-APCI (*m/z*) $[M + H]^+$ calcd for $C_{17}H_{25}N_2OSi^+$, 301.1731; found 301.1729.

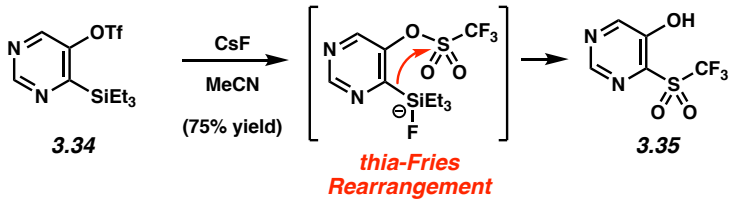


3.33 ***3.34***

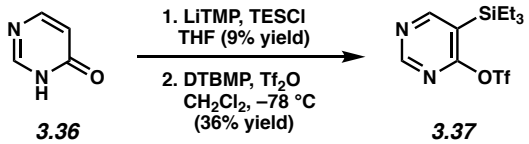
Silyl triflate 3.34 (Scheme 3.3). To a stirred solution of pyrimidine **3.33** (1.00 g, 3.33 mmol, 1.0 equiv) in dry MeOH (20 mL) was added 10% Pd/C (350 mg, 0.330 mmol, 0.1 equiv). The resulting mixture was placed under an atmosphere of H_2 (1 atm) and was allowed to stir at 23 °C for 2 h. The mixture was filtered over celite (MeOH eluent). Evaporation of the solvent under reduced pressure afforded the crude alcohol intermediate, which was used in the subsequent step without further purification.

The alcohol intermediate (510 mg, 2.43 mmol, 1.0 equiv) was dissolved in dry CH_2Cl_2 (7 mL) and freshly distilled 2,2,6,6-tetramethylpiperidine (282 mg, 9.72 mmol, 4.0 equiv) was added dropwise over 10 min. The resulting solution was cooled to –78 °C and a solution of $PhNTf_2$ (714 mg, 2.92 mmol, 1.2 equiv) in CH_2Cl_2 (7 mL) was added dropwise over 15 min. The resulting solution was stirred at –78 °C for 2 h and was then quenched with saturated $NaHCO_3$ (10 mL). The organic layer was separated and the aqueous layer was extracted with CH_2Cl_2 (3 x 20 mL). The combined organic layers were dried with $MgSO_4$ and concentrated under reduced pressure. The resulting oil was further purified by column chromatography (30:1 hexanes:EtOAc) to yield silyl triflate **3.34** as a colorless oil (581 mg, 51% yield, 2 steps). **3.34**: R_f 0.70 (3:1 hexanes:EtOAc); ^1H NMR (500 MHz, $CDCl_3$): δ 9.26 (s, 1H), 8.64 (s, 1H), 0.97 (br s, 15H); ^{13}C NMR (125 MHz, $CDCl_3$): δ 169.7, 156.7, 152.4, 147.0, 118.5 (q, J = 318.2, CF_3),

7.3, 3.0; IR (film): 2960, 2880, 1565, 1428, 1386, 1211 cm^{-1}; HRMS-APCI (*m/z*) $[M + H]^+$ calcd for $C_{11}H_{18}F_3N_2O_3SSi^+$, 343.0754; found 343.0748.



Alcohol 3.35 (Scheme 3.3). To a stirred solution of silyl triflate **3.34** (130 mg, 0.380 mmol, 1.0 equiv) in MeCN (3.8 mL) was added CsF (173 mg, 1.14 mmol, 3.0 equiv). The reaction vessel was sealed and placed in a preheated aluminum heating block maintained at 60 °C for 2 h. After cooling to 23 °C, the reaction mixture was filtered over celite (MeOH eluent, 12 mL). Evaporation under reduced pressure and further purification by preparative thin layer chromatography (100:10:1 CH_2Cl_2:MeOH:Et_3N) afforded **3.35** as a colorless oil (75% yield). **3.35**: R_f 0.76 (MeCN); ^{1}H NMR (500 MHz, MeOD): δ 8.28 (s, 1H), 8.08 (s, 1H); ^{13}C NMR (125 MHz, MeOD): δ 165.6, 161.0, 142.0, 137.6, 122.5 (q, J = 327.9, CF_3); IR (film): 3349, 1643, 1575, 1510, 1445, 1341 cm^{-1}; HRMS-APCI (*m/z*) $[M - H]^-$ calcd for $C_5H_2F_3N_2O_3S^+$, 226.9733; found 226.9750.



Silyl triflate 3.37 (Scheme 3.4). To a stirred solution of freshly distilled 2,2,6,6-tetramethylpiperidine (1.02 g, 7.20 mmol, 1.4 equiv) in THF (10 mL) at 0 °C was added *n*-BuLi in hexanes (2.3 M, 2.94 mL, 6.80 mmol, 1.3 equiv). The resulting solution was stirred at 0 °C for

30 min. A separate flask was charged with 2-pyrimidone **3.36** (500 mg, 5.20 mmol, 1.0 equiv), TESCl (1.97 g, 13.0 mmol, 2.5 equiv), and THF (16 mL). The resulting solution was cooled to 0 °C and the LiTMP solution was added dropwise via cannula over 20 min. The resulting solution was warmed to 23 °C and allowed to stir for 24 h. The solution was then quenched with saturated NH_4Cl (10 mL). The volatiles were removed under reduced pressure and EtOAc (30 mL) was added. The organic phase was separated and the aqueous layer was extracted with EtOAc (3 x 20 mL). The combined organic layers were dried with $MgSO_4$ and concentrated under reduced pressure. The resulting oil was further purified by column chromatography (1:2 to 1:4 hexanes:EtOAc) to yield an alcohol intermediate (100 mg, 9% yield, unoptimized) as a colorless oil.

The alcohol intermediate (90.0 mg, 0.430 mmol, 1.0 equiv) was dissolved in dry CH_2Cl_2 (2 mL) and DTBMP (96.0 mg, 0.470 mmol, 1.1 equiv) was added. The resulting solution was cooled to –78 °C and Tf_2O (133 mg, 0.470 mmol, 1.1 equiv) was added dropwise over 5 min. The resulting solution was allowed to stir at –78 °C for 2 h and was then quenched with saturated $NaHCO_3$ (1 mL). The organic layer was separated and the aqueous layer was extracted with CH_2Cl_2 (3 x 3 mL). The combined organic layers were dried with $MgSO_4$ and concentrated under reduced pressure. The resulting oil was further purified by column chromatography (40:1 hexanes:EtOAc) to yield silyl triflate **3.37** as a colorless oil (55 mg, 36% yield). **3.37**: R_f 0.52 (5:1 hexanes:EtOAc); ^{1}H NMR (500 MHz, $CDCl_3$): δ 9.14 (d, J = 1.2, 1H), 7.29 (d, J = 1.2, 1H), 0.99 (t, J = 7.2, 9H), 0.92–0.86 (m, 6H); ^{13}C NMR (125 MHz, $CDCl_3$): δ 184.2, 162.2, 158.2, 118.6 (q, J = 320.6, CF_3), 117.0, 7.2, 2.6; IR (film): 2959, 2880, 1579, 1511, 1428, 1211 cm^{-1}; HRMS-APCI (*m/z*) $[M + H]^+$ calcd for $C_{11}H_{18}F_3N_2O_3SSi^+$, 343.0754; found 343.0755.

3.8 Spectra Relevant to Chapter Three:

Synthetic Studies Pertaining to the 2,3-Pyridyne and 4,5-Pyrimidyne

Jose M. Medina, Moritz K. Jackl, Robert B. Susick, and Neil K. Garg

Tetrahedron **2016**, *72*, 3629–3634.

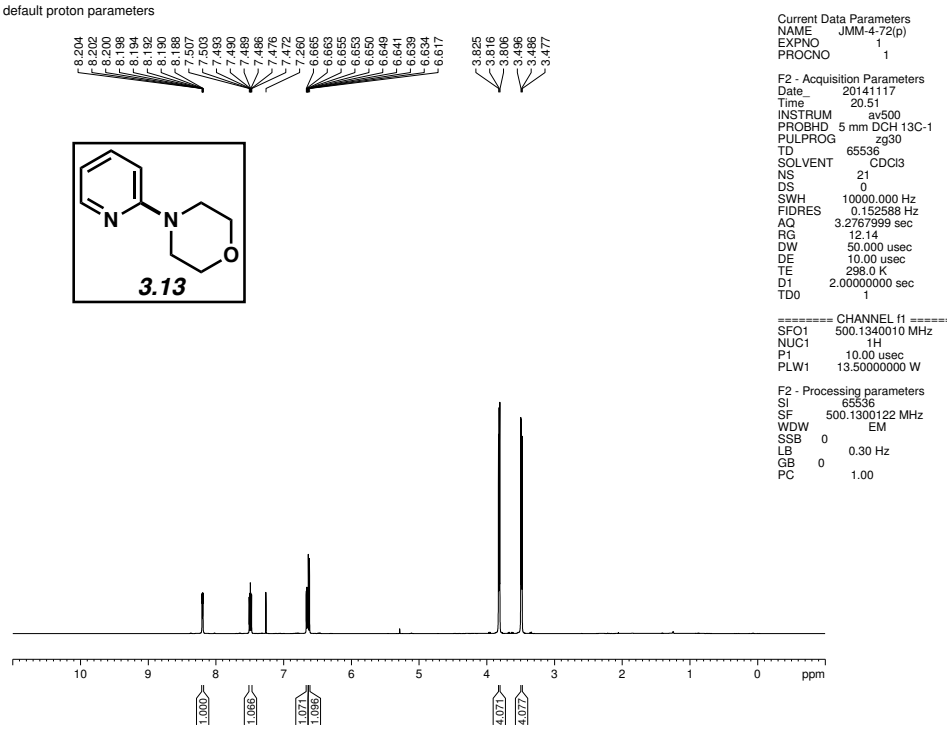


Figure 3.4. ^{1}H NMR (500 MHz, $CDCl_3$) compound **3.13**

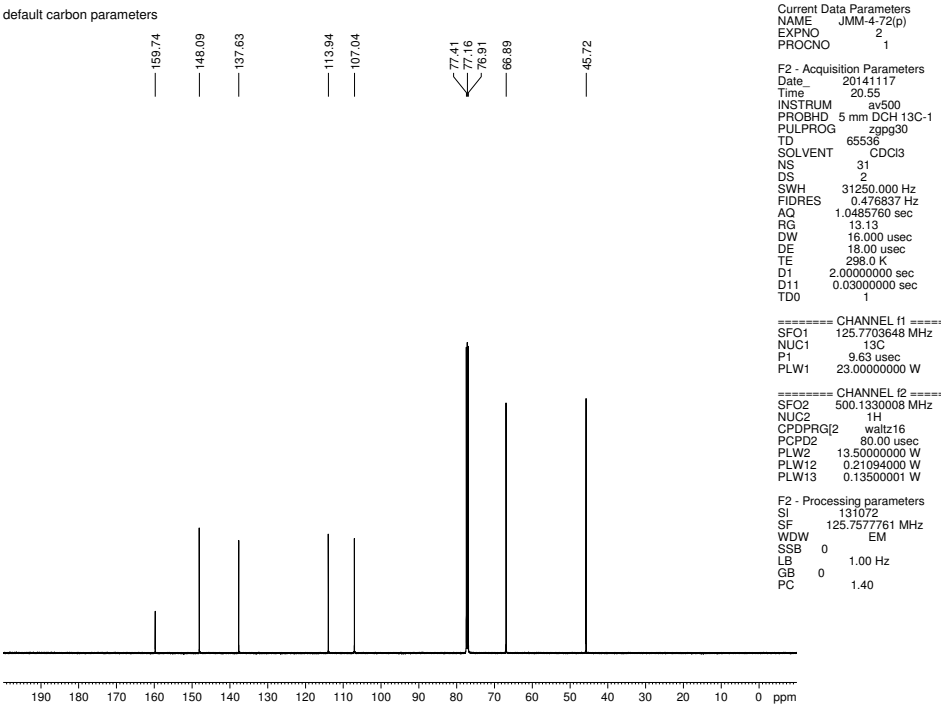


Figure 3.5. ^{13}C NMR (125 MHz, $CDCl_3$) compound **3.13**

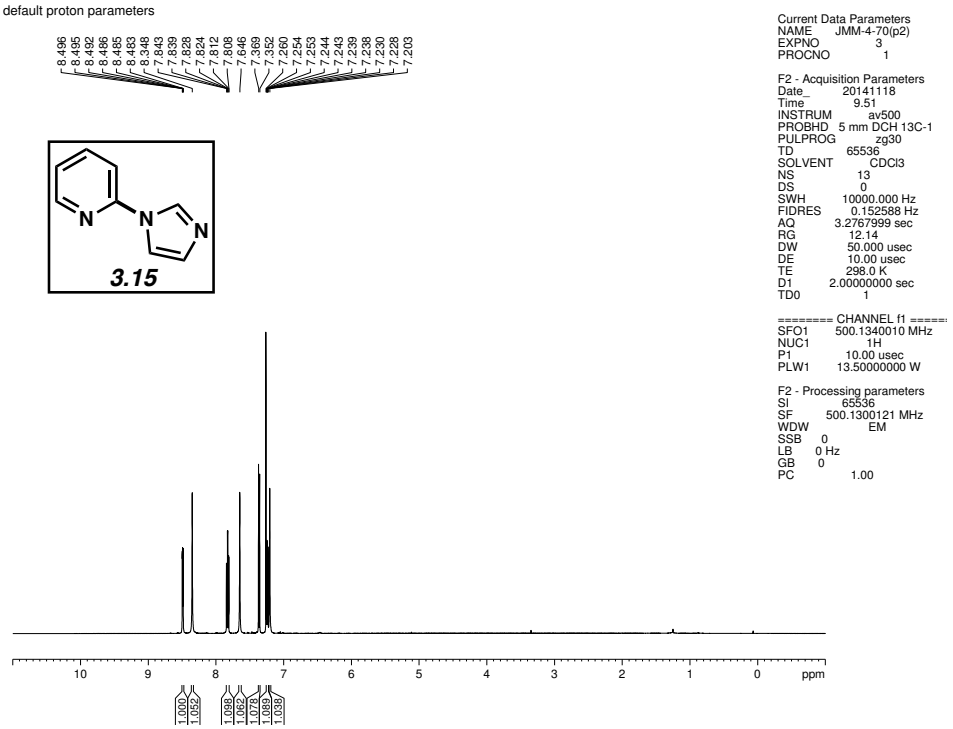


Figure 3.6. ^{1}H NMR (500 MHz, $CDCl_3$) compound **3.15**

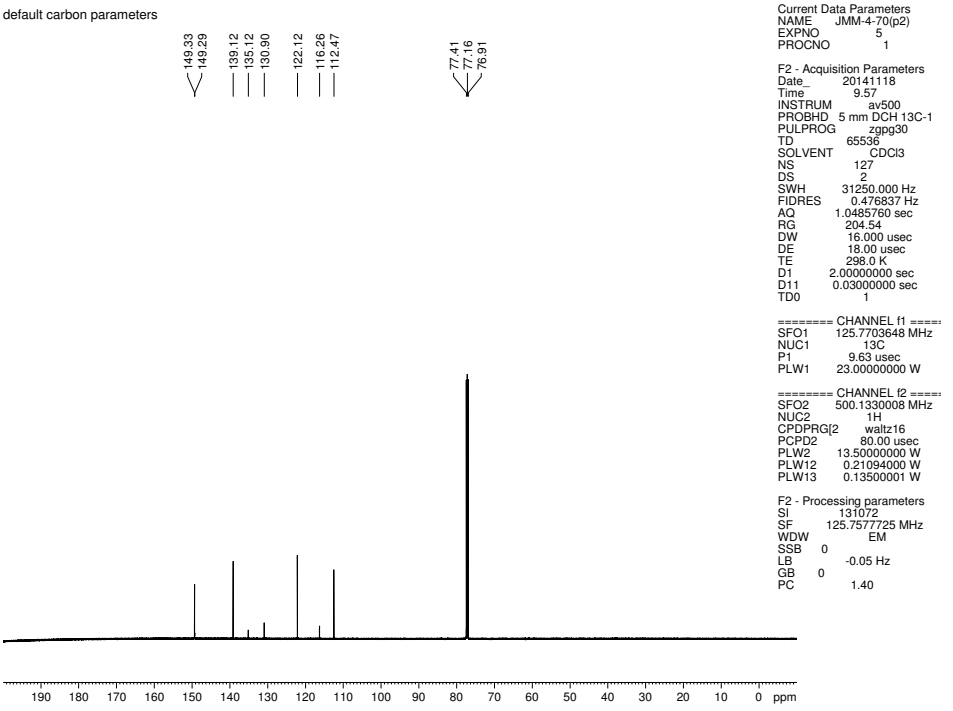


Figure 3.7. ^{13}C NMR (125 MHz, $CDCl_3$) compound **3.15**

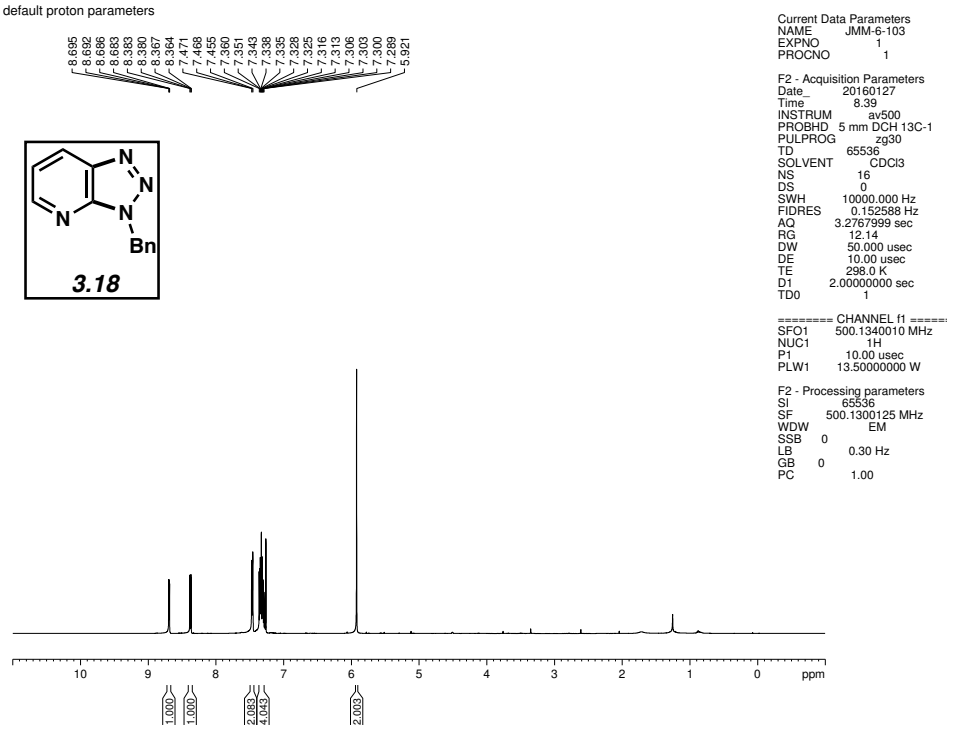


Figure 3.8. ^{1}H NMR (500 MHz, $CDCl_3$) compound **3.18**

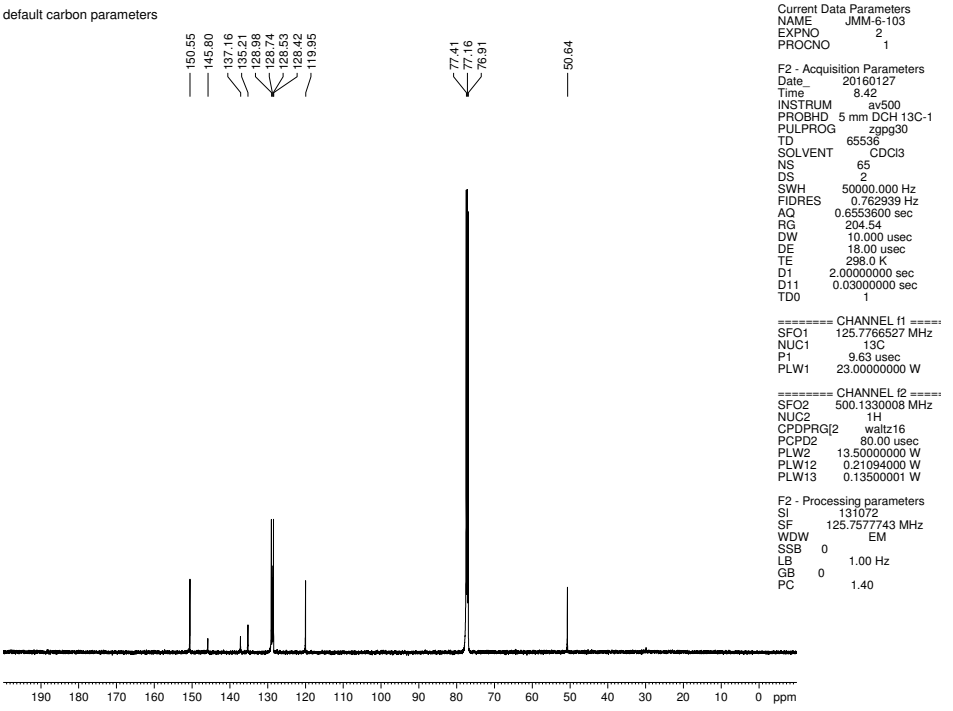


Figure 3.9. ^{13}C NMR (125 MHz, $CDCl_3$) compound **3.18**

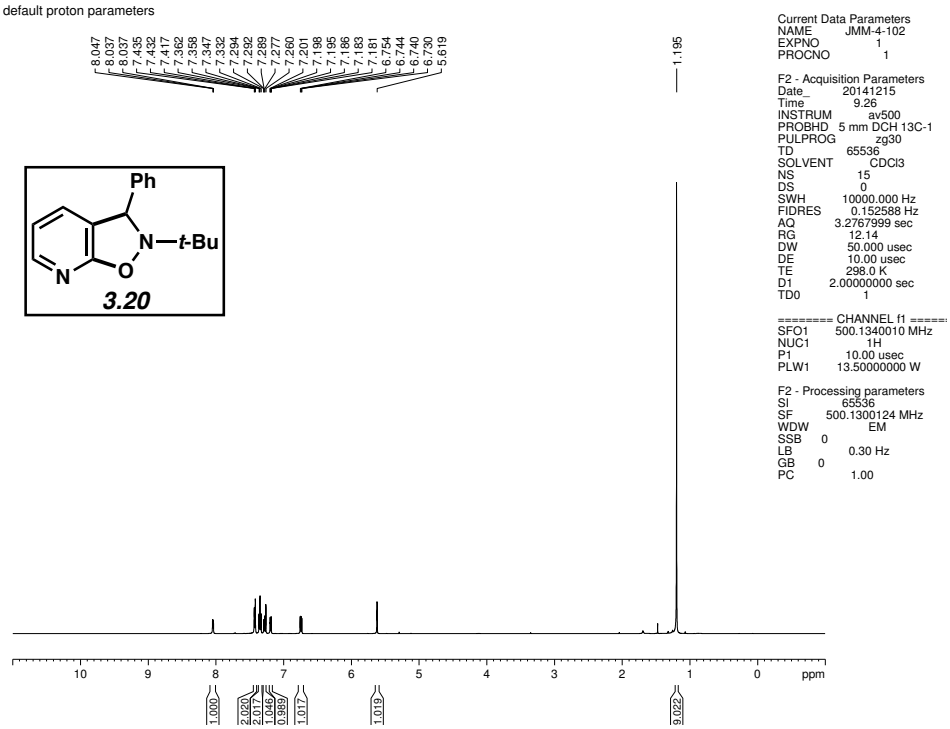


Figure 3.10. ^{1}H NMR (500 MHz, $CDCl_3$) compound **3.20**

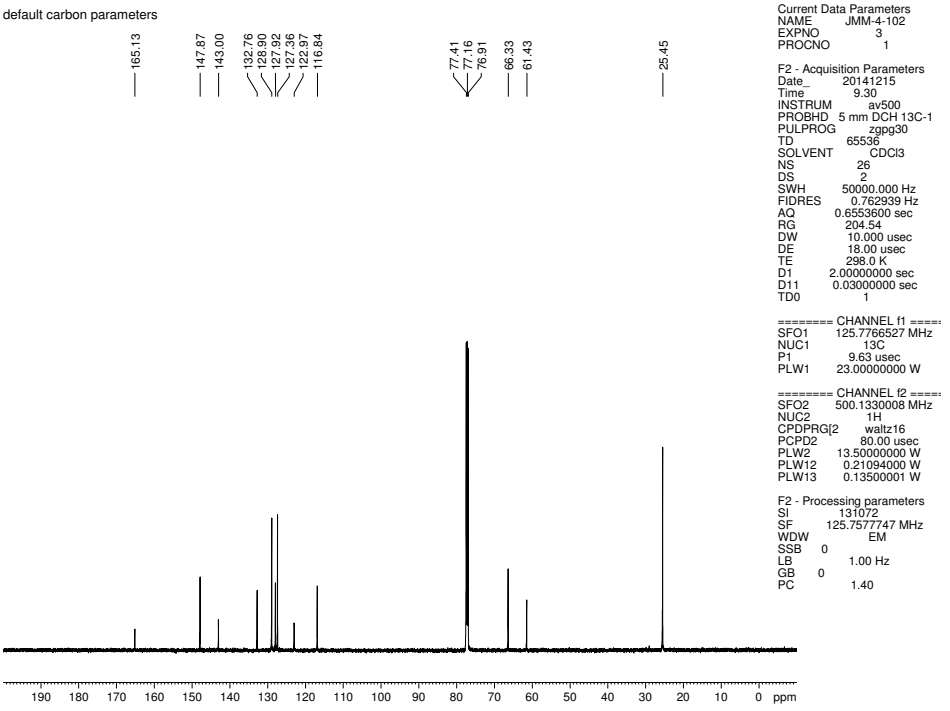


Figure 3.11. ^{13}C NMR (125 MHz, $CDCl_3$) compound **3.20**

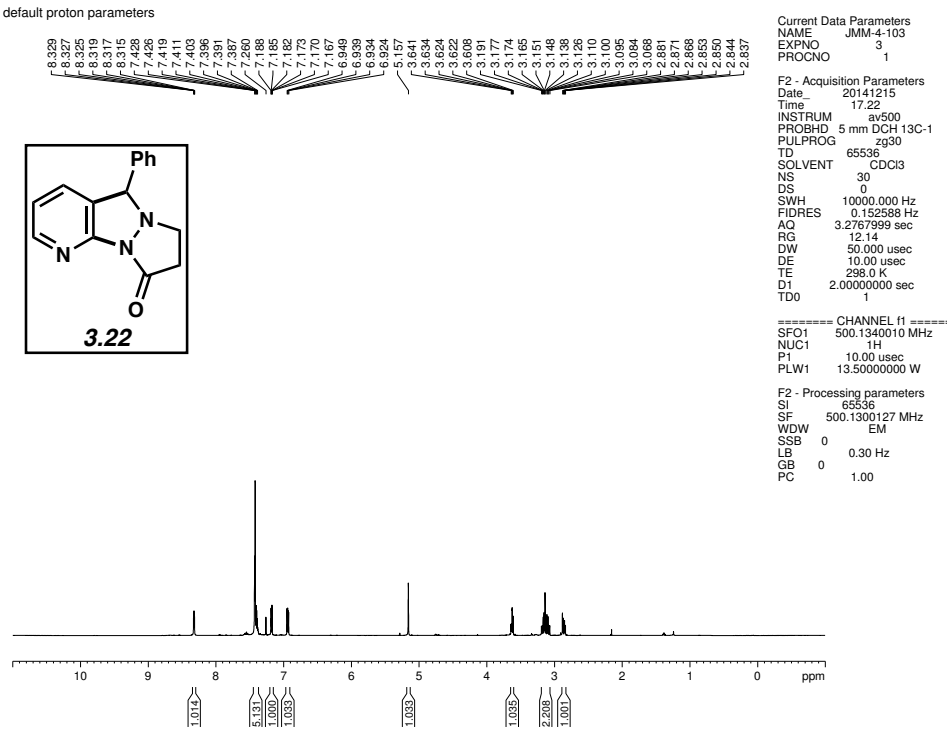


Figure 3.12. ^{1}H NMR (500 MHz, $CDCl_3$) compound **3.22**

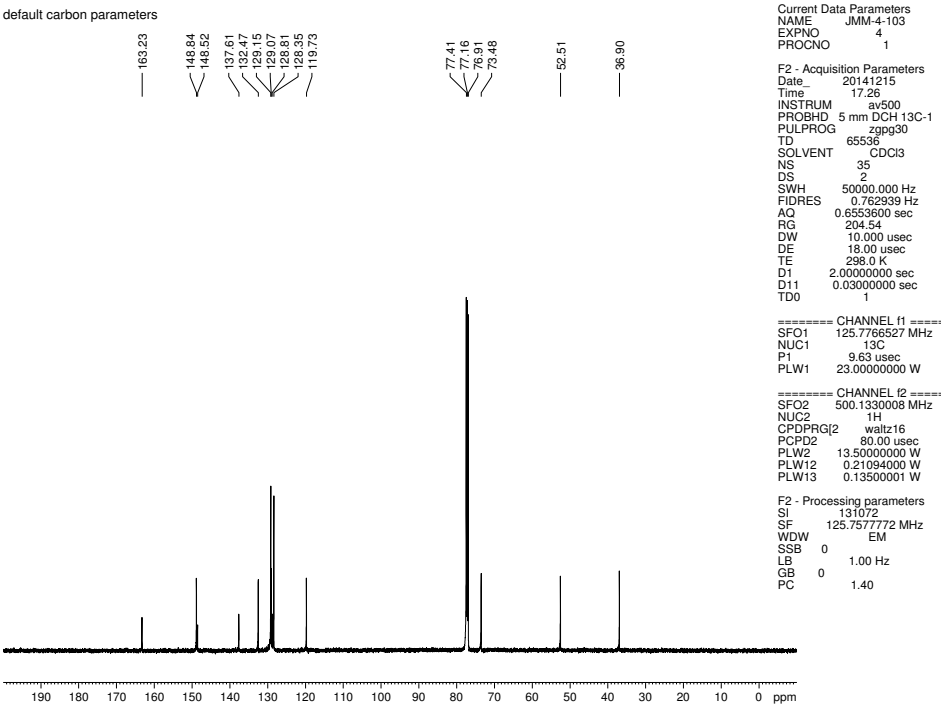


Figure 3.13. ^{13}C NMR (125 MHz, $CDCl_3$) compound **3.22**

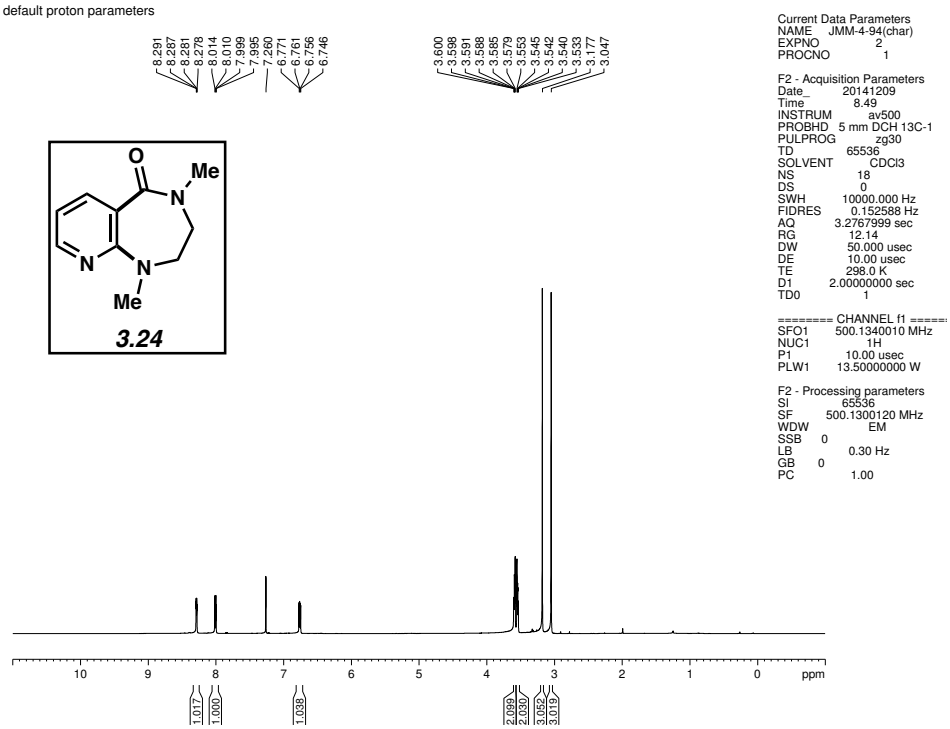


Figure 3.14. ^{1}H NMR (500 MHz, $CDCl_3$) compound **3.24**

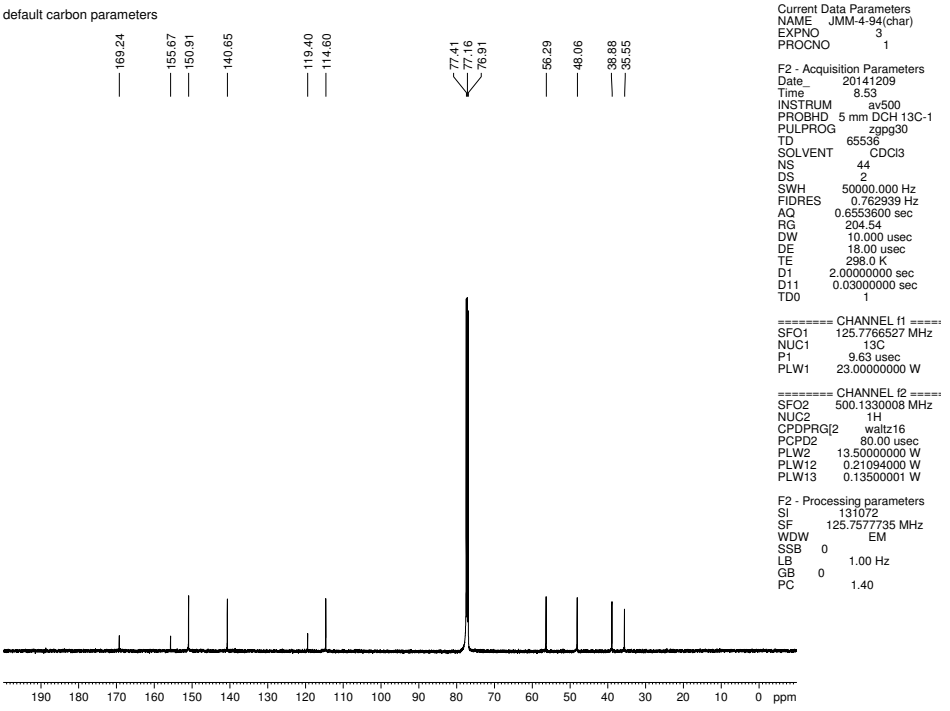


Figure 3.15. ^{13}C NMR (125 MHz, $CDCl_3$) compound **3.24**

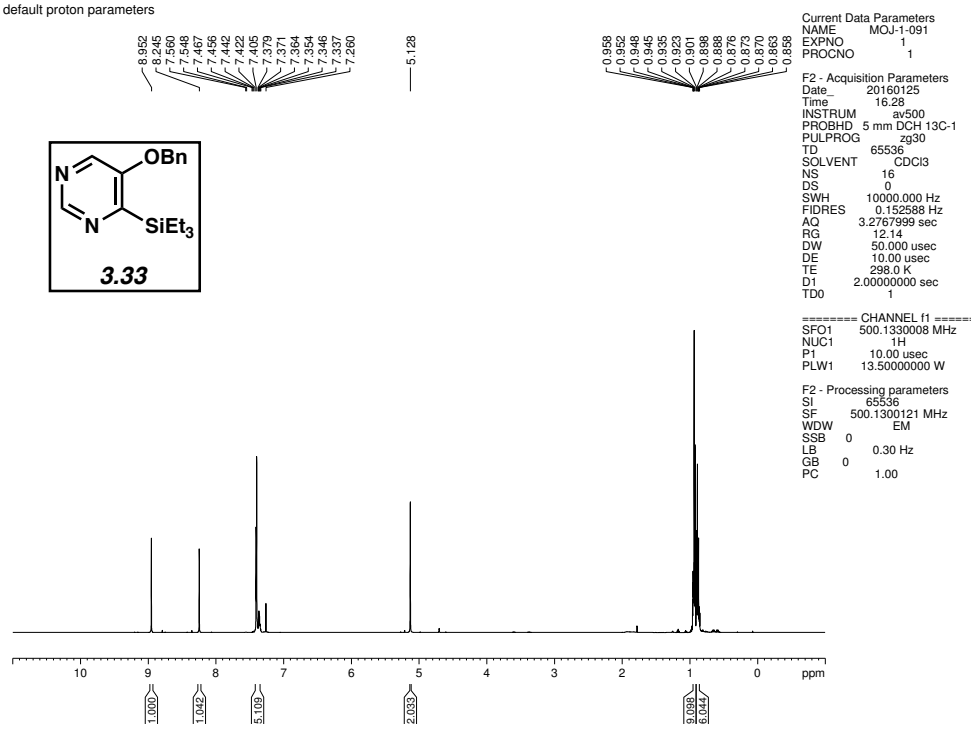


Figure 3.16. ^{1}H NMR (500 MHz, $CDCl_3$) compound **3.33**

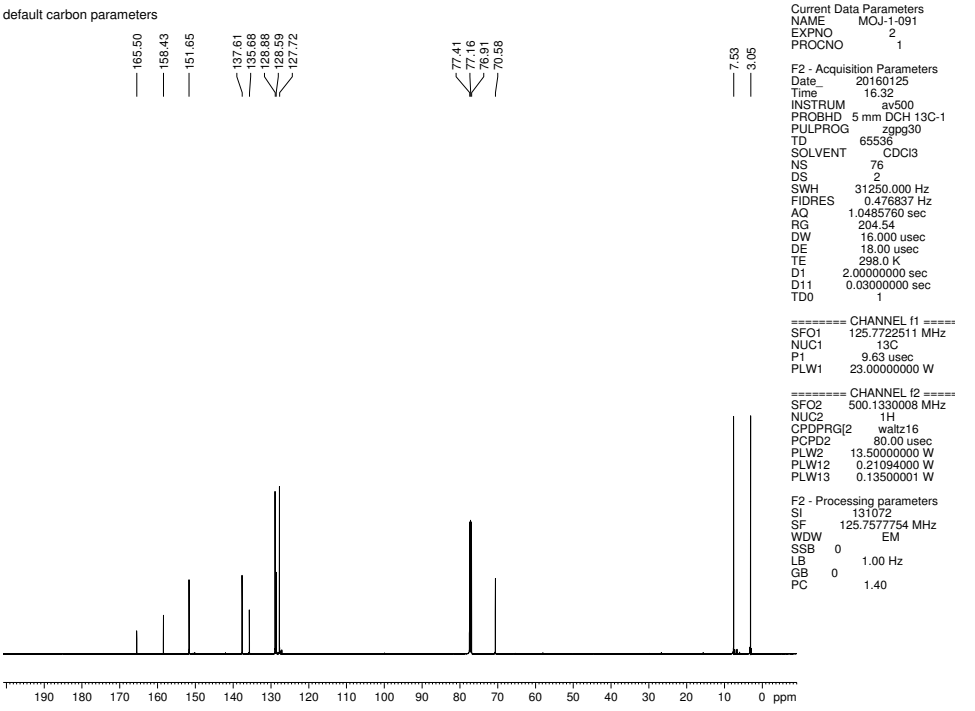


Figure 3.17. ^{13}C NMR (125 MHz, $CDCl_3$) compound **3.33**

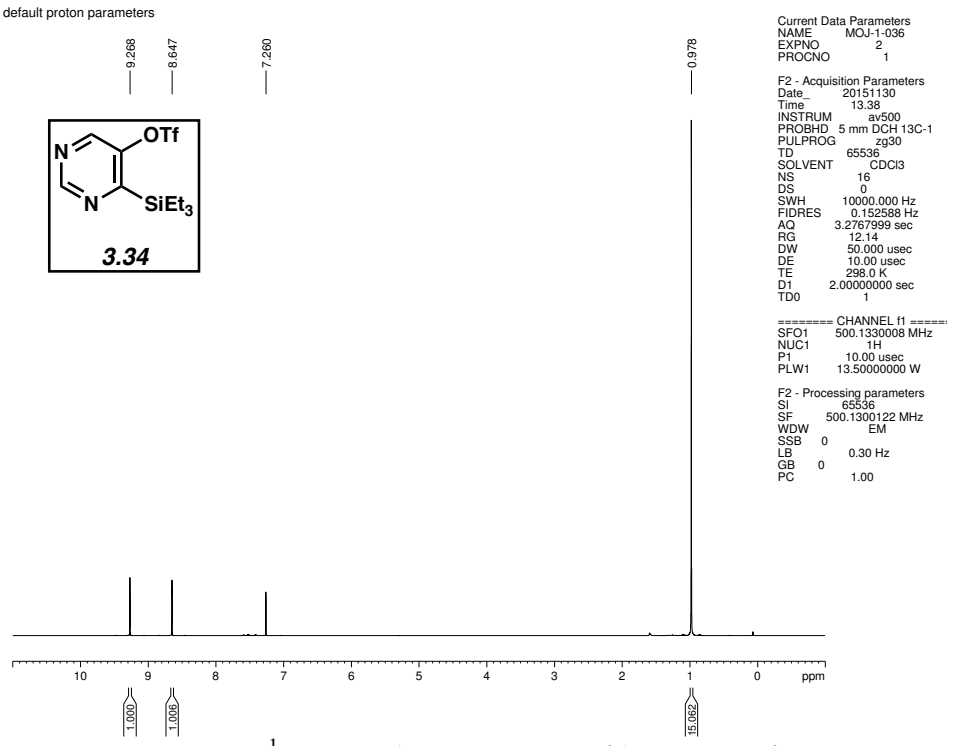


Figure 3.18. ^{1}H NMR (500 MHz, $CDCl_3$) compound **3.34**

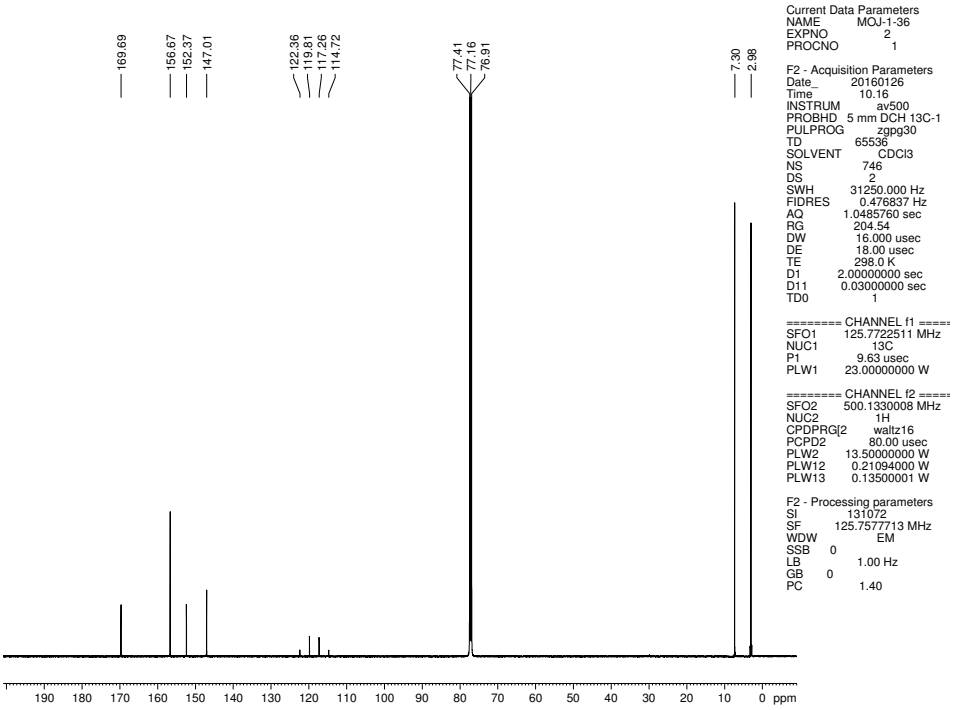


Figure 3.19. ^{13}C NMR (125 MHz, $CDCl_3$) compound **3.34**

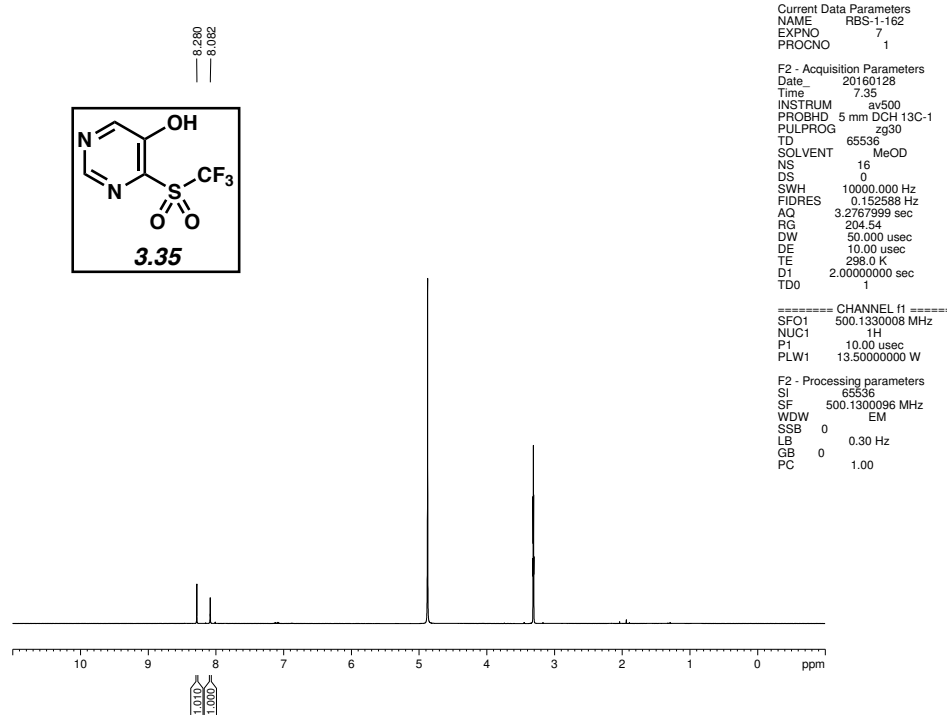


Figure 3.20. ^{1}H NMR (500 MHz, MeOD) compound **3.35**

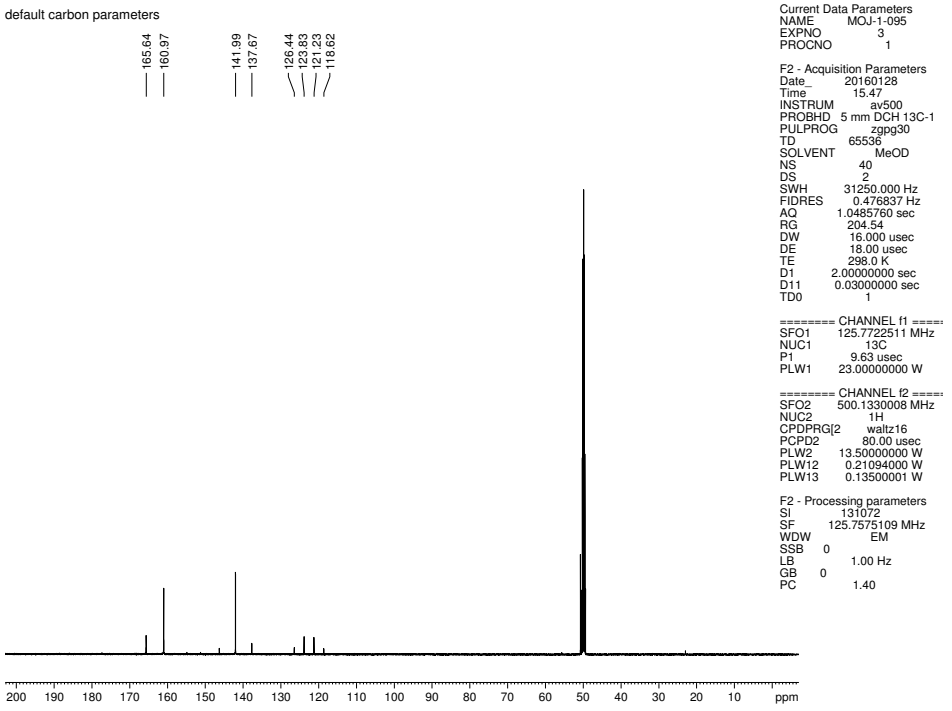


Figure 3.21. ^{13}C NMR (125 MHz, MeOD) compound **3.35**

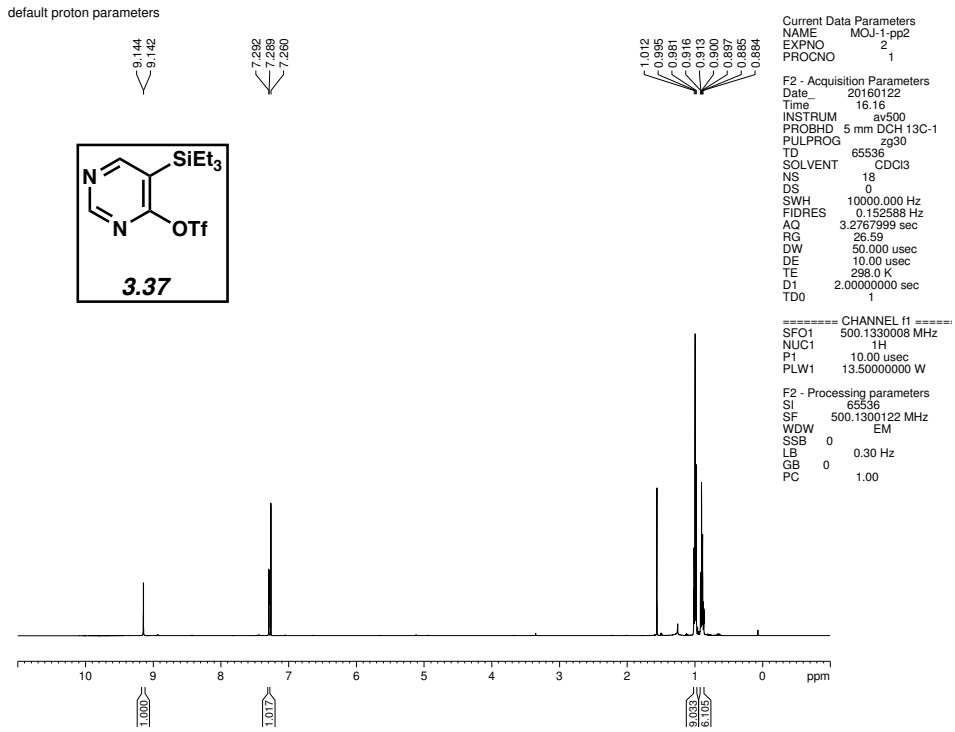


Figure 3.22. ^{1}H NMR (500 MHz, $CDCl_3$) compound **3.37**

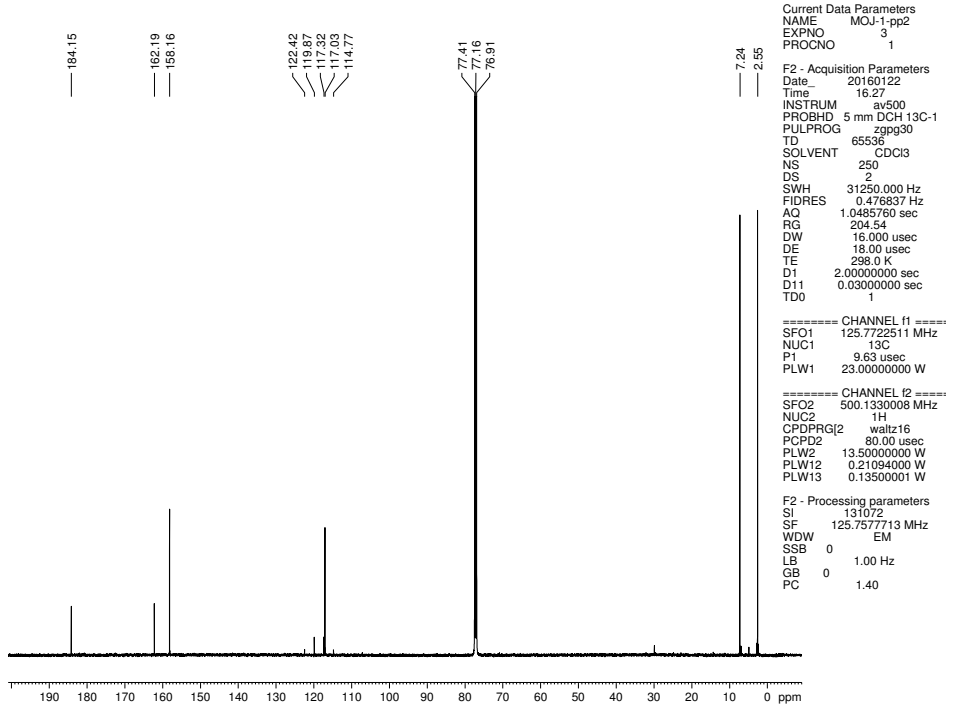


Figure 3.23. ^{13}C NMR (125 MHz, $CDCl_3$) compound **3.37**

3.9 Notes and References

(1) a) Vitaku, E.; Smith, B. R.; Smith, D. T.; Njardarson, J. T. http://njardarson.lab.arizona.edu/sites/njardarson.lab.arizona.edu/files/Top%20US%20Pharmaceutical%20Products%20of%202013.pdf (accessed January 25, 2016). b) McGrath, N. A.; Brichacek, M.; Njardarson, J. T. *J. Chem. Educ.* **2010**, *87*, 1348–1349. c) Dinges, J., Lamberth, C., Eds. *Bioactive Heterocyclic Compounds Classes: Agrochemicals*; Wiley-VCH: Weinheim, 2012. d) Gilchrist, T. L. *J. Chem. Soc., Perkin Trans. 1* **1999**, 2849–2866.

(2) For reviews of hetarynes, see: a) Bronner, S. M.; Goetz, A. E.; Garg, N. K. *Synlett* **2011**, 2599–2604. b) Goetz, A. E.; Garg, N. K. *J. Org. Chem.* **2014**, *79*, 846–851. (c) Goetz, A. E.; Shah, T. K.; Garg, N. K. *Chem. Commun*. **2015**, *51*, 34–45.

(3) For reviews of arynes, see: a) Pellissier, H.; Santelli, M. *Tetrahedron* **2003**, *59*, 701–730. b) Wenk, H. H.; Winkler, M.; Sander, W. *Angew. Chem., Int. Ed.* **2003**, *42*, 502–528. c) Sanz, R. *Org. Prep. Proced. Int.* **2008**, *40*, 215–291. d) Tadross, P. M.; Stoltz, B. M. *Chem. Rev.* **2012**, *112*, 3550–3557. e) Gampe, C. M.; Carreira, E. M. *Angew. Chem., Int. Ed.* **2012**, *51*, 3766–3778. f) Bhunia, A.; Yetra, S. R.; Biju, A. T. *Chem. Soc. Rev.* **2012**, *41*, 3140–3152. g) Yoshida, H.; Takaki, K. *Synlett* **2012**, 1725–1732. h) Dubrovskiy, A. V.; Markina, N. A.; Larock, R. C. *Org. Biomol. Chem.* **2013**, *11*, 191–218. i) Wu, C.; Shi, F. *Asian J. Org. Chem.* **2013**, *2*, 116–125. j) Hoffmann, R. W.; Suzuki, K. *Angew. Chem., Int. Ed.* **2013**, *52*, 2655–2656.

(4) a) Kauffmann, T. *Angew. Chem., Int. Ed.* **1965**, *4*, 543–618. b) Reinecke, M. G. *Tetrahedron* **1982**, *38*, 427–498.

(5) a) Bronner, S. M.; Bahnck, K. B.; Garg, N. K. *Org. Lett.* **2009**, *11*, 1007–1010. b) Cheong, P. H.-Y.; Paton, R. S.; Bronner, S. M.; Im, G-Y. J.; Garg, N. K.; Houk, K. N. *J. Am. Chem. Soc.* **2010**, *132*, 1267–1269. c) Im, G-Y. J.; Bronner, S. M.; Goetz, A. E.; Paton, R. S.; Cheong, P. H.-Y.; Houk, K. N.; Garg, N. K. *J. Am. Chem. Soc.* **2010**, *132*, 17933–17944. d) Bronner, S. M.; Goetz, A. E.; Garg, N. K. *J. Am. Chem. Soc.* **2011**, *133*, 3832–3835. e) Pareek, M.; Fallon, T.; Oestreich, M. *Org. Lett*. **2015**, *17*, 2082–2085. f) Picazo, E.; Houk, K. N.; Garg, N. K. *Tetrahedron Lett*. **2015**, *56*, 3511–3514.

(6) a) Buszek, K. R.; Luo, D.; Kondrashov, M.; Brown, N.; VanderVelde, D. *Org. Lett.* **2007**, *9*, 4135–4137. b) Brown, N.; Luo, D.; VanderVelde, D.; Yang, S.; Brassfield, A.; Buszek, K. R. *Tetrahedron Lett.* **2009**, *50*, 63–65. c) Buszek, K. R.; Brown, N.; Luo, D. *Org. Lett.* **2009**, *11*, 201–204. d) Garr, A. N.; Luo, D.; Brown, N.; Cramer, C. J.; Buszek, K. R.; VanderVelde, D. *Org. Lett.* **2010**, *12*, 96–99. e) Brown, N.; Luo, D.; Decapo, J. A.; Buszek, K. R. *Tetrahedron Lett.* **2009**, *50*, 7113–7115. f) Thornton, P. D.; Brown, N.; Hill, D.; Neuenswander, B.; Lushington, G. H.; Santini, C.; Buszek, K. R. *ACS Comb. Sci.* **2011**, *13*, 443–448. g) Nerurkar, A.; Chandrasoma, N.; Maina, L.; Brassfield, A.; Luo, D.; Brown, N.; Buszek, K. R. *Synthesis* **2013**, *45*, 1843–1852.

(7) For a recent study, see: Goetz, A. E.; Garg, N. K. *Nat. Chem.* **2013**, *5*, 54–60; see also references therein.

(8) http://www.sigmaaldrich.com/technical-documents/articles/technologyspotlights/heterocyclic-aryne-precursors.html (accessed January 25, 2016).

(9) For recent examples of total syntheses using hetarynes, see: a) Huters, A. D.; Quasdorf, K. W.; Styduhar, E. D.; Garg, N. K. *J. Am. Chem. Soc.* **2011**, *133*, 15797–15799. b) Quasdorf,

K. W.; Huters, A. D.; Lodewyk, M. W.; Tantillo, D. J.; Garg, N. K. *J. Am. Chem. Soc.* **2012**, *134*, 1396–1399. c) Styduhar, E. D.; Huters, A. D.; Weires, N. A.; Garg, N. K. *Angew. Chem., Int. Ed.* **2013**, *52*, 12422–12425. d) Weires, N. A.; Styduhar, E. D.; Baker, E. L.; Garg, N. K. *J. Am. Chem. Soc.* **2014**, *136*, 14710–14713. e) Bronner, S. M.; Goetz, A. E.; Garg, N. K. *J. Am. Chem. Soc.* **2011**, *133*, 3832–3835. f) Fine Nathel, N. F.; Shah, T. K.; Bronner, S. M.; Garg, N. K. *Chem. Sci.* **2014**, *5*, 2184–2190. g) Goetz, A. E.; Silberstein, A. L.; Corsello, M. A.; Garg, N. K. *J. Am. Chem. Soc.* **2014**, *136*, 3036–3039. h) Buszek, K. R.; Brown, N.; Luo, D. *Org. Lett.* **2009**, *11*, 201–204. i) Enamorado, M. F.; Ondachi, P. W.; Comins, D. L. *Org. Lett.* **2010**, *12*, 4513–4515.

(10) Arynes have also been used in the synthesis of medicinal agents and to access the fungicide Isopyrazam®. For references, see: a) Carroll, F. I.; Robingson, T. P.; Brieaddy, L. E.; Atkinson, R. N.; Marscarella, S. W.; Damaj, M. I.; Martin, B. R.; Navarro, H. A. *J. Med. Chem.* **2007**, *50*, 6383–6391. b) Shah, F.; Tao, Y.; Tang, C.-Y.; Zhang, F.; Wu, X.-Y. *J. Org. Chem.* **2015**, *80*, 8122–8133. c) Schleth, F.; Vettiger, T.; Rommel, M.; Tobler, H. WO2011131544 A1, 2011.

(11) Levine R.; Leake, W. W. *Science* **1955**, *121*, 780.

(12) a) Bronner, S. M.; Mackey, J. L.; Houk, K. N.; Garg, N. K. *J. Am. Chem. Soc.* **2012**, *134*, 13966–13969. b) Goetz, A. E.; Bronner, S. M.; Cisneros, J. D.; Melamed, J. M.; Paton, R. S.; Houk, K. N.; Garg, N. K. *Angew. Chem., Int. Ed.* **2012**, *51*, 2758–2762. c) Medina, J. M.; Mackey, J. L.; Garg, N. K; Houk, K. N. *J. Am. Chem. Soc.* **2014**, *136*, 15798–15805.

(13) Martens, R. J.; den Hertog, H. J. *Tetrahedron Lett.* **1962**, *3*, 643–645.

(14) Walters, M. A.; Shay, J. J. *Synth. Commun.* **1997**, *27*, 3573–3579.

(15) Fang, Y.; Larock, R. C. *Tetrahedron* **2012**, *68*, 2819–2826.

(16) Yoshida, H.; Shirakawa, E.; Honda, Y.; Hiyama, T. *Angew. Chem., Int. Ed.* **2002**, *41*, 3247–3249.

(17) Nguyen, T. D.; Webster, R.; Lautens, M. *Org. Lett*. **2011**, *13*, 1370–1373.

(18) Saito, N.; Nakamura, K.-i.; Shibano, S.; Ide, S.; Minami, M.; Sato, Y. *Org. Lett*. **2013**, *15*, 386–389.

(19) Lopchuk, J. M.; Gribble, G. W. *Tetrahedron Lett*. **2014**, *55*, 2809–2812.

(20) a) van der Plas, H. C.; Smit, P.; Koudijs, A. *Tetrahedron Lett*. **1968**, *9*, 9–13. b) Tielemans, M.; Areschka, V.; Colomer, J.; Promel, R. *Tetrahedron* **1992**, *48*, 10575–10586.

(21) Several silyl triflate aryne and hetaryne precursors are available from Aldrich Chemical Co., Inc. The 2,3-pyridyne precursor **3.10** is available under catalog number L511641.

(22) Shi, F.; Waldo, J. P.; Chen, Y.; Larock, R. C. *Org. Lett*. **2008**, *10*, 2409–2412.

(23) Matsumoto, T.; Sohma, T.; Hatazaki, S.; Suzuki, K. *Synlett* **1993**, 843–846.

(24) Shi, F.; Mancuso, R.; Larock, R. C. *Tetrahedron Lett*. **2009**, *50*, 4067–4070.

(25) Tambar, U. K.; Stoltz, B. M. *J. Am. Chem. Soc*. **2005**, *127*, 5340–5341.

(26) Nara, S. J.; Jha, M.; Brinkhorst, J.; Zemanek, T. J.; Pratt, D. A. *J. Org. Chem*. **2008**, *73*, 9326–9333.

(27) For lithiation and silylation of pyrimidynes, see: a) Nishiwaki, T. *Tetrahedron* **1966**, *22*, 2401–2412. b) Ple, N.; Turck, A.; Couture, K.; Queguiner, G. *J. Org. Chem*. **1995**, *60*, 3781–3786. c) Wada, A.; Yamamoto, J.; Kanatomo, S. *Heterocycles* **1987**, *26*, 585–589.

(28) We also prepared the nonaflate derivative of **3.34**; however, attempted pyrimidyne generation from this substrate also led to the formation of the corresponding alcohol.

(29) For the thia-Fries rearrangement in attempts to generate arynes, see: a) Hall, C.; Henderson, J. L.; Ernouf, G.; Greaney, M. F. *Chem. Commun.* **2013**, *49*, 7602–7604. b) Zhao, Z.; Messinger, J.; Schon, U.; Wartchow, R.; Butenschon, H. *Chem. Commun*. **2006**, 3007–3009. c) Rasheed, O. K.; Hardcastle, I. R.; Raftery, J.; Quayle, P. *Org. Biomol. Chem*. **2015**, *13*, 8048–8052.

(30) Because **3.37** was deemed an unsuitable precursor to the 4,5-pyrimidyne, the synthetic route to **3.37** was not further optimized.

(31) At present, it is unclear why the silyl triflate approach to the 4,5-pyrimidyne is unsuccessful.

CHAPTER FOUR

Aryne-Driven Approach for the Synthesis and Manipulation of Polypyridyl Metal Complexes

4.1 Abstract

Ruthenium- and iridium-based polypyridyl complexes have remarkable photophysical properties that are utilized across many scientific disciplines. Their broad application across fields such as solar energy conversion, luminescence sensing, and catalysis can be attributed to a highly tunable ligand sphere that controls their photophysical properties. Recently, extended π-conjugation in the ligand sphere has enabled longer excited state lifetimes, thus increasing cytotoxicity in photodynamic therapies and noncovalent π–π interactions for DNA intercalation. Despite decades of study and successful applications, synthetic strategies to access polypyridyl metal complexes are limited to relatively few methods across two major platforms, ligand synthesis and coordination, or direct manipulation of the ligand "on-the-complex". Specifically, annulation reactions that extend the π-conjugation of polypyridyl complexes are limited to C–N bond forming processes. Herein, we report a C–C bond forming annulation directly on polylpyridyl organometallic complexes by harnessing the power of arynes and Pd catalysis. This methodology is also used to generate the first ligand-bound aryne on an organometallic complex, which is trapped via a Diels–Alder cycloaddition to access an exotic ligand.

4.2 Introduction

Since the initial discovery of $[Ru(bpy)_3]^{2+}$ in 1936,[1] the remarkable photophysical properties displayed by ruthenium- and iridium-based polypyridyl complexes have broadly impacted the scientific community. With extensive applications in solar energy conversion,[2] DNA intercalation,[3] and luminescence sensing,[4] transition metal frameworks of this class have demonstrated broad versatility in both photochemical and photophysical applications. More recently, polypyridyl metal complexes such as **4.1**–**4.3** (Figure 4.1) have been implemented as both therapeutics for human disease and as biophysical probes to investigate biomolecules of interest. One recent, compelling example of their therapeutic potential is the ruthenium complex TLD-1433 (**4.1**), which is currently in phase II clinical trials as a photodynamic therapeutic for the treatment of bladder cancer.[5] For the interrogation of biomolecules, Barton and Turro have employed **4.2** as an intercalating agent to study conductivity through stacked DNA nucleobases.[6,3c] Additionally, MacMillan and coworkers recently demonstrated the use of photocatalyst **4.3** to identify protein–protein interactions in live cells.[7] A particularly attractive feature of these polypyridyl metal complexes is the capacity to tune photophysical properties by manipulating the ligand sphere. For example, extended π-conjugation in the ligand sphere has enabled longer photocatalyst excited state lifetimes, thus promoting increased cytotoxicity in photodynamic therapy,[8,9] and noncovalent π–π interactions for DNA intercalation.[3c]

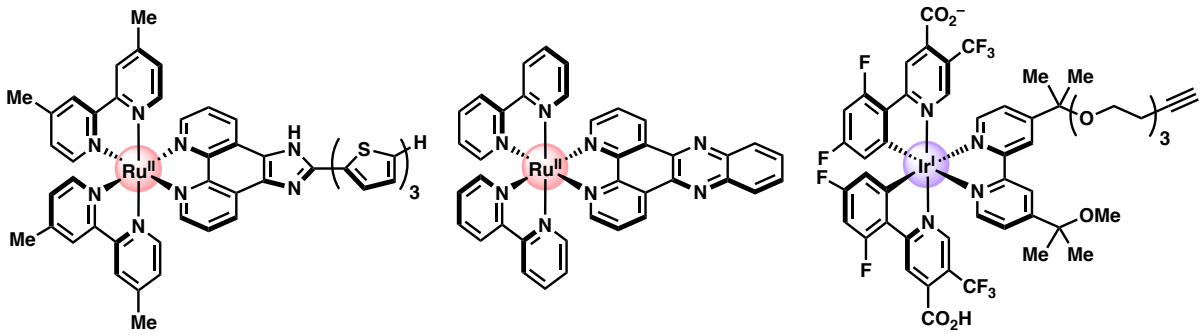


Figure 4.1. Polypyridyl metal complexes used as therapeutics and in bioimaging.

Despite extensive studies to evaluate the photophysical properties of polypyridyl metal complexes, their design is limited to relatively few synthetic platforms. Current strategies for accessing polypyridyl metal complexes largely rely on ligand synthesis followed by metal coordination (Figure 4.2A, reaction *a*, **4.4** + **4.5** → **4.6**). However, this strategy often necessitates long, linear reaction sequences, rendering the process of synthesizing large libraries of Ru- or Ir-based therapeutic targets cumbersome.[10] Moreover, metal-catalyzed processes, though effective in diversifying most arenes, are unproductive in the context of 2,2'-bipyridine ligands. This challenge stems from the strong bidentate chelation properties of 2,2'-bipyridine ligands and their resultant propensity to form stable, catalytically inactive *N*,*N*-chelate complexes.[11] As a result, bipyridyl ligands are unsuitable for the transition metal-catalyzed annulation and cross-coupling reactions that are typically employed to functionalize conjugated organic molecules. Furthermore, the low solubility of highly rigid bipyridyl ligands can complicate their synthesis,[12] rendering traditional ligand synthesis intractable for bipyridine systems bearing extended conjugation.

A synthetic approach that complements traditional coordination chemistry involves so-called, "chemistry-on-the-complex," whereby metal complexes are diversified after coordination

(Figure 4.2A, reaction *b*, **4.7** → **4.6**).[7] Notably, this strategy has proven effective in overcoming challenges manifested in traditional synthetic approaches, but it has rarely been used to access metal complexes bearing annulated bipyridyl ligands. In particular, available protocols for the direct annulation of polypyridyl metal complexes are restricted to C–N bond forming processes.[12b,13] Whereas such protocols have enabled studies revealing the promising photophysical and therapeutic potential of π-extended ligands, they are limited to the formation of quinoxaline and imidazole derivatives. To date, no C–C bond forming annulations exist for coordinated polypyridyl complexes, limiting the electronic nature and design of such ligands.

We questioned if annulated polypyridyl metal complexes could be rapidly accessed through a "chemistry-on-the-complex" strategy involving highly strained aryne intermediates. Strained cyclic intermediates, such as **4.8**–**4.11** (Figure 4.2B), have been harnessed to access various organic targets including heterocycles,[14] phosphine ligands,[15] agrochemicals,[16] and natural products.[17] Given their ability to generate multiple bonds on various cyclic scaffolds, we viewed arynes as uniquely poised for the synthesis and manipulation of polypyridyl metal complexes. Nonetheless, arynes have seen limited use in the manipulation of metal-bound ligands with only two examples reported, both involving Diels–Alder reactions.[18,19] No examples have been demonstrated on polypyridyl metal complexes. Herein, we disclose a platform for the aryne-driven synthesis and manipulation of polypyridyl metal complexes (Figure 4.2C). In one variant, reactions between catalytically generated intermediates **4.12** and fleeting aryne intermediates **4.13** provide one-step conversion to annulated products **4.14**. In a second variant, in situ generation of the first organometallic complex bearing a free aryne **4.15**, followed by trapping with **4.16**, generates cycloadducts **4.17** under mild conditions. Both approaches enable

the formation of multiple C–C bonds in a single operation and offer a divergent means to access functionalized polypyridyl metal complexes, including several exotic structures.

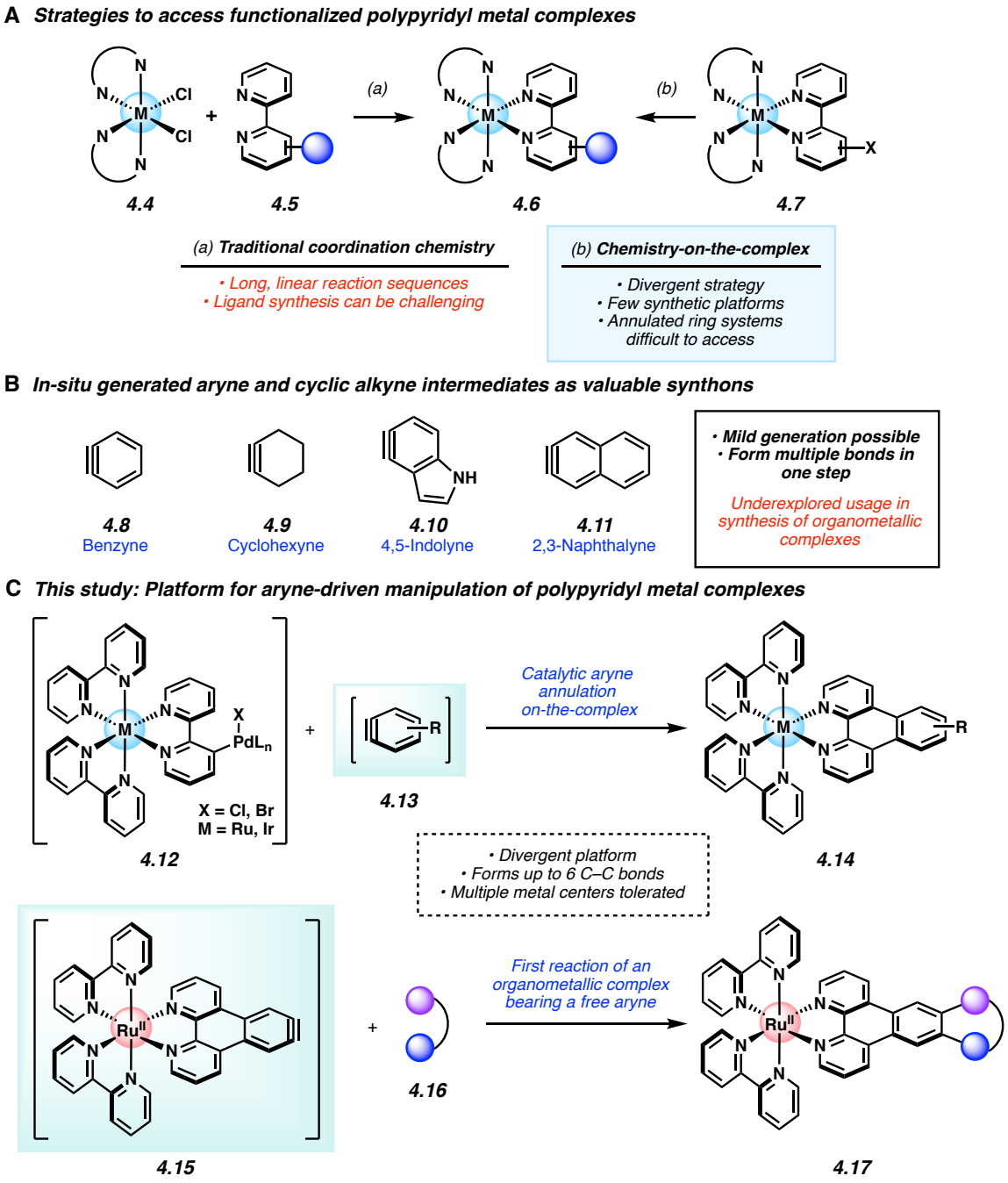
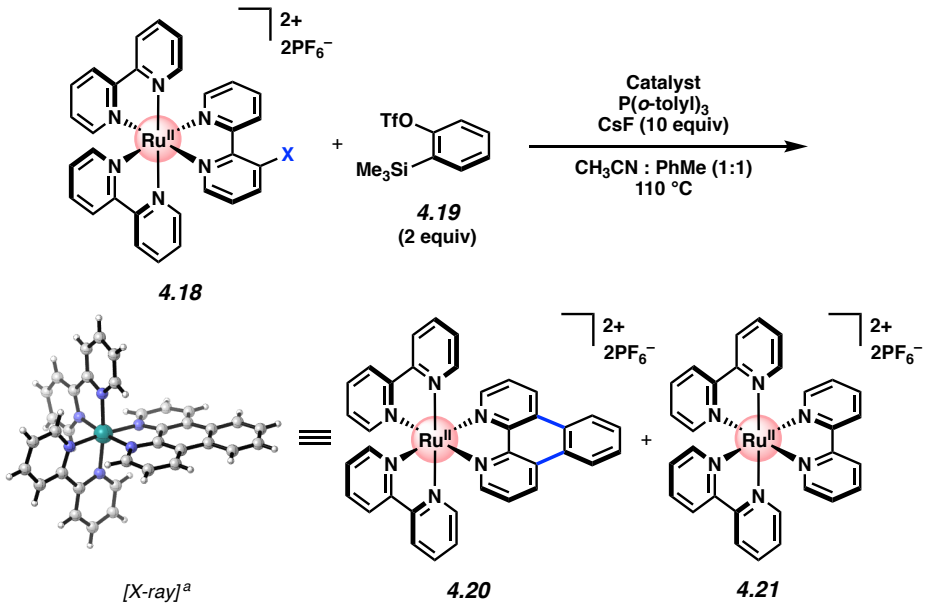


Figure 4.2. A) Strategies for the synthesis of polypyridyl metal complexes. B) Aryne and cyclic alkyne intermediates. C) Synthetic designs for the direct manipulation of photoactive metal complexes using arynes and Pd catalysis.

4.3 Annulation Optimization

We initiated our studies by pursuing a Pd-catalyzed annulation reaction of halogenated $Ru(bpy)_3$ derivative **4.18** and commercially available benzyne precursor **4.19** (Table 4.1). Prior studies by Larock and co-workers established the feasibility of performing Pd-catalyzed annulations of arynes from silyl triflate precursors to furnish organic materials.[20] Our preliminary studies involved the use of $Pd(dba)_2$ and P(*o*-tolyl)$_3$, in the presence of CsF. Under these conditions, we were gratified to observe formation of the desired π-extended adduct **4.20**, albeit in 2% yield (entry 1). Additionally, undesired dehalogenation product **4.21** was observed in 48% yield. Efforts to eliminate this dehalogenation pathway via reduced temperatures and rigorous exclusion of air and moisture proved unfruitful,[21] as did the use of other Pd^0 sources such as $Pd(PPh_3)_4$ (entry 2). Alternatively, $Pd(OAc)_2$ provided a substantial improvement in the yield of the desired π-extended adduct **4.20** to 26% (entry 3). By increasing the catalyst and ligand loadings to 10 mol%, as well as decreasing the reaction duration to 30 minutes, we observed a further increase in yield to 71% (entry 4). The use of modified ratios of the co-solvents, acetonitrile and toluene, resulted in decreased reaction efficiency (entries 5 and 6), highlighting the importance of tuning the rate at which benzyne is generated. Finally, switching from a bromide to a chloride functional handle on the substrate effectively eliminated the dehalogenation pathway and provided the desired product in 78% yield (entry 7). It is worth noting that attempts to perform this transformation on uncoordinated bromo- or chlorobipyridine ligands proved unproductive, potentially owing to the formation of a Pd–*N*,*N*-chelate. The latter result underscores the complementarity of on-the-complex strategies that circumvent issues of unproductive catalyst–substrate chelation.

Table 4.1. Optimization studies for Pd-catalyzed annulation of benzyne onto Ru-polylpyridyl complex **4.18**. [a]PF_6 counterions have been omitted from the X-Ray crystal structure for clarity. [b]Yields were determined by ^1H NMR using 1,3,5-trimethoxybenzene as an external standard.



Entry	*Catalyst*	*X*	*Catalyst Loading*	*Ligand Loading*	*CH_3CN : PhMe*	*Time*	*Yield of **4.20**[b]*	*Yield of **4.21**[b]*
1	$Pd(dba)_2$	Br	5 mol%	5 mol%	1 : 1	2 h	2%	48%
2	$Pd(PPh_3)_4$	Br	5 mol%	5 mol%	1 : 1	2 h	2%	48%
3	$Pd(OAc)_2$	Br	5 mol%	5 mol%	1 : 1	2 h	26%	24%
4	$Pd(OAc)_2$	Br	10 mol%	10 mol%	1 : 1	30 min	71%	16%
5	$Pd(OAc)_2$	Br	10 mol%	10 mol%	3 : 1	30 min	61%	19%
6	$Pd(OAc)_2$	Br	10 mol%	10 mol%	1 : 3	30 min	35%	28%
7	$Pd(OAc)_2$	Cl	10 mol%	10 mol%	1 : 1	30 min	78%	0%

4.4 Scope of Aryne Annulation Partners

Having uncovered optimal conditions for the on-the-complex annulation of benzyne, we then investigated the scope of the methodology with respect to the aryne (Figure 4.3). Benzyne adduct **4.20** could be isolated in 78% yield using standard column chromatography. Notably, the only available protocol to access the diazatriphenylene ligand found in **4.20** involves the use of

hazardous reagents and exceptionally forcing conditions.[22] Heterocyclic arynes were also tolerated, as evidenced by the formation of *N*-Me-4,5-indolyne adduct **4.25** in 75% yield. This result demonstrates the capacity for expedient incorporation of heterocycles directly into the π-framework of polypyridyl metal complexes. 2,3- and 1,2-naphthalyne were also competent under these conditions, leading to the formation of **4.26** and **4.27**, each in 61% yield. Historically, the naphthophenanthroline ligand present in **4.26** has proven challenging to synthesize due to its low solubility. As a result, reported syntheses proceed in very low yields or require multiple steps.[23] In other cases, insolubility has entirely precluded access to the desired naphthophenanthroline ligand, thus necessitating the incorporation of hydrophobic substituents.[12]

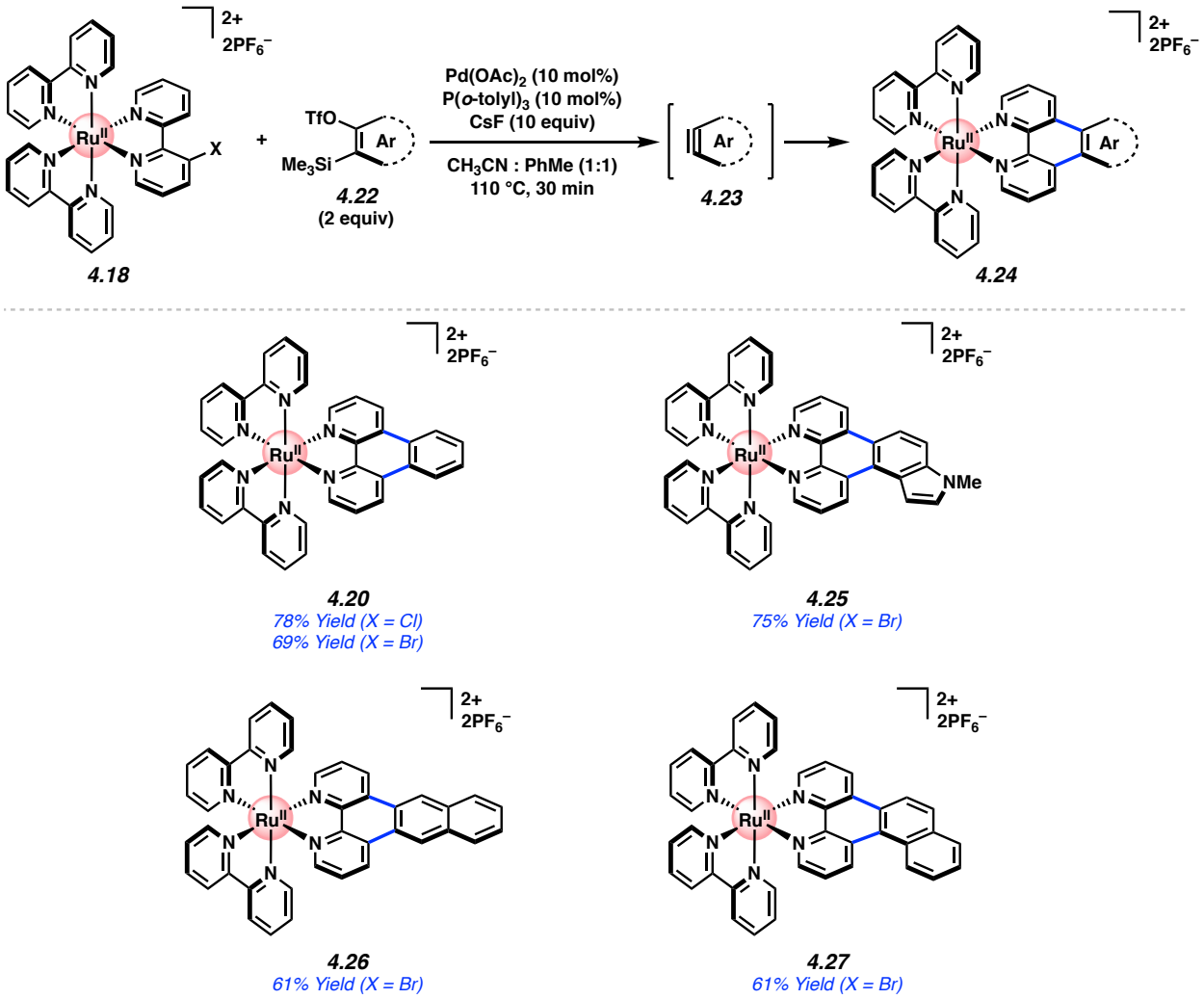


Figure 4.3. Scope of aryne annulation partners.

4.5 Scope of Polypyridyl Annulation Partners

After validating the use of various aryne partners in the methodology, we turned our attention to varying the organometallic substrate (Figure 4.4). We first investigated whether other metal centers could be tolerated under the reaction conditions, as this would provide an entryway to other privileged classes of octahedral complexes. In particular, Ir-centered polypyridyl complexes have demonstrated broad utility as photoactive complexes,[3a,7,24] so we assessed the viability of brominated $Ir(ppy)_2(bpy)$ derivative **4.28**. This substrate underwent the reaction

smoothly to deliver **4.29** in 75% yield. Notably, dehalogenation was not observed in this reaction despite **4.28** bearing the previously problematic C–Br bond. We then questioned if conjugation could be extended across multiple ligands in a single step, thus expanding conjugation of the ligand sphere in multiple directions. Under slightly modified conditions, bis(chlorinated) Ru-complex **4.30** underwent a double annulation in one pot to furnish **4.31** in 54% yield through the formation of four C–C bonds. Finally, tris(chlorinated) Ru-complex **4.32** was treated with six equivalents of benzyne precursor **4.19** to generate triple annulation adduct **4.33** in 57% yield. In this transformation, six new C–C bonds were constructed, three of which resulted from C–H functionalization. These results demonstrate the capacity for arynes to manipulate multiple metal-bound ligands in a single transformation, and in high efficiency per C–C bond formed.

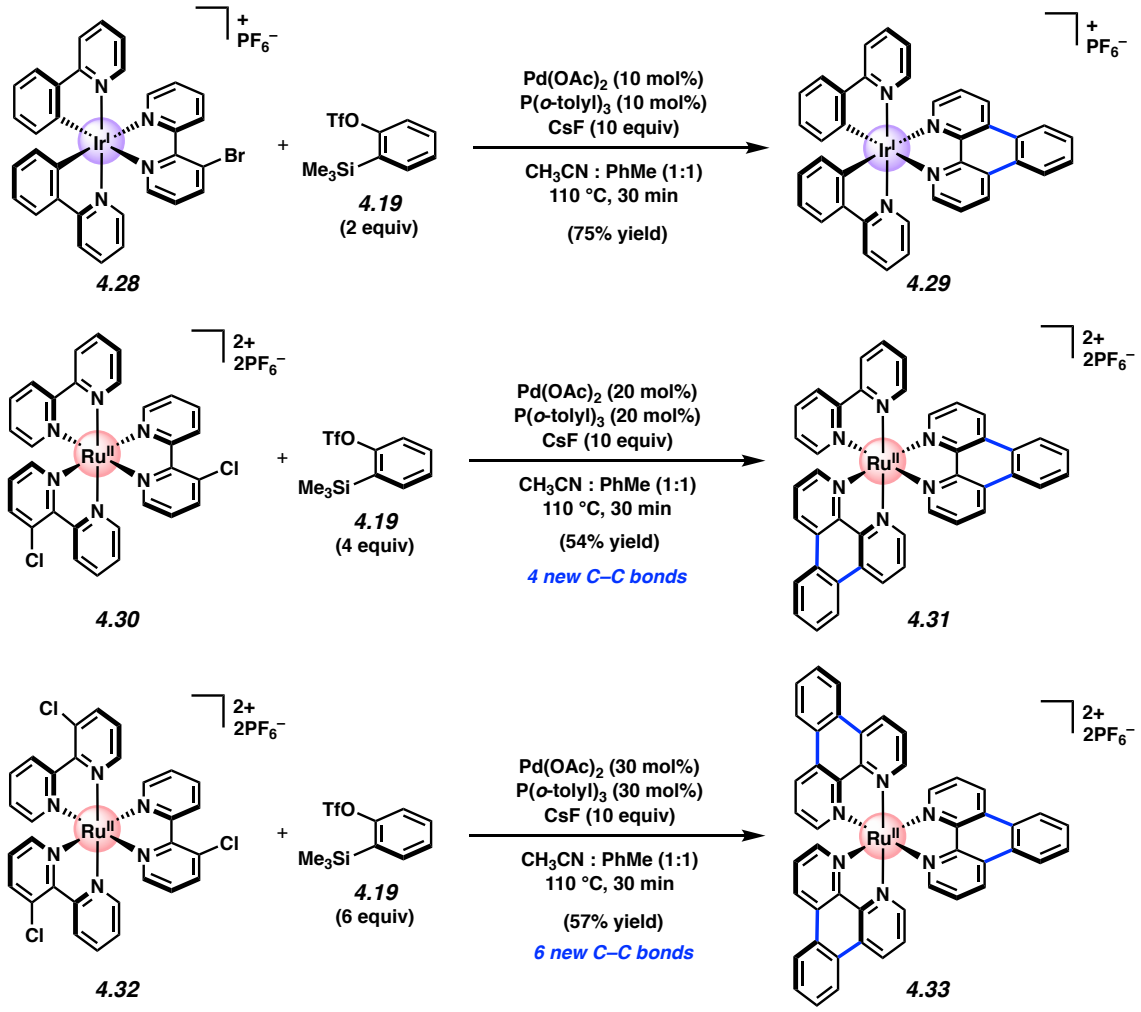


Figure 4.4. Scope of organometallic complex reaction partners.

4.6 Synthesis and Trapping of Ligand-Bound Aryne Precursor

Given the successful union of arynes and organometallic complexes, we next sought to develop a mild and complementary means of decorating polypyridyl organometallic species by generating an aryne on the organometallic complex itself. Doing so would enable a new set of transformations, including those previously validated in the context of organic arynes and cyclic alkynes.[17,25] Toward this end, we first set out to develop a robust route to a suitable silyl triflate precursor (Figure 4.5). Initial attempts to react chlorinated Ru-complex **4.34** with bis(silyl

triflate) **4.35**[26] proved unfruitful in providing access to desired aryne precursor **4.36**. We therefore pursued the use of an unsymmetrical bis(aryne) precursor bearing a silyl triflate and silyl enol ether, the latter of which would not react under fluoride-based reaction conditions.[27] Methoxymethyl (MOM) ether **4.37**, prepared in two steps from commercially available materials, enabled the desired transformation of **4.34** to adduct **4.38** in 80% yield using the Pd-catalyzed aryne annulation. Subsequent mild cleavage of the MOM group using solid-supported $NaHSO_4$•SiO_2, followed by triflation with Comins' Reagent, delivered the desired silyl triflate **4.36** in 73% yield over two steps.

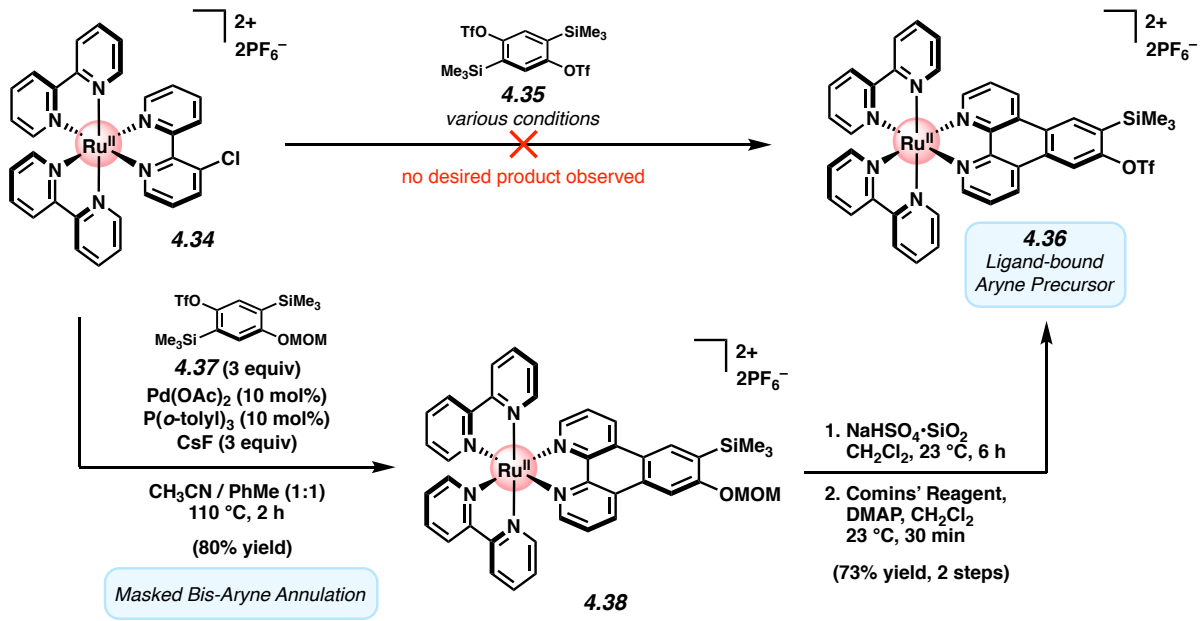


Figure 4.5. Synthesis of Ru-polylpyridyl silyl triflate.

With silyl triflate **4.36** in hand, we then set out to generate a Ru-complex bearing a free aryne and subsequently trap it in a cycloaddition reaction (Figure 4.6). We began by treating **4.36** with 2,5-dimethylfuran (**4.39**) and CsF, and observed the formation of Diels–Alder adduct **4.40** in 59% yield. This represents the first example a free aryne being generated directly on an

organometallic complex. Further studies are underway with trapping partners **4.41**–**4.43** to assess other reaction manifolds such as [3+2]- and [2+2]-cycloadditions. If successful, exotic complexes such as metallotryptycene **4.45** and isoxazoline **4.45** could be obtained in a divergent manner from a common intermediate. Notably, [2+2]-cycloaddition adduct **4.46** would provide a cyclobutane ring and a ketone, the latter of which could be used for further functionalization.

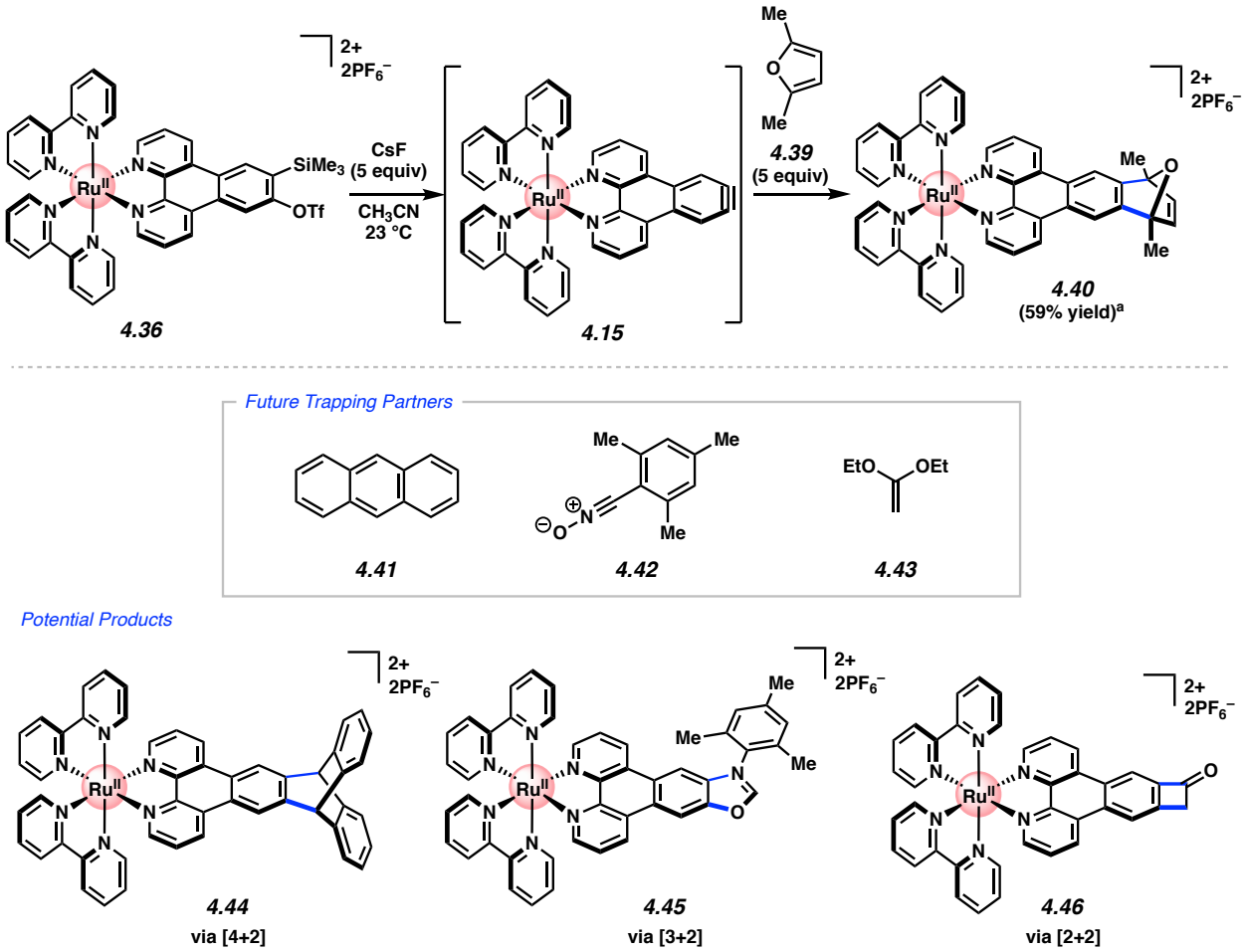


Figure 4.6. Mild generation of the first ligand-bound aryne, and future trapping partners.

[a]Unoptimized yield.

Several salient features of the results presented in Figure 4.6 should be noted. First, the diverse collection of products possible through this approach demonstrates the potential to utilize silyl triflate **4.36** as a common precursor to a library of functionalized metal complexes. Secondly, many of the products potentially accessible through this approach would not be readily accessible by conventional means. Namely, accessing the ligands prior to coordination could be challenging, in part because of the inability to perform Pd catalysis on bipyridyl substrates. Finally, these results demonstrate that a highly strained, free aryne can be generated on an organometallic complex from a silyl triflate precursor under mild reaction conditions.

4.7 Conclusion

In summary, we have developed an aryne-driven strategy for the synthesis and direct manipulation of polypyridyl metal complexes. Our strategy relies on the controlled reactivity of Ru- and Ir-based octahedral complexes with arynes via Pd catalysis. Various arynes can be used to extend the conjugation of Ru-complexes, including a heterocyclic indolyne. The method can also be extended to Ir-complexes, as well as Ru-complexes bearing multiple reactive bipyridyl ligands to construct up to 6 C–C bonds in a single transformation. Lastly, an unsymmetrical bis(aryne) was utilized to access a Ru-based silyl triflate, which was activated to generate a free aryne under mild conditions. Trapping the organometallic aryne with 2,5-dimethylfuran afforded an exotic Diels–Alder adduct, and other cycloaddition partners are currently under investigation. We hope these studies promote the design of novel bipyridyl architectures with the potential for desirable, unique photophysical properties, as well as stimulate future on-the-complex strategies.

4.8 Experimental Section

4.8.1 Materials and Methods

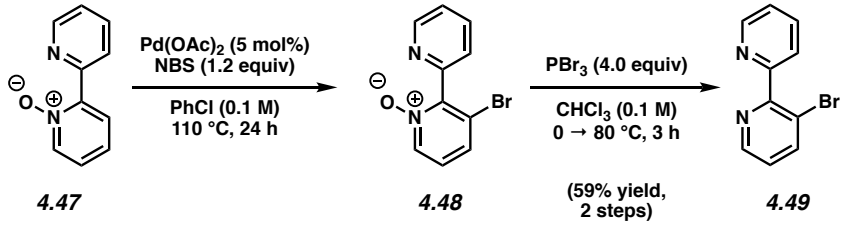
Unless stated otherwise, reactions were conducted in flame-dried glassware under an atmosphere of nitrogen or argon and commercially obtained reagents were used as received. Anhydrous solvents were either freshly distilled or passed through activated alumina columns, unless otherwise stated. Reaction temperatures were controlled using an IKAmag temperature modulator, and unless stated otherwise, reactions were performed at room temperature (approximately 23 °C). Cesium fluoride (CsF), Palladium(II) acetate ($Pd(OAc)_2$), Bis(dibenzylidenacetone)palladium(0) ($Pd(dba)_2$), tetrakis(triphenylphosphine)palladium(0), and Di-μ-chlorotetrakis[2-(2-pyridinyl-kN)phenyl-kC]diiridium(III) were obtained from Strem Chemicals. Methyl iodide was obtained from Spectrum Chemical. Ruthenium(III) chloride trihydrate (**4.54**), 3-(trimethylsilyl)-2-naphthyl trifluoromethanesulfonate (**4.57**), 2,5-dibromohydroquinone (**4.61**), and 2,5-dimethylfuran (**4.39**) were obtained from Combi-Blocks. 1-(trimethylsilyl)-2-naphthyl trifluoromethanesulfonate (**4.58**) was obtained from TCI America. Tri(*o*-tolyl)phosphine ($P(o\text{-tolyl})_3$), Garg 4,5-indolyne precursor (**4.59**), *cis*-bis(2,2'-bipyridine)dichlororuthenium(II) hydrate (**4.52**), phosphorus trichloride (PCl_3), 1,1,1,3,3,3-hexamethyldisilazane (HMDS), and bromomethyl methyl ether (MOMBr) were obtained from Sigma-Aldrich. *N*-bromosuccinimide and *N*-chlorosuccinimide were obtained from Acros Organics. 2,2'-bipyridine *N*-oxide (**4.47**)[28] was prepared according to literature procedures. Thin-layer chromatography (TLC) was conducted with EMD gel 60 F254 pre-coated plates (0.25 mm for analytical chromatography and 0.50 mm for preparative chromatography) and visualized using UV. Silicycle Siliaflash P60 (particle size 0.040–0.063 mm) was used for flash column chromatography. ^{1}H NMR spectra were recorded on Bruker spectrometers (at 400, 500 and 600

MHz) and are reported relative to residual solvent signals. Data for ^{1}H NMR spectra are reported as follows: chemical shift (δ ppm), multiplicity, coupling constant (Hz), integration. Data for ^{13}C NMR are reported in terms of chemical shift (125 MHz). IR spectra were recorded on a Perkin-Elmer UATR Two FT-IR spectrometer and are reported in terms of frequency absorption (cm^{-1}). High-resolution ESI-MS spectra were collected on a Waters LCT Premier mass spectrometer by direct injection. DART-MS spectra were collected on a Thermo Exactive Plus MSD (Thermo Scientific) equipped with an ID-CUBE ion source and a Vapur Interface (IonSense Inc.). Both the source and MSD were controlled by Excalibur software v. 3.0. The analyte was spotted onto OpenSpot sampling cards (IonSense Inc.) using volatile solvents (e.g., chloroform, dichloromethane). Ionization was accomplished using UHP He plasma with no additional ionization agents. The mass calibration was carried out using Pierce LTQ Velos ESI (+) and (–) Ion calibration solutions (Thermo Fisher Scientific).

4.8.2 Experimental Procedures

4.8.2.1 Halobipyridine Organometallic Complex Synthesis

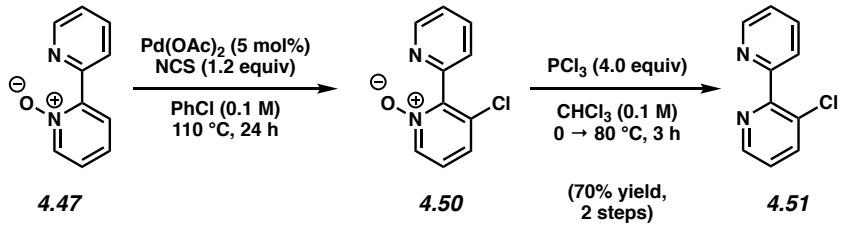
*Note: The following procedures for the synthesis of halobipyridines **4.49** and **4.51** were adapted from a published literature protocol[29] to facilitate gram-scale synthesis.*



2-Bromobipyridine (4.49). To a flask containing 2,2'-bipyridyl *N*-oxide (**4.47**, 1.00 g, 5.81 mmol), $Pd(OAc)_2$ (65.4 mg, 0.291 mmol, 5 mol%), and *N*-Bromosuccinimide (1.24 g, 6.97

mmol, 1.2 equiv) was added PhCl (58 mL, 0.10 M). This suspension was then heated to 110 °C and stirred for 24 h. The reaction was then allowed to cool to 23 °C, at which point it was transferred with CH_2Cl_2 (30 mL) to a separatory funnel containing 1.0 M saturated aqueous NaOH (30 mL). The layers were separated and the aqueous layer was extracted with CH_2Cl_2 (3 x 30 mL). The combined organic layers were then dried over Na_2SO_4, filtered, and concentrated under reduced pressure to afford the corresponding bromobipyridine *N*-oxide **4.48** as a brown oil. This was carried forward without further purification.

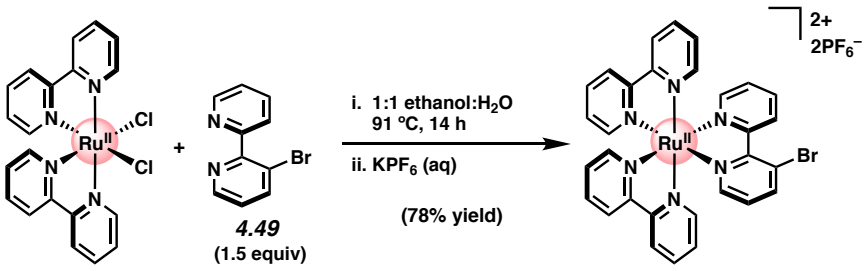
The crude oil was dissolved in $CHCl_3$ (50 mL, 0.10 M) and cooled to 0 °C. To this stirred solution was added PBr_3 (1.98 mL, 21.0 mmol, 4.0 equiv) dropwise over 8 min. The cooling bath was then removed and the reaction was warmed to 80 °C and stirred for 3 h. It was then allowed to cool to 23 °C before being cooled again to 0 °C. The reaction was then quenched by addition of 1.0 M aqueous NaOH (40 mL) over 1 min before being warmed to 23 °C. 6.0 M NaOH (40 mL) was then added and the mixture was stirred at 23 °C for 5 min before being transferred to a separatory funnel. The layers were separated and the aqueous layer was extracted with CH_2Cl_2 (3 x 50 mL). The combined organic layers were then dried over Na_2SO_4, filtered, and concentrated under reduced pressure. The resulting oil was purified by flash chromatography (5% Et_3N in 9:1 hexanes:EtOAc → 5% Et_3N in 7:2 hexanes:EtOAc) using silica gel neutralized with Et_3N to afford 2-bromobipyridine (**4.49**) as a beige solid (800 mg, 59% yield over two steps). **Bromobipyridine 4.49**: R_f 0.31 (10% MeOH in CH_2Cl_2). ^{1}H NMR (500 MHz, $CDCl_3$): δ 8.75 (dd, *J* = 4.9, 0.8, 1H), 8.66 (d, *J* = 4.6, 1H), 8.03 (d, *J* = 7.9, 1H), 7.83 (td, *J* = 7.6, 1.4, 1H), 7.73 (d, *J* = 7.7, 1H), 7.36 (dd, *J* = 7.6, 4.9, 1H), 7.22 (dd, *J* = 8.3, 4.7, 1H). Spectral data match those previously reported in the literature.[29]



2-Chlorobipyridine (4.51). To a flask containing 2,2'-bipyridyl *N*-oxide (**4.47**, 3.81 g, 22.1 mmol), $Pd(OAc)_2$ (248 mg, 1.11 mmol, 5 mol%), and *N*-Chlorosuccinimide (3.55 g, 26.6 mmol, 1.2 equiv) was added PhCl (220 mL, 0.10 M). This suspension was then heated to 110 °C and stirred for 24 h. The reaction mixture was then allowed to cool to 23 °C, at which point it was transferred with CH_2Cl_2 (15 mL) to a separatory funnel containing 1.0 M saturated aqueous NaOH (100 mL). The layers were separated and the aqueous layer was extracted with CH_2Cl_2 (3 x 60 mL). The combined organic layers were then dried over Na_2SO_4, filtered, and concentrated under reduced pressure to afford the corresponding chlorobipyridine *N*-oxide **4.50** as a brown oil. This was carried forward without further purification.

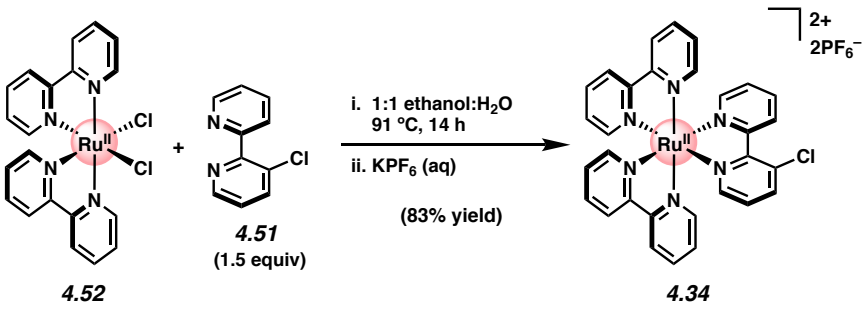
The crude oil was dissolved in $CHCl_3$ (200 mL, 0.10 M) and cooled to 0 °C. To this stirred solution was added PCl_3 (7.28 mL, 83.2 mmol, 4.0 equiv) dropwise at 0 °C over 12 min. The cooling bath was then removed and the reaction was warmed to 80 °C and stirred for 3 h. It was then allowed to cool to 23 °C before being cooled again to 0 °C. The reaction was then quenched by addition of 1.0 M aqueous NaOH (100 mL) over 2 min before being warmed to 23 °C. 6.0 M NaOH (50 mL) was then added and the mixture was stirred at 23 °C for 5 min before being transferred to a separatory funnel. The layers were separated and the aqueous layer was extracted with CH_2Cl_2 (3 x 100 mL). The combined organic layers were then dried over Na_2SO_4, filtered, and concentrated under reduced pressure. The resulting brown oil was purified by flash chromatography (5% Et_3N in 3:1 hexanes:EtOAc → 5% Et_3N in 1:1 hexanes:EtOAc → 5% Et_3N in 1:3 hexanes:EtOAc) using silica gel neutralized with Et_3N to afford 2-chlorobipyridine

(**4.51**) as an off-white solid (2.96 g, 70% yield over two steps). **2-chlorobipyridine** (**4.51**): R_f 0.30 (3:1 EtOAc:hexanes). ^{1}H NMR (400 MHz, CD_3CN): δ 8.77 (d, J = 4.8, 1H), 8.64 (dd, J = 4.8, 1.4, 1H), 7.83 (td, J = 8.7, 1.4, 2H), 7.77 (d, J = 7.9, 1H), 7.36 (ddd, J = 7.7, 4.9, 1.3, 1H), 7.31 (dd, J = 8.31, 4.7, 1H). Spectral data match those previously reported in the literature.[29]



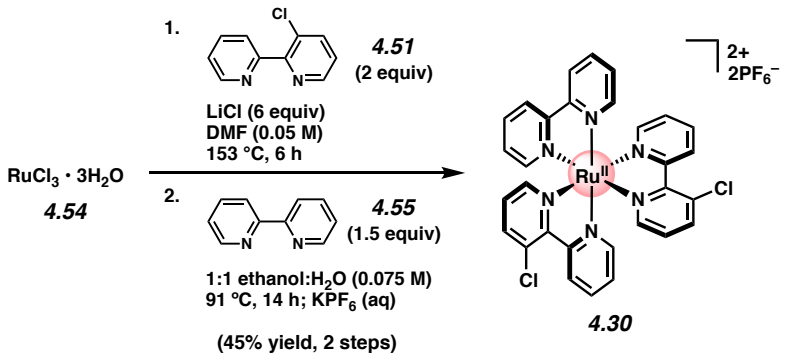
Bromo-Ru(bpy)$_3$[PF$_6$]$_2$ 4.53. To a flask containing *cis*-bis(2,2'-bipyridine)dichlororuthenium(II) hydrate (**4.52**, 899 mg, 1.86 mmol, 1.0 equiv) and bromobipyridine **4.49** (667 mg, 2.84 mmol, 1.5 equiv) was added EtOH (120 mL) and H_2O (120 mL). The reaction mixture was then warmed to 91 °C and stirred for 14 h, during which the solution changed in color from deep purple to red. The reaction was then allowed to cool to 23 °C before saturated aqueous KPF_6 (50 mL) was added over 1 min while stirring to produce a red precipitate. The mixture was then filtered over a pad of celite (packed with Et_2O), washed with Et_2O (3 x 20 mL), and the filtrate was discarded. The remaining solid residue was redissolved in CH_3CN (90 mL) and passed through the same celite plug. The resulting deep red filtrate was then concentrated under reduced pressure and then passed through a pad of neutral alumina with CH_3CN (250 mL). The red band was collected and concentrated under reduced pressure to afford a red semi-solid. This material was then recrystallized from 1:1 MeOH:H_2O (10 mL) and the resulting red crystals were washed with 1:1 MeOH:H_2O (2 x 2 mL, cooled to 0 °C) and dried on high vacuum for 12 h at 60 °C to afford bromo-Ru(bpy)$_3$[PF$_6$]$_2$ **4.53** as a red crystalline solid

(1.36 g, 78% yield based on anhydrous **4.52**). **Bromo-Ru(bpy)$_3$[PF$_6$]$_2$ 4.53**: mp >250 °C; R_f 0.64 (7:2:1 MeCN:H_2O:sat. aq. KNO_3); ^{1}H NMR (400 MHz, CD_3CN): δ 9.56 (dq, *J* = 8.6, 0.7, 1H), 8.49 (dd, *J* = 8.3, 3.4, 4H), 8.30 (dd, *J* = 8.3, 1.3, 1H), 8.10–8.02 (m, 5H), 7.84 (dd, *J* = 5.5, 1.4, 2H), 7.76 (dq, *J* = 5.7, 0.7, 1H), 7.70 (dq, *J* = 5.7, 0.7, 1H), 7.68–7.63 (m, 2H); ^{13}C NMR (125 MHz, CD_3CN, 26 of 30 signals observed): δ 157.79, 157.78, 157.69, 157.65, 157.5, 154.9, 153.2, 152.8, 152.7, 152.5, 152.3, 145.7, 138.93, 138.91, 138.90, 138.0, 129.3, 128.7, 128.64, 128.58, 128.55, 128.46, 127.9, 125.29, 125.28, 121.8; IR (film): 1606, 1467, 1447, 1425, 837, 762 cm^{-1}.



Chloro-Ru(bpy)$_3$[PF$_6$]$_2$ 4.34. To a flask containing *cis*-bis(2,2'-bipyridine)dichlororuthenium(II) hydrate (**4.52**, 4.00 g, 8.26 mmol, 1.0 equiv) and chlorobipyridine **4.51** (2.36 g, 12.4 mmol, 1.5 equiv) was added EtOH (330 mL) and H_2O (330 mL). The reaction mixture was then warmed to 91 °C and stirred for 14 h, during which the solution changed in color from deep purple to red. The reaction was then allowed to cool to 23 °C before saturated aqueous KPF_6 (300 mL) was added over 5 min while stirring to produce a red precipitate. The mixture was then filtered over a pad of celite (packed with Et_2O), washed with Et_2O (3 x 50 mL), and the filtrate was discarded. The remaining solid residue was redissolved in CH_3CN (200 mL) and passed through the same celite plug. The resulting deep red filtrate was then concentrated under reduced pressure and then passed through a pad of neutral alumina with CH_3CN (600 mL). The red band was collected and concentrated under reduced

pressure to afford a red semi-solid. The purified material was then divided into three portions and each was recrystallized from 1:1 MeOH:H_2O (10 mL) and the resulting red crystals were washed with 1:1 MeOH:H_2O (2 x 2 mL for each portion, cooled to 0 °C) and dried on high vacuum for 12 h at 50 °C to afford chloro-Ru(bpy)$_3$[PF_6]$_2$ **4.34** as a red crystalline solid (6.13 g, 83% yield based on anhydrous **4.52**). **Chloro-Ru(bpy)$_3$[PF_6]$_2$ 4.34**: mp >250 °C; R_f 0.60 (7:2:1 MeCN:H_2O:sat. aq. KNO_3); ^{1}H NMR (400 MHz, CD_3CN): δ 9.41 (dq, *J* = 8.5, 0.8, 1H), 8.50 (dd, *J* = 8.2, 1.0, 4H), 8.12–8.02 (m, 6H), 7.86 (dq, *J* = 5.6, 0.7, 1H), 7.81 (dd, *J* = 5.5, 1.3, 1H), 7.76 (dq, *J* = 5.6, 0.7, 1H), 7.70 (dq, *J* = 5.6, 0.7, 1H), 7.68–7.64 (m, 2H), 7.44–7.35 (m, 5H), 7.31 (dd, *J* = 8.4, 5.5, 1H); ^{13}C NMR (125 MHz, CD_3CN, 24 of 30 signals observed) δ 157.80, 157.78, 157.71, 157.67, 157.1, 154.0, 153.2, 152.8, 152.47, 152.45, 151.9, 142.0, 138.94, 138.91, 138.4, 134.2, 129.4, 128.7, 128.65, 128.61, 128.57, 128.5, 128.1, 125.30, 125.29; IR (film): 1604, 1467, 1447, 1427, 1243, 837 cm^{-1}.

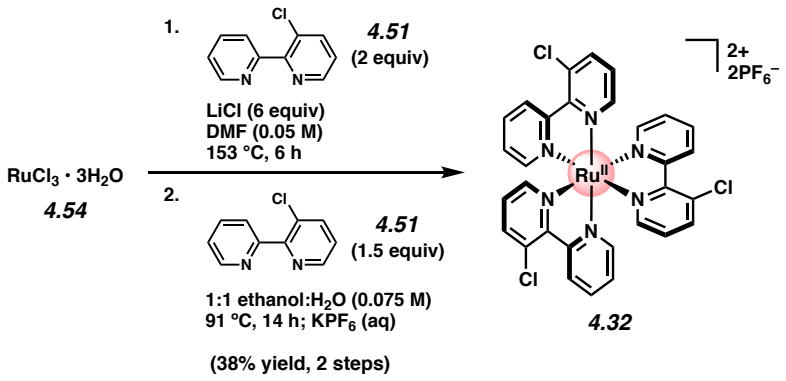


Bis(chloro)-Ru(bpy)$_3$[PF_6]$_2$ 4.30. To a flask containing ruthenium(III) chloride trihydrate (**4.54**, 309 mg, 1.18 mmol, 1.0 equiv), chlorobipyridine **4.51** (559 mg, 2.38 mmol, 2.0 equiv), and LiCl (301 mg, 7.10 mmol, 6.0 equiv) was added DMF (25 mL). The resulting suspension was warmed to 153 °C and stirred for 6 h. The reaction mixture was then allowed to cool to 23 °C before acetone (25 mL) was added and the mixture was added dropwise to vigorously stirring Et_2O (300

mL). The resultant mixture was then filtered over a pad of celite (packed with Et_2O) and washed with Et_2O (3 x 30 mL). The solid residue was then redissolved in CH_2Cl_2 (200 mL) and concentrated under reduced pressure to afford a deep purple solid. This was carried forward without further purification.

To the crude solid was added 2,2'-bipyridine (**4.55**, 281 mg, 1.80 mmol, 1.5 equiv), EtOH (80 mL), and H_2O (80 mL) sequentially. The resulting mixture was then warmed to 91 °C and stirred for 14 h, during which the solution changed in color from deep purple to red. The reaction was then allowed to cool to 23 °C before saturated aqueous KPF_6 (70 mL) was added over 2 min while stirring to produce a red precipitate. The mixture was then filtered over a pad of celite (packed with Et_2O), washed with Et_2O (3 x 30 mL), and the solid residue was redissolved in MeCN (200 mL). The deep red filtrate was then concentrated under reduced pressure and then purified by flash chromatography on neutral alumina (100% MeCN). The red band was collected and concentrated under reduced pressure to afford a red semi-solid. The purified material was then recrystallized from 1:1 MeOH:H_2O (5 mL) and the resulting red crystals were washed with 1:1 MeOH:H_2O (2 x 2 mL, cooled to 0 °C) and dried on high vacuum for 12 h at 60 °C to afford bis(chloro)-Ru(bpy)$_3$[PF_6]$_2$ **4.30** as a red crystalline solid (491 mg, 45% yield over 2 steps). **Bis(chloro)-Ru(bpy)$_3$[PF_6]$_2$ 4.30**: mp >250 °C; R_f 0.63 (7:2:1 MeCN:H_2O:sat. aq. KNO_3); ^{1}H NMR (500 MHz, CD_3CN): δ 9.43–9.39 (m, 2H), 8.50 (d, *J* = 8.2, 2H), 8.13–8.04 (m, 6H), 7.88 (dq, *J* = 5.6, 0.7, 1H), 7.85–7.82 (m, 1H), 7.81–7.77 (m, 1H), 7.75 (ddd, *J* = 5.6, 3.7, 1.4, 1H) 7.71 (app. d, *J* = 5.6, 1H), 7.67–7.63 (m, 1H); ^{13}C NMR (125 MHz, CD_3CN) δ 157.59, 157.57, 157.56, 157.5, 156.92, 156.85, 156.81, 153.85, 153.78, 153.75, 153.3, 153.04, 153.01, 152.64, 152.63, 152.03, 152.02, 151.74, 151.71, 142.24, 142.22, 142.21, 139.13, 139.11, 139.10, 139.09, 138.58, 138.57, 134.32, 134.29, 129.53, 129.51, 128.8, 128.72, 128.67, 128.61, 128.60, 128.5,

128.2, 128.1, 128.0, 125.41, 125.39, 125.37; IR (film): 1603, 1468, 1447, 1419, 1214, 835, 797 cm^{-1}. *Note:* ***4.30*** *was obtained as a mixture of geometric isomers. These data represent empirically observed chemical shifts from the* ^{13}C *NMR spectrum.*

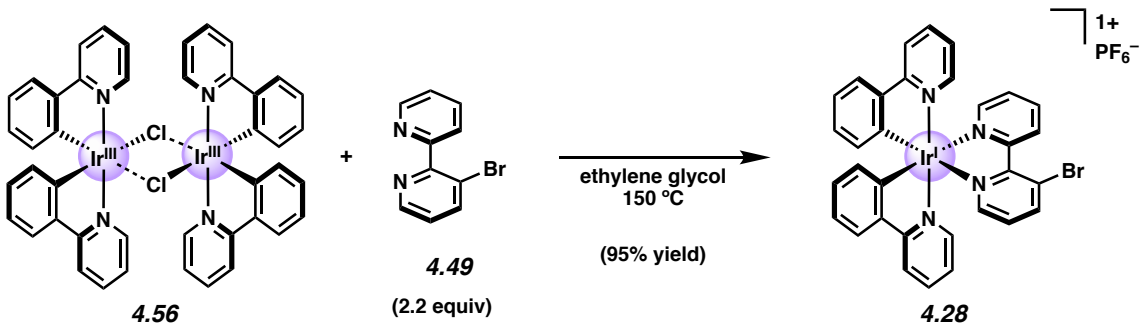


Tris(chloro)-Ru(bpy)$_3$[PF$_6$]$_2$ 4.32. To a flask containing ruthenium(III) chloride trihydrate (**4.54**, 401 mg, 1.54 mmol, 1.0 equiv), 2-chlorobipyridine (**4.51**) (584 mg, 3.07 mmol, 2.0 equiv), and LiCl (390 mg, 9.21 mmol, 6.0 equiv) was added DMF (30 mL). The resulting suspension was warmed to 153 °C and stirred for 6 h. The reaction mixture was then allowed to cool to 23 °C before acetone (35 mL) was added and the mixture was added dropwise to vigorously stirring Et_2O (300 mL). The resultant mixture was then filtered over a pad of celite (packed with Et_2O) and washed with Et_2O (4 x 30 mL). The solid residue was then redissolved in CH_2Cl_2 (250 mL) and concentrated under reduced pressure to afford a deep purple solid. This was carried forward without further purification.

To the crude solid material was added 2-chlorobipyridine (**4.51**) (443 mg, 2.32 mmol, 1.5 equiv), EtOH (100 mL), and H_2O (100 mL) sequentially. The resulting mixture was then warmed to 91 °C and stirred for 14 h, during which the solution changed in color from deep purple to red. The reaction was then allowed to cool to 23 °C before saturated aqueous KPF_6 (70 mL) was added over 2 min while stirring to produce a red precipitate. The mixture was then filtered over a

pad of celite (packed with Et_2O), washed with Et_2O (3 x 30 mL), and the solid residue was redissolved in MeCN (250 mL). The deep red filtrate was then concentrated under reduced pressure and then purified by flash chromatography on neutral alumina (100% MeCN). The red band was collected and concentrated under reduced pressure to afford a red semi-solid. The purified material was then recrystallized from 1:1 MeOH:H_2O (5 mL) and the resulting red crystals were washed with 1:1 MeOH:H_2O (2 x 2 mL, cooled to 0 °C) and dried on high vacuum for 12 h at 60 °C to afford tris(chloro)-Ru(bpy)$_3$[PF_6]$_2$ **4.32** as a red crystalline solid (567 mg, 38% yield over 2 steps). **Tris(chloro)-Ru(bpy)$_3$[PF_6]$_2$ 4.32**: mp >250 °C; R_f 0.69 (7:2:1 MeCN:H_2O:sat. aq. KNO_3); ^{1}H NMR (500 MHz, CD_3CN): δ 9.41 (d, J = 8.5, 3H), 8.14–8.06 (m, 6H), 7.85–7.72 (m, 6H), 7.41–7.38 (qd, J = 6.8, 1.3, 3H), 7.35–7.28 (m, 3H); ^{13}C NMR (125 MHz, CD_3CN) δ 156.7, 156.5, 153.63, 153.62, 153.59, 153.20, 153.18, 151.89, 151.87, 142.40, 142.38, 142.37, 138.74, 138.71, 134.38, 134.36, 134.35, 134.34, 129.61, 129.60, 129.57, 128.83, 128.79, 128.70, 128.66, 128.3, 128.2, 128.13, 128.07; IR (film): 1473, 1428, 1420, 1215, 837, 797 cm^{-1}.

*Note: **4.32** was obtained as a mixture of geometric isomers. These data represent empirically observed chemical shifts from the ^{13}C NMR spectrum.*



4.56 + *4.49* (2.2 equiv) → *4.28*

Bromo-Ir(ppy)$_2$bpy 4.28. To a 1-dram vial was added Di-μ-chlorotetrakis[2-(2-pyridinyl-kN)phenyl-kC]diiridium(III) **4.56** (100.0 mg, 0.093 mmol, 1.0 equiv) in a glovebox. The vial

was removed from the glovebox and placed under nitrogen in a hood. To a separate 1-dram vial was added 3-bromo-2,2'-bipyridine (**4.49**) (48.2 mg, 0.205 mmol, 2.2 equiv) and ethylene glycol (4.0 mL, 0.023 M), then the mixture was sparged with nitrogen for 15 minutes. The solution of 3-bromo-2,2'-bipyridine was then transferred to the vial of diiridium (III) complex. The septa cap was replaced with a Teflon-lined screw cap and the reaction stirred at 150 °C for 15 h. After cooling to 23 °C, the reaction was transferred to a separatory funnel containing deionized water (48 mL). The aqueous phase was washed with hexanes (2 x 24 mL) and then ether (24 mL). The aqueous layer was then heated to 85 °C for 5 minutes to evaporate any remaining organic solvent. The solution cooled to 23 °C, then aq. ammonium hexafluorophospate (12 mL, 0.27 M) was added precipitating orange-yellow crystals. The solid was filtered through a plug of celite (2 x 2 cm) and washed with water (20 mL) to remove ethylene glycol. The pad was then washed with acetonitrile (50 mL) to dissolve the product and the filtrate was collected and concentrated under reduced pressure to afford bromo-Ir(ppy)$_2$bpy complex **4.28** as a dark yellow solid (95% yield). **Bromo-Ir(ppy)$_2$bpy 4.28**. (7:2:1 CH_3CN:H_2O:sat. aq. KNO_3); ^{1}H NMR (600 MHz, CD_3CN): δ 9.42 (ddd, J = 8.4, 1.3, 0.83, 1H), 8.37 (dd, J = 8.4, 1.4, 1H), 8.13 (ddd, J = 8.7, 7.9, 1.8 1H), 8.09 – 8.04 (m, 4H), 7.88 – 7.83 (m, 2H), 7.78 (ddd, J = 7.9, 3.3, 1.1, 2H), 7.73 – 7.70 (m, 2H), 7.49 (ddd, J = 7.7, 5.5, 1.2, 1H), 7.29 (dd, J = 8.6, 5.4, 1H), 7.06 – 7.01 (m, 4H), 6.90 (tdd, J = 7.4, 2.4, 1.3, 2H), 6.22 (ddd, J = 7.6, 4.6, 1.0, 2H); HR-ESI-MS (*m/z*) calcd for $C_{32}H_{23}BrN_4Ir^+$, 735.0735; found 735.0738.

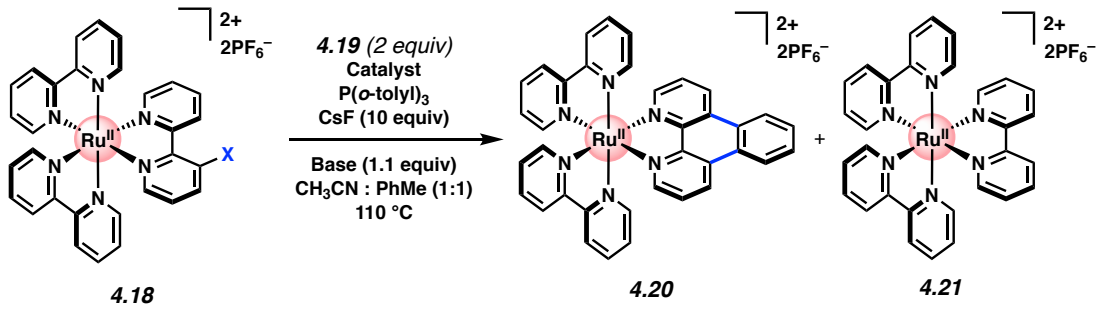
4.8.2.2 Reaction Optimization (Table 4.2)

Representative Procedure for reaction optimization. Benzyne adduct 4.20 (Supplementary Table 4.2, entry 11):

To a 1-dram vial was added $Pd(OAc)_2$ (1.6 mg, 7.3 μmol, 10 mol%), Bromo-$Ru(bpy)_3[PF_6]_2$ **4.53** (68.6 mg, 73.1 μmol, 1.0 equiv), P(*o*-tolyl)$_3$ (2.2 mg, 7.3 μmol, 10 mol%), MeCN (0.5 mL), PhMe (0.5 mL), silyl triflate **4.19** (43.6 mg, 73.1 μmol, 2.0 equiv), an oven-dried magnetic stirbar, and CsF (111 mg, 731 μmol, 10.0 equiv) sequentially. The reaction was then purged with N_2 for 5 min before being sealed with a Teflon-lined screw cap under a flow of N_2, sealed with Teflon tape and electrical tape, and stirred at 110 °C for 30 min. After cooling to 23 °C, the mixture was filtered through a plug of celite with MeCN (6 mL) and concentrated under reduced pressure. The yield was determined by ^{1}H NMR analysis with 1,3,5-trimethoxybenzene as an external standard.

Optimization efforts that deviate from the above conditions are indicated below.

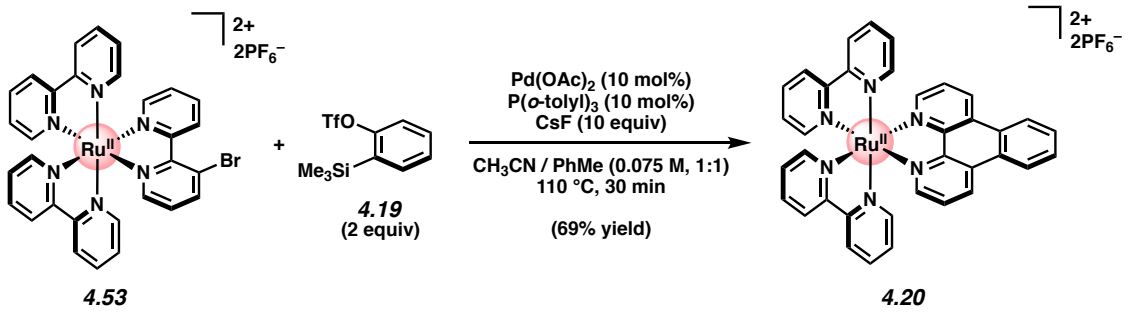
Table 4.2. Optimization studies of Br-Ru(bpy)$_3$ annulation with benzyne. Yields were determined using ^{1}H NMR analysis with 1,3,5-trimethoxybenzene (TMB) as an external standard.



4.18 ***4.20*** ***4.21***

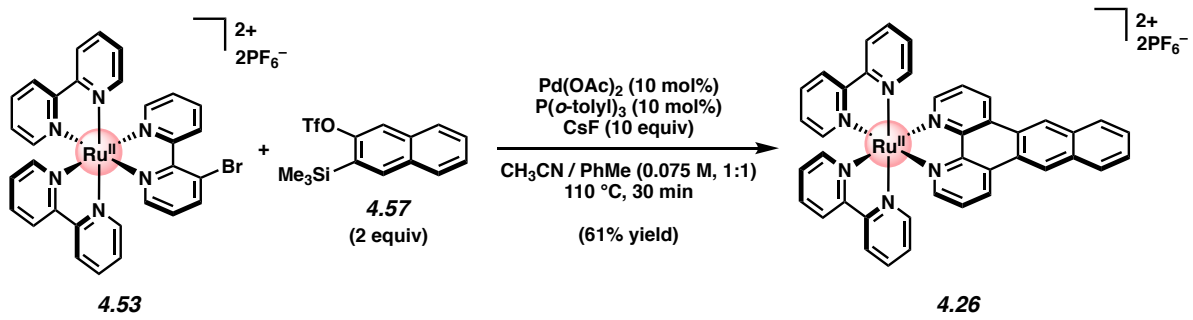
Entry	*Catalyst*	*Ligand*	***X***	*Catalyst Loading*	*Ligand Loading*	*Base*	*CH_3CN : PhMe*	*Time*	*Yield of **4.20***	*Yield of **4.21***
1	$Pd(dba)_2$	P(*o*-tolyl)$_3$	Br	5 mol%	5 mol%	–	1 : 1	2 h	2%	48%
2	$Pd(PPh_3)_4$	P(*o*-tolyl)$_3$	Br	5 mol%	5 mol%	–	1 : 1	2 h	2%	48%
3	XPhos Pd G2		Br	5 mol%	5 mol%	–	1 : 1	2 h	4%	40%
4	$Pd(OAc)_2$	P(*o*-tolyl)$_3$	Br	5 mol%	5 mol%	–	1 : 1	2 h	26%	24%
5	$Pd(OAc)_2$	P(*o*-tolyl)$_3$	Br	10 mol%	30 mol%	–	1 : 1	2 h	60%	18%
6	$Pd(OAc)_2$	P(*o*-tolyl)$_3$	Br	10 mol%	30 mol%	Ag_2CO_3	1 : 1	2 h	54%	16%
7	$Pd(OAc)_2$	P(*o*-tolyl)$_3$	Br	10 mol%	30 mol%	K_2CO_3	1 : 1	2 h	41%	19%
8	$Pd(OAc)_2$	P(4-ClC_6H_4)$_3$	Br	10 mol%	30 mol%	–	1 : 1	2 h	32%	29%
9	$Pd(OAc)_2$	P(4-MeOC_6H_4)$_3$	Br	10 mol%	30 mol%	–	1 : 1	2 h	16%	35%
10	$Pd(OAc)_2$	SPhos	Br	10 mol%	30 mol%	–	1 : 1	2 h	44%	26%
11	$Pd(OAc)_2$	P(*o*-tolyl)$_3$	Br	10 mol%	10 mol%	–	1 : 1	30 min	71%	16%
12	$Pd(OAc)_2$	P(*o*-tolyl)$_3$	Br	10 mol%	10 mol%	–	3 : 1	30 min	61%	19%
13	$Pd(OAc)_2$	P(*o*-tolyl)$_3$	Br	10 mol%	10 mol%	–	9 : 1	30 min	44%	18%
14	$Pd(OAc)_2$	P(*o*-tolyl)$_3$	Br	10 mol%	10 mol%	–	100% CH_3CN	30 min	47%	16%
15	$Pd(OAc)_2$	P(*o*-tolyl)$_3$	Br	10 mol%	10 mol%	–	1 : 3	30 min	35%	28%
16	$Pd(OAc)_2$	P(*o*-tolyl)$_3$	Cl	10 mol%	10 mol%	–	1 : 1	30 min	78%	0%

4.8.2.3 Scope of Pd-Catalyzed Aryne Annulation



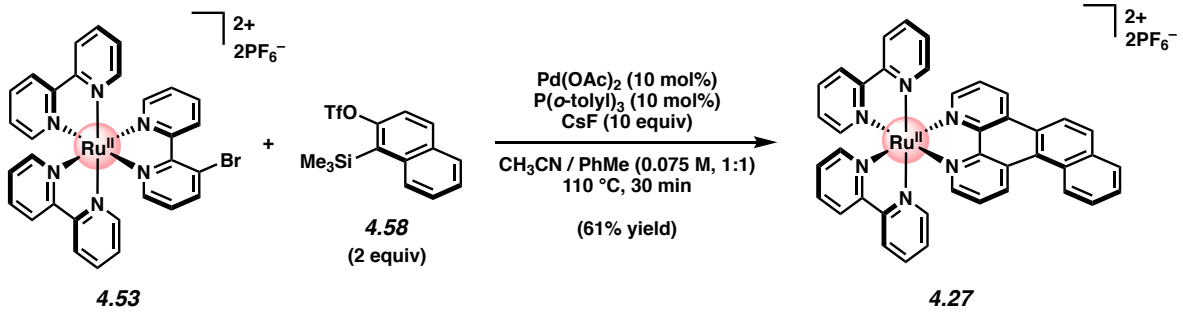
Representative Procedure A for aryne annulations (Figure 4.3, benzyne adduct 4.20 used as an example). To a 1-dram vial was added $Pd(OAc)_2$ (1.5 mg, 6.7 μmol, 10 mol%), Bromo-Ru(bpy)$_3$[PF$_6$]$_2$ **4.53** (62.2 mg, 0.066 mmol, 1.0 equiv), P(*o*-tolyl)$_3$ (2.2 mg, 7.2 μmol, 10 mol%), MeCN (0.5 mL), PhMe (0.5 mL), silyl triflate **4.19** (40.1 mg, 0.134 mmol, 2.0 equiv), an oven-dried magnetic stirbar, and CsF (101 mg, 0.663 mmol, 10.0 equiv) sequentially. The reaction was then purged with N_2 for 5 min before being capped with a Teflon-lined screw cap under a flow of N_2, sealed with Teflon tape and electrical tape, and stirred at 110 °C for 30 min. After cooling to 23 °C, the mixture was filtered through a plug of celite with MeCN (6 mL), and concentrated under reduced pressure. The crude residue was adsorbed onto SiO_2 and purified by flash chromatography (14:2:1 MeCN:H_2O:sat. aq. KNO_3). To the concentrated aqueous mixture was added saturated aqueous KPF_6 (50 mL) to precipitate the desired product, and the resultant mixture was transferred to a separatory funnel with CH_2Cl_2 (50 mL). The layers were separated and the aqueous layer was extracted with CH_2Cl_2 (2 x 50 mL). The combined organic layers were then concentrated under reduced pressure and dried on high vacuum at 100 °C for 12 h to afford benzyne adduct **4.20** as a deep red solid (69% yield, average of two experiments). **Benzyne adduct 4.20**: mp >250 °C; R_f 0.68 (7:2:1 MeCN:H_2O:sat. aq. KNO_3); ^{1}H NMR (500 MHz, CD_3CN): δ 9.23 (d,d *J* = 8.4, 0.9, 2H), 8.92–8.88 (m, 2H), 8.55 (d, *J* = 8.3, 2H), 8.51 (d, *J* = 8.3, 2H), 8.11 (td, *J* = 7.9. 1.5, 2H), 8.07 (dd, *J* = 5.3, 0.9, 2H), 8.02–7.98 (m, 4H), 7.85 (d, *J* =

5.8, 2H), 7.79 (dd, J = 8.2, 5.3, 2H), 7.63 (d, J = 5.6, 2H), 7.46 (td, J = 6.9, 1.3, 2H), 7.23 (td, J = 6.9, 1.2, 2H).

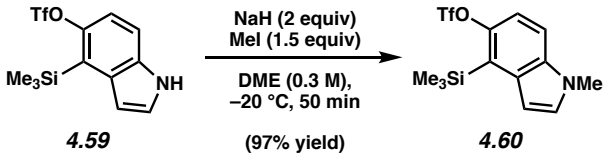


Representative Procedure B for aryne annulations (Figure 4.3, naphthalyne adduct 4.26 used as an example). To a 1-dram vial was added $Pd(OAc)_2$ (1.4 mg, 6.4 μmol, 10 mol%), Bromo-Ru(bpy)$_3$[PF_6]$_2$ **4.53** (60.0 mg, 0.064 mmol, 1.0 equiv), P(*o*-tolyl)$_3$ (2.0 mg, 6.4 μmol, 10 mol%), MeCN (0.5 mL), PhMe (0.5 mL), silyl triflate **4.57** (44.6 mg, 0.128 mmol, 2.0 equiv), an oven-dried magnetic stirbar, and CsF (97.1 mg, 0.639 mmol, 10.0 equiv) sequentially. The reaction was then purged with N_2 for 5 min before being sealed with a Teflon-lined screw cap under a flow of N_2, sealed with Teflon tape and electrical tape, and stirred at 110 °C for 30 min. After cooling to 23 °C, the mixture was filtered through a plug of celite with MeCN (6 mL), and concentrated under reduced pressure. The crude residue was adsorbed onto SiO_2 and purified by flash chromatography (100% EtOAc → 7:2:1 MeCN:H_2O:sat. aq. KNO_3). To the concentrated aqueous mixture was added saturated aqueous KPF_6 (50 mL) to precipitate the desired product, and the resultant mixture was transferred to a separatory funnel with CH_2Cl_2 (50 mL). The layers were separated and the aqueous layer was extracted with CH_2Cl_2 (2 x 50 mL). The combined organic layers were then concentrated under reduced pressure before being redissolved in CH_3CN (10 mL). Activated charcoal (150 mg) was then added the mixture was agitated for 10 seconds before being filtered over celite, concentrated under reduced pressure, and dried on high

vacuum at 100 °C for 12 h to afford naphthalyne adduct **4.26** as a deep red solid (61% yield, average of two experiments). **Naphthalyne adduct 4.26**: R_f 0.57 (7:2:1 CH_3CN:H_2O:saturated aqueous KNO_3); ^1H NMR (500 MHz, CD_3CN): δ 9.41 (s, 2H), 9.29 (dd, *J* = 8.0, 1.2, 2H), 8.56 – 8.51 (m, 4H), 8.30–8.27 (m, 2H), 8.11 (td, *J* = 10, 1.4, 2H), 8.03 – 7.99 (m, 4H), 7.85 (dd, *J* = 5.5, 0.5, 2H), 7.79–7.76 (m, 4H), 7.72 (dd, *J* = 5.6, 0.5, 2H), 7.46 (ddd, *J* = 7.8, 5.7, 1.3, 2H), 7.27 (ddd, *J* = 7.8, 5.7, 1.3, 2H); ^{13}C NMR (500 MHz, CD_3CN): δ 158.1, 157.9, 152.9, 152.8, 152.3, 149.6, 138.8, 138.7, 134.0, 133.0, 132.3, 129.3, 129.1, 128.5, 128.4, 127.7, 126.4, 125.6, 125.2, 125.1; HR-ESI-MS (*m/z*) calcd for $C_{40}H_{27}N_6PF_6Ru^+$, 839.1061; found 839.1050.

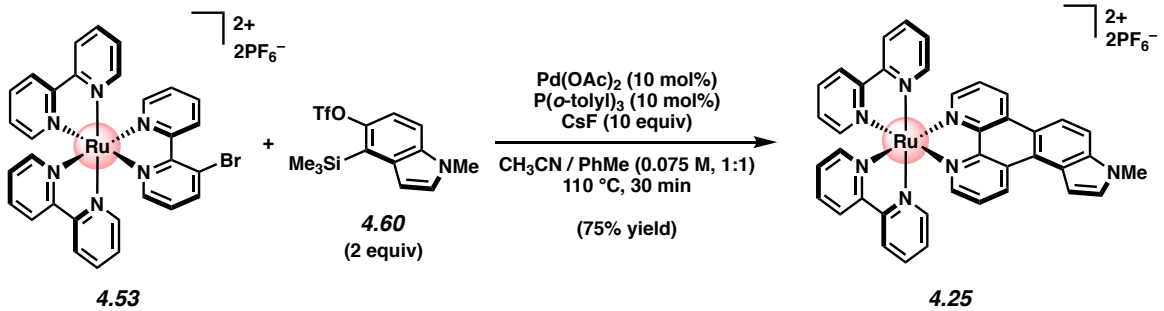


Naphthalyne adduct 4.27. Followed representative procedure B. Purification by flash chromatography (14:2:1 CH_3CN:H_2O:sat. aq. KNO_3) afforded naphthalyne adduct **4.27** (61% yield, average of two experiments) as a red solid. **Naphthalyne adduct 4.27**: R_f 0.70 (7:2:1 CH_3CN:H_2O:sat. aq. KNO_3); (600 MHz, CD3CN): δ 9.52 (d, *J* = 8.7, 1H), 9.29 (d, *J* = 8.7, 1H), 8.96 (d, *J* = 8.3, 1H), 8.82 (d, *J* = 8.7, 1H), 8.57–8.50 (m, 4H), 8.37 (d, *J* = 8.8, 1H), 8.24 (d, *J* = 7.9, 1H), 8.15–8.09 (m, 4H) 8.00 (t, *J* = 7.8, 2H), 7.89–7.78 (m, 6H), 7.69 (d, *J* = 5.2, 1H), 7.64 (d, *J* = 5.6, 1H), 7.49–7.44 (m, 2H), 7.23–7.20 (m, 2H); HR-ESI-MS (*m/z*) calcd for $C_{40}H_{27}N_6PF_6Ru^+$, 839.1061; found 839.1119.



4.59 *4.60*

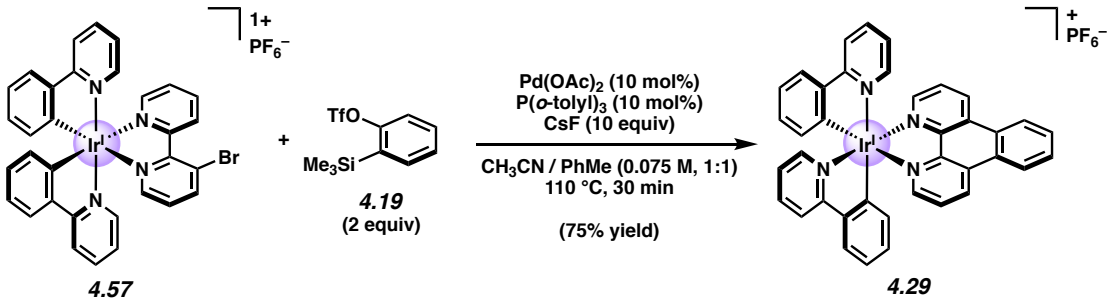
Silyl triflate 4.60. To a solution of Garg 4,5-indolyne precursor (**4.59**, 913 mg, 2.71 mmol, 1.0 equiv) in DME (9 mL, 0.3 M) at –20 °C was added MeI (256 µL, 4.10 mmol, 1.5 equiv) and NaH (60 wt% dispersion in mineral oil; 215 mg, 5.41 mmol, 2.0 equiv) sequentially. The reaction mixture was then stirred at –20 °C for 50 min before being quenched by addition of saturated aqueous NH_4Cl (5 mL). It was then allowed to warm to 23 °C and transferred to a separatory funnel with H_2O (10 mL) and EtOAc (10 mL). The layers were then separated and the aqueous layer was extracted with EtOAc (3 x 15 mL). The combined organic layers were dried over $MgSO_4$, filtered, and concentrated under reduced pressure. The crude residue was then purified by flash chromatography (100% hexanes → 100:1 hexanes:EtOAc → 50:1 hexanes:EtOAc) to afford silyl triflate **4.60** as a viscous, oil (927 mg, 97% yield). ***N*-Me silyl triflate 4.60**: R_f 0.63 (4:1 hexanes:EtOAc). ^{1}H NMR (500 MHz, $CDCl_3$): δ 7.33 (d, J = 9.0, 0.9, 1H), 7.20–7.14 (m, 2H), 6.68 (dd, J = 3.4, 0.6, 1H), 3.81 (s, 3H), 0.50 (s, 9H). Spectral data match those previously reported in the literature.[30]



4.53 *4.60* (2 equiv) *4.25*

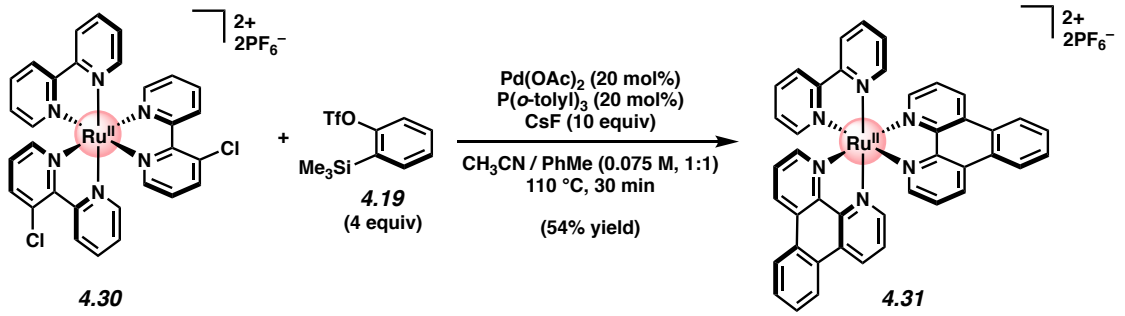
Indolyne adduct 4.25. Followed representative procedure A. Purification by flash chromatography (7:2:1 CH_3CN:H_2O:sat. aq. KNO_3) afforded indolyne adduct **4.25** (75% yield)

as a red solid. **Indolyne adduct 4.25**: R_f 0.63 (7:2:1 CH_3CN:H_2O:sat. aq. KNO_3); ^1H NMR (400 MHz, CD_3CN): δ 9.71 (d, J = 8.0, 1H), 9.25 (d, J = 8.0, 1H), 8.72 (d, 1H), 8.55 – 8.45 (m, 4H), 8.05 – 7.95 (m, 3H), 7.90 – 7.80 (m, 3H), 7.70 – 7.77 (m, 1H), 7.65 – 7.60 (m, 3H), 7.57 (m, 1H), 7.47–7.44 (m, 2H), 7.21–7.17 (m, 2H), 4.24 (s, 3H).

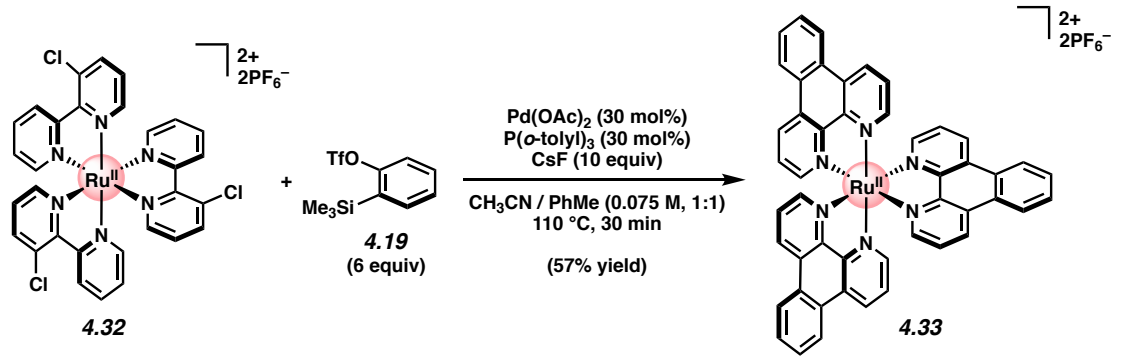


4.57 *4.29*

Ir-benzyne adduct 4.29. Followed representative procedure A. Purification by flash chromatography (9:1 benzene:acetonitrile → 3:2 benzene:acetonitrile) afforded Ir-benzyne adduct **4.29** (75% yield, average of two experiments) as a dark orange solid. **Ir-benzyne adduct 4.29**: ^1H NMR (600 MHz, CD_3CN): δ 9.30 (dd, J = 8.6, 0.9, 1H), 8.92 – 8.88 (m, 1H), 8.29 (dd, J = 5.1, 1.3, 1H), 8.06 (d, J = 8.3, 1H), 8.00 – 7.98 (m, 1H), 7.89 (dd, J = 8.6, 5.1, 1H), 7.84 (dd, J = 8.0, 1.1, 1H), 7.79 (ddd, J = 8.2, 7.6, 1.5, 1H), 7.49 (ddd, J = 6.0, 1.5, 0.7, 1H), 7.29 (dd, J = 8.4, 5.3, 1H), 7.06 – 7.00 (m, 4H), 6.90 (tdd, J = 7.5, 2.5, 1.3, 2H), 6.22 (ddd, 7.5, 4.8, 1.2, 2H); HR-ESI-MS (*m/z*) calcd for $C_{38}H_{26}N_4Ir^+$, 731.1787; found 731.1659.



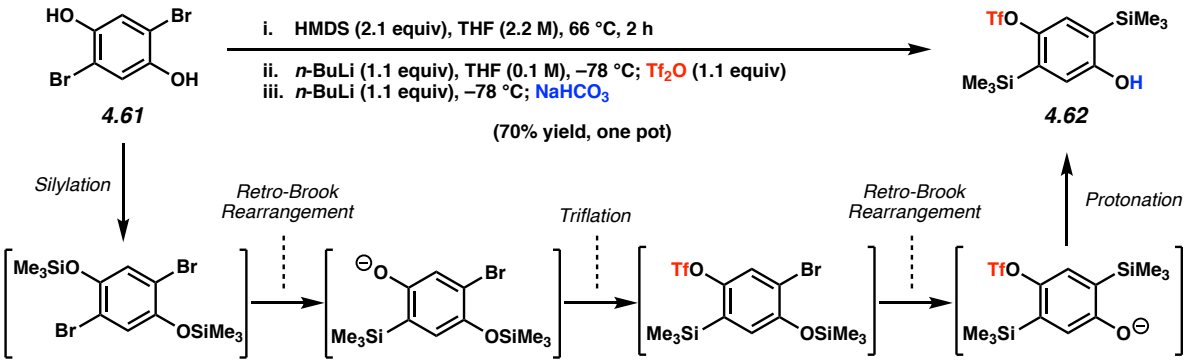
Bis-annulation adduct 4.31. Followed representative procedure A. Purification by flash chromatography (14:1:1 CH_3CN:H_2O:sat. aq. KNO_3) afforded adduct **4.31** (54% yield, average of two experiments) as a red solid. **Bis-annulation adduct 4.31**: mp >250 °C; R_f 0.77 (7:2:1 MeCN:H_2O:sat. aq. KNO_3); ^{1}H NMR (500 MHz, CD_3CN): δ 9.27 (d, J = 8.6, 1H), 9.16 (d, J = 8.6, 1H), 8.96–8.85 (m, 2H), 8.54 (d, J = 8.4, 1H), 8.17 (d, J = 5.2, 1H), 8.07–7.92 (m, 4H), 7.83 (dd, J = 8.5, 5.3, 1H), 7.74 (d, J = 5.3, 1H), 7.61 (dd, J = 8.2, 5.4, 1H), 7.28 (t, J = 6.4, 1H);); ^{13}C NMR (125 MHz, CD_3CN, 19 of 21 signals observed) δ 158.1, 153.1, 152.9, 152.8, 149.0, 148.8, 138.7, 133.2, 133.0, 131.32, 131.26, 131.2, 129.14, 128.3, 127.4, 127.3, 125.64, 125.60, 125.1; IR (film): 1467, 1436, 1407, 840, 762 cm^{-1}.



Tris-annulation adduct 4.33. Followed representative procedure B. Purification by flash chromatography (14:1:1 CH_3CN:H_2O:sat. aq. KNO_3) afforded adduct **4.33** (57% yield, average of two experiments) as a red solid. **Tris-annulation adduct 4.33**: mp >250 °C; R_f 0.78 (7:2:1 CH_3CN:H_2O:sat. aq. KNO_3); ^{1}H NMR (500 MHz, CD_3CN): δ 9.22 (dd, J = 8.7, 0.7, 6H), 8.93–

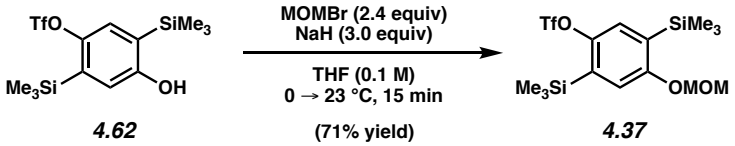
8.90 (m, 6H), 8.08 (dd, J = 5.3, 1.0, 6H), 8.03–7.99 (m, 6H), 7.68 (dd, J = 8.3, 5.3, 6H); ^{13}C NMR (125 MHz, CD_3CN) δ 153.1, 149.0, 133.1, 131.3, 131.2, 129.2, 127.3, 125.6.

4.8.2.4. Synthesis of Ligand-Bound Silyl Triflate and Trapping of Organometallic Aryne

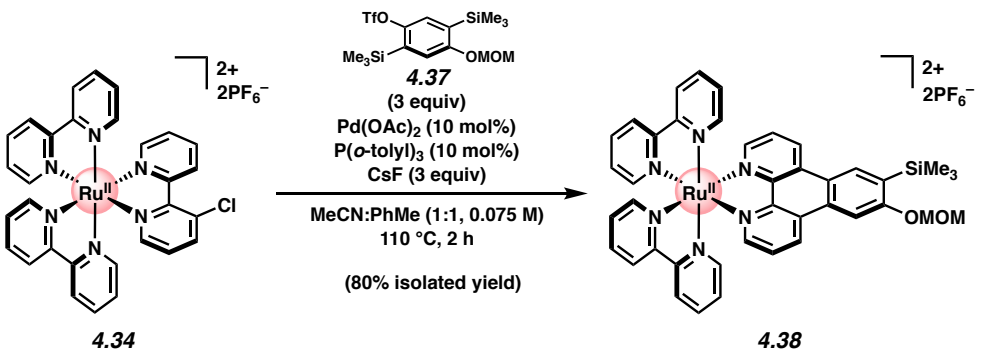


Silyl alcohol 4.62. To a stirred solution of 2,5-dibromohydrone (**4.61**, 2.60 g, 9.71 mmol, 1.0 equiv) in THF (4.40 mL, 2.20 M) was added HMDS (4.25 mL, 20.4 mmol, 2.1 equiv). The mixture was then heated to 66 °C and stirred for 2 h. Then, the reaction mixture was allowed to cool to 23 °C and the volatiles were removed. THF (69.3 mL, 0.14 M) was then added and the mixture was cooled to –78 °C. *n*-BuLi (2.49 M in hexanes; 4.29 mL, 10.7 mmol, 1.1 equiv) was then added dropwise over 8 min. The reaction mixture was then stirred at –78 °C for 25 min. Tf_2O (1.80 mL, 10.7 mmol, 1.1 equiv) was then added dropwise over 5 min at –78 °C, and the mixture was allowed to stir at this temperature for 25 min. *n*-BuLi (2.49 M in hexanes; 4.29 mL, 10.7 mmol, 1.1 equiv) was then added dropwise over 8 min. The reaction mixture was then stirred at –78 °C for 25 min. Finally, the reaction was quenched by addition of sat. aq. $NaHCO_3$ (40 mL) in one portion and the mixture was allowed to warm to 23 °C before being transferred to a separatory funnel with Et_2O (100 mL) and the layers were separated. The aqueous layer was then extracted with Et_2O (2 x 100 mL) and the combined organic layers were then dried over

Na_2SO_4, filtered, and concentrated under reduced pressure. The crude residue was then purified by flash chromatography (100% hexanes → 3% EtOAc in hexanes → 5% EtOAc in hexanes) to afford silyl alchol **4.62** as a viscous yellow oil (2.62 g, 70% yield). **Silyl alcohol 4.62**: R_f 0.39 (9:1 hexanes:EtOAc). ^{1}H NMR (600 MHz, $CDCl_3$): δ 7.23 (s, 1H), 6.74 (s, 1H), 4.88 (s, 1H), 0.35 (s, 9H), 0.31 (s, 9H). Spectral data match those previously reported in the literature.[31]



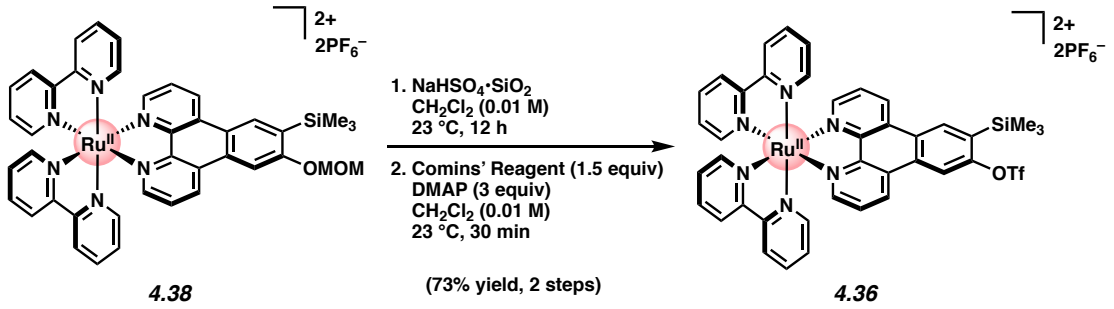
Methoxymethyl ether 4.37. To a stirred solution of silyl alcohol **4.62** (1.03 g, 2.66 mmol, 1.0 equiv) in THF (25 mL, 0.10 M) at 0 °C was added sodium hydride (dry, 95%; 202 mg, 7.99 mmol, 3.0 equiv) in one portion. The solution was then stirred at 0 °C for 15 min, followed by dropwise addition of bromomethyl methyl ether (522 μL, 6.39 mmol, 2.40 equiv) over 1 minute. Following addition, the reaction was allowed to warm to 23 °C and stirred for 15 min before being diluted with Et_2O (30 mL). H_2O (30 mL) was then added over 30 seconds and then mixture was transferred with Et_2O (5 mL) to a separatory funnel. The layers were separated and the aqueous layer was extracted with Et_2O (3 x 30 mL). The combined organic layers were then washed with H_2O (30 mL), dried over Na_2SO_4, and concentrated under reduced pressure. The crude residue was then purified by flash chromatography (100% hexanes) to afford methoxy methyl ether **4.37** as a white solid (814 mg, 71% yield). **Methoxymethyl ether 4.37**: R_f 0.56 (9:1 hexanes:EtOAc). ^{1}H NMR (500 MHz, $CDCl_3$): δ 7.25 (s, 1H), 7.14 (s, 1H), 5.19 (s, 2H), 3.48 (s, 3H), 0.36 (s, 9H), 0.28 (s, 9H). ^{13}C NMR (125 MHz, CD_3CN) δ 160.5, 149.6, 135.3, 132.8, 126.1, 126.0, 119.2, 118.7 (q, J = 320.5), 94.3, 56.3, –0.7, –1.2.



4.34 *4.38*

Methoxymethyl ether adduct 4.38. To a 20 mL scintillation vial was added $Pd(OAc)_2$ (10.1 mg, 44.8 μmol, 10 mol%), chloro-Ru(bpy)$_3$[PF_6]$_2$ **4.34** (400.5 mg, 0.448 mmol, 1.0 equiv), P(*o*-tolyl)$_3$ (13.6 mg, 44.8 mmol, 10 mol%), MeCN (3.0 mL), PhMe (3.0 mL), silyl triflate **4.37** (564 mg, 1.31 mmol, 3.0 equiv), an oven-dried magnetic stirbar, and CsF (204 mg, 1.34 mmol, 3.0 equiv) sequentially. The reaction was then purged with N_2 for 5 min before being sealed with a Teflon-lined screw cap under a flow of N_2, sealed with Teflon tape and electrical tape, and stirred at 110 °C for 2 h. After cooling to 23 °C, the mixture was filtered through a plug of celite with MeCN (10 mL), and concentrated under reduced pressure. The crude residue was adsorbed onto SiO_2 and purified by flash chromatography (100% EtOAc → 14:1:1 MeCN:H_2O:sat. aq. KNO_3). To the concentrated aqueous mixture was added saturated aqueous KPF_6 (100 mL) to precipitate the desired product, and the resultant mixture was transferred to a separatory funnel with CH_2Cl_2 (50 mL). The layers were separated and the aqueous layer was extracted with CH_2Cl_2 (2 x 50 mL). The combined organic layers were then concentrated under reduced pressure before being redissolved in CH_3CN (10 mL). Activated charcoal (500 mg) was then added and the mixture was agitated for 10 seconds before being filtered over celite, concentrated under reduced pressure, and dried on high vacuum at 100 °C for 12 h to afford methoxymethyl ether adduct **4.38** as a red solid (380 mg, 80% yield). **Methoxymethyl ether adduct 4.38**: R_f 0.79 (7:2:1 CH_3CN:H_2O:saturated aqueous KNO_3); ^{1}H NMR (500 MHz, CD_3CN): δ 9.25 (dd, *J*

= 12.0, 8.5, 2H), 8.88 (s, 1H), 8.60 (dd, *J* = 8.2, 2H), 8.56 (dd, *J* = 8.2, 2H), 8.34 (s, 1H), 8.16–8.11 (m, 3H), 8.08 (d, *J* = 5.2, 1H), 8.03 (tt, *J* = 7.9, 1.7, 2H), 7.91 (d, *J* = 5.8, 2H), 7.82 (td, *J* = 8.4, 5.3, 2H), 7.69 (t, *J* = 6.8, 2H), 7.50 (td, *J* = 6.6, 1.0, 2H), 7.28 (dd, *J* = 12.9, 5.5, 2H), 5.58 (q, *J* = 5.5, 2H), 3.54 (s, 3H), 0.48 (s, 9H).

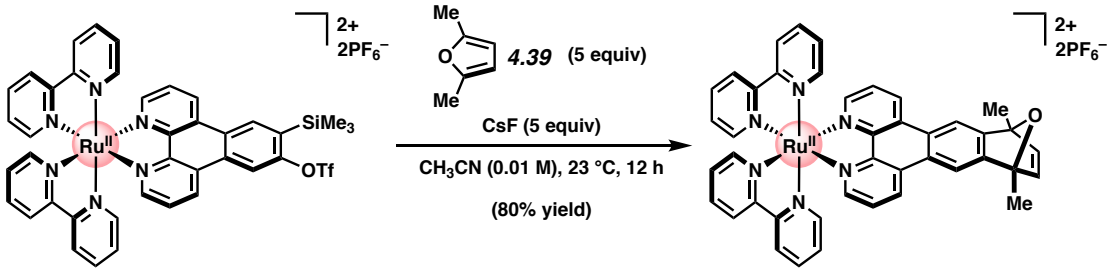


4.38 *4.36*

Silyl triflate 4.36. To a stirred solution of methoxymethyl ether **4.38** (259 mg, 0.243 mmol, 1.0 equiv) in CH_2Cl_2 (25 mL, 0.01 M) at 23 °C was added solid supported catalyst $NaHSO_4$•SiO_2[32] (2.63 g, stored in the oven for >48 h and added while hot) in one portion. The reaction mixture was then stirred for 6 h at 23 °C. The mixture was then filtered through a plug of silica gel with 7:2:1 MeCN:H_2O:sat. aq. KNO_3 (100 mL). The eluate was concentrated under reduced pressure before being crashed out with sat. aq. KPF_6 (100 mL) and transferred to a separatory funnel with CH_2Cl_2 (100 mL). The layers were separated and the aqueous layer was extracted with CH_2Cl_2 (2 x 100 mL). The combined organic layers were then concentrated under reduced pressure to afford the intermediate silyl alcohol as a red solid.

The intermediate silyl alcohol was then dissolved in CH_2Cl_2 (25 mL, 0.01 M) and while stirring at 23 °C, DMAP (89.3 mg, 0.731 mmol, 3.0 equiv) and Comins' reagent (144 mg, 0.366 mmol, 1.5 equiv) were added sequentially, each in single portions. After stirring at 23 °C for 30 min, the reaction was concentrated under reduced pressure and then loaded onto a silica plug. The silica plug was washed with EtOAc (200 mL) before being eluted with 7:2:1

MeCN:H_2O:sat. aq. KNO_3 (100 mL). The red eluate was then concentrated under reduced pressure and transferred with CH_2Cl_2 (100 mL) to a separatory funnel containing 2 M aq. HCl (100 mL). The layers were separated and the organic layer was washed with 2 M aq. HCl (2 x 40 mL). The combined aqueous layers were then back-extracted with CH_2Cl_2 (2 x 100 mL). The organic layers were then combined, dried over Na_2SO_4, and concentrated under reduced pressure. The residue was then filtered over a pad of neutral alumina (200 mL CH_3CN eluent) and concentrated under reduced pressure before being dried on hi-vac at 100 °C for 1 h to afford silyl triflate **4.36** as a red solid (204 mg, 73% yield). **Silyl triflate 4.36**: ^{1}H NMR (500 MHz, CD_3CN): δ 9.29 (d, *J* = 8.6, 1H), 9.11 (d, *J* = 8.5, 1H), 9.02 (s, 1H), 8.69 (s, 1H), 8.53 (d, *J* = 8.2, 2H), 8.49 (d, *J* = 8.2, 2H), 8.13–8.08 (m, 4H), 8.00 (tt, *J* = 7.9, 1.7, 2H), 7.84–7.78 (m, 4H), 7.60 (t, *J* = 5.3, 2H), 7.45 (t, *J* = 6.8, 2H), 7.22 (qt, *J* = 6.6, 1.3, 2H), 0.55 (s, 9H).



4.36 *4.40*

Furan 4.40. To a stirred solution of silyl triflate **4.36** (11.2 mg, 9.71 µmol, 1.0 equiv) and 2,5-dimethylfuran (**4.39**, 10.5 µL, 97.1 µmol, 10.0 equiv) at 23 °C was added CsF (7.4 mg, 48.5 µmol, 5.0 equiv) in one portion. After stirring at 23 °C for 1 h, the reaction was filtered through a plug of celite with CH_3CN (10 mL) and then concentrated under reduced pressure. The crude residue was then adsorbed onto SiO_2 and purified by flash chromatography (100% EtOAc → 14:1:1 MeCN:H_2O:sat. aq. KNO_3). To the concentrated aqueous mixture was added saturated aqueous KPF_6 (100 mL) to precipitate the desired product, and the resultant mixture was

transferred to a separatory funnel with CH_2Cl_2 (50 mL). The layers were separated and the aqueous layer was extracted with CH_2Cl_2 (2 x 50 mL). The combined organic layers were then concentrated under reduced pressure. Further purification by preparative TLC (14:1:1 MeCN:H_2O:sat. aq. KNO_3) afforded furan **4.40** as a red solid (8.0 mg, 80% yield). **Furan 4.40**: ^{1}H NMR (500 MHz, CD_3CN): δ 9.23 (dt, *J* = 8.6, 1.3, 2H), 8.59 (d, *J* = 1.5, 2H), 8.52 (dd, *J* = 8.3, 0.8, 2H, 8.49 (ddt, *J* = 8.3, 3.1, 1.1, 2H), 8.09 (td, *J* = 7.9, 1.5, 2H), 8.04 (ddd, *J* = 5.2, 4.8, 1.1, 2H), 8.01–7.95 (m, 2H), 7.84–7.81 (m, 2H), 7.76 (dd, *J* = 8.5, 5.2, 2H), 7.57 (ddd, *J* = 11.8, 5.7, 1.6, 2H), 7.44 (ddt, *J* = 7.6, 5.7, 1.3, 2H), 7.19 (dddd, *J* = 13.0, 7.6, 5.7, 1.4, 2H), 6.92 (dd, *J* = 6.9, 5.4, 2H), 2.04 (s, 3H), 2.04 (s, 3H); ^{13}C NMR (125 MHz, CD_3CN, 29 of 32 signals observed): δ 158.1, 157.90, 157.88, 156.2, 152.90, 152.89, 152.8, 152.3, 145.6, 147.41, 147.38, 138.8, 138.62, 138.59, 133.3, 131.3, 128.5, 128.33, 128.32, 127.2, 127.1, 125.2, 125.11, 125.09, 114.9, 114.8, 89.6, 15.53, 15.50.

4.9 Spectra Relevant to Chapter Four:

Aryne-Driven Approach for the Synthesis and Manipulation of Polypyridyl Metal Complexes

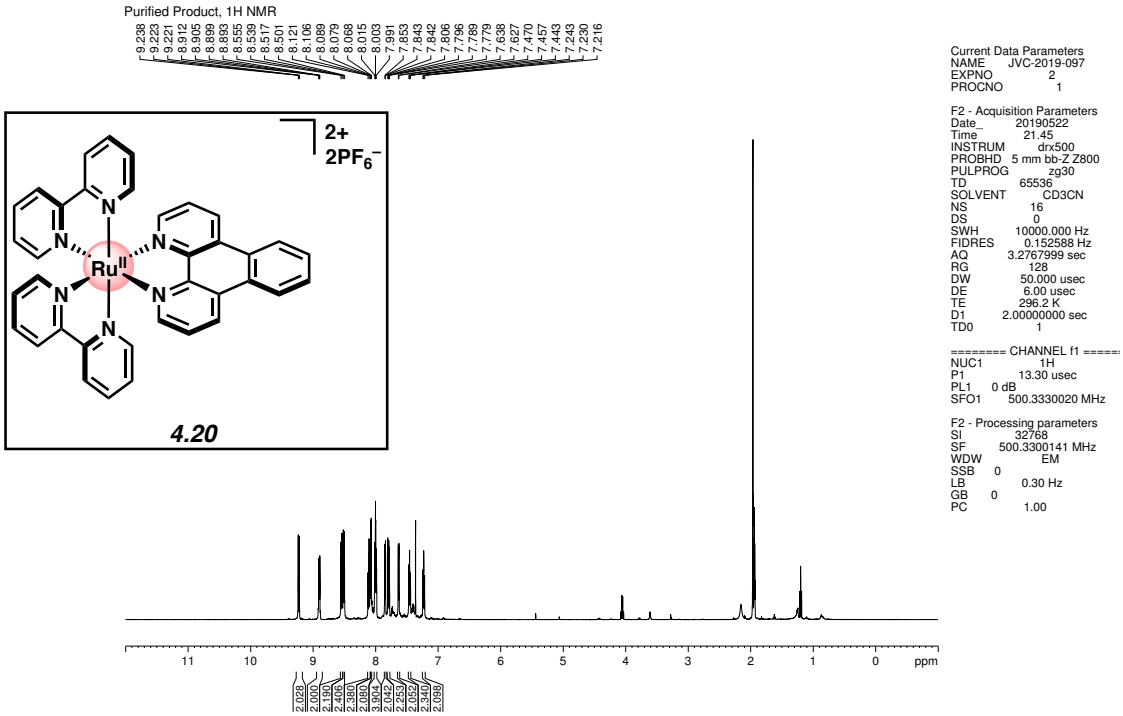


Figure 4.7. ^{1}H NMR (500 MHz, CD_3CN) compound **4.20**

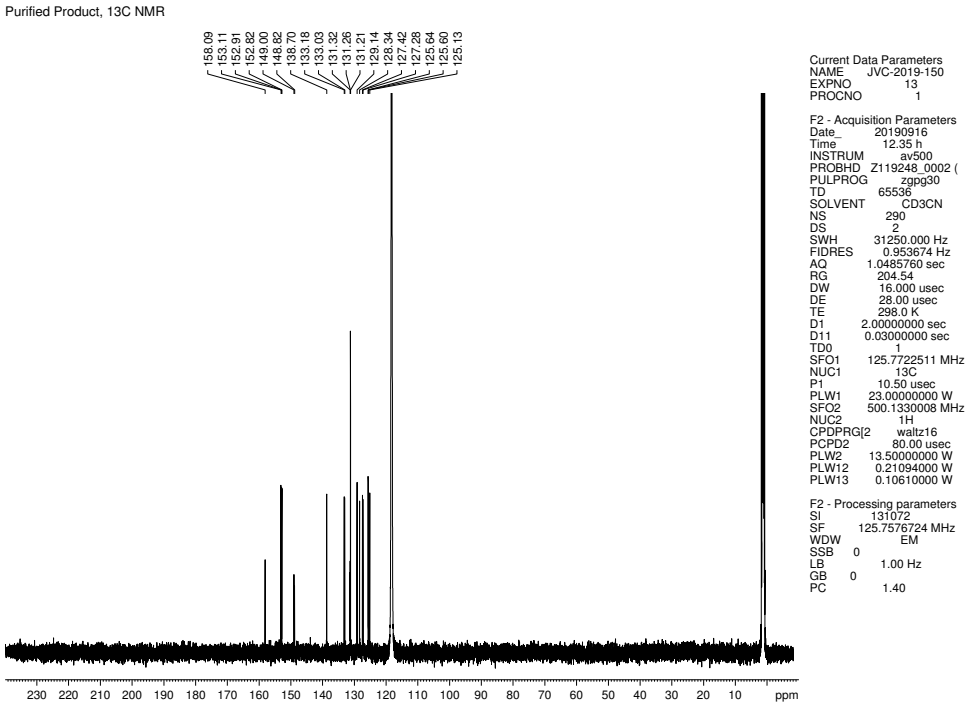


Figure 4.8. ^{13}C NMR (125 MHz, CD_3CN) compound **4.20**

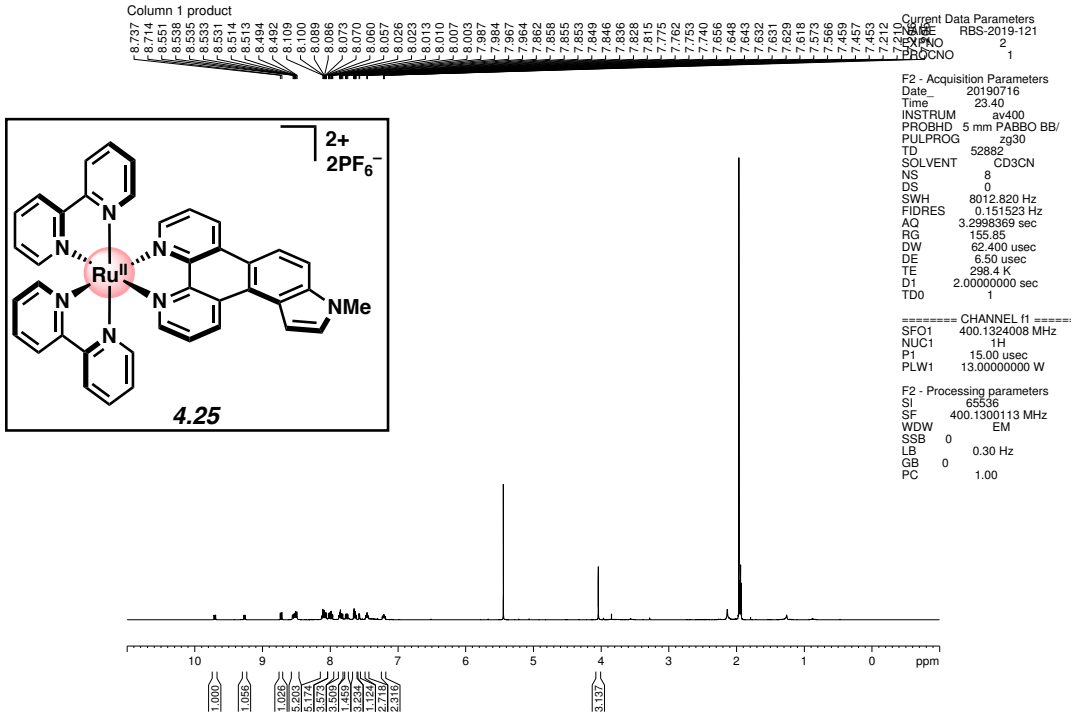


Figure 4.9. ^{1}H NMR (400 MHz, CD_3CN) compound **4.25**

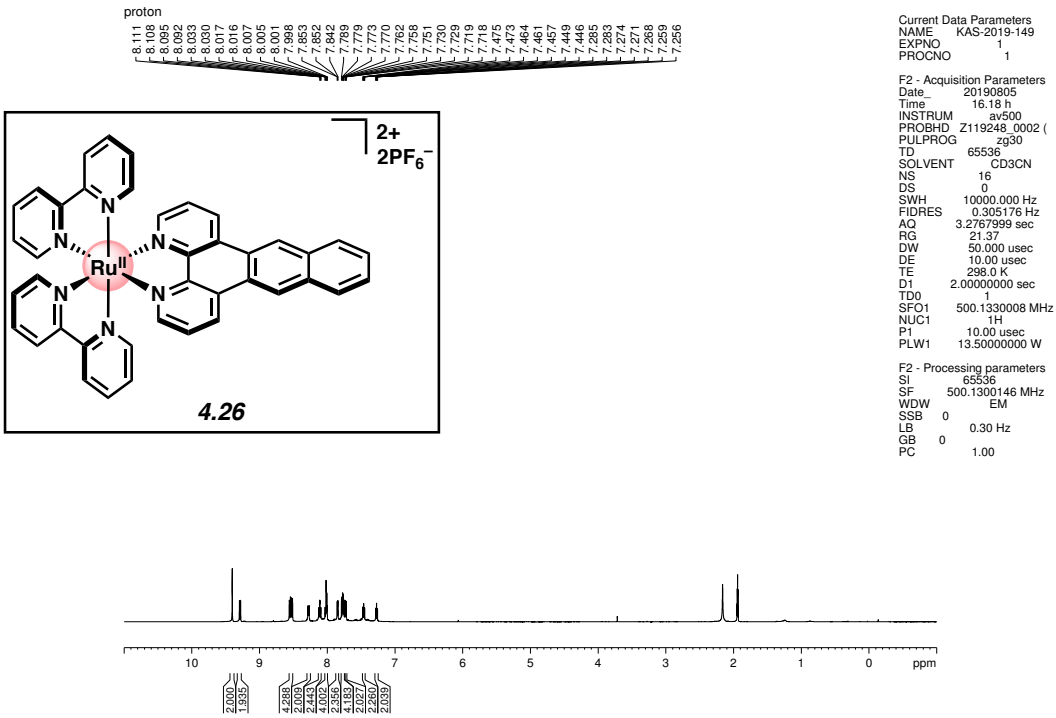


Figure 4.10. ^{1}H NMR (500 MHz, CD_3CN) compound **4.26**

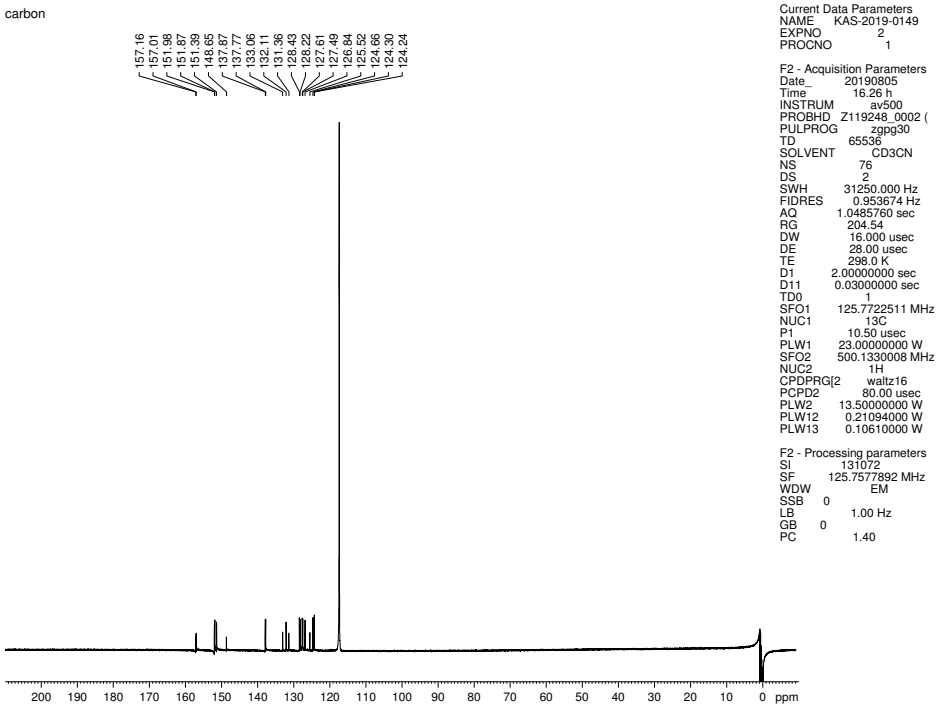


Figure 4.11. ^{13}C NMR (125 MHz, CD_3CN) compound **4.26**

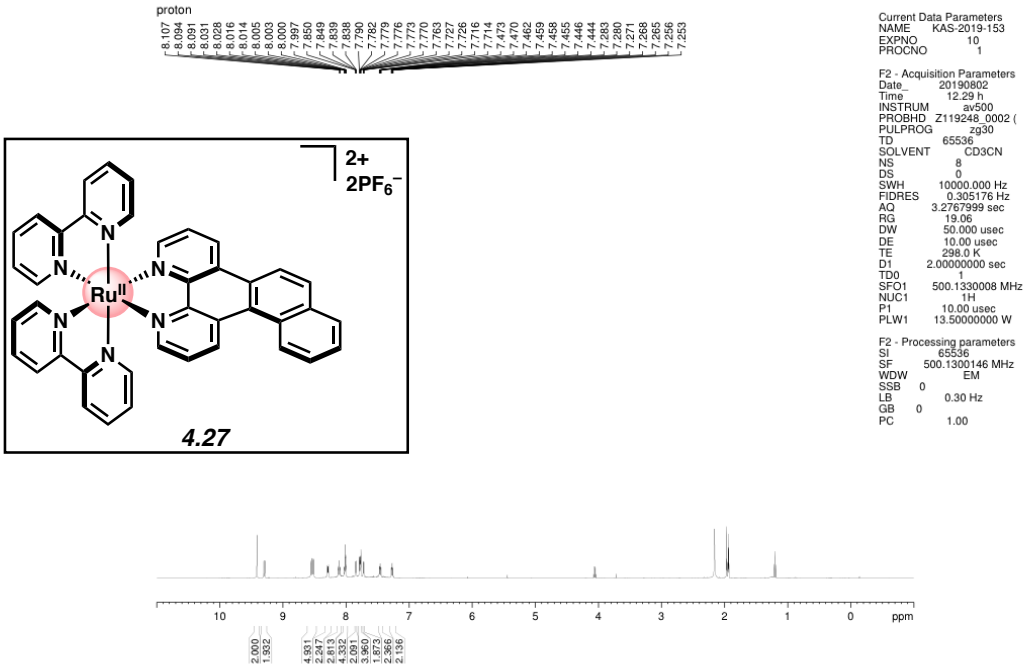


Figure 4.12. ^{1}H NMR (500 MHz, CD_3CN) compound **4.27**

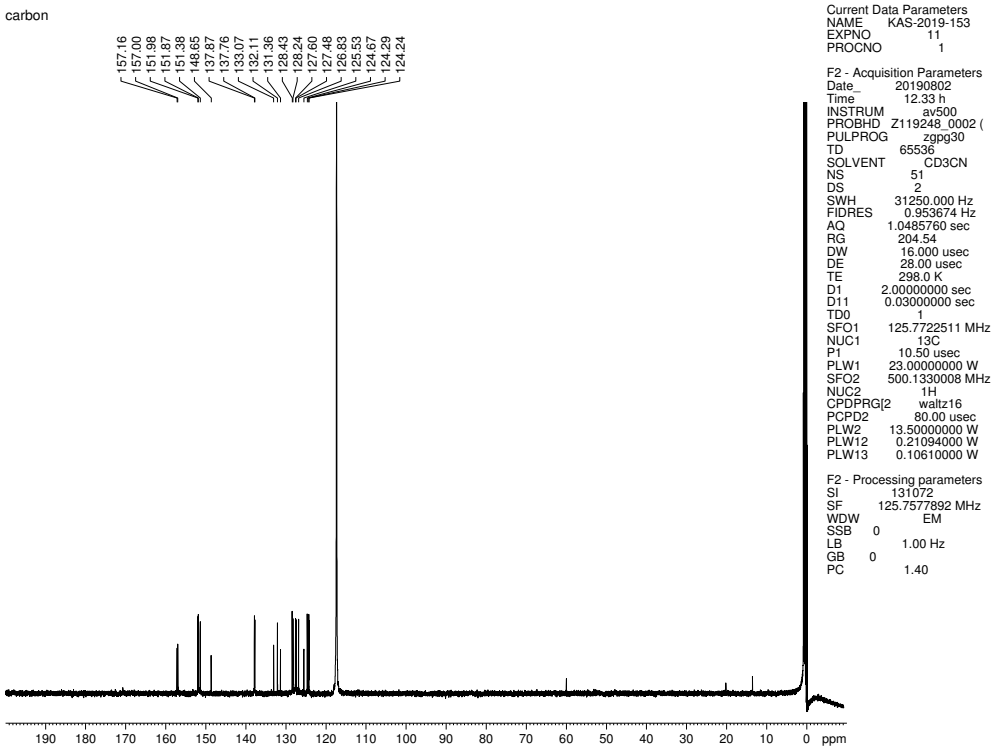


Figure 4.13. ^{13}C NMR (125 MHz, CD_3CN) compound **4.27**

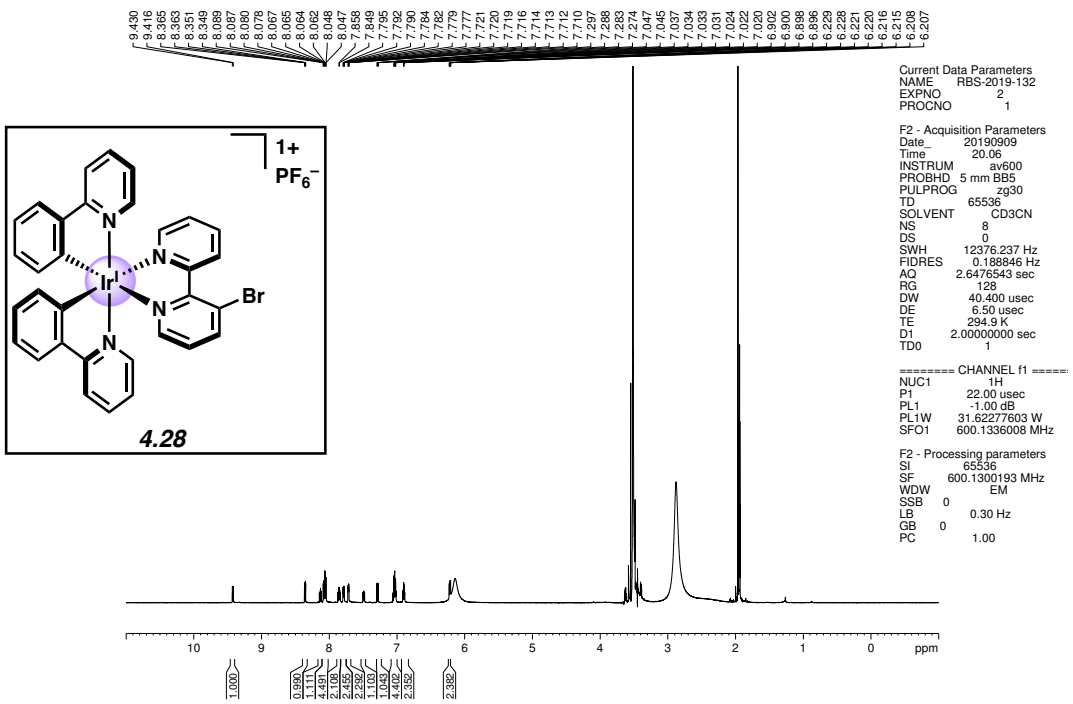


Figure 4.14. ^{1}H NMR (600 MHz, CD_3CN) compound **4.28**

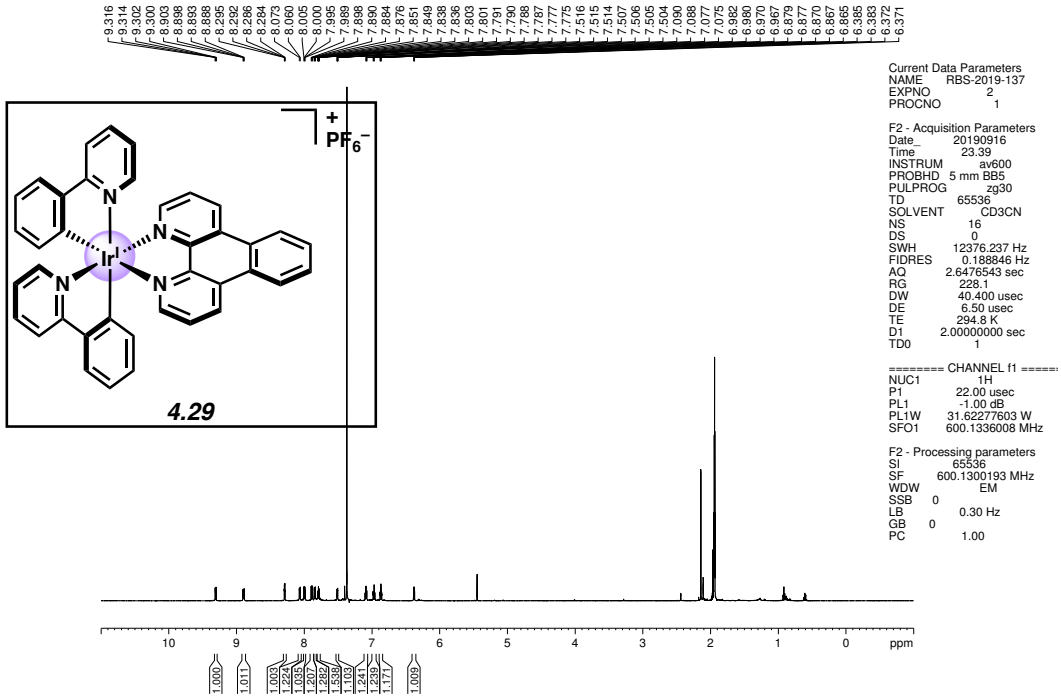


Figure 4.15. ^{1}H NMR (600 MHz, CD_3CN) compound **4.29**

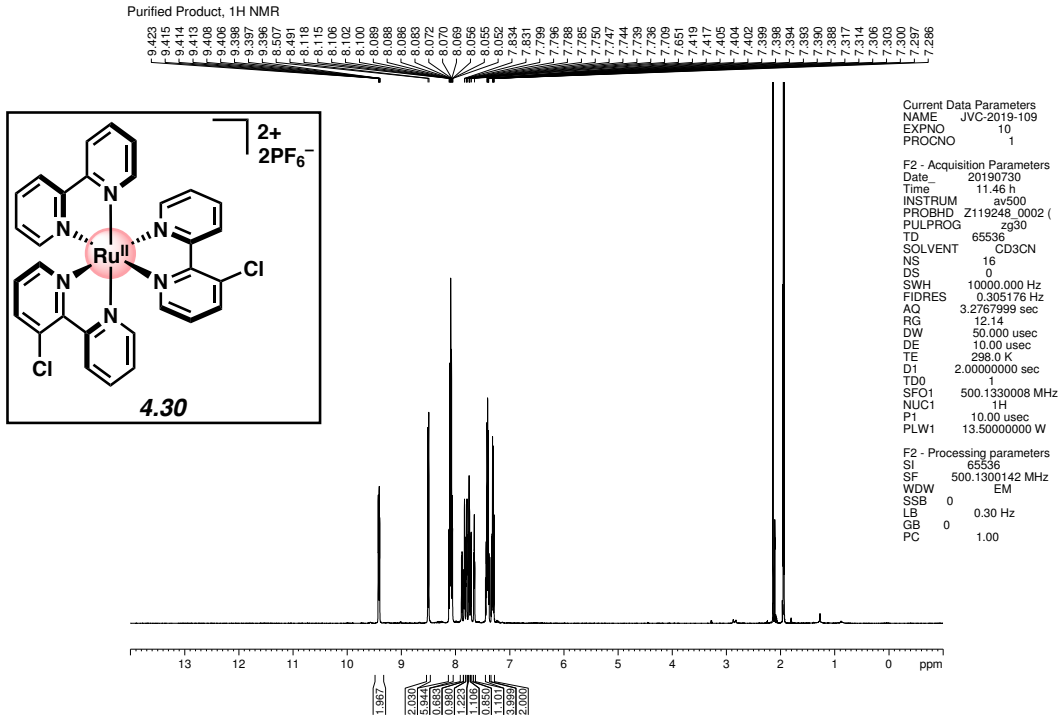


Figure 4.16. ^{1}H NMR (500 MHz, CD_3CN) compound **4.30**

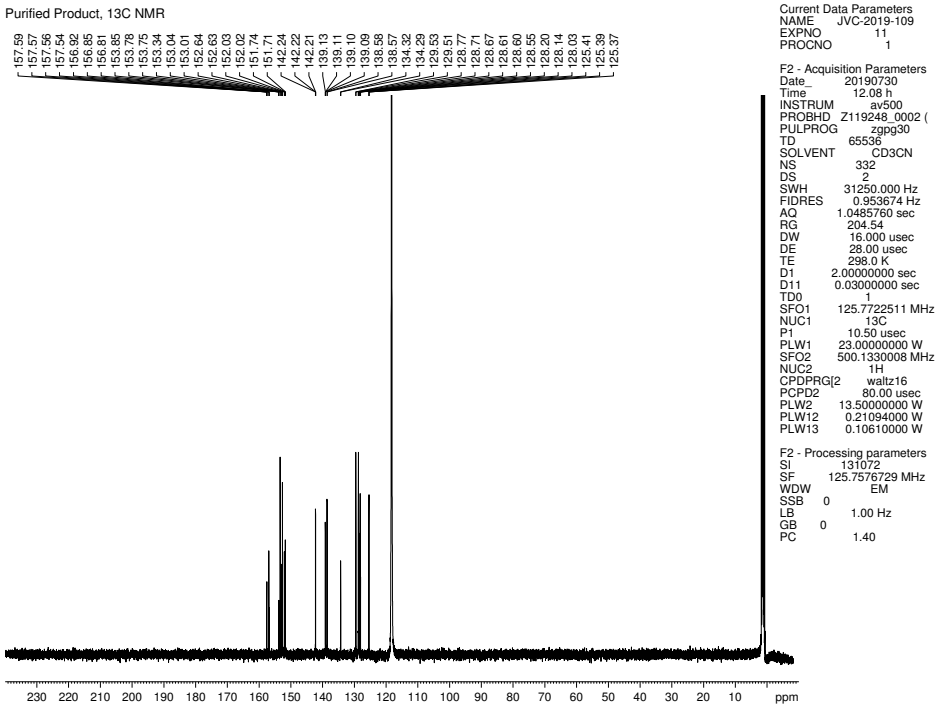


Figure 4.17. ^{13}C NMR (125 MHz, CD_3CN) compound **4.30**

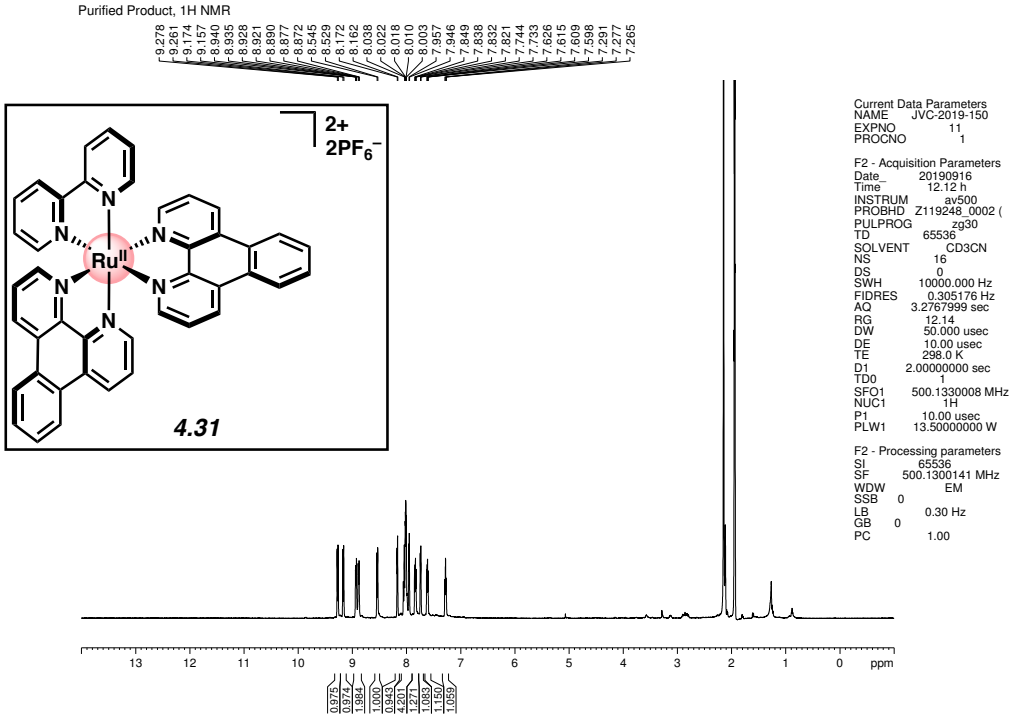


Figure 4.18. ^{1}H NMR (500 MHz, CD_3CN) compound **4.31**

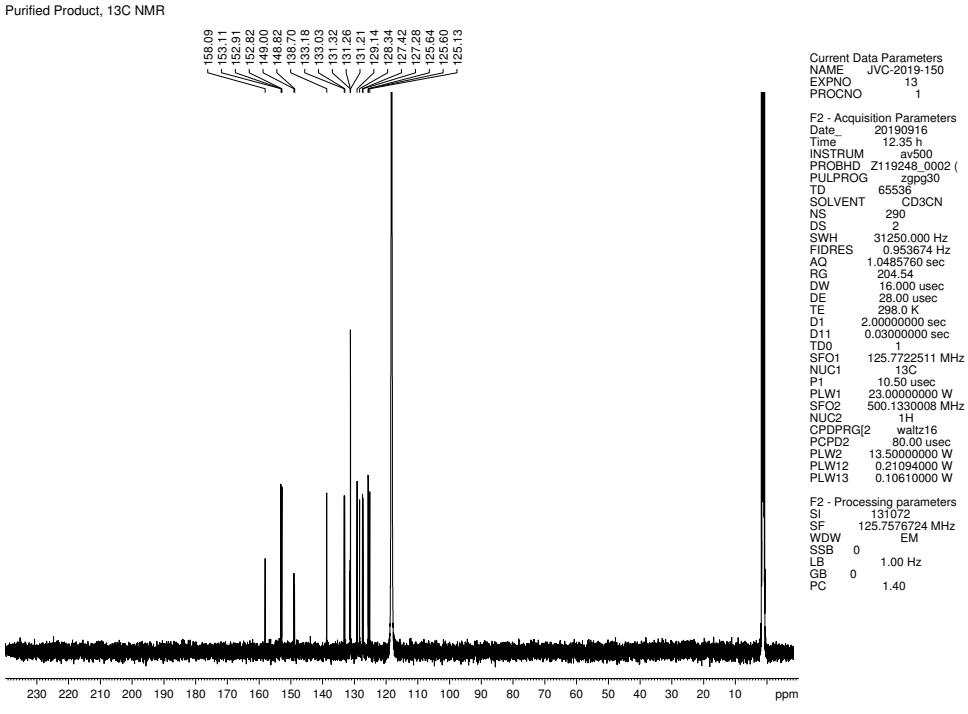


Figure 4.19. ^{13}C NMR (125 MHz, CD_3CN) compound **4.31**

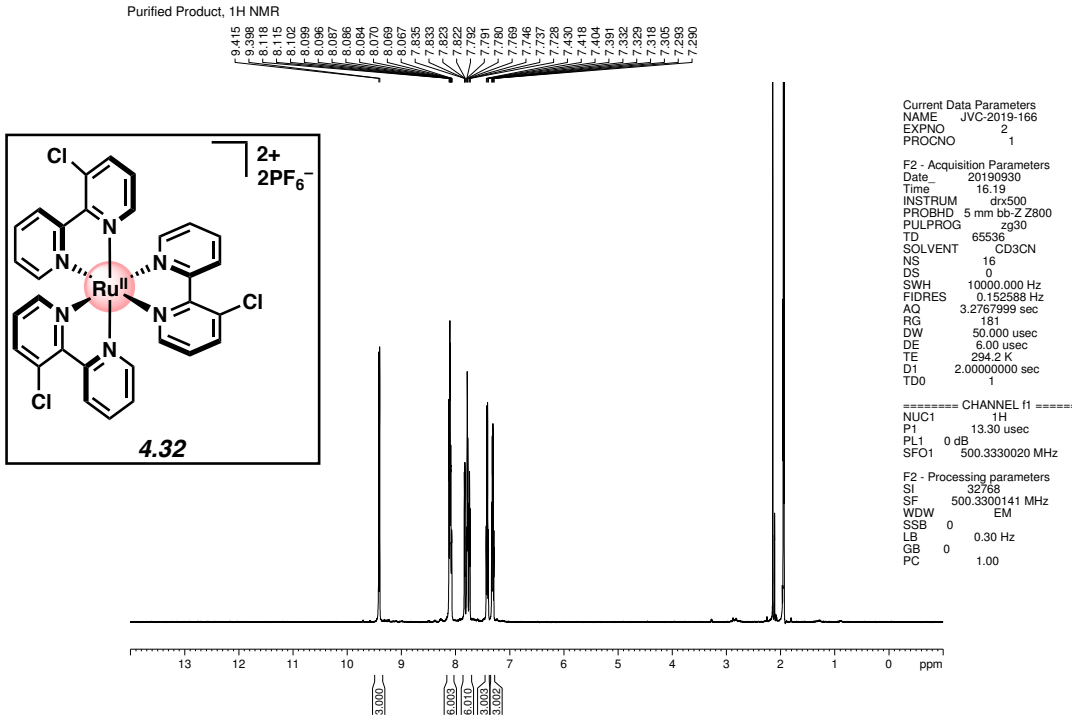


Figure 4.20. ^{1}H NMR (500 MHz, CD_3CN) compound **4.32**

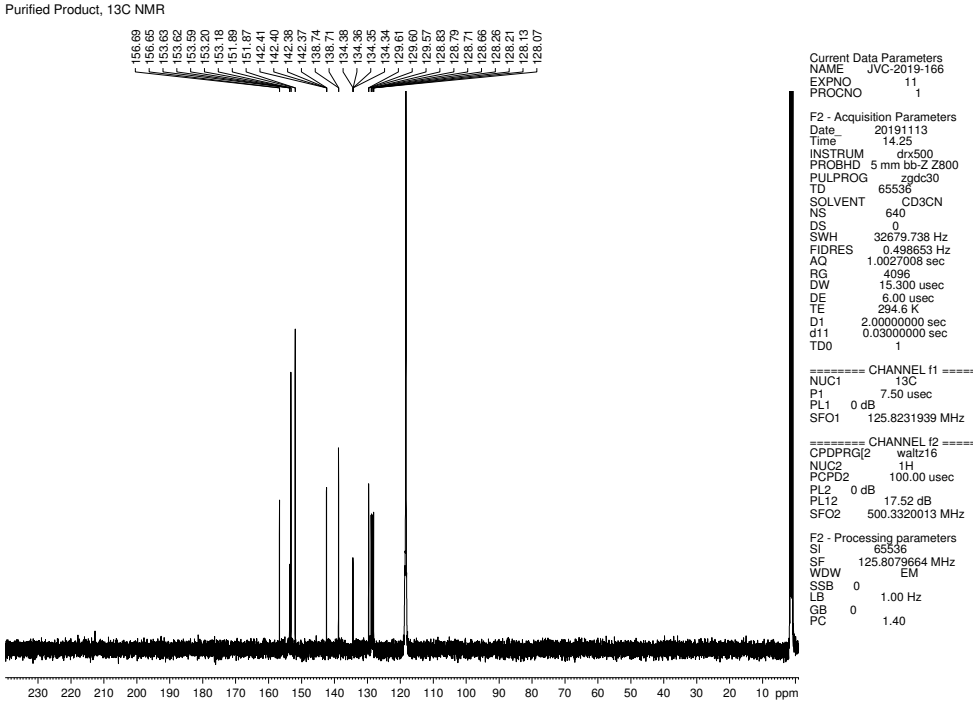


Figure 4.21. ^{13}C NMR (125 MHz, CD_3CN) compound **4.32**

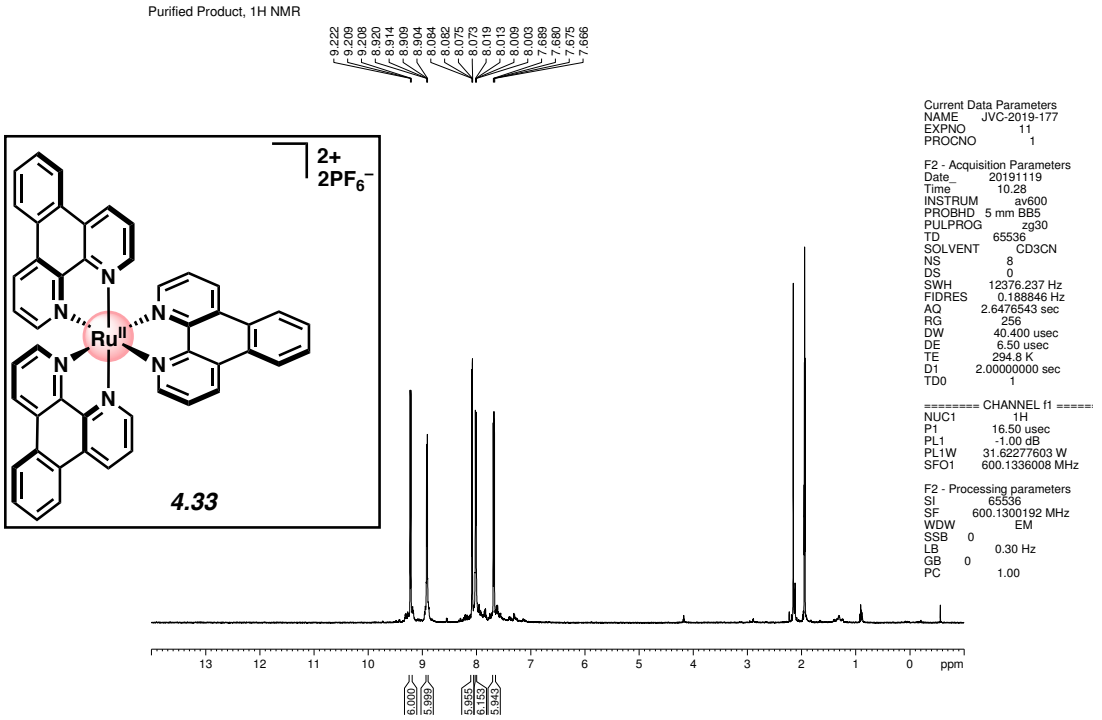


Figure 4.22. ^{1}H NMR (600 MHz, CD_3CN) compound **4.33**

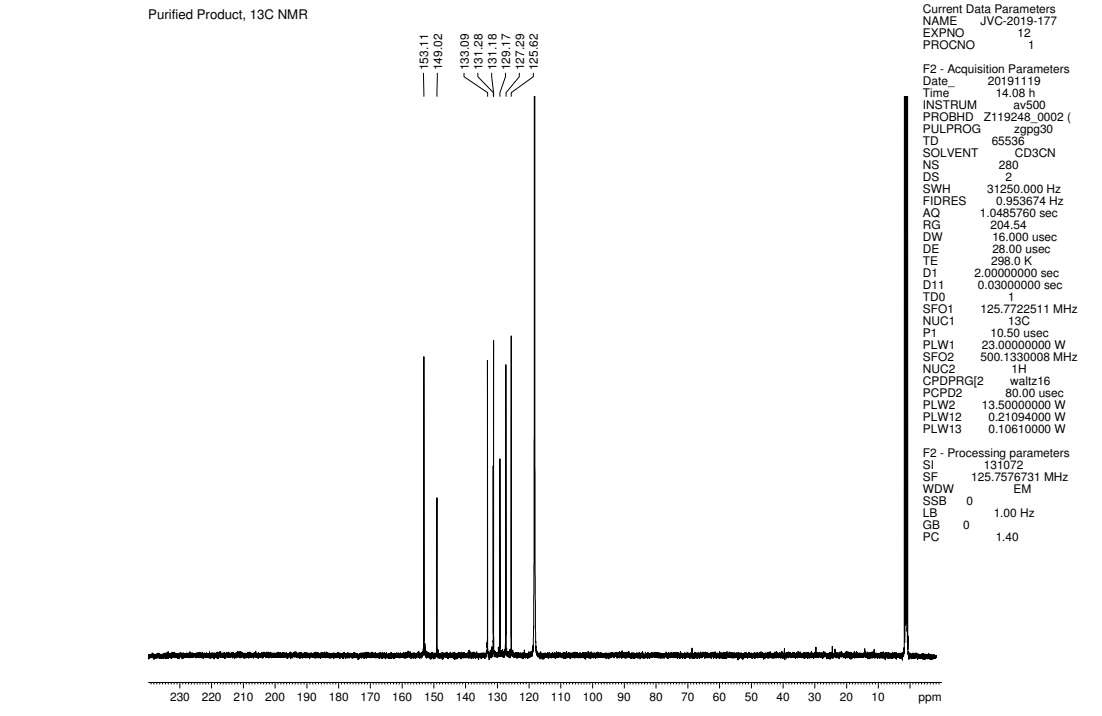


Figure 4.23. ^{13}C NMR (125 MHz, CD_3CN) compound **4.33**

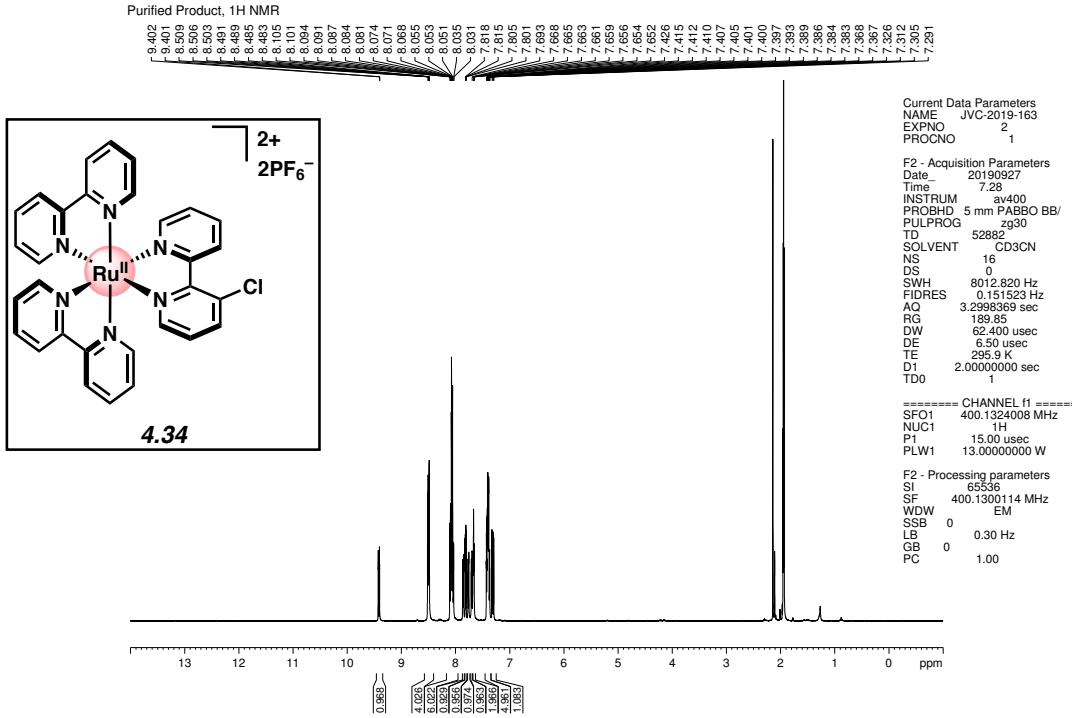


Figure 4.24. ^{1}H NMR (400 MHz, CD_3CN) compound **4.34**

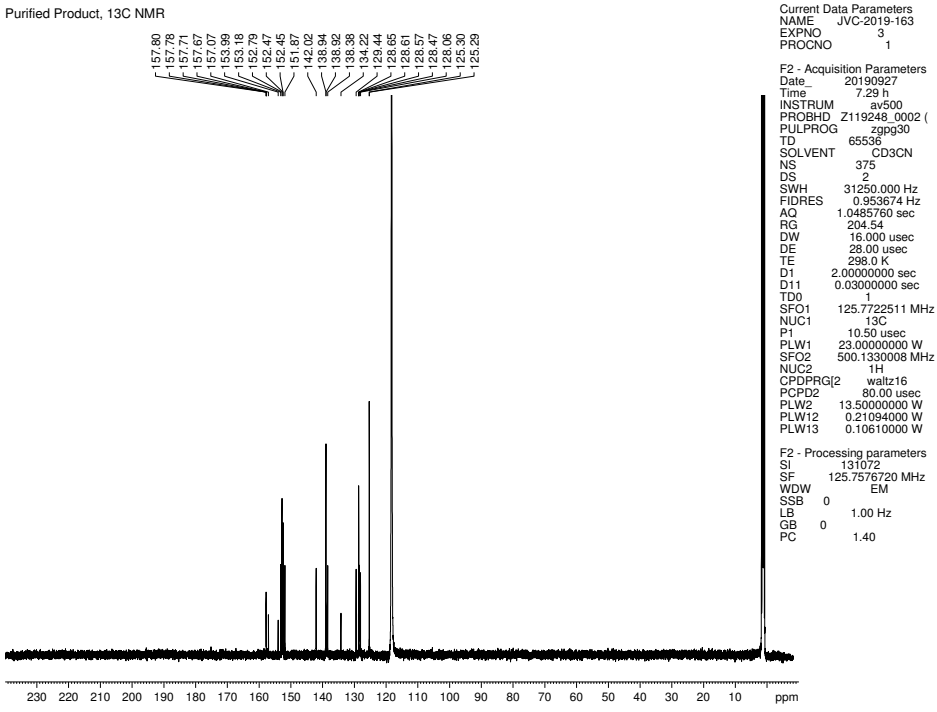


Figure 4.25. ^{13}C NMR (125 MHz, CD_3CN) compound **4.34**

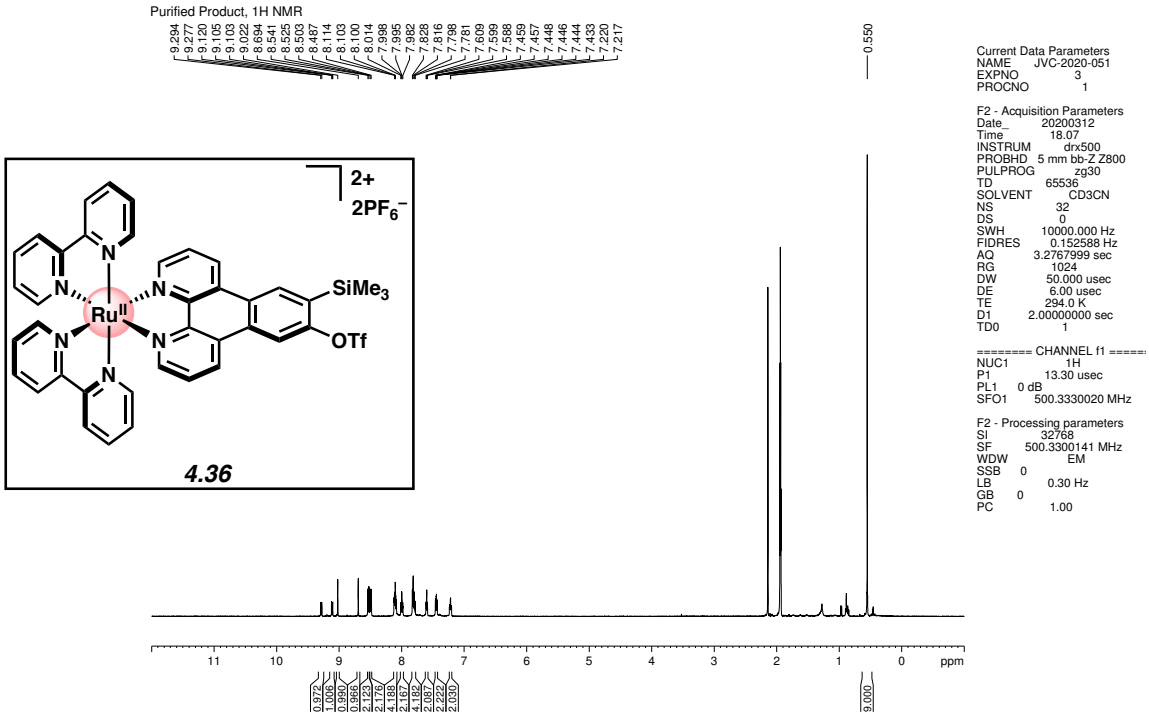


Figure 4.26. ^{1}H NMR (500 MHz, CD_3CN) compound **4.36**

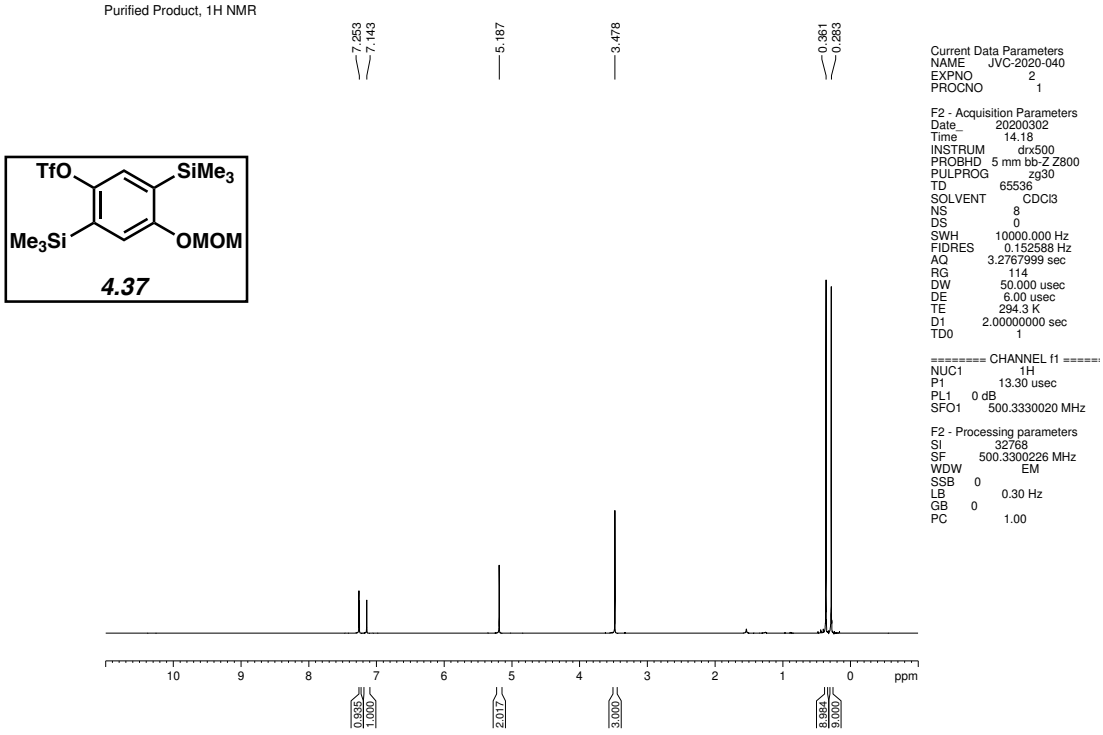


Figure 4.27. ^{1}H NMR (500 MHz, $CDCl_3$) compound **4.37**

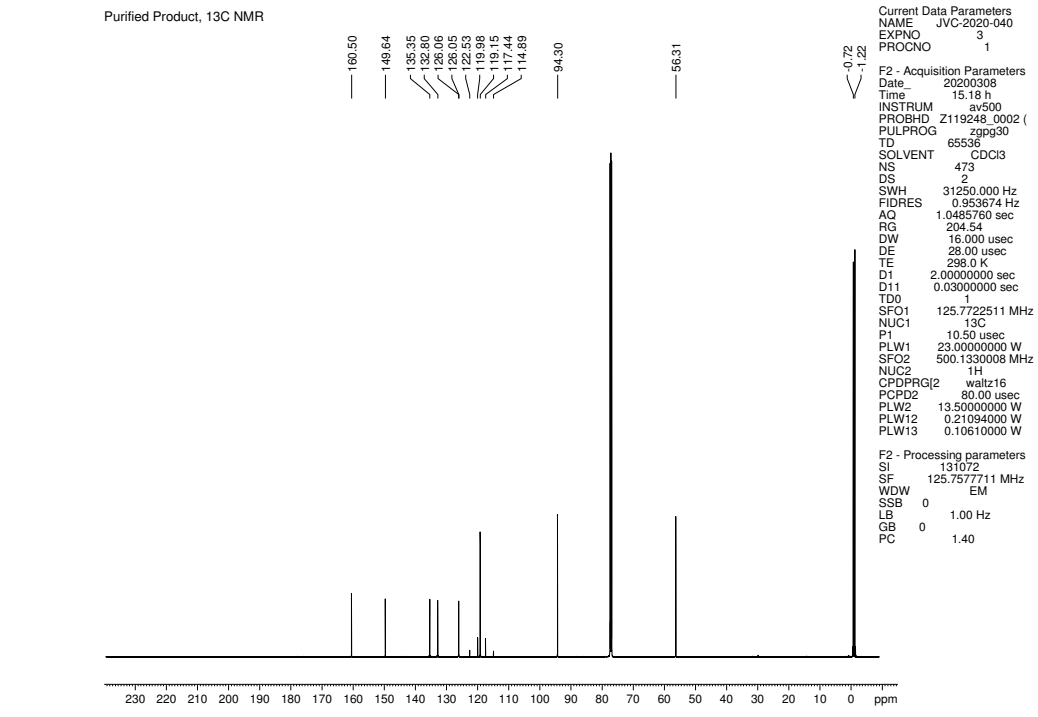


Figure 4.28. ^{13}C NMR (125 MHz, $CDCl_3$) compound **4.37**

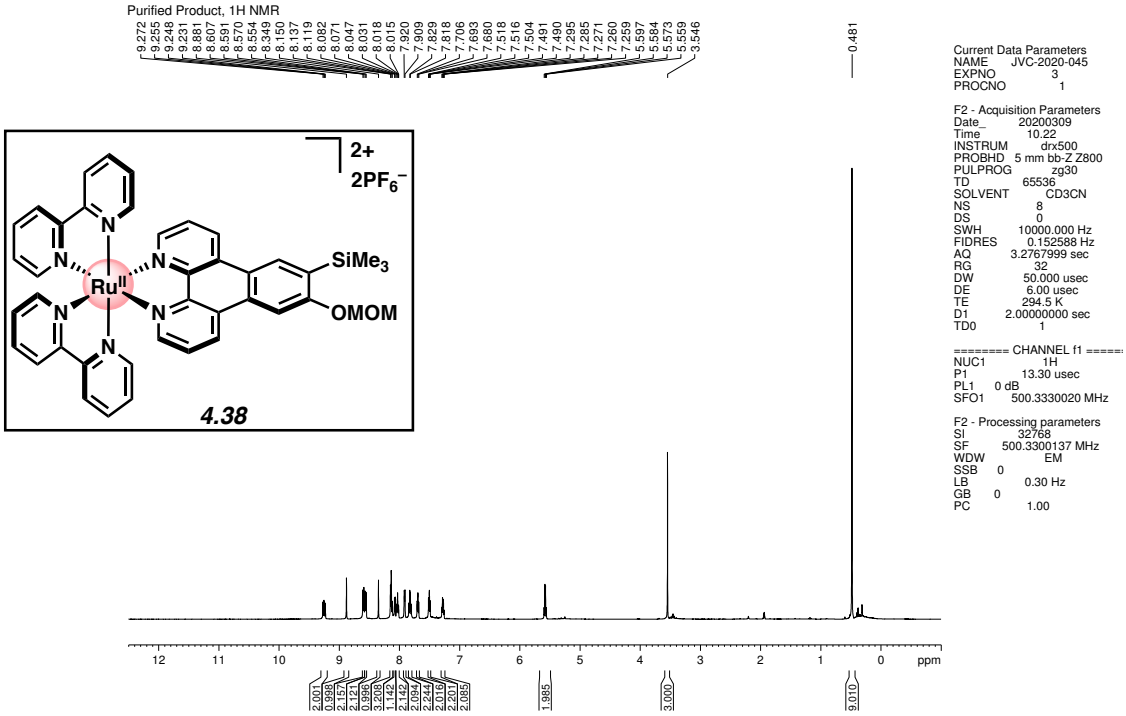


Figure 4.29. ^{1}H NMR (500 MHz, CD_3CN) compound **4.38**

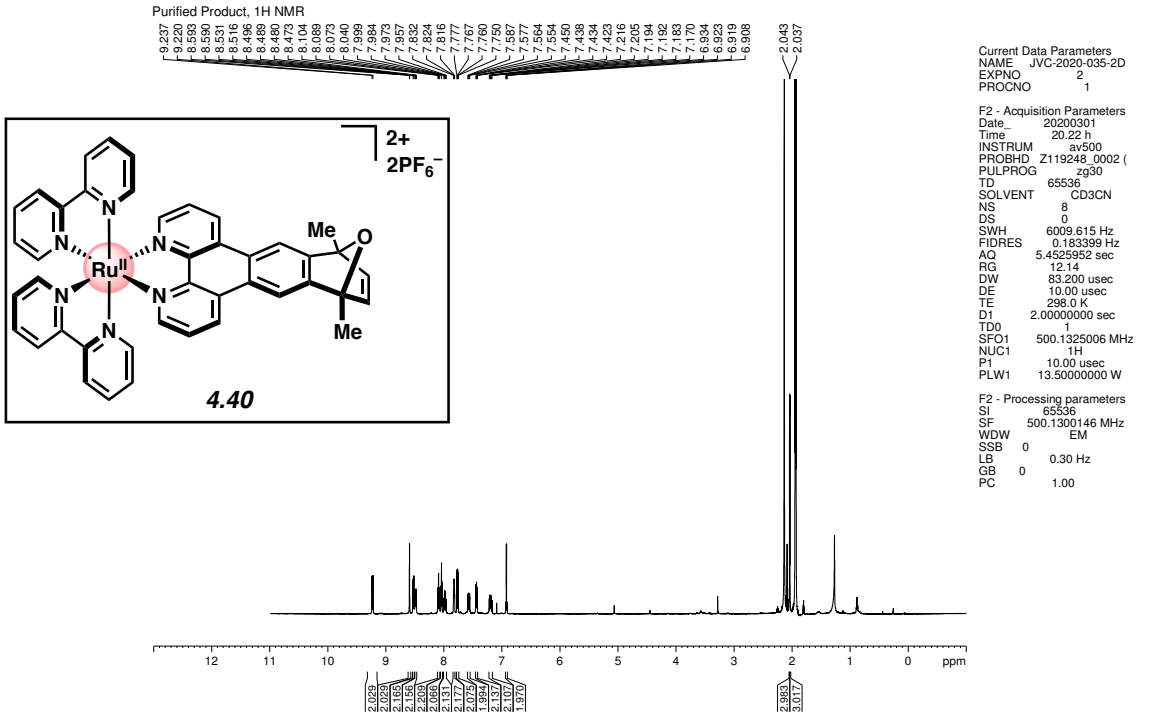


Figure 4.30. ^{1}H NMR (500 MHz, CD_3CN) compound **4.40**

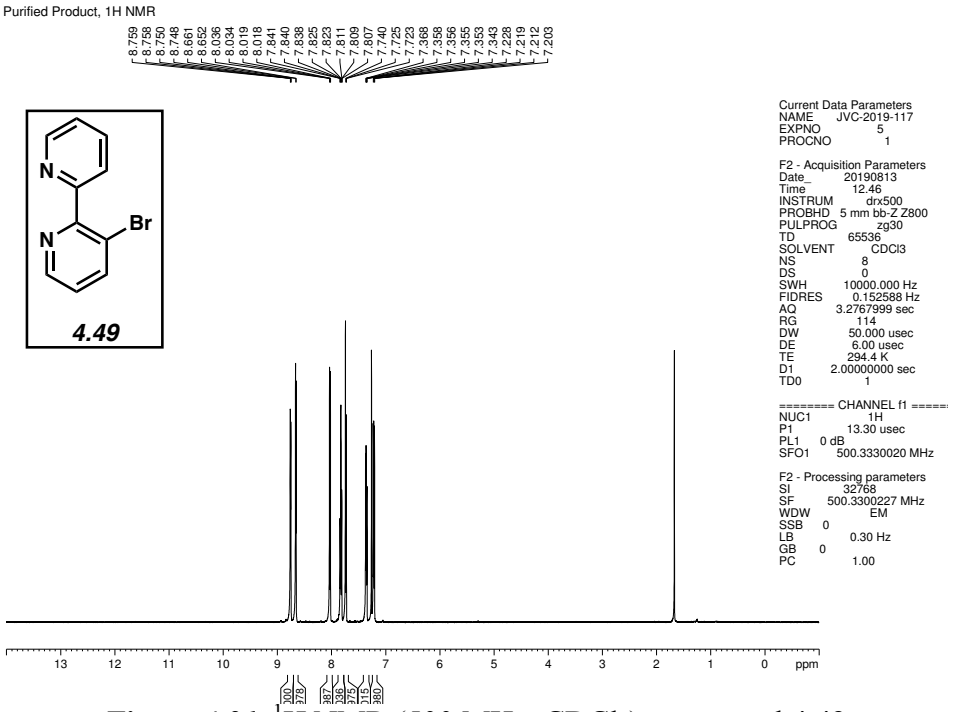


Figure 4.31. ^{1}H NMR (500 MHz, $CDCl_3$) compound **4.49**

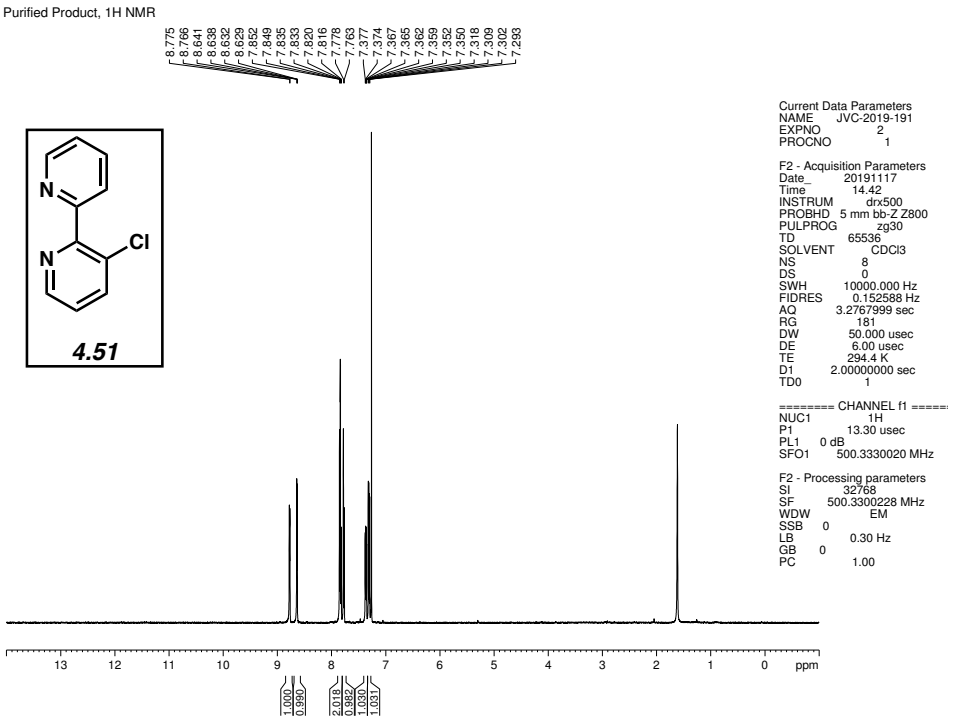


Figure 4.32. ^{1}H NMR (500 MHz, $CDCl_3$) compound **4.51**

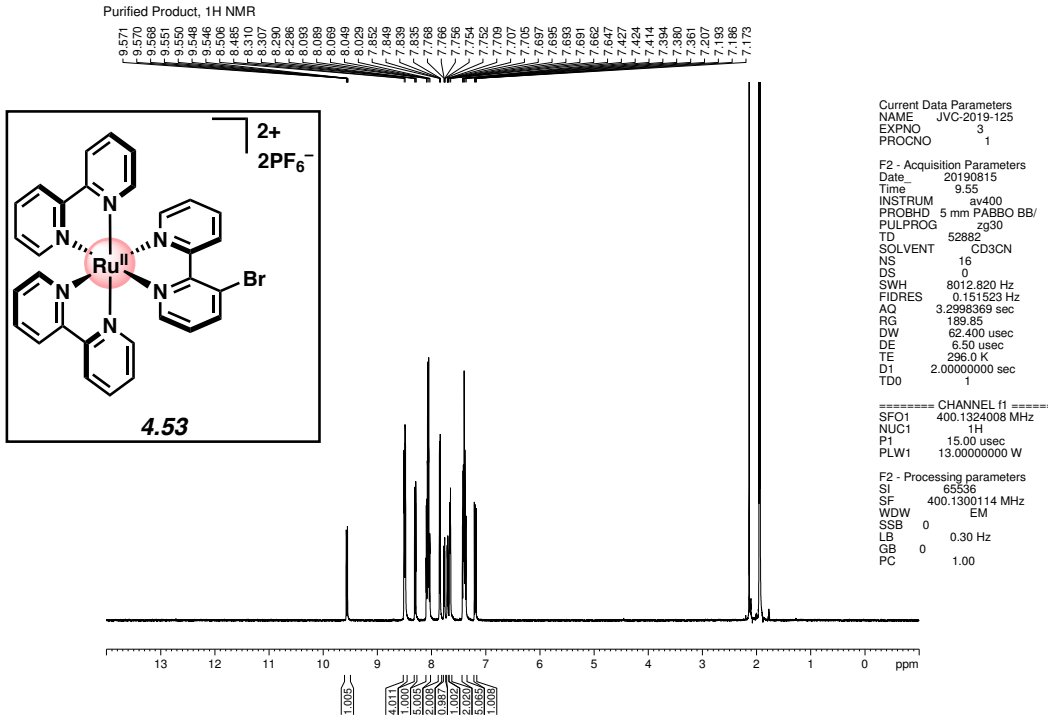


Figure 4.33. ^{1}H NMR (400 MHz, CD_3CN) compound **4.53**

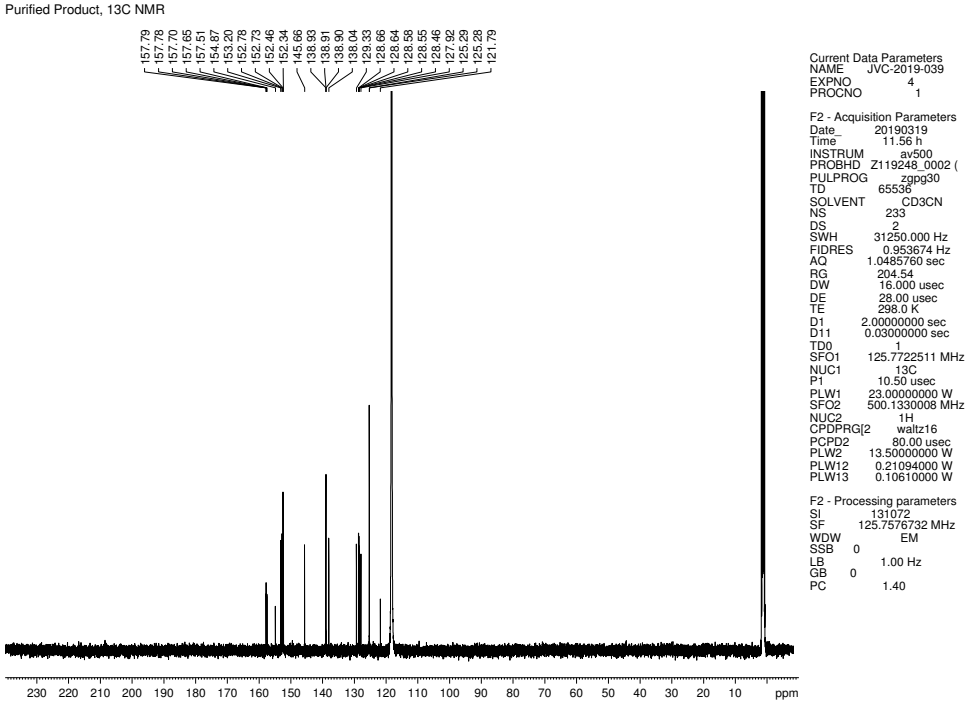


Figure 4.34. ^{13}C NMR (125 MHz, CD_3CN) compound **4.53**

4.10 Notes and References

(1) Burstall, F. H. *J. Chem. Soc.* **1936**, 173–175.

(2) Grätzel, M. *J. Photochem. Photobiol., C* **2003**, *4*, 145−153.

(3) a) Gill, M. R.; Thomas. J. A. *Chem. Soc. Rev.* **2012**, *41*, 3179–3192. b) Zeglis, B.; Pierre, V. C.; Barton, J. K. *Chem. Commun.* **2007**, 4565–4579. c) Song, H.; Kaiser, J. T.; Barton, J. K. *Nat. Chem.* **2012**, *4*, 615–620.

(4) Keefe, M. H.; Benkstein, K. D.; Hupp, J. T. *Coord. Chem. Rev.* **2000**, *205*, 201−228.

(5) Monro, S.; Colón, K. L.; Yin, H.; Roque, J., III.; Konda, P.; Gujar, S.; Thummel, R. P.; Lilge, L.; Cameron, C. G.; McFarland, S. A. *Chem. Rev.* **2019**, *119*, 797–828.

(6) Friedman, A. E.; Chambron, J. C.; Sauvage, J. P.; Turro, N. J.; Barton, J. K. *J. Am. Chem. Soc.* **1990**, *112*, 4960–4962.

(7) Geri, J. B.; Oakley, J. V.; Reyes-Robles, T.; Wang, T.; McCarver, S. J.; White, C. H.; Rodriguez-Rivera, F. P.; Parker, D. L., Jr.; Hett, E. C.; Fadeyi, O. O.; Oslund, R. C.; MacMillan, D. W. C. *Science* **2020**, 367, 1091–1097.

(8) Reichardt, C.; Monro, S.; Sobotta, F. H.; Colón, K. L.; Sainuddin, T.; Stephenson, M.; Sampson, E.; Roque, J., III.; Yin, H.; Brendel, J. C.; Cameron, C. G.; McFarland, S.; Dietzek, B. *Inorg. Chem.* **2019**, *58*, 3156−3166.

(9) Toupin, N. P.; Nadella, S.; Steinke, S. J.; Turro, C.; Kodanko, J. J. *Inorg. Chem.* **2020**, *59*, 3919–3933.

(10) Mede, T.; Jäger, M.; Schubert, U. S. *Chem. Soc. Rev.* **2018**, *47*, 7577–7627.

(11) Zucker, S. P.; Wossidlo, F.; Weber, M.; Lentz, D.; Tzschucke, C. C. *J. Org. Chem.* **2017**, *82*, 5616–5635.

(12) a) Soulis, K.; Gourlaouen, C.; Daniel, C.; Quatela, A.; Odobel, F.; Blart, E.; Pellegrin, Y. *Polyhedron* **2018**, *140*, 42–50. b) Bolger, J.; Gourdon, A.; Ishow, E.; Launay, J.-P. *J. Chem. Soc., Chem. Commun.* **1995**, 1799–1800.

(13) a) Karlsson, E. A.; Lee, B.-L.; Liao, R.-Z.; Åkermark, T.; Kärkäs, M. D.; Becerril, V. S.; Siegbahn, P. E. M.; Zhou, X.; Abrahamsson, M. *ChemPlusChem*, **2014**, *79*, 936–950. b) Herrero, C.; Quaranta, A.; Fallahpour, R.-A.; Leibl, W.; Aukauloo, A. *J. Phys. Chem. C* **2013**, *117*, 9605–9612. c) Karnahl, M.; Tschierlei, S.; Kuhnt, C.; Dietzek, B.; Schmitt, M.; Popp, J.; Schwalbe, M.; Krieck, S.; Görls, H.; Heinemann, F. W.; Rau, S. *Dalton Trans.* **2010**, *39*, 2359–2370. d) Huber, F. L.; Nauroozi, D.; Mengele, A. K.; Rau, S. *Eur. J. Inorg. Chem.* **2017**, 4020–4027.

(14) Goetz, A. E.; Garg, N. K. *J. Org. Chem.* **2014**, *79*, 846–851.

(15) a) Surry, D. S.; Buchwald, S. L. *Angew. Chem., Int. Ed.* **2008**, 47, 6338−6361. b) Mauger, C. C.; Mignani, G. A. *Org. Process Res. Dev.* **2004**, *8*, 1065−1071.

(16) Schleth, F.; Vettiger, T.; Rommel, M.; Tobler, H. WO2011131544 A1, 2011.

(17) Tadross, P. M.; Stoltz, B. M. *Chem. Rev.* **2012**, *112*, 3550–3577.

(18) Wang, B.; Mu, B.; Chen, D.; Xu, S.; Zhou, X. *Organometallics* **2004**, *23*, 6225–6230.

(19) Luo, S; Zhao, X.; Mu, B.; Song, H.; Zu, S.; Wang, B. *Organometallics* **2009**, *28*, 4602–4605.

(20) a) Liu, Z.; Zhang, X.; Larock, R. C. *J. Am. Chem. Soc.* **2005**, *127*, 15716–15717. b) Liu, Z.; Larock, R. C. *J. Org. Chem.* **2007**, *72*, 223–232.

(21) For a prior report of dehalogenation in $Ru(bpy)_3$ derivatives, see: Iranmanesh, H.; Arachchige, K. S. A.; Bhadbade, M.; Donald, W. A.; Liew, J. Y.; Liu, K. T.-C.; Luis, E. T.;

Moore, E. G.; Price, J. R.; Yan, H.; Yang, J.; Beves, J. E. *Inorg. Chem.* **2016**, *55*, 12737−12751.

(22) Hofstraat, J. W.; Reinhoudt, D. N.; Steemers, F. J.; Van der Tol, E. B.; Verboom, W.; Verhoeven, J. W. EP1019401 A1, 1998.

(23) Lu, W.; Vicic, D. A.; Barton, J. K. *Inorg. Chem.* **2005**, *44*, 7970–7980.

(24) a) Colombo, M. G.; Hauser, A.; Guedel, H. U. *Inorg. Chem.* **1993**, *32*, 3088–3092. b) Wang, C.; deKrafft, K. E.; Lin, W. *J. Am. Chem. Soc.* **2012**, *134*, 7211–7214. c) Bolink, H. J.; Coronado, E.; Costa, R. D.; Ortí, E.; Sessolo, M.; Graber, S.; Doyle, K.; Neuberger, M.; Housecroft, C. E.; Constable, E. C. *Adv. Mater.* **2008**, *20*, 3910–3913.

(25) For reviews of arynes, see: a) Nakamura, Y.; Yoshida, S.; Hosoya, T. *Heterocycles* **2019**, *98*, 1623–1677. (b) Pellissier, H.; Santelli, M. *Tetrahedron* **2003**, *59*, 701–730. (c) Wenk, H. H.; Winkler, M.; Sander, W. *Angew. Chem., Int. Ed.* **2003**, *42*, 502–528. (d) Sanz, R. *Org. Prep. Proced. Int.* **2008**, *40*, 215–291. (e) Gampe, C. M.; Carreira, E. M. *Angew. Chem., Int. Ed.* **2012**, *51*, 3766–3778. (f) Bhunia, A.; Yetra, S. R.; Biju, A. T. *Chem. Soc. Rev.* **2012**, *41*, 3140–3152. (g) Yoshida, H.; Takaki, K. *Synlett* **2012**, 1725–1732. (h) Dubrovskiy, A. V.; Markina, N. A.; Larock, R. C. *Org. Biomol. Chem.* **2013**, *11*, 191–218. (i) Wu, C.; Shi, F. *Asian J. Org. Chem.* **2013**, *2*, 116–125. (j) Hoffmann, R. W.; Suzuki, K. *Angew. Chem., Int. Ed.* **2013**, *52*, 2655–2656.

(26) Duong, H. M.; Bendikov, M.; Steiger, D.; Zhang, Q.; Sonmez, G.; Yamada, J.; Wudl, F. *Org. Lett.* **2003**, *5*, 4433–4436.

(27) Suzuki, S.; Itami, K.; Yamaguchi, J. *Angew. Chem., Int. Ed.* **2017**, *56*, 15010–15013.

(28) Young, M. C.; Liew, E.; Ashby, J.; McCoy, K. E.; Hooley, R. J. *Chem. Commun.* **2013**, *49*, 6331–6333.

(29) Zucker, S. P.; Wossidlo, F.; Weber, M.; Lentz, D.; Tzschucke, C. C. *J. Org. Chem.* **2017**, *82*, 5616–5635.

(30) Cheong, P. H.-Y.; Paton, R. S.; Bronner, S. M.; Im, G.-Y. J.; Garg, N, K.; Houk, K. N. *J. Am. Chem. Soc.* **2010**, *132*, 1267–1269.

(31) Suzuki, S.; Itami, K.; Yamaguchi, J. *Angew. Chem., Int. Ed.* **2017**, *56*, 15010–15013.

(32) Breton, G. W. *J. Org. Chem.* **1997**, *62*, 8952–8954.

CHAPTER FIVE

Heterocyclic Aryne Annulations for the π-Extension of Donor Ligands in Two-Coordinate Metal Complexes

5.1 Abstract

Organic light emitting diodes (OLEDs) are crucial for high-performance displays and solid-state lighting applications. Recently, linear two-coordinate metal complexes have been identified as promising dopants with high photoluminescence efficiency and short-lived excited states, whose properties are controlled by the choice of donor and acceptor ligands. Herein, we report a modular platform that leverages a novel carbazolyne precursor to access *N*-containing donor ligands bearing extended π-conjugation. Subsequent photophysical characterization of two-coordinate metal complexes bearing π-extended donors identify a new thermally-activated delayed fluorescence dopant that displays up to 80% photoluminescence efficiency.

5.2 Introduction

Efficient and stable organic light emitting diodes (OLEDs) are crucial for high-performance display technologies and solid-state lighting applications.[1] Despite decades of research in both industry and academia, fundamental discoveries continue to improve the emissive properties and tunability of organometallic phosphors.[2] One recent advancement is the development of thermally-activated delayed fluorescence (TADF) complexes of the general structure donor(carbazole)–M–acceptor(carbene), where M is Cu(I), Ag(I), or Au(I) (**5.1** and **5.2**, Figure 5.1A).[3] The promise of these compounds is evident in their high photoluminescence

efficiencies (up to 100% in both solution and in the solid state), short-lived excited states ($\tau < 1$ μs), as well as an economic advantage over conventional phosphor dopants that rely on precious metals (e.g., Ir and Pt).[4]

The photophysical properties of these TADF complexes can be manipulated by altering both the donor and acceptor ligands.[3c,5] However, a majority of ligand studies have focused on the influence of *N*-heterocyclic carbene (NHC) acceptors, whereas manipulation of the carbazole donor remains limited. Previous donor studies, as summarized in Figure 5.1B, have focused on electronic modification using electron-donating or withdrawing groups (**5.3**), steric hindrance (**5.4**), and structural flexibility (**5.5**), leading to important structure-property relationships.[3b] Extending the conjugation of related systems has also been shown to effect relative HOMO and LUMO energy levels, thereby altering emission color.[6] However, the effect of π-extension on the photophysical properties of donor(carbazole)–M–acceptor(carbene) complexes has not yet been explored.

In this study, we aim to elucidate the effects of extending the π-conjugation of a carbazole donor ligand in two-coordinate metal complexes **5.6 (**Figure 5.1C). We envisioned accessing scaffold **5.6** through a Pd-catalyzed annulation between 2-bromobiphenyl (**5.7**) and 2,3-carbazolyne (**5.8**), followed by coordination with metal–acceptor complex **5.9**. We also demonstrate the versatility of this synthetic platform for the modular synthesis of various *N*-heterocycles with extended conjugation and functional group variability.

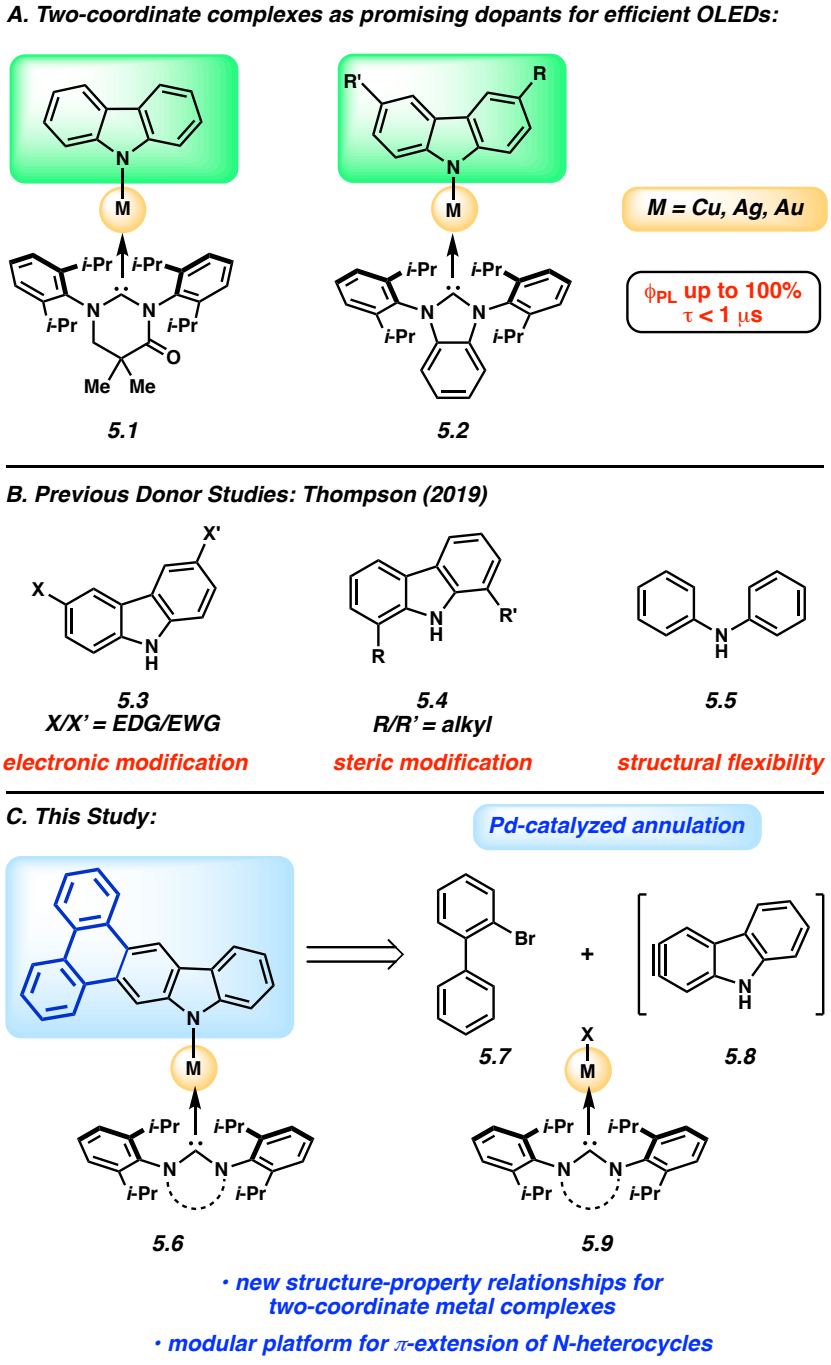


Figure 5.1. (A) Linear two-coordinate metal complexes. (B) Previous donor studies. (C) A modular platform for studying conjugation effects of donors in two-coordinate metal complexes.

5.3 Annulation of Heterocycles

We initiated our synthetic studies by pursuing a Pd-catalyzed annulation reaction of bromobiaryls **5.10** with *N*-Me-4,5-indolyne precursor **5.11** (Figure 5.2). Silyl triflate **5.11**, accessible in only one step from its commercially available N–H derivative, would serve as a model for the corresponding unknown carbazolyne. We were inspired by an analogous annulation strategy previously reported by Larock using benzyne and halobiaryls in the presence of Pd(0),[7] although we found that reaction conditions needed to be modified in order to tolerate our heterocyclic aryne (hetaryne) variant. We determined that 5 mol% $Pd(dba)_2$, a 1:1 ratio of co-solvents, acetonitrile and toluene, and 10 equivalents of cesium fluoride (CsF) were optimal. Presumably, these conditions were ideal for enabling slow generation of the highly reactive hetaryne, such that it can undergo interception of the catalytically-generated Pd intermediates (from **5.10**) without competitive decomposition. Both *N*-Me and *N*-Boc[8] substituted indolynes could be coupled with 2-bromobiphenyl (**5.7**) to give **5.13** and **5.14** in 90% and 61% yields, respectively.[9] Substituted biaryls could also be coupled in good yield, albeit while giving mixtures of regioisomers. For example, methoxy- and nitro-substituted biaryls underwent the annulation smoothly to deliver adducts **5.15** and **5.16** in 62% and 80% yields, respectively. Various heterocycles could also be incorporated into the extended aromatic scaffold, as evidenced by the formation of pyridine **5.17** and pyrrole **5.18** in 76% and 86% yields, respectively. Additionally, fused indole **5.19** could be obtained in 90% yield, as well as indole **5.20** in 57% yield. Not only do these results confirm that hetarynes can be harnessed in annulation reactions with various biaryl substrates, but they also provide a synthetic entryway to electronically and structurally diverse π-extended *N*-heterocycles, which could be of interest in the study of polycyclic aromatic hydrocarbon (PAH)-based materials.

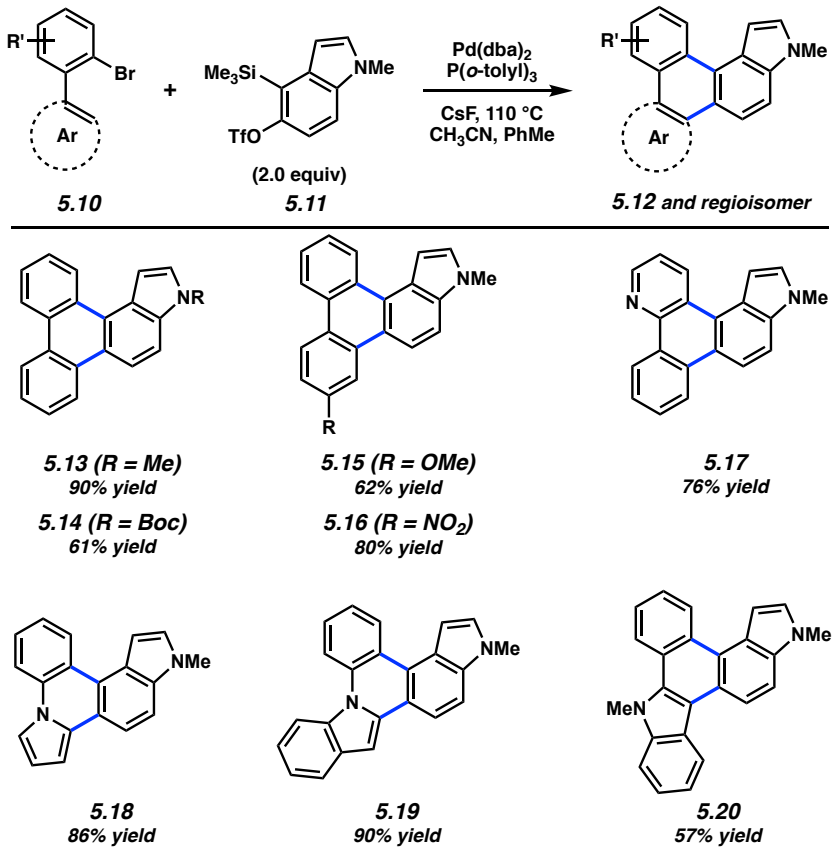
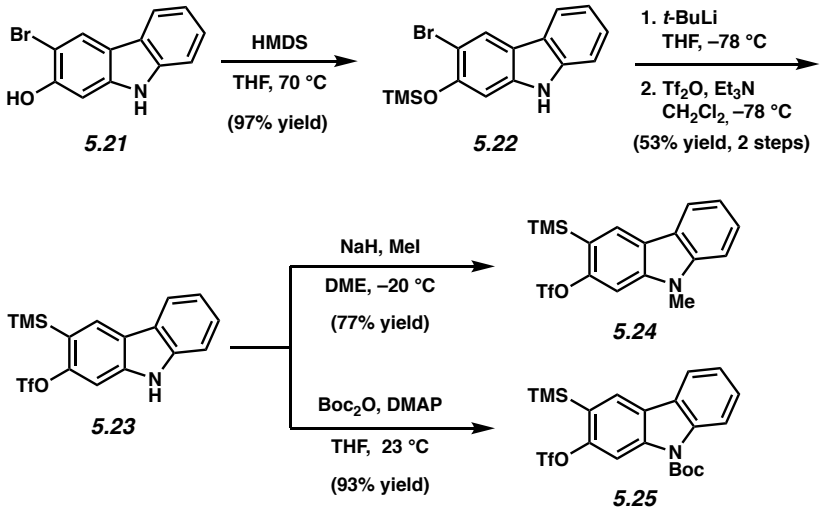


Figure 5.2. Scope of biaryl annulation partners. 5 mol% $Pd(dba)_2$ and P(*o*-tolyl)$_3$ loadings. Yields for **5.15**–**5.20** reflect isolated yields of a mixture of regioisomers (~1–1.5:1; see section 5.8.2 for details).

5.4 Carbazolyne Silyl Triflate Precursor Synthesis

Having validated the use of indolynes in the Pd-catalyzed annulation with halobiaryls, we sought to access a novel carbazolyne silyl triflate precursor that would enable a modular synthesis of carbazole-based donor ligands for two-coordinate metal complexes. Several routes were pursued, ultimately leading to the concise approach shown in Scheme 5.1. Starting from known 3-bromo-2-hydroxycarbazole (**5.21**),[10] treatment with HMDS at elevated temperature afforded silyl ether **5.22** in 97% yield, which was carried forward in a two-step retro-Brook

rearrangement/triflation sequence to afford silyl triflate **5.23** in 53% yield. During our initial annulation studies using indolynes, we observed diminished yields with hetaryne precursors bearing a free N–H, so we opted to protect carbazole **5.23** prior to the annulation. Protection was achieved either through methylation using iodomethane to afford *N*-Me-carbazolyne precursor **5.24** in 77% yield or via Boc-protection using Boc_2O to provide *N*-Boc-carbazolyne precursor **5.25** in 93% yield.



Scheme 5.1. Synthesis of carbazolyne silyl triflate precursors.

5.5 Pd-Catalyzed Carbazolyne Annulations

With suitable carbazolyne precursors in hand, we validated the annulation of 2,3-carbazolyne under our previously optimized conditions (Figure 5.3). 2-Bromobiphenyl (**5.7**) and *N*-Me-carbazolyne precursor **5.24** were coupled in 86% yield to afford π-extended carbazole **5.26**. We also prepared N–H carbazole adduct **5.27** via the union of **5.7** and *N*-Boc carbazolyne precursor **5.25** for subsequent coordination to metal–NHC complexes. The Boc group was cleaved to a minor extent over the course of the annulation reaction. However, extending the

reaction time did not achieve adequate conversion to the free N–H product. Therefore, the annulation was followed by treatment with trifluoroacetic acid (TFA) in dichloromethane to generate the desired π-extended carbazole **5.27** in 65% yield over two steps.

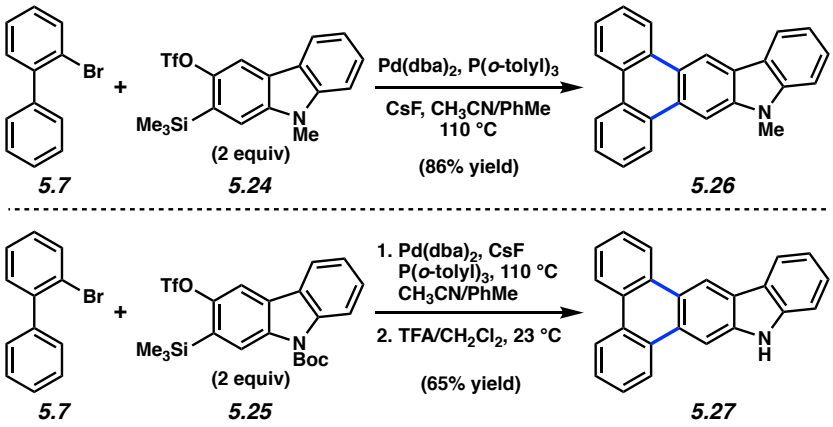


Figure 5.3. Annulation with *N*-substituted carbazolynes.

5.6 Two-Coordinate Metal Complex Synthesis and Photophysical Characterization

With a robust route to the π-extended carbazole ligand, we turned to the synthesis of two-coordinate metal complexes bearing extended π-conjugation (Figure 5.4). We selected known MAC–Au–Cl **5.28**[5] (MAC=1,3-bis(2,6-diisopropylphenyl)-5,5-dimethyl-4-keto-tetrahydropyridylidene) and BZI–Au–Cl **5.30**[11] (BZI=1,3-bis(2,6-diisopropylphenyl)-1-H-benzo[d]imidazole-2-ylidene) complexes as preliminary targets, given the stability of similar Au complexes and the relative acceptor strengths of the BZI and MAC ligands. Treatment of carbazole **5.27** with sodium *tert*-butoxide in the presence of NHC halide complexes **5.28** or **5.30** afforded donor–Au–acceptor complexes **5.29** and **5.31** in 78% and 68% yields, respectively.

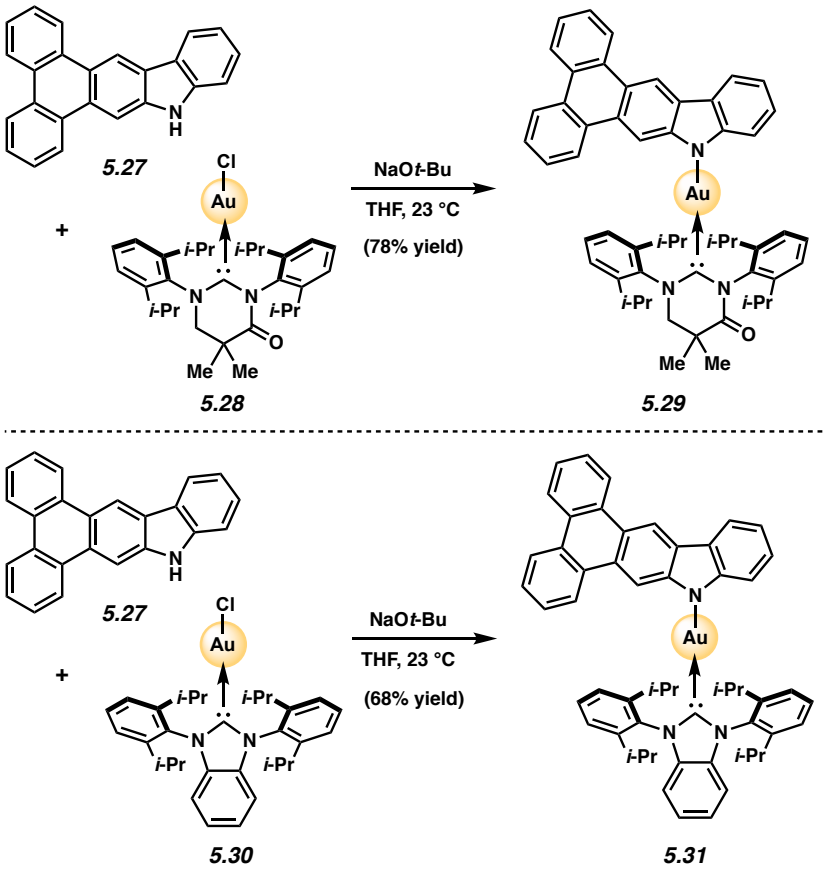


Figure 5.4. Synthesis of novel two-coordinate organometallic complexes.

The photophysical properties of π-extended complexes **5.29** and **5.31** were evaluated in different media and compared to previously studied carbazole-containing complexes **5.32** and **5.33** (Figure 5.5). The absorbance spectra of π-extended carbazole–Au–MAC complex **5.29** (Figure 5.5A) display a solvent-independent, high-energy band at 318 nm, which is attributed to a π-π* transition localized on the carbazole ligand. In addition, the spectra display a broad, negative solvatochromic shift from MeCy (460 nm) to MeTHF (417 nm), which is likely due to inter-ligand charge transfer (ICT) between the π-extended carbazole donor and MAC acceptor ligands. ICT is required to enable efficient TADF emission, and further evidence for ICT in **5.29** is borne out in its emission spectra (Figure 5.5C). Compared to known carbazole–Au–MAC

complex **5.32**,[3c] which undergoes rapid ICT, **5.29** displays a similar emission profile at 298 K, albeit red shifted as a result of the extended conjugation. It is also noteworthy that the emission is red shifted when moving from polar (MeTHF) to non-polar (MeCy and polystyrene film[12]) media. Such solvatochromic behavior is a consequence of dipole moment interactions between the solvent and the complex, in which the dipole of the excited state is larger and opposite relative to the ground state. Emission at 77 K (500 nm) is structured and polarity-independent. In this case, solvent molecules are frozen as a glass around the complex, thus restricting stabilization of the excited charge transfer triplet. Therefore, the triplet state localized on the donor becomes the lowest-lying emissive state and precludes ICT. Notably, **5.29** achieved 80% photoluminescence efficiency in MeTHF (see Table 5.1 for tabulated measurements of complexes **5.29** and **5.32**).

The absorption and emission spectra of π-extended carbazole–Au–BZI complex **5.31** indicate that ICT does not occur between the donor and acceptor ligands. The lower energy bands in the absorption spectra (382 and 416 nm, Figure 5.5A) are more structured and are blue-shifted compared to **5.29**. Unlike the previously studied carbazole–Au–BZI complex **5.33**, the emission spectra of **5.31** are structured and polarity-independent regardless of the temperature (Figure 5.5D). This indicates that the excited state transitions are localized on the donor ligand, rather than undergoing ICT. In other words, the π-extended carbazole–Au–BZI complex **5.31** does not undergo desirable charge transfer and thermally activated fluorescence (TADF), but rather conventional phosphorescence. Further support for this observation is evident in the poor photoluminescence quantum yield (< 5%) and long excited-state lifetime (k_r = 4.2 x 10^2 s^{-1}, see Table 5.2).

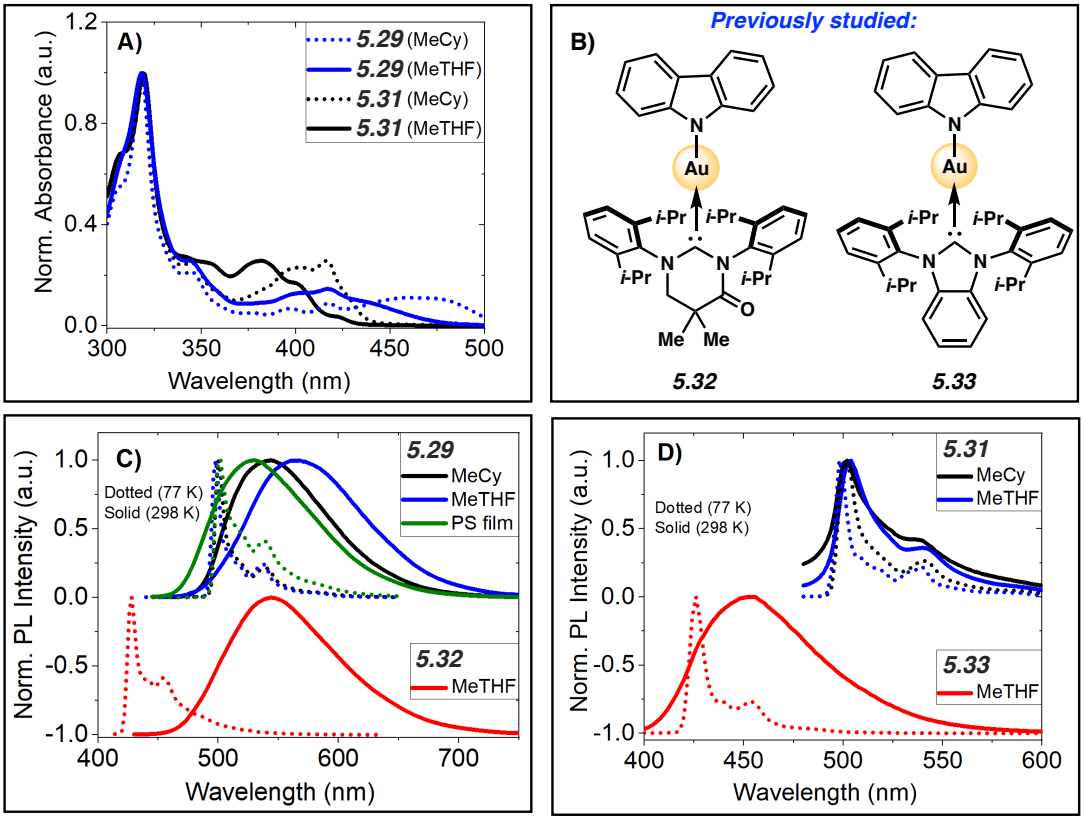


Figure 5.5. A) Absorbance spectra in methylcyclohexane (MeCy) and 2-methyl-tetrahydrofuran (MeTHF). B) Previously studied carbazole–Au–MAC complex **5.32** and carbazole–Au–BZI complex **5.33**. C) Emission spectra of MAC complexes **5.29** and **5.32**. D) Emission spectra of BZI complexes **5.31** and **5.33**.

Table 5.1. Photophysical measurements for MAC-based complexes **5.29** and **5.32**.

	Solvent	λ_{Abs} (CT band)	$\lambda_{Em,\ 298K}$ (λ_{77K})	Yield, ϕ	τ_{298K} (μs)	k_r (s^{-1})	k_{nr} (s^{-1})
5.29	(MeCy)	460	544 (500)	0.80	10.1	7.90×10^4	2.0×10^4
	(1% PS film)	420	529 (500)	0.74	2.27	3.26×10^5	1.15×10^5
	(MeTHF)	417	569 (498)	0.39	31.1	1.30×10^4	2.0×10^4
5.32	(MeTHF)	420	544 (428)	0.50	0.79	6.30×10^5	6.3×10^5

Table 5.2. Photophysical measurements for BZI-based complex **5.31** and **5.32**.

	Solvent	λ_{Abs} (CT band)	$\lambda_{Em,\ 298K}$ (λ_{77K})	Yield, ϕ	τ_{298K} (μs)	k_r (s^{-1})	k_{nr} (s^{-1})
5.31	(MeCy)	416	502 (504)	0.028	29.9	9.36×10^2	3.25×10^4
	(MeTHF)	382	504 (498)	0.024	57.1	4.20×10^2	1.71×10^4
5.33	(MeTHF)	366	452 (426)	0.79	2.63	3.0×10^5	8.0×10^3

In summary, **5.29** is a promising two-coordinate complex achieving up to 80% photoluminescence efficiency via TADF, whereas **5.31** undergoes conventional phosphorescence with ~3% photoluminescence efficiency. The discrepancy in emission type between **5.31** and **5.33** indicates significantly different triplet energies between the π-extended carbazole ligand **5.27** and carbazole. To probe this discrepancy, time-dependent density functional theory (TDDFT) calculations were performed on each ligand, and indeed it was found that the triplet energy of the π-extended carbazole **5.27** is 0.55 eV lower than that of carbazole (see Section 5.8.3 for details). Future studies will focus on the investigation of similar complexes using π-extended indole ligands as well as copper metal centers.

5.7 Conclusion

We have developed a modular platform to access *N*-heterocycles with extended π-conjugation by leveraging hetarynes and Pd-catalysis. The method is tolerant of a variety of bromobiaryls with both structural and electronic diversity. Furthermore, novel π-extended carbazole ligands were synthesized and successfully ligated to give new two-coordinate metal complexes. One of these, **5.29**, displays up to 80% photoluminescence efficiency and therefore shows promise as a TADF emitter for OLED technology. These studies should prompt the further exploration of unique donor ligands in these metal complexes in order to enhance OLED

stability and efficiency, as well as provide access to new *N*-containing polycyclic aromatic hydrocarbon materials.

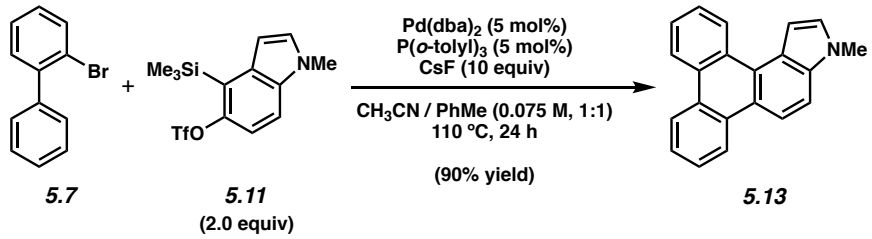
5.8 Experimental Section

5.8.1 Materials and Methods

Unless stated otherwise, reactions were conducted in flame-dried glassware under an atmosphere of nitrogen or argon and commercially obtained reagents were used as received. Anhydrous solvents were either freshly distilled or passed through activated alumina columns, unless otherwise stated. Reaction temperatures were controlled using an IKAmag temperature modulator and, unless stated otherwise, reactions were performed at room temperature (approximately 23 °C). Cesium Fluoride (CsF) and Bis(dibenzylidenacetone)palladium(0) ($Pd(dba)_2$) were obtained from Strem Chemicals and stored in a desiccator. Tri(*o*-tolyl)phosphine ($P(o\text{-tolyl})_3$) was obtained from Sigma Aldrich. 2-Bromobiphenyl (**5.7**) was obtained from Combi-Blocks and purified by flash chromatography (100% Hexanes) prior to use. Bromobiaryl **5.39** was obtained from Combi-Blocks. Bromobiaryls **5.35**,[13] **5.37**,[14] **5.41**,[15] **5.43,**[16] and **5.45**,[17] were prepared according to literature procedures. The silyl triflate precursors to *N*-Me-4,5-indolyne,[18] *N*-Boc-4,5-indolyne,[19] *N*-Me-5,6-indolyne,[19] and were prepared following literature procedures. NHC–Au–Cl complexes **5.28**[5] and **5.30**[11] were prepared following literature procedures. Regioisomeric ratios for annulation products were determined by analysis of the ^{1}H NMR spectra of the crude reaction mixtures. Thin-layer chromatography (TLC) was conducted with EMD gel 60 F254 pre-coated plates (0.25 mm for analytical chromatography and 0.50 mm for preparative chromatography) and visualized using UV. Silicycle Siliaflash P60 (particle size 0.040–0.063 mm) was used for flash column chromatography. ^{1}H NMR spectra were recorded

on Bruker spectrometers (at 400, 500 and 600 MHz) and are reported relative to residual solvent signals. Data for ^{1}H NMR spectra are reported as follows: chemical shift (δ ppm), multiplicity, coupling constant (Hz), integration. Data for ^{13}C NMR are reported in terms of chemical shift (at 101 and 125 MHz). IR spectra were recorded on a Perkin-Elmer UATR Two FT-IR spectrometer and are reported in terms of frequency absorption (cm^{-1}). DART-MS spectra were collected on a Thermo Exactive Plus MSD (Thermo Scientific) equipped with an ID-CUBE ion source and a Vapur Interface (IonSense Inc.). Both the source and MSD were controlled by Excalibur software v. 3.0. The analyte was spotted onto OpenSpot sampling cards (IonSense Inc.) using CH_2Cl_2 as the solvent. Ionization was accomplished using UHP He plasma with no additional ionization agents. The mass calibration was carried out using Pierce LTQ Velos ESI (+) and (–) Ion calibration solutions (Thermo Fisher Scientific). UV-visible absorption spectra were recorded by using Hewlett-Packard 4853 diode array spectrometer. Steady state emission spectra were recorded on Quanta-Master Photon Technology International phosphorescence/fluorescence spectrofluorometer. Emission quantum yields were measured using Hamamatsu C9920 system equipped with a xenon lamp, integrating sphere and model C10027 photonic multichannel analyzer (PMA). Emission lifetimes were acquired on IBH Fluorocube instrument by using time-correlated single photon counting (TCSPC) method.

5.8.2 Experimental Procedures

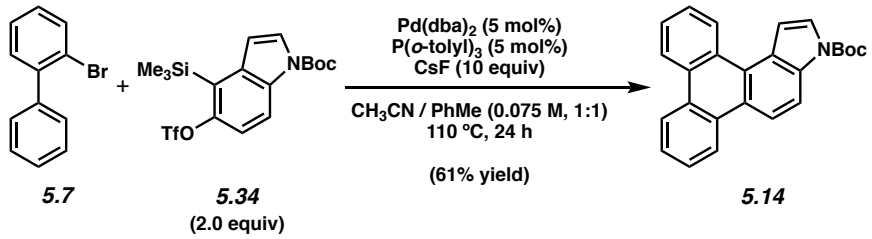


5.7 *5.11* (2.0 equiv) *5.13*

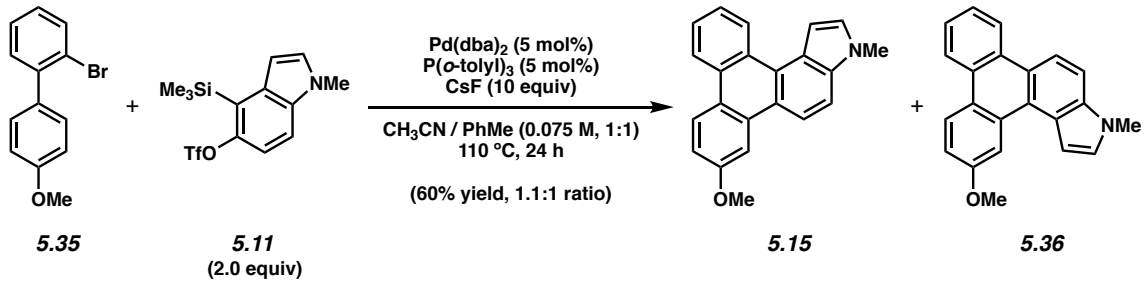
Representative Procedure (Palladium-catalyzed annulation of indolyne precursor 5.11 with 2-bromobiphenyl (5.7) is used as an example). Indole 5.13. A 1-dram vial was charged with $Pd(dba)_2$ (3.7 mg, 0.064 mmol, 5 mol%). Next, toluene (0.86 mL), P(*o*-tolyl)$_3$ (2.0 mg, 0.064 mmol, 5 mol%), 2-bromobiphenyl (**5.7**) (30.0 mg, 0.129 mmol, 1.0 equiv), silyl triflate **5.11** (90.5 mg, 0.257 mmol, 2.0 equiv), and acetonitrile (0.86 mL) were added, followed by an oven-dried magnetic stirbar and then CsF (195 mg, 1.29 mmol, 10.0 equiv). The vial was purged with nitrogen for 3 minutes, then sealed with a Teflon-lined screw cap and stirred at 110 °C for 24 h. After allowing cooling to 23 ºC, the mixture was transferred with CH_2Cl_2 (10 mL) and H_2O (2 mL) to a 150 mL separatory funnel containing brine (15 mL). The layers were separated and the aqueous layer was extracted with CH_2Cl_2 (3 x 15 mL). The combined organic layers were dried over $MgSO_4$, filtered, and concentrated *in vacuo*. The resulting crude product was purified by flash chromatography (100% Hexanes → 200:1 Hexanes:EtOAc) to yield annulation product **5.13** (90% yield, average of two experiments) as an off-white solid. Indole **5.13**: mp: 139–144 ºC; R_f 0.41 (4:1 Hexanes:EtOAc); ^{1}H NMR (500 MHz, $CDCl_3$): δ 9.24 (d, *J* = 8.0, 1H), 8.78 (d, *J* = 8.0, 1H), 8.72 (t, *J* = 7.0, 2H), 8.57 (d, *J* = 9.0, 1H), 7.75 (t, *J* = 7.4, 1H), 7.73–7.62 (m, 4H), 7.53 (d, *J* = 2.8, 1H), 7.28 (d, *J* = 3.0, 1H), 3.92 (s, 3H); ^{13}C NMR (125 MHz, $CDCl_3$): δ 136.4, 131.3, 131.2, 130.4, 128.9, 128.8, 127.17, 127.15, 126.7, 126.4, 125.9, 124.6, 124.1, 123.8, 123.6, 123.3, 123.3, 117.7, 110.5, 104.0, 33.3; IR (film): 3069, 2924, 2850, 1514, 1492, 1441,

1417, 1351, 1248, 754, 740, 718 cm^{-1}; HRMS-APCI (*m/z*) $[M + H]^+$ calcd for $C_{21}H_{16}N^+$, 282.12773; found 282.12717.

Any modifications of the conditions shown in the representative procedure above are specified in the following schemes, which depict all of the results shown in Figure 5.2.

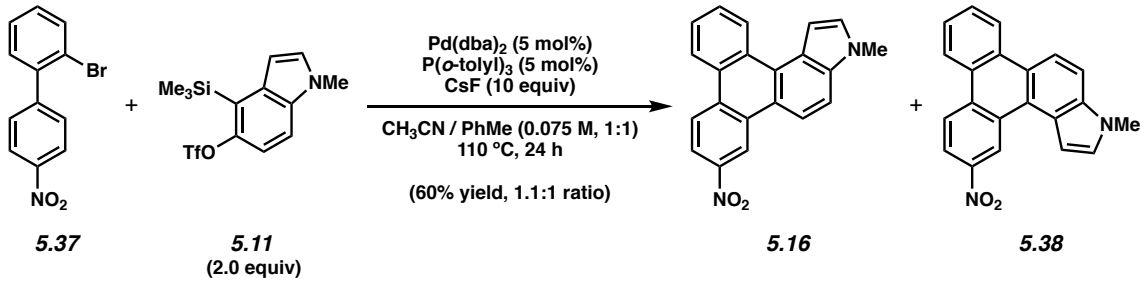


Indole 5.14. Purification by flash chromatography (20% dichloromethane in Hexanes) afforded indole **5.14** (61% yield) as a white solid. Indole **5.14**: R_f 0.45 (9:1 Hexanes:EtOAc); ^{1}H NMR (400 MHz, $CDCl_3$): δ 9.04 – 8.99 (m, 1H), 8.77 – 8.72 (m, 1H), 8.70 (ddd, *J* = 7.8, 5.2, 1.7, 2H), 8.64 (d, *J* = 9.3, 1H), 8.57 (d, J = 9.3, 1H), 7.83 (d, *J* = 3.7, 1H), 7.73–7.64 (m, 4H), 7.62 (d, *J* = 3.8, 1H), 1.74 (s, 9H).



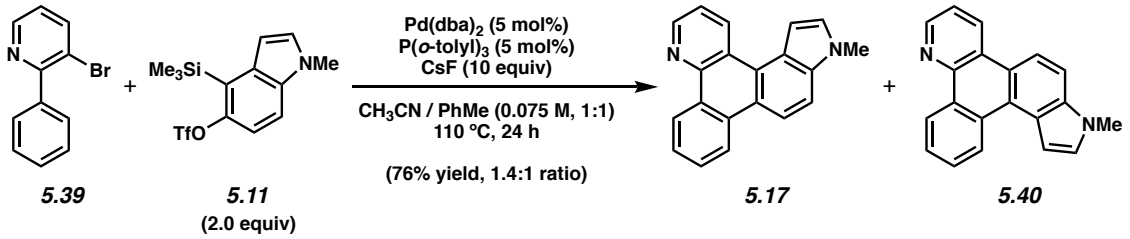
Indoles 5.15 and 5.36. Purification by flash chromatography (50:1 Hexanes:EtOAc) afforded an inseparable mixture of indoles **5.15** and **5.36** (60% yield, average of two experiments, 1.1:1 ratio) as a white solid. Indoles **5.15** and **5.36**: R_f 0.27 (4:1 Hexanes:EtOAc); ^{1}H-NMR (500 MHz,

C_6D_6, combined): δ 9.42 (dd, *J* = 8.3, 1.3, 1H), 8.93 (d, *J* = 2.6, 1H), 8.69 (dd, *J* = 7.9, 1.3, 1H), 8.57– 8.50 (m, 5H), 8.48 (d, *J* = 9.0, 1H), 8.22 (d, *J* = 2.5, 1H), 7.60–7.47 (m, 6H), 7.30–7.26 (m, 3H), 7.21 (dd, *J* = 9.2, 2.6, 1H), 6.72 (d, *J* = 6.7, 1H), 6.69 (d, *J* = 3.2, 1H), 3.61 (s, 3H), 3.55 (s, 3H), 3.001 (s, 3H), 2.995 (s, 3H); ^{13}C-NMR (125 MHz, C_6D_6, combined): δ 159.6, 159.3, 136.7, 136.6, 133.32, 133.31, 131.2, 131.0, 130.8, 129.7, 128.6, 128.5, 127.6, 126.6, 126.4, 126.2, 126.0, 125.8, 125.4, 125.3, 125.2, 125.1, 125.0, 124.6, 124.5, 124.4, 124.0, 123.6, 123.27, 123.25, 118.1, 118.0, 115.5, 115.0, 110.8, 110.5, 110.1, 106.5, 104.5, 104.0, 55.0, 54.9, 32.31, 32.28; IR (film): 2934, 2834, 1614, 1510, 1414, 1246, 1227 cm^{-1}; HRMS-APCI (*m/z*) [M + H$^+$] calcd for $C_{22}H_{18}NO^+$, 312.13829; found 312.13897.



Indoles 5.16 and 5.38. Purification by flash chromatography (50:1 Hexanes:EtOAc → 20:1 Hexanes:EtOAc) afforded an inseparable mixture of indoles **5.16** and **5.38** (80% yield, average of two experiments, 1.4:1 ratio) as a yellow solid. Indoles **5.16** and **5.38**: R_f 0.45 (4:1 Hexanes:EtOAc); ^{1}H-NMR (600 MHz, $CDCl_3$, major): δ 10.10 (d, *J* = 2.4, 1H), 8.79 (d, *J* = 9.1, 1H), 8.71 (d, *J* = 8.3, 1H), 8.66 (d, *J* = 8.2, 1H), 8.55 (d, *J* = 9.2, 1H), 8.41 (dd, *J* = 9.0, 2.3, 1H), 7.78–7.72 (m, 2H), 7.68–7.65 (ddd, *J* = 8.1, 7.0, 1.2, 1H), 7.54 (d, *J* = 3.1, 1H), 7.39 (d, *J* = 3.2, 1H), 4.00 (s, 3H); ^{1}H-NMR (600 MHz, $CDCl_3$, minor): δ 9.54 (d, *J* = 2.3, 1H), 9.21 (d, *J* = 8.3, 1H), 8.75 (d, *J* = 9.1, 1H), 8.70 (d, *J* = 8.3, 1H), 8.55 (d, *J* = 8.9, 1H), 8.35 (dd, *J* = 9.0, 2.3, 1H), 7.82 (ddd, *J* = 8.1, 7.0, 1.3, 1H), 7.76–7.71 (m, 2H), 7.51 (d, *J* = 3.1, 1H), 7.36 (d, *J* = 3.2, 1H),

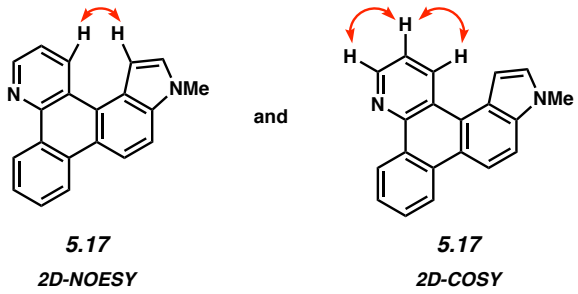
4.00 (s, 3H); ^{13}C-NMR (125 MHz, $CDCl_3$, combined): δ 146.4, 146.0, 136.8, 136.4, 134.8, 133.3, 132.51, 132.48, 131.3, 131.0, 129.9, 129.4, 129.0, 128.7, 128.6, 127.4, 127.3, 126.8, 126.4, 125.2, 124.6, 124.4, 124.21, 124.17, 124.14, 123.8, 123.60, 123.55, 123.5, 123.1, 122.8, 119.9, 119.53, 119.47, 117.5, 117.4, 111.7, 111.1, 104.0, 103.4, 33.4, 33.3; IR (film): 2919, 2852, 1597, 1515, 1346, 854, 747 cm^{-1}; HRMS-APCI (*m/z*) [M + H^+] calcd for $C_{21}H_{15}NO_2^+$, 327.11280; found 327.11387.



Indoles 5.17 and 5.40. Purification by flash chromatography (100% Hexanes → 50:1 Hexanes:EtOAc → 9:1 Hexanes:EtOAc) afforded an inseparable mixture of indoles **5.17** and **5.40** (76% yield, 1.4:1 ratio, average of two experiments) as a pale yellow solid. Indole **5.17**: R_f 0.34 (4:1 Hexanes:EtOAc); ^{1}H-NMR (500 MHz, $CDCl_3$): δ 9.40 (ddd, *J* = 8.2, 4.7, 1.4, 2H), 8.99 (dd, *J* = 4.3, 1.6, 1H), 8.66 (d, 8.2, 1H), 8.54 (d, 8.5, 1H), 7.76 (ddd, *J* = 8.1, 6.9, 1.6, 1H), 7.71 (ddd, *J* = 8.3, 6.8, 1.2, 1H), 7.65 (d, *J* = 9.0, 1H), 7.64–7.60 (m, 1H), 7.38 (d, *J* = 2.9, 1H), 7.27 (d, *J* = 3.2, 1H), 3.91 (s, 3H). Indole **5.17**: R_f 0.34 (4:1 Hexanes:EtOAc); ^{1}H-NMR (500 MHz, $CDCl_3$): δ 9.46 (dd, *J* = 8.1, 1.3, 1H), 9.18 (d, *J* = 8.2, 1H), 8.95 (dd, *J* = 4.3, 1.6, 1H), 8.89 (dd, *J* = 8.4, 1.3, 1H), 8.41 (d, *J* = 9.0, 1H), 7.83 (ddd, *J* = 8.2, 7.0, 1.7, 1H), 7.77 (ddd, *J* = 7.2, 5.6, 1.2, 1H), 7.64–7.60 (m, 1H), 7.55 (dd, *J* = 8.3, 4.3, 1H), 7.53 (d, *J* = 3.1, 1H), 7.29 (d, *J* = 3.2, 1H), 3.90 (s, 3H); ^{13}C-NMR (125 MHz, $CDCl_3$, combined): 147.69, 147.66, 146.9, 145.6, 136.6, 136.3, 134.2, 132.8, 132.7, 131.4, 131.0, 130.1, 129.3, 129.2, 128.8, 128.4, 126.6, 126.4, 126.2, 126.1, 125.8, 125.4, 125.2, 124.6, 124.2, 124.0, 123.9, 123.2, 122.9, 122.8, 122.1, 121.5, 117.7,

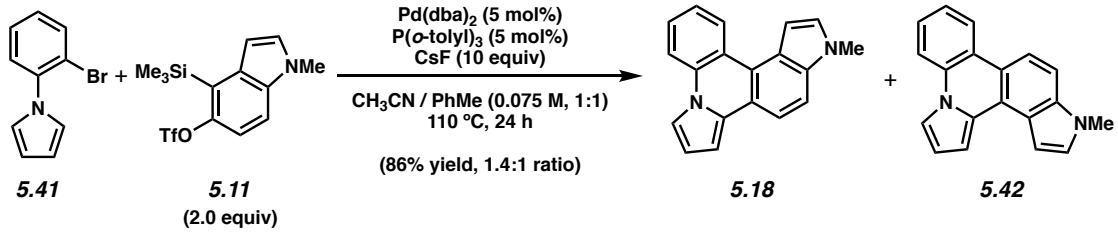
117.3, 111.1, 110.6, 104.0, 103.2, 33.3 (2C); IR (film): 3059, 2920, 1739, 1609, 1579, 1513, 1477, 1444, 1418, 1399, 1349, 1290, 1241 cm^{-1}; HRMS-APCI (*m/z*) [M + H^+] calcd for $C_{20}H_{15}N_2^+$, 283.12297; found 283.11932.

The structure of **5.17** was verified by 2D-NOESY and 2D-COSY of the mixture, as the following interactions were observed:



5.17 ***5.17***

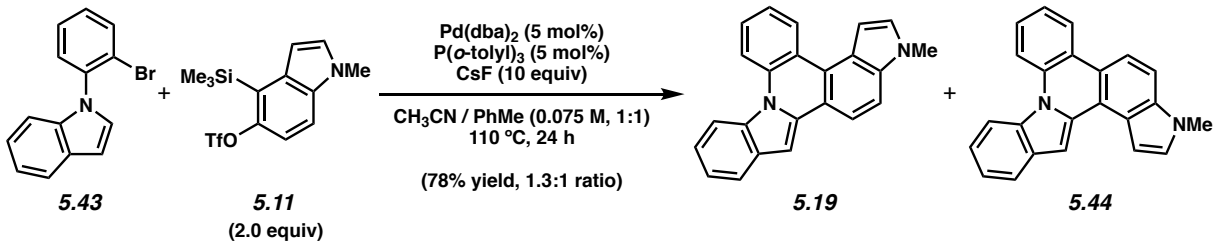
2D-NOESY ***2D-COSY***



5.41 ***5.11*** (2.0 equiv) ***5.18*** ***5.42***

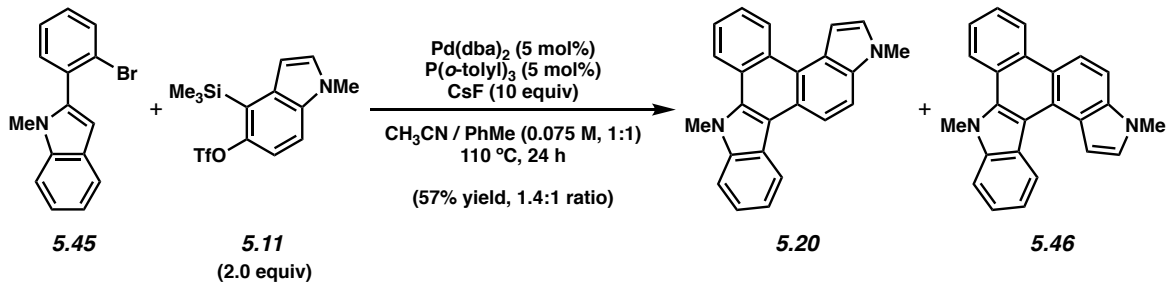
Pyrroles 5.18 and 5.42. Purification by flash chromatography (20:1 Hexanes:Benzene) afforded a mixture of pyrroles **5.18** and **5.42** (86% yield, 1.4:1 ratio, average of two experiments) as a yellow solid, mp: 135–140 ºC. Pyrroles **5.18** and **5.42**: R_f 0.56 (4:1 Hexanes:EtOAc); ^{1}H-NMR (500 MHz, C_6D_6, combined): δ 9.01 (dd, *J* = 8.0, 1.5, 1H), 8.33–8.28 (m, 1H), 8.13 (d, *J* = 8.9, 1H), 8.01 (d, *J* = 8.7, 1H), 7.65 (dd, *J* = 3.0, 1.4, 1H), 7.58 (dd, *J* = 3.0, 1.4, 1H), 7.4 (m, 3H), 7.28 (dd, *J* = 3.2, 0.7, 1H), 7.27–7.23 (m, 2H), 7.22–7.19 (m, 1H), 7.19–7.17 (m, 2H), 7.10 (t, *J* = 0.9, 1H), 7.09 (m, 2H), 6.92 (dd, *J* = 4.0, 2.9, 1H), 6.84 (dd, *J* = 3.9, 2.8, 1H), 6.67 (d, *J* = 3.0, 1H), 6.62 (d, *J* = 3.3, 1H), 2.96 (s, 3H), 2.92 (s, 3H); ^{13}C-NMR (125 MHz, C_6D_6, combined): δ 136.7, 136.2, 134.0, 132.9, 131.5, 129.6, 128.9, 128.8, 127.60, 127.58, 127.0, 124.3, 124.2,

124.0, 123.7, 123.5, 123.4, 122.9, 121.5, 120.4, 118.9, 118.6, 117.9, 117.0, 115.3, 115.2, 113.0, 112.9, 112.7, 112.2, 111.5, 108.8, 105.6, 102.94, 102.88, 101.0, 32.22, 32.19; IR (film): 3102, 2923, 1500, 1441, 1355 cm^{-1}; DART-HRMS (*m/z*) [M + H^+] calcd for $C_{19}H_{15}N_2^+$, 271.12297; found 271.12191.



Indoles 5.19 and 5.44. Purification by flash chromatography (100% Hexanes → 100:1 Hexanes:EtOAc → 25:1 Hexanes:EtOAc → 9:1 Hexanes:EtOAc, followed by a second column of 9:1 Hexanes:EtOAc) afforded an inseparable mixture of indoles **5.19** and **5.44** (78% yield, 1.3:1 ratio) as a bright yellow solid. Indoles **5.19** and **5.44**: R_f 0.32 (4:1 Hexanes:EtOAc); ^{1}H-NMR (500 MHz, $CDCl_3$, major): δ 8.43 (dd, *J* = 8.2, 1.0, 1H), 8.28 (dd, *J* = 8.0, 1.1, 2H), 8.04 (d, *J* = 9.0, 1H), 7.98 (d, *J* = 8.6, 1H), 7.79 (s, 1H), 7.41 (ddd, *J* = 7.8, 6.8, 0.9, 1H), 7.36–7.31 (m, 1H), 7.30–7.17 (m, 3H), 7.08 (dd, *J* = 8.9, 0.6, 1H), 6.63 (d, *J* = 3.2, 1H), 2.94 (s, 3H); ^{1}H-NMR (500 MHz, $CDCl_3$, minor): δ 8.95 (dd, *J* = 8.0, 1.6, 1H), 8.41 (dd, *J* = 8.0, 1H), 8.23 (d, *J* = 8.4, 1H), 7.98 (d, *J* = 7.6, 1H), 7.91 (d, *J* = 7.9, 1H), 7.41 (ddd, *J* = 7.5, 6.9, 0.9, 1H), 7.36–7.31 (m, 1H), 7.30–7.17 (m, 4H), 7.04 (dd, *J* = 8.7, 0.7, 1H), 6.58 (d, *J* = 3.2, 1H), 2.92 (s, 3H); ^{13}C-NMR (125 MHz, C_6D_6, combined): (45 of 46 signals observed) δ 137.6, 137.2, 136.7, 136.5, 135.6, 135.5, 134.1, 133.9, 131.7, 131.6, 129.3, 129.2, 127.6, 127.3, 124.6, 124.3, 124.0, 123.8, 123.7, 123.04, 122.95, 122.3, 122.11, 122.06, 121.6, 121.5, 121.4, 121.05, 120.98, 120.7, 119.9, 118.7, 116.8, 116.7, 116.6, 114.8, 111.3, 110.5, 103.2, 102.9, 99.8, 95.2, 32.2 (2C); IR (film):

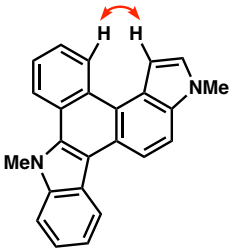
3040, 2923, 1738, 1601, 1550, 1509, 1490, 1447, 1419, 1355; HRMS-APCI (*m/z*) $[M + H]^+$ calcd for $C_{23}H_{17}N_2^+$, 321.13862; found 321.13951.



5.45 ***5.11*** (2.0 equiv) ***5.20*** ***5.46***

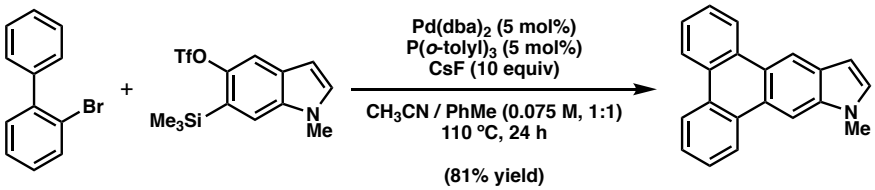
Indoles 5.20 and 5.46. Purification by flash chromatography (100% Hexanes → 200:1 Hexanes:EtOAc → 100:1 Hexanes:EtOAc) afforded an inseparable mixture of indoles **5.20** and **5.46** (57% yield, 1.4:1 ratio, average of two experiments) as a yellow amorphous solid. Indole **5.20**: R_f 0.40 (3:1 Hexanes:EtOAc); ^{1}H-NMR (500 MHz, C_6D_6): δ 9.74 (d, *J* = 8.5, 1H), 9.09 (d, *J* = 8.8, 1H), 8.92–8.88 (m, 1H), 8.48 (dd, *J* = 8.3, 0.9, 1H) 7.70–7.65 (m, 2H), 7.59–7.43 (m, 4H), 7.29 (dd, *J* = 7.5, 1.5, 1H), 6.81 (d, *J* = 3.1, 1H), 3.57 (s, 3H), 3.11 (s, 3H); ^{13}C-NMR (125 MHz, C_6D_6): 141.8, 134.8, 134.2, 132.7, 128.4, 128.2, 125.7, 125.3, 125.2, 124.4, 123.9, 123.8, 123.5, 123.3, 122.6, 122.1, 120.3, 118.8, 115.7, 111.4, 109.9, 103.9, 34.0, 32.4. Indole **5.46**: R_f 0.40 (3:1 Hexanes:EtOAc); ^{1}H-NMR (500 MHz, C_6D_6): δ 9.37 (d, *J* = 8.1, 1H), 8.92–8.88 (m, 1H), 8.68 (d, *J* = 9.1, 1H), 8.38 (dd, 8.4, 0.9, 1H), 7.95 (d, *J* = 3.1, 1H), 7.59–7.43 (m, 3H), 7.40 (ddd, *J* = 7.9, 7.1, 1.1, 1H), 7.34 (dd, J = 9.1, 0.6, 1H), 7.26 (d, *J* = 8.1, 1H), 6.72 (d, *J* = 3.1, 1H), 3.54 (s, 3H), 3.1 (s, 3H); ^{13}C-NMR (125 MHz, C_6D_6, 23 of 24 signals observed): 141.5, 136.4, 136.2, 132.8, 126.3, 125.8, 125.1, 124.8, 124.54, 124.51, 124.46, 123.7, 123.6, 123.1, 121.7, 119.2, 118.3, 115.3, 109.7, 108.1, 105.8, 34.0, 32.4; IR (film, entire mixture): 3055, 2923, 2854, 1737, 1509, 1472, 1374, 1342, 1245, 1102 cm^{-1}; HRMS-APCI (*m/z*) $[M + H]^+$ calcd for $C_{24}H_{19}N_2^+$, 335.15428; found 335.15396.

The structure of **5.20** was verified by 2D-NOESY of the mixture, as the following interaction was observed:



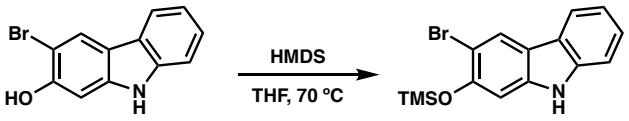
5.20

2D-NOESY



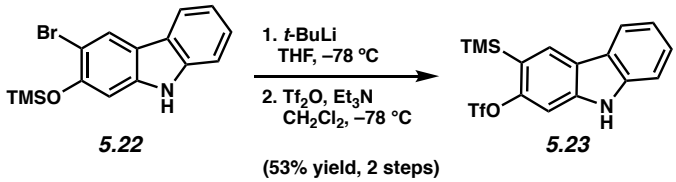
5.7 ***5.47*** (2.0 equiv) ***5.48***

Indole 5.48. Purification by flash chromatography (Hexanes → 1:1 Hexanes/benzene) afforded indole **5.48** (81% yield, average of two experiments) as an off-white solid. Indole **5.48**: R_f 0.25 (9:1 Hexanes:EtOAc); ^{1}H NMR (500 MHz, $CDCl_3$): δ 8.92 (s, 1H), 8.73 (d, J = 8.3, 2H), 8.62 (t, J = 7.7, 2H), 8.51 (s, 1H), 7.66–7.56 (m, 4H), 7.27 (d, J = 2.6, 1H), 6.70 (dd, J = 0.8, 3.1, 1H), 4.00 (s, 3H); ^{13}C NMR (125 MHz, $CDCl_3$): (27 of 28 signals observed) δ 137.4, 132.0, 131.4, 131.2, 129.6, 129.3, 129.0, 127.3, 127.1, 126.6, 126.1, 125.7, 123.56, 123.55, 123.4, 123.22, 123.15, 115.1, 102.3, 101.1, 33.2; IR (film): 3081, 2928, 2811, 1628, 1601, 1520, 1446, 1218, 1085, 754 cm^{-1}; HRMS–APCI (m/z) $[M]^+$ calcd for $C_{21}H_{16}N^+$, 281.11990; found 281.12065.



5.21 *5.22*

Silyl ether 5.22. A scintillation vial was charged with 3-bromo-2-hydroxy carbazole (**5.21**, 4.3 g, 16 mmol, 1.0 equiv) and THF (5.6 mL). 1,1,1,3,3,3-Hexamethyldisilazane (HMDS) (6.9 mL, 2.0 equiv, 33 mmol) was added in one portion, the vial was sealed with a telfon-lined screwcap, and then the vial was placed in a pre-heated aluminum block to stir 70 ºC for 90 min. After the allotted time, the solution was cooled to 23 °C and concentrated under reduced pressure. After drying under high vacuum for 12 hours, the crude product, **5.22**, was carried forward without further purification.



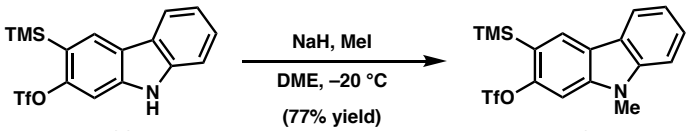
5.22 *5.23*

(53% yield, 2 steps)

Silyl Triflate 5.23. To a scintillation vial was added crude **5.22** (765 mg, 2.29 mmol, 1.00 equiv) and tetrahydrofuran (THF) (8.5 mL). The resulting suspension was purged with nitrogen for 3 minutes, then cooled to –78 ºC. *tert*-Butyllithium (1.70 M, 4.17 mL, 7.09 mmol, 3.1 equiv) was then added dropwise over 10 min. The solution was allowed to stir for 1 hour at –78 ºC. After the allotted time, water (408 μL, 22.5 mmol, 10 equiv) was added dropwise over 2 min. The solution was then allowed to warm to 23 ºC over 10 min and the mixture was transferred to a separatory funnel with water (20 mL) and dichloromethane (20 mL). The layers were then separated and the aqueous layer was extracted with dichloromethane (2 x 20 mL). The combined organic layers were dried over $MgSO_4$, filtered, and concentrated under reduced pressure. The crude residue

was then purified by flash chromatography (100% benzene) to afford an intermediate silyl alcohol as a white solid.

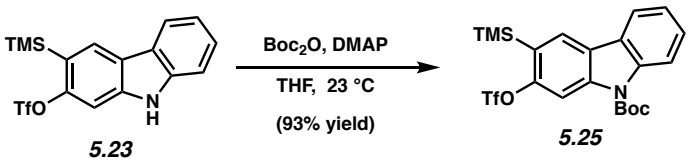
The silyl alcohol from the previous step (403 mg, 1.58 mmol, 1.00 equiv) was suspended in dichloromethane (15 mL) in a scintillation vial. The headspace was purged with nitrogen for 3 minutes, then cooled to –78 ºC. Triethylamine (0.66 mL, 4.7 mmol, 3.0 equiv) was then added in one portion followed by trifluoromethanesulfonic anhydride (400 μL, 2.37 mmol, 1.5 equiv), which was added dropwise over 5 min. The solution was allowed to stir for 1 hour at –78 ºC. After the allotted time, saturated aqueous sodium bicarbonate (20 mL) was added over 1 minute. The solution was then allowed to warm to 23 ºC over 10 min and the mixture was transferred to a separatory funnel with H_2O (10 mL) and dichloromethane (20 mL). The layers were then separated and the aqueous layer was extracted with dichloromethane (2 x 20 mL). The combined organic layers were dried over $MgSO_4$, filtered, and concentrated under reduced pressure. The crude residue was then purified by flash chromatography (100% benzene) to afford silyl triflate **5.23** as a white solid (375 mg, 1.58 mmol, 53% yield over 2 steps). Silyl triflate **5.23**: R_f = 0.59 (benzene); ^{1}H-NMR (600 MHz, $CDCl_3$): δ 8.64 (s, 1H), 7.97 (s, 1H), 7.91 (d, *J* = 8.6, 1H), 7.31 (td, *J* = 7.7, 1.3, 1H), 7.23 (d, J = 7.9, 1H), 7.19 (td, *J* = 7.6, 1.0, 1H), 5.14 (s, 1H), 0.32 (s, 9H); HRMS-APCI (*m/z*) $[M + H]^+$ calcd for $C_{16}H_{17}NOF_3SSi^+$, 388.05723; found 388.05692.



5.23 *5.24*

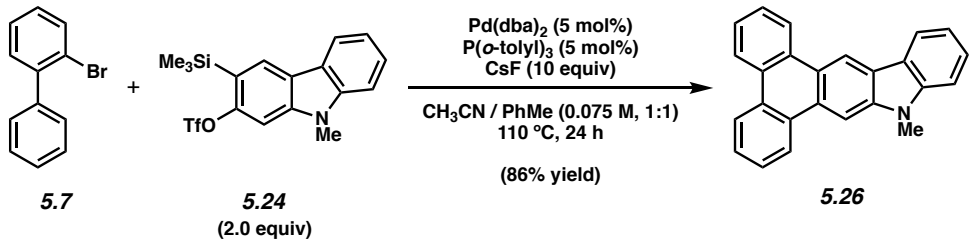
***N*-Me-Carbazole Silyl Triflate 5.24**. To a 2-dram vial was added carbazole silyl triflate **5.23** (196 mg, 0.506 mmol, 1.00 equiv) and DME (1.7 mL, 0.3 M). The resulting mixture was stirred under positive nitrogen pressure. The mixture was cooled to –20 °C in a dry ice water/methanol

bath (7:3) for 5 min. To the cooled solution was added iodomethane (48 μL, 0.76 mmol, 1.5 equiv). Next, the septum was removed and NaH (60% dispersion in mineral oil, 40.5 mg, 1.01 mmol, 2.0 equiv) was added in a single portion, then the septum was quickly replaced. The reaction continued to stir under nitrogen at –20 °C for 2 h, at which point the reaction was quenched with sat. aq. NH_4Cl (5 mL) and allowed to stir at 23 °C for 5 min. The mixture was transferred to a separatory funnel containing water (10 mL) and EtOAc (10 mL). The layers were separated and the aqueous layer was extracted with EtOAc (3 x 10 mL). The organic layers were combined, dried over $MgSO_4$, filtered, and concentrated under reduced pressure to afford a yellow solid. The crude material purified by flash chromatography (dry-loaded using 600 mg of silica, 16:1 Hexanes:benzene) to yield *N*-Me-carbazole silyl triflate **5.24** (156 mg, 77% yield) as a white solid. *N*-Me-carbazole silyl triflate **5.24**: R_f 0.79 (9:1 Hexanes:EtOAc); ^1H NMR (600 MHz, $CDCl_3$): δ 8.18 (s, 1H), 8.11 (d, *J* = 7.9, 1H), 7.53–7.50 (m, 1H), 7.43 (d, J = 8.3, 1H), 7.38 (s, 1H), 7.30 (td, J = 7.5, 0.9, 1H), 3.85 (s, 3H), 0.44 (s, 9H);

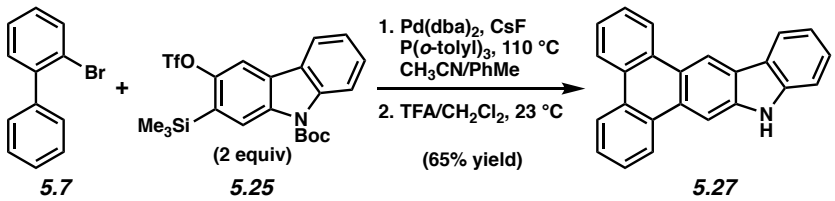


***N*-Boc-Carbazole Silyl Triflate 5.25**. To a 50 mL round bottom flask was added carbazole silyl triflate **5.23** (1.00 g, 2.58 mmol, 1 equiv), THF (13 mL, 0.2 M), 4-dimethylaminopyridine (63 mg, 0.51 mmol, 0.2 equiv), and di-*tert*-butyl dicarbonate (839 mg, 3.84 mmol, 1.5 equiv). The resulting mixture was purged with nitrogen for 3 minutes, then continued to stir under positive nitrogen pressure at 23 °C for 2 h. The mixture was quenched with deionized water (10 mL). The layers were separated and the aqueous layer was extracted with CH_2Cl_2 (3 x 10 mL). The organic

layers were combined, dried over Na_2SO_4, filtered, and concentrated under reduced pressure to afford a yellow solid. The crude material purified by flash chromatography (100:1 Hexanes:EtOAc) to yield *N*-Boc-carbazole silyl triflate **5.25** (1.17 g, 93% yield) as a white solid. *N*-Boc-carbazole silyl triflate **5.25**: R_f 0.57 (9:1 Hexanes:EtOAc); ^{1}H NMR (600 MHz, $CDCl_3$): δ 8.36 (d, J = 8.6, 1H), 8.35 (s, 1H), 8.08 (s, 1H), 8.00 (d, *J* = 7.9, 1H), 7.51 (td, J = 7.6, 1.0, 1H), 7.39 (td, *J* = 7.5, 1.0, 1H), 1.76 (s, 9H).



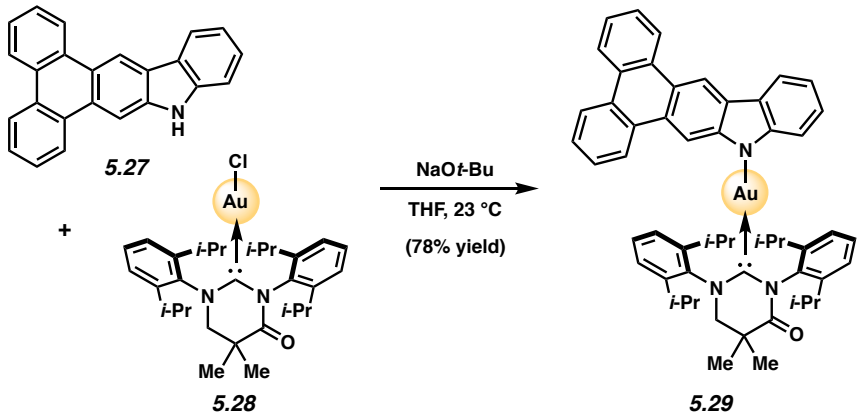
Carbazole 5.26. Follows representative annulation procedure above. Purification by flash chromatography (100% Hexanes → 1:1 Hexanes:Benzene) afforded carbazole **5.26** (86% yield) as an off-white solid. Carbazole **5.26**: R_f 0.74 (4:1 Hexanes:EtOAc); ^{1}H NMR (400 MHz, $CDCl_3$): δ 9.38 (s, 1H), 8.86 (d, *J* = 8.2, 1H), 8.81 (d, *J* = 7.8, 1H), 8.68 (td, *J* = 8.6, 1.5, 2H), 8.54 (s, 1H), 8.31 (dt, *J* = 7.8, 0.9, 1H), 7.72–7.60 (m, 4H), 7.63 (td, *J* = 7.8, 1.1, 1H), 7.58 (td, *J* = 7.8, 1.1, 1H), 7.47 (d, *J* = 8.1, 1H), 7.33 (td, *J* = 7.4, 0.8, 1H), 4.03 (s, 3H); ^{13}C NMR (100 MHz, $CDCl_3$): (27 of 28 signals observed) δ 142.9, 141.3, 131.1, 130.6, 130.0, 128.85, 128.78, 127.4, 127.1, 127.0, 126.8, 126.1, 123.9, 123.6, 123.5, 123.4, 123.1, 123.0, 122.9, 120.8, 119.2, 114.8, 108.5, 101.1, 29.3; IR (film): 3049, 2923, 2854, 1638, 1603, 1500, 1443, 1258, 754 cm^{-1}; HRMS-APCI (m/z) $[M]^+$ calcd for $C_{25}H_{17}N^+$, 331.13555; found 331.13609.



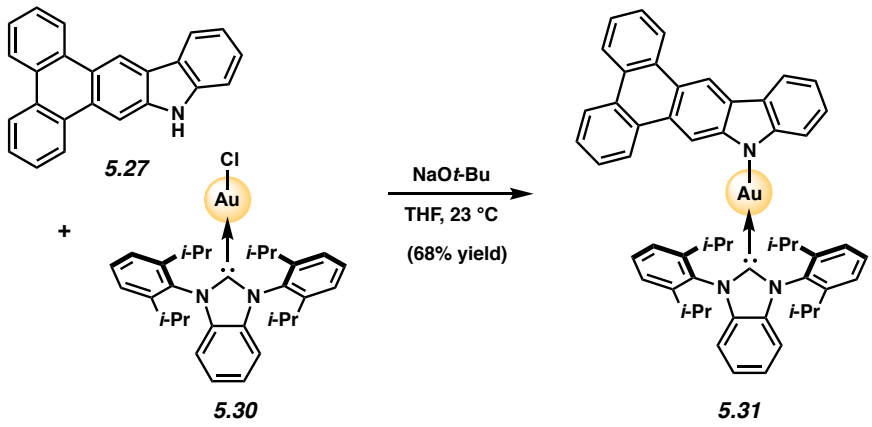
Carbazole 5.27. A 2-dram vial was charged with $Pd(dba)_2$ (7.1 mg, 0.012 mmol, 5 mol%). Next, toluene (1.3 mL), P(*o*-tolyl)$_3$ (3.8 mg, 0.012 mmol, 5 mol%), 2-bromobiphenyl (**5.7**) (58.0 mg, 0.248 mmol, 1.0 equiv), silyl triflate **5.25** (241 mg, 0.495 mmol, 2.0 equiv), and acetonitrile (1.6 mL) were added, followed by an oven-dried magnetic stirbar and then CsF (376 mg, 2.48 mmol, 10.0 equiv). The vial was purged with nitrogen for 3 minutes, then sealed with a Teflon-lined screw cap and stirred at 110 °C for 24 h. After allowing cooling to 23 ºC, the mixture was transferred with dichloromethane (20 mL) and H_2O (10 mL) to a separatory funnel containing brine (15 mL). The layers were separated and the aqueous layer was extracted with dichloromethane (3 x 30 mL). The combined organic layers were dried over Na_2SO_4, filtered, and concentrated under reduced pressure to yield a brown residue that was carried forward without further purification.

The crude material was dissolved in 10:1 CH_2Cl_2:TFA (24.2 mL, 0.01 M) and stirred at 23 °C for 5 h. The reaction was then slowly transferred to a separatory funnel containing sat. aq. sodium bicarbonate (30 mL). The mixture was further diluted with CH_2Cl_2 (10 mL) and the layers were separated. The organic phase was dried over Na_2SO_4 and filtered. To the filtrate was added silica (500 mg). The resulting mixture was dried under reduced pressure until a free flowing solid was obtained. The crude material purified by flash chromatography (100% Hexanes, then 9:1 Hexanes/EtOAc, then 1:1 Hexanes/benzene) to yield carbazole **5.27** (51 mg, 65% yield) as an off-white solid. Carbazole **5.27**. R_f 0.63 (4:1 Hexanes:EtOAc); ^{1}H NMR (600 MHz, DMSO-d_6): δ 11.35 (s, 1H), 9.62 (s, 1H), 9.0 (d, J = 8.0, 1H), 8.82 (d, *J* = 8.3, 1H), 8.76

(dd, J = 12.5, 8.3, 2H), 8.72 (s, 1H), 8.43 (d, *J* = 7.5, 1H), 7.73–7.69 (m, 2H), 7.67 (t, J = 6.9, 1H), 7.62 (t, J = 7.5, 1H), 7.55 (d, J = 8.0, 1H), 7.46 (t, J = 7.5, 1H), 7.24 (t, J = 7.5, 1H); HRMS-APCI (*m/z*) $[M + H]^+$ calcd for $C_{24}H_{16}N^+$, 318.1277; found 318.12843.



Carbazole–Au–MAC 5.29. Sodium *tert*-butoxide (7.3 mg, 76 µmol) was added into a solution of **5.27** (23 mg, 72 µmol) in THF (10 mL). **5.28** (50.2 mg, 73.9 µmol) was added into the reaction flask in one portion and the mixture was left stirring under inert gas at room temperature for 12 hours. The solution was filtered through a plug of celite (2 cm in a 15 mL fritted funnel), washed with THF (10 mL), and the volatiles were removed under reduced pressure. A minimum amount of dichloromethane was added into the residue, followed by 15 mL of dry hexane to precipitate out a solid which was collected by vacuum filtration and washed by more hexane to yield (42 mg, 78% yield). Carbazole–Au–MAC **5.29**: ^{1}H NMR (400 MHz, $CDCl_3$) δ = 9.17 (s, 1H), 8.72 (d, 1H), 8.57 (ddd, *J* = 18.5, 8.3, 1.1 Hz, 2H), 8.39 (d, 1H), 8.08 (d, *J* = 7.4, 1.5, 0.7 Hz, 1H), 7.82 – 7.70 (m, 3H), 7.65 – 7.44 (m, 8H), 7.04 – 6.91 (m, 2H), 5.81 (d, 1H), 3.86 (s, 2H), 3.36 (hept, *J* = 6.5 Hz, 2H), 3.08 (hept, *J* = 6.8 Hz, 2H), 1.45 – 1.33 (m, 18H), 1.26 (d, *J* = 6.8 Hz, 6H).



Carbazole–Au–BZI 5.31. Sodium *tert*-butoxide (6.4 mg, 33 mmol) was added into a solution of **5.27** ligand (20 mg, 63 mmol) in THF (10 mL). **5.30** (44.4 mg, 66.2 mmol, 2.0 equiv) was added into the reaction flask in one portion and the mixture was left stirring under inert gas at room temperature for 12 hours. The solution was filtered through a plug of celite (2 cm in a 15 mL fritted funnel), washed with THF (10 mL), and the volatiles were removed under reduced pressure. A minimum amount of dichloromethane was added into the residue, followed by 10 mL of dry hexane to precipitate out an off-white solid which was collect by vacuum filtration and washed by more hexane to yield (47 mg, 68% yield). Carbazole–Au–BZI **5.31**: ^{1}H NMR (400 MHz, $CDCl_3$) δ 9.25 (s, 1H), 8.77 (dd, J = 8.5, 1.3 Hz, 1H), 8.60 (ddd, J = 16.7, 8.4, 1.4 Hz, 2H), 8.28 (dd, J = 8.5, 1.4 Hz, 1H), 8.17 (dd, J = 7.6, 1.0 Hz, 1H), 8.13 (s, 1H), 7.86 (t, J = 7.8 Hz, 2H), 7.72 (ddd, J = 8.2, 6.9, 1.3 Hz, 1H), 7.65 – 7.56 (m, 6H), 7.52 – 7.47 (m, 3H), 7.29 – 7.26 (m, 2H), 7.16 (ddd, J = 8.2, 7.0, 1.3 Hz, 1H), 7.01 (ddd, J = 7.9, 7.0, 1.0 Hz, 1H), 6.67 (dd, J = 8.1, 0.9 Hz, 1H), 2.60 (hept, J = 6.9 Hz, 4H), 1.40 (d, J = 6.9 Hz, 12H), 1.19 (d, J = 6.8 Hz, 12H).

General Procedure for 1% Polysterene Films. A mixture of polystyrene pellets (99 mg) and toluene (2 mL) was sonicated for 1 h, until all pellets are dissolved. Two-coordinate metal

complex (1 mg) was dissolved in the solution. Using a pipet, ~0.5 mL of the solution was drop-casted onto a glass substrate (2 cm x 2 cm) to achieve an even surface. The film was left to air-dry for 30 min and then placed in the vacuum chamber for further drying overnight. The resulting film was used to acquire the photophysical data.

5.8.3 Computational Data

Density functional theory (DFT) calculations were executed using Q-Chem 5.1 program[20] at the B3LYP/LACVP** level for ground state geometry optimization. Time-dependent density functional theory (TD-DFT) calculations were performed on the ground state optimized geometries at the CAM-B3LYP/LACVP** level for a balanced description of both charge-transfer and locally excited (LE) states (Table 5.3).

Table 5.3. Calculated frontier molecular orbital, singlet (S_1), and triplet (T_1) energies.

	HOMO (ev)	LUMO (eV)	E_{HO-LU} (eV)	S_1 (eV)	T_1 (eV)
carbazole	–5.47	–0.63	4.84	4.56	3.05
5.27	–5.30	–1.14	4.16	4.02	2.50

5.9 Spectra Relevant to Chapter Five:

Heterocyclic Aryne Annulations for the π-Extension of Donor Ligands in Two-Coordinate Metal Complexes

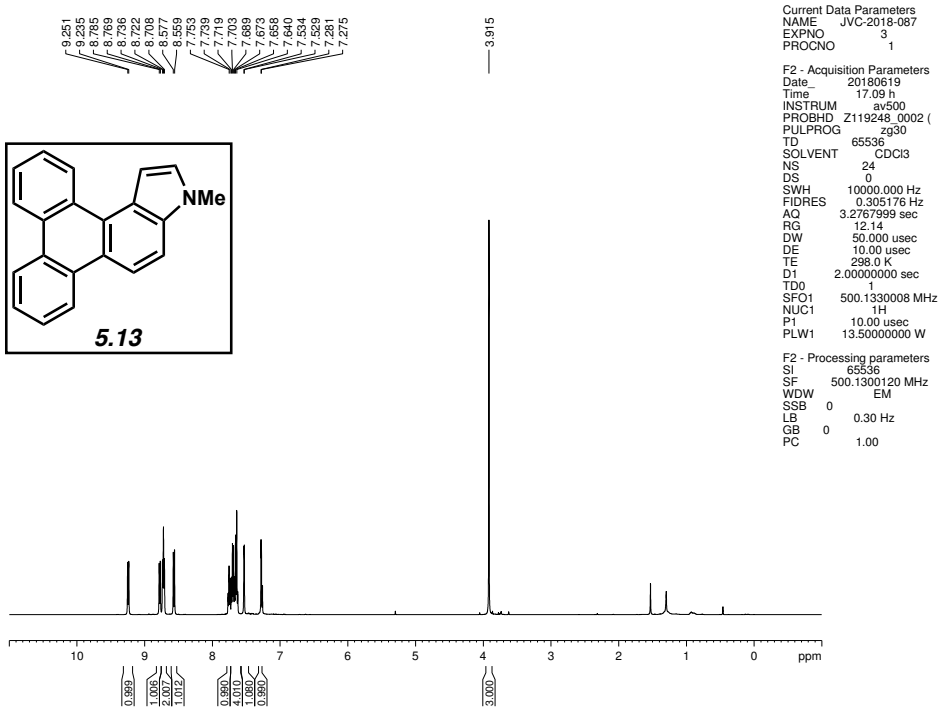


Figure 5.6. ^{1}H NMR (500 MHz, $CDCl_3$) compound **5.13**

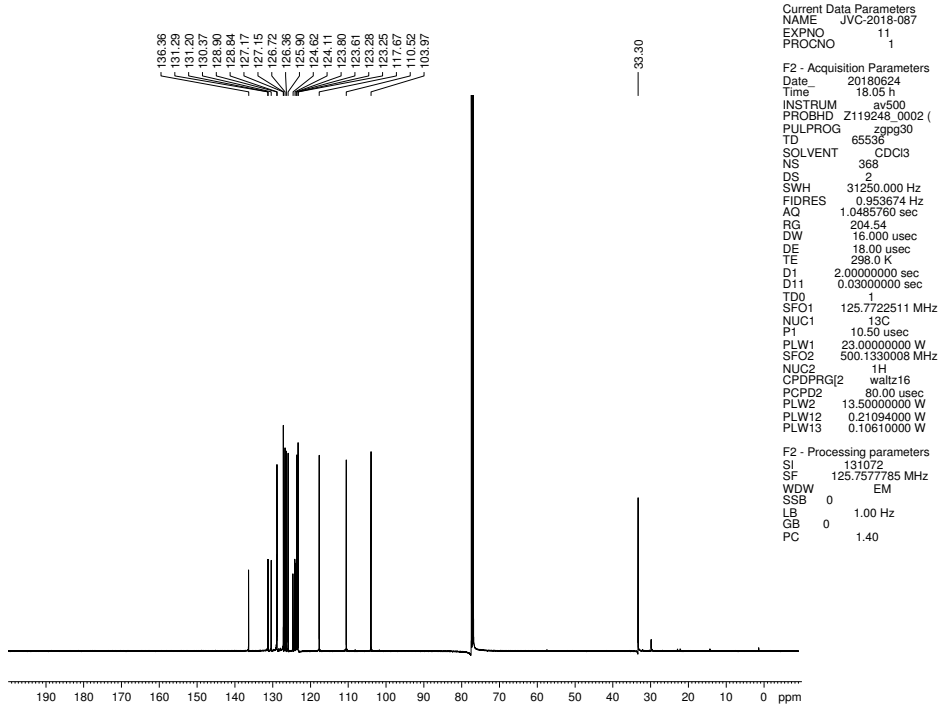


Figure 5.7. ^{13}C NMR (125 MHz, $CDCl_3$) compound **5.13**

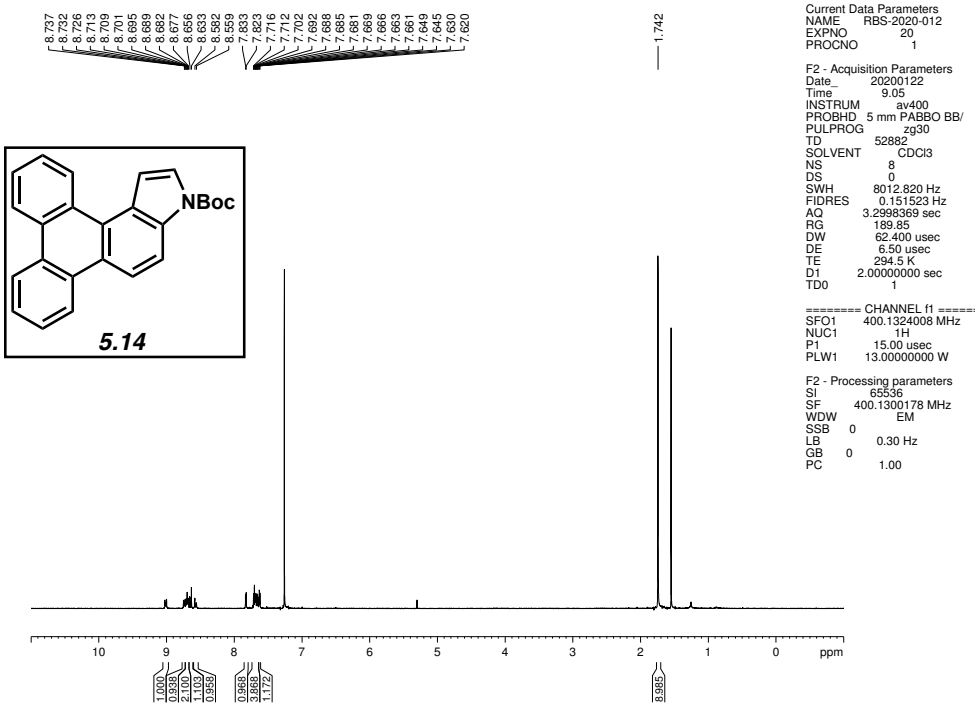


Figure 5.8. ^{1}H NMR (500 MHz, $CDCl_3$) compound **5.14**

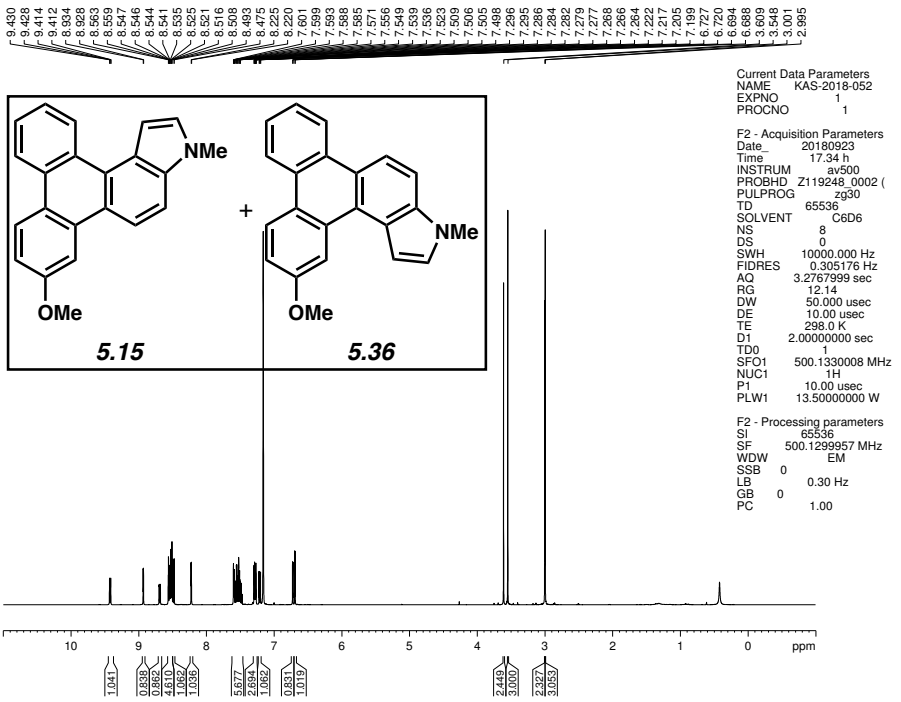


Figure 5.9. ^{1}H NMR (500 MHz, C_6D_6) compound **5.15** and **5.36**

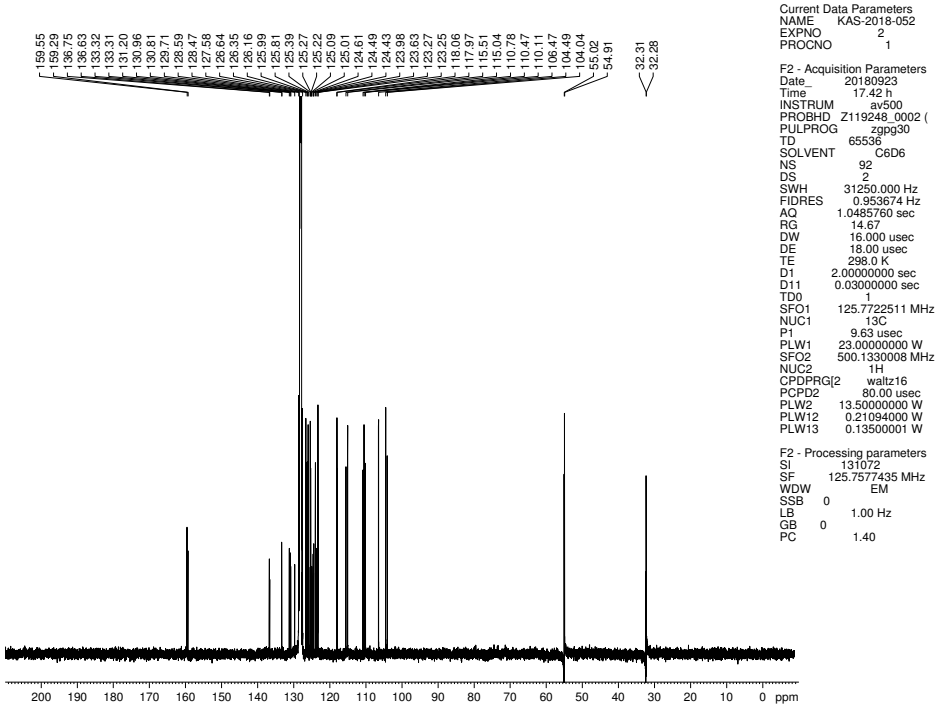


Figure 5.10. ^{13}C NMR (125 MHz, C_6D_6) compound **5.15** and **5.36**

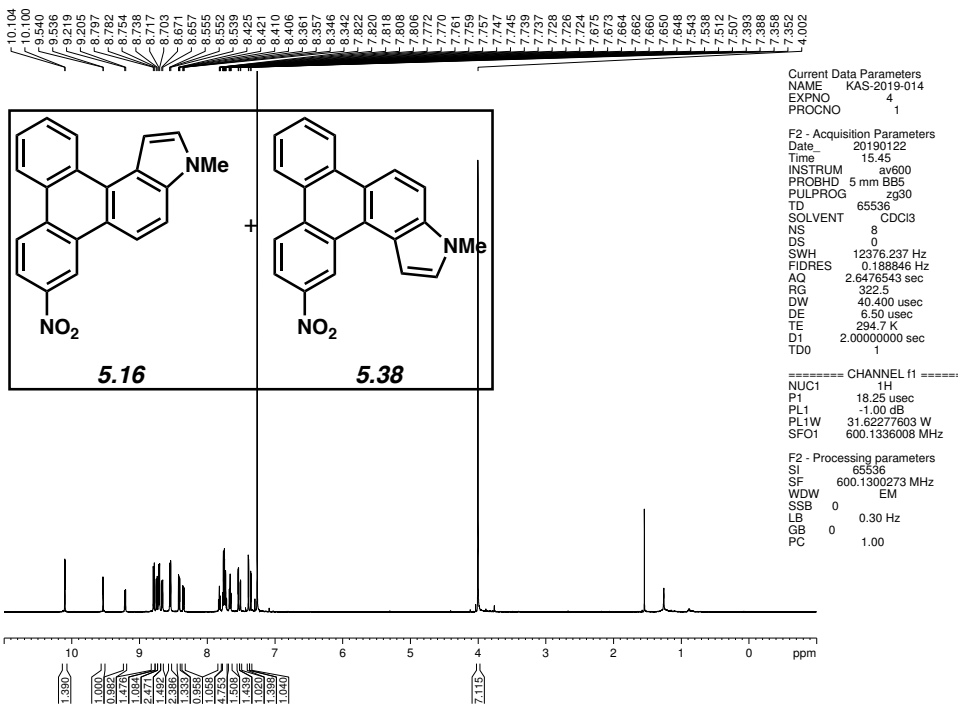


Figure 5.11. ^{1}H NMR (500 MHz, $CDCl_3$) compound **5.16** and **5.38**

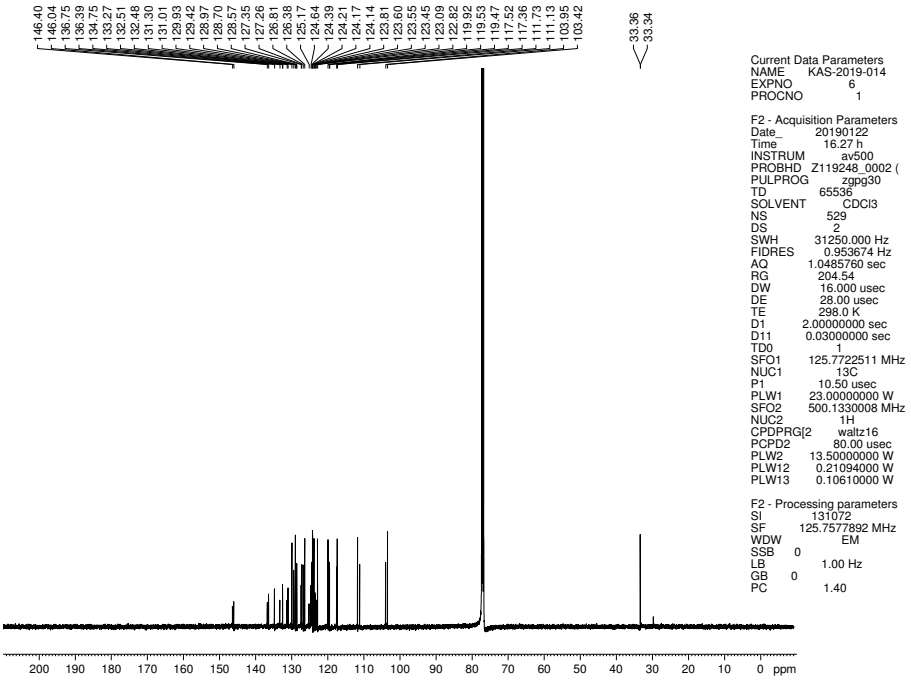


Figure 5.12. ^{13}C NMR (125 MHz, $CDCl_3$) compound **5.16** and **5.38**

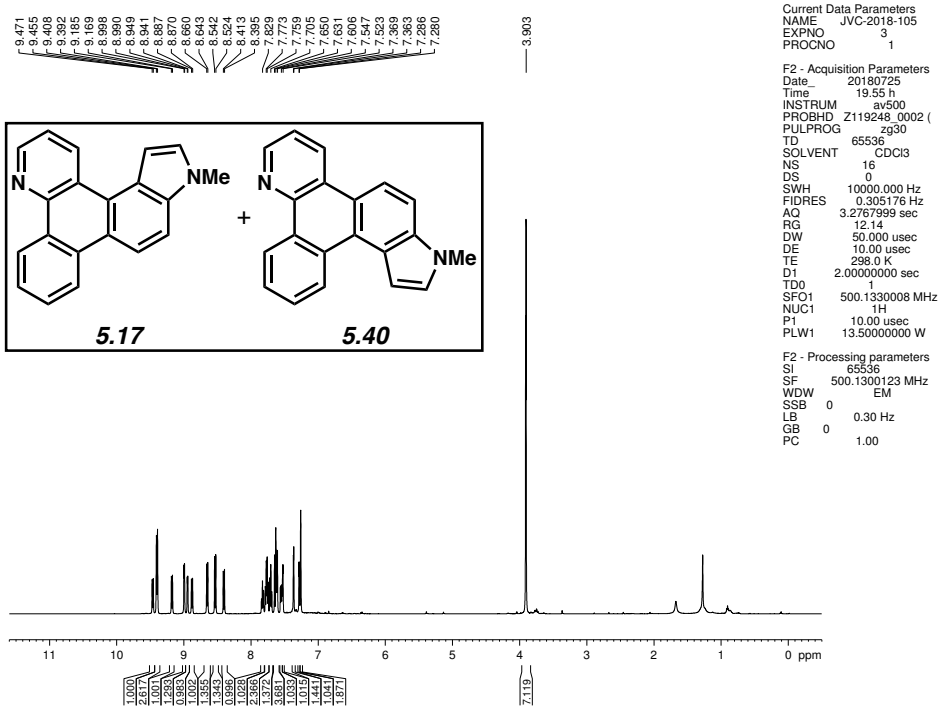


Figure 5.13. ^{1}H NMR (500 MHz, $CDCl_3$) compound **5.17** and **5.40**

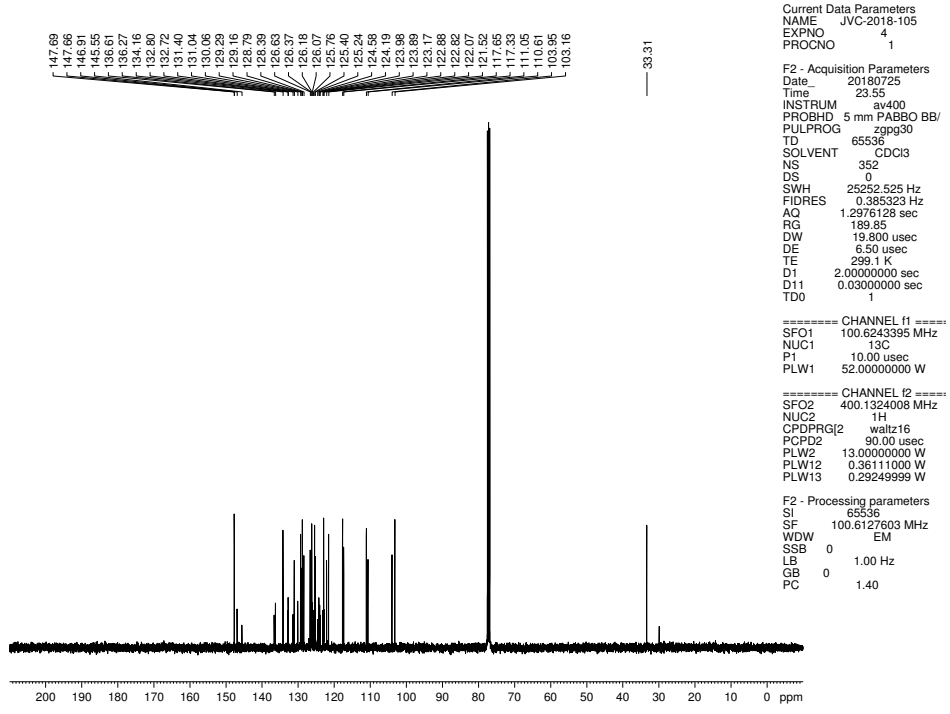


Figure 5.14. ^{13}C NMR (125 MHz, $CDCl_3$) compound **5.17** and **5.40**

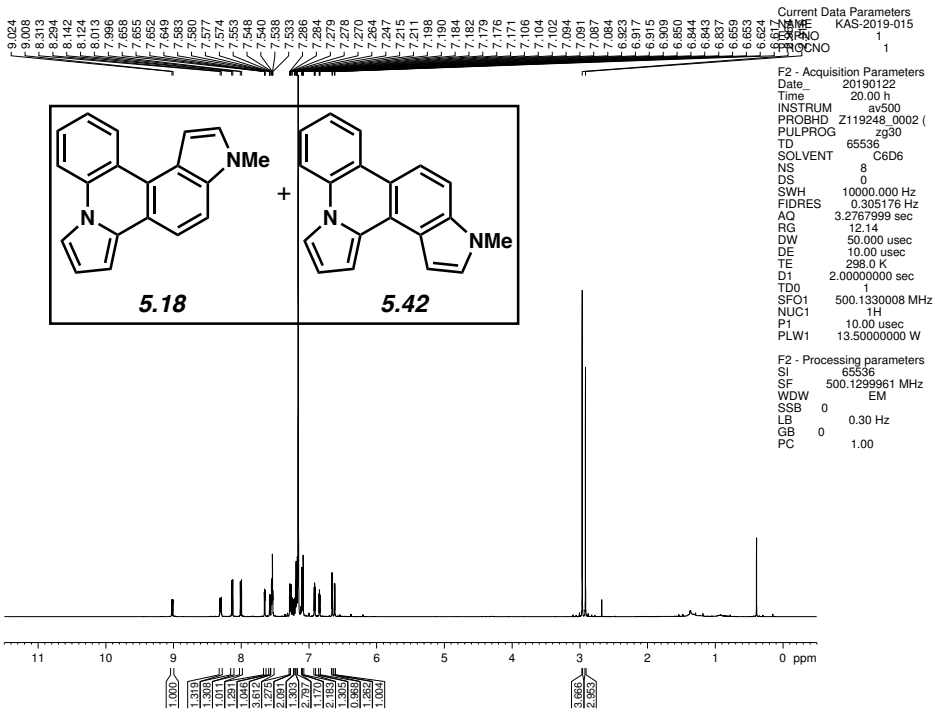


Figure 5.15. ^{1}H NMR (500 MHz, C_6D_6) compound **5.18** and **5.42**

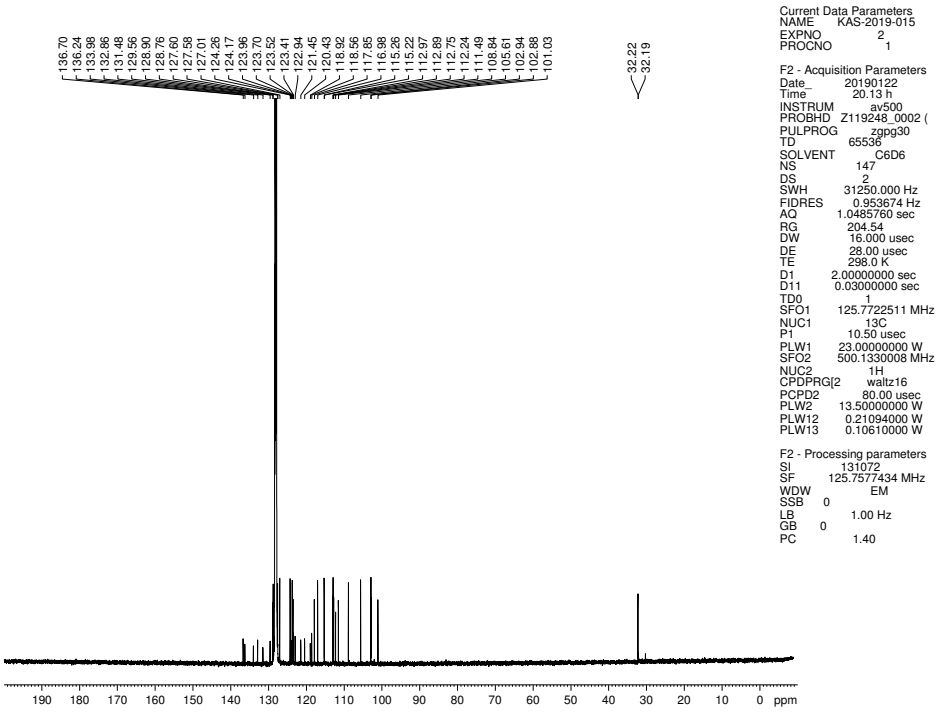


Figure 5.16. ^{13}C NMR (125 MHz, C_6D_6) compound **5.18** and **5.42**

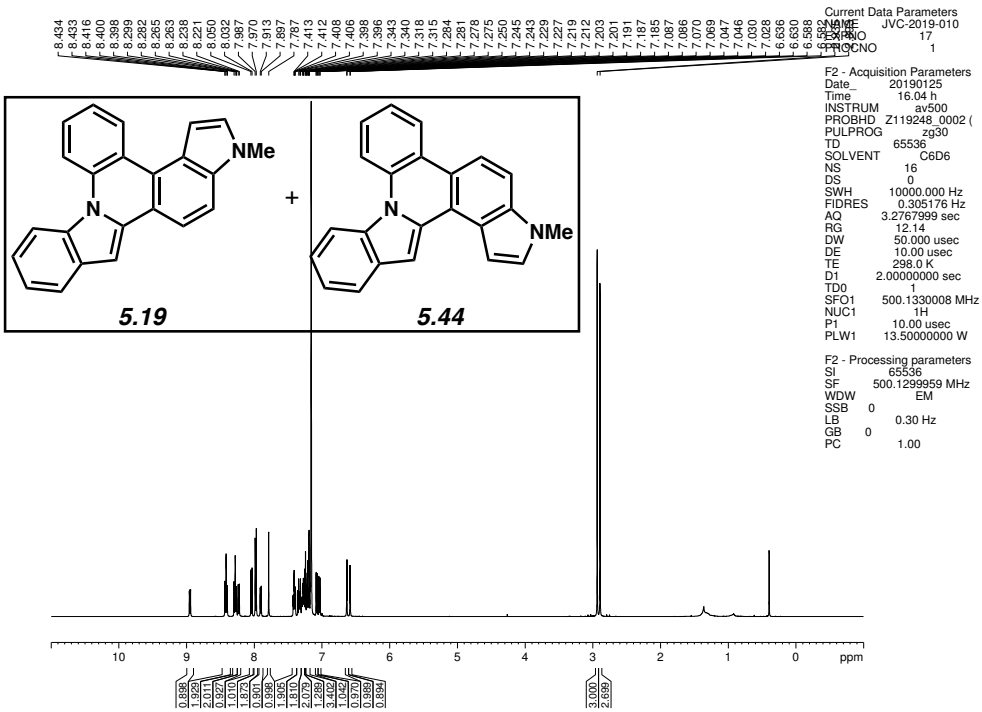


Figure 5.17. ^{1}H NMR (500 MHz, C_6D_6) compound **5.19** and **5.44**

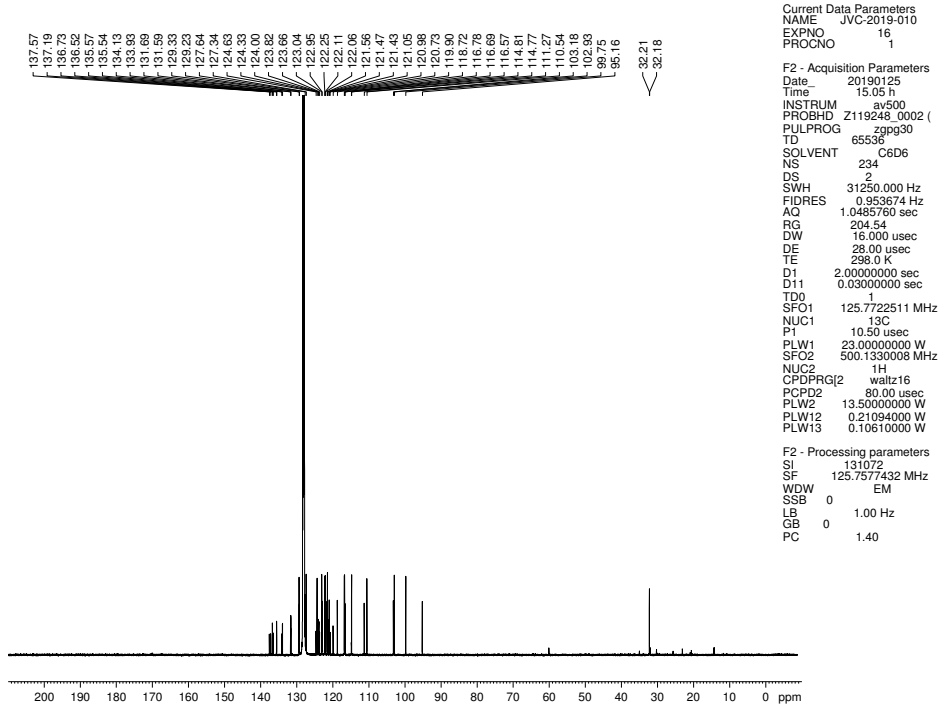


Figure 5.18. ^{13}C NMR (125 MHz, C_6D_6) compound **5.19** and **5.44**

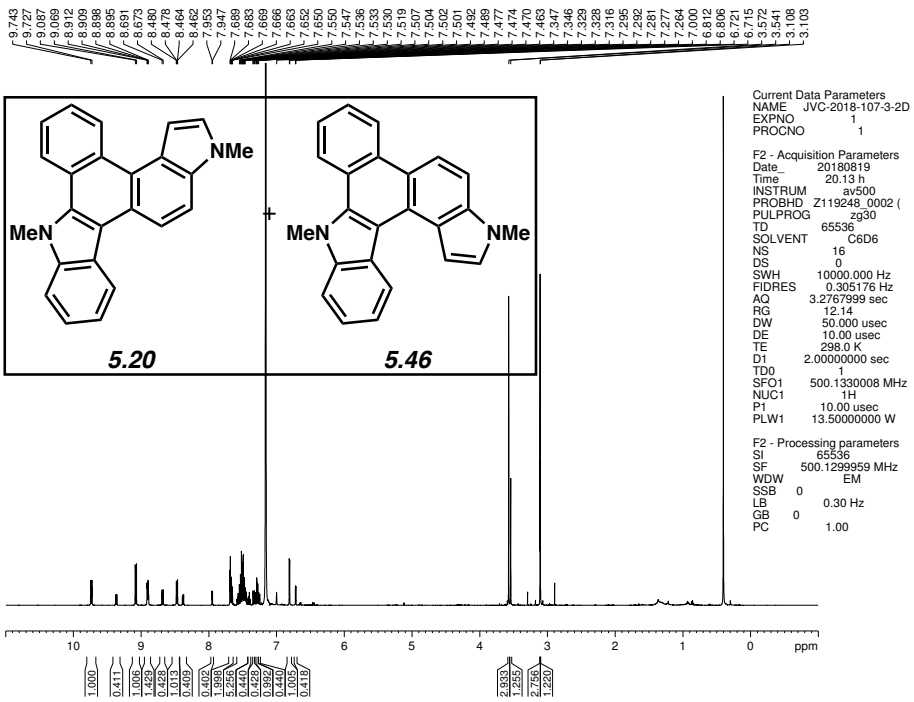


Figure 5.19. ^{1}H NMR (500 MHz, C_6D_6) compound **5.20** and **5.46**

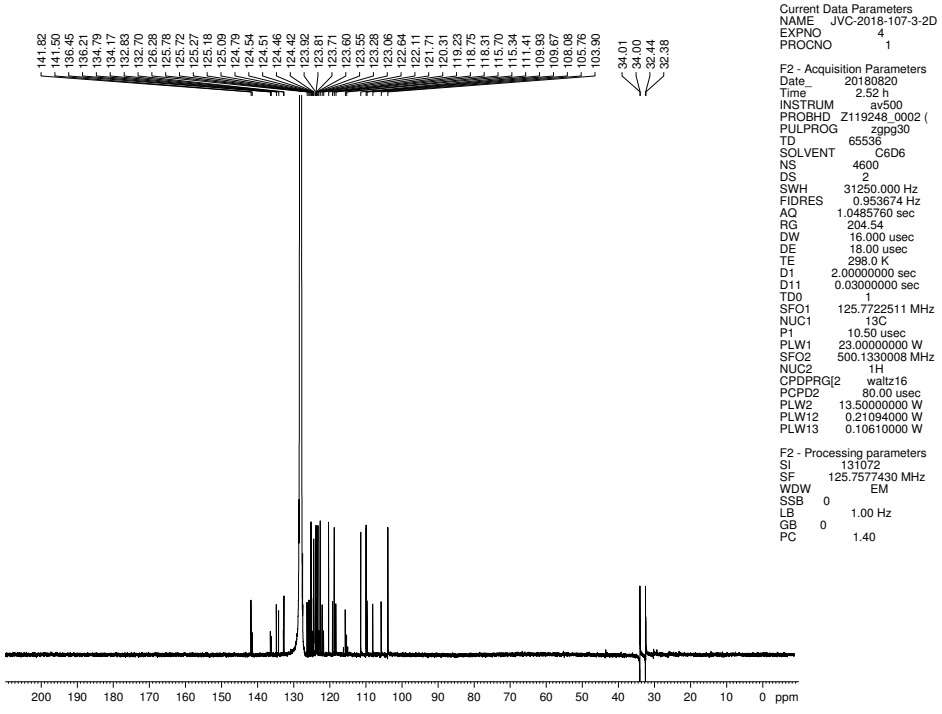


Figure 5.20. ^{13}C NMR (125 MHz, C_6D_6) compound **5.20** and **5.46**

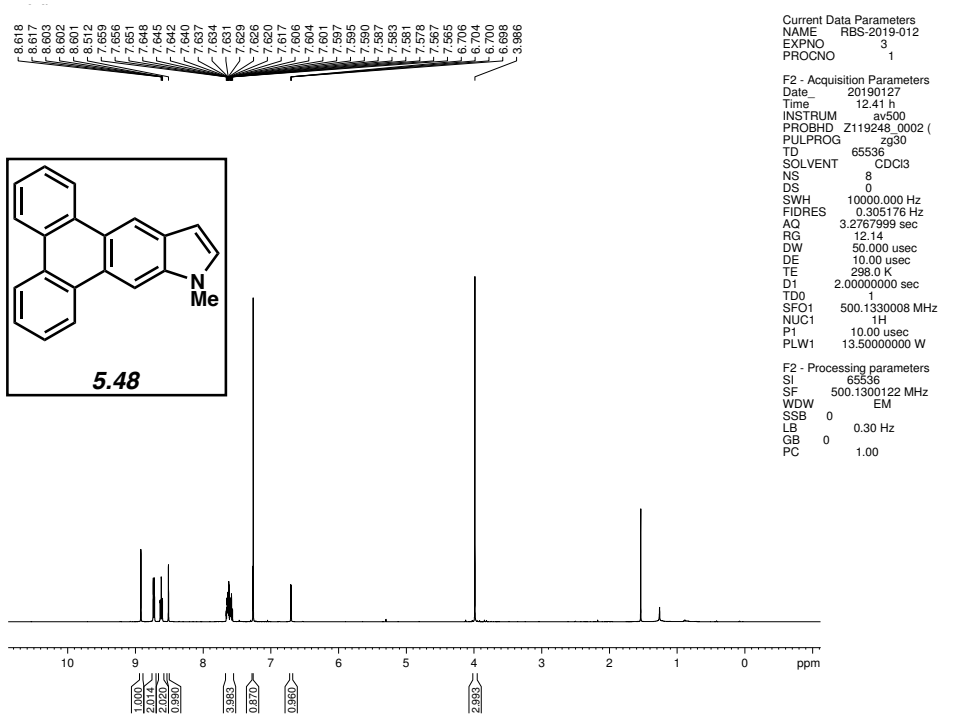


Figure 5.21. ^{1}H NMR (500 MHz, $CDCl_3$) compound **5.48**

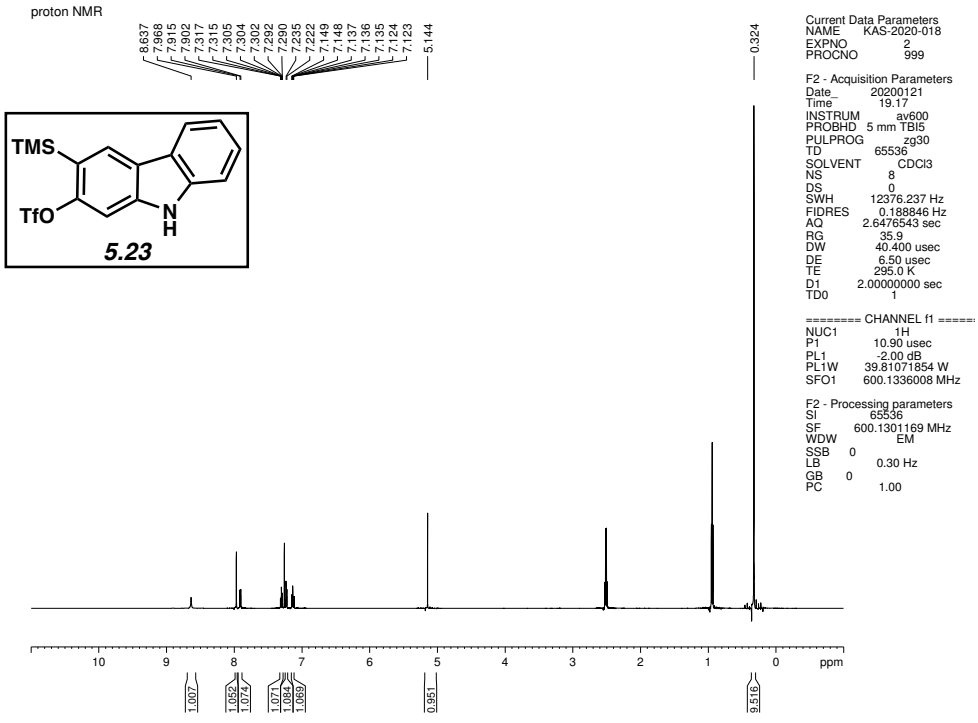


Figure 5.22. ^{1}H NMR (500 MHz, $CDCl_3$) compound **5.23**

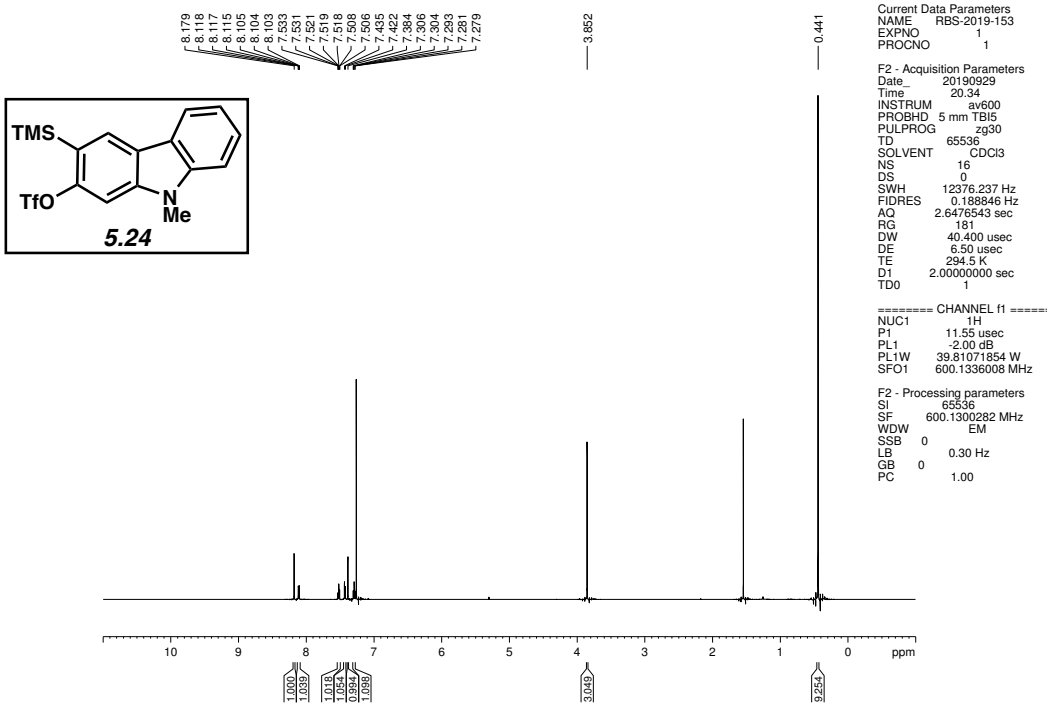


Figure 5.23. ^{1}H NMR (500 MHz, $CDCl_3$) compound **5.24**

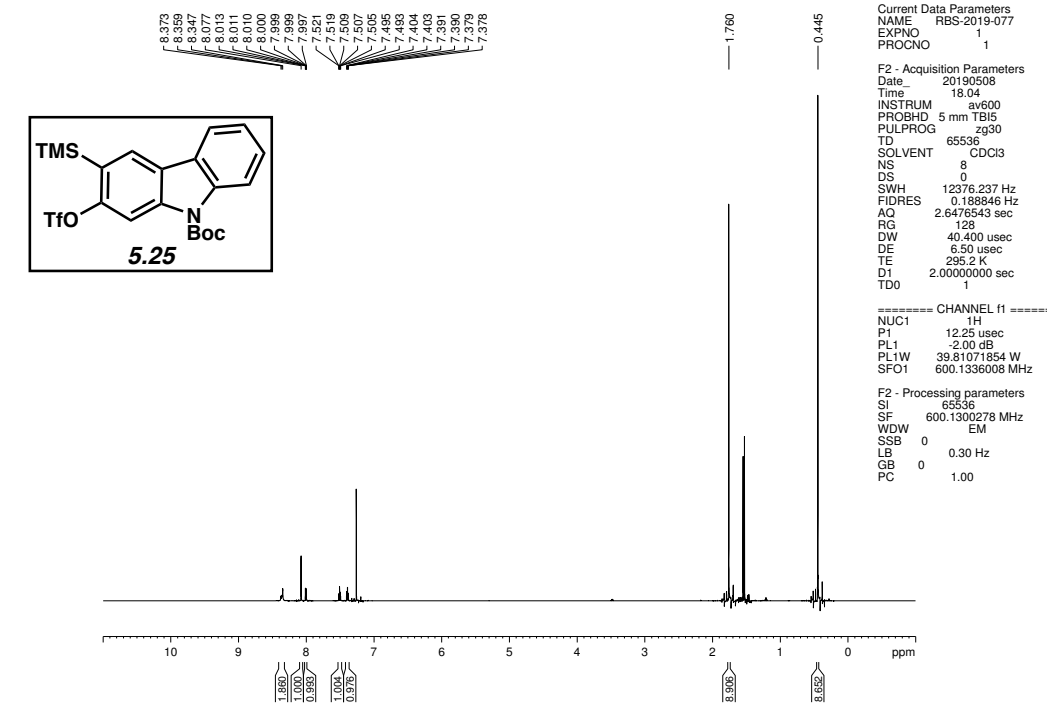


Figure 5.24. ^{1}H NMR (500 MHz, $CDCl_3$) compound **5.25**

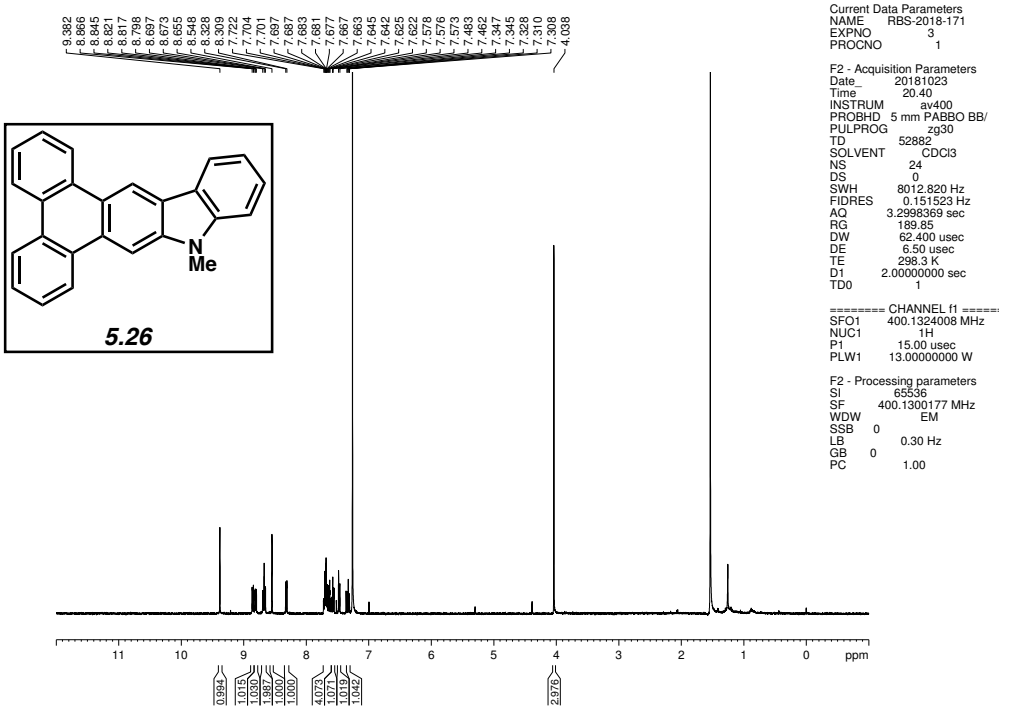


Figure 5.25. ^{1}H NMR (500 MHz, $CDCl_3$) compound **5.26**

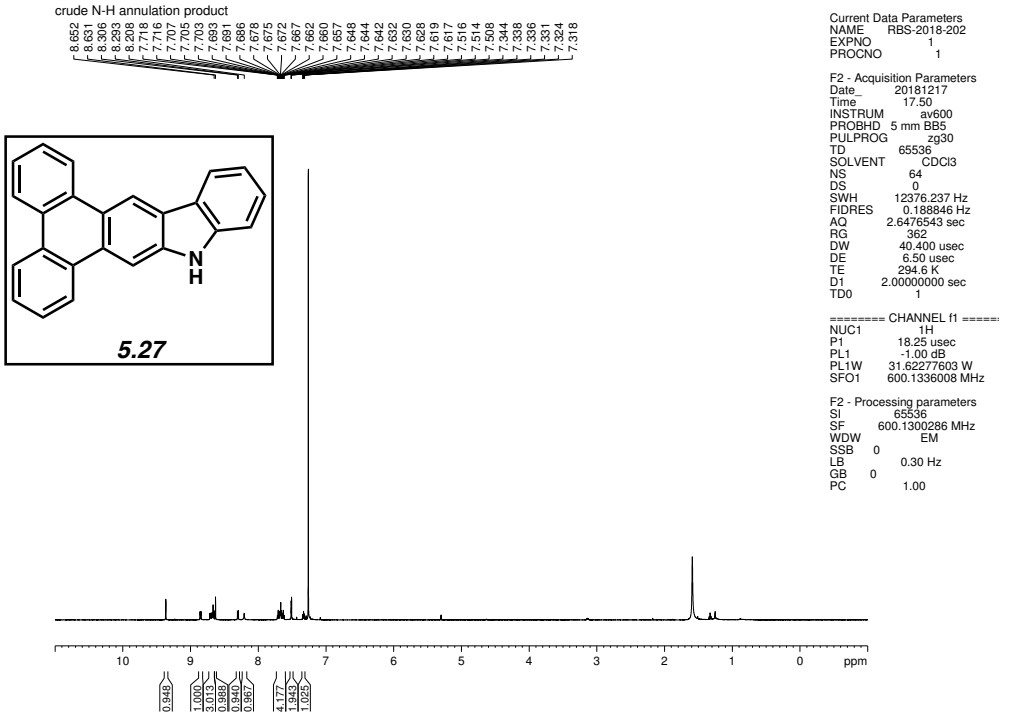


Figure 5.26. ^{1}H NMR (500 MHz, $CDCl_3$) compound **5.27**

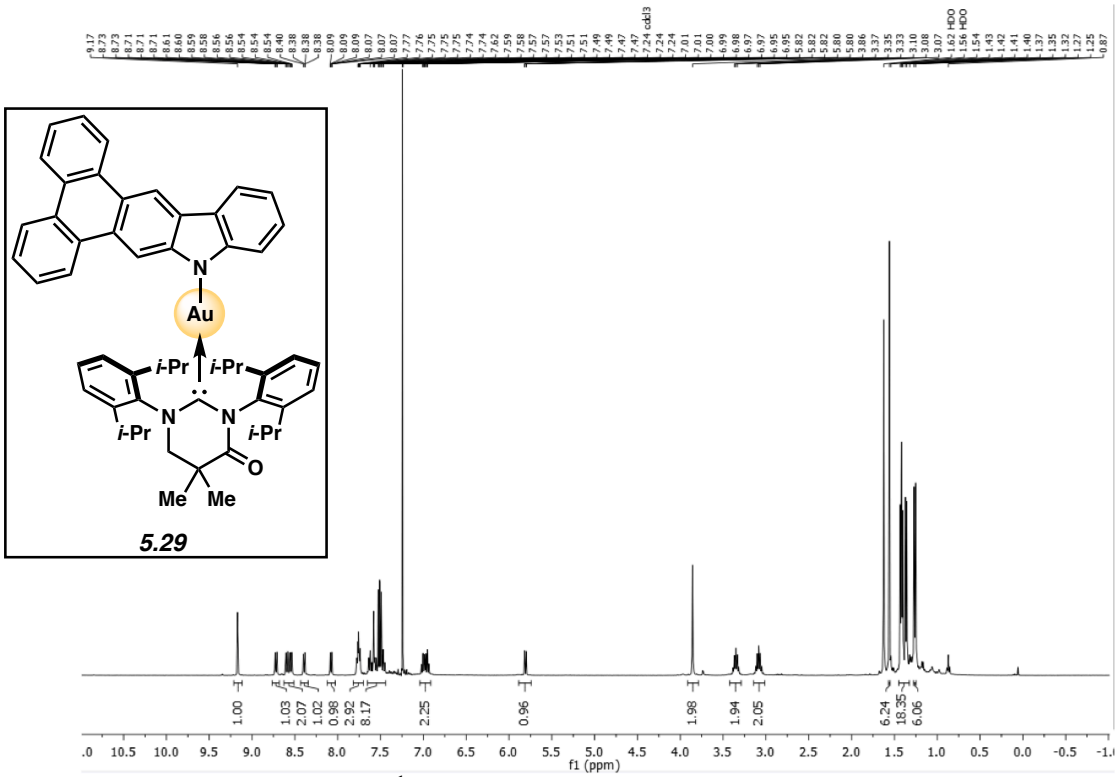


Figure 5.27. ^{1}H NMR (500 MHz, $CDCl_3$) compound **5.29**

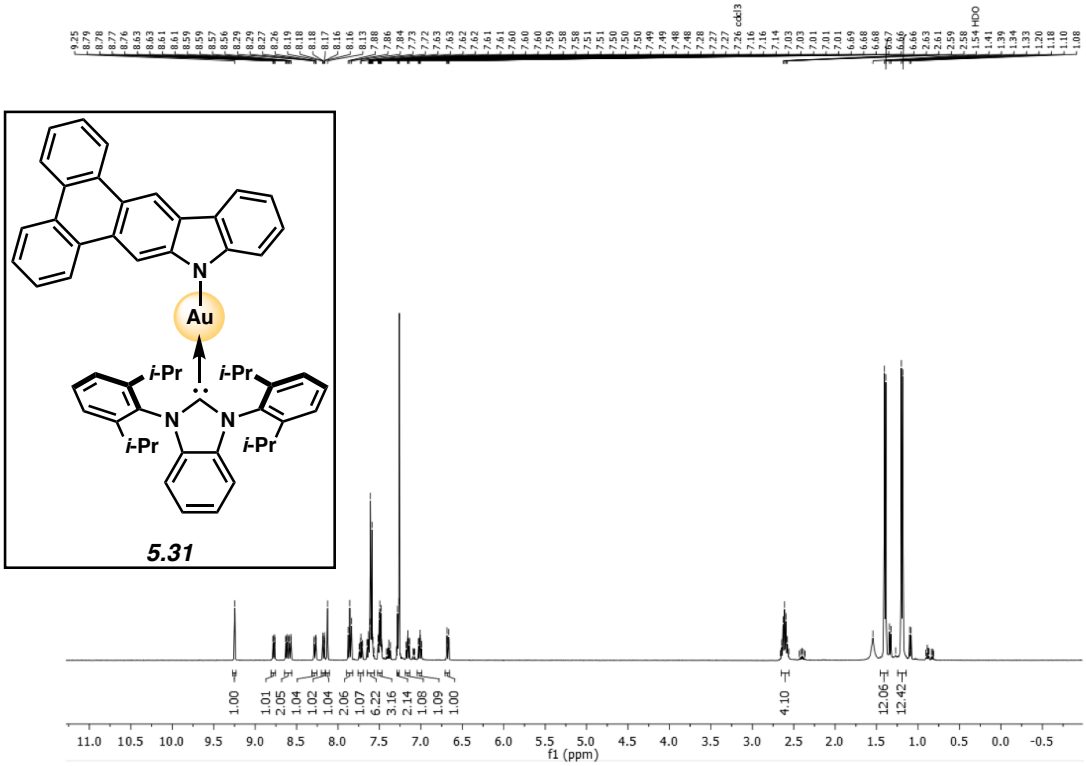


Figure 5.28. ^{1}H NMR (500 MHz, $CDCl_3$) compound **5.31**

5.10 Notes and References

(1) Liu, Y.; Li, C.; Ren, Z.; Yan, S.; Bryce, M. R *Nat. Rev. Mater.* **2018**, *3*, 18020.

(2) For a review on yellow/orange phosphors, see: Fan, C.; Yang, C. *Chem. Soc. Rev.* **2014**, *43*, 6439–6469. For a review on blue phosphors, see: Im, Y.; Byun, S. Y.; Kim, J. H.; Lee, R. D.; Oh, C. S.; Yook, K. S.; Lee, J. Y. *Adv. Funct. Mater.* **2017**, *27*, 1603007.

(3) a) Di, D.; Romanov, A. S.; Yang, L.; Richter, J. M.; Rivett, J. P. H.; Jones, S.; Thomas, T. H.; Jalebi, M. A.; Friend, R. H.; Linnolahti, M.; Bochmann, M.; Credgington, D. *Science* **2017**, *356*, 159–163. b) Hamze, R.; Peltier, J. L.; Sylvinson, D.; Jung, M.; Cardenas, J.; Haiges, R.; Soleilhavoup, M.; Jazzar, R.; Djurovich, P. I.; Bertrand, G.; Thompson, M. E. *Science* **2019**, *363*, 601–606. c) Hamze, R.; Shi, S.; Kapper, S. C.; Ravinson, D. S. M.; Estergreen, L.; Jung, M.-C.; Tadle, A. C.; Haiges, R.; Djurovich, P. I.; Peltier, J. L.; Jazzar, R.; Bertrand, G.; Bradforth, S. E.; Thompson, M. E. *J. Am. Chem. Soc.* **2019**, *141*, 8616–8626.

(4) Yersin, H.; Rausch, A. F.; Czerwieniec, R.; Hofbek, T.; Fischer, T. *Coord. Chem. Rev.* **2011,** *255*, 2622–2652.

(5) Shi, S.; Jung, M. C.; Coburn, C.; Tadle, A.; Sylvinson, D. M. R.; Djurovich, P. I.; Forrest, S. R.; Thompson, M. E. *J. Am. Chem. Soc.* **2019**, *141*, 3576–3588.

(6) Hanson, K.; Roskop, L.; Djurovich, P. I.; Zahariev, F.; Gordon, M. S.; Thompson, M. E. *J. Am. Chem. Soc.* **2010**, *132*, 16247–16255.

(7) a) Liu, Z.; Zhang, X.; Larock, R. C. *J. Am. Chem. Soc.* **2005**, 127, 15716–15717. b) Liu, Z.; Larock, R. C. *J. Org. Chem.* **2007**, *72*, 223–232.

(8) The *N*-H product was also observed as a byproduct of the reaction, but was not isolated.

(9) *N*-Me-5,6-indolyne could also be coupled in 81% yield (see Experimental section 5.8.2 for details)

(10) Goetz, A. E.; Silberstein, A. L.; Corsello, M. A.; Garg, N. K. *J. Am. Chem. Soc.* **2014**, *136*, 3036–3039.

(11) Hamze, R.; Idris, M.; Ravinson, D. S. M.; Jung, M. C.; Haiges, R.; Djurovich, P. I.; Thompson. M. E. *Front. Chem.* **2020**, *8*, 401.

(12) See section 5.8.2 for preparation of 1% by wt polystyrene film.

(13) Zhang, Q.-W.; An, K.; Liu, L.-C.; Guo, S.; Jiang, C.; Guo, H.; He, W. *Angew. Chem., Int. Ed.* **2016**, *55*, 6319–6323.

(14) Wang, T.-F.; Lin, C.-L.; Chen, C.-N.; Wang, T.-C. *J. Chin. Chem. Soc.* **2007**, *54*, 811–816.

(15) Wu, D.; Chen, L.; Ma, S.; Luo, H.; Cao, J.; Chen, R.; Duan, Z.; Mathey, F. *Org. Lett.* **2018**, *20*, 4103−4106.

(16) Panteleev, J.; Geyer, K.; Aguilar-Aguilar, A.; Wang, L.; Lautens, M. *Org. Lett.* **2010**, *12*, 5092–5095.

(17) Wong, S. M.; Yuen, O. Y.; Choy, P. Y.; So, C. M.; Kwong, F. Y. *Org. Synth.* **2016**, *93*, 14–28.

(18) Bronner, S. M.; Bahnck, K. B.; Garg, N. K. *Org. Lett.* **2009**, *11*, 1007–1010.

(19) Im, G.-Y. J.; Bronner, S. M.; Goetz, A. E.; Paton, R. S.; Cheong, P. H.-Y.; Houk, K. N.; Garg, N. K. *J. Am. Chem. Soc.* **2010**, *132*, 17933–17944.

(20) Shao, Y. H.; Gan, Z. T.; Epifanovsky, E.; Gilbert, A. T. B.; Wormit, M.; Kussmann, J.; Lange, A. W.; Behn, A.; Deng, J.; Feng, X. T.; Ghosh, D.; Goldey, M.; Horn, P. R.; Jacobson, L. D.; Kaliman, I.; Khaliullin, R. Z.; Kus, T.; Landau, A.; Liu, J.; Proynov, E. I.;

Rhee, Y. M.; Richard, R. M.; Rohrdanz, M. A.; Steele, R. P.; Sundstrom, E. J.; Woodcock, H. L.; Zimmerman, P. M.; Zuev, D.; Albrecht, B.; Alguire, E.; Austin, B.; Beran, G. J. O.; Bernard, Y. A.; Berquist, E.; Brandhorst, K.; Bravaya, K. B.; Brown, S. T.; Casanova, D.; Chang, C. M.; Chen, Y. Q.; Chien, S. H.; Closser, K. D.; Crittenden, D. L.; Diedenhofen, M.; DiStasio, R. A.; Do, H.; Dutoi, A. D.; Edgar, R. G.; Fatehi, S.; Fusti-Molnar, L.; Ghysels, A.; Golubeva-Zadorozhnaya, A.; Gomes, J.; Hanson-Heine, M. W. D.; Harbach, P. H. P.; Hauser, A. W.; Hohenstein, E. G.; Holden, Z. C.; Jagau, T. C.; Ji, H. J.; Kaduk, B.; Khistyaev, K.; Kim, J.; King, R. A.; Klunzinger, P.; Kosenkov, D.; Kowalczyk, T.; Krauter, C. M.; Lao, K. U.; Laurent, A. D.; Lawler, K. V.; Levchenko, S. V.; Lin, C. Y.; Liu, F.; Livshits, E.; Lochan, R. C.; Luenser, A.; Manohar, P.; Manzer, S. F.; Mao, S. P.; Mardirossian, N.; Marenich, A. V.; Maurer, S. A.; Mayhall, N. J.; Neuscamman, E.; Oana, C. M.; Olivares-Amaya, R.; O'Neill, D. P.; Parkhill, J. A.; Perrine, T. M.; Peverati, R.; Prociuk, A.; Rehn, D. R.; Rosta, E.; Russ, N. J.; Sharada, S. M.; Sharma, S.; Small, D. W.; Sodt, A.; Stein, T.; Stuck, D.; Su, Y. C.; Thom, A. J. W.; Tsuchimochi, T.; Vanovschi, V.; Vogt, L.; Vydrov, O.; Wang, T.; Watson, M. A.; Wenzel, J.; White, A.; Williams, C. F.; Yang, J.; Yeganeh, S.; Yost, S. R.; You, Z. Q.; Zhang, I. Y.; Zhang, X.; Zhao, Y.; Brooks, B. R.; Chan, G. K. L.; Chipman, D. M.; Cramer, C. J.; Goddard, W. A.; Gordon, M. S.; Hehre, W. J.; Klamt, A.; Schaefer, H. F.; Schmidt, M. W.; Sherrill, C. D.; Truhlar, D. G.; Warshel, A.; Xu, X.; Aspuru-Guzik, A.; Baer, R.; Bell, A. T.; Besley, N. A.; Chai, J. D.; Dreuw, A.; Dunietz, B. D.; Furlani, T. R.; Gwaltney, S. R.; Hsu, C. P.; Jung, Y. S.; Kong, J.; Lambrecht, D. S.; Liang, W. Z.; Ochsenfeld, C.; Rassolov, V. A.; Slipchenko, L. V.;

Subotnik, J. E.; Van Voorhis, T.; Herbert, J. M.; Krylov, A. I.; Gill, P. M. W.; Head-Gordon, M. *Mol. Phys.* **2015,** *113*, 184–215.